Satoshi Horikoshi
Graham Brodie
Koichi Takaki
Nick Serpone *Editors*

Agritech: Innovative Agriculture Using Microwaves and Plasmas

Thermal and Non-Thermal Processing

Springer

Agritech: Innovative Agriculture Using Microwaves and Plasmas

Satoshi Horikoshi • Graham Brodie •
Koichi Takaki • Nick Serpone
Editors

Agritech: Innovative Agriculture Using Microwaves and Plasmas

Thermal and Non-Thermal Processing

Springer

Editors
Satoshi Horikoshi
Department of Materials & Life Science
Sophia University
Tokyo, Japan

Graham Brodie
Faculty of Veterinary and Agricultural Sciences
The University of Melbourne
Parkville, VIC, Australia

Koichi Takaki
Faculty of Science and Engineering
Iwate University
Morioka, Iwate, Japan

Nick Serpone
PhotoGreen Laboratory, Dipartimento di Chimica
Universita di Pavia
Pavia, Italy

ISBN 978-981-16-3890-9 ISBN 978-981-16-3891-6 (eBook)
https://doi.org/10.1007/978-981-16-3891-6

This Springer imprint is published by the registered company Springer Nature Singapore Pte Ltd.
The registered company address is: 152 Beach Road, #21-01/04 Gateway East, Singapore 189721, Singapore

Dedication (In Memoriam)

In Memoriam: Marye Anne Fox (1947–2021)

In celebration of the life of **Marye Anne Fox** who passed away on May 9, 2021 after a long illness in Austin, Texas. Chemistry Professor (1974–1998) and Vice-Chancellor Research (1994–1998) at the University of Texas at Austin, Science Advisor to George W. Bush then Governor of Texas, Member of the National Academy of Sciences (1994), Member of the American Philosophical Society (1996), First female Chancellor of North Carolina State University (1998–2004), First female Chancellor of the University of California San Diego (2004–2012), and recipient of the highest honor the National Medal of Science (2010; presented by President Obama)—and many more awards such as the Teaching Excellence Award by the UT College of Natural Sciences, named Rowland Pettit Centennial Professor at UT Austin, and the first UT chemist to hold the M. June and J. Virgil Waggoner Regents Chair in Chemistry (1991). Marye Anne was a public servant and leader beyond academia. She worked hard to advance science policy in the United States.

She was a giant in the Organic Photochemistry and Photoelectrochemistry community, which will sorely miss her. Marye Anne was a role model of women in science—one of her principal goals being "*to build talent in girls—and grit… She had grit and wanted others to have it too….Fox never ran away from criticism. She faced issues—and people—head on* (Gary Robbins, San Diego Union-Tribune, May 11, 2021)." **Mary Anne** also had a softer side that came out in small and modest ways. As Chancellor at UC San Diego, she held events such as *Lunch with the Chancellor* in which attendees were given an old-fashioned lunchbox that carried artwork that depicted her in a humorous way. A former graduate student at UT Austin (Maria Dulay) noted after learning of her passing "*Marye Anne was an amazing Ph.D. advisor. Many of the lessons that she taught me I have carried throughout my scientific career, especially when mentoring students. Her mentorship and counsel has undoubtedly shaped me and has had a profound impact on the scientist that I am today. Marye Anne's legacy burns strong in me and the countless others who have had the privilege to learn from and to work with her."* She was a devoted mother to her children (5), grandchildren (13), and great grandchildren (2).

As a personal note, I have lost a dear friend and colleague with whom we had an occasion to collaborate in the field of semiconductor-based photocatalysis. She was one of the pioneers in the fundamental understanding of TiO_2 both as a semiconductor and as a photocatalyst in environmental remediation. One of my former PhD students, who spent a couple of semesters in Marye Anne's laboratory at UT Austin, said of her: "*She was always very kind and welcoming to me when I went to Austin…Such a smart lady and so hard-working. And a tremendous role model for women in science. A big loss….*" Yes indeed!

May 18, 2021 Nick Serpone

In Memoriam: Bob Schiffmann (1935–2021)

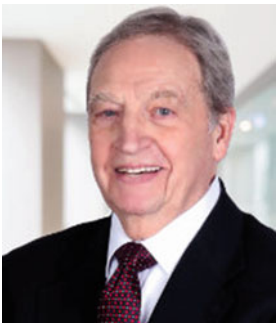

With some sadness, we have also been apprised that following a short illness IMPI's beloved President Bob Schiffmann has passed away on September 4, 2021.

Bob has been known to many in the field of microwaves as the ***microwave guru*** and as the ***go-to guy***, who has made significant contributions into the applications of microwave heating for the past 50 years. During these years, he was closely involved in developing special microwave ovens, in testing and research on microwave ovens, in developing and testing a variety of microwavable food products, as well as in microwave packaging and cookware. Not least, Bob has also been responsible for designing, developing, and constructing a number of industrial microwave heating systems that included the production of muesli, airplane components, bakery products, and extrusion systems, among others (for example: baking ovens, proofers and fryers, granola processing, and sausage manufacturing).

After receiving his BS in Pharmacy from Columbia University (1955) and his MS in Physical and Analytical Chemistry from Purdue University (1959), Bob joined DCA Food Industries, Inc. (1959–1963), followed by a year (1963–1964) as VP Research at Nucleonics Corporation of America, returning to DCA Food Industries, Inc. (1964–1971) during which time he also pursued advanced studies in Biophysics at New York University (1968–1970); he subsequently became a Partner at Bedrosian & Associates (1971–1978). In 1978 he founded and until his passing was the president of R.F. Schiffmann Associates, Inc. a consulting firm with many industry giants as its clients (e.g., Nestle, General Foods, Pillsbury, Proctor and Gamble, American Home Foods, Rubbermaid, and Chlorox among others).

Among his many achievements, Bob found time to devote being President of the Board of the International Microwave Power Institute (IMPI) for 22 years, and with several publications and 28 patents to his name, he also found time to author, co-author, and/or co-edit several books on microwave technology, the most recent one being ***Microwave Chemical & Materials Processing—A Tutorial*** (Springer, 2017). Bob Schiffmann was no doubt the most sought-after consultant in the microwave field that included domestic applications of microwaves as well as industrial applications of microwave energy. In addition he was also a frequent sought-after legal expert witness on all matters related to microwave heating, such as patent infringement, injuries, fires, contracts, and more. He has been the recipient of

several awards and honors, among which are the 2019 AMPERE Gold Medal from the Association for Microwave Power in Europe for Research and Education; the Metaxas Microwave Pioneer Award (as its first recipient); and the Putnam Award for Outstanding Food Process.

Accordingly, this book ***Agritech: Innovative Agriculture Using Microwaves and Plasmas: Thermal and Non-Thermal Processing*** is dedicated to the memory and the many achievements and accomplishments of both Prof. Marye Anne Fox and Dr. Robert F. Schiffmann.

Tokyo, Japan — Satoshi Horikoshi
Parkville, VIC, Australia — Graham Brodie
Morioka, Iwate, Japan — Koichi Takaki
Pavia, Italy — Nick Serpone

Preface

This book describes innovative agricultural methods that make use of the energies from thermal and non-thermal microwaves and plasma.

Humans tended to live a nomadic life in the past, but can now stably obtain food by developments in agriculture, especially over the last several decades. Cities formed as a result of agricultural developments through the centuries. Prior to the 1950s, agriculture relied mostly on natural fertilizers (organic animal-based manure, compost, and dung), crop rotation, and manual removal of weeds by hand, all of which to be replaced by chemical fertilizers, pesticides, and herbicides to increase crop yields and stabilize the food supply. As such, recent years have witnessed significant improvements in crop productivity and diversification and in gene recombination (genetic engineering) as a result of progress in biotechnology that continues to develop further. However, as good as these technologies may have been, they have nonetheless resulted in agricultural soils to be polluted by herbicide and pesticide residues that can pose safety risks. The innovative new developments in agriculture explained in this book are based on the use of microwaves and plasma that do not rely on chemicals and genetic modification to increase crop yields and food safety.

This is one of the first books that focuses on the agricultural usage of microwaves. It is a technical book that also incorporates plasma into agriculture. From this perspective, the book covers microwaves and plasmas, two completely different fields. Consequently, it will be of interest to those readers who wish to acquaint themselves with these alternative technologies and may wish to implement them. Moreover, the book will be useful to a broad readership including researchers and technicians at universities and practitioners in industries. It is accessible to readers across different fields through inclusion of abundant figures and limiting the use of equations to the maximal possible extent.

In the seventeenth century, at the time that Sir Isaac Newton earned his PhD degree, the plague epidemic ravaged across Europe causing many universities to close down, thereby delaying many scientific and technological advances. In the meantime, Newton returned to his hometown and discovered that the forced

"creative vacation" was a stimulus for later advances in science: calculus, the laws of optics, and the law of universal gravitation.

Today, as in Newton's period, the current Covid-19 viral pandemic has limited the progress of much research. Accordingly, it may be time to consider changes and ponder on new research studies over time as Newton did. Thus, it is our hope that this book will trigger novel innovative ideas by researchers during this current "creative period" brought about by the current pandemic.

Finally, the Editors wish to express their gratitude to all the authors who kindly responded to the authors' call and submitted manuscripts in short time. As well, we would also like to thank the staff at Springer Nature for their valuable suggestions prior to publication and for their tremendous support and management.

Tokyo, Japan — Satoshi Horikoshi
Parkville, VIC, Australia — Graham Brodie
Morioka, Iwate, Japan — Koichi Takaki
Pavia, Italy — Nick Serpone

Contents

About the Editors

Satoshi Horikoshi received his PhD degree in 1999 and was subsequently a postdoctoral researcher at the Frontier Research Center for the Global Environment Science in Meisei University (Ministry of Education, Culture, Sports, Science and Technology) until 2006. He joined Sophia University as Assistant Professor in 2006, and then moved to Tokyo University of Science as Associate Professor in 2008, after which he returned to Sophia University as Associate Professor in 2011 and was made Professor in 2020. Currently, he is on the Editorial Advisory Board of the Journal of Microwave Power and Electromagnetic Energy, Molecules, and three other international journals. His research interests involve new functional materials, nanomaterial synthesis, molecular biology, formation of sustainable energy, rubber and plastic recycling, in-liquid plasma chemical synthesis, and environmental protection using microwave- and/or photo-energy. He has co-authored over 200 scientific publications and has contributed to and edited or co-authored 30 books. He frequently explains the role of microwaves on television and in newspapers.

Graham Brodie was awarded his Bachelor of Engineering degree in 1981 and worked in the electrical power industry for some time. In 1997, he joined the Agricultural Department of The University of Melbourne and, after teaching engineering principles to agricultural students for several years, he earned his PhD in 2005. Currently, he is on the Board of Governors for the International Microwave Power Institute; he is on the Research Advisory Board for Chitkara University, Punjab, India; he is an editor with De Gruyter Open; and is the chairman of the Australian Industrial Radio Frequency and Microwave Applications Group. His research interests include using microwave generated plasma to study surface sterilization of materials and agricultural commodities; microwave heating of biomaterials and soil; microwave pyrolysis of plastic and bio-wastes; using microwaves holography for sensing objects in soil and built environments; improving water use efficiency in agriculture; producing and using renewable energy on farms; on-farm animal waste management; and applications of Geographic Information System (GIS) and Remote Sensing technologies in agriculture and archeology.

Koichi Takaki received the B. Eng., M. Eng., and Dr. Eng. degrees in electrical engineering from Kumamoto University, Japan, in 1986, 1988, and 1995, respectively. He joined Oita National College of Technology as a research associate in 1989 and was made an assistant professor in 1993. He moved to the Department of Electrical and Electronics Engineering, Iwate University as a research associate in 1996 and was an associate professor from 2000. During 2000–2001, he was a visiting scientist at the McMaster University, Hamilton, Canada. After that, he was made Professor of Iwate University in 2011. Currently, he is also a Vice-Director of Agri-Innovation Center, Iwate University, and a senior member of IEEE. He received Prizes for Science and Technology in the Commendation for Science and Technology by the Minister of Education, Culture, Sports, Science, and Technology in April 2016. He frequently explains the role of high-voltage technologies, general sciences, and electrostatic phenomena on 34 TV and radio programs including NHK (Ohayo-Nippon, Asa-Ichi, NHK world), TBS (Yumeno-Tobira

+, Evening-wide), etc. His current research interests include pulsed power technology such as pulsed ion technology, agricultural applications (plant growth acceleration, fruition of mushrooms, retaining freshness of fruits and vegetables), and environmental applications (water purification, gas remediation, ozone production). He has research experiences of triggering lightning using water jets, ceramic joining using exploding foil, and exhaust gas processing in atmospheric pressure such as reduction of NOx and PFCs. He has co-authored 219 scientific publications and has contributed to and edited or co-authored 27 books.

Nick Serpone Cornell University (Ithaca, N.Y., PhD, 1968); Professor of Chemistry (1968–1998), Founder and Director of the Canadian Picosecond Laser Spectroscopy Center (1981–1990, 1994–1998), University Research Professor (1998–2004), and Professor Emeritus (2000–. . .) at Concordia University, Montreal, Canada; Professore a Contratto (2002–2005) and Visiting Professor at the University of Pavia, Italy (2005–. . .); Visiting Professor at the Universities of Bologna (1975–1976), Ferrara (1997–1998), and Tokyo University of Science (2008); Professeur Invité (École Polytechnique Fédérale de Lausanne, 1983–1984); Visiting Professor and Research Director (École Centrale de Lyon, 1990–1991); Guest Lecturer (University of Milan, 2015); Director of the IBO Program at the U.-S. National Science Foundation (Arlington, VA, 1998–2001); Consultant to the 3M Company (USA, 1986–1996). His principal research interests focused on the photochemistry and photophysics of coordination compounds, photochemistry of sunscreen active ingredients, fundamental photophysics of semiconductor photocatalysts, imaging science for which he was the co-recipient of the *Best Paper Award* from the Society for Imaging Science and Technology (1997), heterogeneous photocatalysis for environmental remediation, and most recently microwave-assisted chemistry. He has co-edited/co-authored over 12 books, contributed 35 chapters and published over 490 articles (citation index $h = 104$, Google Scholar). In 2010, he was elected Fellow of the European Academy of Sciences and was Head of its Materials Science Division (2014–2020).

Part I
Tutorial

Chapter 1
Microwave Thermal and Nonthermal Processes

Satoshi Horikoshi and Nick Serpone

Abstract The microwave heat process and the microwaves heating mechanism are outlined. With regard to the thermal process, both the heating principles and features are summarized. In addition, nonthermal processes are presented, defined, and paraphrased as ***electromagnetic wave processes***. In other words, some of the effects that microwaves display are introduced—particularly at weak microwave power levels that do not generate heat—rather than electromagnetic wave processes that occur in combination with thermal utilization of the microwaves.

Keywords Microwaves · Thermal processes · Nonthermal processes · Electromagnetic wave effects · Electromagnetic wave processes

1.1 Microwave Thermal Processes

1.1.1 Microwave Heating Mechanism

There are tens, if not hundreds of research studies that have been carried out on the thermal use of microwaves, together with their innovative use described in this book. Consequently, herein we examine the principle and the characteristic features of microwave heating.

Microwave radiation is electromagnetic radiation that spans a frequency in the range from 300 GHz to 300 MHz (i.e., from a wavelength of 1 mm to 1 m). It is used widely in communications and in heating, especially in the heating of foodstuff.

S. Horikoshi (✉)
Department of Materials and Life Sciences, Faculty of Science and Technology, Sophia University, Chiyodaku, Tokyo, Japan
e-mail: horikosi@sophia.ac.jp

N. Serpone
PhotoGreen Laboratory, Dipartimento di Chimica, Universita di Pavia, Pavia, Italy
e-mail: nick.serpone@unipv.it

S. Horikoshi et al. (eds.), *Agritech: Innovative Agriculture Using Microwaves and Plasmas*, https://doi.org/10.1007/978-981-16-3891-6_1

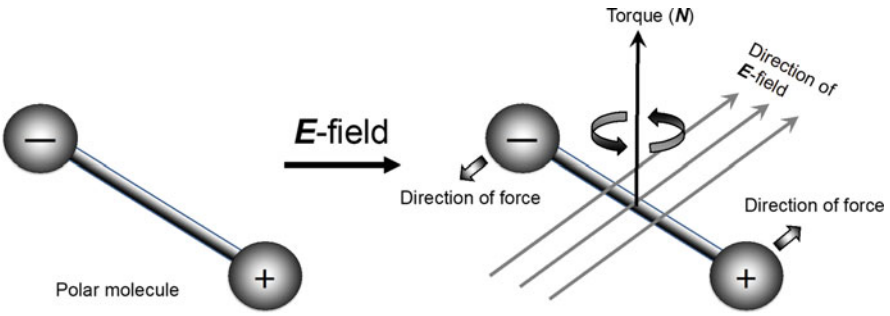

Fig. 1.1 Image illustrating a dipole rotation of a polar molecule in an electric field (***E***-field)

When microwave heating is applied to polar molecules or clusters of molecules, it affects the electrical equilibrium that was originally relaxed within those assemblies. When microwaves are applied to a molecule or cluster, the microwaves' electric field will have a noninsignificant influence on the electric dipole of the molecule or cluster (Fig. 1.1) [1]. The microwaves' electric field (***E***-field) exercises a torque (***N***) on the electric dipole of the molecule such that its dipole will consequently rotate to align itself with the applied electric field thus causing orientation polarization to occur [2]. If the field changes direction, the torque will also change. The orientation polarization changes through a vibration in a microwave electric field. A time difference occurs between the frequency of the microwave electric field and the electric dipole of molecules or cluster. At the general frequency of 2.45-GHz, the microwaves vibrates at 2,450,000,000 times per second, so that a molecular cluster cannot follow this vibration through the power chain with the surrounding molecules. This delay changes to heat energy (i.e., kinetic energy) as loss of the electromagnetic wave energy. The heat generated by such changes is referred to as ***dielectric heating*** (dielectric loss heating). The friction accompanying the orientation of the dipole will contribute to dielectric losses. Alignment polarization (molecular alignment) occurs only when the polarity of the molecules is affected by the electric field because of their permanent dipoles. A substance with a partial electric charge (dielectric) can also act as an insulator of solid substances. A slight distortion of the atomic positions (lattice points) in a structure lattice may cause a lattice strain of a crystalline solid substance such that it cannot follow the changing time of the microwave electric field. As a result, microwave heating of a solid substance develops by these phenomena [3].

Generally, microwave heating is thought of as dielectric loss heating; however, there exist two other heating mechanisms: (i) ***magnetic loss heating***, and (ii) ***Joule heating***. The heating of solid substances possessing magnetic dipole moments occurs by the microwaves' magnetic field component. The heating process is a similar phenomenon as by the microwaves' electric field [4]. Generation of heat by magnetic loss heating is expected only in magnetic (solid) materials. Joule heating progresses by the interaction of microwaves with an ionic solution, or with activated carbon possessing conductivity-like metallic properties [5].

The three types of heating phenomena caused by microwaves are summarized in Eq. (1.1) [1]. The thermal energy $\boldsymbol{P}$ produced per unit volume originates from microwave radiation. The first term in Eq. (1.1) expresses ***conduction loss heating***; the second term denotes ***dielectric loss heating***, whereas ***magnetic loss heating*** is given by the third term.

$$P = \frac{1}{2}\sigma|E|^2 + \pi f \varepsilon_0 \varepsilon_r''|E|^2 + \pi f \mu_0 \mu_r''|H|^2 \tag{1.1}$$

where $|\boldsymbol{E}|$ and $|\boldsymbol{H}|$ denote the strength of the microwaves' electric and magnetic fields, respectively; $\boldsymbol{\sigma}$ is the electrical conductivity; $\boldsymbol{f}$ is the frequency of the microwaves; $\boldsymbol{\varepsilon_o}$ is the permittivity in vacuum; $\boldsymbol{\varepsilon_r''}$ is the relative dielectric loss factor; $\boldsymbol{\mu_o}$ is the magnetic permeability in vacuum; and $\boldsymbol{\mu_r''}$ is the relative magnetic loss. These heating mechanisms are related to the electrical properties of a substance: dielectric loss, magnetic loss, and conductivity, and their magnitude determines the microwave heating efficiency. Heating with 2.45-GHz microwaves in a liquid is the sum of dielectric heating and Joule heating. In addition, as the frequency decreases, the contribution from dielectric heating relative to Joule heating increases.

When considering microwave heating efficiency, is it relevant to query whether everything follows Eq. (1.1)? When microwaves are actually used in a process, their penetration depth into the substrate(s) must be taken into consideration. Just like light, microwaves are electromagnetic waves that are attenuated by the absorption of energy by the substrate(s). The penetration depth ($\boldsymbol{D_p}$) refers to the distance from which the microwave power density (W/cm^2) decreases by 36.8% ($1/e$) from the surface; $\boldsymbol{D_p}$ can be obtained from Eq. (1.2).

$$D_p = \frac{\lambda}{4\pi}\left[\frac{2}{\varepsilon'\left(\sqrt{1+(\varepsilon''/\varepsilon')^2}-1\right)}\right]^{1/2} \tag{1.2}$$

where $\boldsymbol{\lambda}$ is the wavelength of the radiation, $\lambda_{(2.45\text{GHz})} = 12.24$ cm, $\boldsymbol{\varepsilon}$' is the dielectric constant and $\boldsymbol{\varepsilon}$" is the dielectric loss factor. Inasmuch as the dielectric constant and the dielectric loss are components of this equation, we can expect that the penetration depth will change with an increase of temperature. For example, since the penetration depth at 25 °C is ca. 1.8 cm for water, even if we used a 10-cm (diameter) reactor, the microwaves would not reach the center of the reactor. However, at 50 °C, the penetration depth is 3.1 cm, and at 90 °C it is 5.4 cm so that now the microwaves can and do reach the center of the water sample [6].

1.1.2 Features of Microwave Heating

How is microwave different from existing heating methods? In microwave heating, the heating efficiency is determined by how much microwave energy is absorbed by

or has penetrated into the substance and how much is lost. Therefore, heat generation progresses at the molecular level and cluster level without depending on heat transfer. The advantages of microwave heating can be broadly classified into the following items:

Internal heating: Many dielectrics have low thermal conductivity. Thus, it takes a long time to heat the center of the sample. Microwaves do not depend on heat conduction because the sample self-heats. Therefore, even if the sample possessed a complicated shape, it could nevertheless be uniformly heated from the inside in a short time.

High-precision heating control: Since the sample self-heats in microwave heating, the sample cools rapidly when microwave irradiation is stopped because of the surrounding atmospheric environment (atmosphere or container). Therefore, precise temperature control can be performed by repeatedly turning ON and OFF the microwaves.

Selective heating: Since the heat generation efficiency of microwaves is determined by the relative permittivity loss of substances, the heating efficiency of each substance differs greatly when a heterogeneous mixture with a large difference of such loss is irradiated with microwaves. Therefore, even if the sample consisted of a mixture, only the target substance can be selectively heated. In addition, it is also possible for local hot spots to occur.

Energy saving: Microwave heating, in which the sample generates heat directly, does not require extra energy because it does not need to heat the furnace assembly or the atmospheric environment. Also, if there is a space (air) between the container and the sample, it will take a long time to heat the sample inside because the thermal conductivity of the reactor may be rather poor from the outside to the inside of the container. Nonetheless, microwaves can propagate in space gap and can heat the sample directly.

Low environmental load: Microwave heating is electrically driven and does not require fossil fuels. In any case, in order to master microwave heating, it is necessary to understand the problems of microwave heating. The problems with general microwave heating are summarized below; solving these problems will make the use of microwaves in Microwave Chemistry run more smoothly.

Electric discharge phenomenon: When a conductive substance such as metal is contained in the sample, microwaves may concentrate and discharge on the surface of the conductive substance. The latter may then cause burning of the sample or else may ignite the volatile solvent.

Penetration depth: Since the heating of a substance proceeds due to the loss of microwave energy, there is a limit to the distance that microwaves can reach (penetration depth). This is because the sample with higher heating efficiency has a shallower penetration depth.

Nonuniform heating: It is difficult to uniformly heat nonuniform mixed samples with different relative permittivities. In addition, since the surface of the sample cools depending on the container and the atmospheric environment, it is necessary to devise measures such as heat insulation.

Temperature measurement: It is difficult to measure the temperature accurately because the measuring thermometer may not be able to follow the temperature response.

Radio leakage: The use of microwaves is controlled by the Radio Law. It is necessary to comply with relevant laws and regulations and consider electromagnetic interference (EMI) to any peripheral equipment. Generally, it is necessary to place the sample in a microwave cavity (metal box) surrounded by a metal.

1.2 Microwave Nonthermal Processes

1.2.1 General Nonthermal Processes

In general, a nonthermal process can be viewed as a weak energy level that does not change the temperature of a sample when various energies such as an electric field, a magnetic field, pressure, or ultrasonic waves act on the sample. However, it is nonetheless an epoch-making effect. It has already been put into practical use in the food field from the viewpoint of sample denaturation by heat and energy saving [7]. The kinds of nonthermal processes are: (a) pulsed electrical fields, (b) ultraviolet radiation, (c) ionizing radiation, (d) cold plasma, (e) supercritical carbon dioxide, (f) pulsed light with UV to NIR radiations, (g) high hydrostatic pressure processing (HPP), (h) ultrasound, and (i) chemical reaction with oxidative species.

Nonthermal processes are also pervasive in the environmental field. For example, in water treatment, purification using ultraviolet rays is performed worldwide, and it is possible to realize an energy-saving procedure as compared with sterilization of water using, for instance, high-temperature disinfection. To sterilize a large amount of water (hundreds of tons), heat sterilization requires an enormous amount of energy. However, with UV light, sterilization is completed in a very short time, and can be done in a flow process [8]. The wavelengths for UV treatments range from 100 nm to 400 nm. The germicidal properties of UV radiation are mainly due to DNA mutations induced through absorption of UV light by the DNA molecules. UV light may be used in combination with other alternative processing technologies, including various powerful oxidizing agents such as ozone and hydrogen peroxide. In the case of drinking water, for example, it can be sterilized for a longer time and lasts longer than by boiling the water.

1.3 Microwave Nonthermal Effects

1.3.1 Restrictions on the Use of Microwaves in the Environment

In the last decade, the human population has been exposed increasingly to radiation from microwave-operating devices: for example, radars, diathermic devices, and cellular or cordless phones. As well, the rate of penetration of mobile phones into the market place has increased worldwide between 2000 and 2013. In India, for example, the number of mobile phones have increased by a factor of 247.8, while the global penetration of mobile phones increased from 12.1% in 2000 to 94.4% in 2013 (see Table 1.1) [9].

Both humans and microorganisms living on the human body are exposed to significant doses of microwave radiation in everyday life. How and whether or not microwave radiation could influence the viability and growth of microorganisms is of course a matter of some debate. Under these circumstances, the existence of nonthermal effects of microwaves has been discussed for a long time in addition to the thermal effects of microwaves.

Electromagnetic exposures depend on several factors not least of which are: power (specific absorption rate, incident power density), wavelength/frequency, near field/far field, polarization (linear, circular) continuous wave and pulsed waves (pulse repetition rate, pulse width or duty cycle, pulse shape, pulse to average power, etc.), modulation (amplitude, frequency, phase, complex), static magnetic field and electromagnetic stray field at the place of exposure, overall duration and intermittence of exposure (continuous, interrupted), and finally acute and chronic exposures [10]. With increased absorption of energy, thermal effects of microwaves

Table 1.1 Global mobile phone penetration statistics compiled from data given by the Ministry of Internal Affairs and Communications of Japan [9]

Countries/continents	Number of mobile phones		Rate of increase/ times
	2000	2013	
Japan	66,784,374	149,561,007	2.2
USA, Canada	118,205,031	334,102,000	2.8
Europe	296,106,468	787,728,453	2.7
Asia Pacific (excluding Japan, China, and India)	84,692,157	1,231,504,515	14.5
China	85,260,000	1,229,113,000	14.4
India	**3,577,095**	**886,304,245**	**247.8**
Latin America/Mexico	58,300,965	674,907,938	11.6
Russia region (CIS)	4,976,051	381,311,610	76.6
Arab countries	9,035,241	407,704,505	45.1
Africa	11,326,972	580,569,307	51.3
World	**738,264,354**	**6,662,806,580**	**9.0**
Global penetration rate	**12.1%**	**94.4%**	**—**

are usually observed that deal with microwave heating. A measure of determining the safety of the microwaves' specific absorption rate has been defined as a ***specific absorption rate*** (SAR). In Japan, the measure for assessing thermal effects refers to the whole-body average SAR, with a guideline of the whole-body average SAR set at 0.08 Watts per kilogram, which includes the safety factor. For instance, when the energy density of microwaves transmitted into the living body through the skin reaches 100 mW/cm^2 or more, some irreversible changes may occur in the living tissues. In addition to this, SAR has been decided from various studies based on the microwave output power. SAR can cause burns due to the heat of the human body irradiated with microwaves. Previous studies of the nonthermal effect of microwaves suggested that the thermal effect occurs before the nonthermal effect begins. For this reason, the nonthermal effects from weak microwaves have not been the object of many investigations.

As a strategy in innovation technologies, one may wish to utilize the nonthermal effect as a positive use of microwaves at weak output power levels under conditions such that the temperature does not rise. In this regard, nonthermal effects at the cellular level have been investigated over the last decade [11]. Some of the observed results now include effects that cannot otherwise be obtained from thermal effects. While research studies were intended to avoid deleterious damage caused by microwaves to the human body, from a different perspective they also revealed that nonthermal effects may well prove useful in industrial processing. Can these effects of the microwaves then be used to enrich our lives? This is something to think about.

1.3.2 Active Use of Nonthermal Effects as Electromagnetic Wave Effects

While microwave heating may be required in the fields of agriculture and biology, it may necessitate the use of the energy of electromagnetic waves from the microwave radiation. In general, this temperature-independent effect is referred to as a nonthermal process. This expression comes from nonthermal plasma in the plasma field. It is understood that this is not a thermal effect of the microwaves. But then what is it? Briefly, the nonthermal effect in microwaves can be considered as an effect that acts directly on the electromagnetic energy. In this chapter, microwave nonthermal effects are reworded as ***microwave electromagnetic wave effects***. In other words, it is necessary to actively utilize this electromagnetic wave effect in the process, but for what usage? There have been many research studies on the use of this effect in pest control.

In this regard, Yanagawa and coworkers [12] reported that the effect on termites placed in an ESR (Electron Spin Resonance) cavity. The effect was examined by measuring the number of free radicals while irradiating with weak microwaves. Miyakoshi [13] confirmed that free radicals are formed when pests are irradiated with microwaves, and to the extent that such formation does not occur with simple

heat, it was inferred that the effect resulted from a nonthermal action of the microwaves. Insects contain such paramagnetic substances as manganese, copper, and iron. It has been reported that because of these nonthermal effects, the electrical properties of the molecules that make up the living body, including lipids in insects, are affected by the influence of the microwaves' magnetic field and thus could prove useful in pest control. Common termite exterminations in homes typically use chemicals and heat, which are not without safety problems to humans, to the deterioration of wood, and to wasteful energy consumption. Various problems could be solved if termites were exterminated simply by the use of microwave radiation using its electromagnetic wave effect.

Related to this, Tanner and coworkers [14] reported that when chickens were exposed to ***slightly thermal*** microwave fields of 20 to 50 mW/cm^2, they responded with an escape or avoidance reaction within a few seconds of the onset of microwave radiation. Note that an important difference between thermal and nonthermal effects is a matter of timescale. Such effects have been considered for use at airports as a way to prevent disastrous accidents from birds' strikes. On the positive side, the growth of plants in agriculture can be controlled by the nonthermal effects of the microwaves (see Chap. 5).

1.3.3 Summary of Electromagnetic Wave Processes

The problems in electromagnetic wave processes are that the electromagnetic wave effects of microwaves are not well defined, and that the relevant principles have not been elucidated nor systematized. In addition, it is necessary to separate the thermal effect from the nonthermal effect at the molecular level. At present, the existence of the microwave electromagnetic wave effect is not clear, even though many phenomena attributed to this effect have been reported [15]. However, many of the studies on this topic have used typical domestic microwave ovens, for which the microwave output is too strong to carry out related experiments, not to mention that the magnetron and power supply of the microwave oven cannot reproduce the microwave radiation conditions. Regardless, several articles have reported that microwave processing is a nonthermal process, not just a thermal process. However, it is difficult to separate the nonthermal effects of microwaves described in many of these studies, because these nonthermal effects also appear with thermal effects. In this regard, Apollonio and coworkers [16] have offered a critical literature review of the models of the interaction mechanisms involving microwaves, together with an overview of all the publications that reported positive results in in vitro and in vivo studies. This kind of scrutiny was necessary.

The microwaves' "weak energy" could be put to optimal use in innovative novel technologies such as ***AGRITECH*** (agriculture technology) and ***FOODTECH*** (food technology). In addition, when it comes to targeted animals, plants, and microorganisms (among others) in agriculture and the food industry, the energy level is such as to make the temperature of these objects remain unchanged.

References

1. Horikoshi S, Schiffmann RF, Fukushima J, Serpone N. Microwave chemical and materials processing: a tutorial. Japan: Springer; 2017.
2. Agilent basics of measuring the dielectric properties of materials, Application Note, June 26, 2006.; http://www3.imperial.ac.uk/pls/portallive/docs/1/11949698.PDF. Accessed March 2021.
3. Metaxas AC, Meredith RJ. Industrial microwave heating. London: Peter Peregrinus; 1983.
4. Peng Z, Hwang J-Y, Andriese M. Magnetic loss in microwave heating. Appl Phys Express. 2012;5:027304-1-3.
5. Horikoshi S, Sumi T, Serpone N. Unusual effect of the magnetic field component of the microwave radiation on aqueous electrolyte solutions. J Microwave Power Electromagn Energy. 2012;46:215–28.
6. Horikoshi S, Serpone N. In: de la Hoz A, Loupy A, editors. Microwaves in organic synthesis. Chapter 9. 3rd ed. Weinheim: Wiley-VCH Verlag GmbH; 2012.
7. Martín-Belloso O, Soliva-Fortuny R, Elez-Martínez P, Marsellés-Fontanet RA, Vega-Mercado H. In: Motarjemi Y, Lelieveld H, editors. Food safety management. London., Chapter 18: Elsevier; 2014. p. 443–6.
8. Poepping C, Beck SE, Wright H, Linden KG. Evaluation of DNA damage reversal during medium-pressure UV disinfection. Water Res. 2014;56:181–9.
9. https://www.soumu.go.jp/johotsusintokei/whitepaper/ja/h27/html/nc123110.html. (in Japanese). Accessed March 2021.
10. Belyaev IY. Nonthermal biological effects of microwaves: current knowledge, further perspective, and urgent needs. Electromagn Biol Med. 2005;24:375–403.
11. Yanagawa A, Kajiwara A, Nakajima H, Desmond-Le Quemener E, Stayer J-P, Lewis V, Mitani T. Physical assessments of termites (Termitidae) under 2.45 GHz microwave irradiation. Sci Rep. 2020;10:5197.
12. Miyakoshi J. Radiofrequency biology: in vitro. In: Kato M, editor. Electromagnetics in biology. Japan: Springer; 2006. p. 305–16.
13. Frenkel RB. Magnetic guidance of organisms. Annu Rev Biophys Bioeng. 1984;14:85–103.
14. Tanner JA, Romero-sierra C, Davie SJ. Non-thermal effects of microwave radiation on birds. Nature. 1967;216:1139.
15. Kubo MT, Siguemoto ÉS, Funcia ES, Augusto PE, Curet S, Boillereaux L, Sastry SK, Gut JA. Non-thermal effects of microwave and ohmic processing on microbial and enzyme inactivation: a critical review. Curr Opinion Food Sci. 2020;35:36–48.
16. Apollonio F, Liberti M, Paffi A, Merla C, Marracino P, Denzi A, Marino C, d'Inzeo G. Feasibility for microwaves energy to affect biological systems via non-thermal mechanisms: a systematic approach, IEEE Trans. Microwave Theory Tech. 2013;61:2031–45.

Chapter 2
Plasma Thermal and Nonthermal Technologies

Kunihito Tanaka

Abstract A space called plasma containing charged particles is generally formed by using an electric discharge. Therefore, charged particles (mainly electrons) having very high energy exist in the plasma, and gas molecules are dissociated by the electrons having the high energy. Various radicals generated by this action promote chemical reactions that do not occur in ordinary chemical reaction fields. Taking advantage of this feature, the use of plasma as a new reaction field is expanding.

Keywords Electric discharge · Corona discharge · Silent discharge · Creepage discharge · Glow discharge · Atmospheric pressure glow discharge · Arc discharge

2.1 What Is Plasma?

The words *solid*, *liquid,* and *gas* are words to express the state of a system. The word *plasma* is one of the words to express the state of the system as well as those words, too. A rough explanation of the state of the system represented by plasma is "an ionized gas that contains ions and electrons and is electrically neutral as a whole." Inaccuracies are undeniable, but they are sufficient for understanding how they are used in agriculture.

If a gas contains charged particles, it becomes plasma, so if energy is applied to gas molecules to cause ionization, plasma can be obtained. The ionization energy of general gas molecules is 10–25 eV degree. As a method of giving the energy, heating, light irradiation, and electric discharge can be considered.

When a material is heated, it changes from solid to liquid and gas, and eventually becomes plasma. However, a temperature of 10,000 K is required to ionize 1% of 1 bar of nitrogen molecules. Such high temperature plasma cannot be used for all purposes, not limited to agriculture. In the first place, it is unrealistic to heat a

K. Tanaka (✉)
Department of Materials and Life Sciences, Faculty of Science and Technology, Sophia University, Chiyoda-ku, Tokyo, Japan
e-mail: tanaka@sophia.ac.jp

S. Horikoshi et al. (eds.), *Agritech: Innovative Agriculture Using Microwaves and Plasmas*, https://doi.org/10.1007/978-981-16-3891-6_2

material to such a high temperature. Therefore, the method of heating is not suitable as a method of obtaining a plasma state.

Next, a method of obtaining a plasma state by light irradiation will be examined. The wavelength of light corresponding to the ionization energy of 10–25 eV is vacuum ultraviolet light of 50–100 nm. It is extremely difficult to prepare a light source having such a short wavelength and to irradiate the space to be in a plasma state. Therefore, the generation of a plasma state by light irradiation is also unrealistic.

The electric discharge can be easily generated by simply applying a voltage of several kV to the electrodes placed in the gas. Since it is clear that charged particles are flowing in the space shining by the electric discharge, the space is plasma state. In addition, by changing the structure of the electrode and the atmosphere (type of gas and pressure) in the vicinity of the electrode, it can be easily changed to various discharge types. This indicates that when plasma is used for agriculture, it leads to a great advantage that an appropriate discharge type can be freely selected according to the processing target.

2.2 Classification of Discharge Type and Plasma State

The discharge type and plasma state vary depending on the electrode structure, power supply, pressure, type of gas in the discharge field, and so on. Electrodes and power supplies affect the electric field formed in the discharge field. The pressure and the type of gas affect the degree of ionization.

Table 2.1 shows a summary of typical discharge types and plasma states. Typical discharge types include corona discharge, glow discharge, and arc discharge. Of these, corona discharge and glow discharge are classified as nonequilibrium plasma (or nonthermal plasma). The electrons in the plasma have enough energy to ionize gas molecules. When this energy is converted into temperature, it becomes 100,000 K or more. On the other hand, the temperature of these discharge-type gases is around room temperature. Since the thermal equilibrium is not established between the electron and the gas, it is called nonequilibrium plasma. The arc discharge is classified as a thermal equilibrium plasma (or thermal plasma) because the gas temperature is about 10,000 K, although the thermal equilibrium is not completely established.

Table 2.1 Plasma and discharge types

Thermodynamic equilibrium (temperature)	Discharge type	Degree of ionization
Nonequilibrium plasma (cold plasma)	Corona discharge	Weakly ionized plasma
	Glow discharge	
Thermal equilibrium plasma (thermal plasma)	Arc discharge	Strongly ionized plasma

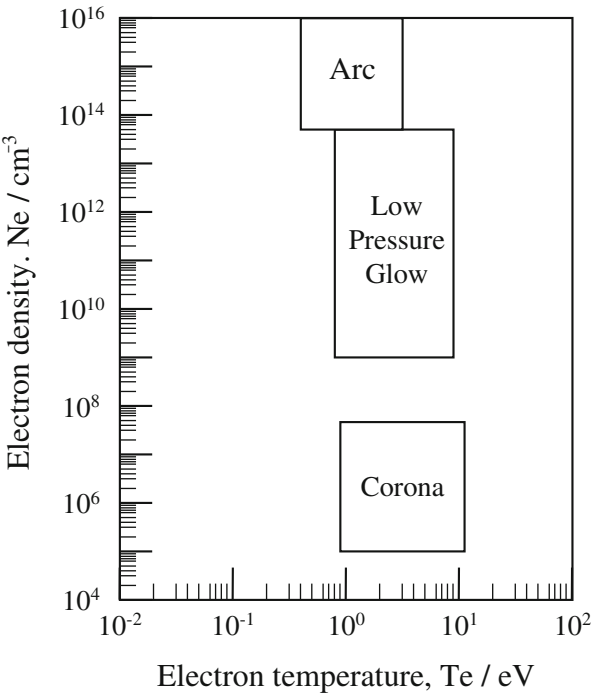

Fig. 2.1 Plasma types by electron temperature and density

Understanding how much gas molecules in the plasma are ionized is an important factor in selecting the appropriate discharge type for the purpose. Figure 2.1 shows the approximate distribution of electron temperature and density during each discharge. Corona discharge and silent discharge, which are weakly ionization plasmas, are discharges generated under atmospheric pressure, and the degree of ionization is about 10^{-11} to 10^{-14}. Glow discharge, which is also weakly ionization plasma, is a discharge generated under a low pressure of about 1 to 100 Pa, and the degree of ionization is about 10^{-4} to 10^{-9}. The degree of ionization of the arc discharge, which is strong ionization plasma, is about 10^{-3} to 10^{-9}, which shows that the degree of ionization is quite high.

Ionization in plasma occurs mainly by collisions between electrons and gas molecules. Collision between electrons and gas molecules causes not only ionization but also excitation of gas molecules and dissociation reaction of gas molecule bonds, and various active species such as electronically excited gas molecules and radicals are generated. The density of these active species is not equal to the density of electrons, but the density of electrons is clearly proportional to the density of active species. Thus, it seems that arc discharge and glow discharge are more advantageous than corona discharge and silent discharge when considering only the amount of active species. However, it can be seen that there are many objects for which arc discharge and glow discharge are difficult to use when considering the conditions for

generating arc discharge and glow discharge. In order to understand this, the conditions and characteristics of each discharge will be described.

2.3 Inelastic Collision Process in Plasma

As mentioned above, the density of electrons and active species in plasma is an important factor in estimating the effect when plasma is used for processing. Therefore, understanding how these particles are generated and how they disappear is an important basis for understanding the processing results.

It is impossible to explain all of the inelastic collision processes in plasma, and there are many processes that are unnecessary to understand the contents of this book, so only the important processes will be explained.

2.3.1 Ionization

In order to generate a plasma state, ionization must first occur. Ionization in the discharge field begins with the collision of electrons with gas molecules. The electrons in the discharge field are accelerated by the electric field and gradually store energy. If the electron has enough energy, it collides with a gas molecule and direct ionization (Eq. 2.1) occurs. If the electron does not have sufficient energy, it excites a gas molecule, and electrons collide with the excited gas molecule again, resulting in cumulative ionization (Eq. 2.2). These two ionizations are the main processes involving electrons.

$$\text{Direct ionization} : \mathrm{A} + \mathrm{e}^- \rightarrow \mathrm{A}^+ + \mathrm{e}^- + \mathrm{e}^- \tag{2.1}$$

$$\text{Cumulative ionization} : \mathrm{A}* + \mathrm{e}^- \rightarrow \mathrm{A}^+ + \mathrm{e}^- + \mathrm{e}^- \tag{2.2}$$

When the number of positive ions and excited gas molecules increases, ionization also occurs due to collision with these active molecules. Positive ions are also accelerated by the electric field, so they collide with gas molecules and cause ionization, but this process is negligible in many cases. Ionization due to collision with excited gas molecules can be considered in the Eqs. (2.4) and (2.5), and Eq. (2.5), called Penning ionization, plays a relatively important role in the plasma process.

$$\text{Ionization by positive ion} : \mathrm{A} + \mathrm{A}^+ \rightarrow \mathrm{A}^+ + \mathrm{A}^+ + \mathrm{e}^- \tag{2.3}$$

$$\text{Ionization by excited molecule} : \mathrm{A}* + \mathrm{A}* \rightarrow \mathrm{A}^+ + \mathrm{A} + \mathrm{e}^- \tag{2.4}$$

$$\text{Penning ionization} : \mathrm{B} + \mathrm{A^m} \rightarrow \mathrm{B^+} + \mathrm{A} + \mathrm{e^-} \tag{2.5}$$

Penning ionization is an ionization caused by collision with a gas molecule in a metastable excited state. A typical gas that can take a metastable excited state is a noble gas (usually argon or helium), and the energy of the metastable state of those noble gases is about 10–20 eV. Therefore, not only the ionization of gas molecules but also the excitation and dissociation reactions can occur at the same time. In addition, since the metastable excited state is characterized by a long lifetime, the energy supplied from the power source can be efficiently used by adding the noble gas to the process gas.

2.3.2 Recombination

As the number of charged particles increases, positive ions are recombined with electrons or anions accordingly, and the charged particles disappear. The energy generated by the recombination reaction is released as light or heat, and is also used for the dissociation reaction of gas molecules.

$$\text{Radiative recombination} : \mathrm{A^+} + \mathrm{e^-} \rightarrow \mathrm{A} + h\nu \tag{2.6}$$

$$\mathrm{A^+} + \mathrm{B^-} \rightarrow \mathrm{A} + \mathrm{B} + h\nu \tag{2.7}$$

$$\text{Dissociative recombination} : \mathrm{AB^+} + \mathrm{e^-} \rightarrow \mathrm{A} + \mathrm{B} \tag{2.8}$$

2.3.3 Excitation

Collisions between electrons and gas molecules cause not only ionization but also excitation and dissociation reactions.

$$\text{Excitation} : \mathrm{A} + \mathrm{e^-} \rightarrow \mathrm{A} * + \mathrm{e^-} \tag{2.9}$$

$$\text{Dissociation} : \mathrm{AB} + \mathrm{e^-} \rightarrow \mathrm{A} \cdot + \mathrm{B} \cdot + \mathrm{e^-} \tag{2.10}$$

$$\mathrm{AB} + \mathrm{C^m} \rightarrow \mathrm{A} \cdot + \mathrm{B} \cdot + \mathrm{C} \tag{2.11}$$

If the charged particles in the plasma are to be utilized, it is important how to increase the degree of ionization and increase the number of charged particles. On the other hand, plasma is used as a chemical reaction field in many use cases. As shown in Eqs. (2.8), (2.10), and (2.11), gas molecule dissociation reactions also occur in plasma, and the radicals generated in that process are the main chemical reactions. Therefore, what kind of radicals are required for the desired chemical

reaction, what kind of substance should be introduced into the plasma to supply the radicals, and how to use the plasma as a chemical reaction field. Such a viewpoint becomes important.

2.4 Generation and Characteristics of Each Discharge Type

2.4.1 Corona Discharge

Corona discharge is a type of discharge that occurs when a high voltage is applied using electrodes shaped like needles, fine wires, or knife edges, and ordinary flat plate-shaped electrodes. Due to the extremely biased electrode shape, the applied electric field is concentrated near the electrode with the smaller surface area. Due to its local high electric field, electrons can easily obtain the high energy required for ionization, so that corona discharge is easily obtained under atmospheric pressure. Schematic diagrams of the corona discharge apparatus are shown in Fig. 2.2, and a summary of the generation conditions is shown in Table 2.2. The pressure does not need to be atmospheric pressure, which means that neither pressurization nor decompression is required.

Since corona discharge is easily generated by a simple device, it is widely used as a surface treatment for polymer materials and as an electron supply device. The purpose of the surface treatment is often a hydrophilic treatment for improving adhesiveness and coatability. As an electron supply device, it is widely used in electrostatic precipitators, copiers, and the like.

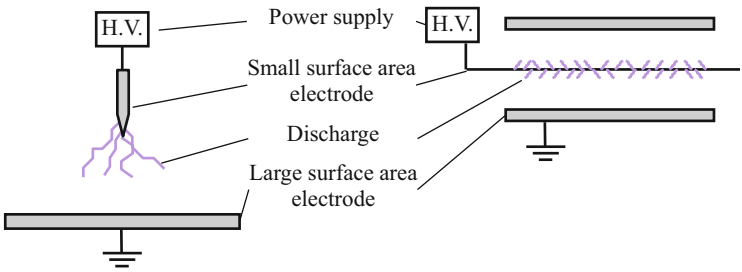

Fig. 2.2 Schematic diagrams of corona discharge apparatus

Table 2.2 Occurrence conditions of corona discharge

Electrodes	Needle or thin wire and flat plate electrodes
Pressure	Atmospheric pressure
Gas	All gases. Air or oxygen gas for industrial use
Power supply	DC and AC power supplies are available

2.4.2 Dielectric Barrier Discharge

Dielectric barrier discharge (DBD) occurs when a dielectric such as glass is inserted between the electrodes so as to cover the electrode surface and a high voltage is applied. Schematic diagrams of the DBD apparatus are shown in Fig. 2.3, and a summary of the generation conditions is shown in Table 2.3.

The discharge generated by the left-side apparatus shown in Fig. 2.3 is called silent discharge, and thin linear discharges are sparsely generated over the entire electrode in the silent discharge. Since the discharge occurs only sparsely and the discharge gap is generally only a few mm, silent discharge is not used for surface treatment. However, silent discharge is used as the most energy efficient ozone generation method.

As shown on right side in Fig. 2.3, the device of the electrode structure made it possible to almost uniformly generate DBD over a relatively wide area. Since the shape of the generated discharge is similar to corona discharge or silent discharge, it is difficult to use this discharge for the completely uniform surface treatment, but it is considered to be more effective than corona discharge as a source of radicals and electrons. Although the DBD's electrodes are more difficult to make than corona discharge apparatus, it is worth considering the use of DBD for agriculture.

2.4.3 Glow Discharge

When the pressure in the space where the high voltage is applied drops to about 1000 Pa, the discharge type becomes glow discharge regardless of other conditions.

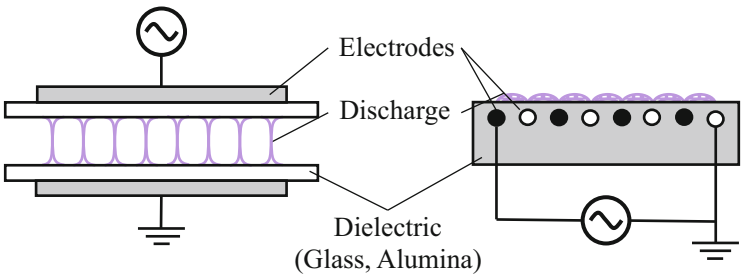

Fig. 2.3 Schematic diagram of silent discharge apparatus

Table 2.3 Occurrence conditions of silent discharge

Electrodes	Insert dielectric(s) between metal electrodes
Pressure	Atmospheric pressure
Gas	All gases. Air or oxygen gas for industrial use
Power supply	Only an AC power supply is available

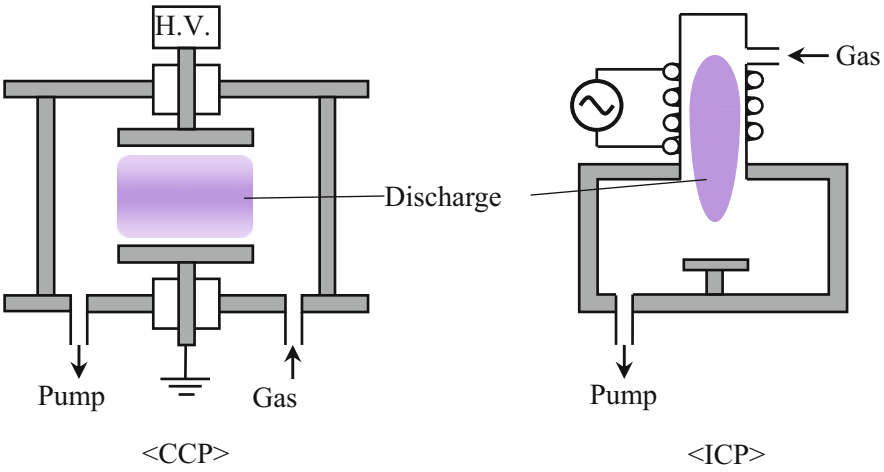

Fig. 2.4 Schematic diagrams of glow discharge apparatus

Table 2.4 Occurrence conditions of glow discharge

Electrodes	Many electrode types
Pressure	Low pressure. About 0.1–100 Pa
Gas	All gases
Power supply	DC and AC power supplies are available

The advantages of glow discharge are that the discharge field spreads spatially uniformly, the density of electrons and radicals is higher than that of corona discharge and silent discharge, and the temperature of the gas is low (about room temperature to 200 °C). These advantages lead to the ability to treat a solid surface uniformly, at high speed, and without denaturing the solid itself. Therefore, when plasma is used as a manufacturing technique, it is first considered to use glow discharge. Schematic diagrams of the glow discharge apparatus are shown in Fig. 2.4, and a summary of the generation conditions is shown in Table 2.4.

There are so many types of glow discharge apparatus that have been developed, but I will introduce two typical ones. One is called capacitively coupled plasma (CCP), which is a very simple apparatus that only prepares two flat plates. The other is called inductively coupled plasma (ICP), which is a method of supplying energy to electrons by a magnetic field to generate a discharge. Compared to CCP, ICP is used for a powerful process because it can easily supply high power.

Glow discharge is widely used as a technique for manufacturing ICs, such as surface modification that changes the chemical state of the surface, thin film deposition that creates a thin film, and etching treatment that changes the surface shape.

2.4.4 Atmospheric Pressure Glow (APG) Plasma

The biggest drawback of using glow discharge as a manufacturing technique is that the sample must be placed under low pressure: the processing equipment is expensive because a vacuum device is required to reduce the pressure; the process is a costly batch process as the sample must be placed under low pressure; if the sample cannot be put into a low pressure, it is impossible to process.

This drawback can be overcome if glow discharge can be generated under atmospheric pressure, but the discharge under atmospheric pressure is usually corona discharge or arc discharge. Therefore, it has been considered impossible to generate a glow discharge under atmospheric pressure. Kogoma et al. presented the successful development of atmospheric pressure glow (APG) plasma [1, 2]. Schematic diagrams of the APG discharge apparatus are shown in Fig. 2.5, and a summary of the generation conditions is shown in Table 2.5. Left- and right-side apparatuses shown in Fig. 2.6 are commonly used for silent discharge and atmospheric pressure plasma jet, respectively.

As shown in Table 2.5, glow discharge occurs even under atmospheric pressure by filling the discharge space with a noble gas using the DBD apparatus [3–6]. Glow discharge is maintained even if a few percent of other gas is added to the noble gas. If too much other gas is added to the noble gas, discharge will gradually turn into a silent discharge.

From this presentation, the treatment by the atmospheric pressure discharge has been reviewed, and the treatment by the pure N_2 atmospheric pressure discharge is now widely used in the industry [7–12]. Since APG plasma has the same density of active species as low-pressure glow plasma, higher processing effect can be expected

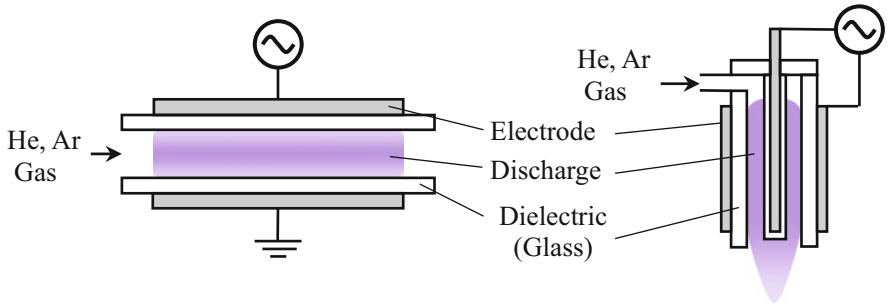

Fig. 2.5 Schematic diagram of APG discharge apparatus

Table 2.5 Occurrence conditions of APG discharge

Electrodes	Dielectric barrier electrodes
Pressure	Atmospheric pressure
Gas	Noble gas or high purity N_2
Power supply	Only an AC power supply is available

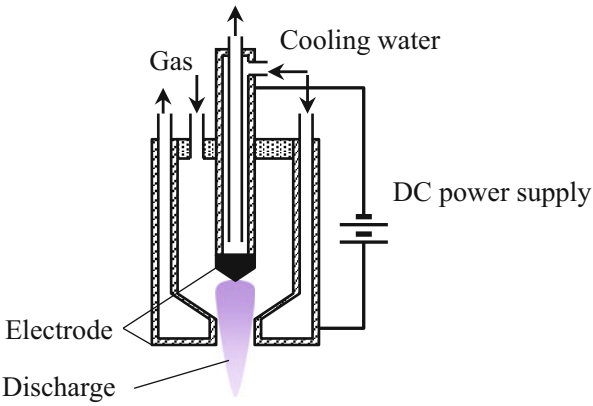

Fig. 2.6 Schematic diagram of arc discharge apparatus

Table 2.6 Occurrence conditions of arc discharge

Electrodes	Many electrode types
Pressure	Atmospheric ~ low pressure
Gas	All gases
Power supply	DC and AC power supplies are possible

compared to corona discharge and silent discharge. When high active species density is required, it may be worth considering the use of APG plasma.

2.4.5 Arc Discharge

When a discharge is generated using a power source capable of passing a large current and an electrode that can withstand high temperatures, the temperature of the electrode rises to a temperature at which thermo electrons are emitted from the electrode surface. At the same time, the temperature of the gas in the discharge field also rises, and thermo ionization begins to occur in the gas. When the discharge field is maintained at a high temperature, the plasma can be maintained even if there is not much ionization action due to collision between electrons and gas molecules. Such a discharge is called an arc discharge. A schematic diagram of the arc discharge apparatus is shown in Fig. 2.6, and a summary of the generation conditions is shown in Table 2.6. The apparatus diagram shown in Fig. 2.6 is an example, and different apparatuses are often used.

Depending on the conditions, the gas temperature of the arc discharge reaches several 1000–10,000 K. Arc discharge is widely used for welding and melting by utilizing this high temperature. Since the substance introduced into the discharge field is dissociated to the atomic state, it is also used in the production of ceramics and ultrafine powders.

The use of arc discharge is limited due to the high gas temperature, but on the other hand, the high density of active species is a very attractive point. Therefore, in

recent years, a process using a discharge type called gliding arc discharge, in which the gas temperature rises only to about 1000 K, has been performed.

2.5 Summary

When considering plasma as a tool, active species such as charged particles and radicals are obtained from plasma. By clarifying which active species is required for the treatment and how much active species is required, it is possible to determine which discharge type is appropriate.

Considering the application to agriculture, the treatment target is the plant itself or seeds. Then, there is no choice but to select a discharge type that can be generated under atmospheric pressure. Also, considering the ease of supply of active species and the low processing cost, corona discharge or N_2 atmospheric pressure plasma (although it cannot be classified as glow discharge, the density of active species is higher than corona discharge) is seem optimal. In some cases, gliding arc discharge may also be considered.

The greatest advantage of plasma processing is that almost all the bonds of substances introduced into the plasma are dissociated by electron collisions, so almost all possible radicals can be generated. And it is possible to cause an unthinkable reaction in the generally chemical reaction. Of course, the generated radicals often do not react as expected, using plasma is difficult. But there is a possibility that new discoveries that cannot be obtained by conventional methods will be born. It would be fun to use plasma.

References

1. Kanazawa S, Kogoma M, Moriwaki T, Okazaki S. Carbon film formation and surface modification by cold plasma at atmospheric pressure. Proc 8th Int Symp Plasma Chem. 1987;3:1839–44.
2. Kanazawa S, Kogoma M, Moriwaki T, Okazaki S. Stable glow plasma at atmospheric pressure. J Phys D Appl Phys. 1988;21(5):838–40.
3. Yokoyama T, Kogoma M, Moriwaki T, Okazaki S. The mechanism of the stabilisation of glow plasma at atmospheric pressure. J Phys D Appl Phys. 1990;23(8):1125–8.
4. Yokoyama T, Kogoma M, Kanazawa S, Moriwaki T, Okazaki S. The improvement of the atmospheric-pressure glow plasma method and the deposition of organic films. J Phys D Appl Phys. 1990;23(3):374–7.
5. Kanda N, Kogoma M, Uchiyama H, Okazaki S, Jinno H. Atmospheric pressure glow plasma and its application to the surface treatment and film deposition II, Development of a new method. Proc 10th Int Symp Plasma Chem. 1991;3.2–20:1–6.
6. Okazaki S, Kogoma M, Uehara M, Kimura Y. Appearance of stable glow discharge in air, argon, oxygen and nitrogen at atmospheric pressure using a 50 Hz source. J Phys D Appl Phys. 1993;26(5):889–92.

7. Massines F, Gadri RB, Decomps P, Rabehi A, Segur P, Mayoux C. Atmospheric pressure dielectric controlled glow discharges: diagnostics and modelling. AIP Conf Proc. 1996;363:306–15.
8. Segur P, Massines F, Rabehi A, Bordage M. Proceedings of the Eighth International Symposium on Gaseous Dielectrics, Virginia Beach, VA; 1998: 141–146.
9. Massines F, Rabehi A, Decomps P, Ben Gadri R, Segur P, Mayoux C. Experimental and theoretical study of a glow discharge at atmospheric pressure controlled by dielectric barrier. J Appl Phys. 1998;83(6):2950–7.
10. Gat E, Gherardi N, Lemoing S, Massines F, Ricard A. Quenching rates of N (C,ν') vibrational states in N and He glow silent discharges. Chem Phys Lett. 1999;306:263–8.
11. Ricard A, Decomps P, Massines F. Kinetics of radiative species in helium pulsed discharge at atmospheric pressure. Surf Coat Technol. 1999;112:1–4.
12. Gouda G, Massines F. Annual report – Conference on Electrical Insulation and Dielectric Phenomena. 1999;2:496–9.

Chapter 3
High-Voltage and Pulsed Power Technologies

Koichi Takaki

Abstract Recently, applications of high-voltage technologies including plasma have been newly developed for agricultural and food processing. Repetitively operated, compact high-voltage power supplies with moderate peak power have been developed for controlling discharge plasmas and electric field distribution in the applications. These applications are mainly based on the biological effects of a spatially distributed electric field and the chemically active species produced by the plasma. For the applications it is essential to generate, in a controlled way, repetitive high voltages, with precise voltage amplitude and waveform shapes, in order to deliver well-defined energy packages to biologic loads. This energy flow can be based on relatively simple circuits consisting of passive discrete resistive-inductive-capacitive elements, transformers, and switches, which convert the energy stored in the electric fields of capacitors or magnetic fields of coils into well-defined voltage outputs. Here, at first, a basis of high electric field phenomena is outlined. After that, generations of high voltage are described. The transient phenomena of single and stack circuits are also described as a basis of the generation and handling of high-voltage pulses, i.e., pulsed power. These include direct capacitive discharge, comprising a single switch or an association of circuits to circumvent the still voltage and current limitation of semiconductors, which include inductively multiplied circuit and Marx generator. Also, the utilization of pulse transmission lines (PFL) and pulse-forming network (PFN) to generate and format pulses into well-defined loads is explained.

Keywords Plasma · High-voltage · Agriculture · Food processing · Pulsed power · Pulse electric field

K. Takaki (✉)
Faculty of Science and Engineering, Iwate University, Morioka, Iwate, Japan
e-mail: takaki@iwate-u.ac.jp

S. Horikoshi et al. (eds.), *Agritech: Innovative Agriculture Using Microwaves and Plasmas*, https://doi.org/10.1007/978-981-16-3891-6_3

3.1 Introduction

The food supply chain from farm to fork is an important topic in a sustainable society. The agricultural and food industries must continually adapt to meet the demands of a growing population, both in terms of nutrition and consumer expectations. This must be achieved within the confines of the resources available and the regulatory requirements. Innovative technologies with regard to food production and processing are required to meet the emerging challenges of global food security and the complexities of the modern food supply chain. The study of possible agricultural and food processing applications of ionized gas plasmas and intense electric fields is experiencing rapid growth by researchers worldwide [1]. In the applications, the repetitively operated, compact high-voltage power supplies with moderate peak power have been developed for controlling discharge plasmas and electric field distribution. These applications are mainly based on the biological effects of a spatially distributed electric field and the chemically active species produced by the plasma [2, 3].

The intense pulse electric fields (PEFs) that have biological effects are caused by applying pulse voltage between the electrodes. When the applied voltage exceeds the corona discharge criterion, discharge plasmas that produce free radicals, ultraviolet (UV) radiation, an intense electric field, and shock waves are generated by the accelerated electrons within the intense electric field in a gas or liquid medium [4]. Different high voltages and plasmas may have different biological effects on substrates via the electric field and reactive species. For instance, intense electric fields form pores on the cell membrane (i.e., electroporation) or influence the nucleus [5]. The agricultural applications of plasma are categorized as seed germination promotion [6], plant growth acceleration [7], the inactivation of bacteria in soil and liquid hydroponic media [5, 8], and the promotion of fruit-body formation such as in mushrooms and fruits in the preharvest phase [5, 9]. In the postharvest phase, maintaining the freshness of agricultural products is important for a sustainable food supply chain. High-voltage and plasma technologies can contribute to maintaining freshness by decontaminating the air and liquid in agricultural products storage containers [5, 10]. In the food processing phase, an intense PEF can be used to extract juice, nutritional agents, and antioxidant metabolites such as vitamin, carotenoids, and polyphenols from fruits and vegetables [11]. Some foods and liquors are made by fermenting a food substance. Fermentation is a metabolic process enabled by yeast and bacteria, the activity of which can be controlled by an intense electric field [5, 12].

For the applications it is essential to generate, in a controlled way, repetitive high voltages, with precise voltage amplitude and waveform shapes, in order to deliver well-defined energy packages to biologic loads. This static or transient energy flow can be based on relatively simple circuits consisting of passive discrete resistive-inductive-capacitive elements, transformers or transmission lines, and switches, which convert the energy stored in the electric fields of capacitors or magnetic fields of coils into well-defined voltage outputs. Here, at first, a basis of high electric field

phenomena is outlined. After that, generations of high voltage are described. The transient phenomena of single and stack circuits are also described as a basis of the generation and handling of high-voltage pulses, i.e., pulsed power. These include direct capacitive discharge, comprising a single switch or an association of circuits to circumvent the still voltage and current limitation of semiconductors, which include inductively multiplied circuit and Marx generator. Also, the utilization of pulse transmission lines (PFL) and pulse-forming network (PFN) to generate and format pulses into well-defined loads is explained. As the behavior of the load can influence greatly the shape of the voltage waveform applied to the load, the type of load will be outlined in relation to the most common type of biological type loads, with resistive or capacitive behavior, respectively.

3.2 High Electric Field Phenomena

Here, a basis of high electric field phenomena is outlined. The high electric field is usually generated as electrostatic or induction fields. The electric field accelerates charged particles by the Coulomb force. As a result, an electron avalanches are formed and are developed in direction of the electric field. The electron avalanches cause an electrical breakdown (or discharge onset) between the electrodes when the electric field has enough amplitude to cause the electrical breakdown [13]. Plasma is commonly defined as a state of ionized gas and is generated by the electrical discharge (breakdown) in medium, gas, liquid, and solid materials.

3.2.1 Electrostatic Fields and Potentials

The relationship between magnetic and electric fields is completely described by the set of four Maxwell's equations [14];

$$\nabla \times \mathbf{E} = -\frac{\partial \mathbf{B}}{\partial t} \tag{3.1}$$

$$\nabla \times \mathbf{H} = \mathbf{J} + \frac{\partial \mathbf{D}}{\partial t} \tag{3.2}$$

$$\nabla \cdot \mathbf{B} = 0 \tag{3.3}$$

$$\nabla \cdot \mathbf{D} = \rho \tag{3.4}$$

where, **E** is the electric field strength, **B** is the magnetic flux density, **H** is the magnetic field strength, **J** is the current density, **D** is the electric flux density, ρ is the charge density. Equation (3.1) describes how a time-varying magnetic field generates an electric field. It explains how electrical generators work. It is the

differential form of Faraday's law of induction. Equation (3.2) describes how electrical currents produce magnetic fields. It explains how electromagnets and motors work. Equation (3.3) describes the shape of the magnetic field. It implies that magnetic monopoles do not exist. Equation (3.4) describes the shape of the electric field in the presence of electrical charges. Both point and diffuse charges can exist. It is the differential form of Gauss's law.

If no magnetic fields are present, Eq. (3.1) becomes $\nabla \times \mathbf{E} = 0$, which means no induction electric field. The definition of electric field is the rate at which the scalar potential ϕ varies with distance as follows;

$$\mathbf{E} = -\nabla\phi \tag{3.5}$$

The electric field and electric displacement field (electric flux density) are related by the electrical permittivity ?:

$$\mathbf{D} = \varepsilon\mathbf{E} \tag{3.6}$$

Substituting Eq. (3.5) and Eq. (3.6) into Eq. (3.4) gives Poisson's equation:

$$\nabla^2\phi = -\frac{\rho}{\varepsilon} \tag{3.7}$$

If no charges are present, Eq. (3.7) becomes Laplace's equation:

$$\nabla^2\phi = 0 \tag{3.8}$$

Laplace's equation can be used to calculate the electric fields present in different geometries. Figure 3.1 shows potential and electric field distributions between the electrode in three different geometries calculated using Eqs. (3.8) and (3.5), respectively. In case of an infinite parallel plate, the electric field is homogeneous in gap between the electrodes. However, in cases of a point electrode and an infinite coaxial line, the electric field strength changes with the distance from the electrode with small radius of curvature.

3.2.2 Electrical Discharges

Electrical discharges are used to create plasma as source of ion and chemically active species such as radical oxygen species (ROS) and radical nitrogen species (RNS). The electrical discharges can be initiated in localized regions of high field strength, then continue to propagate into regions where the field is not strong enough to start a discharge, but it is strong enough to allow the discharge to continue to propagate. Whether the discharge is transient or continuous can also depend on how the discharge gets its power.

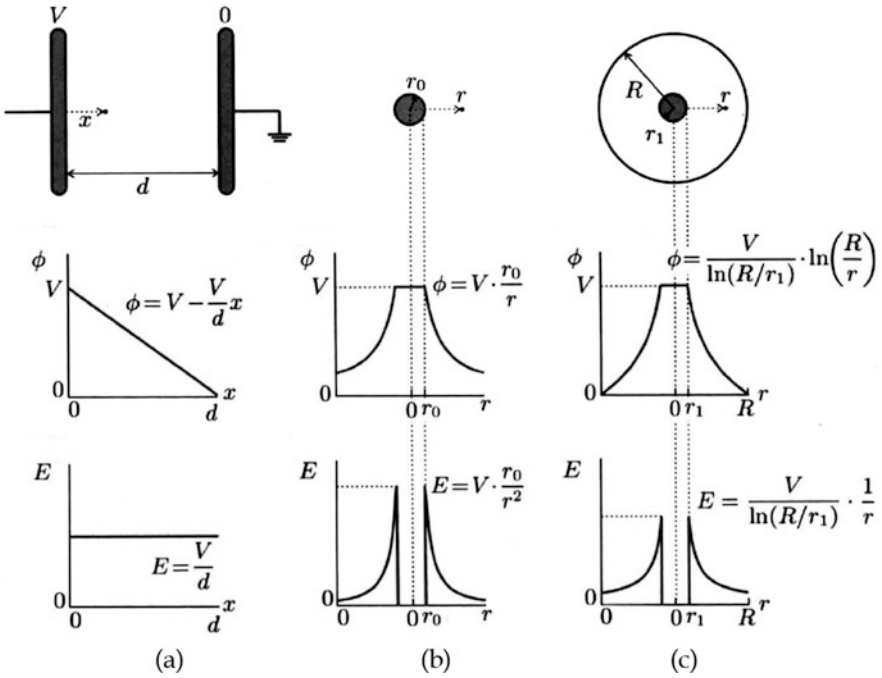

Fig. 3.1 Potential and electric field distributions between the electrode in three different geometries; (**a**) infinite parallel plate, (**b**) point electrode, and (**c**) infinite coaxial line

Electrical discharges are fundamentally ionizing materials (gases, liquids or solids) to produce charge carriers (electrons and ions). There is always a low level of background ionization occurring due to background radiation, which comes mainly from natural sources such as radon gas and cosmic rays. The most important ionization mechanism in electrical discharges is electron impact ionization. Free electrons impact on the outer electron orbitals of atoms and molecules all the time. If the free electrons have enough energy, they can knock the outer electron out of its orbital, leaving a positive ion and another free electron. The free electrons get their energy from externally applied fields. The field applied to create a discharge is usually the electric field; however, a magnetic field can also be applied in the case of inductively coupled discharges [15].

There are many names for the basic phenomenon that comprise electrical discharges, such as avalanches, streamers, corona, leaders, glows, and arcs [13]. These will all be defined in this section. They cover a huge range of different currents. To provide a conceptual landscape in which these discharges exist, it is useful to consider a simple set-up with two electrodes shown in Fig. 3.2a. A d.c. voltage can be applied between the electrodes and the resulting current measured. The general exact shape of the curve depends on the type of gas, pressure, electrode geometry, electrode temperatures, electrode materials, and any magnetic fields present. At low voltages, the current between two electrodes is extremely small,

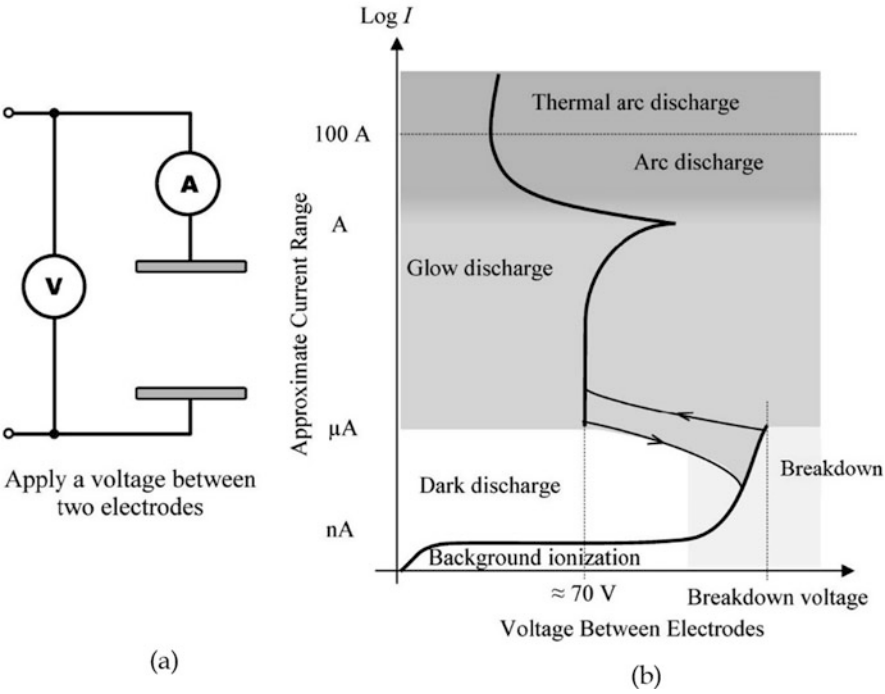

Fig. 3.2 Current–voltage characteristic of a typical electrical discharge between two electrodes [13]

but it slowly increases as the voltage between the electrodes increases (as shown in the bottom left corner of the graph in Fig. 3.2b). This tiny current comes from charge carriers produced by background ionization. They are swept out of the gap by the electric field between the electrodes that is created by the applied voltage. There are only enough charge carriers produced by background radiation for a few nanoamps of current, so the current quickly saturates. The voltage can then be increased with no increase in current. The ions and electrons are pulled towards the electrodes through the gas molecules interacting with them as they go.

3.2.3 Electron Multiplication: Avalanche Process

The voltage between the electrodes is increased until the applied electric field is high enough to accelerate the electrons to the ionization energy of the gas. At this point the current rapidly increases, as shown in the bottom right corner of the graph in Fig. 3.2b. The electrons ionize the neutral atoms and molecules, producing more electrons. These additional electrons are accelerated to ionize even more atoms, producing even more free electrons in an avalanche build-up process. This is the

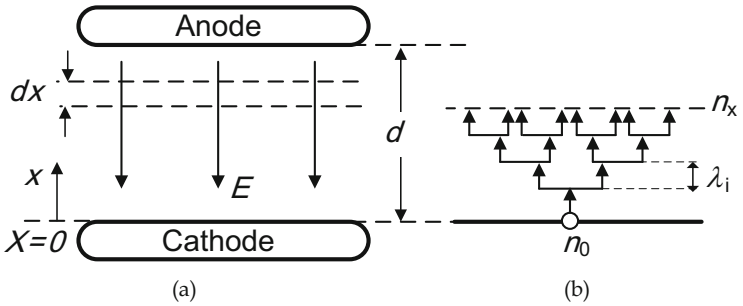

Fig. 3.3 Schematics representation of electron multiplication (**a**) gap arrangement, (**b**) electron avalanche

moment of inception of a high-voltage breakdown, and if the conditions are right, it can cause complete flashover of the electrodes [16].

The avalanche process was first mathematically described by Townsend in 1897. Consider an avalanche discharge between two electrodes. The position between the electrodes is given by the variable x, which defined as distance from negative (or grounded) electrode as shown in Fig. 3.3a. The number of additional free electrons dn_x produced in a distance dx depend on the number of electrons at that point n_x and the Townsend's (primary) ionization coefficient α:

$$dn_x = n_x \alpha \, dx \tag{3.9}$$

The primary ionization coefficient α is the number of additional electrons produced per unit length. By integration and the fact that $n_x = n_0$ at $x = 0$, this gives.

$$n_x = n_0 e^{\alpha x} \tag{3.10}$$

The number of free electrons (and ions) increase exponentially in the avalanche.

The increase of electron number (avalanche growth) shown in the diagram (Fig. 3.3b) would be $n_x = n_0 e^k$, with k = number of ionizing steps expressed as $k = x/\lambda_i$. Townsend related the ionization mean free path to the total scattering mean free path λ by treating it as being a process activated by the drift energy gained from the electric field $E\lambda$, with an activation energy eV_i, where V_i means ionization potential. This leads to a formula analogous to that of Arrhenius for thermally activated processes, giving rate constant known as Townsend's ionization coefficient [15];

$$\alpha = \frac{1}{\lambda_i} = \frac{\text{constant}}{\lambda} \exp\left(\frac{-V_i}{E\lambda}\right) \tag{3.11}$$

Since the mean free path is inversely proportional to pressure p, the coefficient can be written as;

$$\alpha = Ap \cdot \exp\left(\frac{-Bp}{E}\right) \tag{3.12}$$

Where the constants A and B are properties of the gas.

3.2.4 Transition to Self-Sustained Discharge: The Townsend Mechanism

Townsend also considered secondary ionization processes. In addition to electron impact ionization process, secondary electron emission process should also be considered. Acceleration of the positive ions in the electric field leads to secondary emission of electrons from the negative electrode, when they reach there, at a rate of γ electrons per indicate ion (γ: secondary ionization coefficient). The process of secondary emission and multiplication will become self-sustaining if the ions from multiplication between $x = 0$ and $x = d$ release from the cathode sufficient secondary electrons to exactly replenish population of ions in the gap. According to Eq. (3.10), n_0 initial electrons will produce $n_0 e^{\alpha x}$- n_0 ions at position x. Across the gap therefore there will be generated n_0 ($e^{\alpha d}$-1) ions. To be self-sustaining.

$$\gamma n_0 \left(e^{\alpha d} - 1\right) = n_0 \tag{3.12}$$

or

$$\alpha d = \ln\left(1 + \frac{1}{\gamma}\right) \tag{3.13}$$

In general, Townsend breakdown (self-sustaining discharge onset) criterion of αd value is obtained as 8–10 [16].

The breakdown voltage of a gas between two flat electrodes depends only on the electron mean free path and the distance between the electrodes. The electron mean free path is the average distance the electrons travel before hitting atoms, so it is the key factor defining the growth of an electron avalanche. It is directly related to pressure. Figure 3.4 shows how the breakdown voltage of several gases varies with the product of pressure p and distance d between electrodes. This was first stated in 1889 by Paschen.

An analytical expression for breakdown voltage V_s in uniform field gaps as a function gap length d and gas pressure p can be derived from the Townsend's criterion Eqs. (3.13) and (3.12) by expressing the ionization coefficient α/p as a function field strength and gas pressure as follows [15];

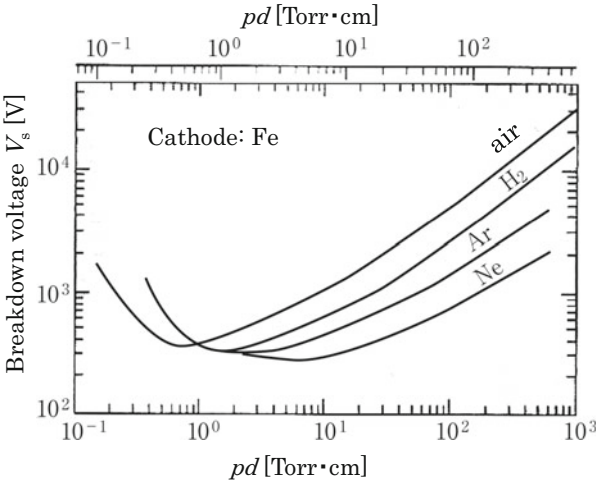

Fig. 3.4 Schematic breakdown curve for variable gases

$$V_s = \frac{B \cdot pd}{\ln\left(A \cdot pd/\phi\right)}, \text{where } \phi = \ln\left(1 + \frac{1}{\gamma}\right), \tag{3.14}$$

At very high pressures, the mean free path is very short. This means that the electrons never have enough time to be accelerated to the ionization energy before hitting an atom or molecule. This means that the breakdown voltage is high at very high pressures. At very low pressures, the mean free path between collisions is longer than the distance between the electrodes. So, although the electrons can be accelerated to ionizing energies, they are unlikely to hit anything other than the anode. This means that the breakdown voltage is very high at very low pressures. This is why vacuum is such a good insulating medium.

Between these two extremes is a minimum whose position depends on the type of gas and the electrode material. This "Paschen minimum" leads to a counterintuitive phenomenon: operating just below this minimum, electrodes further apart will have a lower breakdown voltage than those closer together. This is because, in a longer gap, there is more space for the electron avalanches to develop. The Paschen curves for all gases in Fig. 3.4 are very similar, with slightly different Paschen minima, ranging from 0.5 to 5 Pa cm and 200 to 400 V.

3.2.5 Streamer Mechanism of Spark

Figure 3.5a shows the distribution of particles in a single avalanche [13]. The discharge has a negative head, comprising the avalanche of free electrons, and a positive tail, comprising the positive ions left behind after the ionization avalanche has passed. The ions are at least 1800 times heavier than the electrons so they take

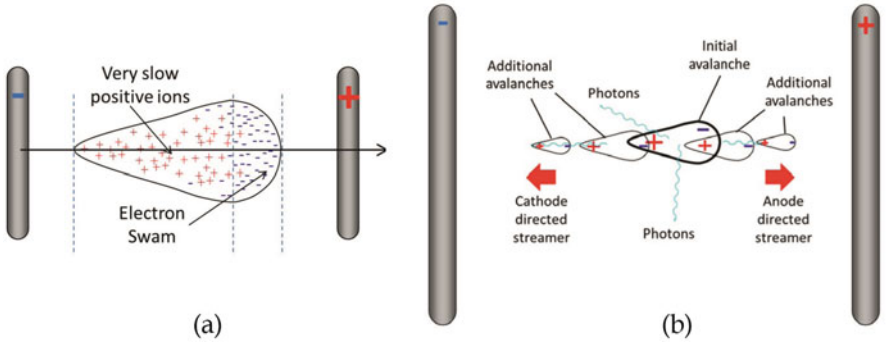

Fig. 3.5 Schematics of (**a**) distribution of particles in a single avalanche discharge, (**b**) streamer formation made up of a series of avalanches propagating in both directions from the initial avalanche [13]

much longer to accelerate than the electrons. Compared to the fast free electrons, the ions only move a tiny distance from where they were born.

The difference in mobility of the ions and electrons creates the charge distribution, which in turn produces the electric field distribution. If the discharge was not present, the electric field between the electrodes would be *V*/*d*. Even though the total amount of positive and negative particles is approximately equal, the distribution of charges in the avalanche causes an increase in the field in front of and behind the discharge. This is caused by the negative electron avalanche being closer to the positive electrode and the positive ions being closer to the negative electrode. The avalanche emits photons that can ionize nearby atoms creating free electrons. Any free electrons created in the higher-field region in front of or behind the initial avalanche will go on to produce additional avalanches.

Each additional avalanche creates more photons and further enhances the electric field. In this way a chain of avalanches propagates from the head and tail of the initial avalanche. The name for this chain of avalanches is a streamer. Streamers propagate in both directions, as shown in Fig. 3.5b. Eventually the chain of avalanches bridges the gap between the electrodes, creating an ionized conductive channel. This is the moment the gap actually flashes over. As much current flows from one electrode to the other as the power supply can deliver.

On the basis of an experimental observations and some simple assumptions, Raether developed an empirical expression for the streamer spark criterion of the form.

$$\alpha x_c = 17.7 + \ln x_c + \ln \frac{E_r}{E} \tag{3.15}$$

where E_r is the space charge field strength directed radially at the head of avalanche, as shown in Fig. 3.6, E is the externally applied field strength [16]. The resultant field strength in front of the avalanche is thus $(E + E_r)$ while in the positive ion region just

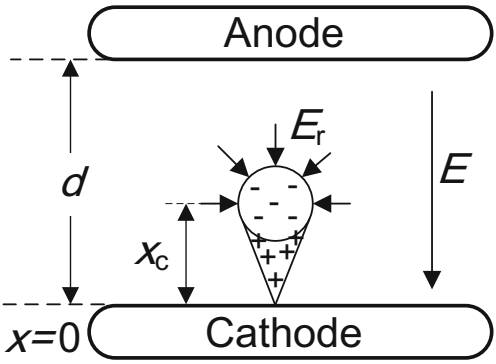

Fig. 3.6 Space charge field (E_r) around avalanche head

behind the head, the field is reduced to a ($E - E_r$). It is also evident that the space charge increases with the avalanche length ($e^{\alpha x}$).

The condition for the transition from avalanche to streamer assumes that space charge field E_r approaches the externally applied field ($E_r \fallingdotseq E$), hence the breakdown criterion Eq. (3.15) becomes.

$$\alpha x_c = 17.7 + \ln x_c \tag{3.16}$$

The minimum breakdown value for a uniform field gap by streamer mechanism is obtained on the assumption that the transition from avalanche to streamer occurs when the avalanche has just crossed the gap d. Then Raether's empirical expression for this condition takes.

$$\alpha d = 17.7 + \ln d \tag{3.17}$$

The streamer criterion for spark formation requires a value of 18–20, $\alpha d = \alpha x_c = \ln 10^8 \cong 20$, with $x_c \leq d$. In session 3.2.4, we have seen that the Townsend criterion for spark formation is satisfied when the product αd reaches a value 8–10 as $\alpha d = \ln (1 + 1/\gamma) = 8 - 10$. Therefore, under certain experimental conditions there will be a transition from Townsend to streamer mechanism. This transition is brought about by increased gas pressure and gap length, and in practice it occurs in the region of $pd \geq 1 - 2$ bar cm [16].

3.3 Generation of High Voltage

Here, a basis of high voltage (HV) generation is outlined. Generally, commercially available HV generators are not only used for testing electric power equipments such a transformer, bushing, and cables, but also used in many branches of natural sciences of other technical applications based on discharge plasmas and high electric

field. In this session, the generation of direct (DC) voltages, alternating (AC) voltages, and transient voltage is outlined.

3.3.1 Direct Voltages

High DC voltages are even more extensively used in applied physics (accelerators, electron microscopy, etc.), electromedical equipment (X-rays), industrial applications (precipitation and filtering of exhaust gases in thermal power stations and the cement industry; electrostatic painting and powder coating, etc.), or communications electronics (TV, broadcasting stations). Therefore, the requirements on voltage shape, amplitude, and current rating, short- or long-term stability for every HVDC generating system may differ strongly from each other. With the knowledge of the fundamental generating principles, it will be possible, however, to select proper circuits for a special application [16].

The DC voltages are generally obtained by means of rectifying circuits applied to AC voltage (or electrostatic generation). For a clear understanding of all AC to DC conversion circuits, the single-phase half-wave rectifier with voltage smoothing is of basis interest as shown in Fig. 3.7a. If we neglect the leakage reactance of the transformer and the small internal impedance of the diodes during conduction (this will be done throughout unless otherwise stated), the reservoir or smoothing capacitor C is charged to the maximum voltage $V_{\max}$ of the AC voltage of the transformer, when D conducts. If load current $i_L = 0$, i.e., the output load being zero ($R_L = \infty$), the DC voltage across C remains constant ($V_{\max}$), whereas v_{ac} oscillates between $\pm V_{\max}$. However, the output voltage V does not remain any more constant of the circuit is leaded. During one period, $T = 1/f$ of the AC voltage, where f means frequency, a charge stored in the capacitor is transferred to the load R_L. The DC voltage V includes ripple as shown in Fig. 3.7b.

The demands in some applications for very high DC voltages forced the improvement of rectifying circuits quite early. It is observed that every multiplier circuit in which transformers, rectifiers, and capacitor units have only to withstand a fraction

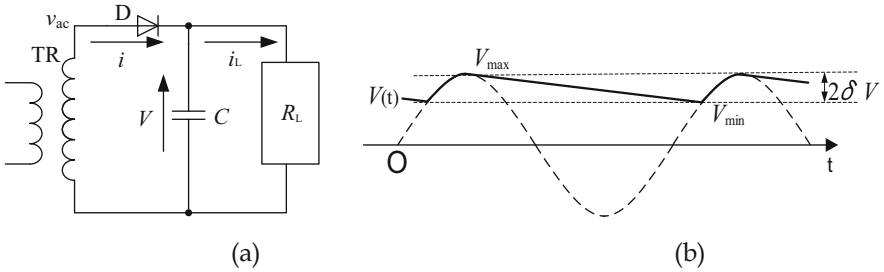

Fig. 3.7 Single-phase half-wave rectifier with reservoir capacitance C; (**a**) circuit, (**b**) voltages with load R_L

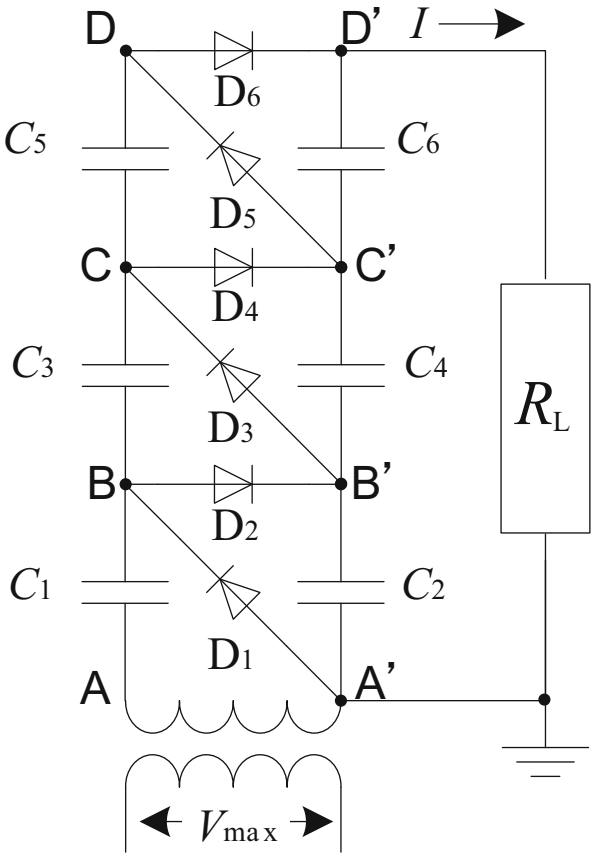

Fig. 3.8 Cascade circuit according to Cockcroft-Walton

of the total output voltage will have great advantages. Today there are many standard cascade circuits available for conversion of modest AC to high DC voltage. In 1920, Greinacher published a circuit which was improved in 1932 by Cockcroft and Walton to produce high-energy positive ion [16]. A six-stage single-phase cascade circuit of the "Cockcroft-Walton type" is shown in Fig. 3.8. If load current $I = 0$, i.e., the output load being zero ($R_L = \infty$), the capacitor C_1 is charged up to $V_{\max}$ through a half-wave rectifier circuit if the potential A has reached the lowest potential, $-V_{\max}$. If C_2 is still uncharged, the rectifier D_2 conducts as soon as applied voltage increases. As the potential of point B′ swings up to $2V_{\max}$ during one period, $T = 1/f$ of the AC voltage. Therefore, all capacitors are charged up to $V_{\max}$ in the steady state and the potential of point D′ reaches $6V_{\max}$. The use of several stages arranged in this manner enables very high voltages to be obtained.

3.3.2 Alternating Voltages

As electric power transmission with high AC voltages predominates in our transmission and distribution systems, the most common form of testing HV apparatus is related to AC voltages. It is obvious then that most research work in electrical insulation systems has to be carried out with this type of voltage. In general, all AC voltage tests are made at the nominal power frequency of the test objects. The power frequency single-phase transformer is the most common form of HVAC generation apparatus. Deigned for operation at the same frequency as the normal working frequency of the test objective (i.e., 50 or 60 Hz), they may also be used for higher frequencies with rated voltage, or for lower frequencies, if the voltages are reduced in accordance to frequency, to avoid saturation of the core [16].

Figure 3.9 shows illustration and diagram of single-phase transformer. The primary winding n_1 is usually rated for low voltages of $V_1 \leqq 1$ kV, but might often be slip up in two or more windings which can be switched in series of parallel to increase the regulation capabilities. The iron core is fixed at ground potential as well as one terminal of each of the two windings. The secondary winding n_2 is usually rated for high voltages V_2. The secondary output voltage and current are simply expressed as

$$V_2 = \frac{n_2}{n_1} V_1, I_2 = \frac{n_1}{n_2} I_1 \tag{3.18}$$

3.3.3 Impulse Voltages

Disturbances of electric power transition and distribution systems are frequently caused by two kinds of transient voltages whose amplitudes may greatly exceed the peak values of the normal AC operation voltage. The first kind is lightning

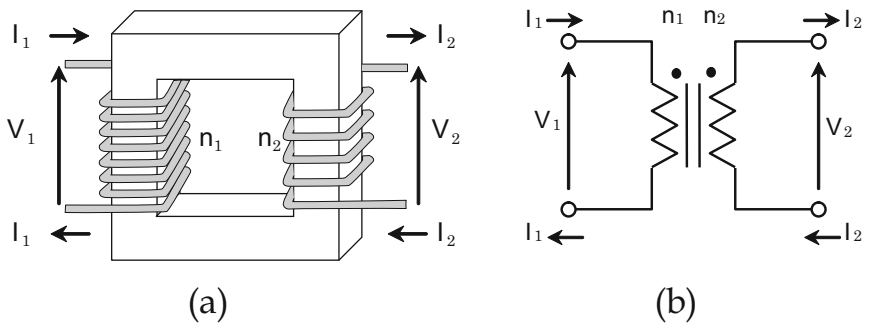

Fig. 3.9 Single-phase transformer, (**a**) schematics and (**b**) diagram

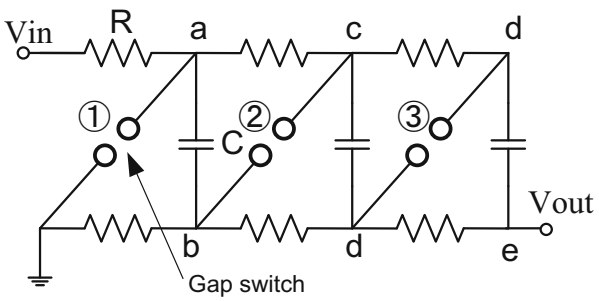

Fig. 3.10 Basic circuit of a three-stage impulse generator (Marx generator)

overvoltage, originated by lightning strokes hitting the phase wires of overhead lines or the busbars of outdoor substations. The second kind is caused by switching phenomena. Although the actual shape of both kinds of overvoltages varies strongly, it becomes necessary to simulate these transient voltages by relatively simple means for testing purpose. For most applications of lightning impulse voltages, the front time T_1 is 1.2 μs, and the time to half-value T_2 is 50 μs (1.2/50 impulse). For applications of switching impulse voltages, the time to peak T_P and the time to half-value T_2 are 250 and 2500 μs, respectively (250/2500 impulse) [16].

The difficulties encountered with spark gaps for switching of very high voltages, the increase of the physical size of the circuit elements, the efforts necessary in obtaining high DC voltages to charge capacitor, the difficulties of suppressing corona discharges from the structure and leads during the charging period make the one-stage circuit inconvenient for higher voltage. In order to overcome these difficulties, in 1923 Marx suggested an arrangement where a number of condensers are charged in parallel through high ohmic resistances and then discharged in series through spark gap as shown in Fig. 3.10 (three-stage Marx generator). The DC voltage V_{in} charges the equal stage capacitors C in parallel through the high value charging resistors R. The discharge or firing of the generator is initiated by the breakdown of the lowest gap switch ① which is followed by a nearly simultaneous breakdown of all remaining gap switches. This circuit gives an output voltage $(-3V_{in})$ with a polarity opposite to that of the charging voltage.

One basic circuit for single-stage impulse generators is shown in Fig. 3.11a. The capacitor C is slowly charged from a DC source until the spark gap switch breakdowns. An ignition time (time to voltage breakdown) of the gap switch is very short in comparison to the front time (T_1). After the gap switch is closing, the output voltage between the resistance R can be roughly expressed as shown in Fig. 3.11b at $\left(\frac{R}{L}\right)^2 - \frac{4}{LC} \gg 0$. The time constants for rise and fall of output voltage are roughly estimated as L/R and RC, respectively, under condition of $\left(\frac{R}{L}\right)^2 - \frac{4}{LC} \gg 0$. Therefore, we can control the waveform with choosing values of resistance R, capacitance C, and inductance L.

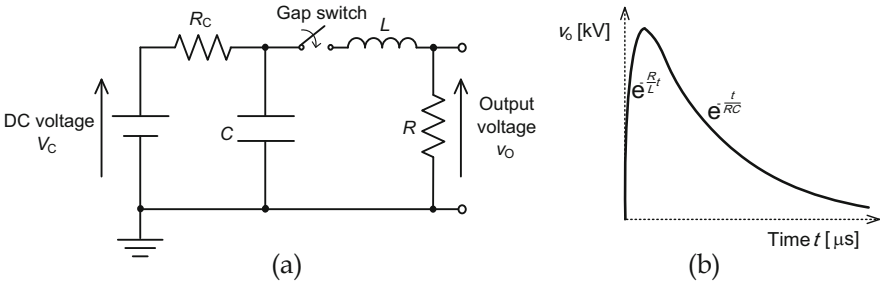

Fig. 3.11 Single-stage impulse generator; (**a**) circuit, (**b**) waveform of output voltage at $\left(\frac{R}{L}\right)^2 - \frac{4}{LC} \gg 0$

3.4 Generation of Pulsed Power

Pulsed power refers to the science and technology of accumulating energy over a relatively long period of time and releasing it as a high-power pulse composed of high voltage and current over short period of time; as such, it has extremely high power but moderately low energy [2, 17, 18]. Pulsed power is produced by transferring energy generally stored in capacitors and inductors to a load very quickly through switching devices. Applications of pulsed power continue expansion into fields including the environment, recycling, energy, defense, material processing, medical treatment, plasma medicine, and food and agriculture. Building upon the development of pulsed power generators which offer both high repetition and performance, scientists are now able to investigate efforts of pulsed power on living organisms, and their research has expanded to encompass a new field. This session summarizes pulsed power generation with a focus on this new field.

3.4.1 Basic Circuit for Pulsed Power

Figure 3.12 shows familiar circuits combining a capacitor of an inductor and switches. Capacitors and inductors (known as reactive elements) store electrical energy in form of electric field ($0.5\varepsilon E^2$ [J/m^3], where ε dielectric constant, E electric field strength) and magnetic fields ($0.5\mu H^2$ [J/m^3], where μ magnetic permeability, H magnetic field strength), respectively.

In the capacitor-resister circuit (capacitive energy storage system) shown as Fig. 3.12a, the electrical energy $0.5CV_0^2$ (V_0 initial charging voltage) is stored in a capacitor and then dumped into a load resistor R_L through a closing switch S. The load voltage and current after closing the switch S are obtained as follows using continuity of current in the circuit;

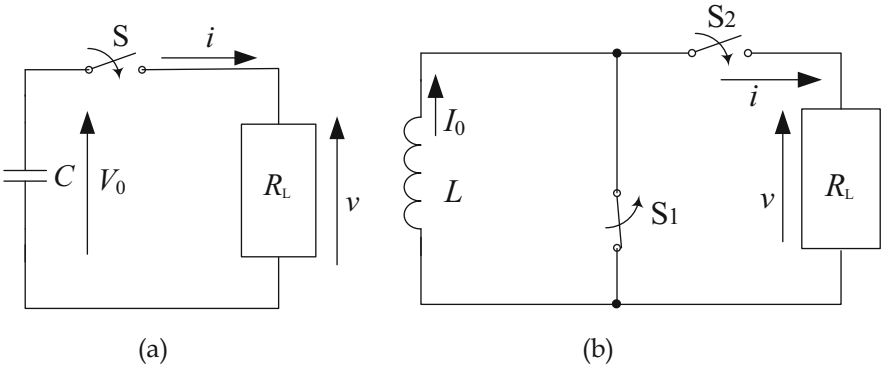

Fig. 3.12 Basic circuits for pulsed power; (**a**) capacitive and (**b**) inductive energy storage system

$$v(t) = V_0 \exp\left(-t/R_L C\right) \tag{3.19}$$

$$i(t) = \frac{V_0}{R_L} \exp\left(-t/R_L C\right) \tag{3.20}$$

where t time after closing switch S.

In the inductor-resister circuit (inductive energy storage system) shown as Fig. 3.12b, the magnetic energy $0.5LI_0^2$ (I_0 initial current in the inductor) is stored in a inductor and then dumped into a load resistor R_L by opening switch S_1 and closing switch S_2. The load voltage and current after closing the switch S_2 are obtained as follows using Kirchhoff's voltage law;

$$v(t) = R_L I_0 \exp\left(-\frac{t}{L/R_L}\right) \tag{3.21}$$

$$i(t) = I_0 \exp\left(-\frac{t}{L/R_L}\right) \tag{3.22}$$

3.4.2 Transmission Line

Most applications for pulse modulators require a constant voltage during period of pulse width. The critically damped waveform is the closest a modulator with a single capacitor and inductor can approach constant voltage. Better waveforms can be generated by modulators with multiple elements; such circuits are called pulse-forming networks (PFNs), whose transmission line (distributed constant circuit) is the contentious limit of PFN. Here, we analyze pulse transmission lines (PFLs) by a lumped element description rather than the direct solution of the Maxwell equations. Discrete elements PFNs are treated in Sect. 3.4.3.

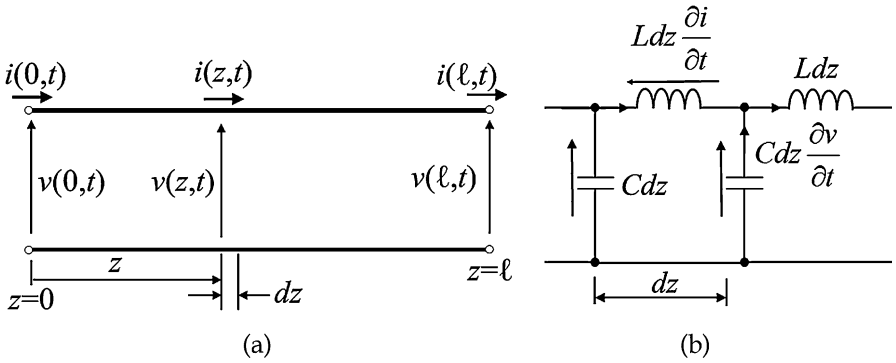

Fig. 3.13 Transmission line; (**a**) distributed circuit and (**b**) its lumped circuit element analogue

Figure 3.13a shows a diagram of a transmission line as distribution circuit with differential elements of length dz. Figure 3.13b shows its model using lamped circuit elements *L*dz and *C*dz, where *L* [*H/m*] and *C* [*F/m*] are inductance and capacitance per unit length, respectively. Based on Kirchhoff's voltage and current laws, the voltage and current differences between two points can be approximated in terms of the function as contentious partial differential equations when dz. is small,

$$\frac{\partial v}{\partial z} = -L\frac{\partial i}{\partial t}, \frac{\partial i}{\partial z} = -C\frac{\partial v}{\partial t} \tag{3.23}$$

The two above equations are called telegraphist's equations and can be combined to give wave equations for voltage and current of the form

$$\frac{\partial^2 v}{\partial t^2} = \left(\frac{1}{LC}\right)\frac{\partial^2 v}{\partial z^2}, \frac{\partial^2 i}{\partial t^2} = \left(\frac{1}{LC}\right)\frac{\partial^2 i}{\partial z^2} \tag{3.24}$$

The two above equations are mathematical expressions of the properties of a transmission line. It can easily be verified as follows

$$v(z,t) = v_f(z - vt) + v_b(z + vt) \tag{3.25}$$

$$i(z,t) = \frac{1}{Z_0}\left\{v_f(z - vt) - v_b(z + vt)\right\} \tag{3.26}$$

where v_f and v_b are forward and backward voltage waves, respectively, Z_0 characteristic impedance of line ($Z_0 = \sqrt{L/C}$) and v phase velocity ($v = 1/\sqrt{LC}$). Figure 3.14 shows typical transmission lines. The capacitance C and inductance L can be calculated geometrically. The phase velocity is expressed as using geometrically obtained L and C values

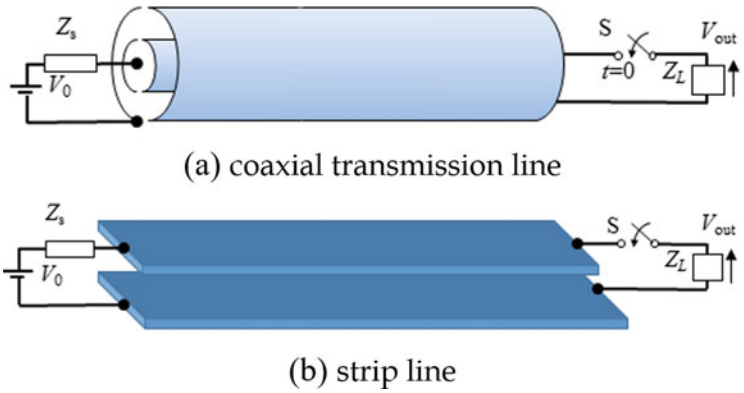

Fig. 3.14 Typical transmissions lines

$$v = 1/\sqrt{\epsilon\mu} \tag{3.27}$$

Figure 3.15 shows snapshots of the voltage distribution in the line and the output voltage when the end of the transmission line is terminated by a load with an impedance of Z_L. The reflection coefficient k at transmission line end is

$$k = \frac{Z_L - Z_0}{Z_L + Z_0} \tag{3.28}$$

The above equation indicates that the condition of $Z_0 = Z_L$ results in $k = 0$, i.e., no reflection results, and all electromagnetic energy is absorbed in the load as shown in Fig. 3.15. This situation of no reflection is called a matching between load and transmission line.

3.4.3 Pulse-Forming Network

Transmission lines are well suited for output pulse lengths in range $5\,\text{ns} < \Delta t_p < 200\,\text{ns}$ but are impractical for pulse lengths above 1 μs. Discrete element circuits are usually used for long pulse lengths as they achieve better output waveforms than the critically damped circuit due to their use of more capacitors and inductors. Discrete element circuits providing a shaped waveform are called pulse-forming networks. The derivations of Sect. 3.4.2 suggest that the circuit Fig. 3.16 can provide a pulse with an approximately constant voltage. A transmission line is simulated by a finite number N of inductor-capacitor units. Following the derivation of Sect. 3.4.2, the resistance of matched load is $Z_0 = \sqrt{L/C}$, where the quantities L and C are the inductance and capacitance of discrete elements. The Z_0 is called as impedance of PFN. The single transient time of an electromagnetic pulse through the network is

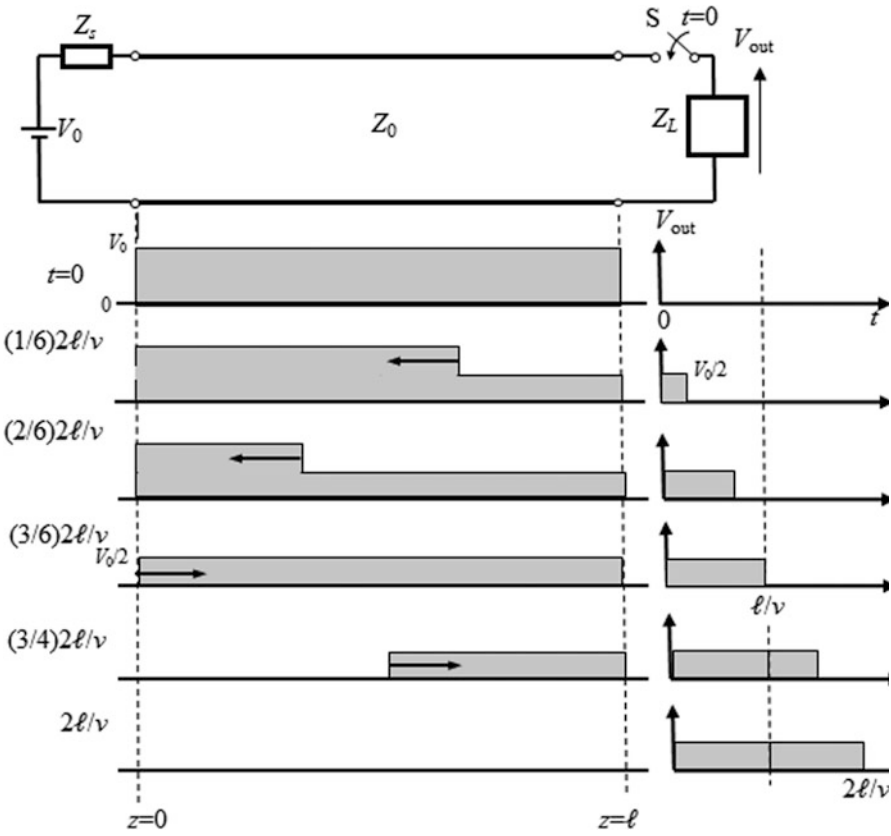

Fig. 3.15 Snapshots of the voltage distribution in the line and the output voltage at $Z_0 = Z_L$

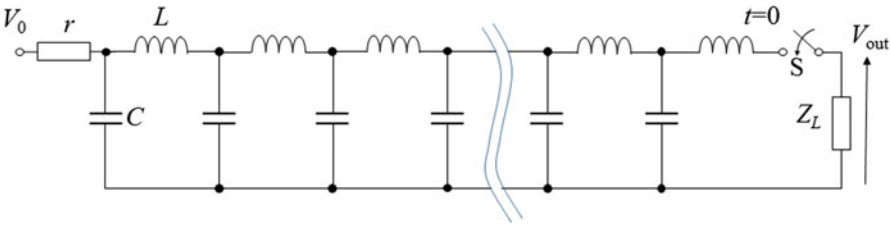

Fig. 3.16 Diagram of pulse-forming network

approximately $N\sqrt{LC}$. The output voltage pulse has average magnitude $V_0/2$ and duration of

$$\Delta t_p = 2N\sqrt{LC} \tag{3.29}$$

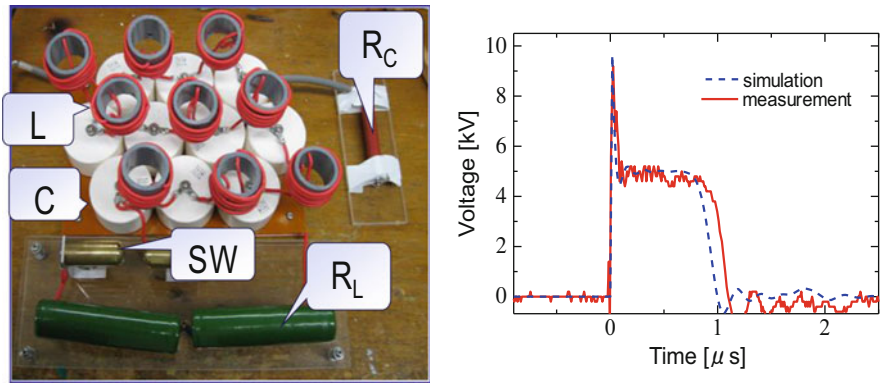

Fig. 3.17 Schematics of deigned PFN (**a**) and its output voltage (**b**) with connecting a load resistance of $Z_0 = Z_L$ at $C = 2$ nF, $L = 1.25$ μH, and $N = 10$

Figure 3.17 shows the example of deigned PFN and its output voltage with connecting a load resistance of $Z_0 = Z_L$ (matching condition; no reflection at the end of PFN). The PFN consists of 2 nF capacitor and 1.25 μH with $N = 10$. The charging voltage is 10 kV. The pulse length is calculated as

$$\Delta t_p = 2 \times 10\sqrt{1.25 \times 10^{-6} \times 2 \times 10^{-9}} = 1\,\mu s$$

The pulse length is almost same with calculating result as shown in Fig. 3.17b. The output voltage is almost constant and is 5 kV ($=V_0/2$).

3.4.4 Generator Using Power Semiconductor Device

Both the rise and fall times of switches and switching loss have decreased with the development of power semiconductor devices used as switches. Pulsed power generator is possible by direct switching ac, a DC power source (including AC/DC converter) with high voltage and current. Figure 3.18a shows a schematic circuit composed of AC/DC converter circuit, H-bridge connected four insulated gate bipolar transistors (IGBTs), and pulse transformer which is used for amplifying voltage to 10 kV. The pulse width and the pulse repetition rate are controlled with timing of gate trigger of the semiconductor switching devices. Duty factor (ratio of on time per pulse cycle) can also be controlled by the gate-trigger timing as shown in Fig. 3.18b [19].

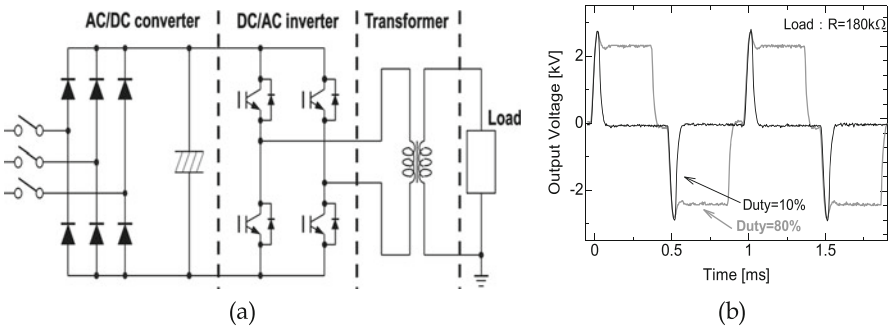

Fig. 3.18 Schematic circuit composed of AC/DC, H-bridge connected four insulated gate bipolar transistors, and pulse transformer (**a**) and its output voltage waveforms (**b**)

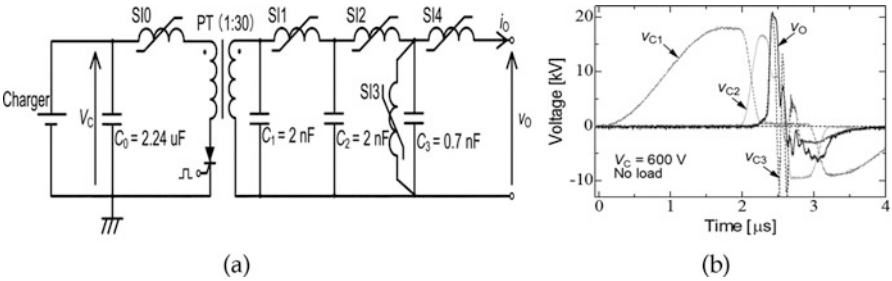

Fig. 3.19 Schematic diagram of a pulse power generator using a magnetic compression circuit (**a**) and its output voltage waveforms (**b**)

3.4.5 Magnetic Pulse Compression

Figure 3.19a shows a schematic diagram of a pulse power generator using a magnetic pulse compression circuit. After the capacitor C_0 is charged to V_C, semiconductor switching device is switched-on. Since the saturable inductor SI_0 has large value in inductance, current of the semiconductor switching device remains low during its initiation. Therefore, switching loss calculated from voltage and current of the switching device is minimized. When the capacitor C_1 is charged to nV_C, where n is the amplification factor of the pulse transformer PT, the stored energy of C_1 transfers to C_2 through the saturable inductor SI_2. Subsequently, the energy transfer from C_2 to C_3 occurs concurrently through the saturable inductor SI_3. The energy transfer from C_3 to the load occurs in same way. These energy transfers are summarized in Fig. 3.19b. The risetime of voltage decreases gradually because of $SI_1 > SI_2 > SI_3$.

3.5 Concluding Remarks

The introduction of intense electric fields and plasmas into agricultural and food processing practices is not only a big challenge for interdisciplinary research at the interface between high-voltage plasma physics and biosciences but also an option to develop new, sustainable food supply chain strategies for several of today's leverage points in food supply systems.

For the applications of high-voltage technologies in agriculture and food processing, it is essential to generate DC, AC, and transient voltages, with precise voltage amplitude and waveform shapes, in order to deliver well-defined energy packages to biologic loads. The energy flow was described in this chapter based on relatively simple circuits consisting of passive discrete resistive-inductive-capacitive elements, transformers or transmission lines, and switches, which convert the energy stored in the electric fields of capacitors or magnetic fields of coils into well-defined voltage outputs. As the behavior of the load influenced the shape of the voltage pulse applied to the load, the type of load was described in relation to biological type loads with resistive or capacitive behavior.

Even though the high-voltage and plasma application in agriculture field is new and still mainly in the experimental stage of development, the first signs of its potential are evident. The plasma-agriculture research community has the responsibility to address legitimate public expectations with responsible and reliable research, but without inspiring the hope of easy, short-term solutions for all problems including cost. Since the field of plasma agriculture is young, the long-term study issues still remain, which can be addressed by worldwide collaboration between diverse specialized researchers.

Acknowledgments The authors of this chapter confirm that they have received permission to reuse all the tables and figures in their current work.

References

1. Takaki K, Hayashi N, Wang D, Ohshima T. High-voltage technologies for agriculture and food processing. J Phys D Appl Phys. 2019;52:473001.
2. Akiyama H, Heller R, editors. Bioelectrics. Tokyo: Springer; 2017.
3. Graves DB. The emerging role of reactive oxygen and nitrogen species in redox biology and some implications for plasma applications to medicine and biology. J Phys D Appl Phys. 2012;45:263001.
4. Weltmann K, Kindel E, von Woedtke T. Atmospheric pressure plasma sources: prospective tools for plasma medicine. Pure Appl Chem. 2010;82:1223–37.
5. Zimmermann U. Electric field-mediated fusion and related electrical phenomena Biochem. Biophys Acta. 1982;64:227–77.
6. Eing CJ, Bonnet S, Pacher M, Puchta H, Frey W. Effects of nanosecond pulsed electric field exposure on Arabidopsis thaliana. IEEE Trans Dielectr Electr Insul. 2009;16:1322–8.
7. Takahata J, Takaki K, Satta N, Akahashi K, Fujio T, Sasaki Y. Improvement of growth rate of plants by bubble discharge in water. Jpn J Appl Phys. 2015;54:01AG07.

8. Okumura T, Saito Y, Takano K, Takahashi K, Takaki K, Satta N, Fujio T. Inactivation of bacteria using discharge plasma under liquid fertilizer in a hydroponic culture system. Plasma Med. 2016;6:247–54.
9. Takaki K, Yoshida K, Saito T, Kusaka T, Yamaguchi R, Takahashi K, Sakamoto Y. Effect of electrical stimulation on fruit body formation in cultivating mushrooms. Microorganisms. 2014;2:58–72.
10. Koide S, Nakagawa A, Omoe K, Takaki K, Uchino T. Physical and microbial collection efficiencies of an electrostatic precipitator for abating airborne particulates in postharvest agricultural processing. J Electrost. 2013;71:734–8.
11. Yang N, Huang K, Lyu C, Wang J. Pulsed electric field technology in the manufacturing processes of wine, beer, and rice wine: a review. Food Control. 2016;61:28–38.
12. Ohshima T, Tamura T, Sato M. Influence of pulsed electric field on various enzyme activities. J Electrost. 2007;65:156–61.
13. https://arxiv.org/abs/1404.0952
14. Jackson JD. Classical electrodynamics. 3rd ed. Hoboken, NJ: John Wiley & Sons Inc.; 1999. p. 237.
15. Braithwaite NSJ. Introduction to gas discharges. Plasma Sources Sci Technol. 2000;9:517–27.
16. Kuffel E, Zaengl WS, Kuffel D. High-voltage engineering: fundamentals. 2nd ed. Oxford: Elsevier; 2000.
17. Lehr J, Rpn P. Foundations of pulsed power technology. Hobson: John Wiley & Sons; 2017.
18. Bluhm H. Pulsed power system. Berlin: Springer; 2006.
19. Miura T, Sato T, Arima K, Mukaigawa S, Takaki K, Fujiwara T. Duty factor effect on ozone production using dielectric barrier discharge reactor driven by IGBT pulse modulator. J Adv Oxid Technol. 2007;10:311–5.

Chapter 4
Agricultural Engineering

Graham Brodie

Abstract A viable agricultural system, producing adequate and healthy food is essential for human society to continue. Transformational changes in agricultural production have been possible because of the adoption of technologies, as they became available. Engineers have been integral in the development and deployment of technologies into agriculture, including some novel applications of electromagnetic energy. This chapter presents a brief overview of the importance of agriculture and the contribution of engineers to this important industry.

Keywords Human population · Food production · Industrial revolutions · Engineering · Agricultural production

4.1 Introduction

Modern agriculture is the foundation of society and culture. Without adequate supplies of food and fibre, society has insufficient energy to do more than simply survive [1]. When supplies of food and fibre fall below the threshold levels needed to sustain a population, chaos and population collapse ensue [1].

Humanity's ability to produce enough food to sustain its current population is mostly due to adoption of new methods and technologies by the agricultural industries as they became available [2]. Mechanisation has transformed agricultural practices [3], allowing the industrialisation of agriculture. Mechanisation has been achieved and guided by agricultural engineers [4].

Engineering is an ancient profession, with several major innovations such as wedges, wheels, leavers and the harnessing of animals dating to well before 3000 BC [4]. More recently, the industrialisation of agriculture has transformed the world.

G. Brodie (✉)
Faculty of Veterinary and Agricultural Sciences, The University of Melbourne, Parkville, VIC, Australia
e-mail: grahamb@unimelb.edu.au

S. Horikoshi et al. (eds.), *Agritech: Innovative Agriculture Using Microwaves and Plasmas*, https://doi.org/10.1007/978-981-16-3891-6_4

Agricultural and mechanical innovations accelerated in the Middle Ages releasing surplus wealth and energy in Europe for exploration [5].

The English word 'engineer' is derived from the Latin word 'ingenium,' meaning creative or ingenious [3]. The modern profession of engineering can be loosely described as the practical application of science and knowledge [3]; therefore, an engineer is someone who can apply available knowledge to improve the human state. Because the universe appears to be mathematical in its nature [6], engineers necessarily have a good mastery of mathematics and use this tool to solve problems to improve the long-term prospects of humanity.

This chapter will outline some of the grand challenges facing the sustenance of humanity. These challenges are not trivial and require significant effort and investment to overcome; however, history has demonstrated that humanity is both resilient and resourceful. Engineering has played an important role in the achievements of humanity and will continue to do so into the future. Therefore, this chapter will also highlight how engineering, and particularly agricultural engineering, can help address these grand challenges.

4.2 The Malthusian Catastrophe

Malthus [1] studied population growth in Europe. He estimated that population was increasing exponentially, and resources were only increasing linearly; therefore, population was increasing faster than food production. Malthus believed that agricultural output could not keep up with the exponential growth in human population. Inevitably, famine would result, standards of living would fall and wars over scarce resources would ensue. His conclusion was that global starvation and universal struggle and poverty were inevitable.

Malthus based his analysis on three major assumptions:

1. Malthus assumed that there was a limit to agricultural productivity. In reality, since 1800, farm mechanisation, and better fertiliser usage have increased the output per farmer by more than 400 time in developed countries. While there has been some increase in global land use for agricultural production, this increase has been of the order of 0.5% per annum, since 1960 (Fig. 4.1). Crop yield increases of approximately 23% per annum have been achieved during the same period (Fig. 4.2).
2. Without overtly stating it, Malthus assumed that there would be no significant changes to agricultural technologies in the future; however, thanks to ongoing innovations, agricultural productivity has kept pace with human population growth. For example, cereal crop productivity in the United Kingdom has increased in proportion with human population growth over the past 220 years (Fig. 4.2), thanks to ongoing adoption and adaptation of emerging technologies. The adoption of technologies into agriculture has kept productivity aligned with human population growth (Fig. 4.2).

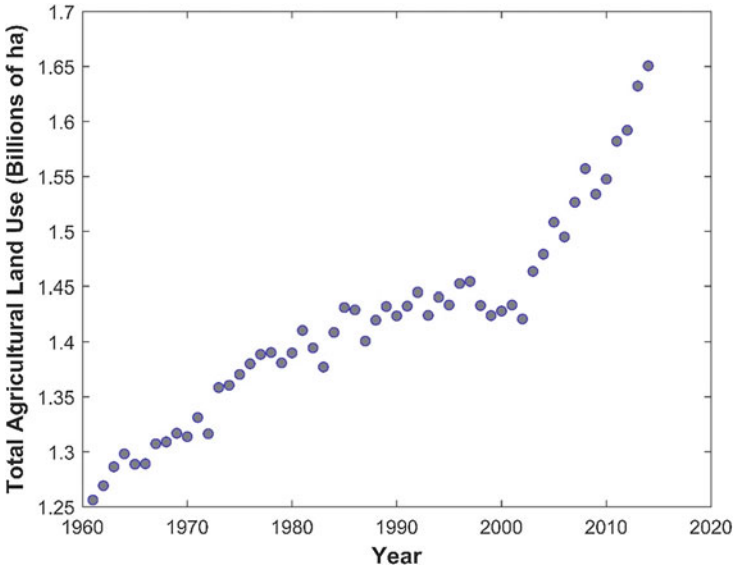

Fig. 4.1 Change in global crop production land use as a function of time (Source: https://ourworldindata.org/)

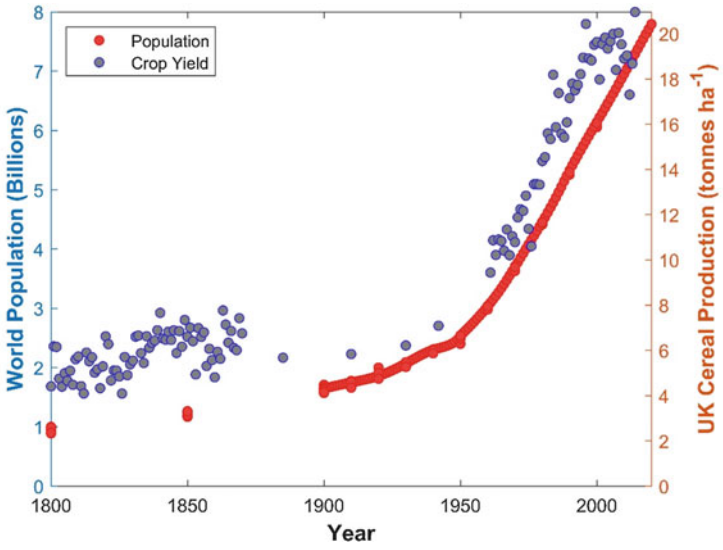

Fig. 4.2 Comparison of cereal crop productivity in the UK with global human population growth as a function of time (Source: https://ourworldindata.org/)

3. Malthus assumed that population would continue to grow at an exponential rate until limited by a resource crisis; however, *demographic transition* has occurred in which healthier and wealthier people tend to have fewer children [7]. Non-imigrant population growth rates are negative in many countries, including Japan and much of Europe. World population growth peaked at 2.1% in the 1960s. Now, the world population growth rate is 1.2% and falling. Demographers predict that the human population is likely to plateau at 9.5–12 billion in the year 2100 [8].

Demographic transition has profoundly affected the agricultural sector. Over the past 200 years, the number of people who are directly involved in agriculture have dramatically declined. In the 1800s, nearly 80% of the employed population was directly involved in agriculture; by the 1900s only 35% of the employed population were directly involved in agriculture [9]. In the year 2000, only 4 to 5% of the employed population of Australia were directly involved in agriculture [9]. These employment trends are common across other developed countries. Increased agricultural productivity from significantly fewer agricultural workers has only been possible through mechanisation and more recently automation of agricultural systems.

Recent systematic studies of famine and starvation around the world have revealed that, although famines have occurred ever since the development of agriculture, many of the worst famines in recent history must be attributed to political instability, poor distribution systems and wastage of adequate food supplies, rather than the ravages of natural disaster and the consequences of population growth outstripping food production [10]. Therefore, it can be concluded that the adoption of technology, especially through the industrial revolution, green revolution and the advent of new technologies, such as precision agriculture, fostered by ongoing research by agricultural scientists and technology transfer by scientists and agricultural and biological engineers, have avoided Malthus' dire predictions.

4.3 Yield Gaps

Yield potential (Yp) is the yield of a crop cultivar when grown in an environment to which it is adapted, with non-limiting water and nutrient supplies, and with pests, weeds and diseases effectively excluded [11]. Crop growth is determined by such things as solar radiation, temperature, atmospheric CO_2 concentration, sowing date, cultivar maturity and plant density [11]. Management practices also impact crop yield potential. Yield gaps are the difference between practically achieved yield and the yield potential for each crop.

Affholder et al. [12] studied the estimated yield gaps of rainfed crops across systems in Senegal (millet, subsistence-oriented systems), central Brazil (maize, market-oriented systems) and Vietnam (maize, market-oriented systems and upland rice, subsistence-oriented systems). They used a simple crop simulation model (potential yield estimator, PYE) to determine Yp for each crop in each environment

and determined that the yield gaps were 15% for millet in Senegal, 33% for upland rice in Vietnam, 26% for maize in Vietnam and 46% for maize in Brazil.

Bridging these yield gaps will increase agricultural efficiency and output, without requiring more agricultural land. Ongoing study of production systems and application of new technologies will help close these yield gaps. Farm mechanisation and automation will play an important role in bridging yield gaps around the world.

4.4 Agricultural and Food Chain Waste

Gunders [13] stated that getting food from the farm to consumers uses 10% of the total energy budget of the United Sates. Food production uses 50% of U.S. land and 80% of all freshwater consumed in the United States, yet 40% of food produced in the United States goes uneaten, due to wastage or spoilage, costing the equivalent of $165 billion each year. This financial impact of agricultural waste is supported by a study by Pimentel [14].

A study of the Australian fresh mango industry by Ridoutt et al. [15] demonstrates that there was significant distribution and spoilage waste in the food chain and that there was an annual waste of 26.7 Gl of green water (the portion of precipitation that is stored in the soil) and 16.6 Gl of blue water (water withdrawn for irrigation from rivers, lakes and aquifers). Their study revealed that between 2004 and 2010, Australian mango growers have despatched an average of 44,692 t year^{-1} of fresh mango and 15,260 t year^{-1} of processing mango. Waste in the distribution stage was estimated at 14,709 t year^{-1} and avoidable waste of fresh mango by Australian households was estimated at 5642 t year^{-1}; therefore, approximately 46% of the fresh fruit was wasted.

Reducing food waste is a significant challenge. Historically, the introduction of canning, refrigeration, faster transportation and pasteurisation technologies has greatly improved the preservation and distribution of food; however, more is needed. Reducing waste and improving biosecurity are areas of great need. New technologies may hold the key to reducing this waste and further improving the food security of the world's population.

Waste will not be eliminated. Currently, significant quantities of organic waste find their way into land fill where it undergoes anaerobic decomposition and contributes methane to the atmosphere. Methane has a high greenhouse heating potential; therefore, diverting this waste to other purposes would be environmentally beneficial. Fermentation to produce fuel alcohol, chemical extraction to recover valuable pharmaceuticals and pyrolysis to recover biochar (a very stable carbon material that can benefit soil and crop growth), bio-oil (equivalent to crude oil) and syngas (similar to coal gas or natural gas) could provide renewable offsets for fossil fuels [16–19].

4.5 Adoption of Technology

In most cases, human progress has been associated with dominion over the physical world through the harnessing of ideas and energy [20]. Ancient humans mastered natural systems by harnessing human physical effort, including slaves, animals and energy sources such as moving water, wind and fire [20]. During this time, various machines were used to help amplify the effort of nature, men and beasts; however, each machine was an artisan effort and somewhat unique in design and efficacy. Engineering effort was intimately involved in the design and construction of these machines.

Between 1750 and 1850, the first Industrial Revolution dominated the development of engineering in Western Europe. It was significantly influenced by the development of inanimate power sources, such as steam engines, and later internal combustion engines. Machinery for the mass production of goods; and mass rapid transit using railways and steam ships were developed by engineers like Stephenson, Brunel and others. Mass production also introduced the idea of product uniformity and standards in production processes. Agricultural machinery, such as mechanical harvesters and stump-jump ploughs [21], and the use of engines rather than horses as a primary power source were also major legacies of this period.

The second Industrial Revolution, also known as the Technological Revolution, occurred between 1871 and 1914. It is mostly linked to the harnessing and adoption of electricity and electrical technologies into industry and daily human life [22]. This resulted in the development of reliable lighting, electric motors and the installation of extensive telegraph networks, which allowed for faster transfer of ideas. Electronics became prominent through the work of James Clerk Maxwell and Heinrich Hertz in the late nineteenth century. Major advances came with the development of the vacuum tube by Lee De Forest in the early twentieth century and the invention of the transistor, by William Shockley, John Bardeen and Walter Brattain, in the mid-twentieth century. In the late twentieth century, electrical and electronic engineers outnumbered all other forms of engineers in the world.

The Third Industrial Revolution, also known as the Digital Revolution, occurred in the late twentieth century. It was marked by a shift from mechanical and analogue electronic controllers to digital electronics [23]. This revolution was possible because of the development of the transistor and integrated circuits. Gordon Moore, the co-founder of Fairchild Semiconductor and co-founder of Intel, famously projected in 1965, that the number of components per integrated circuit would double every year. He later revised this prediction, in 1975, to a doubling every 2 years (Fig. 4.3).

This digital transformation also introduced robotics into the manufacturing process [24]. According to Glaser [25], about 8000 industrial robots per year were sold in North America between 1994 and 1996; however, between 2004 and 2006, the number of sales had risen to 12,000 units per year. While industrial robots are fast and precise when doing repetitive tasks, they lack ‘adaptability,’ and usually do not

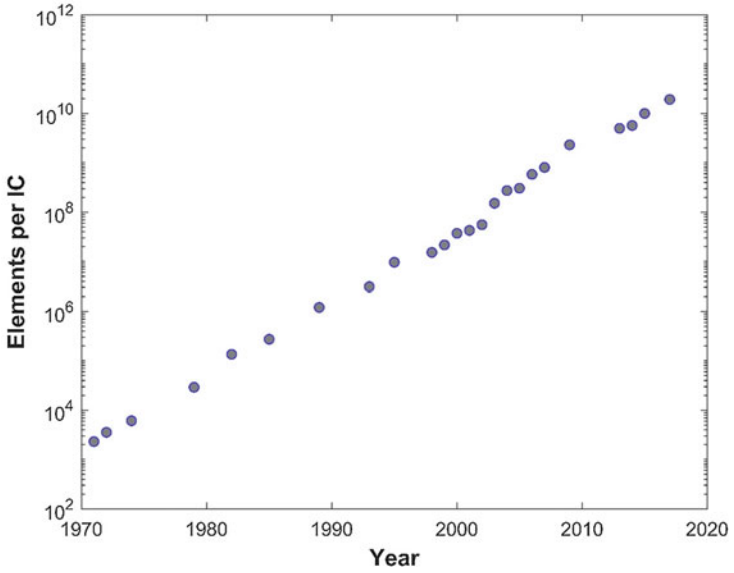

Fig. 4.3 Elements per Integrated Circuit (IC) chip as a function of time (Data sourced from: https://ourworldindata.org/)

co-habit with human workers because of the risk of humans being injured by robot performing their pre-programmed motions.

The Fourth Industrial Revolution, called 'Industrie 4.0' (Industry 4.0), began as a high-tech strategy by the German Government [26]. The objectives of Industry 4.0 were to promote the computerisation of manufacturing. The keys to this strategy are the customisation of products through highly customisable (mass-) production. This becomes possible through the adoption of automation technology, which incorporates self-optimisation, self-configuration, self-diagnosis, machine vision, cognition and artificial intelligence to support workers in their increasingly complex work environments.

Effectively, these phases in the 'Industrial revolution' have progressed from artisan manufacture, through mass production (with consequent needs for uniformity), back to more flexible customisation of products and processes. To a large extent, agriculture has mirrored these same steps. Ancient agriculture relied on care of individual plants and animals. Industrialisation of agriculture promoted the development of uniformity in plant and animal breeding to be compatible with mechanised production systems. As has been shown earlier, agricultural productivity increased significantly as a result of intensification, mechanisation and automation [24]. Recent developments in drone technologies, remote sensing and field robotics, under the banner of precision agriculture, are returning agriculture to the individual care of plants and animals, without the associated loss of productivity.

Arguably, the tractor must be one of the most important developments in agriculture. Fawkes produced a steam tractor that could pull eight ploughs through soil at

4.8 km h^{-1} [27]. Tractors with internal combustion engines first appeared in 1907 [27]. Based on a detailed survey of 115 Australian farms in the 1920s, Perkins [28] demonstrated that one 24 H.P. (18.75 kW) tractor could replace 11.4 horses on an average South Australian farm; thus freeing additional cropping land that was previously used to grow feed for work animals. The transition from using animals to using machinery for farm power has been profound.

Although many other machines predate the adoption of tractors, farm mechanisation has allowed fewer agricultural workers to produce more food for a growing population. Ploughs, rotary hoes, mechanical harvesters, mechanical milking machines and electric sheering machines have all been adopted to improve productivity and, in many cases, improve comfort and lifestyle for farmers [3]. In more recent years, the newer engineering discipline of mechatronics is being added to traditional agricultural engineering disciplines as many of these machines are becoming automated and operating autonomously. Industrial robots are being redesigned to produce commercially viable robotic milking machines [29]. Research is currently under way on developing robotic sheering machines and several agribusinesses have pilot scale or even commercially available field robots, which operate autonomously on farms [24].

Irrigation has also transformed agricultural production. Irrigation has been used in agricultural practices since ancient times. Clearly, irrigation overcomes crop moisture stresses and improves production. For example, Huang et al. [30] demonstrate that irrigation significantly increases crop production, except in the case of rice production, which usually involves flooding the field. Irrigation modernisation and automation projects, which are based on modern information and communication technology, are being deployed in many parts of the world. Design, construction and management of irrigation systems require high level engineering expertise.

Agricultural engineers will continue to invent, develop and adapt technology to solve agricultural and food distribution problems. More traditional areas of study, including hydraulics, electricity, machinery, thermodynamics, animal handling and post-harvest systems will continue to be important to agricultural engineering; however, newer interest such as mechatronics, information technology, remote sensing, autonomous field robotics and applications of diverse forms of electromagnetic, chemical and physical energy to agricultural problems will be added to the agricultural engineer's tool kit.

4.6 Conclusion

Humanity's ability to produce enough food is mostly due to adoption of new methods and technologies by the agricultural industries, as they became available. New information, communication, high-speed processing and precision agriculture technologies are transforming the agricultural industry. Many of these technologies incorporate radiofrequency and microwave radiation into their systems [2]. Some of the technologies that incorporate radiofrequency and microwave radiation include

insect and decay detection and treatment [31], moisture monitoring, radar imaging [4], dielectric heating [32], innovative weed management [33–36], treatment of animal fodder [37] and microwave assisted extraction [38]. Other technologies and applications are at various stages of development. This book will introduce the reader to some of these developments.

References

1. Malthus T. An essay on the principle of population. London: J. Johnson, in St. Paul's Church-Yard; 1798.
2. Brodie G, Jacob M, Farrell P. Microwave and radio-frequency Technologies in Agriculture: an introduction for agriculturalists and engineers. Warsaw/Berlin: De Gruyter Open Ltd.; 2016.
3. Studman C. Agricultural and horticultural engineering. Wellington: Butterworth's Agricultural Books; 1990.
4. Brodie GI. Ingenious devices and systems: engineering for landscape managers. Saarbruecken: VDM Verlag; 2009.
5. Adas M, Chan MA. Machines as the measure of men : science, technology, and ideologies of Western dominance. Ithaca, NY: Cornell University Press; 2015.
6. Tegmark M. Our mathematical universe: my quest for the ultimate nature of reality. New York: Knopf; 2015.
7. Nakamura T. Solow meets stone–Geary: technological progress and the demographic transition. Metroeconomica. 2018;69(4):768–90.
8. United Nations. World Population Prospects 2019. 12th December, 2020, 2021. 2019. https://population.un.org/wpp/Graphs/Probabilistic/POP/TOT/900
9. Australian Bureau of Statistics. Year book Australia. Canberra: Australian Bureau of Statistics; 2000.
10. Scrimshaw NS. The phenomenon of famine. Annu Rev Nutr. 1987;7(1):1–22.
11. Edreiraa JIR, Mourtzinis S, Conley SP, Roth AC, Ciampitti IA, Licht MA, Kandel H, Kyveryga PM, Lindsey LE, Mueller DS, Naeve SL, Nafziger E, Specht JE, Stanley J, Staton MJ, Grassini P. Assessing causes of yield gaps in agricultural areas with diversity in climate and soils. Agric For Meteorol. 2017;247:170–80.
12. Affholder F, Poeydebat C, Corbeels M, Scopel E, Tittonell P. The yield gap of major food crops in family agriculture in the tropics: assessment and analysis through field surveys and modelling. Field Crop Res. 2013;143:106–18.
13. Gunders D. Wasted: how America is losing up to 40 percent of its food from farm to fork to landfill. Natural Resources Defense Council; 2012.
14. Pimentel D. Environmental and social implications of waste in U.S. agriculture and food sectors. J Agric Ethics. 1990;3(1):5–20.
15. Ridoutt BG, Juliano P, Sanguansri P, Sellahewa J. The water footprint of food waste: case study of fresh mango in Australia. J Clean Prod. 2010;18(16–17):1714–21.
16. Aimin J, Yan C, Hongya L, Zuguo Q. A review on pyrolysis technology and characters of products from sewage sludge. Appl Mech Mater. 2013;295-298:1419–24.
17. Antunes E, Jacob MV, Brodie G, Schneider PA. Microwave pyrolysis of sewage biosolids: dielectric properties, microwave susceptor role and its impact on biochar properties. J Anal Appl Pyrolysis. 2018;129:93–100.
18. Bhatta Kaudal B, Aponte C, Brodie G. Biochar from biosolids microwaved-pyrolysis: characteristics and potential for use as growing media amendment. J Anal Appl Pyrolysis. 2018;130:181–9.
19. Brodie G, Duan A, Doronila A, Antunes E, Jacob M. Bio-oil from microwave-assisted pyrolysis of sewage biosolid. AMPERE Newsletter. 2018;96:1–7.

20. Ubbelohde AR. Man and energy. Harmondsworth, Middlesex: Penguin Books Ltd.; 1963.
21. Neumann B. The Smith brothers and the stump jump plough. 2nd ed., rev. ed. Maitland: National Trust of South Australia, Central Yorke Peninsula Branch; 1986.
22. Smith RJ. Circuits, devices and systems. 3rd ed. New York: Wiley International; 1976.
23. Parker C. Understanding computers: today and tomorrow. Fort Worth: The Dryden Press; 2000.
24. Bechar A, Vigneault C. Agricultural robots for field operations: concepts and components. Biosyst Eng. 2016;149:94–111.
25. Glaser A. Industrial robotics - how to implement the right system for your plant; 2009.
26. Bundesministerium für Bildung und Forschung. Industrie 4.0: Innovationen im Zeitalter der Digitalisierung. Bundesministerium fur Bilung und Forschung; 2020
27. Goering CE. Celebrating a century of tractor development. Resource. 2008;15(7):5–6.
28. Perkins AJ. A critical glance at some aspects of tractor farming in Australia. J Dep Agric S Aust. 1929;33:224–36.
29. Osei-Amponsah R, Dunshea FR, Leury BJ, Cheng L, Cullen B, Joy A, Abhijith A, Zhang MH, Chauhan SS. Heat stress impacts on lactating cows grazing Australian summer pastures on an automatic robotic dairy. Animals. 2020;10(869):1–12.
30. Huang Q, Rozelle S, Lohmar B, Huang J, Wang J. Irrigation, agricultural performance and poverty reduction in China. Food Policy. 2006;31(1):30–52.
31. Brodie G, Thanigasalam DB, Farrell P, Kealy A, French JRJ, Ahmed (Shiday), B. An in-situ assessment of Wood-in-Service using microwave technologies, with a focus on assessing hardwood power poles. Insects. 2020c;11(568):1–15.
32. Metaxas AC, Meredith RJ. Industrial microwave heating. London: Peter Peregrinus; 1983.
33. Brodie G, Khan MJ, Gupta D, Foletta S, Bootes N. Understanding the energy requirements for microwave weed and soil treatment. Global J Agric Innov Res Dev. 2020a;6:11–24.
34. Brodie G, Pchelnikov Y, Torgovnikov G. Development of microwave slow-wave comb applicators for soil treatment at frequencies 2.45 and 0.922 GHz (theory, design, and experimental study). Agriculture. 2020b;10(12):10.00604.
35. Wayland J, Merkle M, Davis F, Menges RM, Robinson R. Control of weeds with UHF electromagnetic fields. Unkrautbekämpfung mit elektromagnetischen UHF-Feldern. 1975;15 (1):1–5.
36. Wayland JR, Davis FS, Merkle MG. Toxicity of an UHF device to plant seeds in soil. Weed Sci. 1973;21(3):161.
37. Brodie G, Bootes N, Dunshea F, Leury B. Microwave processing of animal feed: a brief review. Trans ASABE. 2019;62(3):705–17.
38. Morales S, Canosa P, Rodriguez I, Rubi E, Cela R. Microwave assisted extraction followed by gas chromatography with tandem mass spectrometry for the determination of triclosan and two related chlorophenols in sludge and sediments. J Chromatogr. 2005;1082(2):128–35.

Part II
Microwave Applications

Chapter 5
Improvement and Effective Growth of Plants' Environmental Stress Tolerance on Exposure to Microwave Electromagnetic Wave Effects

Satoshi Horikoshi, Nobuhiro Suzuki, and Nick Serpone

Abstract The usage of microwaves in cooking, in radar, and in communications is well known to most people who cook, and who use mobile phones. We have discovered that microwave energy can be used in agriculture, albeit the outcome does not only appear to be a thermal energy source but also a medium to carry information. Consequently, this chapter introduces the reader to the influence that microwaves have in plant growth. A peculiar feature of the microwave stimulus is that it suffices to irradiate the plant seeds, or else the first plant leaf for a very short time, after which plant growth follows its natural course. In addition to the discussion of the enhancement of plant growth by microwaves, pest repellents, and heat resistance, among others, the chapter also describes a novel method to irradiate plants with the use of drones to deliver the microwave radiation.

Keywords Microwaves · Electromagnetic wave effects · Growth enhancement · Environmental stress tolerance

5.1 Brief Review of Research on Plants with Microwave Irradiation

Most reports that examined the effects of irradiating plants with microwaves using WiFi and mobile phones have noted a negative growth of plants when subjected to the microwaves emitted from these sources. In this regard, Soran and coworkers [1]

S. Horikoshi (✉) · N. Suzuki
Department of Materials and Life Sciences, Faculty of Science and Technology, Sophia University, Chiyodaku, Tokyo, Japan
e-mail: horikosi@sophia.ac.jp; n-suzuki-cs6@sophia.ac.jp

N. Serpone
PhotoGreen Laboratory, Dipartimento di Chimica, Universita di Pavia, Pavia, Italy
e-mail: nick.serpone@unipv.it

S. Horikoshi et al. (eds.), *Agritech: Innovative Agriculture Using Microwaves and Plasmas*, https://doi.org/10.1007/978-981-16-3891-6_5

studied the influence of microwave radiation at bands corresponding to a wireless router (WLAN) and mobile devices (GSM) on leaf anatomy, on the essential oil content, and on the volatile emissions from such plants as *Petroselinum crispum* (Parsley), *Apium graveolens* (Celery), and *Anethum graveolens* (Dill). It appears that microwave irradiation resulted in thinner cell walls, and smaller chloroplasts and mitochondria as well as enhanced emissions of volatile compounds, particularly the monoterpenes and green leaf volatiles. Seemingly, the effects were stronger for the WLAN-frequency microwaves. Additionally, they found a direct relationship between microwave-induced structural and chemical modifications of the three plant species investigated, and concluded that their collective data demonstrated that pollution from generated microwaves may constitute a stress to the plants. On the other hand, only a few studies [1–3] have reported positive effects of microwaves with regard (i) to the enhancement of essential oil content by the GSM-frequency microwaves, albeit the effect of WLAN-frequency microwaves was inhibitory [1], and (ii) to the continuous microwave irradiation during the entire period from germination to the growth of plants such as, for example, the enhanced growth of roots in spinach and green beans [2, 3].

In a related study, Verma et al. [4] exposed the tomato fruit with a double dose of 9.3-GHz microwave radiation that yielded high lycopene content, total protein content, together with phenolic and flavonoid content in unripe, ripe, and overripe stages of two tomato varieties (NS-585 and NS-2535). Moreover, the activity of cell-wall degrading enzymes, such as polygalacturonase, pectinmethylesterase, and β-galactosidase, decreased in the double-dosed microwave irradiated fruit of both varieties. As well, postharvest exposure to microwaves could be applied to increase the shelf-life of the tomato fruit [4].

A recent study by Miler and Kulus [5] examined the ambiguous impact of microwaves on the DNA of plant cells, as they recognized that the usage of this electromagnetic radiation (e.g., 2.45 GHz, 800 W cm^{-2}) as a source of variation in mutation breeding could be very advantageous. Accordingly, their goal was to examine the influence of microwave radiation on the in vitro regeneration and acclimatization efficiencies as well as on the genetic and phenotypical variation of chrysanthemum *Alchemist*. Thus, they subjected leaf explants, with or without callus, to a microwave treatment for various periods and in different environments. It appears that microwave irradiation affected negatively shoot formation if it were applied for long periods, although it did not affect the rooting and acclimatization steps that were fully successful. Chrysanthemums produced from microwave-treated explants had longer shoots with inflorescences of greater diameter and altered shapes [5]. They further noted that the microwave treatment affected the generative phase by prolonging the bud coloration period. Approximately 22% of the plants regenerated from the microwave-treated explants, which demonstrated that band profiles were different from the reference control. The authors concluded that microwaves are an efficient and easy-to-access tool in mutation breeding of chrysanthemum *Alchemist* [5].

Several studies have considered that microwave effects are mainly due to a temperature increase on microwaving potting soils and plants. Nonetheless, there

is also a report by Saitou et al. [2] and Iguchi et al. [3] that considered the temperature rise to be extremely small, and that the effect was a peculiarity of the microwaves. In other words, any effects by the microwaves were nonthermal in nature. However, neither of these studies noted that there was no evidence for a nonthermal microwave effect.

5.2 The Obvious Question Is Then: Can Microwaves Affect Plant Growth?

First of all, it is relevant to recall that the term *Microwave* is a general term that describes electromagnetic waves at wavelengths between 1 m and 1 mm – i.e., electromagnetic waves with frequencies from 300 MHz to 300 GHz. These microwaves are used, for example, in communications such as mobile phones, satellites, and television broadcasting, and for heating and cooking as done in microwave ovens [6]. Our recent research has focused toward the application of the microwaves' electromagnetic wave energy to chemical reactions, to the synthesis and processing of (nano)materials, and to biological fields that involve physics and chemistry. In particular, to maximize the advantages of the microwaves' electromagnetic wave energy, we carried out several investigations from which we discovered and/or proposed applications of microwave-specific phenomena that could not be imitated by conventional heat sources, nor by any other type of energy sources.

The series of researches in the use of microwave electromagnetic wave effects led us to consider a new avenue of investigation as to how plants might be affected and how they might perform if they were exposed to weak microwaves at output microwave power of several μ-Watts. The objective here was that if plants felt microwaves as a stress, they may not relax that stress as humans normally would. Accordingly, the question relates as to how plants change to relieve that stress. Will the plants die/wither if irradiated with microwaves or will they show no change? Our first approach to answer this query then was to use the *Arabidopsis thaliana* (Columbia-0) plant that we had available 14 days after sowing. Using our 2.45-GHz microwave synthesis device, we proceeded to irradiate this plant with these microwaves initially for 1 h using the lowest possible output power so as to minimize/suppress any temperature rise that might otherwise affect the plant as thought by others [7]. For comparison, a control experiment was also carried out on the *Arabidopsis thaliana* plant that was sown and allowed to grow for a 14-day period but was not exposed to microwave radiation. The growth of the two plants was then observed in a growth chamber (artificial meteorological device) in which we could control the temperature, the humidity, the illuminance, and adjust the light/dark cycles to optimal conditions for growth. While no changes were expected, it was not what we observed. In fact, the *Arabidopsis thaliana* plant that had been microwave-irradiated revealed an enhanced growth rather than the expected *no change*. Nonetheless, we continued to observe the extent to which the difference

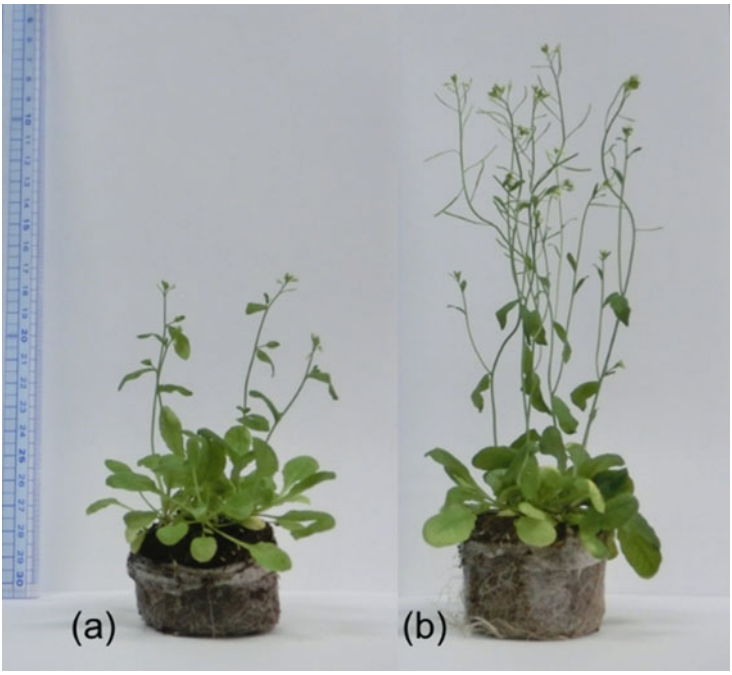

Fig. 5.1 Growth comparison of *Arabidopsis thaliana* after 1-h irradiation of microwave (photograph taken 38 days after sowing) [7]: (**a**) nonirradiated with microwaves (control), (**b**) irradiated with microwaves

in growth might be between the two plants. The results displayed in Fig. 5.1 show a photograph of the two *Arabidopsis thaliana* plants 38 days after sowing [7]. Despite being grown under the same environmental conditions, irradiating one of the plants with microwaves for just 1 h and subsequently allowed the plant growth to continue its normal course showed that the microwaves promoted its growth by nearly a factor of two (Fig. 5.1b) compared to the control *Arabidopsis thaliana* plant that had not been exposed to microwave radiation (Fig. 5.1a). The average inflorescence length of the microwaves was ca. 16 cm, while for the control plant it was on average about 8 cm.

We also discovered that irradiation with microwaves promoted the transition of *Arabidopsis thaliana* to the reproductive growth phase. In other words, microwaves had a positive effect on plant growth and should thus be considered as a kind of ***microwave-induced stimulation***. Subsequent to these early experimental observations, and as a result of conducting additional screening experiments under various conditions of microwave power, irradiation timing, and irradiation times, among others, we found recently that a 1-s irradiation period is in fact sufficient to influence plant growth. Thus, contrary to our initial approach of irradiating for a 1-h period, it appears that the plants need not be exposed to microwave radiation for such a long period.

The significance of social and academic contributions of our research efforts is not inconsequential. As a social significance, it is important to note that the change in the growth rate by irradiating for just 1-s period with weak microwaves is indeed remarkable. That is, if seedling companies were to irradiate the seeds with microwaves in advance, even for just a very short time, the farmers need not then irradiate plant constituents with microwaves to enhance plant growth. On the other hand, the academic significance is that irradiation with microwaves for only 1 s, and then only once, can have a lasting and significant effect on plant growth in the future. As well, a comprehensive analysis of the plant genes [8] revealed that *Arabidopsis thaliana* irradiated with microwaves at μ-Watts output power suffered no genetic modification. In this regard, it is worth noting that the quantum energy of microwaves is 10^{-5} eV, so that chemical bonds cannot be broken by the microwaves.

Examination and use of electromagnetic wave effects have been a long-standing goal of our research efforts. Two decades ago we discovered that when a photocatalyst, whose extensive use has been in environmental remediation, is irradiated with microwaves together with UV-light, its photocatalytic activity was enhanced several times [9]. The photocatalyst referred to is titanium dioxide (TiO_2), an *n*-type semiconductor that whenever the nanoparticles are irradiated with less than 387 nm UV-light (band gap energy: 3.2 eV [10]) in aqueous media leads to the oxidative decomposition of water (H_2O) and generates reactive oxygen active species such as the •OH radicals, which can oxidatively decompose organic pollutants in aqueous media using only photon energy. In general, it is possible to decompose not only pollutants in aqueous ecosystems but also atmospheric pollutants. In spite of the thousands of academic studies and patents, however, water purification by the photocatalytic method has hardly been put into practical use because this treatment method is slow compared to other chemical purification methods that use, for example, ozone or hypochlorous acid. In other words, our efforts succeeded in enhancing the catalytic activity of the photocatalyst on exposure to both microwaves and UV/Visible light energy. The significance of that study [9] was that the photocatalytic activity was not a response to heat. Stated differently, the reaction efficiency of photocatalysts cannot be enhanced without utilizing the electromagnetic wave effects of the microwaves.

As an example, the degradation of the rhodamine-B (RhB) dye in aqueous media with dispersed TiO_2 semiconductor nanoparticles under both UV and microwave irradiation [11, 12] is reported in Fig. 5.2 [13]. Some decolorization was observed in the decomposition of RhB by TiO_2 irradiated only with UV light (TiO_2/UV). On the other hand, the photodegradation of RhB is clearly accelerated on exposing the TiO_2 simultaneously to both UV light and microwave radiation (TiO_2/UV/MW). Heating the RhB aqueous solution in which the TiO_2 dispersion was heated using a conventional heater while also irradiating with UV-light showed no enhancement of the activity of the photocatalyst (TiO_2/UV/CH) [11], even though the temperature of the water matched the heating rate from a solution exposed to microwave radiation. Moreover, no accelerated reaction was observed when the temperature was greater than the temperature reached on microwave heating. Accordingly, it appears that the role(s) of the microwaves was to streamline electron transfer inside the photocatalyst

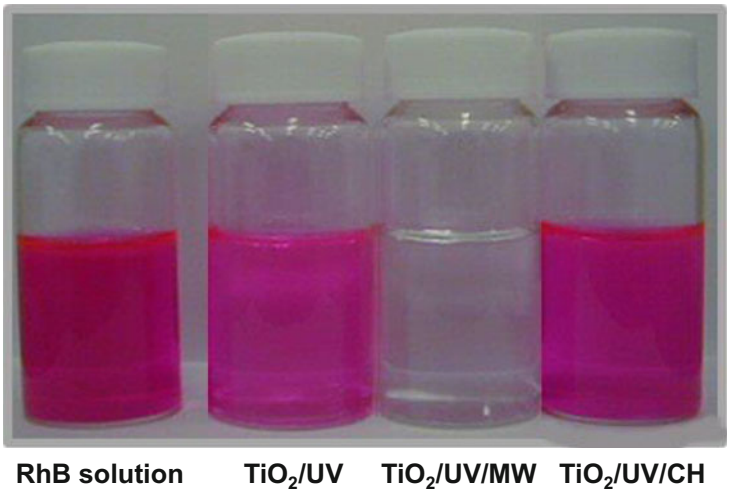

Fig. 5.2 Visual comparison of color fading in the degradation of RhB solutions (0.05 mM) subsequent to being subjected to various degradation methods for 150 min. From left to right: initial RhB solution; RhB subjected to photo-assisted TiO_2 degradation (TiO_2/UV); RhB subjected to integrated microwave−/ photo-assisted TiO_2 degradation (TiO_2/UV/MW); RhB subjected to photo- and thermal-assisted TiO_2 degradation (TiO_2/UV/CH). Reproduced from [13]. Copyright 2009 by Elsevier B.V

TiO_2 particles and suppress the recombination of the photogenerated electrons with the photogenerated holes [14]. Seemingly, microwave compatibility is good for reactions that require light energy, because they both consist of electromagnetic waves. The series of photocatalytic studies led us to envisage the existence of phenomena other than thermal effects from the microwaves as electromagnetic waves. In addition, we imagine next that microwaves are likely to affect what is originally driven by the electromagnetic waves from UV-Visible light photon energy.

We should not forget that microwaves are commonly used daily as a heat source (microwave ovens). However, we may hypothesize intuitively as to what the actual role of microwaves is in plant growth – thus the question: how does microwave electromagnetic energy directly affect plants?

5.3 Are Microwaves Used as Electromagnetic Energy?

Is the role of microwaves on plants simply as an electromagnetic wave source, or is it simply a heat source? We have recently been conducting multifaceted research on this question. For example, while the *Arabidopsis thaliana* on the 14th day after sowing was irradiated with microwaves for 1 h, we patiently monitored any changes in temperature using a plurality of optical fiber thermometers, and not least by

thermography. We noted that the maximum temperature change under microwave irradiation for 1 h was about 1.4 °C, from which we infer there was no thermal effect by the microwave irradiation. The expressions of heat shock protein (HSP), which is a heat response gene of *Arabidopsis thaliana*, and its regulator, HSF, were analyzed after microwave irradiation. There were no changes in these even when irradiated with microwaves. That is, under the conditions of the experiment, the temperature of the *Arabidopsis thaliana* plant increased neither macroscopically nor microscopically even when they were exposed to microwave radiation.

5.4 What Then Is the Role of Microwaves?

Since the growth of inflorescence stems of plants was enhanced by the microwaves, we proceeded to analyze the expression of genes and proteins involved in plant flowering induction and formation of reproductive organs. Results showed that the expression of the FT (FLOWERING LOCUS T) gene, which controls flowering induction by microwave stimulation, increased at 18 days after sowing. Similarly, we found that the expression of the FT protein also increased. In addition, since the expressions of the MYB30 gene and the FT gene (which are involved in flowering induction) increased, the stimulation of plants by microwaves promoted the flowering induction.

Next, the autofluorescence of chlorophyll was examined immediately after microwave irradiation on *Arabidopsis thaliana* 14 days after sowing (Fig. 5.3) in order to investigate the effect of microwaves on photosynthesis. Chlorophyll fluorescence is

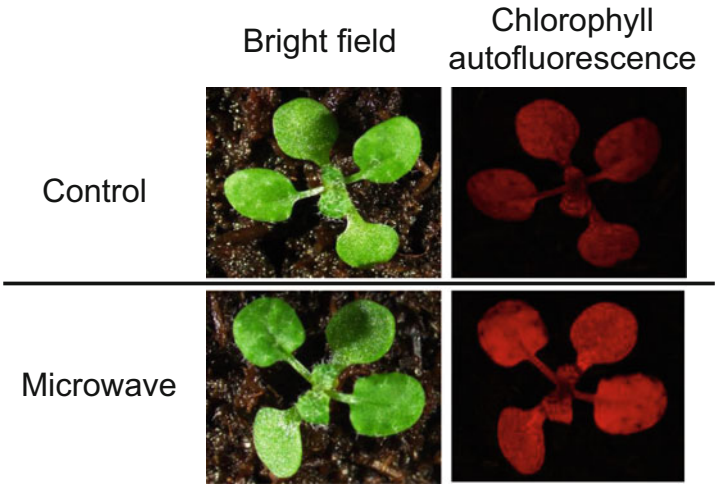

Fig. 5.3 Observation of chlorophyll autofluorescence from the *Arabidopsis thaliana* plant using a fluorescence microscope: Upper panel: control (nonirradiated microwave plant) and Lower panel: Microwave (plant irradiated with microwaves)

light that is re-emitted by the chlorophyll molecules during their decay from an excited state to their ground state. It is used as an indicator of photosynthetic energy conversion in higher plants, algae, and bacteria. In our case, microwave-treated plants revealed greater chlorophyll autofluorescence intensity compared to the nonmicrowave treated plant control. Chlorophyll autofluorescence is also known as a way for chlorophyll to dissipate excess energy not used for photosynthesis, but the plant appears to dissipate light energy even more when it is irradiated with microwaves. Even with its condensing antennae, chlorophyll is unable to capture microwave energy as the wavelength of the 2.45-GHz microwaves used is 12.24 cm, and thus chlorophyll cannot initiate its normal function of storing and using light energy to convert carbon dioxide (absorbed from the air) and water into glucose. In fact, however, we do find that microwaves do have some effect on the photosynthetic process.

5.5 Can Microwaves Improve Environmental Stress Tolerance?

5.5.1 General Situation of Plant Growth when Exposed to Environmental Stresses

It is well-known that the actual crop yields are within about 65 to 87% of the maximum value, assuming that the crop yields have reached their maximal value when the plants grow under ideal environmental conditions. However, the crop yields are reduced when plants are subjected to environmental stresses. Within this context, Table 5.1 shows the loss yields resulting from environmental biotic stresses

Table 5.1 Worldwide highest harvest yields, average harvest yields, and average loss yields of crops caused by environmental stresses on eight types of grains. Average loss yields from environmental stresses increased with both biological loss (disease, insect damage, and weeds) and nonbiological loss (drought, salt damage, flooding, and low temperatures) [15]

Grain	Highest harvest yields (kg/ha)	Average harvest yields (kg/ha)	Average loss yields from environmental stresses (kg/ha)	
			Biological losses	Nonbiological losses
Corn	19,300	4600	1952	12,700
Wheat	14,500	1880	726	11,900
Soybean	7390	1610	666	5120
Sorghum	20,100	2830	1051	16,200
Oats	10,600	1720	924	7960
Barley	11,400	2050	765	8590
Potato	94,100	28,300	17,775	50,900
Sugar beet	121,000	42,600	17,100	61,300

(biological stresses such as disease, insect damage, weeds) and abiotic stresses (nonbiological stresses such as drought, salt damage, flooding, and low temperatures) for eight types of grains [15]. The results show that environmental stresses do play a noninsignificant role that reduces crop yields. In particular, the yield loss due to abiotic (nonbiological) factors exceeds 50%. Accordingly, new technologies are required for increasing plant production under environmental stresses. Microwaves are thought and are expected to elicit results that are more resistant to these environmental stresses.

5.5.2 *Heat Stress*

Global temperature increases year by year as a result of global warming, and thus both the natural environment and the ecosystems are likely to undergo some associated changes. Because of this warming effect, some crops are being replaced by varieties that are resistant to temperature increases. Accordingly, can microwaves help to overcome this challenge? As a consequence, the following experiment was conducted in response to this challenge. To do so, Arabidopsis plants with and without microwave irradiation were subjected to high temperature (44 °C for 7 days) and scored in survival rate. We found that irradiation with microwaves improved the survival rate by $\geq$30%, even in a high temperature environment (see Fig. 5.4).

Next, it is relevant to describe possible molecular biological changes resulting from the application of microwaves through an analysis using a DNA microarray of the *Arabidopsis thaliana* plant subjected to microwave irradiation for 1 h at 14-day period after sowing. We confirmed an increased expression of the abscisic acid signaling genes Nced3, Abi2, and Abi3 that play an important role in the regulation of heat tolerance, and of the bZip28 gene that is involved in response of plants to various stress conditions including heat. Accordingly, we inferred that the heat response mechanism of plants was not activated by the microwave treatment,

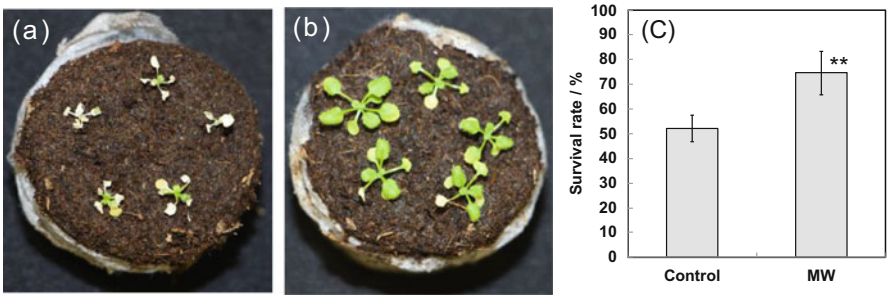

Fig. 5.4 Photographs that confirm the survival rate of *Arabidopsis thaliana* (**a**) unirradiated and (**b**) microwave irradiated in a high temperature environment (44 °C, for 7 days); (**c**) comparison of the survival rate of *Arabidopsis thaliana* after 7 days ($n = 20$; **: Significant at 1% level of t-test; bars show standard error) [8]

Fig. 5.5 Photograph of strawberries after a daytime temperature exceeding 30 °C. (**a**) Fruits from nonirradiated microwave strains, (**b**) fruits from microwave-irradiated strains [8]

although the mechanism of protecting plant cells from various stresses, including heat, was indeed activated.

As a further experiment, we examined the heat tolerance using strawberries as the commercial plant. Strawberry plants in the reproductive growth period were cultivated outdoors after irradiating them with microwaves for a 1-h period. Strawberries are known to shift from reproductive growth to vegetative growth at temperatures above 25 °C. Therefore, strawberries are not suitable for fruiting in a high temperature environment. Consequently, it was relevant and instructive to examine the presence or absence of any improvement in plant growth that might have been caused by microwaves. We found that the duration of fruiting was significantly longer, and the size of fruits was larger for the Strawberries that had been subjected to microwave irradiation than for the nonirradiated Strawberries. In addition, 51 days after planting, the temperature continued to exceed 30 °C; this caused the control strawberries to preclude harvesting the fruits after this period. By contrast, however, the strawberries that had been irradiated with microwaves continued fruiting after this period and were of excellent quality (see, for example, Fig. 5.5).

Currently, only 12% of the land worldwide is cultivated, as other lands are unsuitable for cultivation owing to present temperature conditions. In addition, global warming may well reduce arable land in the future. Even in such land and harsher conditions, however, we predict that agriculture could benefit if seeds and seedlings were preirradiated with microwaves.

5.5.3 Stresses from Pests

Agricultural chemical products have brought about prosperity to humanity because of their many effects on plant growth and increased crop yields to satisfy the never ending demands to feed the ever increasing world population. However, agricultural chemicals that previously consisted of natural products (such as manure or compost) now consist of chemically synthesized pesticides, especially since World War II, and over the years their effects on agriculture have improved significantly, albeit some beneficial and others deleterious. In this context, the negative societal image of

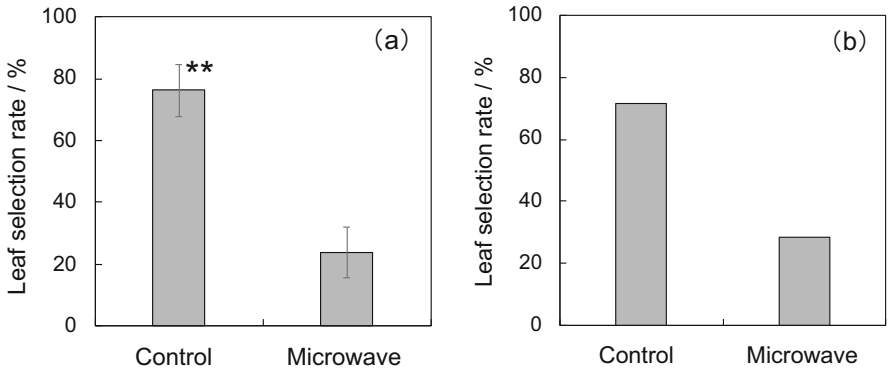

Fig. 5.6 Leaf selection rate by cabbage white butterfly larva ($n = 21$; **: Significant at 1% level of t-test; vertical bars refer to standard error); (**a**) *Arabidopsis thaliana,* (**b**) Arugula [8]

pesticides on commercial plants has grown, so much so that vegetables are now being marketed as being "pesticide-free" and are considered as higher value-added products (note the label "biological" and more costly products in your supermarkets). Accordingly, it was relevant for us to begin examining the pest repellent effect of microwave-irradiated plants following our many years of research on Microwave-assisted Chemistry and microwave effects on materials syntheses and processing. The principal motivation for starting this research is that plants grown by irradiating with microwaves might show an increase in external stress resistance. Pests also cause external stresses, which may thus increase the amount of various chemical repellent substances that plants produce. Indeed, when plants are injured by insects, the plants have a natural tendency to protect themselves (i) by releasing the insect damage/injury-resistant plant hormone known as Jasmonic Acid, (ii) by inducing the herbivore-induced plant volatile (HIPV), and (iii) by producing well-known reactive oxygen species [16]. At this juncture, our recent studies are focused on investigating whether irradiation with microwaves for a given time period of plant growth would affect these three defense responses. Accordingly, we conducted leaf preference tests using *Arabidopsis thaliana* and Arugula as our model plants and cabbage white butterfly larvae (*Pieris rapae*) as our model feeding pests.

In our experiments, the cabbage white butterfly larva was placed at the center between the *Arabidopsis thaliana* that had been irradiated with microwaves for 1 h and the nonirradiated *Arabidopsis thaliana*. Then, we assessed which plant the larva selects between these two cases (Fig. 5.6a). Figure 5.6b shows the results of a preference test using Arugula grown for 1 month after sowing the seeds that has been irradiated with microwaves. Results showed that microwave irradiation reduced the feeding damage caused by the cabbage white larvae. Similar results were observed from the data of the pest repellent rate of strawberries and Komatsuna (Japanese mustard spinach) in actual alley cultivation. An egg-laying preference test using the cabbage white butterfly was also conducted, results from which the proportion of the cabbage white butterfly, selected as the spawning plant, was

reduced by 1/3 or less by irradiating with microwaves. Furthermore, irradiation with microwaves significantly increased the synthesis of the amount of pest repellent produced. A sensory evaluation of vegetable foods subjected to microwaves and without exposure to microwave radiation revealed no difference in the five human sensorial responses, including taste. Since the repellent effect can be improved by electrical power used to generate microwave radiation, it would thus be possible to secure a safe and plentiful crop production without worrying about residual pesticides.

5.6 Microwave Irradiation Methodology

The advantages of our technique are that irradiation is achieved using only weak microwave power for a short time period at the beginning of plant growth, or else at some stage on the seeds, such that no further treatment would be required. Therefore, it is not necessary to arrange for microwave irradiation for the whole life of plant growth. In addition, it is not necessary to install a microwave device in an open cultivation field, in a greenhouse cultivation field, or in a plant factory, or in similar venues. Two types of microwave irradiation methods can be considered at the production site, one of which is a method of fixing the microwave irradiation port and performing the irradiation treatment while moving the plant. For example, a production process could be constructed by placing the buds (or seeds) in their early growth stage on a conveyor belt and irradiating them with a microwave irradiation device. Our second method would involve irradiating a fixed plant while moving the microwave irradiation port. In the latter case, the production process could be constructed by continuously applying microwave stimulation by irradiating with microwaves using a moving object such as a drone (Fig. 5.7).

Currently, attempts are being actively made to convert agriculture to IoT, a platform where embedded devices are connected to the internet, so they can collect and exchange data with each other. In addition, this platform enables the devices to interact, collaborate, and learn from each other's experiences as humans do daily. To the extent that this method is also entirely powered by electricity, it would be easy to incorporate it into the IoT agriculture. As well, to the extent that various phenomena can be controlled and expressed by changing the microwave irradiation pattern, it is possible to carry out detailed production according to the number of plants and the order for each habitat.

5.7 Concluding Remarks

There is a saying in Japan that states "Stepping on wheat seeds makes the sprouts grow stronger". This saying likens the phenomenon of deepening the roots and thickening the stems by stepping on the sprout of wheat. It is also a saying that can be applied to the difficulties and hardships faced by the young generation that should be

Fig. 5.7 Photograph illustrating a drone connected to a compact GaN semiconductor microwave generator with an antenna used to continuously apply a microwave irradiation pattern to the plants [8]

taken as an investment toward their future growth. The microwaves stress technology is similar to this. It is a technology that induces and activates the original power of plants by microwave irradiating their seeds or sprouts. In other words, the significance of microwave irradiation is that microwaves act as a trigger, that is, as a kind of catalyst that raises the potential of plants and their growth.

References

1. Soran M-L, Stan M, Niinemets Ü, Copolovici L. Influence of microwave frequency electromagnetic radiation on terpene emission and content in aromatic plants. J Plant Phys. 2014;171:1436–43.
2. Saitou H, Miyasaka J, Ohdoi K, Nakashima H, Hashimoto K, Shinohara N, Mitani T. Effects of 2.45GHz microwave on the plant growth rate - Promotion of germination, root elongation, and synthesis of the chlorophyll. Tech Rep IEICE (Japanese). 2007;2:7–14.
3. Iguchi H, Nakashima H, Miyasaka J, Ohdoi K, Ogawa Y, Shimizu H, Shinohara N, Mitani T. Effects of 2.45GHz microwave on the plant growth rate - Measurement of spinach seed growth by image processing. Tech Rep IEICE (Japanese). 2011;3:11–4.
4. Verma S, Sharma V, Kumari N. Microwave pretreatment of tomato seeds and fruit to enhance plant photosynthesis, nutritive quality and shelf life of fruit. Postharvest Biol Technol. 2020;159:111015.
5. Miler N, Kulus D. Microwave treatment can induce chrysanthemum phenotypic and genetic changes. Sci Hortic. 2018;227:223–33.
6. https://en.wikipedia.org/wiki/Microwave. Accessed January 2021.
7. Horikoshi S, Hasegawa Y, Suzuki N.. Growth stimulation system of plants using microwave irradiation and elucidation of its molecular mechanisms, Proceedings of IMPI's 50th annual

microwave power symposium, The Caribe Royale All-Suite Hotel & Convention Center, Orlando, Florida, USA, June 21–23, 2016.
8. Horikoshi S, et al., to be published (2021).
9. Horikoshi S, Hidaka H. Enhancement for retardation of dye rhodamine B by cooperation of microwave with UV-illumination in TiO_2 aqueous dispersion., Proceedings 5-st International Conference on Photocatalytic Purification and Treatment of water and Air, June 25–30, 2000, London, ON, Canada.
10. Strehlow WH, Cook EL. Compilation of energy band gaps in elemental and binary compound semiconductors and insulators. J Phys Chem Ref Data. 1973;2:163–93.
11. Horikoshi S, Hidaka H, Serpone N. Environmental remediation by an integrated microwave/UV-illumination method. 1. Microwave-assisted degradation of rhodamine-B dye in aqueous TiO dispersions. Environ Sci Technol. 2002;36:1357–66.
12. Horikoshi S, Hidaka H, Serpone N. Environmental remediation by an integrated microwave/UV illumination method. V. Thermal and nonthermal effects of microwave radiation on the photocatalyst and on the photodegradation of rhodamine-B under UV/Vis radiation. Environ Sci Technol. 2003;37:5813–22.
13. Horikoshi S, Serpone N. Photochemistry with microwaves Catalysts and environmental applications. J Photochem Photobiol C: Photochem Rev. 2009;10:96–110.
14. Horikoshi S, Tsutsumi H, Matsuzaki H, Furube A, Emeline AV, Serpone N. *In situ* picosecond transient diffuse reflectance spectroscopy of opaque TiO systems under microwave irradiation and influence of oxygen vacancies on the UV-driven/microwave-assisted TiO photocatalysis. J Mater Chem C. 2015;3:5958–69.
15. Shimamoto K, Shinozaki K, Shirasu K, Shinozaki W. Response to environmental and biological stress (in Japanese). Tokyo: Kyoritsu Shuppan Co., Ltd.; 2007.
16. Boyes DC, Zayed AM, Ascenzi R, McCaskill AJ, Hoffman NE, Davis KR, Görlach J. Growth stage-based phenotypic analysis of Arabidopsis: a model for high throughput functional genomics in plants. Plant Cell. 2001;13:1499–510.

Chapter 6
Food Processing

Donglei Luan

Abstract Heating is a very common operation in food processing. In conventional heating, the force of heat transfer is temperature gradient. Due to the low thermal conductivity of food materials, the efficiency of heating operation is limited. Microwave could provide volumetric heating for food materials and obviously improve the heating efficiency. Microwave heating has been widely applied in food drying, thawing, precooking, and thermal processing. With the assistance of microwave heating, the processing time could be significantly reduced, which would improve product quality and save energy. Among these processing techniques, microwave thermal processing (sterilization and pasteurization) is the most promising technology. After approval by the Food and Drug Administration (FDA) of the USA, microwave processing is on the way to commercialization. The major challenge in microwave processing is the nonuniform heating, which is intensified at higher microwave power. This chapter describes the theory and application of microwave heating in food processing.

Keywords Microwave assisted drying · Microwave assisted thawing · Sterilization · High temperature · Short times

6.1 Introduction

Microwave heating could provide volumetric heating for dielectric materials, such as foods. Foods are dielectric materials with low conductivity and also low thermal conductivity. During food processing, heating is a very common and important operation. However, low thermal conductivity of food materials is an inevitable problem during conventional heating, which results in long processing times and thermal deterioration of food quality. With a fast heating rate, microwave heating

D. Luan (✉)
College of Food Science and Technology, Shanghai Ocean University, Shanghai, China
e-mail: dlluan@shou.edu.cn

S. Horikoshi et al. (eds.), *Agritech: Innovative Agriculture Using Microwaves and Plasmas*, https://doi.org/10.1007/978-981-16-3891-6_6

can shorten the processing time and improve product quality. Thus, microwave heating has a great application potential in food processing. Numerous scientific studies and industrial applications of microwave heating are being undertaken and developed to solve the problems in traditional food processing.

Microwaves can propagate into food materials and provide energy through the interaction between alternating electromagnetic fields and food ingredients. It provides an obvious energy transfer rate than traditional heating can. Thus, most of the traditional food processing could be improved by microwaves, including drying, thawing, tempering, and thermal processing, i.e., pasteurization and sterilization.

6.2 Drying

Drying is a process that removes the majority of water from food by the application of heat. Water is separated from food through evaporation or sublimation in the case of freeze drying [1]. Hot air is the most widely used heat medium during conventional drying processes. It provides heat for increasing the temperature of foods and the energy required for latent heat of water evaporation. The drying rate is significantly affected by the condition of hot air. Higher air temperature and lower relative humidity provide more energy and driving force for water evaporation. Furthermore, an increase in air velocity also brings about a faster evaporation of water from the food surface. A typical drying rate curve of foods is shown in Fig. 6.1. Once the water at the surface starts evaporating, a moisture gradient forms from the interior to the surface, which causes the water migrating from the food interior to the surface. At first, the drying rate increases rapidly. Subsequently, a constant rate period starts when the amount of water moves from the interior to the surface equal to that of

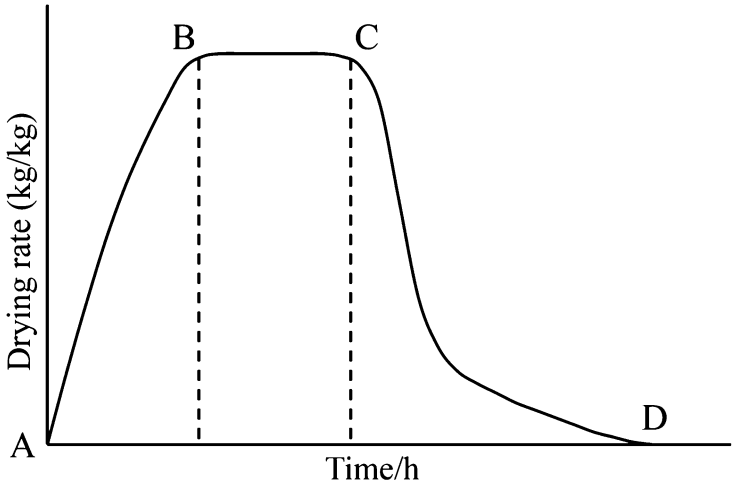

Fig. 6.1 The curve of a typical drying rate of foods

evaporating to the hot air. During this period, adjusting air conditions can increase the drying rate. The parameters that decide and limit the rate of drying in the constant rate period are the state of the air, such as temperature, relative humidity, and air velocity [2]. By altering these factors, the process can be accelerated.

However, when the moisture content of food reaches a critical point (point C in Fig. 6.1), the amount of water moving from the interior to the surface cannot provide sufficient water for evaporating, so that the drying process then enters into a falling rate period. During this falling rate period, it is the characteristics of food that controls the drying rate. Within this period, heat from air increases the surface temperature first and then the heat is transferred from the food surface to the interior via a lower conduction heat transfer rate. The force of heat transfer is due to a temperature gradient established between the surface and the interior, which causes a barrier to be erected for the interior water to migrate to the surface. As a result, the falling rate period is the most time and energy consuming section [3]. Besides, other drying methods such as freeze drying and vacuum-drying also encounter the same problem of low heat transfer rate. This restricts the energy supply for the evaporation and sublimation and leads to long processing times and more energy consumption. Microwave heating could provide a fast energy transfer rate, which would accelerate the drying speed and save energy [4].

6.2.1 Microwave-Assisted Hot Air Drying

In conventional hot-air drying, the drying speed is limited by the rate of water diffusing from the interior to the evaporating surface. Water diffuses by a capillarity action, which is controlled by the size and structure of food materials. This phenomenon is more obvious at the falling rate period of the drying process. Although adjusting the air conditions (higher velocity and temperature and lower relative humidity) could increase surface evaporation, it does not change the characteristics of food materials. Fast drying speed may over dry the surface and lead to cracks and hardening. In turn, however, this changes the diffusion path of the interior water and impedes its migration. With the assistance of microwave volumetric heating, a different water diffusion mechanism is applied within food materials. The temperature distribution within the microwave-heated food is totally different from that of hot air. The internal temperature will be higher than that at the surface, thereby forming an internal pressure gradient [5]. Furthermore, water has a higher loss factor than other ingredients, which have the capacity to absorb more microwave energy. Within foods, the part with high moisture is heated faster than the dried part; this is known as microwave selective heating, which also brings a pressure gradient between the high and low moisture parts. The pressure gradient improves water diffusion from the interior to the surface [6]. The hot air plays a role in removing the vapor. Thus, the temperature of hot air could be reduced properly to save energy and retain food quality. A typical application of microwaves in the falling rate period of hot-air drying is in the baking of cookies [7]. However, for some heat-sensitive food

materials other than cookies, applied microwave heating in the falling rate period may sharply increase the temperature and cause quality deterioration. Thus, for some food materials with low thermal resistance, it is more suitable to apply low power intermittent microwave heating [4, 8].

Besides the falling rate period, microwaves can also be utilized at the beginning of hot-air drying to preheat the product. This could help the food product to reach the drying temperature in a very short time. As a result, the temperature gradient from the surface to the interior in hot-air drying is reduced, which is conductive to water diffusion and drying speed.

In addition, to maximize the utilization of energy, some studies have reported the advantage of using a two-stage drying process that involves an initial forced-air convective drying followed by microwave drying or an initial input power of microwave drying followed by a changed input power of microwave drying [4]. Under different microwave power conditions, the time and energy consumption was reduced and the quality of dried carrots was improved. Microwave-assisted hot-air drying is widely applied in drying fruits and vegetables [9–11].

6.2.2 Microwave-Assisted Vacuum Drying

Vacuum drying is applied to alleviate the deterioration of food quality during hot-air drying. A lower pressure in vacuum drying reduces the boiling point of water and promotes the rate of water diffusion and evaporation. Lower temperatures and the absence of oxygen make vacuum drying suitable for heat-sensitive and oxygen-sensitive foods [12]. Generally, vacuum-dried food products have a higher porosity and less shrinkage. Furthermore, the rehydration is clearly greater than hot-air drying. Consequently, vacuum drying brings high sensory and nutritional quality (color, texture, and flavor) with less drying time. During vacuum drying, heat is also required for water evaporation. Different from convection heat transfer in hot-air drying, heat is transferred by conduction to food from the hot surface of the drier or hollow shelves [13]. The temperature of the surface is carefully controlled so as to balance the energy supply and product quality. The limitation of vacuum drying is related to the conduction heat transfer rate. Different heat transfer models have been developed for various vacuum-drying equipment. However, the mechanisms of these heat transfer models are the same, which restricts the heat transfer efficiency. Thus, microwaves are always combined with vacuum drying to improve the drying efficiency through volumetric heating [5].

Microwave-assisted vacuum drying shows significant advantages for food materials of large sizes and low thermal conductivities. Hu, Zhang, Mujumdar, Xiao, & Sun [14, 15] investigated drying damage of the hot air and vacuum microwave drying and found that the sequential combination of hot-air drying and vacuum microwave drying provided better results compared to vacuum microwave drying or air drying. Greater preserved color and less toughness were obtained for microwave vacuum-dried strawberries [16]. In addition, within a vacuum environment, foods

avoid exposure to oxygen and microwave vacuum drying displays great advantages in reducing oxidation of nutrients in chicken fillets, for example [17].

6.2.3 *Microwave-Assisted Freeze Drying*

Freeze drying is a special type of vacuum drying, which is performed at a temperature lower than the freezing point. In freeze drying, the frozen water in the food materials changes directly to vapor, known as sublimation. The speed of sublimation is improved by vacuum. Freeze drying has been developed for heat-sensitive materials [5]. The product quality of freeze drying is obviously better than other drying methods owing to the much lower drying temperature and lack of oxidation.

However, sublimation is a very time-consuming process even through a vacuum-assisted process. Furthermore, food should be frozen first, which also costs time and energy. As a result, freeze drying is an expensive process with long times and energy consumption and lower output [18, 19]. Similar to normal vacuum drying, the efficiency of heat supply during the freeze drying process limits the speed of water sublimation. Microwave-assisted freeze drying could lead to short processing times and to better food quality [20].

In microwave heating, the characteristics of food materials will affect the absorption of microwaves and product quality [21]. The dielectric loss factor of ice is much lower than that of water, which implies that the capacity of microwave energy absorption by water is much higher than that by ice [17]. For example, bananas with different maturity have different sugar and starch content, which requires different microwave operating conditions to retain quality [22, 23]. Thermal runaway may occur at the melting location. Also, arcing might occur in high power industrial applications of microwave-assisted freeze drying. As a result, product quality may be deteriorated due to thermal runaway and arcing. To avoid these problems, microwave power and the pressure should be carefully controlled. During the microwave-assisted freeze drying of sea cucumber, the pressure is in the range of 50–100 Pa, so that a reduced microwave power at low moisture content was recommended to avoid arcing. Furthermore, lower microwave frequencies could help to alleviate the nonuniform heating and arcing due to the longer penetration depth of the microwaves. As such, 915-MHz microwaves have been suggested to replace the 2450-MHz microwaves.

6.3 Thawing and Tempering

In the food industry, thawing is a very important process, while freezing has been widely applied for preserving food, especially for meat and aquatic materials. Conventional thawing processes require long times due to the low heat transfer efficiency. Quality degradation occurs during the long thawing process because of

microbial spoilage and drip loss [24]. With volumetric heating of whole frozen foods, microwave thawing displays greater advantages compared with conventional processing [25]. Microwave thawing has the potential to significantly reduce the thawing times. However, nonuniform heating remains a major problem. Microwave nonuniform heating is due to the uneven electric field distribution within the foods. The electric field distribution is controlled by the microwave heating cavity and the characteristics of the treated foods. With higher microwave power, microwave nonuniform heating will be worse, because the microwave heating rate is proportional to the square of the electric field intensity [26]. Furthermore, water absorbs much faster microwave energy than does ice due to a large difference in the dielectric loss factors [25, 27]. As a result, the point of greatest heating will melt first and absorb more energy than the frozen part. This also enhances the nonuniform heating. The microwave nonuniform heating in the thawing process may lead to quality degradation, while some parts may be cooked and others may still be frozen.

A novel technology was developed by Fathi, Lauf, and Mcmillan [28] for frozen liquid or semiliquid foods. A shielded region was designed for the thawed material that flowed to the region without microwaves. Although many studies have been carried out to improve the heating uniformity during the microwave thawing process, there are still some barriers in the industrial application that requires high microwave power [25].

However, instead of increasing the temperature of the frozen food above the freezing point, microwave tempering is a more effective operation. In tempering, the hard frozen food is warmed from −10 °C to 18 °C or lower to −5 °C or −2 °C. Within this temperature range, the food is softened so as to be easily sliced, ground, or otherwise processed. Microwave tempering is the most successful industrial application of microwave heating [29]. Commercial microwave tempering systems are primarily used for frozen meat, fish, and poultry.

For long-distance shipment and long-time storage, meat is frozen and packaged in cartons with a weight of 30–60 kg. Microwaves can penetrate through the carton to temper the frozen material, which saves labor and handling [29]. The power of microwaves used for tempering can be in the hundreds of kilowatts. Concerning the frequency, 915 MHz is a widely used frequency for tempering frozen food of large size. Compared to the 2450 MHz frequency, the 915-MHz microwaves have a much longer wavelength and larger penetration depth. For frozen food with temperature higher than −60 °C, there still exist unfrozen water molecules and high concentration of dissolved salts. These water molecules and ions severely absorb microwave energy, which limits the penetration depth of the 2450-MHz microwaves and thus their industrial application.

6.4 Microwave Sterilization and Pasteurization

Traditionally, sterilization and pasteurization are thermal processing operation to extend product shelf-life by inactivating spoilage and pathogenic micro-organisms. Canned foods are the typical sterilized products, which can be stored at room temperature. Food materials are packaged first and then treated with thermal processing to destroy the micro-organisms that concern food spoilage and public health. The hermetic environments within the packaged prevent the growth of other micro-organisms and the recontamination from the storage environment. Although many novel technologies are being investigated for sterilization and pasteurization, thermal processing remains the most efficient and most widely used method. For conventional thermal processing, steam or hot air is utilized as the heating medium. Heat is transferred from the heating medium to the surface of packaged foods and then to the interior. Temperature gradient from the surface to the interior is the driving force of heat transfer. However, because of poor thermal conductivity of food materials and the decreasing temperature gradient, a long time is required to achieve sterilization process. To ensure food safety, the cold spot location (i.e., the part of food that receives the lowest heating rate) should reach a sufficient thermal processing level.

6.4.1 High Temperature Short Time Process

Thermal processing is a combined action of time and temperature. To evaluate the thermal inactivation of a target micro-organism, the thermal lethality value (F) was defined by eq. 6.1 based on the recorded time-temperature profiles [30],

$$F = \int_0^t 10^{\frac{T(t)-T_{\text{ref}}}{z}} dt, \tag{6.1}$$

where $T(t)$ is the measured time-temperature profiles at the cold spot location (°C); T_{ref} is the reference temperature, which is 121.1 °C for sterilization (F_0) and 90 °C for pasteurization (F_{90}) process; z is the thermal resistance of the target micro-organism known as the z-value. The general z-value of bacteria is around 7–12 °C (Table 6.1).

Long-time thermal processing could not only destroy micro-organisms but also the food ingredients that cause quality degradation. Similar to micro-organisms, the thermal degradation values of nutritional ingredients have also been developed based on their z-values. The item for estimating nutrient loss is referred as cook values, or C values. Mansfield [32] first proposed the C values for aseptic processing determined from the following equation:

Table 6.1 Kinetic data on the thermal destruction of microbial spores and quality factors. (Used with permission from [31])

	Temperature range (°C)	T_{ref} (°C)	z-value (°C)
Bacillus stearothermophilus			
TH 24 aqueous	120–160	120	7.3
NCIB 8710 phosphate buffer	100–140	121	12.1
Bacillus subtilis			
5230 aqueous	105–132	121	8.3
5230 aqueous	124–140	121	14.1
Clostridium botulinum			
Type A aqueous	115.6–121	121	10
213 phosphate buffer	120–140	120	10
Clostridium thermosaccharolyticum			
S9 McIlvaine spore form	99–127	121	14.7
S9 acid spore form	99–127	121	9.76
Putrefactive anaerobe			
PA 3679 white corn purée	110–127	121	8.8
PA 3679 aqueous	110–132.2	121	9.8
Vitamin A			
Beef liver purée	103–127	122	23.0
Vitamin B1, thiamin			
Buffer solution pH 6	109–150	109	24.0
Vitamin B6			
Pyridoxine hydrochloride			
Pyridoxamine	105–133	118	26.0
Pyridoxal	105–133	118	30.0
Vitamin C, ascorbic acid			
Peas	110–132	121.1	18.2
Model solution			
Buffer pH 4	110–127	120	39.4

$$C = \int_0^t 10^{\frac{T(t)-T_{\text{ref}}}{Zc}} dt \tag{6.2}$$

where $T(t)$ is the measured time-temperature profiles at the recorded location (°C); T_{ref} is the reference temperature, which is 100 °C for C_0; and z_c is the thermal resistance of the nutrients. In general, the range of z_c is around 25–45 °C (Table 6.1); 33.1 °C is always used to calculated C.

The kinetic data on thermal destruction of some microbial spores and quality factors are reported in Table 6.1. Compared with micro-organisms, food ingredients are more resistant to heat. Figure 6.2 shows the variations of C values, while ensuing the same thermal lethality values of $F_0 = 3$ and 6 min. The thermal lethality values are calculated at constant temperature, and the same time-temperature combination

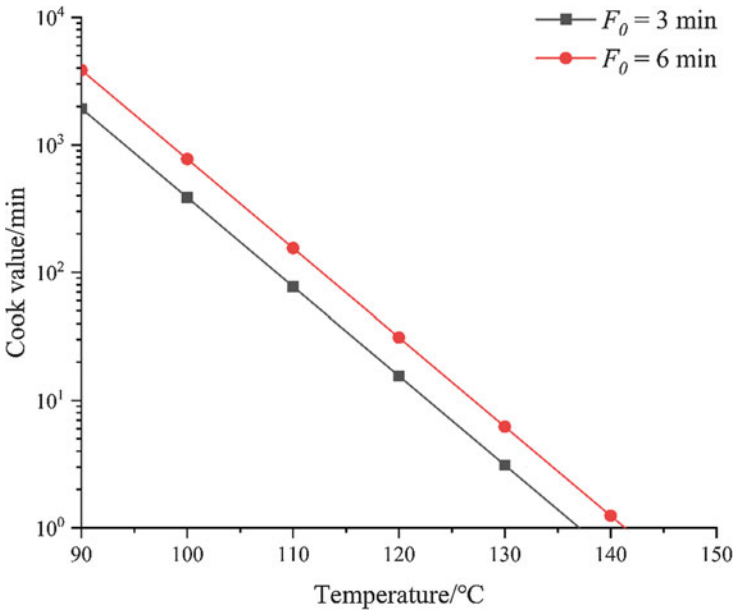

Fig. 6.2 Variations of *C* values for a constant thermal processing level processed at different temperatures

was used to calculate the *C* values. In Fig. 6.2, the *C* values decrease logarithmically with increasing temperature levels. This indicates that, theoretically, a high temperature/short time (HTST) process can significantly improve product quality, while ensuring food safety.

6.4.2 Microwave Thermal Processing

Microwave volumetric heating has the potential to achieve the HTST process for solid or semisolid foods to produce high-quality shelf-stable products. Traditionally, with steam or hot water heating, a thermal process is established based on the theory in calculating the *F* value. There are two essential parameters that must be confirmed: the thermal resistance of the target micro-organisms and the time-temperature profiles recorded at the cold spot location. The procedure for measuring the thermal resistance of micro-organisms and the recording (or predicting) of the time-temperature profiles have been described in detail by Holdsworth & Simpson [33]. To ensure food safety, microwave thermal processing – i.e., sterilization and pasteurization – follows the same principle as conventional processing. The microwave nonthermal effects on microbial inactivation are not taken into consideration as they could not yet be evaluated quantitatively, which could be regarded as an extra protection [34]. Thus, only the thermal effect is used to evaluate the thermal lethality

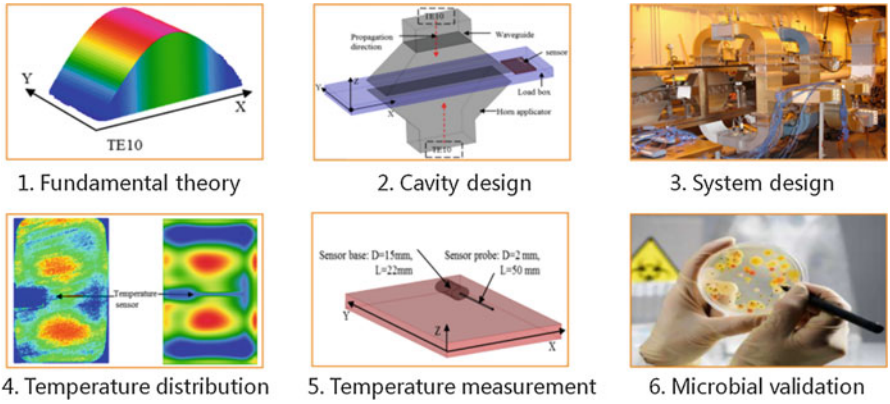

Fig. 6.3 Protocol for developing a microwave thermal process. (Revised from [36, 37])

in microwave processing. As well, the same thermal kinetics data from conventional processing of micro-organisms are applied in microwave processing [35].

Although the domestic microwave oven has been a common appliance in modern kitchens, the first microwave sterilization process was not approved by the United Sates FDA until 2009. The system for achieving this process was developed at Washington State University, now referred to as the Microwave-Assisted Thermal Sterilization (MATS) system. It is a 915 MHz single-mode microwave heating system. The major challenge for microwave thermal processing is obtaining the time-temperature profiles at the cold spot to ensure microbial food safety. In an early reported study, unstable and unpredictable heating patterns were the key problems. The cold spot location remained changing and was unpredictable in varying the heating pattern. As a result, it was impossible to design a safe thermal processing. Many studies have investigated theoretically and practically verified the microbial safety of microwave thermal processing. The protocol to establish a microwave thermal process and meet the regulatory requirements is shown in Fig. 6.3.

Within a microwave heating cavity, microwaves propagate and are reflected by the metal wall. The electric field distribution within the cavity is determined by the cavity's size and the microwave frequency. Solutions are obtained by solving Maxwell equations with boundary conditions of the cavity. Each solution is a mode of the electric field distribution, which has a unique matched microwave frequency. The electric field distribution keeps changing as the microwave frequency varies. This type of microwave heating cavity is known as a multimode cavity. Multimode microwave heating cavities are not available for developing microwave thermal processing, because there is no stable cold spot location [38]. Thus, a single-mode microwave heating cavity with predictable heating pattern is the prerequisite for microwave thermal processing. Theoretically, to design a single-mode cavity, there should be at least one dimension of the cavity to be much smaller than the microwave wavelength [35]. This guarantees that only one

solution of the Maxwell equations exists with the boundary conditions. The electric field distribution within this single-mode cavity is stable and predictable.

6.4.2.1 Design of Microwave Heating Systems

In Europe, 2450-MHz microwave sterilization systems have been reported since the 1990s [39, 40]. Later, processing plants were developed in the Tops Foods plant in Olen, Belgium, and at the Otsuka Chemical Co. [41]. Details of the microwave sterilization process based on the 2450-MHz system in Tops Foods were reported by Tang & Chan [42]. The system consists of four sections: loading, microwave heating, holding, and cooling. Compressed air was used to maintain the inner pressure of the system. There is a gate design between the loading and the microwave heating section, as well as holding and cooling section. For the operating process, packaged food products are placed in the loading section and compressed air is used to increase the pressure at the same level as in the microwave heating section. After opening the gate, the loaded food products are transported to the microwave heating section. The temperature is sharply increased to the desired level in several minutes, while these food products move through the microwave heating section. The temperature is maintained for a sufficient length of time at the holding section to achieve sterilization. Subsequently, the gate between the holding and cooling sections is opened to move the food products to the cooling section. Cold air is used to cool down the sterilized products. Because of the large difference in dielectric constant between the food (around 50–60) and air (ca. 1), edge heating becomes unavoidable. The unexpected edge heating may cause much higher temperatures and inner pressures within the packages. Consequently, to avoid package breaking, a lower microwave power and higher pressures of compressed air is applied.

In the United States, the commercial operation of microwave sterilization is still ongoing. So far, all the investigations have been carried out to meet the rigorous requirements of the FDA on the food safety of sterilized low acid food products. With lower safety requirements, there are a few microwave commercial pasteurization systems established in the United States. However, all the reported commercial systems use a 2450-MHz magnetron [35].

A pilot plant that included a 915-MHz single-mode microwave heating system was developed at Washington States University to solve the problem on the possible commercialization of microwave sterilization in the United States [43–45]. The system was also designed with four sections: preheating, microwave heating, holding, and cooling. To reduce edge heating, the packaged food products are immersed within a thin water bed during the microwave processing. Circulating water at different temperatures is used to achieve the preheating, holding, and cooling process. With this single-mode cavity design, this system could provide predictable and stable heating patterns for developing a sterilization process.

6.4.2.2 Determining the Heating Pattern

The heating pattern refers to the temperature distribution within the heated foods. The volumetric temperature distribution of the microwave process is controlled by the electric field distribution within the foods. However, for thermal processing of packaged food products, samples are taken out of the microwave heating system after cooling. To map the experienced thermal process during microwave processing, a noninvasive chemical marker method was developed by the U.S. Army Natick Soldier Center [46, 47]. It is based on the formation of a brownish color owing to the products from the Maillard reactions occurring in the thermal processed foods. The color changes in the Maillard reactions are due to the production of intrinsic chemical markers; these reactions are irreversible. In normal food materials, the products from the Maillard reactions are too few to accurately display the heating pattern. Homogenous food models with additives of substrates for the Maillard reactions were developed to accelerate the reactions and to display acceptable color changes [48–50]. However, the dielectric properties of food products could affect the electric field distribution and bring about variations in the heating pattern. To obtain a correct heating pattern, the dielectric properties of the food models should be the same as the food it tries to model. A production of the M-2 marker was suitable for the mapping of the volumetric heating pattern for the microwave sterilization process. Besides, a computer visual method was combined with the chemical maker method to clearly show the heating pattern of microwave processing [51, 52]. The location with the least thermal processing level can be determined by the color intensity displayed on the heating pattern. This location is known as the cold spot in microwave processing. Temperature sensors should be used to confirm the cold spot location.

6.4.2.3 Temperature Measurement

The time-temperature profiles at the cold spot location are the essential data to evaluate the thermal lethality value and establish a thermal process. In general, a fiber optical sensor is the best option for temperature measurements in microwave environments because it contains no metallic parts that may interact with microwaves [44, 53]. However, it is not suitable for moving packages in a high pressure environment owing to the long delicate wires. The application of a metallic mobile temperature sensor in a continuous microwave sterilization process was explored at Washington State University. Based on systematic studies, the sensor proved to be suitable for temperature measurements of the MATS system. Both computer simulation and experimental results showed that the sensor did not affect the electric field distribution [36]. The application of the sensor in high-power commercial systems was also investigated using a computer simulation [37]. Results showed that the accuracy is acceptable, while the sensor probe is oriented such that it is perpendicular to the electric field intensity.

6.4.2.4 Microbial Validation

Microbial validation is the last procedure to ensure the safety in the establishment of microwave thermal processing. To do so, the target micro-organisms were inculcated at the cold spot location of the food samples, after which the samples were then packaged and processed followed by acquiring the parameters. The calculated thermal lethality value and the measured population reduction need to be verified. For the commercial sterilization of low acid food products (pH $>$ 4.6, Aw $>$ 0.85), the spores of *Clostridium botulinum* type A and B (proteolytic) were the target bacteria, while they have the highest thermal resistance; the z value is 10 °C [54]. For commercial sterilization, a thermal lethality value of $F_0 = 3$ min should be achieved to obtain a minimum of 12-log reduction of the spores. However, in practical experiments of microbial validation, the *Clostridium sporogenes* strain PA 3679 spores were used as the surrogates for the *Clostridium botulinum* spores type A and B. The *Clostridium sporogenes* PA 3679 has the same thermal resistance, and it generates no toxin [55, 56].

Provided with supplemental data, a filing for homogeneous food of mashed potatoes processed by an MATS system was accepted for the first time by the FDA in October 2009. Later, the processing of salmon fillets was accepted in January 2011. In the industry, the military ration supplier AmeriQual Foods (Evansville, Ind., U.S.A.) established a third process filing for mashed potatoes, which was accepted by the FDA in 2014. This indicates that the filing protocols for microwave sterilization processes are well established to ensure food safety and fulfill the established requirements of the regulations. A detailed description for the supporting documents was described by Tang [35]. These accepted filings indicate that protocols for establishing a microwave thermal processing are valid and effective. Future work should focus on a processing design for different food materials, a sensory and nutritional quality of microwave processed products and heating uniformity improvement for high power industrial microwave processing systems.

6.5 Other Processing

Numerous applications of microwave volumetric heating have successfully been applied in specific food processing. Although these applications draw little attention from scientific research, they are commercially successful. These successful applications include cooking sausage patties, baking of potato chips, and precooking of bacon and chickens [29]. Krieger [57] suggested a set of criteria for a successful adoption, which involves high energy transfer rate, better quality and great yields, selective heating for the target materials, and an electronic monitoring system. Based on these criteria, microwave thermal processing has limited applications compared with other types of processing. However, compared with other processing, microwave sterilization and pasteurization processes are the most promising applications

in the food industry. They could provide high-quality and long shelf-life products, which fulfill the demands of modern society.

References

1. Grandison A. Food processing technology: principles and practice[J]. Int J Dairy Technol. 2011;64(3):455.
2. Joardder M, Kumar C, Karim A. Multiphase transfer model for intermittent microwave-convective drying of food: considering shrinkage and pore evolution. Int J Multiphase Flow. 2017;95:101–19.
3. Azzouz S, Guizani A, Jomaa W, Belghith A. Moisture diffusivity and drying kinetic equation of convective drying of grapes. J Food Eng. 2002;55(4):323–30.
4. Zhao D, An K, Ding S, Liu L, Xu Z, Wang Z. Two-stage intermittent microwave coupled with hot-air drying of carrot slices: drying kinetics and physical quality. Food Bioprocess Technol. 2014;7(8):2308–18.
5. Zhang M, Tang J, Mujumdar AS, Wang S. Trends in microwave-related drying of fruits and vegetables. Trends Food Sci Technol. 2006;17:524–34.
6. Rakesh V, Seo Y, Datta AK, McCarthy KL, McCarthy MJ. Heat transfer during microwave combination heating: computational modeling and MRI experiments. AICHE J. 2010;56:2468–78.
7. Roddy D. Handbook of microwave technology for food applications[M]. (Bookshelf). CRC Press; 1978. 536 p.
8. Zhao G, Hu C, Luo H. Effects of combined microwave hot air drying on the physicochemical properties and antioxidant activity of rhodomyrtus tomentosa berry powder. J Food Measur Charact. 2020;14(3):1433–42.
9. Łechtańska J, Szadzińska M, Kowalski J, S. J. Microwave-and infrared-assisted convective drying of green pepper: quality and energy considerations. Chem Eng Process Process Intensif. 2015;98:155–64.
10. Maskan M. Microwave/air and microwave finish drying of banana. J Food Eng. 2000;44:71–8.
11. Maskan M. Drying, shrinkage and rehydration characteristics of kiwifruits during hot air and microwave drying. J Food Eng. 2001;48:17–182.
12. Reis R, Felipe. Vacuum drying for extending food shelf-life[M]. New York: Springer International Publishing; 2014. p. 72.
13. Dilip PM. Vacuum drying: basics and application. Chem Eng. 2015;122(4):48–54.
14. Hu Q, Zhang M, Mujumdar AS, Xiao G, Sun J. Drying of edamames by hot air and vacuum microwave combination. J Food Eng. 2006;77:977–82.
15. Hu Q, Zhang M, Mujumdar AS, Xiao G, Sun J. Performance evaluation of vacuum microwave drying of edamame in deep-bed drying. Dry Technol. 2007;25:731–6.
16. Bruijn J, Rivas F, Rodriguez Y, Loyola C, Flores A, Melin P, Borquez R. Efect of vacuum microwave drying on the quality and storage stability of strawberries. J Food Process Preserv. 2015;40(5):1104–15.
17. Qiu L, Zhang M, Tang J, Adhikari B, Cao P. Innovative technologies for producing and preserving intermediate moisture foods: a review. Food Res Int. 2019;116:90–102.
18. Duan X, Zhang M, Mujumdar AS, Wang R. Trends in microwave-assisted freeze drying of foods. Dry Technol. 2010;28:444–53.
19. Duan X, Zhang M, Mujumdar AS, Wang R. Microwave freeze drying of sea cucumber (*Stichopus japonicus*). J Food Eng. 2010;96:491–7.
20. Wang D, Zhang M, Wang Y, Martynenko A. Effect of pulsed-spouted bed microwave freeze drying on quality of apple cuboids. Food Bioprocess Technol. 2018;11(5):941–52.

21. Wang R, Zhang M, Mujumdar AS. Effect of food ingredient on microwave freeze drying of instant vegetable soup. LWT Food Sci Technol. 2010;43:1144–50.
22. Jiang H, Zhang M, Mujumdar AS. Microwave freeze-drying characteristics of banana crisps. Dry Technol. 2010;28:1377–84.
23. Jiang H, Zhang M, Mujumdar AS. Physico-chemical changes during different stages of MFD/FD banana chips. J Food Eng. 2010;101:140–5.
24. James SJ, James C. Freezing/thawing. Chapter 5. In: Toldrà F, editor. Handbook of meat processing. Ames: Wiley-Blackwell; 2010. p. 105–24.
25. Zhang R, Wang Y, Wang X, Luan D. Study of heating characteristics for a continuous 915 MHz pilot scale microwave thawing system. Food Control. 2019;104:105–14.
26. Luan D, Tang J, Pedrow PD, Liu F, Tang Z. Analysis of electric field distribution within 352 a microwave assisted thermal sterilization (MATS) system by computer simulation. J Food Eng. 2016;188:87–97.
27. Regier M, Knoerzer K, Schubert H. The microwave processing of foods. Woodhead Publishing Series in Food Science, Technology and Nutrition[M]. 2nd ed. Woodhead Publishing; 2016. 484 p.
28. Fathi Z, Lauf RJ, Mcmillan AD. Microwave thawing apparatus and method. US Patent application, 20030192884; 2004.
29. Schiffmann RF. Chapter 9. Microwave processes for the food industry. In: Handbook of microwave technology for food applications. CRC Press; 2001. p. 299–377.
30. Awuah GB, Ramaswamy HS, Economides A. Thermal processing and quality: principles and overview. Chem Eng Process. 2007;46(6):584–602.
31. Holdsworth SD, Simpson R. Kinetics of thermal processing. Food Engineering, Chapter 3. Boston, MA: Springer; 2007. p. 87–122.
32. Mansfield T. High temperature-short time sterilization. Proceedings of the 1st International Congress on Food Science and Technology, vol. 4. London; 1962. p. 311–6.
33. Holdsworth SD, Simpson R. Thermal processing of packaged foods[M]. Blackie Academic & Professional, Springer Science & Business Media; 1997. 407 p
34. Guo C, Wang Y, Luan D. Non-thermal effects of microwave processing on inactivation of *Clostridium Sporogenes* inoculated in salmon fillets. LWT Food Sci Technol. 2020;133: 109861.
35. Tang J. Unlocking potentials of microwaves for food safety and quality. J Food Sci. 2015;80(8): E1776–93.
36. Luan D, Tang J, Pedrow PD, Liu F, Tang Z. Using mobile metallic temperature sensors in continuous microwave assisted sterilization (MATS) systems. J Food Eng. 2013;119 (3):552–60.
37. Luan D, Tang J, Pedrow PD, Liu F, Tang Z. Performance of mobile metallic temperature sensors in high power microwave heating systems. J Food Eng. 2015;149:114–22.
38. Luan D, Wang Y, Tang J, Jain D. Frequency distribution in domestic microwave ovens and its influence on heating pattern. J Food Sci. 2017;82(2):429–36.
39. Harlfinger L. Microwave sterilization. Food Technol. 1992;46(12):57–61.
40. Schlegel W. Commercial pasteurization and sterilization of food products using microwave technology. Food Technol. 1992;46(12):62–3.
41. Decareau RV. Microwaves and foods newsletter, 6(1), 5. Trumbull: Food and Nutrition Press Inc; 1996.
42. Tang J, Chan TV. Microwave and radio frequency in sterilization and pasteurization applications. Heat transfer in food processing-recent developments and applications. Southampton: Wessex Institute Of Technology (WIT) Press; 2007. p. 101–57.
43. Herve AG, Tang J, Luedecke L, Feng H. Dielectric properties of cottage cheese and surface treatment using microwaves. J Food Eng. 1998;37(4):389–410.
44. Lau MH, Tang J. Pasteurization of pickled asparagus using 915 MHz microwaves. J Food Eng. 2002;51(4):283–90.

45. Lau MH, Tang J, Taub IA, Yang TCS, Edwards CG, Mao R. Kinetics of chemical marker formation in whey protein gels for studying high temperature short time microwave sterilization. J Food Eng. 2003;60(4):397–405.
46. Kim HJ, Taub IA. Intrinsic chemical markers for aseptic processing of particulate foods. Food Technol. 1993;47(1):91–7. 99
47. Kim HJ, Taub IA, Choi YM, Prakash A. Principles and applications of chemical markers of sterility in high-temperature-short-time processing of particulate foods. In: Lee TC, Kim HJ, editors. Chemical markers for processed and stored foods. Washington, DC: American Chemical Society; 1996. p. 54–69.
48. Auksornsri T, Bornhorst ER, Tang J, Tang Z, Songsermpong S. Developing model food systems with rice based products for microwave assisted thermal sterilization. LWT Food Sci Technol. 2018;96:551–9.
49. Wang Y, Tang J, Rasco B, Wang S, Alshami AA, Kong F. Using whey protein gel as a model food to study the dielectric heating properties of salmon (*Oncorhynchus gorbuscha*) fillets. LWT Food Sci Technol. 2009;42:1174–8.
50. Zhang W, Luan D, Tang J, Sablani SS, Rasco B, Lin H, Liu F. Dielectric properties and other physical properties of low-acyl gellan gel as relevant to microwave assisted pasteurization process. J Food Eng. 2015;149:195–203.
51. Pandit RB, Tang J, Liu F, Pitts M. Development of a novel approach to determine heating pattern using computer vision and chemical marker (M-2) yield. J Food Eng. 2007;78(2):522–8.
52. Pandit RB, Tang J, Liu F, Mikhaylenko G. A computer vision method to locate cold spots in foods in microwave sterilization processes. Pattern Recogn. 2007;40(12):3667–76.
53. Tang Z, Mikhaylenko G, Liu F, Mah JH, Pandit R, Younce F, Tang J. Microwave sterilization of sliced beef in gravy in 7-oz trays. J Food Eng. 2008;89(4):375–83.
54. Stumbo CR. Thermal resistance of bacteria. Thermobacteriology in food processing. 2nd ed. New York: Academic Press Inc.; 1973. p. 93–120.
55. Naim F, Zareifard MR, Zhu S, Huizing RH, Grabowski S, Marcotte M. Combined effects of heat, nisin and acidification on the inactivation of *Clostridium Sporogenes* spores in carrot-alginate particles: from kinetics to process validation. Food Microbiol. 2008;25(7):936–41.
56. Reddy NR, Marshall KM, Morrissey TR, Loeza V, Patazca E, Skinner GE, et al. Combined high pressure and thermal processing on inactivation of type a and proteolytic type B spores of *Clostridium botulinum*. J Food Prot. 2013;76(8):1384–92.
57. Krieger B. Commercialization: steps to successful applications and scale-up, microwaves: theory and applications in materials processing. III. Ceramic transactions, vol. 59. Westerville, OH: The American Ceramic Society; 1995. p. 17–21.

Chapter 7
Stimulating the Aging of Beef with Microwaves

Satoshi Horikoshi and Nick Serpone

Abstract Originally, microwave ovens and foods have had a long-standing relationship that has been going on for more than half a century. In this regard, the purpose of microwave ovens was simply to reheat cooked foods. Is that really all? Under the theme ***Foodtech*** (Food technology), this chapter describes the accelerated hydrolysis reaction of casein (a model protein) using the papain enzyme (major industrial enzyme) and nonfluctuating microwave radiation investigated with respect to both activity and autolysis. The effect of microwaves on their interaction with beef was investigated in vivo using this papain enzyme. This chapter summarizes the characteristics of various electromagnetic wave components and conditions (e.g., electric field, magnetic field, pulsed microwave radiation, and continuous microwave radiation). Microwave heating showed different effects from conventional heating that occurs via heat conduction. These effects were emphasized by pulsed microwave irradiation. It was expected that there would also be an effect of the electromagnetic waves. Consequently, microwaves were applied to the aging of beef. Under microwave heating, the inner parts of the beef could be heated, while the the surface remained cool owing to the surrounding cool atmosphere. A microwave meat aging machine prevents surface spoilage and matures the inside of the meat. Electromagnetic and heat effects are therefore introduced as an application.

Keywords Food technology · Microwave aging · Aging · Beef · Enzyme · Papain · Electromagnetic field effect · Continuous microwave irradiation · Pulsed microwave irradiation

S. Horikoshi (✉)
Department of Materials and Life Sciences, Faculty of Science and Technology, Sophia University, Chiyodaku, Tokyo, Japan
e-mail: horikosi@sophia.ac.jp

N. Serpone
PhotoGreen Laboratory, Dipartimento di Chimica, Universita di Pavia, Pavia, Italy
e-mail: nick.serpone@unipv.it

S. Horikoshi et al. (eds.), *Agritech: Innovative Agriculture Using Microwaves and Plasmas*, https://doi.org/10.1007/978-981-16-3891-6_7

7.1 Introduction

The interaction of electromagnetic fields with various life processes has intrigued scientists since the 1800s. Of current interest are the electromagnetic fields present in microwave radiation, which spans a frequency from 300 GHz to 300 MHz (i.e., from a wavelength of 1 mm to 1 m). Microwaves are used widely in communications and in heating, particularly in the heating of foodstuffs. This nonionizing electromagnetic radiation is absorbed at the molecular level causing changes in the vibrational energy of the molecules; it also manifests itself as heat [1]. In the interaction between microwaves and a substance, the enzymatic reactions involving microwaves have been the object of active investigations in the latter half of the twentieth century, with the first such study reported in the early 1970s. For instance, microwave radiation to inactivate the enzymes in the brain of animals has been used widely since Stavinoha and coworkers first introduced it in 1970 [2]. Inactivating the enzymes made it possible to sample and measure many enzymatically destroyed brain neurochemicals, thereby reducing the influence of postmortem changes [3]. Usage of microwaves has succeeded in stopping enzymatic activity selectively with minimal damage to other cells and/or proteins under in vivo conditions, for which equipment is now commercially available. Moreover, investigations have also been carried out into the promoting effect of microwaves in the enzymatic activity of in vitro systems at the molecular level [4]. In this regard, Young et al. [5] reported that hyperthermophilic enzymes can be activated at temperatures far below their optimal temperature, presumably through a microwave-induced conformational flexibility. This finding offered the prospect of using hyperthermophilic enzymes at ambient temperatures to catalyze reactions with thermally labile substrates and products. Additionally, microwaves could also be used to regulate biocatalytic rates of enzymes at very low temperatures from less thermophilic sources [5]. Parenthetically, Damm and coworkers [6] critically evaluated microwave-assisted proteomic protocols. Upon examining microwave heating versus conventional heating, these authors [6] asserted that nonthermal effects (i.e., microwave specific effects) had no influence on the structure and on the enzymatic digestion of proteins. More recently, studies on the use of microwave radiation have spanned several different fields of science and engineering [7]. For instance, Parker and coworkers [8] reported on organic syntheses involving microwave-assisted enzymatic reactions, while the accelerated proteolytic cleavage of proteins under controlled microwave irradiation was investigated by Pramanik and coworkers [9]. Elhafi et al. [10] examined microwave treatment as a satisfactory method for inactivating a virus in preserving nucleic acid for the identification of the polymerase chain reaction (PCR). A novel microwave-assisted protein digestion method using trypsin-immobilized magnetic nanoparticles (TIMNs) has been developed by Lin and coworkers [11], while Shaw et al. [12] performed the polymerase chain reaction (PCR) in a microfluidic device with microwave heating using 8-GHz microwaves.

The use of microwaves on enzymes and proteins in foodstuffs [13] is also attracting considerable attention. However, the number of research reports in the

literature is rather limited on this point. In addition, most of the research is on the deterioration of food in microwave ovens. Nonetheless, many experiments have not been without problems; for example, reproducibility is one such issue in experiments that involve a microwave oven, particularly when using strong microwave output power. In addition, temperature measurements are difficult to perform with any accuracy. Therefore, in discussing the effects of these microwaves, precise temperature measurements and irradiation with stable microwaves must be assured. Our purpose is not to clarify the negative effects of microwaves on enzymes and foods. Rather, our goal has been to actively take advantage of the fascinating effects of microwaves on food enzymes, with the aim of using them to process and cook foods via an innovative methodology—***Foodtech*** (food technology).

This chapter describes the use of a device that can perform microwave irradiation without fluctuation (i.e., continuous microwaves) and precise temperature measurement: (i) the interaction between the microwave and the enzyme was performed with the parameters of the microwave added (e.g., *electric field, magnetic field, continuous microwaves, and pulsed microwaves*), which clarified whether microwaves are effective for carrying out enzymatic reactions, and (ii) consideration of the data on interactions between "in vitro" and "in vivo". Results demonstrated that microwaves can be used meaningfully in enzymatic reactions, as evidenced by the improvement of the Umami component by actually aging the edible meat subsequent to being exposed to microwaves. Furthermore, the effect was improved by performing pulsed microwave irradiation. The microwave-promoted beef aging machine (Aging booster) is that the Umami component of meat can be improved by promoting the enzyme activity in the meat through microwave internal heating, while keeping the surface of the meat at 0 °C.

7.2 Device Capable of Precise Temperature Measurement and Microwave Irradiation

Many experiments of enzyme reactions use microwave ovens, and many of the results cannot be reproduced. The reason for this has been attributed to the usage of different microwave generators and power supplies. The frequency distribution of the microwave radiation from the magnetron generator in microwave cooking oven is reported in Fig. 7.1a, which shows that the frequency of the microwaves is distributed over a large frequency range of 2.25–2.60 GHz [14]. Also, the shape of this spectrum changes over time. Moreover, the distribution of the microwave frequency changes depending on the characteristics of the microwave generator equipment. How can this problem be solved? One of the possible solutions is the use of a semiconductor generator that produces microwaves only within the very narrow frequency range of 2.4500 ± 0.0025 GHz (Fig. 7.1b). In the case of the magnetron generator, the microwave input power distribution reflects the widely dispersed frequency distribution. Therefore, the output of the actual 2.45-GHz

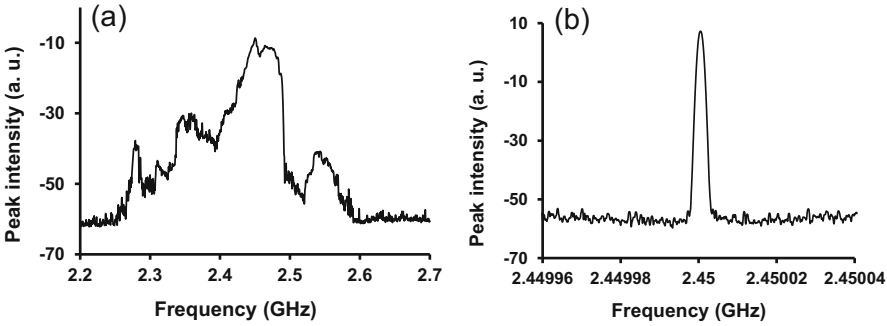

Fig. 7.1 Frequency spectral distribution of the 2.45-GHz microwave radiation emitted from the (**a**) magnetron generator and (**b**) the semiconductor generator. Reproduced from [14] with permission

microwaves is smaller than the input power. Additionally, when using a semiconductor microwave generator, the heating can progress efficiently because the microwave input power is concentrated at the 2.45000 GHz frequency and because most microwave ovens cannot emit microwaves below ca. 200 W. This is clearly too strong for biological samples. Also, this output is not constant with the power supply of the microwave oven. By contrast, the semiconductor generator can be set from a stable output of less than 0.1 W. In our studies, we used a semiconductor oscillator that did not fluctuate and with the equipment illustrated in Fig. 7.2a that can strictly monitor the temperature with no temperature unevenness throughout the sample.

The schematics and an actual photograph of the microwave device used in our experiments are illustrated in Fig. 7.2a. The microwave generator utilized a semiconductor-type microwave generator system {SPC Electronics Corp.: maximum output power, 240 W}. The continuous microwave irradiation (CMI) and pulsed microwave irradiation (PMI) were obtained from the semiconductor microwave generator under PMI conditions. The incident microwaves were absorbed with a dummy load; under the conditions used, none of the microwaves were reflected. The reason for this was to prevent nonuniform temperatures at the samples owing to unevenness of the electromagnetic wave at the samples' position originating from resonance conditions. Also, a power sensor was connected between the sample and the dummy load to monitor the power of the microwave passing through it. Moreover, the experiments were carried out at maximal electric or magnetic field density in a single-mode TE103 cavity (transverse electric 103 mode) as schematically illustrated in Fig. 7.2b; also included in the equipment used were a short plunger, an iris, a three-stub tuner, power sensors, and an isolator. The resonance of the microwaves was adjusted with the iris and the plunger at 1.5 cycles [15].

Heating the enzyme solution was achieved by locating the quartz tube reactor in the single-mode microwave apparatus (Fig. 7.2b) within the waveguide at positions either of maximal electric field (position (i)) or magnetic field (position (ii)) density. The maximal position of the *E* field from the iris was located at 3/4 the wavelength of the standing wave in the waveguide (i.e., at 11.09 cm) [15]. An electric field monitor

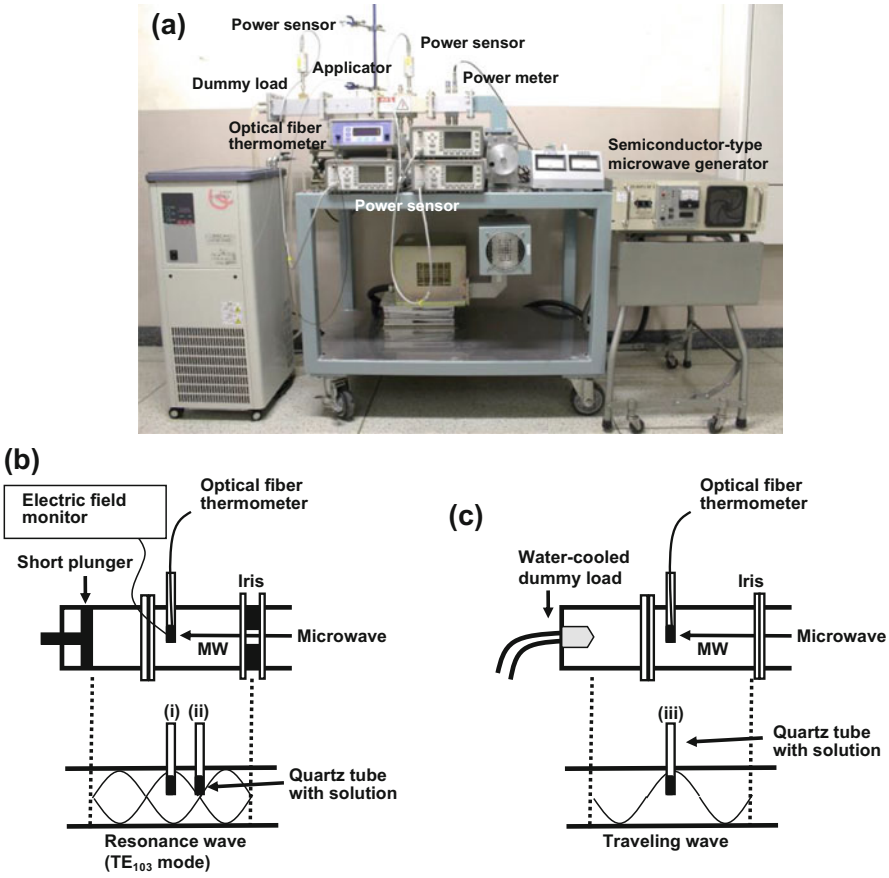

Fig. 7.2 (**a**) Photograph of the microwave heating system using a microwave semiconductor generator, a single channel power meter and a power sensor, isolator, single-mode applicator, and a dummy load. (**b**) detailed illustration of the experimental setup and positioning of the samples in the single-mode TE_{103} cavity with resonance wave; (i) maximal position of the electric field (*E*-field) density; (ii) maximal position of the magnetic field (*H*-field) density; (**c**) detailed illustration of the experimental setup and positioning of the samples in the single-mode cavity with traveling wave; (iii) position of electric/magnetic field (*E*/*H*-field). Reproduced from [16] with permission

(Fuji Electronic Industrial Co. Ltd.) was used to maintain the sample tube at the maximal position of the *E*-field density, as the reproducibility of such experiments is often diminished if such operations were neglected. A water-cooled dummy load was connected to the tip of the applicator (for *E/H*-field-CMI and *E/H*-field-PMI methods); the sample was subsequently irradiated with a traveling wave without resonating the microwaves (Fig. 7.2c). The experiment involving conventional heating was conducted using a water bath with stirrer; the temperature of water in the water bath was fixed at 60 °C. Experiments for microwave heating and water-bath heating were repeated not less than six times; the average of the data

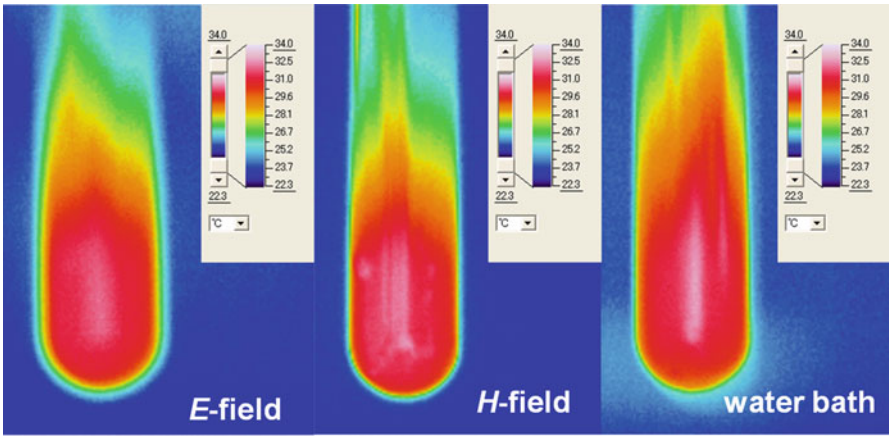

Fig. 7.3 Temperature distribution in a reactor containing the solution exposed to maximal electric field (***E***-field) or maximal magnetic field (***H***-field) density for microwave heating; also shown is the distribution under conventional water heating (WB). Reproduced from [17] with permission

was reported. The sample solution was contained in a branched test tube made of quartz (inner diameter, 12 mm); a reflux tube was connected to the top of the test tube; the temperature was measured using a fiber optic thermometer (Anritsu Meter Co., Ltd.). In preliminary experiments, we confirmed that the difference in temperature with respect to the vertical direction of the solution due to microwave irradiation was less than 1 °C. We also confirmed that during the experiments the reflection of microwaves was zero according to the power sensor.

The temperature distribution of the aqueous sample, subsequent to being exposed to microwaves and conventional heating after a reaction time of 6 min, was determined by thermography (Fig. 7.3) after taking out the quartz reactor with the sample from either the waveguide or the water bath; the color from the thermography ascertained the temperatures. The ambient temperature was 24 °C. Thermography measurements could not be done after heating with the multimode applicator, however, because of the configuration of the microwave equipment.

Temperature profiles were assessed at the center of the solution using an optic fiber thermometer. Results for ***E***-field, ***H***-field, and multimode microwave heating, and for water bath heating to 37 °C are displayed in Fig. 7.4. The temperature difference between ***E***-field/***H***-field heating and conventional heating was less than 1 °C.

In the present instance, the penetration of the 2.45-GHz microwaves into the solution was estimated to be ca. 17 mm at 37 °C (internal diameter of quartz reactor, 10 mm). Accordingly, the microwaves permeated sufficiently into the center of the solution, and thus, temperature fluctuations in the solution were negligible as the sample was continually stirred (magnetic bar).

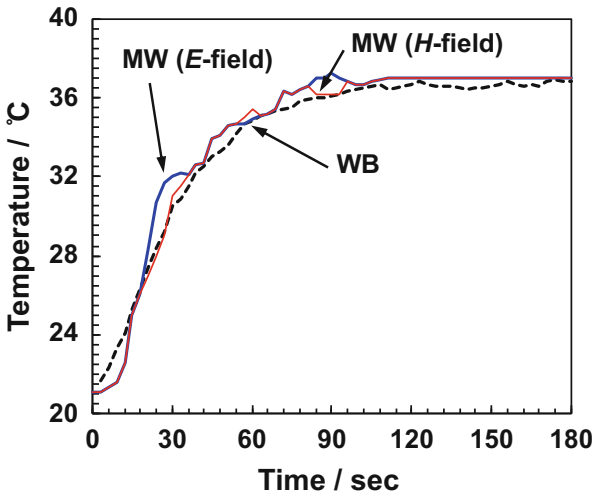

Fig. 7.4 Temperature profiles at the center of the solutions under ***E***-field (blue solid line) and ***H***-field (red solid line) microwave heating, multimode microwave heating (red solid line), and water bath heating (WB; black dashed line). Reproduced from [17] with permission

7.3 Microwave Electromagnetic Wave Effect(s) Enzyme Reaction in "in vitro"

To evaluate the possible microwaves' electromagnetic field effects in an in vitro case, we examined the hydrolysis of ***casein*** (a model protein) in the presence of the ***papain enzyme*** (a model enzyme) performed with microwave elements. The increase in the efficiency of the papain-assisted hydrolysis of casein after 5, 15, and 30 min heating against 0 min is shown in Fig. 7.5 with respect to the heating method, namely, (a) *E*-field and *H*-field microwave heating, (b) water-bath heating (WB), (c) *E/H*-field heating under continuous microwave irradiation (CMI), and (d) under pulsed microwave irradiation (PMI; 20-ms pulses); the temperature was in all cases 60 °C.

In the first case, we looked at the effects that the microwaves' electric field (*E*-field) and magnetic field (*H*-field) heating might have on such an in vitro process. As evident in Fig. 7.5, there was no significant difference in the rate of hydrolysis of casein at all three heating times by *E*-field heating, *H*-field heating, and water-bath heating. The only significant difference by the t-test was 5 min of *E*-field. Moreover, within experimental error, no enhancement of the hydrolysis of casein was seen in the presence of the papain enzyme under microwave and conventional heating. A comparison between *E*/*H*-field (CMI) and *E*/*H*-field (PMI) conditions, as done for the in vivo case (see below), shows that the efficiency of the hydrolytic process was greater under PMI than WB heating. However, the efficiency of the papain enzymatic reaction under PMI conditions did not increase dramatically—the only significant difference by the t-test was 15 and 30 min under *E*/*H*-field. Under CMI conditions, the efficiency was below that of WB heating. Apparently, the promotion of enzyme activity by microwaves is more clearly demonstrated by pulsed

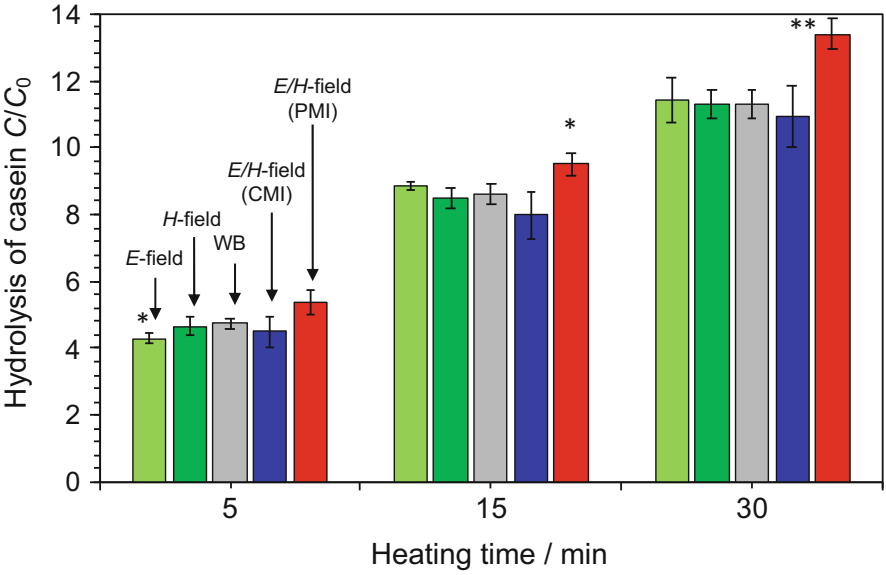

Fig. 7.5 Hydrolysis of casein by the papain enzyme monitored by the UV absorption at 275 nm after 5, 15, and 30 min heating (C) against 0 min (C_0); the reactor was located at the maximal position of the electric field density (E-field), at the maximal position of the magnetic field density (H-field), by water-bath heating (WB), by electric/magnetic field heating (E/H-field) under continuous microwave (CMI) or pulsed microwave (PMI; 20-ms pulse) irradiation; temperature was in all cases 60 °C. Note that * and ** refer to the significance of the student's t-test for $p < 0.05$ and $p < 0.01$, respectively, compared to WB. Reproduced from [16] with permission

irradiation. Furthermore, the effect was even greater with long-term irradiation rather than during the initial stage of microwave irradiation.

The question then is: where did the promoting effect of microwaves originate? To resolve this issue, we next focused on events that may occur within the enzyme itself. Protease enzymes, such as papain, typically hydrolyze proteins, yet at the same time, papain seems to be an atypical enzyme as it may undergo self-digestion (autolysis), as evidenced by the quantity of enzyme remaining in solution that decreased with reaction time.

The heating of aqueous solutions containing only the papain enzyme (without the casein) at 60 °C was also carried out using each of the heat sources reported in Fig. 7.6, which also displays the extent of self-digestion of the enzyme monitored by absorption spectra recorded at 0, 5, 15, and 30 min. A comparison between the microwaves' E-field and H-field heating reveals that the self-digestion of the enzyme was suppressed under E-field heating; in fact, changes in absorption in the spectra were hardly observed under the latter condition. Under H-field heating conditions, however, the extent of self-digestion increased with heating time. Most significant, under water-bath heating, the extent of self-digestion of papain was significantly greater vis-à-vis microwave heating and remained unchanged with heating time.

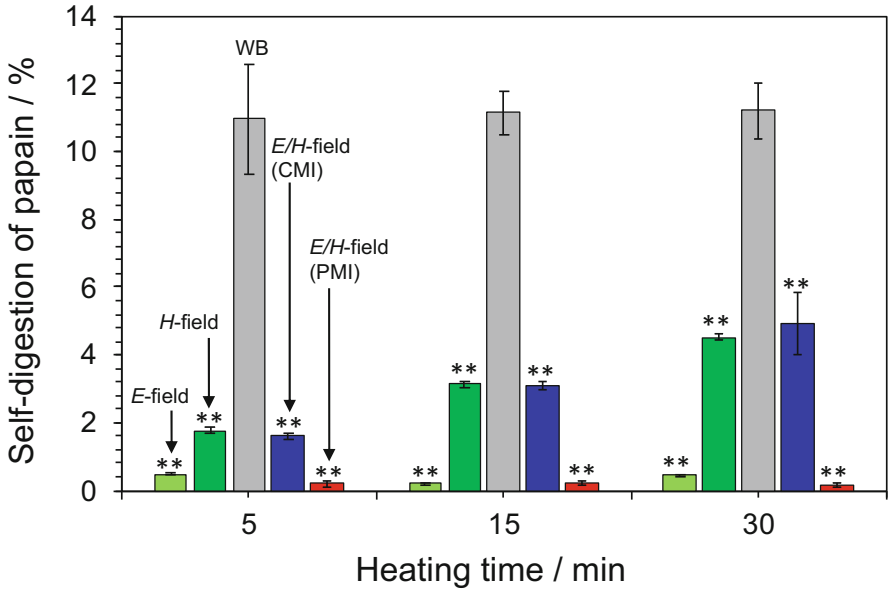

Fig. 7.6 Percent of self-digestion of papain monitored by the UV absorption at 245 nm for 5, 15, and 30 min heating against 0 min; the reactor was located at the maximal position of the electric field density (*E*-field), at the maximal position of the magnetic field density (*H*-field), by water-bath heating (WB), by electric/magnetic field heating (*E/H*-field) under continuous microwave (CMI) or pulsed microwave (PMI; 20-ms pulses) irradiation at 60 °C. Note that * and ** refer to the student's t-test for $p < 0.05$ and $p < 0.01$, respectively, compared to WB. Reproduced from [16] with permission

Results from the self-digestion experiments of aqueous solutions of papain (no casein) subjected to microwave *E*/*H*-field irradiation under CMI and PMI conditions showed that the self-digestion of this enzyme under PMI was significantly inhibited relative to CMI. Since an apparent pulsed microwave effect was observed at 60 °C, we considered that suppression of the self-digestion of papain was affected by the electromagnetic field—note that in all the experimental data, the *t*-test showed a significant difference of less than 0.01). Yet even with cooling, inhibition of the self-digestion of papain was remarkably absent compared with *E/H* fields with CMI. For the in vitro case, although the microwaves' electromagnetic fields had no influence in the hydrolysis of casein by the papain enzyme, they likely did play a role in the attenuation/inhibition of the self-digestion of this protease enzyme. This was taken to mean that the self-digestion of papain was not an aqueous media event, but rather it was an intramolecular event within the enzyme.

To summarize, the advantage of the enzymatic reaction given by microwaves is that it does not contribute much to the promotion of the enzymatic reaction itself, but rather extends the life of the enzyme itself. Such characteristics may affect the reaction of papain enzymes in beef, for example. In other words, for the in vivo case, the amount of enzyme was significantly smaller than that of substrates such as

proteins. Thus, extending the lifetime of the enzyme was considered advantageous for the overall enzyme reaction.

7.4 Microwave Electromagnetic Wave Effect(s) Enzyme Reaction in "in vivo"

In a practical in vivo experiment, a 10-mg powdered sample of the papain enzyme was used to cover the whole surface of the pieces of beef (dimensions ca. 20 × 20 × 50 mm). Microwave radiation was subsequently used to heat these pieces with 11-Watt (continuous wave) and 20-Watt (pulse wave) microwaves in a system consisting of a single-mode microwave applicator (traveling microwave wave) that was kept at a temperature of 45 °C for 10 min. In pulsed microwave heating, the microwaves emitted from the semiconductor microwave generator were turned ON and OFF every 20 ms. This pulse condition was the pulse width generated by most of the magnetrons driven by a 50 Hz power supply as the commercial power frequency. That is, it imitates the oscillation of most microwave ovens and industrial microwave irradiation equipment. For comparison, the beef/papain samples were also heated and kept at ca. 45 °C for 10 min in an electric furnace previously brought to this temperature. In electric furnace heating, the temperature of the beef specimens was controlled and the potential overshoot of the temperature beyond 45 °C was prevented by opening and closing the door of the electric furnace. The temperature of all the beef/papain samples was measured at locations 3 mm below the surface of the beef sample using a fiber optic thermometer. Most of the beef samples were cut into 20 × 20 × 50 mm rectangularly-shaped specimens as illustrated in Fig. 7.7a-i, a-ii that display the initial papain-free beef sample.

The papain-treated beef samples were subjected to pulsed microwave irradiation (PMI; 20-ms pulses; Fig. 7.7b-i) and to continuous-wave microwave irradiation (CMI; Fig. 7.7c-i). Under microwave heating, the papain-treated samples of Fig. 7.7b-i, c-i softened in a manner suggestive of liquefied jelly when compared to the nonirradiated papain-free initial sample (Fig. 7.7a-i). That is, it shows that exposing the papain-coated beef specimens to microwave heating enhanced the decomposition of the protein(s) on the beef surface. We also observed that the degree of softness of the beef surface under PMI conditions was, to some extent, greater than under CMI. By contrast, upon being subjected to heating in an electric furnace at 45 °C for 10 min, the papain-treated beef sample of Fig. 7.7d-i softened much less than under microwave irradiation. Moreover, after the conventional heat treatment, the specimen's surface was unlike the jelly-like surface displayed by the samples of Fig. 7.7b, c. Experiments were also conducted at 50 °C (+5 °C) and 40 °C (−5 °C) in the electric furnace to examine whether errors in temperature measurements could explain this difference. There were no differences at both these temperatures. Accordingly, despite the same temperature conditions (45 °C), the

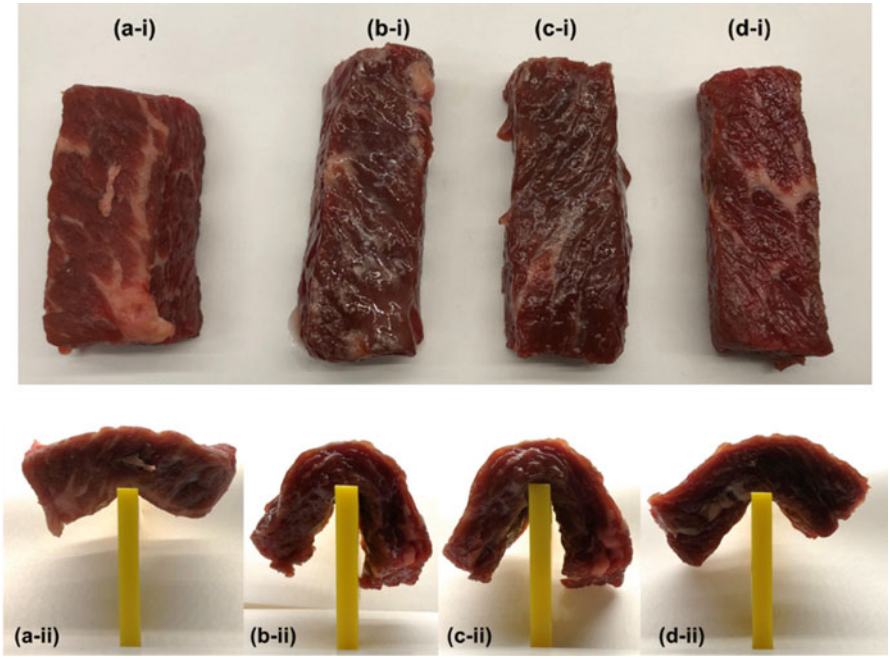

Fig. 7.7 Observations of the surface changes (i) and the degree of softening (ii) of beef samples after applying papain to the beef: (**a**) control experiment with no papain used on the beef, (**b**) papain-treated beef sample after heating with pulsed microwave irradiation (PMI) and maintaining it at 45 °C for 10 min, (**c**) papain-treated beef sample subjected to continuous microwave irradiation (CMI) under otherwise identical conditions as in (**b**), and (**d**) papain-treated beef sample subjected to heating in an electric furnace at 45 °C for 10 min. Reproduced from [16] with permission

microwaves promoted the activity of papain on the beef surface that we attributed to the microwaves' electromagnetic fields.

A closer look at the photographs in Fig. 7.7abcd-i shows that the sizes of the samples differed after their treatment. After microwave heating (Fig. 7.7b-i, c-i) and electric furnace heating (Fig. 7.7d-i), their longitudinal and lateral sizes were longer and narrower relative to the untreated beef specimen (Fig. 7.7a-i). The two beef specimens exposed to PMI and CMI irradiation were longer by about 2 cm, while the specimen heated in the electric furnace was ca. 1 cm longer than the untreated beef. These changes are due to the papain-assisted hydrolysis that cleaved the beef's internal protein chains with the efficiency expected to increase under the microwaves' electromagnetic fields relative to conventional heating. To confirm the cleavage of the internal protein chains, we examined the effect that gravity had on the heated and nonheated samples. To do so, we placed all four samples at the center of a vertical yellow plastic plate (5 mm thick and 10 mm wide) in a manner reminiscent of a seesaw.

The papain-free untreated beef sample remained firm to gravity as illustrated in Fig. 7.7a-ii, that is, there was no change in shape even though the sample was left

standing for 5 min in this state. By comparison, it is clear from Fig. 7.7b-ii, c-ii that the papain-treated beef specimens subjected to microwave irradiation were unable to counter the gravity as they drooped down considerably compared to the untreated specimen of Fig. 7.7a-ii. It also became clear that they could not keep their initial flattened shape for more than 20 s, which confirmed the cleavage of the protein chains inside the beef (softening) by the papain enzyme. A comparison of the extent of drooping in Fig. 7.7b-ii, c-ii shows that the hydrolysis of the beef protein was somewhat greater when the sample was subjected to PMI hydrolysis than with CMI. These experiments were repeated no less than four times, and in every instance, the hydrolysis reaction was more pronounced under PMI than under CMI conditions. Upon being subjected to heating in an electric furnace at 45 °C for 10 min, the papain-treated beef sample softened somewhat, but significantly less than the microwaved specimens by the electromagnetic fields as evident from comparing the specimen of Fig. 7.7d-ii with the specimens of Fig. 7.7bc-ii after 5 min standing in that state.

The results afford two possible mechanistic considerations. In the first instance, the hydrolysis of the beef protein(s) by the papain enzyme was enhanced under PMI compared to CMI conditions, as the microwaves applied power for PMI was 1.8 times higher than that of CMI (11 W). Evidently, the microwave power level influences the papain's activity and, not to be precluded, by the instantaneous electric field and magnetic field enhancement under pulsed microwave irradiation (PMI). In the second instance, microwave heating occurred first in the inner core of the beef samples and to the extent that the surface temperature was that of the surrounding atmosphere, thus cooler than within the inner core, a temperature gradient was established under microwave heating. Consequently, some of the moisture contained within the bulk moved to the surface, thus causing the enzymatic hydrolysis reaction to occur mostly at the specimens' surface, as the extent of diffusion of the papain enzyme into the beef was limited. Thus, migration of the water in the bulk of the specimens to the surface had little, if any consequence on any reaction occurring in the bulk. For the conventionally heated specimen, because the temperature inside the electric furnace was high, any moisture on the surface of the beef sample tended to evaporate, thereby causing the hydrolysis reaction at the surface to be inhibited, as evidenced by the results shown in Fig. 7.7d-ii relative to Fig. 7.7bc-ii.

In summary, compared to conventional heating, microwave heating presents certain features that promote the activity of the papain enzyme in the in vivo case that we attributed to the accelerating effect of the electromagnetic fields of the microwave radiation.

7.5 Microwave-Accelerated Meat Aging Device (Aging Booster)

Aging of beef can increase its commercial value, but in many cases, aging for 40–180 days is required by strictly adjusting the storage method, storage temperature, and storage humidity. However, managing these parameters requires experience and skill, which are difficult to automate. For this reason, dry aging and Vacuum-Aged are known for easier aging. Among these, dry aging can yield higher quality beef aging than other aging methods [18]. In addition, aging is possible in a shorter time than existing aging methods and is completed in 14–35 days. However, aging for 2 weeks or more has a risk of causing meat spoilage, and since dry aging maintains a temperature of 0–4 °C for a long period of time, it takes an air conditioning feed during this period. For this reason, there is a need to reduce the risk of meat spoilage and saving of electricity costs. How can microwaves solve this problem? This question was solved by the fact that microwave heating can be parallel to cooling. Since microwaves can self-heat the sample itself instead of traditional heating that depends on heat conduction, the atmosphere in which the sample is placed can be cooled. [19]. Our previous studies demonstrated this effectiveness in chemical reactions. A radical chemical reaction requires energy to start the reaction and gives heat energy to the reaction system, but as the reaction proceeds, this heat energy leads to a runaway of the chemical reaction. Therefore, while cooling the reaction system with hexane that does not absorb microwaves cooled with dry ice, electromagnetic energy was continuously applied by the microwaves [20]. Even with continuous microwave irradiation, the cooled hexane prevented the sample from rising in temperature and kept the sample at room temperature. As a result, microwaves gave only the energy required to start the reaction, and the reaction system remained cold; hence, the chemical reaction did not run out of control. As a result, a higher synthesis yield could be obtained than by the conventional method.

A microwave device that solves the problems (long time) of the meat aging process (keywords: *cooling and heating*) would be most desirable if it could irradiate the meat inside the refrigerator with microwaves while it is being stored. While cooling the beef placed inside the device from −5 to 10 °C, it is possible to irradiate with microwaves to improve only the temperature inside the meat (Fig. 7.8a). This microwave-promoted beef aging machine (Aging booster) is equipped with a semiconductor microwave generator and has been prototyped by Shikoku Instrumentation Co., Ltd. The semiconductor generator can irradiate the meat using either continuous-wave microwave radiation (CMI) or pulsed microwave irradiation (PMI). Both the temperature of the meat placed within the aging machine and the temperature of the atmosphere inside the refrigerator can be monitored using an optic fiber thermometer.

The configuration of this device was divided into an upper stage and a lower stage that have a refrigerating function, and since it was designed for preliminary experiments, the microwaves irradiated only the contents in the upper stage. The

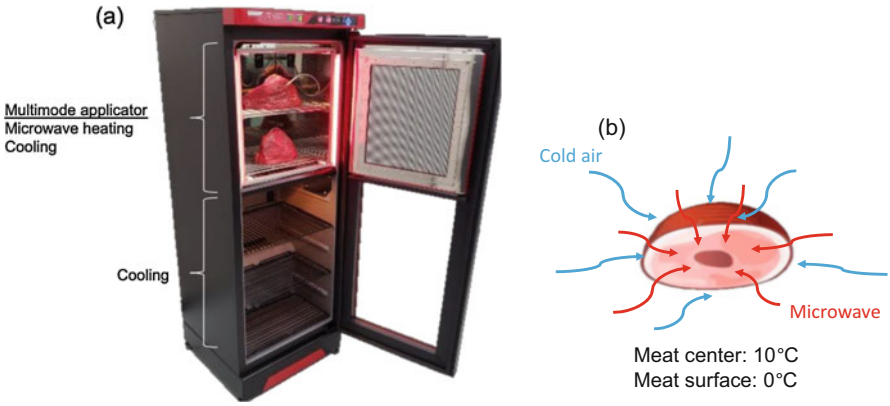

Fig. 7.8 (**a**) Photograph of a microwave-promoted beef aging machine (aging booster) with beef (Shikoku Instrumentation Co., Ltd., Aging booster); (**b**) cartoon illustrating the benefits of meat aging

microwave oscillator was a semiconductor generator, and the generated microwaves could irradiate inside the refrigerator using an antenna. As shown in Fig. 7.8b, the surface of the meat was chilled, and the inside of the meat was heated by the microwaves. Therefore, the cooling of the surface of the meat prevents the growth of bacteria, and the inside of the meat can be aged at an appropriate temperature. In addition, by irradiating with microwaves, the enzyme activity contained inside the meat can be extended by the electromagnetic wave effect or the life span can be extended, and the Umami component (for example, L-glutamic acid or inosinic acid) can be increased from the protein. Note that heating the inside of the meat does not expose it to oxygen, which can significantly reduce the growth of the fungus. As a feature of this device, the lower stage matches the temperature and humidity conditions, and it is possible to simultaneously produce controlled beef without microwave irradiation. The extent of aging could thus be evaluated relative to the control. Note that in the experiments described in this section, no papain enzyme was introduced into the beef as we expected some activity from the original enzyme present in the beef.

In this experiment, commercially available beef thighs (1 kg) from Japan, the United States, and Australia were placed in a microwave aging device, and the tips of the optical fiber thermometers were fixed at the surface and at the center of the beef thighs. Microwave irradiation of the samples lasted about 5 days. For evaluation purposes, the change in the taste of the meat was assessed by examining the increase in the amount of L-glutamic acid (mg) with respect to 1 kg of beef. Microwave irradiation was performed with continuous-wave microwave irradiation (CMI) and pulsed microwave irradiation (PMI). The 1-s PMI pulse wave consisted of 0.1 s with the microwaves ON and 0.9 s with the microwaves OFF, while for the 10-s PMI pulse, the microwaves were ON for 1 s and OFF for 9 s; for the 30-s PMI pulses, the microwaves were ON for 3 s and OFF for 27 s. Under all microwave irradiation

Table 7.1 Comparison of the temperatures at the beef center and the microwave applied power (continuous-wave microwave irradiation; atmospheric temperature fixed at 0 °C)

Microwave applied power/Watt	Temperature at the center of the meat/°C
1	2.8
3	5.9
5	11.2
10	14.5

conditions, the cooler inside the applicator and the microwave heating output were set such that the temperature on the surface of the meat was 2 °C and the temperature inside the meat was 7 °C.

The relationship between the microwave output and temperature consumed by the microwave-promoted beef aging machine was investigated further. The temperature inside the microwave-promoted beef aging machine was set to 0 °C, while the microwave output under continuous-wave microwave irradiation (CMI) conditions was set at 1, 3, 5, and 10 W; temperature changes at the center and at the surface of beef were monitored. Since the core temperature of the beef becomes constant several hours after microwave irradiation, the temperature was monitored every 30 min; the average temperature is reported in Table 7.1. Since the ambient temperature was set to 0 °C, the surface temperature of the beef was 0 ± 2 °C. However, by irradiating with microwaves, the central part of the beef was heated to 2.8 °C with irradiating using 1-W microwaves, to 5.9 °C with 3-W microwaves, 11.2 °C with 5-W microwaves, and 14.6 °C with 10-W microwaves and then kept warm. In addition, the temperature at the center of the beef could be kept above 10 ° C with a power consumption of only 5 W.

Accordingly, four types of microwave irradiation were performed, and the aging degree of the meat was evaluated from the amount of L-glutamic acid present. By monitoring the temperature changes on the surface and inside the meat from the cooling and the microwave irradiation for 5 days, the temperature on the surface of the meat was adjusted to 2 ± 2 °C and the temperature inside the meat was adjusted to 6 ± 4 °C. Figure 7.9 shows the color change of the meat after 5 days. Before aging, all the samples showed a bright red color attributable to myoglobin; however, after aging, the meat sample turned dark brown under all microwave irradiation conditions owing to the formation of metmyoglobin. In particular, the very surface was dry and hardened. It should also be noted that the drying of the inside of the meat did not occur as much as it occurred at the surface.

Changes in the amount of L-glutamic acid in the beef that had been irradiated under each of the microwave conditions for 5 days were consequently assessed. Since the measurements were expected to change depending on the part of the beef, the dry and hardened parts of the meat surface were removed.

The amount of L-glutamic acid was measured by dividing the remaining portion into a surface (about 0.5 cm from the surface) and an inside (about 1.5 cm from the surface) (see Fig. 7.10). In addition, the amounts of L-glutamic acid at the same positions were also measured for nonirradiated beef samples (control conditions) by

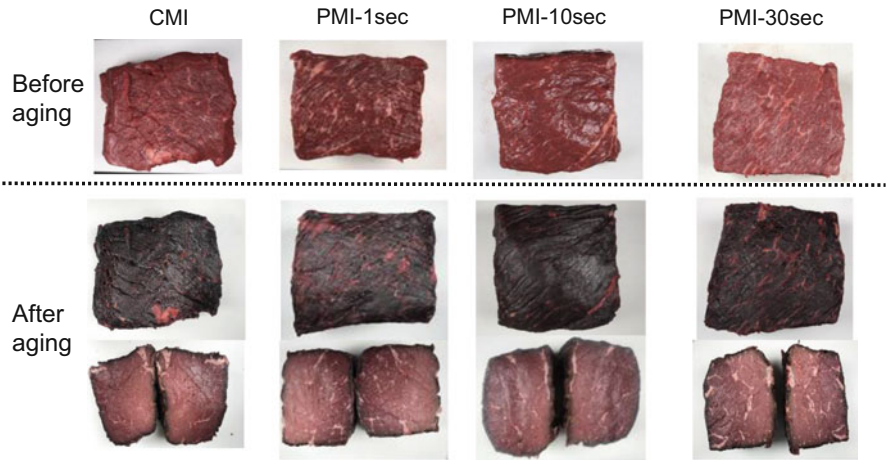

Fig. 7.9 Photographs of meat before aging and after aging by microwave irradiation at an atmospheric temperature of 0 °C. Upper part: photographs of the meat surface before microwave irradiation (i.e., before aging). Middle part: photographs of the meat surface after aging for 5 days. Lower part: photographs of the cross sections after aging for 5 days. Continuous-wave microwave irradiation (CMI). Pulsed microwave irradiation: PMI-1 sec with 0.1 sec microwaves ON and 0.9 sec microwaves OFF; PMI-10 sec with 1 sec microwaves ON and 9 sec microwaves OFF; and PMI-30 sec with 3 sec microwaves ON and 27 sec microwaves OFF

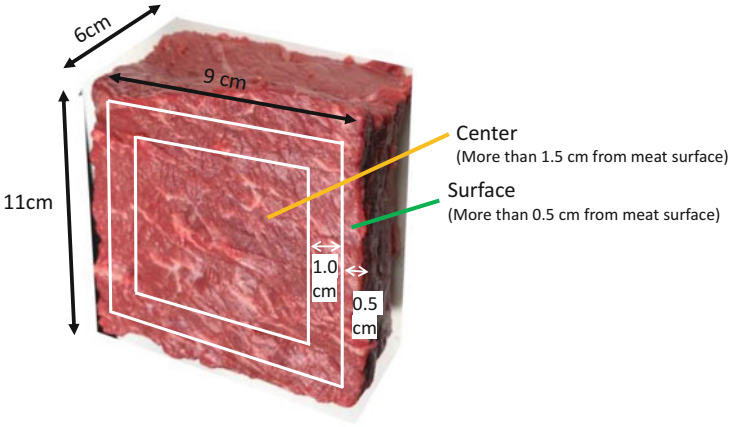

Fig. 7.10 Definition of the positions of meat sampling after removing the dried and solidified parts of the meat surface. Surface sample: ca. 0.5 cm from the surface; inside ca. 1.5 cm from the surface

matching the temperature conditions. Measurements were performed no less than three times; the average quantities of the L-glutamic acid are reported in Fig. 7.11.

The increase in the amount of L-glutamic acid in beef under the control conditions was 1.03 times on the inside and 1.04 times on the surface. Clearly, the increase in the amount of L-glutamic acid was negligible. On the other hand, continuous-wave

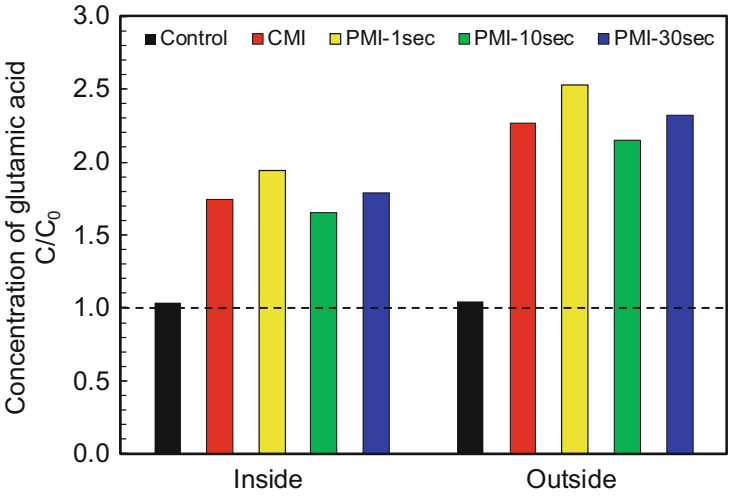

Fig. 7.11 Quantities of L-glutamic acid in the internal (inside) and at the surface (Outside) of the beef samples (1 kg) after aging for 5 days under various microwave irradiation conditions using a microwave-promoted beef aging machine. The temperature on the surface of the meat was 2 °C, and the temperature inside the meat was 7 °C. Continuous-wave microwave irradiation (CMI); pulsed waves: PMI-1 sec with 0.1 sec microwaves ON and 0.9 sec microwaves OFF, PMI-10 sec with 1 sec microwaves ON and 9 sec microwaves OFF, and PMI-30 sec with 3 sec microwaves ON and 27 sec microwaves OFF

microwave irradiation (CMI) increased the quantity by a factor of 1.8 inside the meat sample and 2.3 times at the surface. Microwave irradiation clearly increased the amount of L-glutamic acid, especially on the surface. By comparison, when pulsed microwave irradiation was performed, the quantity of L-glutamic acid increased by about a factor of ca. 2.0 inside and by a factor of ca. 2.5 at the surface in the area where the 1-s pulsed microwaves were the highest. In addition, the power consumption of the PMI can be lower than that of the CMI. The difference is small, but when you put together the 5 days, the advantage of power consumption using pulses seems to be great. L-Glutamic acid showed a higher increase on the surface than in the central part. We thus infer that this is due to the penetration depth of the microwaves. That is, although the internal temperature was to some extent kept at the same temperature as at the surface, the penetration depth of the microwaves into the beef before aging was 0.86 cm, whereas the penetration depth at the surface after 2 days was 4.70 cm. In the early stage of aging, the microwaves irradiated up to about 1 cm from the surface of the meat, following which heating proceeds to the center by heat diffusion. Therefore, the promotion of enzymes by the electromagnetic wave effect of the microwaves occurs about 1 cm from the surface of beef. Consequently, we conclude that the inside is aged by heat in the same manner as normal heating. As the aging of beef progressed, the water content decreased allowing the microwaves to penetrate further inside. Thus, as the microwave reached the center of the beef, the original beef enzyme was activated both thermally and

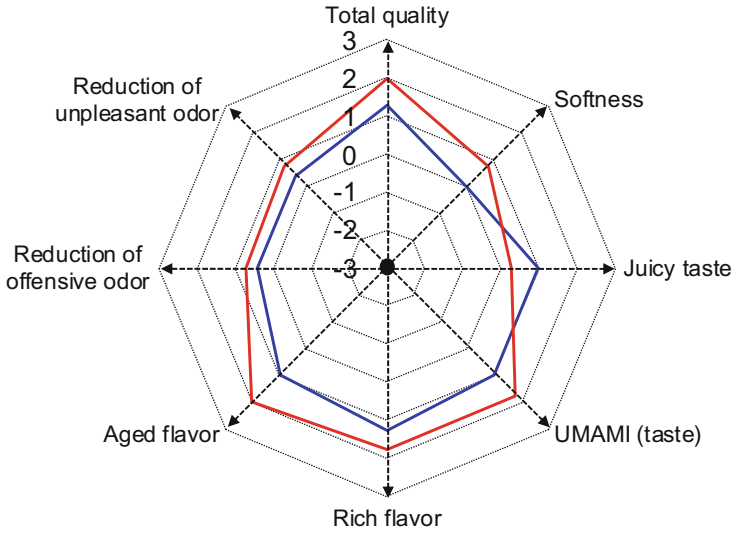

Fig. 7.12 Sensory test of thigh meat in Holstein aged for 5 days by a microwave aging method (continuous-wave microwave irradiation; red line) and a conventional dry aging method (stored at an ambient temperature of 0 °C. while blowing air; blue line). Total quality and 7 viewpoints using a score from −3 to +3 (softness, juicy taste, Umami (taste), rich flavor, aged flavor, reduction of offensive odor and reduction of unpleasant odor) were examined; see http://www.agingbooster.com/#Potential

electromagnetically so as to further enhance the amount of L-glutamic acid. A proper amount of L-glutamic acid improves the Umami (i.e., the taste) and also improves the quality of meat tasting.

Thigh meat from Holstein cattle was aged for 5 days by a microwave aging method and by a more conventional dry aging method (stored at an ambient temperature of 0 °C while blowing air) to conduct the sensory test. The evaluation was made by three inspectors from the Japan's Meat Science & Technology Institute, with beef before aging (counts as a 0 point) and after aging on the basis of 7 viewpoints using a score from −3 to +3 points: (1) softness, (2) juicy taste, (3) Umami, (4) rich flavor, (5) aged flavor, (6) reduction of offensive odor, and (7) reduction of unpleasant odor. Figure 7.12 shows the average of the results from the three inspectors. The taste of beef before aging is represented by the dotted line at position 0 on the radar chart. In all items except juiciness, the microwave aging method was highly evaluated. In particular, the Umami, rich flavor, and aged flavor scored highest.

7.6 Prospects for the Future

Changes in enzyme activity using microwaves and its application to food technology are expected. The microwave specific heating and electromagnetic effect(s) seem to provide a food culture that cannot be achieved by conventional concepts. In particular, the promotion of enzymes by the microwaves' electromagnetic wave effect is valuable for the use of microwaves in food technology. For example, the microwave-promoted beef aging machine can heat the beef in a cooled state. That is, the surface of the beef can be cooled to prevent the meat from spoiling, and the inside of the meat can be aged with electromagnetic wave energy and heat energy. In the next stage, it will be necessary to elucidate the principle of the interaction(s) between microwaves and biological samples such as enzymes. While pursuing innovation as a new food culture of food processing and cooking, it will also be necessary to elucidate the mechanism in order to increase efficiency and pursue new phenomena.

Acknowledgements We wish to thank Mr. H. Soga of Shikoku Instrumentation Co., Ltd. (Japan) for technical support.

References

1. Banik S, Bandyopadhyay S, Ganguly S. Bioeffects of microwaves – a brief review. Bioresour Technol. 2003;87:155–9.
2. Stavinoha WB, Pepelko B, Smith PW. Microwave radiation to inactivate cholinesterase in the rat brain prior to analysis for acetylcholine. Pharmacologist. 1970;12:257.
3. Stavinoha WB, Weintraub ST, Modak AT. The use of microwave heating to inactivate cholinesterase in the rat brain prior to analysis for acetylcholine. J Neurochem. 1973;20:361–71.
4. Yoshimura T, Mineki S, Ohuchi S. Microwave-assisted enzymatic reactions. In: Horikoshi S, Serpone N, editors. Microwaves in catalysis: methodology and applications. Chapter 11. Weinheim: Wiley-VCH Verlag GmbH Co. KGaA; 2015. isbn:978-3-527-33815-3.
5. Young DD, Nichols J, Kelly RM, Deiters. A. Microwave activation of enzymatic catalysis. J Am Chem Soc. 2008;130:10048–9.
6. Damm M, Nussholds C, Cantillo D, Rechberger GN, Gruber K, Sattler W, Kappe CO. Can electromagnetic fields influence the structure and enzymatic digest of proteins? A critical evaluation of microwave-assisted proteomics protocols. J Proteomics. 2012;75:5533–43.
7. Roy I, Gupta MN. Applications of microwaves in biological sciences. Curr Sci. 2012;85:1685–93.
8. Parker M-C, Besson T, Lamare S, Legoy M-D. Microwave radiation can increase the rate of enzyme-catalysed reactions in organic media. Tetrahedron Lett. 1996;37:8383–6.
9. Pramanik BN, Mirza UA, Liu YH, Bartner PL, Weber PC, Bose AK. Microwave-enhanced enzyme reaction for protein mapping by mass spectrometry: a new approach to protein digestion in minutes. Protein Sci. 2002;11:2676–87.
10. Elhafi G, Naylor CJ, Savage CE, Jones RC. Microwave or autoclave treatments destroy the infectivity of infectious bronchitis virus and avian pneumovirus but allow detection by reverse transcriptase-polymerase chain reaction. Avian Pathol. 2004;33:303–6.
11. Lin S, Yun D, Qi D, Deng C, Li Y, Zhang X. Novel microwave-assisted digestion by trypsin-immobilized magnetic nanoparticles for proteomic analysis. J Proteome Res. 2008;7:1297–307.

12. Shaw KJ, Docker PT, Yelland JV, Dyer CE, Greenman J, Greenway GM, Haswell SJ. Rapid PCR amplification using a microfluidic device with integrated microwave heating and air impingement cooling. Lab Chip. 2010;10:1725–172.
13. Ponne CT, Bartels PV. Interaction of electromagnetic energy with biological material – relation to food processing. Radiat Phys Chem. 1995;45:591–607.
14. Horikoshi S, Osawa A, Abe M, Serpone N. On the generation of hot-spots by microwave electric and magnetic fields and their impact on a microwave-assisted heterogeneous reaction in the presence of metallic pd nanoparticles on an activated carbon support. J Phys Chem C. 2011;115:23030–5.
15. Cronin NJ. Microwave and optical waveguides. Great Britain: Institute of Physics Publishing; 1995. p. 27–40.
16. Horikoshi S, Watanabe T, Narita A, Suzuki Y, Serpone N. Probing the effect(s) of the microwaves' electromagnetic fields in enzymatic reactions. Sci Rep. 2019;9:8945.
17. Horikoshi S, Watanabe T, Narita A, Suzuki Y, Serpone N. Effect of microwave radiation on the activity of catalase. Decomposition of hydrogen peroxide under microwave and conventional heating. RSC Adv. 2016;6:48237–44.
18. Savell JW. Dry-aging of beef executive summary. https://www.beefresearch.org/Media/BeefResearch/Docs/dry_aging_of_beef_08-20-2020-28.pdf
19. Horikoshi S, Schiffmann RF, Fukushima J, Serpone N. Microwave chemical and materials processing: a tutorial. Japan: Springer; 2017.
20. Horikoshi S, Tsuzuki J, Kajitani M, Abe M, Serpone N. Microwave-enhanced radical reactions at ambient temperature. Part 3. Highly selective radical synthesis of 3-cyclohexyl-1-phenyl-1-butanone in a microwave double cylindrical cooled reactor. New J Chem. 2008;32:2257–62.

Chapter 8
Controlling Weeds with Microwave Energy

Graham Brodie

Abstract Herbicide resistance has prompted interest in microwave weed management as an alternative weed control strategy. Microwave energy can heat soil to deactivate the weed seed bank in the soil, or it can be used to directly heat already emerged weeds, causing death of the plants. This chapter explores the prospects for both soil treatment and plant treatment in the quest for an alternative weed management technology.

Keywords Weeds · Weed seeds · Soil treatment · Microwave heating

8.1 Introduction

Weeds can be defined as plants that are not valued where they are growing. For example, in some production systems, such as grazing systems, plants like annual ryegrass (*Lolium rigidum* Gaudin) is valued for stock grazing [1]; however, in a cropping system, this species is a significant weed [2, 3].

Weed management, in modern agricultural and environmental systems, usually relies on herbicide application. Glyphosate is the world's most widely used herbicide [3], because it controls a broad spectrum of annual and perennial weeds. Unfortunately, herbicide resistance, especially resistance to glyphosate in many weed species, is becoming a wide spread problem [4–6], and multiple herbicide resistances in several economically important weed species have also been widely reported [2]. The loss of herbicide efficacy has a significant impact on crop yield potential.

G. Brodie (✉)
Faculty of Veterinary and Agricultural Sciences, The University of Melbourne, Parkville, VIC, Australia
e-mail: grahamb@unimelb.edu.au

S. Horikoshi et al. (eds.), *Agritech: Innovative Agriculture Using Microwaves and Plasmas*, https://doi.org/10.1007/978-981-16-3891-6_8

8.2 Weed Impacts on Crop Production

Crop yield gaps are a significant issue for food security and agricultural sustainability. Crop yield gaps are defined as the differences between the optimal yield potential of a crop and its actual yield [7]. Although there are many contributors to crop yield gaps, weeds make a significant contribution to this gap. Weeds compete with crop plants for sunlight, moisture, and nutrients. Some crop ecology studies have demonstrated that competition from weeds can reduce the potential yield of some crops by 35–55% [8, 9]. In some extreme cases, the crop plants are outcompeted by weeds and potential yield falls to practically zero.

Modern weed science is based on the chemistry that emerged from the Second World War [10]. Herbicide-based weed management has helped establish minimum till cropping systems [3]. According to Menalled et al. [10], herbicide-based weed management is founded on (1) the precautionary principle, where the most lethal treatment is generally adopted; (2) the desire for rapid and effective response to the treatment; and (3) an expectation of complete eradication. Unfortunately, as Menalled et al. [10] point out, the success of this approach and the reluctance to conduct integrated and multidisciplinary research have resulted in strong selection pressure for herbicide-resistant biotypes.

It is over 60 years since Harper predicted the development of resistance to herbicides [11]. Globally, there are over 400 weed species that have developed resistance to herbicides [6]. The development of resistance is an inevitable consequence of reliance on chemistry for weed control [10].

System analysis techniques have been applied to an agricultural cropping system to better understand the impact of weeds on crop production [12]. Equation (8.1) approximates the crop yield potential in response to weed infestation and herbicide application. This model also attempts to account for herbicide resistance within the weed population and the potential toxicity of the herbicide to the crop itself,

$$Y = Y_o \left\{ 1 - \frac{I \cdot [W(1-N-D_o) - E_m + I_m] \cdot \left[1 - S \cdot e^{\frac{-ag^2}{2}} + S \cdot e^{\frac{-ag^2}{2} - \lambda H} \right]}{100 \left\{ e^{ct} \left[1 + e^{-\left(\frac{t-t_o}{d}\right)} \right] + \frac{I \cdot [W(1-N-D_o) - E_m + I_m] \cdot \left[1 - S \cdot e^{\frac{-ag^2}{2}} + S \cdot e^{\frac{-ag^2}{2} - \lambda H} \right]}{A_w} \right\}} + aH^2 - bH \right\}, \tag{8.1}$$

where I is the percentage yield loss as the weed density tends towards zero (= 0.38 [13]), W is the viable seed bank, N is the natural death rate for the whole population (Note: this is expressed as a fraction of the initial seed bank population W_o), D_o is a fraction of the seed population developing dormancy (Note: this is expressed as a fraction of the initial seed bank population W_o), E_m is the seed emigration out of the area of interest, I_m is the seed immigration into the area of interest, S is the initial portion of the weed population that is susceptible to herbicides, a is the selection

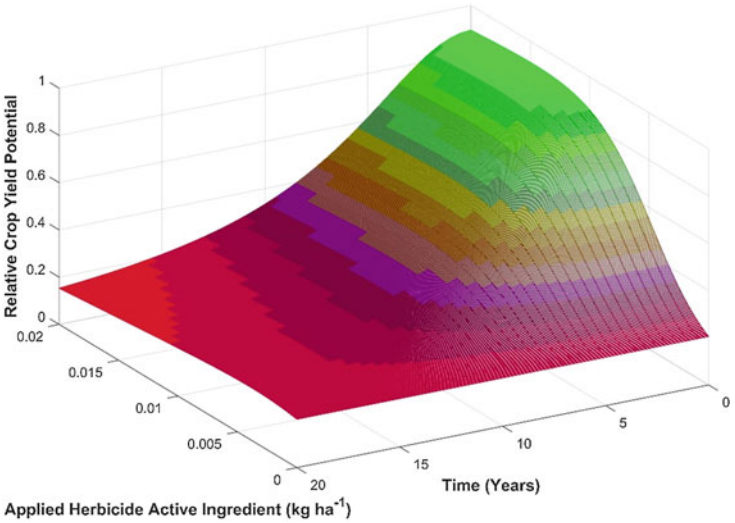

Fig. 8.1 Response surface for potential crop yield as a function of both herbicide application and generational change in the weed population

pressure for herbicide resistance in the system, g is the number of weed generations in the study period, c is the rate at which I approaches zero as time approaches ∞ (= 0.017 [13]), t is the time difference between crop emergence and weed emergence, t_o is the time for 50% germination of the viable seed bank, d is the slope of the seed bank recruitment curve at to, λ is the efficacy of the herbicide killing action, H is the herbicide dose, and A_w is the percentage yield loss as weed density approaches ∞ (= 38.0 [13]).

Equation (8.1) was coded into a simple cropping system model using the MatLab® software platform. Using data published by Bosnić and Swanton [13] and Yin et al. [14] for Rimsulfuron herbicide and assuming an initially small resistant population (i.e. $S = 0.9999$), a seed mortality rate of 10% each year, and a slightly positive selection coefficient of ($a = 0.002$) for herbicide resistance [15], the system transfer function was used to analyse the effect of a single herbicide application on crop yield potential. The transfer function was also used to forecast the long-term crop yield potential, if only a single herbicide type was used during this time.

It is possible to visualise the influence of both herbicide application and generational development of herbicide resistance in a response surface, as shown in Fig. 8.1. This illustrates that initially, there is a significant response in crop yield potential to the application of herbicides; however, the transfer function also predicts that significant herbicide resistance will occur within 15 generations (Fig. 8.1), as was also predicted by Thornby and Walker [16]. This is apparent when looking at how the relative crop yield potential reduces with time in Fig. 8.1. After 15–20 years

of using the same herbicide control system, the model outlined in Eq. (8.1) suggest that further herbicide application will be ineffectual.

In addition to growing issues with herbicide resistance, the International Agency for Research on Cancer (IARC), which is part of the World Health Organisation (WHO), has also concluded that glyphosate is probably carcinogenic to humans [17]. Other authors have also highlighted the potential hazard to human health of long-term exposure to herbicides and pesticides [18–23]; therefore, there has been growing interest in non-herbicidal control of weeds.

8.3 Tillage

Prior to the introduction of herbicides in the 1940s, weed control was often achieved through tillage [24]. Hand hoeing of weeds has probably been undertaken since agriculture began; however, Giampietro and Pimentel [25] suggested that adult males can sustain a power output of only 90 W, whilst adult women can sustain a 60 W power output. It has also been shown that humans require approximately 100 J of food energy to produce 1.0 J of work; therefore, it has been estimated that hand hoeing requires newly 11 GJ of energy per hectare [26]. Giampietro and Pimentel [27] demonstrate that using a 50-HP tractor for weed scarifying can reduce this energy investment to about 4.1 GJ ha^{-1}.

Tillage usually results in intense soil disturbance, which often leads to soil degradation, erosion, and loss of productivity [24]; therefore, modern agriculture is focused on reducing tillage. Therefore, weed management strategies need to be effective, but without engaging the soil.

8.4 Thermal Weed Control

Thermal weed control applies heat directly to the weed, which quickly raises the temperature of the moisture in the plants' cambium cells. The rapid expansion of this moisture causes the cell structure to rupture, preventing nutrients and water from entering the stalk and leaves [28]. Several strategies for thermal weed control are being explored. These include flaming, steam treatment, applying infra-red radiation, applying ultraviolet radiation, using lasers, and microwave weed treatment.

Flaming, steam, and infra-red radiation treatments are the most common thermal weed control methods; however, these methods rely on the application of heat to the surface of the plants, followed by conduction of this heat into the plant material. The final temperature profile in the plants depends on the material's thermal diffusion properties [29] and the influence of moisture transport, which often hinders the convective heating process [30]. Unlike conventional heating systems, one key benefit of microwave heating is speed. The origin of this speed is the volumetric interactions between the microwave's electric field and the material [31].

8.5 Microwave Weed Management

It has been known since the 1920s that high-frequency electromagnetic waves affect plants [32]. Many of the earlier experiments explored radio frequency (RF) effects on seeds [32]. Low energy treatment of seeds can increase germination and vigour of the emerging seedlings [33–35]. Similar increases in plant vigour and maturation have also been reported when young plants are exposed to low energy doses of electromagnetic radiation [36, 37].

Magone [38] studied duckweed (*Spirodela polyrhiza*) grown in flasks, which were located 2 km from a radio station transmitter. The frequency and intensity of the radiation used were 156–162 MHz and 0.1–1.8μW cm^{-2}. Generally, the vegetative reproduction rate of plants that were exposed to the electromagnetic radiation for between 24 and 88 h was accelerated by between 105% and 195%, compared with the control plants, during the first 20 days after exposure. This phenomenon has also been observed by Grundler et al. [39] in yeast exposed to 40 to 60 GHz microwave fields.

High energy doses result in seed death [32, 40, 41]. Davis et al. [42, 43] were amongst the first to study the lethal effect of microwave heating on seeds. They developed a set of field prototypes, called "Zappers." Their final prototype, the Zapper III, operated at a frequency of 2.45 GHz and successfully demonstrated that microwave treatment could both kill weed seeds in the soil and emerged weed plants [44, 45].

Later, Brodie and Hollins [46] demonstrated that microwave treatment kills both emerged weed plants and their seeds in the soil. Seed treatment requires higher energy applications than emerged plant treatment and is conceptually like soil fumigation treatments. Microwave treatment of growing plants requires far less energy than seed treatment and can therefore be compared to the application of herbicide.

8.6 Soil Treating for Weed Seed Control

Microwave treatment of the soil, using a horn antenna as the applicator, can inactivate weed seeds at various depths [45–48]. The efficacy of the treatment depended on the soil type, the seed burial depth, the microwave treatment energy density at the soil surface, and whether the soil had been irrigated prior to treatment (Fig. 8.2). Irrigation increases the dielectric properties of the loam soil [49], used by Wayland et al. [45], resulting in shallower microwave heating; therefore, seeds that were buried deeper in the soil were less affected by the microwave heating when the soil was moist [45, 48].

Brodie and Hollins [46] also found that moisture content of soil affected the susceptibility of seeds to microwave treatment when using a 2.45 GHz microwave system feeding into a horn antenna (Fig. 8.3); however, the sandy soil they used

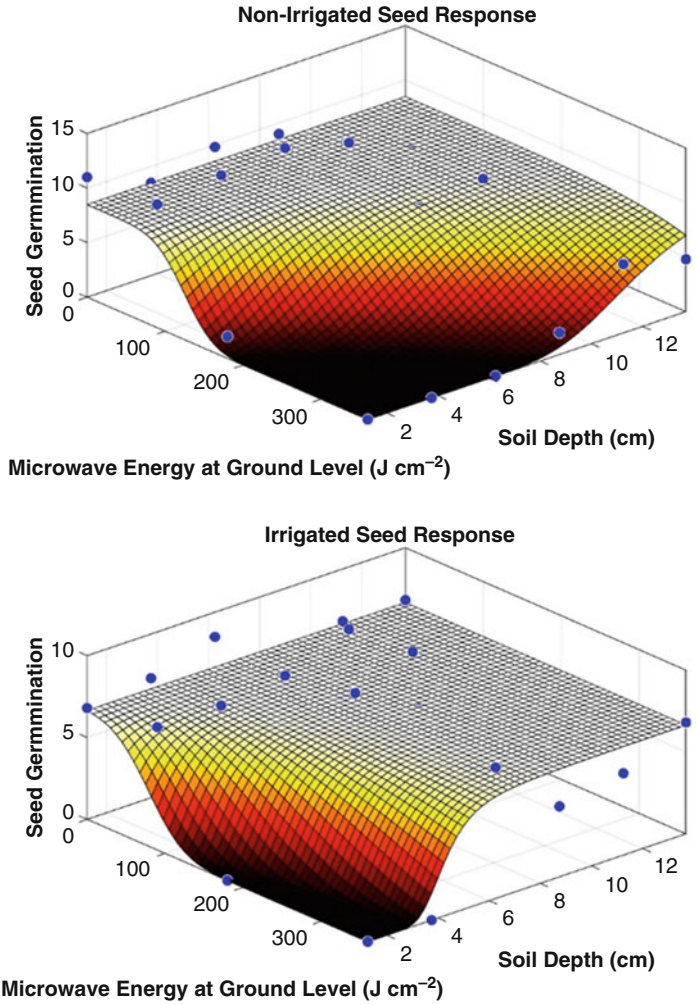

Fig. 8.2 Response of weed seeds in the clay-loam soil to microwave energy, as a function of applied energy density, burial depth, and irrigation status (Sources: [45, 48])

allowed substantial heating to 10 cm depth, when it was moist. The loam soil, used by Wayland, et al. [45], restricted heating to the top 5 cm when it was moist.

Analysis of these data reveals that 150–500 J cm^{-2} of microwave energy, at the soil surface, can control weed seeds in the top 4–6 cm of soil. This is equivalent to between 15 and 50 GJ ha^{-1} of microwave energy.

The impact of microwave treatment on weed seeds, as a function of applied microwave energy and seed depth, can be described by

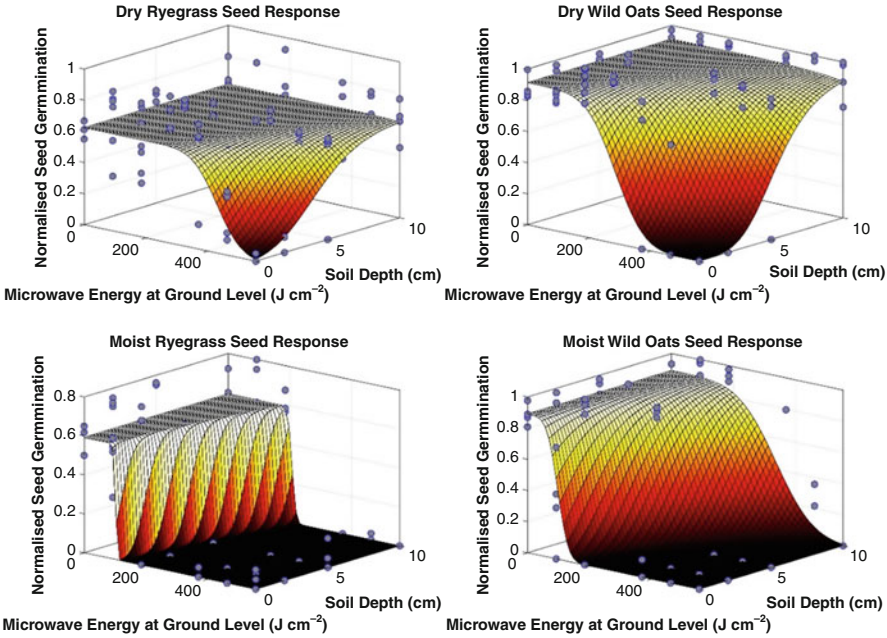

Fig. 8.3 Response of weed seeds in the sandy soil to microwave energy, as a function of applied energy density, burial depth, and irrigation status (Sources: [41, 50])

$$S = S_o \cdot erfc\left\{a\left[\Psi \cdot e^{-2\alpha d}\right] - b\right\}, \tag{8.2}$$

where S_o is the natural survival rate of seeds in the soil, Ψ is the applied microwave energy density (J cm^{-2}), α is the attenuation factor for the microwave field in the soil, d is the depth in the soil (m), a and b are constants that are determined for each weed seed species, and $erfc(z) = 2\int_z^\infty \frac{e^{-u^2}}{\sqrt{\pi}} \cdot du$. The attenuation factor is determined by

$$\alpha = \frac{\omega}{c}\sqrt{\frac{\kappa'}{2}\left[\sqrt{1+\left(\frac{\kappa''}{\kappa'}\right)^2} - 1\right]}, \tag{8.3}$$

where ω is the angular frequency of the microwave fields (Rad s^{-1}), c is the speed of light (m s^{-1}), κ' is the dielectric constant of the soil, and κ" is the dielectric loss factor for the soil.

Microwave soil heating reduces weed emergence. Microwave soil treatments provide weed-free conditions for extended periods of up to 400 days without seedling emergence [51]. Soil treatment also improves crop yield, with crop yield increases of between 21% and 84%, compared with hand weeded plots, under field

conditions [52]. Other unpublished longitudinal studies have shown weed-free conditions for more than 250 days.

8.7 Effect of Soil Treatment on Crop Yield

In various pot experiments, it has been demonstrated that, in addition to significantly reducing weed emergence, microwave soil treatment significantly increases crop yield, for crops that are planted into the treated soil after it has cooled [52–54]. Table 8.1 presents a summary of an extensive experimental study programme investigating the impact of microwave soil heating on the yield of crops planted into the treated soil. Two of the pot trials, listed in Table 8.1, included longitudinal studies where a single microwave treatment was imposed, but crops were grown in the same undisturbed pots for 2 or 3 years after treatment.

The application of microwave energy to the soil achieves weed seed bank deactivation; however, this strategy also changes the soil biota and nutrient profile in favour of higher crop yield, when crops are planted into microwave-treated soil. In multiple field trials, an application of approximately 320 J cm^{-2} of microwave energy achieves a 70–80% reduction in weed establishment. In addition, there was a significant increase in crop yield, which in one of the trials achieved a ten-fold increase in nitrogen use efficiency, and a 37% higher water use efficiency [61]. There is also evidence that the soil treatment provided persistent effects, beyond a single season [60] both in pot experiments and in field conditions.

The effects of microwave soil treatment are not due simply to the depletion of the weed seed bank and reduced competition from weeds. In several of the experiments, reported in Table 8.1, a hand-weeded control was included in the experiment. In these cases, the yield of the highest microwave treatment was significantly higher than this hand-weeded control. There is growing evidence that microwave soil treatment also changes the soil biota and nutrient profile in favour of increases in crop yield [61]. In recent experiments, it has been shown that microwave soil treatment significantly changes the soil microbial community. Initially, the total number of bacterial and fungi is significantly reduced [47, 62, 63]; however, although MW treatments alters the soil microbial community, beneficial soil microbes exhibit faster recovery over time [63], providing benefits to the growing crops and leading to higher yields.

Although there is evidence that microwave soil treatment can provide significant weed seed deactivation and improvements in crop yield, with even prolonged effects being observed in pot and field experiments, the long-term efficacy of a single microwave treatment event needs to be better understood.

Table 8.1 Summary of multiple pot and field experiments investigating the impact of microwave soil treatment on subsequent crop yield (Sources: [54–60]). Some unpublished data are also included in this table

Treatment		Untreated control	Herbicide	Hand weeded	Microwave treatment (J cm^{-2})			LSD ($P = 0.05$)	Change from hand weeded/control
					80	160	320		
Pot trials									
Canola yield (g pot^{-1})		0.27[a]	–	0.56[a]	0.36[a]	1.25[b]	1.95[c]	0.55	250%
Wheat yield (g pot^{-1})		0.66[a]	–	0.67[a]	0.68[a]	0.75[a]	1.25[b]	0.30	87%
Longitudinal wheat experiment	Year 1 yield (g pot^{-1})	5.1[a]	–	–	–	–	7.5[b]	0.83	47%
	Year 2 yield (g pot^{-1})	16.0[a]	–	–	–	–	23.5[b]	1.79	47%
	Year 3 yield (g pot^{-1})	12.8[a]	–	–	–	–	16.5[b]	1.48	29%
Rice grain yield (g pot^{-1})		40.0[a]	–	41.3[a]	43.3[a]	59.0[ab]	64.0[b]	18.9	55%
Longitudinal rice experiment	Year 1 yield (g pot^{-1})	16.0[a]	–	–	–	22.4[b]	28.7[c]	1.5	79%
	Year 2 yield (g pot^{-1})	28.4[a]				32.2[b]	39.5[c]	1.4	39%
Maize (g pot^{-1})		5.3[a]	–	6.6[a]	–	10.3[ab]	12.8[b]	4.8	92%
Strawberries (fruit pot^{-1})		2.5[a]	–	–	–	–	5.0[b]	2.1	100%
Field trials									
Rice (t ha^{-1})—Field experiment 1 (2015/2016)		7.5[a]	–	–	–	–	10.1[b]	2.0	35%
Rice (t ha^{-1}) field experiment 2—(2016/2017)—Cold affected		2.1[a]	–	–	–	–	3.9[b]	1.3	84%
Rice (t ha^{-1})—Field experiment 3 (2016/2017)		7.7[a]	–	–	–	–	9.1[b]	1.2	19%
Wheat (t ha^{-1})		5.7[a]	6.2[a]	6.7[b]	–	–	7.8[b]	1.4	16%

(continued)

Table 8.1 (continued)

Treatment	Untreated control	Herbicide	Hand weeded	Microwave treatment (J cm^{-2})			LSD ($P = 0.05$)	Change from hand weeded/control
				80	160	320		
Tomato (t ha^{-1})	64.1[a]	65.2[a]	–	–	–	89.6[b]	24.7	37%
Strawberry runner (plants m^{-1})	53.8[a]	–	–	–	–	74.0[b]	10.5	38%

8.8 Long-Term Efficacy

Weed control is closely linked to seed bank depletion. Neve et al. [64] suggested that the recruitment of seedlings from the seed bank can be described by

$$S = \frac{W(1 - N - D_o) - E_m + I_m}{\left[1 + e^{-\left(\frac{t - t_o}{d}\right)}\right]}, \tag{8.4}$$

where W is the viable seed bank, N is the natural death rate for the whole population (Note: this is expressed as a fraction of the initial seed bank population W_o), D_o is a fraction of the seed population developing dormancy (Note: this is expressed as a fraction of the initial seed bank population W_o), E_m is the seed emigration out of the area of interest, I_m is the seed immigration into the area of interest, t is the time, t_o is the time for 50% germination of the viable seed bank, and d is the slope of the seed bank recruitment curve at t_o.

These recruited seedlings, if they grow to maturity, replenish the seed bank in accordance with [64]

$$W = \frac{g_s \cdot S}{\left[1 + \frac{g_s \cdot S}{B}\right]}, \tag{8.5}$$

where g_s is the number of seeds shed per plant and B is the maximum number of seeds that can be produced per square metre.

Using quite moderate values for the various parameters in Eqs. (8.4) and (8.5), as outlined in Table 8.2, Fig. 8.4 illustrates the impact of significantly reduced seed bank densities on weed seedling recruitment over time. In this illustration, when the initial weed seed bank is reduced to 2–4 seeds per square metre, the potential weed density after 2 years may be slightly reduced, compared with higher weed seed densities; however, by the third year, there is no significant reduction in weed

Table 8.2 Parameter values used in the model for weed recruitment over time

Parameter	Description	Value in model
N	Natural death rate of seeds in the seed bank	0.1
t	Time to plant maturity	120 days
t_o	Time for 50% germination of the viable seed bank	38 days [64]
d	Slope of the seed bank recruitment curve at t_o	10.25 seedlings per day [64]
g	Mean seed production per weed plant	500
B	Maximum number of seeds that can be produced per m^2	58,300
D_o	Seeds entering dormancy each year	20% of the new seeds
E_m	Emigration of seeds out of the area of interest	30% of the new seeds
I_m	Immigration of seeds into the area of interest	2 seeds m^{-2}

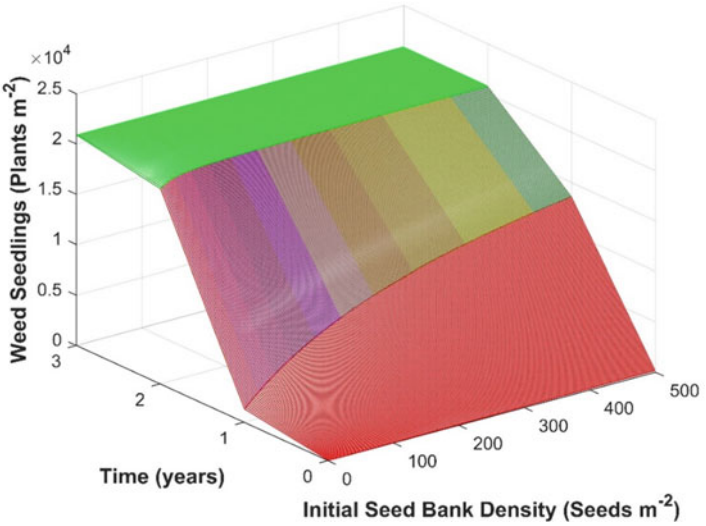

Fig. 8.4 Seedling recruitment from the weed seed bank as a function of initial seed density and time

populations compared with higher initial seed bank populations. Therefore, a once-off soil seed bank treatment will not have a long-term effect on weed numbers in a treated area. Therefore, ongoing weed management is needed. Microwave treatment of emerged weed plant could provide a viable weed control option.

8.9 Treating Emerged Weeds

Microwave heating depends on the interaction of the microwave's electric field with a dielectric material; therefore, the dielectric properties of the heated material have a profound effect on the heating potential. Because water plays such an important role in many organic systems, the dielectric properties of these materials are dependent on the water content (Fig. 8.5). It is evident that fresh vegetation has very high dielectric properties; therefore, microwave fields interact strongly with fresh plant material.

A meta-study (Fig. 8.6) of published data [45, 46, 48, 65] reveals that microwave treatment of emerged weed plants, including eleven species, with a stationary horn antenna, can be described by equations of the form

$$S = a \cdot erfc[b(\Psi - c)], \tag{8.6}$$

where S is the survival rate and a, b, and c are constants appropriate for each species of weed.

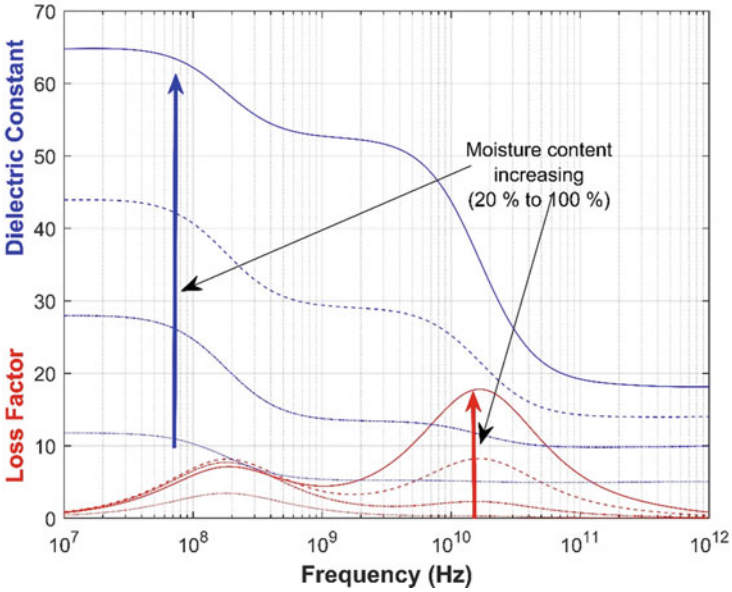

Fig. 8.5 Dielectric properties of vegetative materials as a function of frequency and moisture content

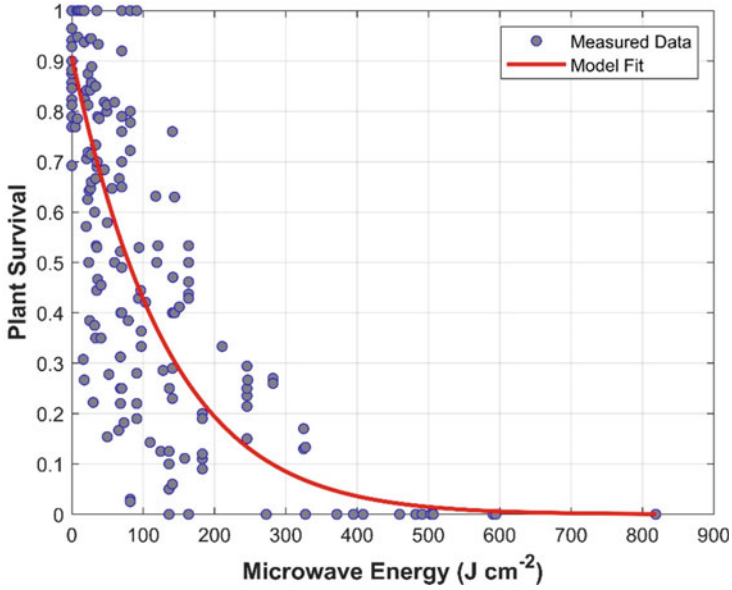

Fig. 8.6 Response of 11 species of weed to microwave energy, delivered using a stationary horn antenna fed from a 2.45 GHz microwave source (Sources: [45, 46, 48, 65])

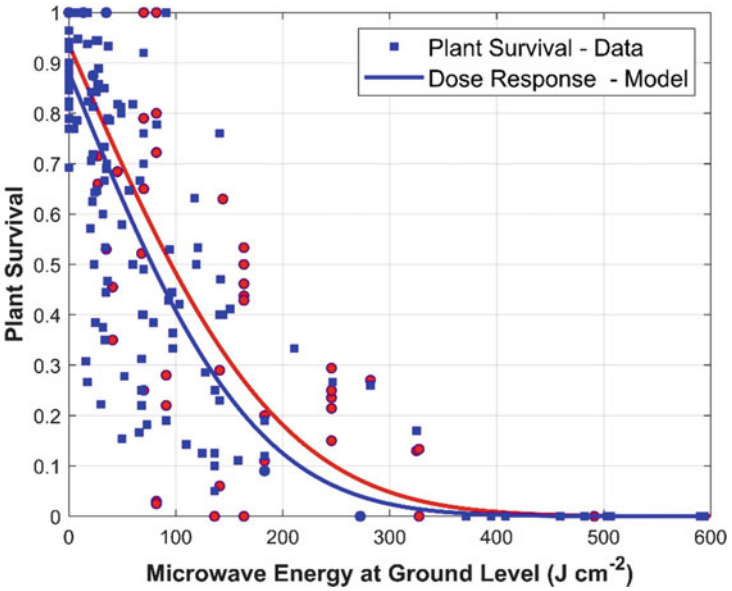

Fig. 8.7 Response of grasses (blue) and broad-leafed weeds (red) to microwave energy (Sources: [45, 46, 48])

When the weed species are separated into categories of broad leafed and grasses, it appears that broad leafed plants require slightly more microwave energy to achieve treatment efficacy, compared with grasses (Fig. 8.7). Moving the horn antenna relative to the weeds does not appear to change the energy requirements for effective weed control.

It is apparent from Figs. 8.2, 8.3, 8.6, and 8.7 that the energy requirements at ground level for weed seed control and for emerged weed control are practically the same, when using a horn antenna. This is because a horn antenna projects microwave energy vertically into the soil profile, whether it is used to kill emerged weeds or their seeds. Improvements in weed control can be achieved by developing an applicator that projects the microwave fields horizontally along the soil surface, rather than projecting them vertically into the soil. In this way, the necessary energy intensity to kill weeds can be achieved, whilst the treated 'footprint' on the ground can be greatly increased.

8.10 Novel Microwave Applicators for Weed Management

Traditional microwave applicators, such as horn antennas, have been used for heating semi-infinite materials that cannot be contained in a resonant cavity. Antennas cannot restrict their heating effect to the surface layers, and energy usually

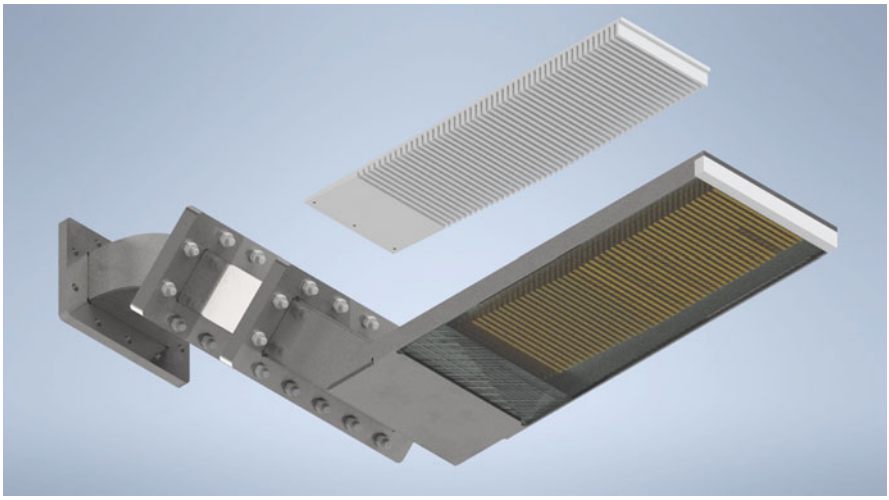

Fig. 8.8 Slow-wave applicator assembly, showing detail of the slow-wave comb element, which fits into the applicator housing. This design is for a 2.45 GHz applicator with a comb length of approximately 370 mm

penetrates deeply into the material in accordance with Maxwell's Equations, which describe the exponentially decaying propagation of electromagnetic fields into semi-infinite lossy media [66], where energy from the microwave field is converted into heat. In this scenario, much more material is being heated than is necessary to kill weed plants. In many cases, especially in zero till cropping systems, the soil seed bank is confined to the upper 2 cm of soil [67, 68]; therefore, confining the microwave field to the soil surface can provide more efficient weed management and weed seed deactivation in many agricultural systems.

Slow-wave comb (SWC) structures, which are often called "surface wave" structures, provide an opportunity to intensely treat the soil surface, without irradiating deeply into the soil. Slow-wave structures have a characteristic comb structure (Fig. 8.8), which constrains the microwave field to be near the comb surface.

Extensive testing of the new slow-wave applicator has shown that the effective energy density needed to kill weeds, when the applicator is stationary, is approximately 100 J cm^{-2} for grasses and 80 J cm^{-2} for broad leafed weeds (Fig. 8.9). This compares very favourably with using a stationary horn antenna, where the energy density required to kill weeds was between 400 and 500 J cm^{-2}.

Because of the unique way that the slow-wave applicator distributes microwave energy along the length of the applicator, when the applicator is in motion, plants are exposed to the microwave field, whilst the slow-wave structure moves over the plant. This extended exposure time can effectively reduce the total microwave energy density needed to treat individual weeds. In a dynamic test, using an adjustable 3.0 kW microwave, 2.45 GHz, source mounted in a trolley (Fig. 8.10), the slow-wave applicator was able to treat approximately 0.5 m^2 of grass per minute

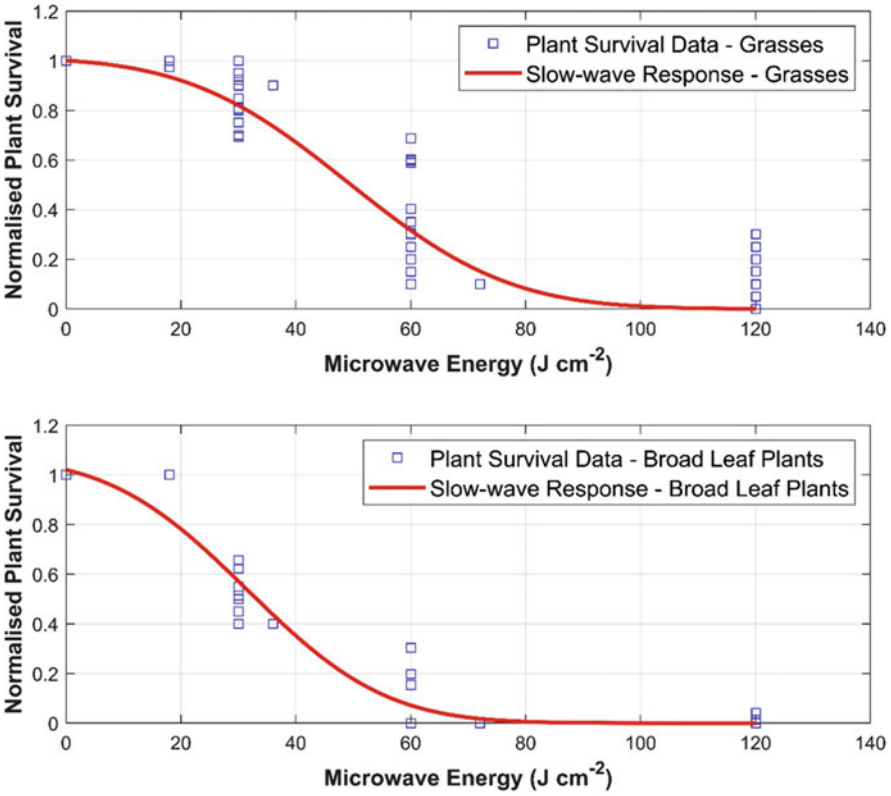

Fig. 8.9 Combined normalised plant survival data for 7 species of weeds treated with a stationary slow-wave applicator, powered by a 2 kW, 2.45 GHz, microwave source. Data separated according to whether the weeds were grasses (top) or broad leafed (bottom) (Data not previously published)

(Fig. 8.11), when the output power of the microwave generator was adjusted to 2.0 kW. This implies that the effective treatment energy density was 24 J cm^{-2}, which was significantly less than the energy density needed when using a horn antenna.

Subsequently, a 5.0 kW prototype system has been developed and tested. It also uses a slow-wave applicator for delivery of the microwave energy to the weeds. In recent field tests, it required 21.4 J cm^{-2} to control grass weeds in long strips across the test area.

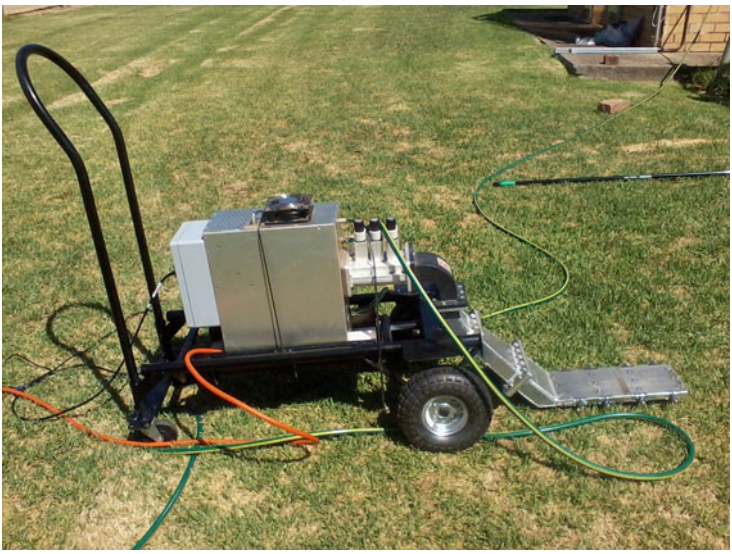

Fig. 8.10 Trolley mounted, 3 kW microwave generator, operating at 2.45 GHz, with a slow-wave applicator attached

Fig. 8.11 Grass test area (**a**) immediately after treatment and (**b**) after 3 days (Unpublished results)

8.11 Conclusions

The development of herbicide resistance and concerns about environmental pollution from chemicals has prompted interest in alternative weed management technologies. Several options are being explored, with microwave weed control being one of these options. The volumetric heating associated with microwave fields can heat soil and vegetation; therefore, microwave energy can be used to deactivate weed seeds in the soil or kill weed plants. Microwave soil treatment is comparable to soil fumigation and requires between 300 and 500 J cm^{-2} of applied energy to control

weed seeds. In addition to reducing weed emergence, microwave soil treatment also significantly increases subsequent crop growth and yield; however, long-term weed control from a single treatment is unlikely. Microwave energy can also be used to kill already emerged weed plants. By adopting novel microwave applicators, like the slow-wave structure, energy requirements for emerged weed control can be significantly reduced, making the technology potentially viable for commercial application.

References

1. Molle G, Decandia M, Fois N, Ligios S, Cabiddu A, Sitzia M. The performance of Mediterranean dairy sheep given access to sulla (Hedysarum coronarium L.) and annual ryegrass (Lolium rigidum Gaudin) pastures in different time proportions. Small Rumin Res. 2003;49(3):319–28.
2. Owen M, Walsh M, Llewellyn R, Powles S. Widespread occurrence of multiple herbicide resistance in Western Australian annual ryegrass (Lolium rigidum) populations. Aust J Agric Res. 2007;58(7):711–8.
3. Yu Q, Cairns A, Powles S. Glyphosate, paraquat and ACCase multiple herbicide resistance evolved in a Lolium rigidum biotype. Planta. 2007;225(2):499–513.
4. Heap IM. The occurrence of herbicide-resistant weeds worldwide. Pestic Sci. 1997;51 (3):235–43.
5. Heap I. Herbicide resistance – Australia vs. the rest of the world. Proc. 13th Australian Weeds Conference proceedings: weeds 'threats now and forever'. 645-649.Sheraton Perth Hotel, Perth, Western Australia; 2002.
6. Heap IM. International survey of herbicide resistant weeds. 25th September, 2016; 2016. http://www.weedscience.org/
7. Edreiraa JIR, Mourtzinis S, Conley SP, Roth AC, Ciampitti IA, Licht MA, Kandel H, Kyveryga PM, Lindsey LE, Mueller DS, Naeve SL, Nafziger E, Specht JE, Stanley J, Staton MJ, Grassini P. Assessing causes of yield gaps in agricultural areas with diversity in climate and soils. Agric For Meteorol. 2017;247:170–80.
8. Cathcart RJ, Swanton CJ. Nitrogen management will influence threshold values of green foxtail (Setaria viridis) in corn. Weed Sci. 2003;51(6):975–86.
9. Mondani F, Golzardi F, Ahmadvand G, Ghorbani R, Moradi R. Influence of weed competition on potato growth, production and radiation use efficiency. Notulae Scientia Biologicae. 2011;3 (3):42–52.
10. Menalled F, Peterson R, Smith R, Curran W, Páez D, Maxwell B. The eco-evolutionary imperative: revisiting weed management in the midst of an herbicide resistance crisis. Sustainability. 2016;8(12):1297.
11. Harper JL. The evolution of weeds in relation to resistance to herbicides. Proc. The 3rd British Weed Control Conference. 179–188. Farnham, UK; 1956.
12. Brodie G. Derivation of a cropping system transfer function for weed management: part 1 – herbicide weed management. Global J Agric Innov Res Dev. 2014;1(1):11–6.
13. Bosnić AČ, Swanton CJ. Economic decision rules for Postemergence herbicide control of Barnyardgrass (Echinochloa crus-galli) in corn (Zea mays). Weed Sci. 1997;45(4):557–63.
14. Yin XL, Jiang L, Song NH, Yang H. Toxic reactivity of wheat (Triticum aestivum) plants to herbicide Isoproturon. J Agric Food Chem. 2008;56(12):4825–31.
15. Baucom RS, Mauricio R. Fitness costs and benefits of novel herbicide tolerance in a noxious weed. Proc Natl Acad Sci U S A. 2004;101(36):13386–90.
16. Thornby DF, Walker SR. Simulating the evolution of glyphosate resistance in grains farming in northern Australia. Ann Bot. 2009;104(4):747–56.

17. Guyton KZ, Loomis D, Grosse Y, El Ghissassi F, Benbrahim-Tallaa L, Guha N, Scoccianti C, Mattock H, Straif K. Carcinogenicity of tetrachlorvinphos, parathion, malathion, diazinon, and glyphosate. Lancet Oncol. 2015;16(5):490–1.
18. Duke SO. Herbicide and pharmaceutical relationships. Weed Sci. 2010;58(3):334–9.
19. Hernández AF, Parrón T, Tsatsakis AM, Requena M, Alarcón R, López-Guarnido O. Toxic effects of pesticide mixtures at a molecular level: their relevance to human health. Toxicology. 2013;307:136–45.
20. Mačkić S, Ahmetović N. Toxicological profiles of highly hazardous herbicides with special reference to carcinogenicity to humans. Herbologia. 2011;12(2):55–60.
21. Peighambarzadeh SZ, Safi S, Shahtaheri SJ, Javanbakht M, Forushani AR. Presence of atrazine in the biological samples of cattle and its consequence adversity in human health. Iran J Public Health. 2011;40(4):112–21.
22. Troudi A, Sefi M, Ben Amara I, Soudani N, Hakim A, Zeghal KM, Boudawara T, Zeghal N. Oxidative damage in bone and erythrocytes of suckling rats exposed to 2,4-dichlorophenoxyacetic acid. Pestic Biochem Physiol. 2012;104(1):19–27.
23. Wickerham EL, Lozoff B, Shao J, Kaciroti N, Xia Y, Meeker JD. Reduced birth weight in relation to pesticide mixtures detected in cord blood of full-term infants. Environ Int. 2012;47:80–5.
24. Price A, Kelton J. In: Larramendy M, editor. Weed control in conservation agriculture in herbicides, theory and applications 3–16. InTech: Rijeka, Croatia; 2011.
25. Giampietro M, Pimentel D. Assessment of the energetics of human labor. Agric Ecosyst Environ. 1990;32(3):257–72.
26. Brodie G, Jacob M, Farrell P. Microwave and radio-frequency technologies in agriculture: an introduction for agriculturalists and engineers. Warsaw/Berlin: De Gruyter Open Ltd.; 2016.
27. Giampietro M, Pimentel D. Energy efficiency: assessing the interaction between humans and their environment. Ecol Econ. 1991;4(2):117–44.
28. Gourd T. Controlling weeds using propane generated flame and steam treatments in crop and non croplands. Organic Farming Research Foundation; 2002.
29. Holman JP. Heat transfer. 10th ed. New York: McGraw-Hill; 1997.
30. Crank J. The mathematics of diffusion. Bristol: J. W. Arrowsmith Ltd.; 1979.
31. Patil NG, Rebrov EV, Eränen K, Benaskar F, Meuldijk J, Mikkola J-P, Hessel V, Hulshof LA, Murzin DY, Schouten JC. Effect of the load size on the efficiency of microwave heating under stop flow and continuous flow conditions. J Microw Power Electromagn Energy. 2012;46 (2):83–92.
32. Ark PA, Parry W. Application of high-frequency electrostatic fields in agriculture. Q Rev Biol. 1940;15(2):172–91.
33. Nelson SO, Ballard LAT, Stetson LE, Buchwald T. Increasing legume seed-germination by VHF and microwave dielectric heating. Trans ASAE. 1976;19(2):369–71.
34. Nelson SO, Stetson LE. Germination responses of selected plant species to RF electrical seed treatment. Trans ASAE. 1985;28(6):2051–8.
35. Tran VN. Effects of microwave energy on the strophiole, seed coat and germination of acacia seeds. Aust J Plant Physiol. 1979;6(3):277–87.
36. Horikoshi S, Hasegawa Y, Suzuki N. Benefitting of plants using microwave genetic activation method and its applications. Proc. IMPI's 51st Annual Microwave Power Symposium (IMPI 51). 35-36.Miami, FL, USA; 2017.
37. Horikoshi S, Suzuki N, Hasegawa Y. Plant cultivation method. Patent No. US 2018/0153105 A1; 2018.
38. Magone I. The effect of electromagnetic radiation from the Skrunda radio location station on Spirodela polyrhiza (L.) Schleiden cultures. Sci Total Environ. 1996;180(1):75–80.
39. Grundler W, Keilmann F, Fröhlich H. Resonant growth rate response of yeast cells irradiated by weak microwaves. Phys Lett A. 1977;62(6):463–6.
40. Bebawi FF, Cooper AP, Brodie GI, Madigan BA, Vitelli JS, Worsley KJ, Davis KM. Effect of microwave radiation on seed mortality of rubber vine (Cryptostegia grandiflora R.Br.),

parthenium (Parthenium hysterophorous L.) and bellyache bush (Jatropha gossypiifolia L.). Plant Prot Q. 2007;22(4):136–42.
41. Brodie G, Harris G, Pasma L, Travers A, Leyson D, Lancaster C, Woodworth J. Microwave soil heating for controlling ryegrass seed germination. Trans Am Soc Agric Biol Eng. 2009;52 (1):295–302.
42. Davis FS, Wayland JR, Merkle MG. Ultrahigh-frequency electromagnetic fields for weed control: phytotoxicity and selectivity. Science. 1971;173(3996):535–7.
43. Davis FS, Wayland JR, Merkle MG. Phytotoxicity of a UHF electromagnetic field. Nature. 1973;241(5387):291–2.
44. Davis F. Neew techniques in weed control via microwaves. Proc. Western session- southeastern Nurserymen's conferences 75-78. Nacogdoches, Texas; 1974.
45. Wayland J, Merkle M, Davis F, Menges RM, Robinson R. Control of weeds with UHF electromagnetic fields. Unkrautbekämpfung mit elektromagnetischen UHF-Feldern. 1975;15 (1):1–5.
46. Brodie G, Hollins E. The effect of microwave treatment on ryegrass and wild radish plants and seeds. Global J Agric Innov Res Dev. 2015;2(1):16–24.
47. Cooper AP, Brodie G. The effect of microwave radiation and soil depth on soil pH, N, P, K, SO4 and bacterial colonies. Plant Prot Q. 2009;24(2):67–70.
48. Menges RM, Wayland JR. UHF electromagnetic energy for weed control in vegetables. Weed Sci. 1974;22(6):584–90.
49. Kabir H, Khan MJ, Brodie G, Gupta D, Pang A, Jacob MV, Antunes E. Measurement and modelling of soil dielectric properties as a function of soil class and moisture content. J Microw Power Electromagn Energy. 2020;54(1):3–18.
50. Brodie G, Pasma L, Bennett H, Harris G, Woodworth J. Evaluation of microwave soil pasteurization for controlling germination of perennial ryegrass (Lolium perenne) seeds. Plant Prot Q. 2007;22(4):150–4.
51. Brodie G, Khan MJ, Gupta D, Foletta S, Bootes N. Understanding the energy requirements for microwave weed and soil treatment global journal of agricultural innovation. Res Dev. 2020;6:11–24.
52. Brodie G, Khan MJ, Gupta D. Microwave soil treatment and plant growth. In: Filho MCMT, Hasanuzzaman M, editors. Sustainable crop production. London: IntechOpen; 2019.
53. Khan MJ, Brodie G, Cheng L, Liu W, Jhajj R. Impact of microwave soil heating on the yield and nutritive value of rice crop. Agriculture. 2019;9(134):1–7.
54. Khan MJ, Brodie G, Gupta D. Effect of microwave (2.45 GHz) treatment of soil on yield components of wheat (Triticum aestivum L.). J Microw Power Electromagn Energy. 2016;50 (3):191–200.
55. Brodie G, Bootes N, Reid G. Invited paper. Plant growth and yield of wheat and canola in microwave treated soil. Proc. IMPI's 49th Microwave Power Symposium. 40-41.San Diego, California, USA; 2015.
56. Brodie GI, Khan MJ, Gupta D, Foletta S. Microwave weed and soil treatment in agricultural systems. Global J Agric Innov Res Dev. 2018;5(2):1–14.
57. Khan MJ, Brodie G, Dorin G. The effect of microwave soil treatment on rice production under field conditions. Trans Am Soc Agric Biol Eng. 2017;60(2):517–25.
58. Khan MJ, Brodie G, Gupta D. Potential of microwave soil heating for weed management and yield improvement in rice cropping. Crop Pasture Sci. 2019;70(3):211–7.
59. Khan MJ, Brodie GI, Gupta D, Foletta S. Microwave soil treatment improves weed management in Australian dryland wheat. Trans Am Soc Agric Biol Eng. 2018;61(2):671–80.
60. Khan MJ, Brodie GI, Gupta D, He J. Microwave soil treatment increases soil nitrogen supply for sustained wheat productivity. Trans ASABE. 2019c;62(2):355–62.
61. Khan MJ, Brodie GI. Microwave weed and soil treatment in Rice production. In: Shah F, et al., editors. Rice crop - current development, 99–127. Vienna: InTech; 2018.
62. Brodie G, Grixti M, Hollins E, Cooper A, Li T, Cole M. Assessing the impact of microwave treatment on soil microbial populations. Global J Agric Innov Res Dev. 2015;2(1):25–32.

63. Khan MJ, Jurburg SD, He J, Brodie G, Gupta D. Impact of microwave disinfestation treatments on the bacterial communities of no-till agricultural soils. Eur J Soil Sci. 2019d;71(6):1006–17.
64. Neve P, Norsworthy JK, Smith KL, Zelaya IA. Modelling evolution and management of glyphosate resistance in Amaranthus palmeri. Weed Res. 2011;51(2):99–112.
65. Brodie G, Hamilton S, Woodworth J. An assessment of microwave soil pasteurization for killing seeds and weeds. Plant Prot Q. 2007;22(4):143–9.
66. Liu CM, Wang QZ, Sakai N. Power and temperature distribution during microwave thawing, simulated by using Maxwell's equations and Lambert's law. Int J Food Sci Technol. 2005;40 (1):9–21.
67. Chauhan BS. Ecology and management of weeds under no-till in southern Australia. Unpublished PhD thesis. Roseworthy: University of South Australia; 2006.
68. Chauhan BS, Gill G, Preston C. Influence of tillage systems on vertical distribution, seedling recruitment and persistence of rigid ryegrass (Lolium rigidum) seed bank. Weed Sci. 2006;54 (4):669–76.

Chapter 9
Soil Modifications

Muhammad Jamal Khan and Graham Brodie

Abstract The presence of toxins, pests, and pathogens in soil can significantly hinder the growth and production of crops. Soil sanitisation can overcome many of these crop inhibiting issues. Chemical soil fumigation has been employed for many years to sanitise agricultural soils; however, concern over the environmental impact of these chemicals has led to bans and reductions in the use of several key chemical disinfectants, particularly Methyl bromide. Soil heating has been considered as an alternative to chemical fumigation. Microwave soil treatment has the potential to thermally sanitise the soil. This chapter explores the fundamentals of in situ soil heating with microwave energy. This chapter also explores the impact of microwave heating on soil health, nutrition, and biology.

Keywords Soil · Fumigation · Microwave heating · Soil nutrition · Soil biota

9.1 Introduction

Soil is the basis of almost all agricultural endeavours, with the exception of hydroponic and aeroponic production systems [1]. Plant growth and crop yields depend on healthy soils, with a good supply of nutrients and water; however, the presence of toxins, pests, and pathogens in the soil can significantly hinder growth and production [2]. Various strategies have been employed to address soil deficiencies in order to increase plant growth and bridge the yield gap between ideal yield potential and actual yield response [3]. Modelling by Brodie et al. [2] suggests that pre-sowing soil sanitation could provide a crop yield increase (compared with untreated soil) of 133% or more. Practical experience in field conditions confirms this yield response [2].

M. J. Khan · G. Brodie (✉)
Faculty of Veterinary and Agricultural Sciences, The University of Melbourne, Parkville, VIC, Australia
e-mail: mkhan3@student.unimelb.edu.au; grahamb@unimelb.edu.au

S. Horikoshi et al. (eds.), *Agritech: Innovative Agriculture Using Microwaves and Plasmas*, https://doi.org/10.1007/978-981-16-3891-6_9

Various chemical disinfectants have been applied to soil to reduce pest and pathogen loads. Historically, chemical controls have been employed; however, there is growing concern about the ongoing use of chemicals and some options, such as Methyl bromide, have been banned due to their impact on the atmosphere and the environment. Methyl bromide has been classified as a Class I ozone-depleting chemical [4]; therefore, it should no longer be used for soil fumigation. Soil heating, through solarisation or the application of steam, has been considered as an alternative for chemical fumigation. Solarisation is slow and the transfer of heat from steam to soil is hindered by the thermal conductivity of the soil, which can be quite low, especially in dry soil [5].

Microwave soil heating has been considered for weed control for some time [6–8]; however, it has only become apparent in recent times that microwave soil heating has the potential to disinfect soil [9–11] and modify its nutritional profile [12]. This chapter explores how microwave treatment modifies the physical, nutritional, and biological parameters of soils.

9.2 Microwave Energy Distribution in Soil

Soil is a heterogeneous three-dimensional matrix, and heat transfer is highly variable due to non-uniform texture and water content [5]. The propagation of microwave energy through soil depends upon the gravimetric (θ_g) and volumetric (θ_v) moisture content [13], bulk density [14], organic matter content [15], soil texture [16], and specific heat of soil. Soil moisture percentage has three major impacts on microwave dielectric heating: (1) bond water increases the soil surface reflectivity [17], which ultimately reduced the microwave penetration into the soil [18]; (2) moist soil readily absorbs microwave energy to generate heat [18], and thus, less total microwave energy propagates into the soil; and (3) moisture is also responsible for heat-diffusing phenomena in the soil profile [19].

An initial understanding of microwave heating requires an understanding of the dielectric properties of the material being heated. It has been reported that the dielectric constant (ε') of known soil at known θ_g is proportional to the bulk density of soil. The dependence of soil dielectric constant on the bulk density is due to the direct dependence of bulk density on the volumetric soil moisture fraction [20]. The textural composition of soil (particles' size distribution) also affects the dielectric constant (ε'), because soil texture determines the water holding capacity of the soil. A higher percentage of clay particles (with bulk density range of 1.0–1.6 g cm^{-3}) increases the dielectric constant of soil [14], because clay particles are small and plate-shaped, with a high surface area to volume ratio. This high surface area holds more hygroscopic water, therefore increasing the thermal heat capacity [21] and dielectric properties of the soil [22]. As a consequence, this will increase the absorption of microwave energy by the soil.

The expected temperature (T) distribution, as a function of applied microwave energy in soil profile, was explained by [16]. Based on the work done by Ayappa

et al. [23], the heat evolved in a thick dielectric slab, like soil, can be described by (Eq. 2.1)

$$Q = \frac{\omega \varepsilon_o k'' \tau^2 E_o^2 e^{-2\beta z'}}{2} \tag{2.1}$$

where ω is the angular frequency of the electromagnetic field (Rad s^{-1}), ε_o is the electrical permittivity of free space (F m^{-1}), κ" is the dielectric loss factor of the material, τ is the transmission coefficient of the irradiated surface, E_o is the strength of the electric field (V m^{-1}), β is the attenuation rate of the propagating electromagnetic field (m^{-1}), and z' is the distance into the irradiated material (m).

Using this evolved heat profile, the temperature distribution in the soil, from a horn antenna, can be described by Eq. (2.2) [24]

$$T = \frac{n\omega\varepsilon_0 k''\tau^2\left(e^{4\gamma\beta^2 t}-1\right)}{4k\beta^2}\left[e^{-2\beta z}+\left(\frac{h}{k}+2\beta\right)z\times e^{-z^2/4\gamma t}\right] \times \left[\frac{E_a}{4\pi}\int_{-B/2}^{B/2}\int_{-A/2}^{A/2}\cos\left(\frac{\pi}{A}x'\right)\frac{e^{-j\beta_o\left(\sqrt{(x-x')^2+(y-y')^2+z^2}+\sqrt{R_o{}^2+(x')^2}+\sqrt{R_o{}^2+(y')^2}\right)}}{\sqrt{(x-x')^2+(y-y')^2+z^2}}.\mathrm{d}x'.\mathrm{d}y'\right]^2, \tag{2.2}$$

where n is the scaling factor associated with simultaneous heat and moisture movement in the microwave heated soil [25, 26], γ is the thermal diffusivity of the heated soil, accounting for simultaneous heat and moisture movement (m^2 s^{-1}), h is the convective heat transfer coefficient of the soil surface, k is the thermal conductivity of the heated soil (W m^{-1} K^{-1}), t is the heating time (s), E_a is the strength of the electric field in the aperture of the horn antenna (V m^{-1}), A is the width of the long face of the horn antenna (m), B is the height of the short face of the horn antenna (m), x' is the unit dimension across the width of the horn antenna (m), and y' is the unit dimension up the height of the horn antenna (m).

The temperature distribution in the soil, for microwave heating durations of up to 150 s, using the horn antenna, has been confirmed by Brodie et al. [19]. The highest temperature in the microwave soil heating pattern occurred along the centre line of horn antenna (core heating) and between 0.02–0.05 m below the soil surface, depending on the soil texture and moisture content. Therefore, microwave soil heating can be used in many ways in agriculture due to its rapid and volumetric heating mechanism, which makes it more effective over numerous thermal pest management technologies.

A horn antenna is a very simple and convenient applicator for soil heating; however, the depth of heating in soil depends entirely on the field attenuation rate (β) in the soil, which given by (Eq. 2.3)

$$\beta = \frac{\omega}{c}\sqrt{\frac{\kappa'}{2}\left[\sqrt{1+\left(\frac{\kappa''}{\kappa'}\right)^2}-1\right]}, \tag{2.3}$$

where c is the speed of light in a vacuum (m s^{-1}) and κ' is the real part of the dielectric constant of the soil.

For some soil heating applications, it is preferable to maintain shallow heating. In this case, a novel microwave applicator is required, which restricts the propagation of the electromagnetic field into the soil. Recently, Brodie et al. [27] developed a slow-wave applicator based on a metallic comb structure, which limits the field penetration into the soil. The temperature distribution in the soil below the slow-wave applicator will be of the form (Eq. 2.4).

$$T = \frac{n\omega\varepsilon_o\kappa {E_o}^2}{8k\alpha^2}\left(e^{4\gamma\alpha^2 t}-1\right)\left[e^{-2\alpha x}+\left(\frac{h}{k}+2\alpha\right)x\cdot e^{\frac{-x^2}{4\gamma t}}\right]\cdot U(y,t)\cdot e^{-2\tau_2 z} + T_o \tag{2.4}$$

The Voigt Function $U(y,t)\Re\left\{\frac{e^{\upsilon^2}}{8t\sqrt{\gamma}}\cdot erfc(\upsilon)\right\}$, where $\upsilon = \frac{1-\frac{jxy}{A}}{2\sqrt{\gamma t}}$. It is useful to note that $\lim_{t\to 0} U(y,t) = \frac{1}{1+\left(\frac{xy}{A}\right)^2}$.

If the applicator is protected by a dielectric plate with a dielectric constant κ'_1, and the medium to be heated has a dielectric constant of κ'_2, then the field dispersion in the second medium is described by Eq. (2.5) [27]

$$\tau_2 = -k^2\Psi_\tau\frac{\kappa'_1}{2\tau_1}+\sqrt{\left(k^2\Psi_\tau\frac{\kappa'_1}{2\tau_1}\right)^2+{\tau_1}^2+k^2\kappa'_1}, \tag{2.5}$$

where $\Psi_\tau = \frac{\tau_1\kappa'_2}{\tau_2\kappa'_1}$ and the subscripts correspond to the two materials.

$$\tau_1 = \sqrt{{\tau_2}^2+k^2\left(\kappa'_2-\kappa'_1\right)}, \tag{2.6}$$

where k in these equations is the wave number of the microwave field. The value of τ_2 needs to be solved iteratively, using Eqs. (2.5) and (2.6). In this case, κ'_2 is the dielectric constant of the soil. As a starting point for this iterative calculation, it is assumed that $\tau_1 = k\kappa'_1\tan(\mathrm{kd})$.

In this applicator, the depth of heating in the soil is controlled by the physical depth of the teeth (d) in the comb of the slow-wave structure.

9.3 Impact of Microwave Soil Treatment on Soil Properties and Biota

Within this context, the pre-emergence microwave soil treatment for weed seedbank devitalisation will also have some impact on the soil properties. Soil is a complex heterogeneous environment [5]. Accordingly, the influence of transient temperature-induced changes in the soil nutrient profile and biologically important taxa are of interest and should be explored. Relevant to soil nutrient, it has been reported that microwave soil heating facilitates organic nitrogen (N) mineralisation [28, 29] and ultimately increases the plant available N. The availability of indigenous soil N for crop productivity is an integral component of the farming system [30]. The higher N mineralisation, due to soil heating [31], will benefit the N use efficiency of crops.

Increases in crop productivity, resulting from microwave soil heating, have been reported previously [32, 33]; however, the exact phenomenon behind this scenario has yet to be explored rigorously. Changes in N within a crop management strategy seems to be important as it would reflect the influence of a single management approach on crop productivity. In this regard, a study is needed to explore the heating influence on soil N behaviour and its impact on the long-term productivity of soil.

Additionally, when considering microwave soil heating for killing the weed seedbank, the soil microbiota cannot be ignored, as initially suggested by Nelson [13]. The bacterial community's resistance, an immediate response to heating disturbance [34], resilience, and recovery process following microwave heating [35] may favour the practicability of this technology. In general, soil heating is detrimental to microorganisms [36]; however, numerous safeguarding strategies within the soil microaggregates can harbour the biologically important taxa from heating disturbance [37]. Relevant to indigenous N supply for crop growth, the role of ammonia is critical in nitrifying bacteria and archaea. They are responsible for nitrification in the majority of soils [38]. However, their response to microwave soil heating is largely unclear, although the literature (mostly evaluated by classical cultural-dependent techniques) suggests that they are resistant to microwave energy [11].

From this viewpoint, the extent of temperature sensitivity varies from species to species [39] and complete soil sterilisation at $\leq$200 °C is not achievable with microwave heating [40]. In an earlier glasshouse soil sterilisation study, Eglitis and Johnson [41] demonstrated that dielectric heating of the soil within a temperature range of 86–101 °C was effective in controlling fungi without any serious damage being caused to the nitrogen-fixing bacteria. Moreover, Vela et al. [11] documented that soil nitrifying bacterial groups survived much higher dosage levels of microwave exposure (40,000 J cm^{-2}) than those needed for soil seedbank deactivation (180–350 J cm^{-2}) [42]. Similarly, Ferriss [9] reported that *Prokaryotes* showed higher resistivity to microwave soil heating than Fungi. Recently, Nunes et al. [43] employed various microwaving doses (2–3 min) for soil bacterial community shift; they reported that there was no significant effect of heating on the

potentially active bacteria. Finally, they confirmed the survival of nitrogen-fixing bacteria, after an exposure of 2–3 min of soil microwave heating using a high-throughput sequencing analysis. Overall, the adaptability of soil microbiota to management regimes gives a framework for understanding the potential of the system (i.e. microwave weed management).

For this reason, the proposed peak soil temperature for weed seedbank suppression is in the range of 75–80 °C. However, it is expected that this temperature regime will alter the soil biota to some extent. The extent of immediate bacterial response to soil heating is relevant and mostly unexplored in the case of microwave soil heating. However, a part of this undertaking has explored the effect of microwave soil heating on the bacterial community shift and on the total abundance of ammonia oxidising bacteria (AOB) and archaea (AOA) using the quantitative polymerase chain reaction (qPCR) and the Next-generation Sequencing.

9.4 Effect of Microwave Soil Heating on Nutrient Profile

Microwave soil heating was first considered for weed seed bank control; however, soil heating also induces changes in the soil organic matter (SOM), which also alters the plant growth limiting nutrients and elements [36]. Notably, two important conditions, which are critical to thermal treatment of soil, are the heating temperature and time. In the case of microwave weed management, 80 °C is the desirable threshold temperature required to kill from 60–80% of the weed seedbank in the top soil (0–6 cm) layer, regardless of cropping regimes [44, 45]; however, there will be some effect of this short-term heat disturbance on the soil nutrient profile.

The dynamics of key soil nutrients is explained by the size and turnover rate of organic constituents, such as C–N type compounds, cellulose, hemicellulose, and lignin. The soil-microwave interaction is a function of various soil properties such as texture, moisture, salinity, bulk density, temperature [14, 16, 20], and thermal conductivity. Microwave soil interactions also decide the degradation and distillation fate of organic contents of the soil [46].

The response of the soil nutrient profile, following microwave heating, is not very well investigated. Cooper and Brodie [47] investigated the effect of different durations of microwave treatment and soil depth on soil nutrient status and pH. In their investigation, the microwave treatments had no significant effect on nitrogen, phosphorus, potassium, and sulphate concentrations in all the treatment combinations, albeit there was an increase in nitrite concentration following 120 s of microwave soil treatment. There was a nitrate reduction in the irradiated soil, which could be the principal cause of nitrite formation [48]. Wainwright et al. [28] tested the effect of microwave soil treatment (20 s; 20 g soil; 40% water content) on the nitrification rate and sulphur oxidation of an organic loamy soil. They found that microwave heating had no strong effect on the total bacterial count; however, there was a decrease in NO_3^--N concentration in the heated soil, which reflects the susceptibility of ammonia oxidisers. Although an increase in NH_4^+-N content in

irradiated soil may favour the soil quality and ultimately the speed of plant growth and development, additionally, this short exposure significantly stimulated S-oxidation. Similarly, Speir et al. [49] examined the effect of microwave energy (600 W; 2.45 GHz) on low fertility soil (100 randomly selected cores at a depth of 50 mm) microbial biomass C, N, phosphorus, and phosphatase activity. They reported that an increase in microwave treatment duration (90 s) dramatically increased the extractable N level (106μg N g^{-1} soil) but the microbial biomass C (μg C g^{-1} soil) and phosphorus concentration declined with increasing irradiation time (90 s). The higher flush in soil N is of a microbial origin as microwave heating has a broad-spectrum biocidal effect [50, 51].

Yang et al. [29] tested the nutrient extractability effect of microwave heating (0–240 s) on soil and then incubated the soil for 0–12 days at 20 °C. When fresh soil was exposed to microwave energy, a dramatic increase in the NH_4^+-N concentration was observed for an extended treatment of 120 s. They concluded that this effect was partially from non-microbial processes, either from site exchange or from fixed positions in inorganic collides (clay minerals). Additionally, a decrease in NO_3^--N concentration in the soil reflected the prevention of nitrification at high temperature. Alphei and Scheu [52] evaluated the effect of various biocidal treatments on mull-structured soil (600 g) fauna, microbiota, and nutritional dynamics over a period of 120 days after heating. Of the tested treatments, microwave soil heating (2.45 GHz, 700 W, 180 s) had an appreciably detrimental effect on soil fauna, but did not completely eliminate the soil microbial communities. They also found an increasing trend of NH_4^+-N (100–200μg g^{-1} soil) with microwave soil treatment compared with the unheated soil (≥100μg g^{-1} soil); however, a decrease in the NO_3^--N (≥40μg g^{-1} soil) content of the soil gave an indication that there was no nitrification occurring. The phosphorous content gradually increased over time. Increases in soil C and N mineralisation [53], NH_4^+-N, and sulphur oxidation were also reported by Wainwright et al. [28].

Independent of heating methodology, some studies have reported the effect of heating on soil properties. For instance, Glass et al. [31] verified the effect of high temperature, associated with surface fire severity, on soil health. The concentration of ammonium ions (NH_4^+) was greatly increased with high temperature treatment and duration, whilst the concentration of nitrate ions (NO_3^-) responded variably among various soil types, but generally increased with high soil water content. It was concluded that a low-intensity fire ($100 \leq °C \leq 200$) can considerably alter the NH_4^+ and NO_3^- concentrations without any change in total N or C. Similarly, Certini [54] explained the possible mechanisms and changes induced by fire on the soil quality. He reported that the transient changes in soil pH and available nutrients after the fire depend on the severity and duration of the heating. Some hydrophobicity was induced by the fire, which can reduce the soil water holding capacity and ultimately increase erosion. However, numerous studies reported an increase in soil organic matter (SOM) with fire and this would have enhanced the soil structure, which would have led to an increase in water holding capacity. In contrast, Yi et al. [55] reported that low-temperature remediation of oil-contaminated soil decreased the organic matter and total N, while phosphorous, microbial count, enzyme activity

(dehydrogenase) and water holding capacity increased. Based on these studies, soil heating has the potential to alter the soil nutrient availability; therefore, the effect depends on the heating duration and intensity.

9.5 Response of Soil Microorganisms to Microwave Heating

Bacterial and fungal communities' responses are a key challenge in the adaptation of microwave technology for weed and pathogen control in agricultural systems. It is important to note that the target temperature for microwave soil heating is 75–80 °C and so the response of soil biota must be considered for this temperature range.

Farming systems are expected to face new production and management techniques for sustainable food production. However, the influence of these new management practices on soil microbial composition and activity is unclear [56]. For instance, the role of soil microbiota in protecting and regulating the key soil processes, under increased environmental changes, is poorly understood [57]. Therefore, the effect of microwave heating on soil microbiota is still in question and has very limited literature.

Vela et al. [11] treated different types of soil to check the instant effect of microwave heating on soil microorganisms. Small soil samples (250 g) were subjected to microwave heating for 5, 10, 20, and 40 s in a 1-kW microwave oven. This distinct range of exposure achieved an overall temperature gradient of 80 °C. The results from all the soil types showed that only fungal colonies were significantly reduced by microwave irradiation. They found that soil nitrifying bacteria were highly resistant to microwave energy applied to the soil surface at a rate of 40,000 J cm^{-2}. They further found that bacteria could survive an exposure of 480 s when in the soil; however, the bacteria could not bear a 20-s treatment in an isolated aqueous culture. Their bacterial population was reduced from 1.3×10^6 to 2.9×10^3 g^{-1} of soil. The authors [11] collected soil from one of the pre-emergent weed management field experimental sites. The soil was irradiated with the Zapper III (60 kW; four independently controlled microwave generators) with energy densities of 200, 400, and 800 J cm^{-2} to check on the microbiota damage and recovery. These tested energy densities were effective for killing weed populations without any serious damage to the soil microflora.

In a parallel study, Ferriss [9] documented that the treatment time, soil moisture content, and soil load collectively dictate the fate of soil microorganisms. In Ferriss' study, there was no pronounced effect of microwave heating on the *Prokaryotes* population measured in colony-forming units (CFU) 1 day after soil treatment in a 625-W microwave oven operating at a frequency of 2.45 GHz. Additionally, Ferriss demonstrated the relative susceptible ranking of soil biota to microwave heating: nematodes > fungi > bacteria and thermophiles.

For soil steaming treatment, Bollen [39] found a similar susceptibility index of soil microflora to heating, independent of the heating methodology employed. In his study, Ferriss concluded that a small amount of soil ($\leq$1 kg) can easily be sterilised

with microwave heating although the complete sterilisation of large soil volume was difficult to achieve [9]. Under extreme conditions, the difference in temperature sensitivity of soil microflora [39], with fungi being more sensitive than bacteria [58], triggers competitive dynamics and new microbiota reassembly scenarios.

Transient heat (50 or 80 °C for 1 h) induces a rearrangement of bacterial communities [59], which ultimately favours the rapid recovery of slow-growing thermophilic taxa [60]. Wainwright et al. [28] treated small amounts of contrasting soils (20 g) in a 1-kW microwave oven operating at 2.45 GHz, for 10–30 s to check the instant effect of heating on soil microorganisms. This short-term heating progressively reduced nitrification with an abrupt increase in soil NH_4^+-N. Additionally, a 20-s exposure considerably increased sulphur oxidation (two- to three-fold) compared with the untreated control soil at day 28. They reported a rapid reduction in fungi, from 30,000 g^{-1} to 0 g^{-1} with similar exposure time without any profound detrimental effect on the heterotrophic bacteria measured at day 28 after the microwave soil treatment. This result was for organic loam soil. Similarly, Lyon et al. [61] heated small soil samples (25 g; organic loam) in a 1-kW microwave oven (equivalent to 11 J cm^{-3} s^{-1} dissipated in a 40-ml water load) for a maximum of 30, 120, and 360 s. Fungal colonies were completely eradicated with the 30-s exposure, although bacterial communities remained unaffected with this short exposure. They found a slight reduction in the bacterial colonies at 120 s; however, 360 s of exposure completely killed them all.

To deal with field soil, Chen et al. [62] verified the efficacy of microwave soil heating on the total bacterial count and found that bacterial taxa were undetectable with soil heating of 6 minutes at 3.3% moisture content. The reduction pattern was 1.48×10^6 (with 2 min) to 0.021×10^6 (at 6 min) CFU g^{-1} of soil. Therefore, the results of these previous studies give some good insight into the interaction of microwave energy with soil microorganisms; however, the limitations with these studies is the culture-dependent soil microbiota assays after soil heating; they are limited in what they can reveal. The majority of soil bacteria are unable to be cultured.

Recently, Jurburg et al. [63] subjected 120 soil microcosms (50 g; 45% field capacity) to treatment in an 800-W microwave oven for 90 s, achieving a maximum temperature of 85.5 °C, to check the community shift after this transient heat disturbance. Samples were assessed over 50 days by sampling independently incubated microcosms. They found that the total potentially active bacteria, based on the cDNA/DNA copies of the 16S rRNA gene, were reduced moderately following microwave heating, but reached pre-heating levels at day 29 (stability phase). In general, soil heating is detrimental to microorganisms [36]; however, a transient heat disturbance kills some species and favours others via various resistance mechanisms.

In other domains, the effect of microwave heating was observed on the disintegration of microbes in a solid medium upon being treated up to the maximum temperature [64, 65]. Microwave-induced disintegration of cells increases the amount of intracellular and extracellular components in the solid medium, thereby increasing the soluble organic content. This is a direct effect of heating on the microbes in a less complex material; however, if microwave energy were applied

to a very complex substance such as, for example, soil, the disintegration scenario would then be different.

A temporary disturbance (i.e., in the case of microwave heating) alters the community composition by killing various vulnerable species [66]. Because of this, the newly available niches may favour competitive dynamics, for instance, secondary succession [67]. In summary, there is a pronounced effect of microwave heating on the soil microbiota. Nonetheless, the rapid recovery of microbes after microwave heating has been reported by numerous studies [11, 36, 63, 67–69].

Post-heating conditions stimulate the microbial community, because it is mostly controlled by soil moisture and organic matter. Accordingly, culture-independent research is needed to elucidate the effect of soil heating on the population dynamics of beneficial soil microbiota. A part of this research has explored the effect of microwave soil treatment on the community of ammonia oxidising bacteria (AOB) and archaea (AOA), as well as their activity in the field soil of various cropping regimes using the quantitative polymerase chain reaction (qPCR). Ammonia oxidisers are responsible for the conversion of ammonium ions (NH_4^+) to nitrate ions (NO_3^-; nitrification), via a nitrite intermediate in terrestrial ecosystems [38, 70]. However, the relative contribution of AOA and AOB to soil nitrification is highly uncertain. AOA is found to be numerically higher than AOB but functionally less dominant [38]. The ammonia monooxygenase α-subunit (*amoA* gene), carried by all know ammonia oxidisers, is involved in the first step of nitrification and is widely used to study the community size of AOA and AOB. A comprehensive study is needed to understand the effect of microwave heating on the soil beneficial microbiota, particularly AOA and AOB and their role in soil nitrogen cycling. The response of soil biota, at various soil depths, after microwave heating is also crucial to understand the downstream impact of penetration depth for pathogen control in production systems. For soil nematodes, O'Bannon and Good [71] treated a root knot nematode (*Meloidogyne* spp.) infected soil (90 g; 11% water content) in a 1.25-kW microwave oven for 30–300 s and found that short exposure ($\leq$30 s) severely hindered their activity. A similar reducing trend was found when a larger soil load (400 g) was treated for nematodes elimination.

9.6 Conclusion

Microwave soil heating can sanitise soil and provide many of the benefits of soil fumigation; however, microwave heating does not sterilise the soil. There is considerable evidence that some beneficial organisms in the soil, especially nitrifying organisms such as AOA and AOB, are resilient to microwave heating. This modifies the soil microbiota and leads to significant changes in the soil nutrient cycling and often leads to changes in key soil nutrient profiles.

References

1. Tavan M, Wee B, Brodie G, Fuentes S, Pang A, Gupta D. Optimising sensor-based irrigation management in a soilless vertical farm for growing microgreens. Front Sust Food Syst. 2021;4:1–12.
2. Brodie G, Khan MJ, Gupta D. Microwave soil treatment and plant growth. In: Filho MCMT, Hasanuzzaman M, editors. Sustainable crop production. London: IntechOpen; 2019.
3. Edreiraa JIR, Mourtzinis S, Conley SP, Roth AC, Ciampitti IA, Licht MA, Kandel H, Kyveryga PM, Lindsey LE, Mueller DS, Naeve SL, Nafziger E, Specht JE, Stanley J, Staton MJ, Grassini P. Assessing causes of yield gaps in agricultural areas with diversity in climate and soils. Agric For Meteorol. 2017;247:170–80.
4. Samtani JB, Gilbert C, Ben Weber J, Subbarao KV, Goodhue RE, Fennimore SA. Effect of steam and solarization treatments on pest control, strawberry yield, and economic returns relative to methyl bromide fumigation. HortScience. 2012;47:64–70.
5. Lu Y, Lu S, Horton R, Ren T. An empirical model for estimating soil thermal conductivity from texture, water content, and bulk density. Soil Sci Soc Am J. 2014;78:1859–68.
6. Davis FS, Wayland JR, Merkle MG. Ultrahigh-frequency electromagnetic fields for weed control: phytotoxicity and selectivity. Science. 1971;173:535–7.
7. Davis FS, Wayland JR, Merkle MG. Phytotoxicity of a UHF electromagnetic field. Nature. 1973;241:291–2.
8. Menges RM, Wayland JR. UHF electromagnetic energy for weed control in vegetables. Weed Sci. 1974;22:584–90.
9. Ferriss R. Effects of microwave oven treatment on microorganisms in soil. Phytopathology. 1984;74:121–6.
10. Mahdi WM, Al-Badri KSL, Al-Samarrai GF. Use of microwave radiation in soil sterilization and effects on the Bacteria, Fungi and growth characteristics of chickpea plant (Cicer arietinum L.). Plant Arch. 2019;19:2064–9.
11. Vela G, Wu J, Smith D. Effect of 2450 MHz microwave radiation on some soil microorganisms in situ. Soil Sci. 1976;121:44–51.
12. Khan MJ, Brodie GI, Gupta D, He J. Microwave soil treatment increases soil nitrogen supply for sustained wheat productivity. Trans ASABE. 2019;62:355–62.
13. Nelson S. A review and assessment of microwave energy for soil treatment to control pests. Trans ASAE. 1996;39:281–9.
14. Hallikainen MT, Ulaby FT, Dobson MC, El-Rayes MA, Wu L-K. Microwave dielectric behavior of wet soil-part 1: empirical models and experimental observations. IEEE Trans Geosci Remote Sens. 1985:25–34.
15. O'Neill P, Jackson T. Observed effects of soil organic matter content on the microwave emissivity of soils. Remote Sens Environ. 1990;31:175–82.
16. Brodie G, Ryan C, Lancaster C. Microwave technologies as part of an integrated weed management strategy: a review. Int J Agron. 2012;2012:1–14.
17. Von Hippel AR. Dielectrics and waves; 1954.
18. Metaxas AA, Meredith RJ. Industrial microwave heating. IET; 1983.
19. Brodie G, Hamilton S, Woodworth J. An assessment of microwave soil pasteurization for killing seeds and weeds. Plant Protect Q. 2007;22:143.
20. Dobson MC, Ulaby FT, Hallikainen MT, El-Rayes MA. Microwave dielectric behavior of wet soil-part II: dielectric mixing models. IEEE Trans Geosci Remote Sens. 1985;GE-23:35–46.
21. Nidal H. Thermal properties of soils as affected by density and water content. Biosyst Eng. 2003;86:97–102.
22. Kabir H, Khan MJ, Brodie G, Gupta D, Pang A, Jacob MV, Antunes E. Measurement and modelling of soil dielectric properties as a function of soil class and moisture content. J Microw Power Electromagn Energy. 2020;54:3–18.
23. Ayappa K, Davis H, Crapiste G, Davis E, Gordon J. Microwave heating: an evaluation of power formulations. Chem Eng Sci. 1991;46:1005–16.

24. Brodie G. Derivation of a cropping system transfer function for weed management: part 2. Microwave weed management. Global J Agric Innov Res Dev. 2016;3:1–9.
25. Brodie G. Simultaneous heat and moisture diffusion during microwave heating of moist wood. Appl Eng Agric. 2007;23:179–87.
26. Henry PSH. The diffusion of moisture and heat through textiles. Discuss Faraday Soc. 1948;3:243–57.
27. Brodie G, Pchelnikov Y, Torgovnikov G. Development of microwave slow-wave comb applicators for soil treatment at frequencies 2.45 and 0.922 GHz (theory, design, and experimental study). Agriculture. 2020;10:10.00604.
28. Wainwright M, Killham K, Diprose M. Effects of 2450 MHz microwave radiation on nitrification, respiration and S-oxidation in soil. Soil Biol Biochem. 1980;12:489–93.
29. Yang JE, Skogley EO, Schaff BE. Microwave radiation and incubation effects on resin-extractable nutrients: I. Nitrate, ammonium, and Sulphur. Soil Sci Soc Am J. 1990;54:1639–45.
30. Cassman K, Peng S, Olk D, Ladha J, Reichardt W, Dobermann A, Singh U. Opportunities for increased nitrogen-use efficiency from improved resource management in irrigated rice systems. Field Crop Res. 1998;56:7–39.
31. Glass DW, Johnson DW, Blank RR, Miller WW. Factors affecting mineral nitrogen transformations by soil heating: a laboratory-simulated fire study. Soil Sci. 2008;173:387–400.
32. Brodie G, Bootes N, Reid G. Plant growth and yield of wheat and canola in microwave treated soil. IMPI's 49th microwave power symposium. USA; 2015.
33. Gibson F, Fox FM, Deacon J. Effects of microwave treatment of soil on growth of birch (Betula pendula) seedlings and infection of them by ectomycorrhizal fungi. New Phytol. 1988;108:189–204.
34. Hodgson D, Mcdonald JL, Hosken DJ. What do you mean,'resilient'? Trends Ecol Evol. 2015;30:503–6.
35. Shade A, Peter H, Allison S, Baho D, Berga M, Buergmann H, Huber D, Langenheder S, Lennon J, Martiny J, Matulich K, Schmidt T, Handelsman J. Fundamentals of microbial community resistance and resilience. Front Microbiol. 2012;3
36. O'Brien PL, Desutter TM, Casey FX, Khan E, Wick AF. Thermal remediation alters soil properties–a review. J Environ Manag. 2018;206:826–35.
37. Nie M, Pendall E, Bell C, Wallenstein MD. Soil aggregate size distribution mediates microbial climate change feedbacks. Soil Biol Biochem. 2014;68:357–65.
38. Banning NC, Maccarone LD, Fisk LM, Murphy DV. Ammonia-oxidising bacteria not archaea dominate nitrification activity in semi-arid agricultural soil. Sci Rep. 2015;5:11146.
39. Bollen G. The selective effect of heat treatment on the microflora of a greenhouse soil. Neth J Plant Pathol. 1969;75:157–63.
40. Bárcenas-Moreno G, Bååth E. Bacterial and fungal growth in soil heated at different temperatures to simulate a range of fire intensities. Soil Biol Biochem. 2009;41:2517–26.
41. Eglitis M, Johnson F. Control of seedling damping-off in greenhouse soils by radio frequency energy. Plant Dis Rep. 1970;54:268–71.
42. Wayland J, Davis F, Merkle M. Toxicity of an UHF device to plant seeds in soil. Weed Sci. 1973;21:161–2.
43. Nunes I, Jurburg S, Jacquiod S, Brejnrod A, Salles JF, Priemé A, Sørensen SJ. Soil bacteria show different tolerance ranges to an unprecedented disturbance. Biol Fertil Soils. 2018;54:189–202.
44. Brodie G. The use of physics in weed control. In: Non-chemical weed control. London: Elsevier; 2018. p. 33–59.
45. Khan MJ, Brodie GI, Gupta D, Foletta S. Microwave soil treatment improves weed management in Australian dryland wheat. Trans ASABE. 2018;61:671–80.
46. González-Pérez JA, González-Vila FJ, Almendros G, Knicker H. The effect of fire on soil organic matter—a review. Environ Int. 2004;30:855–70.
47. Cooper A, Brodie G. The effect of microwave radiation and soil depth on soil pH, N, P, K, SO_4 and bacterial colonies. Plant Prot Q. 2009;24:67–70.

48. Cawse P, Crawford D. Accumulation of nitrite in fresh soils after gamma irradiation. Nature. 1967;216:1142–3.
49. Speir T, Cowling J, Sparling G, West A, Corderoy D. Effects of microwave radiation on the microbial biomass, phosphatase activity and levels of extractable N and P in a low fertility soil under pasture. Soil Biol Biochem. 1986;18:377–82.
50. Shamis Y, Patel S, Taube A, Morsi Y, Sbarski I, Shramkov Y, Croft RJ, Crawford RJ, Ivanova EP. A new sterilization technique of bovine pericardial biomaterial using microwave radiation. Tissue Eng Part C Methods. 2009;15:445–54.
51. Shamis Y, Taube A, Shramkov Y, Mitik-Dineva N, Vu B, Ivanova EP. Development of a microwave treatment technique for bacterial decontamination of raw meat. Int J Food Eng. 2008;4
52. Alphei J, Scheu S. Effects of biocidal treatments on biological and nutritional properties of a mull-structured woodland soil. Geoderma. 1993;56:435–48.
53. Zagal E. Effects of microwave radiation on carbon and nitrogen mineralisation in soil. Soil Biol Biochem. 1989;21:603–5.
54. Certini G. Effects of fire on properties of forest soils: a review. Oecologia. 2005;143:1–10.
55. Yi YM, Park S, Munster C, Kim G, Sung K. Changes in ecological properties of petroleum oil-contaminated soil after low-temperature thermal desorption treatment. Water Air Soil Pollut. 2016;227:108.
56. Smith P, House JI, Bustamante M, Sobocká J, Harper R, Pan G, West PC, Clark JM, Adhya T, Rumpel C. Global change pressures on soils from land use and management. Glob Chang Biol. 2016;22:1008–28.
57. Nemergut DR, Shade A, Violle C. When, where and how does microbial community composition matter? Front Microbiol. 2014;5:497.
58. D'ascoli R, Rutigliano FA, De Pascale RA, Gentile A, De Santo AV. Functional diversity of the microbial community in Mediterranean maquis soils as affected by fires. Int J Wildland Fire. 2005;14:355–63.
59. Mendes R, Kruijt M, De Bruijn I, Dekkers E, Van Der Voort M, Schneider JH, Piceno YM, Desantis TZ, Andersen GL, Bakker PA. Deciphering the rhizosphere microbiome for disease-suppressive bacteria. Science. 2011;332:1097–100.
60. Voort M, Kempenaar M, Driel M, Raaijmakers JM, Mendes R. Impact of soil heat on reassembly of bacterial communities in the rhizosphere microbiome and plant disease suppression. Ecol Lett. 2016;19:375–82.
61. Lyon A, Hackam R, and Benson F Partial soil sterilisation and soil and leaf moisture content measurement by microwave radiation. Proc. 1978 British Crop Protection Conference-Weeds. November. Brighton, UK; 1978, pp. 491–498.
62. Chen S, Dickson D, Mitchell D. Effects of soil treatments on the survival of soil microorganisms. J Nematol. 1995;27:661–3.
63. Jurburg SD, Nunes I, Stegen JC, Le Roux X, Priemé A, Sørensen SJ, Salles JF. Autogenic succession and deterministic recovery following disturbance in soil bacterial communities. Sci Rep. 2017;7:1–11.
64. Woo IS, Rhee IK, Park HD. Differential damage in bacterial cells by microwave radiation on the basis of cell wall structure. Appl Environ Microbiol. 2000;66:2243–7.
65. Zhou BW, Shin SG, Hwang K, Ahn J-H, Hwang S. Effect of microwave irradiation on cellular disintegration of gram positive and negative cells. Appl Microbiol Biotechnol. 2010;87:765–70.
66. Lennon JT, Aanderud ZT, Lehmkuhl B, Schoolmaster DR. Mapping the niche space of soil microorganisms using taxonomy and traits. Ecology. 2012;93:1867–79.
67. Jurburg SD, Nunes I, Brejnrod A, Jacquiod S, Priemé A, Sørensen SJ, Van Elsas JD, Salles JF. Legacy effects on the recovery of soil bacterial communities from extreme temperature perturbation. Front Microbiol. 2017;8:1–13.

68. Brodie G, Grixti M, Hollins E, Cooper A, Li T, Cole M. Assessing the impact of microwave treatment on soil microbial populations; 2015.
69. Vela G, Wu J. Mechanism of lethal action of 2,450-MHz radiation on microorganisms. Appl Environ Microbiol. 1979;37:550–3.
70. He J-Z, Shen J-P, Zhang L-M, Di HJ. A review of ammonia-oxidizing bacteria and archaea in Chinese soils. Front Microbiol. 2012;3:1–7.
71. O'Bannon J, Good J. Applications of microwave energy to control nematodes in soil. J Nematol. 1971;3:93.

Chapter 10
Microwave Application for Animal Feed Processing to Improve Animal Performance

Md Safiqur Rahaman Shishir, Graham Brodie, Brendan Cullen, and Long Cheng

Abstract Feed nutritive value and its utilization by the animal are the two important factors that influence the profitability and sustainability of animal production systems. Microwave (MW) technology is one of the efficient technologies being used for physical processing of feed to improve feed nutritive value in the animal digestive system. Previous research has demonstrated that MW treatment may have been useful for improving feed digestibility and changing its utilization in animals' bodies. Crude protein (CP) is one of the most important nutrients, MW treatment is effective at reducing concentrate feed CP rumen degradability, potentially leading to more efficient utilization of protein in the ruminant intestine. It reduces the anti-nutritional factors present in the feeds, which can limit animals' intake and utilization. In this chapter, the application of MW treatment for feed processing and the prospects for the future use of MW technology in animal production systems will be discussed.

Keywords Digestibility · Forage · Concentrate · Processing · Ruminant · Crude protein digestibility

M. S. R. Shishir (✉)
Faculty of Veterinary and Agricultural Sciences, The University of Melbourne, Parkville, VIC, Australia

Department of Animal Nutrition, Bangladesh Agricultural University, Mymensingh, Bangladesh
e-mail: mshishir@student.unimelb.edu.au; shishir.an@bau.edu.bd

G. Brodie · B. Cullen · L. Cheng
Faculty of Veterinary and Agricultural Sciences, The University of Melbourne, Parkville, VIC, Australia
e-mail: grahamb@unimelb.edu.au; bcullen@unimelb.edu.au; long.cheng@unimelb.edu.au

S. Horikoshi et al. (eds.), *Agritech: Innovative Agriculture Using Microwaves and Plasmas*, https://doi.org/10.1007/978-981-16-3891-6_10

10.1 Introduction

Globally, ruminant farming plays a vital role in providing high-quality animal origin food products (e.g., meat and milk) to the human diet [1]. With the rapid growing human population, animal production systems' continuous advancement is increasingly important [2]. Feed is considered to be the most important input to animal production systems [3], as it often accounts for more than 50% of the total production cost [4]. For ruminant livestock producers, obtaining high-quality feed at an affordable price is often challenging due to the competition from non-ruminant animal production systems and humans. Therefore, to achieve a sustainable and profitable ruminant production, careful use of feed resources and advancement in processing techniques, to improve feed quality, are important.

Feed processing technologies have been used to enhance the feeding value (voluntary feed intake $\times$ feed nutritive value [5]) of various feed resources [6]. Feed processing includes physical, chemical, and/or biological alteration of feed to improve its nutritive value, maximize the nutritional outputs, and reduce animal production costs [7]. In addition, feed processing can improve shelf life, detoxify poisonous substances, and deactivate anti-nutritional factors present in the feed [8]. Feed processing in the livestock industries has a long history and was commenced in the early 1800s. Early examples of feed processing include soaking flint and dent corn in water to reduce its hard and flinty texture prior to it being fed to beef cattle [9].

The most common physical treatment method used to improve fibrous feed resources' utilization capability is grinding and pelleting [10]. Extrusion is commonly used for fish feed production in the twenty-first century. This increases starch gelatinization and the cross-linking of proteins within the matrix, which improves the overall feed digestibility [11]. The other physical treatment method is steam treatment, which has proved to be effective in improving the digestibility of low-quality roughage feed [12, 13]. However, it requires considerably higher energy and a sophisticated high-pressure container.

Chemical treatment methods include treatment of roughage with urea, sodium hydroxide, or urea molasses; this is widely used in developing countries where roughage like straw is the basal diet for large ruminants [14]. On the other hand, the ensiling of forages, using different biological additives for improving their nutritive value, is an example of biological processing [14]. More recently, research has concentrated on modifying the chemistry of feed to improve the feed's nutrient availability [15] rather than only transforming the physical form of feed. While chemical processing has its merit, physical treatment is usually easier to implement. Microwave (MW) treatment is one of the physical treatment methods that has potential to achieve the abovementioned goal from feed processing and support the development of the animal industry.

10.2 Microwave Processing Techniques

Microwave (MW) treatment is a nonionizing electromagnetic physical processing technique that has been commonly used in the human food industry [16] due to its quick and energy-efficient heating for the improvement of food product quality [17], while having little or no negative impact on the chemical composition of the foods. The MW treatment has also been applied in the animal feed industry in recent years, specifically for concentrate and roughage feed processing to improve nutritive value [18–21]. Previous research showed that in conjunction with sodium hydroxide, pretreatment use of MW treatment reduced sugar content and removed the lignin, hemicellulose, and silicon from rice straw [22]. In addition, MW treatment has been used to dry feed samples for further chemical analysis [23] and preservation purposes [8].

10.2.1 Microwave Treatment Effect on Feed Cell Microstructure

Rapid heating and steam explosions inside the cell during the MW treatment of plant material can have a considerable effect on the cell microstructure [24]. The MW treatment causes rapid intercellular moisture/bound water evaporatation that lead to steam explosions inside the cell [25–27].

For example, Torgovnikov et al. [27] demonstrated that there was a microcellular fracture in timber when treated with intense MW energy. Choi et al. [26] found that MW treatment caused the destruction of the microstructure of soybean grain cells, which eventually increased the extraction of soluble soy protein. A similar result was also observed in rapeseed, which facilitated a better oil extraction due to MW heat treatment [28, 29]. A recent study showed MW heating also increased the microporosity of the plant material, which improved the permeability of moisture and enzymatic accessibility [78]. In the case of roughage feed, MW treatment significantly increased cell microstructure destruction (Fig. 10.1). In addition, analysis of microscopic images of treated and untreated forage hay revealed that the intensity variance is much higher in MW-treated forage hay than untreated forage hay [21]. The intensity variance in the image indicated that each pixel's smoothness of the MW-treated hay image is lower than the untreated forage hay image, which attributed to microcellular structure changes due to MW treatment [30].

Pretreatment of plant fiber with MW weakens the intercellular strength. Brodie [31] found that MW pretreatment was effective in juice extraction from sugarcane. Sugarcane compressive strength was reduced by about 18% of its initial strength after MW treatment. Therefore, it is reasonable to assume that the energy required

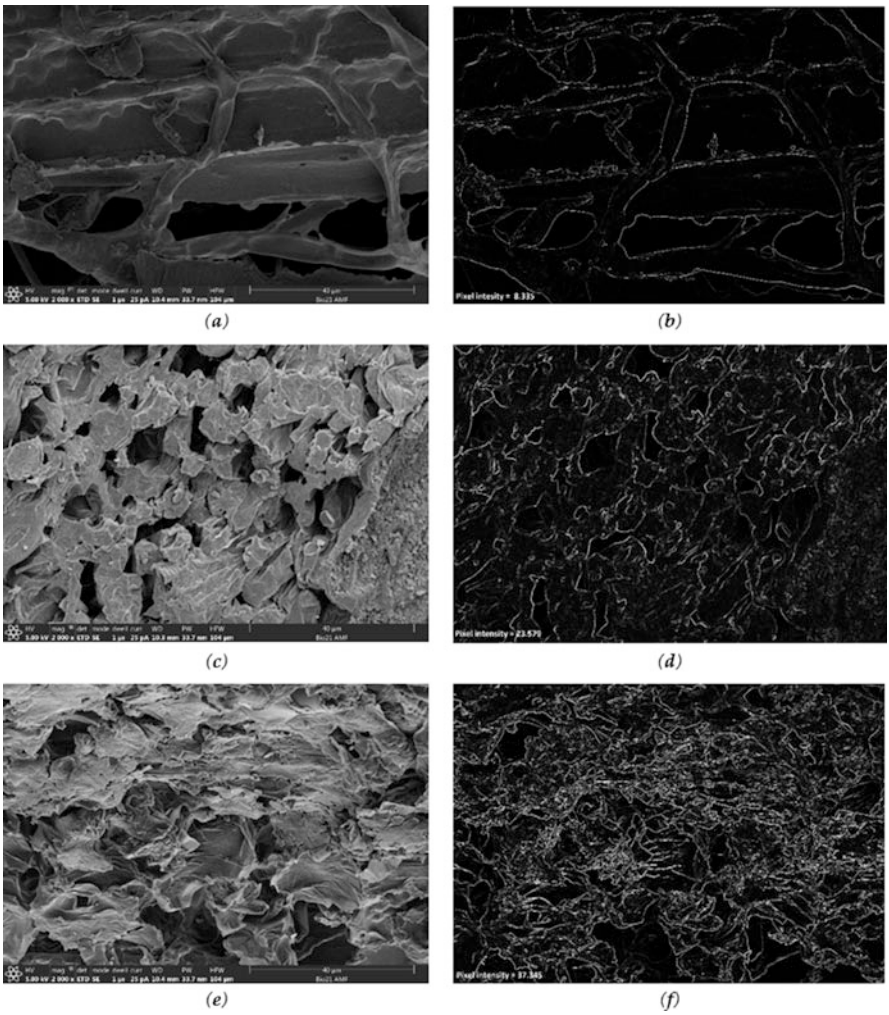

Fig. 10.1 Scanning electron microscope images of wheat hay, (**a**, **b**) SEM and Fiji analytical image of untreated hay, respectively, (**c**, **d**) SEM and intensity variance image of MW treated (taken from the top of the sample), respectively, (**e**, **f**) MW treated (taken from the center core of the sample), respectively. [21]

for crushing and breaking down the MW-treated plant fiber may be less during feed intake and digestion [32].

10.3 Microwave Treatment and Feed Nutritive Value

The effect of MW treatment on different feed resources' nutritive values is shown in Table 10.1.

Table 10.1 Effect of MW heat treatment on different feed resources' nutritive value and animal performance

Target feed resources	MW power (W)	Treatment time (seconds)	Moisture added	CP	Non-fiber CHO	NDF	ADF	In vitro DMD (Pepsin-cellulase)	*In saco* effective rumen DM degradability	In vitro gas production	In vitro intestinal CP digestibility	Animal trial	References
Roughage feed resource													
Lucerne hay	750	0, 40, and 80	No	ND	NM	NM	NM	↑	NM	NM	NM	↑ LWG (sheep)	[18]
Lucerne hay	1100	0, 20, 40, 60, and 80	No	ND	NM	ND	ND	↑	NM	NM	NM	NM	[21]
Canola hay				↑		ND	ND	↑					
Pasture hay				ND		↓	ND	↓					
Oat hay				↑		↑	ND	↓					
Wheat hay				ND		ND	ND	↑					
Wheat straw	750	0, 240, and 480	No	ND	NM	NM	ND	NM	↑(Yak's rumen)	NM	NM	NM	[37]
Concentrate feeds resource													
Canola meal	800	0, 120, 240, and 360	Yes	NM	NM	NM	NM	NM	↓	NM	↑	NM	[20]
Canola seed	800	0, 120, 240, and 360	Yes	ND	NM	ND	ND	NM	↓	NM	↑	NM	[50]
Soybean meal	800	0, 120, 240, and 360	Yes	NM	NM	NM	NM	NM	↓	NM	↑	NM	[39]

(continued)

Table 10.1 (continued)

Target feed resources	MW power (W)	Treatment time (seconds)	Moisture added	CP	Non-fiber CHO	NDF	ADF	In vitro DMD (Pepsin-cellulase)	*In saco* effective rumen DM degradability	In vitro gas production	In vitro intestinal CP digestibility	Animal trial	References
Corn/ maize	800	0, 180, 300, and 420	Yes	NM	NM	NM	NM	NM	↓	NM	NM	NM	[51]
Barley	800	0, 180, 300, and 420	Yes	NM	NM	NM	NM	NM	↓	NM	NM	NM	[52]
Cotton seed meal	800	0, 120, 240, and 360	Yes	NM	NM	NM	NM	NM	↓	NM	↑	NM	[53]
Safflower seed	900	0, and 180	Yes	NM	NM	NM	NM	NM	↓	↑	↑	NM	[54]
Sunflower seed	1000	0, and 360	NS	NM	NM	NM	NM	NM	NM	↑	NM	NM	[55]
Sorghum	900	0, 180, 300, and 420	Yes	NM	NM	NM	NM	NM	NM	↑	NM	↑ DMD/ OMD (sheep)	[56]
Sorghum	900	0, 180, 300, and 420	Yes	NM	NM	NM	NM	NM	NM	↑	NM	NM	[57]
Wheat				NM	NM	NM	NM	NM	NM	↑	NM		
Sorghum	900	0, 180, and 300	NS	NM	NM	NM	NM	NM	NM	↑	NM	NM	[46]
Corn/ maize				NM	NM	NM	NM	NM	NM	↑	NM	NM	
Wheat				NM	NM	NM	NM	NM	NM	ND	NM	NM	
Guar meal	900		Yes	NM	NM	NM	NM	NM	ND	↓	↑	NM	[19]

		0, 120, 240, and 360											
Oak nut	900	0, 120, 240, and 360	No	ND	NM	NM	NM	NM	↑	↑	NM	NM	[58]
Wheat*	1100	0, 15, 30, 45, and 60	No	↑	NM	↑	↑	ND	NM	NM	NM	NM	*(Shishir et al.)
Faba bean *			No	↑	NM	↑	↑	↑	NM	NM	NM	NM	

CP crude protein, *Non-fiber CHO* non-fiber carbohydrate (starch, sugar, etc.), *NDF* neutral detergent fiber, *ADF* acid detergent fiber, *DM* dry matter, *DMD* dry matter digestibility, *OMD* organic matter digestibility, *LWG* live weight gain, *NM* not measured or mentioned, ↑ increasing; ↓ decreasing, *ND* no difference. *Data was presented orally in 55 International Microwave Power Institute. The data will be published as proceeding

10.3.1 Microwave Treatment Effect on Roughage Feed Nutritive Value

For ruminants, roughage feeding is a significant portion of the total ration. Fresh forage is the most common form of roughage, where ruminant animals directly graze pastures and grasslands. However, due to seasonal variation, year-round fresh forage feeding is not always possible. As a result, alternative forms of roughage feed resources, such as hay or straw, are used by the farmers to fill feed gaps. Considering the fact that, hay and straw normally have low to moderate quality compared with fresh forage, farmers have been urged for decades to develop alternative processing techniques to improve low-quality roughages.

Over time, researchers have studied different processing techniques (chemical, physical, or biological) to improve dry roughage quality [33–36]. However, despite quality improvements, most of the efficient methods are not sustainable for commercial use due to their high processing cost, being hazardous to humans and the environment, their longer operating time, and/or their higher energy consumption/cost. Several studies suggested that MW treatment of forage hay has potential to improve feed quality. Dong et al. [37] suggested that MW treatment can improve the ruminal organic matter degradability of wheat straw by 20% vs. control. This was found in an *in sacco* degradability experiment with yak-fed wheat straw that was MW treated in a 750 W power oven, operating with a frequency of 2.45 GHz, for up to 480 s. Another interesting finding of this study was that acid detergent fiber digestibility improved by 62% without creating any negative effect on other chemical components of the treated wheat straw.

In a small-scale pepsin cellulase in vitro study, Brodie et al. [18] found that dry matter digestibility (DMD) of lucerne hay increased by 15% when it was MW treated for up to 80 s using a 750 W MW oven, operating at a frequency 2.45 GHz. Brodie et al. [18] treated lucerne hay in larger quantity (25 kg bags) with a 6 kW, 2.45 GHz, MW chamber for 450, 900, 1350, and 1800 s in a larger scale experiment. This experiment also found an improvement in DMD %; however, the level of DMD increase (i.e. 6%) was less than the aforementioned small-scale pepsin cellulase study.

In a follow-up sheep growth trial, Brodie et al. [18] found that this 6% improvement of DMD in the 25 kg bags of MW-treated lucerne hay led to an 8.1% increase in liveweight gain in the sheep fed the MW-treated lucerne hay in comparison with the sheep being fed the untreated lucerne hay. After calculating energy efficiency, Brodie et al. [18] found that the bulk treatment of lucerne hay samples (25 kg bag for 900 s with 6 kW power) consumed approximately 216 kJ kg^{-1} of equivalent energy to achieve a 6% increase in pepsin-cellulase DMD, compared with the control, which provided an extra 540 kJ kg^{-1} of metabolizable energy (ME) to the sheep during the growth trial (considering that lucerne hay contained approximately 9.16 MJ kg^{-1} ME according to El-Meccawi et al. [38]).

Furthermore, in simple economic analysis, Brodie et al. [18] demonstrate that providing the extra 540 kJ kg^{-1} of ME to the sheep led to an additional AU$6.50 per

head for the sheep that were fed with the MW-treated lucerne hay over the 5 weeks, considering all the treatment and other costs.

Recently in a multi-forage hay pepsin cellulase in vitro study, Shishir et al. [21] treated five forage hays (lucerne, canola, wheat, pasture, and oat) for five treatment times of 0, 20, 40, 60, and 80 s with MW power of 1.1 kW in an oven operating at 2.45 GHz. He found that lucerne, canola, and wheat hay digestibility of organic matter in the dry matter (DOMD) was increased by 14, 12, and 8%, respectively. However, the improvement occurred in the forage hays after different MW treatment times (lucerne 60 s, canola 20 s, and wheat 40 seconds). Shishir et al. [21] also found a strong positive relationship ($r^2 = 0.79$; $p < 0.001$) between crude protein (CP) content of the untreated forage hays and the MW energy requirement for their optimal DMD improvement. This finding provides an approach to calculating the MW energy requirement for hay treatment to achieve increased DMD when the CP content of the selected forage is known.

The review of these studies demonstrates that MW treatment has the potential to improve the quality of low-quality roughage for better ruminant production. However, the limited number of studies is a major drawback. More research is required to understand the effects of MW treatment of hay under different conditions to develop MW processing method further.

10.4 MW Treatment Effect on Concentrate Feed Nutritive Value

Feeding concentrate to the animals is considerably more complicated in comparison with roughage feeding. Certain criteria need to be considered while feeding concentrate feed resources, including the type of animal (ruminant vs. nonruminants), the availability and price of the feed resource, and the presence of anti-nutritional factors (e.g., trypsin inhibitor in soybean meal, gossypol in cottonseed meal, etc.). Therefore, the effect of MW treatment application on concentrate feed resources' nutritive value needs to be considered for both ruminant and nonruminant animals.

10.5 Microwave Treatment on Concentrate Feed's Ruminal Degradation and Fermentation Characteristics

Rumen degradability of feed nutrients is used to describe the supply of available nutrients to the anaerobic microbes and body tissues of ruminant animals [1]. The MW heat treatment effect on effective rumen degradability of dry matter (DM) and CP of different grains were measured in several studies (Table 10.1). All the studies found that DM and CP's ruminal degradability were decreased significantly ($P < 0.05$) when treated with MW compared with the control. However, the level

of reduction on DM and CP degradability was not the same across different grain types. A previous study showed soybean meal treated with MW reduced both in vitro DM and CP degradability by 40% compared with untreated soybean meal [39].

On the other hand, barley grain showed only a 4.4 and 17% reduction in in vitro DM and CP degradability, respectively. The magnitude of changes can be attributed to the variation in the nutrients present and the morphological structure of the feed type. For example, the lower degradability of DM in MW-treated grain was attributed to the reduction in effective protein degradation. This may link to the MW heat treatment of feed increased the feed protein's enzyme resistance [40]. Besides, Banik et al. [41] suggested that there may be some non-thermal effect of MW heat treatment on protein alteration and transformation.

It is a well-established fact that the protein's denaturation and unfolding due to heating could break the bond that stabilizes the protein's tertiary structure. As a result, hydrophobic groups of proteins get exposed to enzymes, which reduces the protein solubility [42] and ruminal protein degradability. This statement is also supported by Prestløkken [43] with an *in sacco* study, where pelleted and expander-treated barley were suspended in three non-lactating dairy cows. Prestløkken [43] reported that hydrophobic amino acids degraded less in the rumen than hydrophilic amino acids.

One of the important concentrate feeds used in animal production is sorghum; however, a major limitation to the use of sorghum is that its starch digestibility is comparatively lower than other cereal grains. This is due to peripheral endosperm layer resistance that encloses the starch granule [44]. The MW heating can help to disrupt the complex protein–starch bond by migrating and liberating hygroscopically bound water within the organic complexes [45].

In an in vitro rumen fermentation study, Bootes et al. [46] treated three-grain sorghums, maize, and wheat grains in a 900 W, 2.45 GHz MW oven for 180 and 300 s. The results showed that the maximum amount of ruminal gas production was increased by 6.9% in sorghum and 5.5% in maize, but not in wheat when treated for 180 s. The gas production indicated the microbial fermentation characteristics due to feeding various types of feed resources. It also helped predict the range and rate of digestion of different feed resources [47]. However, no changes occurred beyond 180 s of MW treatment. This result demonstrated that MW treatment could improve rumen in vitro gas production of sorghum and maize when correct treatment time was applied.

In another study, sorghum and broom sorghum were treated with MW. The MW heat treatment significantly increased in vitro gas production. The maximum gas production with 3, 5, and 7 min treatment time for sorghum increased by 10, 13, and 8%, respectively, in MW-treated sorghum [48].

10.6 MW-Treatment Effect on Concentrate Intestinal Crude Protein Digestibility in Ruminant

In case of ruminant production systems, by-pass protein plays an important role. By-pass protein is a portion of dietary proteins that by-pass or escape the rumen degradation process and are made available for intestinal digestion [49]. In addition, there are other different protein sources available for intestinal digestion, such as microbial protein synthesized in the rumen and endogenous proteins from the animal's body. Over the last century, animal researchers have tried to develop some physical or chemical techniques that can manipulate the degradable nature of CP to prevent the degradation of protein in the rumen [49]. Table 10.1 showed that, physical techniques like MW treatment have been proven to decrease CP's degradability in the rumen and increase CP digestibility in the intestine at the same time.

In addition to that, Fig. 10.2 demonstrated that, MW studies with canola seed [50], canola meal [20], cottonseed meal [53], and soybean meal [39] increased intestinal CP digestibility by 7–25%, with some differences between feed sources and MW treatment times. The mechanism for MW heat treatment to increase intestinal CP digestibility may be due to enhance the protein denaturation and unfolding of the tertiary structure, which exposes hydrophobic amino acid with positional group active sites for enzymes like pepsin and trypsin present in the small intestine [76, 77]).

10.7 Microwave Treatment Effect on Anti-Nutritional Factors Present in Feed

Anti-nutritional factors are the chemical compounds, or their secondary metabolites, found in feedstuff, which intervene in feed utilization, digestive processes, or metabolic utilization of feed [59]. There are different types and levels of anti-nutritional factors in feeds that can cause problems during feed ingestion and

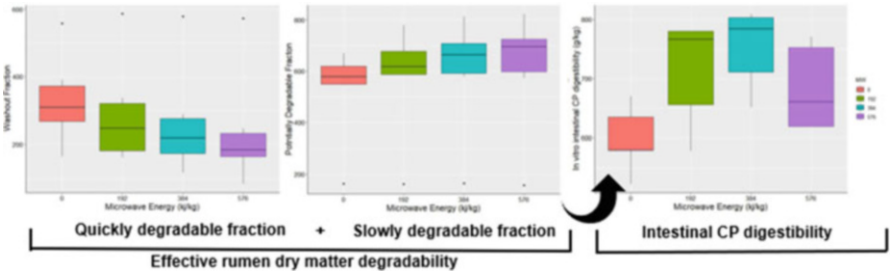

Fig. 10.2 Graphical presentation of the effect of MW heat treatment on ruminal DM degradability and intestinal CP digestibility of concentrate feeds (canola seed, canola meal, soybean meal, and cottonseed meal) (Shishir et al., unpublished)

utilization in animals. As a result, many physical and chemical methods have been applied to reduce the harmful effects of anti-nutritional factors of plant feed components on animals (e.g., heating, chemical treatment, extraction, etc.) [60, 61]. Physical treatments, like MW heat treatment, have been effective in completely removing trypsin inhibitors from legume seed [62]. In addition, other anti-nutritional factors like tannins and phytic acid in legume seeds are also significantly reduced by MW treatment [62]. The reduction in these anti-nutritional factors due to MW treatment may be partly due to their heat-labile nature and the formation of insoluble chemical complexes [63, 64].

Increased animal performance by reducing anti-nutritional factors in feed by MW treatment was demonstrated in nonruminant animals by Xian and Farrell [65]. In this study, MW-treated raw soya bean had reduced trypsin inhibitor and urease activity after 330 s of MW treatment with 14.1 kW conveyor-type MW oven. When fed to chickens, the apparent digestibility for MW-processed raw soybean was significantly higher, except for nitrogen retention. On the other hand, feed intake (DM and CP intake) was lower in the MW-processed soybean diet than the raw diet. The growth rate of chicken fed MW-processed soybean diet was 76% higher than the control group. In a rat feeding trial, significant increases in growth rate were observed due to being fed a MW-processed soybean diet, which led to higher efficiency in feed conversion ratio (FCR). But, no effect was observed in feed intake. In the case of rabbits, no significant effect was found in performance whatsoever. The results demonstrated that positive responses can be achieved for nonruminant animals, like poultry, due to the reduction of anti-nutrition factors. However, more extensive research is needed to understand the MW treatment's effect on a broader range of anti-nutritional factors in feed resources.

10.8 Microwave-Treated Concentrate Feed Effect on Ruminant Animal Performance

In regard to ruminant animal feeding trials with MW treatment concentrate feed resources, only the in vivo study conducted by Khajehdizaj et al. [56] on sheep fed on MW-treated sorghum observed the effect on sheep nutrient utilization, blood metabolites, and fermentation characteristics. The apparent digestibility of DM, organic matter, and starch increased linearly when treated with 900 W of MW power, operating at 2.45 GHz, for 300 s. In the rumen fermentation characteristics, the concentration of volatile fatty acid in the rumen fluid was significantly higher in the MW-treated sorghum. On the other hand, ammonia nitrogen was linearly reduced with increasing MW treatment time, from 0 to 300 s. However, no significant effect was observed on the blood parameters due to feeding MW-treated sorghum. The lack of in vivo studies of MW-treated feed highlights an important knowledge gap.

10.9 Microwave Drying

There is a wide range of drying applications that have been used in processing animal feed and animal origin food products (e.g., meat and egg). Many studies have investigated MW drying applications to various feed resources. Irrespective of the purpose of drying, MW heating showed some favorable aspects in each case. To preserve quality during storage and avoid spontaneous combustion, drying of forage or concentrate feeds with MW can be useful [45]. The MW drying proved to be more convenient due to its high energy efficiency and quick-drying and less effect on the product quality than conventional hot air drying [66]. In many cases, MW drying even improved the products' quality because rapid energy absorption in the material during MW heating, due to dielectric properties, led to quick evaporation of moisture [24], which causes less damage to the product quality. The MW drying has also been extensively used for moisture determination in the lab [67, 68] and to help preserve the sample for further chemical analysis [23, 69] since it has been found in research that MW heating has minimal effects on the nutrient composition of the material [70, 71].

10.10 Microwave Soil Treatment Effect on Crop Growth and Yield

Wheat and rice can be utilized as a grazing crop for animal production. Previous studies suggested that soil MW treatment increased wheat and rice biomass yield by 33% and 22%, respectively [72, 73]. This indicates that there is a potential to offer more feed to the grazing animal in the form of grazed forage by considering MW heat-treated paddocks vs. non-treated paddocks, which may lead to increased animal production performance. On the other hand, a recent paper published by Khan et al. [74] showed that MW soil treatment did not alter rice crop (plant and grain) nutritive value. However, an increase in total nitrogen and DM accumulation in the rice crop was observed under field conditions. The higher DM production of MW-treated soil may support higher stocking rates and animal production if it is grazed by livestock; however, experimental work with grazing animals on the MW-heat-treated paddocks or small plots is required to validate this hypothesis. Further work in pastures and grasslands is required to examine if yield increases also occur in those systems to increase animal performance.

10.11 Prospect of MW Technology in Animal Production System

It is plausible to predict that the future advancement of any technology must consider three points to become useful and sustainable at the same time. These points are time efficiency, energy efficiency, and being relatively risk-free. The MW technology

potentially fulfills all these criteria and has already been proven in many fields, like the technical, agriculture, medical industries, etc. [17]. The MW techniques may be a prospective technique that can possibly replace existing drying techniques in the feed milling industry worldwide. Furthermore, the potentiality of MW techniques regarding the removal or reduction of anti-nutritional factors will help develop techniques that can increase the storage life of animal feed and animal products.

Moreover, improving the nutritive value of feed may lead to lower energy losses in the form of methane from ruminant animals [75]. This will reduce the enteric greenhouse gas contribution from the ruminants. However, MW treatment's possible effect on the conversion rate of methane has not yet been studied. Future work needs to determine the optimal MW treatment energy level (kW), time, frquency to improve feed quality, yield and animal performance. Mathmatical model need to build to support the decision making process of optimal MW treatment selection.

10.12 Conclusion

In a sustainable animal production system, the feed will always be the most important input. The MW treatment is a processing technique that may help to achieve maximum nutritional benefits from the animal feed from the intake and utilization point of view. In order to gain more comprehensive knowledge on how MW heat treatment may impact on feed quality parameters in forage/conserved forage, further research needs to be conducted. In addition, the exploration of the mechanisms that underpin previously observed feed quality changes in grain/meals is also needed. The level of MW power used, application duration (time), feed physical/chemical structure, and their interactive effects on feed quality and animal performance are the key areas to be understood. While in vivo animal study is essential to validate the use of MW application in the animal industry, the in vitro study will continue to be a time/cost-effective approach to conduct a preliminary analysis to recognize the usefulness of MW heat treatment in animal production.

References

1. Chaudhry AS. Forage based animal production systems and sustainability, an invited keynote. Rev Bras Zootec. 2008;37(Special Issue):78–84.
2. Tona GO. Current and future improvements in livestock nutrition and feed resources. Anim Husb Nutr. 2018:147–69.
3. Behnke KC. Feed manufacturing technology: current issues and challenges. J Anim Feed Sci Technol. 1996;62(1):49–57.
4. Moran J. Tropical dairy farming: feeding management for small holder dairy farmers in the humid tropics. Melbourne: CSIRO Publishing; 2005.
5. Chapman D, Lee J, Waghorn G. Interaction between plant physiology and pasture feeding value: a review. J Crop Past Sci. 2014;65(8):721–34.

6. Coffey D, Dawson K, Ferket P, Connolly A. Review of the feed industry from a historical perspective and implications for its future. J Appl Anim Nutr. 2016:4.
7. Rosentrater K, Evers A. Feed and industrial uses for cereals. Cambridge: Woodhead Publishing; 2018.
8. Stein H, Bohlke R. The effects of thermal treatment of field peas (Pisum sativum L.) on nutrient and energy digestibility by growing pigs. J Anim Sci. 2007;85(6):1424–31.
9. Matsushima JK. History of feed processing. Proceeding of Cattle Grain Proccessing Symposium; 2006, p. 1–16.
10. Uden P. The effect of grinding and pelleting hay on digestibility, fermentation rate, digesta passage and rumen and faecal particle size in cows. J Anim Feed Sci Technol. 1988;19 (1–2):145–57.
11. Riaz MN. Chapter 16: Food extruders. In: Kutz M, editor. Handbook of farm, dairy and food machinery engineering. 2nd ed. San Diego, CA: Academic Press; 2013. p. 427–40.
12. Liu J-X, Orskov E, Chen X. Optimization of steam treatment as a method for upgrading rice straw as feeds. J Anim Feed Sci Technol. 1999;76(3–4):345–57.
13. Rai S, Mudgal V. Synergistic effect of sodium hydroxide and steam pressure treatment on composition changes and fibre utilization of wheat straw. J Biol Wastes. 1988;24(2):105–13.
14. Ørskov ER. Feed science. Madison, WI: Elsevier Science Publishers, The University of Wisconsin; 1988.
15. Wagner JJ, Archibeque SL, Feuz DM. The modern feedlot for finishing cattle. J Ann Rev Anim Biosci. 2014;2(1):535–54.
16. Chandrasekaran S, Ramanathan S, Basak T. Microwave food processing—A review. Food Res Int. 2013;52(1):243–61.
17. Ayappa K, Davis H, Crapiste G, Davis E, Gordon J. Microwave heating: an evaluation of power formulations. Chem Eng Sci. 1991;46(4):1005–16.
18. Brodie G, Rath C, Devanny M, Reeve J, Lancaster C, Doherty T, Harris G, Chaplin S, Laird C. The effect of microwave treatment on animal fodder. J Microw Power Electromagn Energy. 2012;46(2):57–67.
19. Narimani S, Taghizadeh A, Sis NM, Parnian F, Nobari BB. Effects of compound treatment of exogenous feed enzymes and microwave irradiation on in vitro ruminal fermentation and intestinal digestion of guar meal. Indian J Anim Sci. 2014;84(4):436–41.
20. Sadeghi A, Shawrang P. Effects of microwave irradiation on ruminal degradability and in vitro digestibility of canola meal. Anim Feed Sci Technol. 2006;127(1–2):45–54.
21. Shishir MSR, Brodie G, Cullen B, Kaur R, Cho E, Cheng L. Microwave heat treatment induced changes in forage hay digestibility and cell microstructure. J Appl Sci. 2020;10(22):8017.
22. Singh R, Tiwari S, Srivastava M, Shukla A. Microwave assisted alkali pretreatment of rice straw for enhancing enzymatic digestibility. J Energy. 2014:2014.
23. Higgins T, Spooner A. Microwave drying of alfalfa compared to field-and oven-drying: effects on forage quality. Anim Feed Sci Technol. 1986;16(1–2):1–6.
24. Brodie G. Simultaneous heat and moisture diffusion during microwave heating of moist wood. Appl Eng Agric. 2007;23(2):179–87.
25. Brodie G, Rath C, Devanny M, Reeve J, Lancaster C, Harris G, Chaplin S, Laird C. Effect of microwave treatment on lucerne fodder. Anim Prod Sci. 2010;50(2):124–9.
26. Choi I, Choi SJ, Chun JK, Moon TW. Extraction yield of soluble protein and microstructure of soybean affected by microwave heating. J Food Process Preserv. 2006;30(4):407–19.
27. Torgovnikov G, Vinden P, Folz D, Booske J, Clark D, Gerling J. In: Folz DC, Booske JH, Clark DE, Gerling JF, editors. Innovative microwave technology for the timber industry. Microwave and radio frequency applications: proceedings of the third world congress on microwave and radio frequency applications'; 2003. p. 349–56.
28. Ponne CT, Möller AC, Tijskens LM, Bartels PV, Meijer MM. Influence of microwave and steam heating on lipase activity and microstructure of rapeseed (Brassica napus). J Agric Food Chem. 1996;44(9):2818–24.

29. Wroniak M, Rękas A, Siger A, Janowicz M. Microwave pretreatment effects on the changes in seeds microstructure, chemical composition and oxidative stability of rapeseed oil. J LWT Food Sci Technol. 2016;68:634–41.
30. Aparna R, Josemartin MJ. Application of image intensity local variance measure for analysis of distorted images. 2017 International Conference on Networks & Advances in Computational Technologies (NetACT), 20–22 July 2017; 2017, pp. 382–386.
31. Brodie G. Microwave heating in moist materials. In: Advances in induction and microwave heating of mineral and organic materials. Vienna: IntechOpen; 2011.
32. Brodie, G., Jacob, M.V., Farrell, P. 2016. Microwave and radio-frequency Technologies in Agriculture: an introduction for agriculturalists and engineers. Walter de Gruyter GmbH & Co KG.
33. Ajila C, Brar S, Verma M, Tyagi R, Godbout S, Valéro J. Bio-processing of agro-byproducts to animal feed. J Crit Rev Biotechnol. 2012;32(4):382–400.
34. Ghasemi E, Khorvash M, Ghorbani GR, Emami MR, Karimi K. Dry chemical processing and ensiling of rice straw to improve its quality for use as ruminant feed. J Trop Anim Health. 2013;45(5):1215–21.
35. Hartley R. Chemical constitution, properties and processing of lignocellulosic wastes in relation to nutritional quality for animals. J Agric Environ Microbiol. 1981;6(2–3):91–113.
36. Viola E, Zimbardi F, Cardinale M, Cardinale G, Braccio G, Gambacorta E. Processing cereal straws by steam explosion in a pilot plant to enhance digestibility in ruminants. J Bioresour Technol. 2008;99(4):681–9.
37. Dong S, Long R, Zhang D, Hu Z, Pu X. Effect of microwave treatment on chemical composition and in sacco digestibility of wheat straw in yak cow. Asian Australas J Anim Sci. 2005;18 (1):27–31.
38. El-Meccawi S, Kam M, Brosh A, Degen A. Heat production and energy balance of sheep and goats fed sole diets of. Acacia Saligna Medicago Sativa. 2008;75(2–3):199–203.
39. Sadeghi A, Nikkhah A, Shawrang P. Effects of microwave irradiation on ruminal degradation and in vitro digestibility of soya-bean meal. Anim Sci. 2005;80(3):369–75.
40. Englard S, Seifter S. Precipitation techniques. In: Deutscher MP, editor. Methods in enzymology, vol. 182. New York: Academic Press; 1990. p. 285–300.
41. Banik S, Bandyopadhyay S, Ganguly S. Bioeffects of microwave—a brief review. J Bioresour Technol. 2003;87(2):155–9.
42. Voragen A. Effects of some manufacturing technologies on chemical, physical and nutritional properties of feed. J Rec Adv Anim Nutr. 1995
43. Prestløkken E. Ruminal degradability and intestinal digestibility of protein and amino acids in barley and oats expander-treated at various intensities. J Anim Feed Sci Technol. 1999;82 (3–4):157–75.
44. Rooney L, Pflugfelder R. Factors affecting starch digestibility with special emphasis on sorghum and corn. J Anim Sci. 1986;63(5):1607–23.
45. Brodie G, Bootes N, Dunshea F, Leury B. Microwave processing of animal feed: A brief review. Trans ASABE. 2019;62(3):705–17.
46. Bootes NG, Brodie G, Leury B, Russo VM, Dunshea F. Microwaving improves in vitro rumen fermentation of sorghum.. 8 th INRA-Rowett Symposium on Gut Microbiology Gut microbiota: friend or foe? , June 2012, Polydome Congress Centre Clermont-Ferrand. INRA and Rowett Institutes of Nutrition and Health; 2012, pp. 110.
47. Getachew G, DePeters E, Robinson P. In vitro gas production provides effective method for assessing ruminant feeds. J Cali Agric. 2004;58(1):54–8.
48. Parnian F, Taghizadeh A. Evaluation of microwave irradiation effects on nutritive value of broom sorghum grain using an in vitro gas production technique. Proceedings of the British Society of Animal Science. Cambridge University Press; 2009, pp. 182–182.
49. Kempton T, Nolan J, Leng R. Principles for the use of non-protein nitrogen and by-pass proteins in diets of ruminants. Rome: Food and Agricultural Organization; 1977.

50. Ebrahimi S, Nikkhah A, Sadeghi A. Changes in nutritive value and digestion kinetics of canola seed due to microwave irradiation. Asian Australas J Anim Sci. 2010;23(3):347–54.
51. Sadeghi A, Shawrang P. Effects of microwave irradiation on ruminal protein and starch degradation of corn grain. Anim Feed Sci Technol. 2006;127(1-2):113–23.
52. Sadeghi A, Shawrang P. Effects of microwave irradiation on ruminal dry matter, protein and starch degradation characteristics of barley grain. Anim Feed Sci Technol. 2008;141 (1–2):184–94.
53. Sadeghi A, Shawrang P. Effects of microwave irradiation on ruminal protein degradation and intestinal digestibility of cottonseed meal. Livest Sci. 2007;106(2–3):176–81.
54. Paya H, Taghizadeh A, Janmohammadi H, Moghaddam GA, Khani AH, Alijani S. Effects of microwave irradiation on in vitro ruminal fermentation and ruminal and post-ruminal disappearance of safflower seed. J Biodivers Environ Sci. 2014;5(2):349–56.
55. Maheri-Sis N, Baradaran-Hasanzadeh A, Salamatdoust R, Khosravifar O, Agajanzadeh-Golshani A, Dolgari-Sharaf J. Effect of microwave irradiation on nutritive value of sunflower meal for ruminants using in vitro gas production technique. J Anim Plant Sci. 2011;2 (12):126–31.
56. Khajehdizaj FP, Taghizadeh A, Nobari BB. Effect of feeding microwave irradiated sorghum grain on nutrient utilization, rumen fermentation and serum metabolites in sheep. J Livest Sci. 2014;167:161–70.
57. Parnian F, Taghizadeh A, Nobari BB. Use of in vitro gas production technique to evaluate the effects of microwave irradiation on sorghum (Sorghum bicolor) and wheat (Triticum sp.) nutritive values and fermentation characteristics. J BioSci Biotechnol. 2013;2(2):125–30.
58. Emrah K, Atalay AI, Kamalak A, Özer K, Salih MJM, Zangana DN. Determination of effects of microwave irradiation on fermentation of oak nut (Quercus coccifera) using Hohenheim gas production technique. KSU J Nat Sci. 2016;19(3):268.
59. Soetan KO, Oyewole OE. The need for adequate processing to reduce the anti-nutritional factors in plants used as human foods and animal feeds: a review. Afr J Food Sci. 2009;3 (9):223–32.
60. Mubarak A. Nutritional composition and antinutritional factors of mung bean seeds (Phaseolus aureus) as affected by some home traditional processes. J Food Chem. 2005;89(4):489–95.
61. Yacout M. Anti-nutritional factors & its roles in animal nutrition. J Dairy Vet Anim Res. 2016;4 (1):237–9.
62. Khattab R, Arntfield S. Nutritional quality of legume seeds as affected by some physical treatments 2. Antinutritional factors. LWT Food Sci Technol. 2009;42(6):1113–8.
63. Rakić S, Petrović S, Kukić J, Jadranin M, Tešević V, Povrenović D, Šiler-Marinković SJFC. Influence of thermal treatment on phenolic compounds and antioxidant properties of oak acorns from. Serbia. 2007;104(2):830–4.
64. Udensi E, Ekwu F, Isinguzo J. Antinutrient factors of vegetable cowpea (Sesquipedalis) seeds during thermal processing. Pak J Nutr. 2007;6(2):194–7.
65. Xian J, Farrell D. The nutritive value of microwave-processed raw soya beans determined with chickens, rats and rabbits. J Anim Feed Sci Technol. 1991;34(1–2):127–39.
66. Vadivambal R, Jayas D. Changes in quality of microwave-treated agricultural products—a review. Biosyst Eng. 2007;98(1):1–16.
67. Altan A. Effects of pretreatments and moisture content on microstructure and physical properties of microwave expanded hull-less barley. Food Res Int. 2014;56:126–35.
68. Nirmaan A, Prasantha BR, Peiris BJC. Comparison of microwave drying and oven-drying techniques for moisture determination of three paddy (Oryza sativa L.) varieties. Chem Biol Technol Agric. 2020;7(1):1–77.
69. Goossen C, Bosworth S, Darby H, Kraft J. Microwave pretreatment allows accurate fatty acid analysis of small fresh weight (100 g) dried alfalfa, ryegrass, and winter rye samples. Anim Feed Sci Technol. 2018;239:74–84.

70. Lenaerts S, Van Der Borght M, Callens A, Van Campenhout L. Suitability of microwave drying for mealworms (Tenebrio molitor) as alternative to freeze drying: Impact on nutritional quality and colour. Food Chem. 2018;254:129–36.
71. Pradeep P, Abdullah SA, Choi W, Jun S, Oh S, Ko S. Potentials of microwave heating technology for select food processing applications-a brief overview and update. J Food Process Technol. 2013;4(11):278.
72. Khan MJ, Brodie G, Gupta D. Potential of microwave soil heating for weed management and yield improvement in rice cropping. J Crop Past Sci. 2019;70(3):211–7.
73. Khan MJ, Brodie GI, Gupta D, He J. Microwave soil treatment increases soil nitrogen supply for sustained wheat productivity. J Trans ASABE. 2019;62(2):355–62.
74. Khan MJ, Brodie G, Cheng L, Liu W, Jhajj R. Impact of microwave soil heating on the yield and nutritive value of rice crop. J Agric. 2019;9(7):134.
75. Eckard R, Grainger C, De Klein C. Options for the abatement of methane and nitrous oxide from ruminant production: a review. J Livestock Sci. 2010;130(1–3):47–56.
76. Alajaji SA, El-Adawy TA. Nutritional composition of chickpea (Cicer arietinum L.) as affected by microwave cooking and other traditional cooking methods. J Food Com Anal. 2006;19 (8):806–12.
77. Negi A, Boora P, Khetarpaul N. Effect of microwave cooking on the starch and protein digestibility of some newly released moth bean (Phaseolus aconitifolius Jacq.) cultivars. J Food Com Anal. 2001;14(5):541–6.
78. Chen C, Aita G, Boldor D. Enhancing enzymatic digestibility of sweet sorghum by microwave-assisted dilute ammonia pretreatment. In: 2010 Pittsburgh, Pennsylvania, June 20 - June 23, 2010, St. Joseph, MI: ASABE; 2010.

Chapter 11
Microwave Heating for Grain Treatment

Saeedeh Taheri, Graham Ian Brodie, and Dorin Gupta

Abstract Microwave radiation as an emerging technology has shown a great potential in food and agriculture. Microwave as a source for thermal treatment of grains will be discussed in this chapter. The applications of microwave heating for fungi control (disinfection), insect control (disinfestation), drying, modification of seed quality and seed germination enhancement will be reviewed, and any challenges of industrialization will be discussed. Overall, microwave heating has a great potential in grain industry, but special considerations should be taken into account for having a uniform heating of the grains to maintain their quality attributes, especially the seed viability which is of great importance for those with sowing purposes.

Keywords Microwave · Grains · Drying · Disinfection · Insect control · Dielectric properties

11.1 Introduction

The increasing world population needs much more food than ever before. With diminishing resources in the world, the food and agriculture industry must devise new strategies to meet the demand. One way of responding to the growing demand for food is to reduce waste of agriculture products pre- and post-farmgate. Food loss and wastage in the world consists of approximately 1.3B tonnes of food or one-third of edible food produced for consumption [1]. Reduction of this loss would mean providing more food for the fast-growing world population, which will need 60% more food by 2050 [2].

S. Taheri (✉) · G. I. Brodie · D. Gupta
School of Agriculture and Food, Faculty of Veterinary and Agricultural Sciences, The University of Melbourne, Melbourne, VIC, Australia
e-mail: saeedeh.taheri@unimelb.edu.au; grahamb@unimelb.edu.au; dorin.gupta@unimelb.edu.au

S. Horikoshi et al. (eds.), *Agritech: Innovative Agriculture Using Microwaves and Plasmas*, https://doi.org/10.1007/978-981-16-3891-6_11

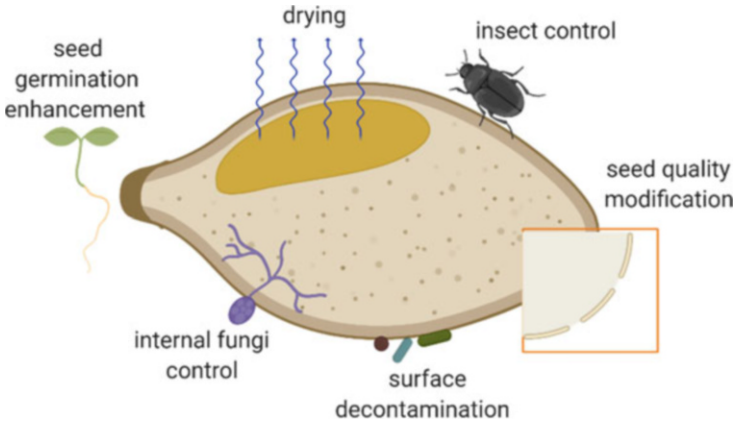

Fig. 11.1 Summary of the applications of microwave heating for grain seeds (created in Biorender.com)

Emerging technologies are defined as the new technologies that are in the phase of research and development and will significantly affect the business and social environment in the near future (5–10 years) [3]. These technologies aim to reduce energy consumption, create a sustainable food production, and meet the modern consumers' demand for safer, healthier, fresher, and more natural food with a less detrimental impact on the environment [3, 4].

Microwave heating is one of these emerging clean-energy technologies which is still under investigation in the food and agriculture sectors. It is defined as a type of electromagnetic energy with a frequency range of 300 MHz to 300 GHz with the most used frequencies being 915 MHz and 2450 MHz. It has been tried for different applications in food and agriculture and has shown a great potential for drying, sterilization, disinfestation, enzyme extraction, waste management, and many others. Utilizing microwave's thermal and nonthermal potential in the food and agriculture industry could be a step toward replacing conventional methods with a more environmentally friendly technology.

Despite many advantages of electromagnetic energy, it has not been commercialized in some sections of food and agricultural industry. One of these sections is the grain industry, which has many potential applications of microwave energy. Therefore, the aims of this review are to summarize the principles and applications of dielectric heating (with a focus on microwaves) for the treatment of grains with the aim of safe storage and reduction of post-gate grain losses, food security, increasing the value for end users, and finally to discuss the challenges and future works for taking advantage of microwave radiation in this sector. A summary of the applications of microwave heating for grain treatment is illustrated in Fig. 11.1.

11.2 Microwave Heating Principles and Dielectric Properties

Microwave energy is converted to heat in a dielectric material by affecting their polar molecules. Dipolar molecules start to align with the oscillating electromagnetic field and rotate in proportion to the applied frequency of the electromagnetic fields. These movements cause intermolecular friction and heating of the material. Microwave heating is a volumetric process, and it can be modeled as an internal heat source in the heat balance equation of a system and the dissipated microwave power itself can be described by Eq. (11.1)

$$P = 2\pi f \varepsilon_0 \varepsilon'' E^2 V \tag{11.1}$$

where P is dissipated microwave power (W); f is electromagnetic field frequency; ε_0 is permittivity of free space (F m^{-1}); ε'' is loss factor of the material; E is electric field strength (V m^{-1}); and V is the volume of the material (m^3).

For treating a material by means of the microwave, the dielectric properties of the workload should be known. Dielectric properties regulate the behavior of the material, exposed to electromagnetic energy, and are expressed using the relative complex permittivity, $\varepsilon = \varepsilon' - j\varepsilon''$. The real part ($\varepsilon'$) is called the dielectric constant and the imaginary part (ε'') is the loss factor. The dielectric constant expresses the potential of a material to store energy and the loss factor shows the loss of electromagnetic energy in the form of heat. These properties depend on the frequency, temperature, moisture content, and the composition of the material. They also depend on the bulk density for particles [5].

Penetration depth, which is defined by Eq. (11.2), is expressed as the depth in a material where microwave power drops to $1/e$ ($e = 2.718$) or 36.8% of its initial value. In this equation, c is the speed of light in free space and equals to 3 is^8 m s^{-1} and f is frequency (Hz). Penetration depth is negatively correlated with frequency and thus at higher frequencies, energy penetrates less in the material and more surface heating occurs. The wavelength is another important factor, which is calculated by Eq. (11.3) using the dielectric properties. By knowing the penetration depth and wavelength, heat uniformity of a particular geometry during microwave treatment can be predicted [6, 7].

$$d_p = \frac{c}{2\Pi f \sqrt{2\varepsilon' \left[\sqrt{1 + (\varepsilon''/\varepsilon\prime)^2} - 1\right]}} \tag{11.2}$$

$$\lambda_m = \frac{c\sqrt{2}}{f\sqrt{\sqrt{\varepsilon\prime^2 + \varepsilon''^2} + \varepsilon'}} \tag{11.3}$$

Methods of measurement of dielectric properties of some grains and the models developed for them are summarized in Table 11.1. By knowing dielectric properties, it is possible to define the penetration depth and predict heat uniformity or determine the proper thickness of the grains for achieving good heat uniformity at a specific frequency. It is also possible to predict if there could be any selective heating between the materials and the pests by comparing their dielectric constant and loss factor. However, it appeared to be more beneficial to develop a model, which relates dielectric properties to the moisture content of the material and processing temperature at a specific frequency. This model should be used in simulations of the process to find the electric field and temperature distribution and define proper process parameters as well as the best design for the electromagnetic applicator.

Finally, as grains (and seeds in general) are discrete particles, it is difficult to measure their exact penetration depth. Most studies have tried to measure the dielectric properties of ground samples, which are usually less dense than the seeds and contain some air inside. Guo et al. [15] suggested that the ground sample should be compressed to reach the true density of the seeds to overcome this problem. However, the particles are a mixture of seeds and air with known bulk density. The other point is that heat transfer in the sample is by conduction through contact points from one particle to the next, which can make the simulation of the process more complicated as the seeds can have more than one contact points in reality.

11.3 Microwave Drying for Safe Storage of Grains

Grains are usually harvested at relatively high moisture contents to prevent any physical damage during postharvest practices. Weather condition is another reason which forces farmers to harvest grains earlier before they can dry out. Storage of the seeds at high moisture contents, depending on the storage temperature, leads to negative changes in seed physiological and biochemical properties and has a high risk of insects and fungi invasion. Therefore, artificial drying is one of the common postharvest practices to remove excess seed moisture for safe storage of grains and has benefits including long-time seed storage with no damage to seed quality, continuous supply of the grains throughout the year, maintenance of seed viability until the next sowing season, and enabling early harvest to prevent physical damages [16]. It should also be noted that safe storage seed moisture contents are different among different grains as well as different climate and storage conditions.

The conventional nonchemical method of artificial drying of grains includes applying airflow at a specific temperature to remove the excess moisture of the seeds. This can be done by batch or continuous flow of the grains in different patterns such as cocurrent, countercurrent, or crossflow [17]. However, this conventional method of drying has the drawback of low thermal efficiency and very long time required for drying, which is the reason why grain drying is still reliant on desiccants. It has turned the researcher's attention to exploring new technologies in

Table 11.1 Dielectric properties of some grains [a]

Grain	MC%	T (°C)	Frequency (MHz)	Method	Main result	Reference
Chickpea	7.9–20.9	20–90	10–1800	Open-ended coaxial-line probe & impedance analyzer	$\varepsilon''/\rho = 0.4552\ \varepsilon'/\rho - 0.8046$ ($f = 1800$ MHz)	[8]
Green pea	10.8–21.6	20–90	10–1800	Open-ended coaxial-line probe & impedance analyzer	$\varepsilon''/\rho = 0.4410\ \varepsilon'/\rho - 0.6241$ ($f = 1800$ MHz)	
Lentil	8.4–21.5	20–90	10–1800	Open-ended coaxial-line probe & impedance analyzer	$\varepsilon''/\rho = 0.4609\ \varepsilon'/\rho - 0.6347$ ($f = 1800$ MHz)	
Soybean	8.9–19.9	20–90	10–1800	Open-ended coaxial-line probe & impedance analyzer	$\varepsilon''/\ \rho\ = 0.5048\ \varepsilon'/\rho - 0.8869$ ($f = 1800$ MHz)	
Mung bean, black eyed pea	10.2–22.3 8.8–20.9	20–60	10–1800	Open-ended coaxial probe and impedance analyzer	Differential heating between insects and legume at RF frequencies	[9]
Cereal grains			5000–15,000	Development of models for existing data	$\varepsilon' = \varepsilon'_0 + a \times logf + b \times MC$ $\varepsilon'' = \varepsilon''_0 + c \times f + d \times MC$ for each of them a, b, c, d is defined	[10]
Common bean	4–13.5		3000–10,600	Free space transmission	ε' remained constant & ε" decreased with frequency	[11]
Barley, corn, Sorghum, wheat		20–60	915,2450, 5800	Free space transmission	ε' slightly increased & ε" remained constant over the range of temperature	[12]
Common bean	8.8–12.3	20–60	800–2500	Free space transmission	ε' and ε" decreased by increasing f, increased by increasing T, ε' increased, and ε" remained constant by increasing MC	[13]
Chickpea	8–20	24–85	700–7000	Open-ended coaxial probe	$\varepsilon' = 60.76 - 6.05 \log f + 0.165\ T$ $\varepsilon'' = 2.707 - 6.985 \times 10^{-11}$ $f + 0.001578\ T - 2.049 \times 10^{-12} f\ T + 0.000456\ T^2$ (MC = 19.8%)	[14]
Red lentil	8–20		700–7000	Open-ended coaxial probe	$\frac{\varepsilon''}{\rho} = 0.3994 \frac{\varepsilon'}{\rho} - 0.9185$ ($f = 1800$ MHz)	[14]

[a] *MC* moisture content, *T* temperature, ρ grain true density, *f* frequency

grain drying such as infrared and dielectric heating as faster and more energy-efficient methods. Some of these technologies, such as microwave drying, are still in the phase of research and development and one of the reasons is that the effect of the process on the quality attributes of the grains has not been fully discovered, though it is well documented that by adding microwave to conventional method of air drying, drying time decreases dramatically.

Soybean seed drying in microwave-assisted dryers was reported several times in references. Shivhare et al. [18] studied drying of soybean seeds by a combination of microwave radiation and air at $30^{\circ}C$ passing through the soybean bed and concluded that microwave at 0.13 W g^{-1} could be applied to dry soybean seeds without any seed viability loss. Wang et al. [19] designed a new hybrid microwave dryer for soybean drying. They used a rotary drum dryer inside a microwave oven with convective air passing through the soybean seeds and showed that the cracking ratio of the soybean seeds was the lowest at the drum speed of 15–20 rpm. It increased with increasing airflow and microwave power. Drying rate, in their process, was reported to increase dramatically by increasing microwave power. Simulation and validation of soybean drying in a microwave-assisted fluidized bed dryer were investigated by Zare and Ranjbaran [20]. They confirmed that time saving of 83.39–98.07% and an energy saving of 82.07–95.22% could be achieved for drying of soybeans from the moisture content of 18.32–12% (db) by adding microwave to a conventional fluidized bed dryer. Soybean drying kinetics in a microwave fluidized bed dryer and their possible quality changes were later examined by Khoshtaghaza et al. [21]. They stated that addition of microwave heating reduced the soybean cracking rate and increased the rehydration rate compared with conventional fluidized bed dryer.

Lentil seeds drying in a microwave oven was investigated at different microwave powers between 300–800 W and it was concluded that the least energy consumption could be achieved at the microwave power of 550 W [22]. It was also observed that there was no change in the crude protein of the seeds after drying, while crude oil content increased at all power levels. Drying kinetics of lentil seeds were later studied in a combined convective-infrared-microwave dryer [23]. Lentil's drying rate increased by increasing air temperature, infrared radiation, and microwave power.

Microwave drying of rice was another field, which has shown a great potential to be applied in the rice industry. Microwave drying of a thin layer of rice was firstly evaluated in a microwave-vacuum dryer [24] and it was reported that there was no change in cooking and physicochemical characteristics of dried rice. Later, Kaasova et al. [25] compared conventional and microwave oven drying of rice and concluded that low-power microwave did not affect total starch content of the rice but increasing microwave power increasingly damaged starch. However, they observed that the damaged starch was minimum when the initial moisture content of the rice was less than 23%. Sangdao et al. [26] proposed a new applicator, comprising of perpendicular waveguides on a concentric cavity, for continuous microwave fluidized bed drying of paddy with improved heating uniformity. They suggested that this system had an efficiency of 61.5% and with a maximum capacity of 3.1 kg h^{-1}, its energy

consumption and cost were 5.2 kJ and US$47.7 ton^{-1}, respectively. Horrungsiwat et al. [27] compared microwave hot air and steam drying of paddy rice and stated that both processes could be used for rice drying with increasing rice antioxidant activity. They concluded that microwave at 4–6 W g^{-1} and steam at 400 °C could be used for rice drying without a change in sensorial attributes, though they slightly increased rice hardness. Deep bed rice drying has been recently investigated in an industrial microwave with a frequency of 915 MHz [28], and it was suggested that drying rice from 23% to 17% could be done by applying microwave specific energy of 400 kJ kg^{-1} without any significant difference in head rice yield compared with gentle drying with air at room temperature. It was concluded that microbial populations decreased, and milling quality of rice was optimum by employing this level of energy.

Drying of wheat and corn seeds, using the microwave and microwave-assisted technology, was examined by several authors. Drying of corn at initial seed moisture contents of 9.6–32.5% (db, dry base) in a microwave oven with different power levels between 140 and 700 W (total energy of 84 kJ) was reported to have lower viscosity of flour suspension, which was concluded to be due to changes in protein and starch structure [29]. It was added that milling energy reduced as a result of this drying process. Corn drying, with an initial moisture content of 18.3–42.3% (db) at the microwave power of 245 W, was indicated to increase seed stress crack and reduce seed germination, but applying 70 W of microwave power for kernel drying-preserved germination [30]. Seeds' viability, with higher initial moisture contents, was also reported to be more susceptible to higher microwave power. Winter wheat drying at initial seed moisture contents of 15%, 20%, and 25% was possible in a microwave oven at a power of 245 W with less than 2 min of exposure time and without seed viability loss. However, higher powers (490 and 910 W) could reduce seed germination and was not advisable for drying of wheat seeds [31].

There have been some suggestions about the apparatus which could be used for grain drying in the field or in storage [32]. Snaper [33] patented an apparatus consisting of microwave magnetrons and convective air for grain drying. They recovered heat from the internal combustion engine of the harvester machine to warm up the air and make the process more cost-effective. This apparatus could be used online during harvesting of the crop and before transferring them to the storage.

It can be concluded from the literature that microwave-assisted hot air is a promising, fast, and efficient method for grain drying. Microwave speeds up the drying process and hot air, either by blowing over the seeds or by fluidizing them, helps to make the microwave heating uniform. However, there is still a lack of data in the literature on the quality assessment of most grains, especially pulses, after drying with this method. This could have been a setback to commercialize the process as an artificial method of grain drying. Also, there have not been enough investigations on optimizing the process parameters such as proper initial moisture content, microwave power, air temperature, and air speed in the references. The other point is that, although there are sufficient data on the study of drying and drying kinetics of important grains using microwave and microwave-assisted

processing, there have been few investigations of simultaneous drying and disinfection/disinfestation of grains [34, 35].

11.4 Seed Germination Enhancement

The use of good-quality seeds is a key factor in agricultural production. High-quality seeds have high germination and growth potential as well as being free from pests and pathogens. There are several nonchemical methods for seed vigor enhancement, which can be generally divided into three groups including physical, physiological, and biological [36]. Among physical treatments, ionizing irradiation and microwave are the most promising methods [37].

There are few works which reported the potential of microwave radiation in seed germination enhancement. Germination and vigor of lentil seeds at high moisture content increased after 30 s exposure to microwave power of 450 W [38, 39]. Tylkowska et al. [40] observed that treatment of 50 bean seeds with 9.5% moisture content in a microwave oven (650 W) for up to 120 s increased germination capacities but had no effect on the final germination. Jakubowski [41] reported the increase of germination, vigor, and fresh plant mass of bean seeds after 10 s exposure to microwave treatment at 100 W. However, a 60-s exposure to this microwave power had adverse effects on plant mass. Kontar et al. [42] investigated the effect of microwave pretreatment of grains and vegetable seeds. They stated that microwave processing at 1.8 kW kg^{-1} for 15 s or 0.9 kW kg^{-1} for 45 s can enhance grain crops' yield and germination of watermelon seeds. They also concluded that microwave treatment helps to form the Hydrogen and Hydroxyl ions, which leads to maltose hydrolysis and formation of glucose and increase in germination. They additionally observed that this information transmits from activated to dormant seeds.

Generally, to design a microwave process with the aim of seed enhancement, absorbed power by the seeds and the final temperature as well as moisture content of them should be considered. For each seed, depending on their size and characteristics of the seed coat, a specific level of microwave power and final temperature can break the dormancy and increase viability. However, after a threshold, embryo will be negatively affected, which lead to viability loss and seed damage. Unfortunately, there is not enough information about this potential of microwave in literature to draw a firm conclusion about the possibility of seed vigor enhancement.

11.5 Modification of Seed Quality for End Users

A summary of the application of microwave heating for seed quality modification is illustrated in Fig. 11.2. Legumes are efficient sources of protein, as they need less input energy per kilogram of produced protein compared with meat [43]. However,

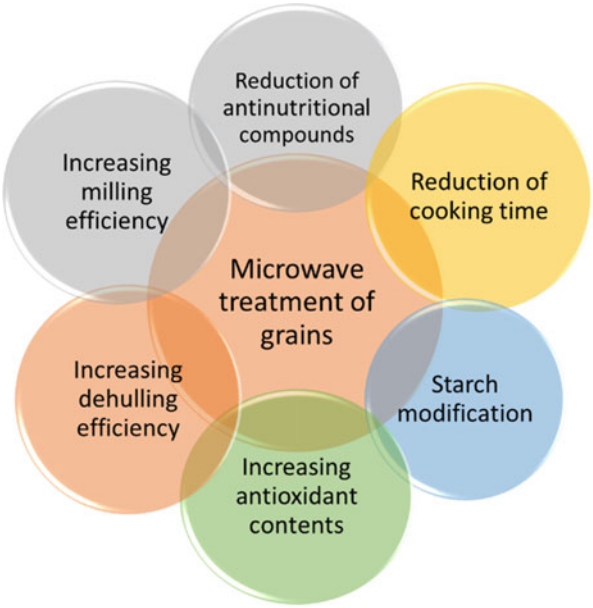

Fig. 11.2 Microwave heating applications for grain quality modification

they contain some antinutritional compounds, which can cause digestive problems. These compounds include protein types such as lectin or agglutinins, trypsin inhibitor, chymotrypsin inhibitor, and nonprotein types such as alkaloids, phytic acid, and phenolic compounds (tannins, saponins) [44]. The effect of microwave treatment on antinutritional compounds of legumes was studied by Hernandez-Infante et al. [45]. In this study, microwave cooking was compared with conventional cooking in water to explore their effects on the reduction of trypsin inhibitor and hemagglutinins. They observed that microwave heating was effective in reducing the antinutritional factors of all legumes except for common bean and its efficiency was the same as conventional cooking. Zhong et al. [46] compared microwave, radiofrequency, and high-pressure processing in reducing antinutritional compounds and protein digestibility of soybeans. For this experiment, 250 g black soybean, which was previously soaked in water, cooked in vacuum microwave and RF (27 MHZ) at, respectively, 1 kW and 6 kW powers for 30 min. They stated that microwave and RF did not have a significant effect on total essential amino acids but were more effective in reducing antinutrients. They also reported that microwave and high pressure were more efficient than RF in enhancing protein digestibility.

Poor cooking quality of legumes is another problem related to its consumption. Microwave radiation has shown good potential in improvement of cooking quality of grains. Marconi et al. [47] showed that microwave heating not only reduced cooking time of legumes, but also it decreased cooking loss compared with conventional boiling in water. Less vitamin and mineral loss, as a result of microwave cooking compared with conventional cooking, was also reported by other

researchers [48, 49]. However, Ertas [50] stated that ultrasound was more effective than microwave cooking in reducing mineral loss.

Microwave pretreatment of grains and legumes can be an efficient way to reduce the hardness of the seeds, which facilitates the dehulling process of grains [51] and reduction of their cooking time [52]. López-Perea et al. [53] investigated the effect of microwave radiation at 1450 W, on 100 g of barley seeds for 4–25 s. They reported that microwaving barley seeds for 4 sec, which raised the temperature to about $35^{\circ}C$, decreased hardness and lead to having higher and better quality malt extract from the barley seeds while 8 s of treatment increased their hardness. Velu et al. [54] reported that microwave drying of maize in a domestic oven (390 W, 3–16 min) improved its milling properties and decreased its flour's viscosity, which could be the result of change in protein and starch structure. Divekar et al. [52] showed that there were some fissures on the seed coat after microwave treatment of pulses, which could be the result of vaporization of moisture content from the cotyledon and the moisture loss from starch granules. These made some holes on the seed coat, leading to more water uptake and reducing cooking time. However, they reported significant change in protein secondary structure because of this treatment. The same result for reduction of cooking time and increasing dehulling and milling efficiency of mung bean after microwave treatment was reported [55].

Microwave processing is able to increase phenolic content and antioxidant activities of legumes. Randhir and Shetty [56] suggested that microwave treatment of fava bean could increase phenolic content and its antioxidant activity during germination. They exposed fava bean to microwave for 15–60 s and reported changes from day one to day eight of germination. According to their results, on the first day of germination, antioxidant activity of microwave-processed seeds were higher than control and after 7 days, sprouts of those seeds treated for 30 s, showed the most antioxidant activity as well as producing the highest phenolic contents. It was concluded that this high antioxidant activity was related to the high amount of phenolic compound, which was induced by microwave treatment. Enhancing phenolic contents and antioxidant activity of chickpea, roasted at 450–900 W for 5–15 min in microwave, was also reported [57].

Modification of grain's starch is another potential application of microwave heating as it was confirmed for lentil's starch [58]. The isolated lentil's starch was processed by microwave power of 650 W, at 85 $^{\circ}$C for 6 min and it was concluded that this process was able to decrease starch retrogradation, which made it more beneficial to be used in the baking industry as high retrogradation of legume starch is an inhibitory factor for their application in bakery formulations.

Conclusively, microwave treatment is a promising method of modulating the characteristics of legumes and grains to make them more nutritional or pave the way for having more efficient food processing. It is also helpful to eliminate those problematic properties of legume, which are preventive to make them as an alternative source of protein. However, there is still ambiguity about the effect of this process on the protein secondary structure as well as the mechanism of these changes, which can be further studied.

11.6 Disinfestation/Disinfection of Grains by Microwave Heating

One of the most important contributions to annual world food loss, which mostly occurs in developing countries, is postharvest losses of grain crops, including cereals and legumes, due to contamination or physical damage during several operations after harvest. However, in many cases, the contamination of the crops starts from the field, where they grow and include insects, fungi, and bacteria among which insects can cause more than 50% losses.

Decontamination of grains (disinfestation, disinfection) is still heavily reliant on chemical fungicides, herbicides, and insecticides. These chemicals are used for either preventing or controlling biotic stresses during post-gate storage of grains. According to FAOSTAT [1], countries around the world spent more than US$29B on different pesticides for crop protection in 2016. However, there are many concerns regarding this huge usage of pesticides, including the chemical residues in the grains, adverse effects on the environment. and development of chemical resistance by pests and pathogens [59]. For instance, there have been several reports that new and stronger resistances against Phosphine are emerging among insects and much effort has been devoted to understanding the impact of these resistances [60]. Therefore, replacing chemicals with natural or physical methods with little impact on the environment and low risk of resistance development seems to be a necessity. Among these safe alternatives is thermal treatment including dielectric heating using the microwave.

Thermotherapy is one of the oldest methods of eradication of micro and macroorganisms from grains, which can decrease the reliance on fungicides and protect the environment. There are some reviews on thermotherapy for pest control in grains [61–63]. Nevertheless, conventional ways of thermotherapy, such as hot air and hot water, have the drawbacks of long processing times or drying of the seeds after treatment [62]. As a result of these drawbacks, high-temperature short-time treatment, which can be provided by dielectric heating has been considered [64].

Advantages of dielectric heating over conventional heating for grain processing have been explained by many researchers. Firstly, it provides selective and volumetric heating mechanisms [65] and intrinsically heats the pests, like insects, at a higher rate than the host due to their higher moisture content and higher dielectric properties than the host materials [66]. This difference in absorbing energy will be more obvious at lower frequencies, which help to remove the pests before affecting the grain quality. Secondly, dielectric processing tends to heat inside and outside of the commodity at the same time, while the mechanism of conventional heat treatment is convection from the surface and then conduction inside the sample. Hence, in dielectric heating, it is more probable that the pests, inside the product, could be eradicated before damaging seed quality. Finally, dielectric heating is much faster than conventional heating, which makes it a better choice for industrial processing. More details of research on insect and pathogen control using microwave heating are provided below.

11.6.1 Insect Control (Disinfestation)

Insect pests are the most important threat to stored products. They not only spoil the products directly but also could be a way of transferring fungal contamination. The cost of postharvest loss due to insect infestation contributes considerably to the overall annual world food loss, which is approximately 1.3B tonnes of food or one-third of edible food produced for consumption [1]. Additionally, the cost of insect disinfestation, as well as the development of new chemicals due to insects' resistance to the previous insecticides, are very high [67], which has necessitated investing in research and development of insect pest control, especially nonchemical methods, in stored grains.

Electromagnetic radiation is among the nonchemical methods of insect control, which have recently gained a lot of attention among researchers. When comparing dielectric properties of dry grains and their related insects, it can be concluded that the real and imaginary parts of permittivity at all stages of insect growth are higher than their hosts [5]. This could probably be due to the higher moisture content of the insects compared with the commodities, which leads to faster heating of the insect to a higher temperature than the host. However, this difference in absorbed electromagnetic energy is higher at lower frequencies (RF compared with microwave) and thus lower frequencies have been recommended for this purpose [66, 68].

A summary of the insect control in grains, using microwave energy, is represented in Table 11.2. There are a number of thorough reviews on RF and microwave insect control [66, 81, 82]. Based on the literature, microwave has a good potential to eradicate the major insect pests of important grain crops including bruchids in legumes and rice weevil in cereal grains. However, the impact of these processes on all aspects of grain quality, as well as the proper types of process and process parameters, such as frequency, power, and exposure time, needs to be explored more. The process and process parameters need to be optimized to have more energy efficiency, more heating uniformity, and least quality change. It might demand a combination of microwave heating with other conventional methods if the cost of operation is reasonable. There has recently been an investigation of hot air-assisted microwave treatment of chickpea and green gram seeds, at a seed moisture content of 7.5–9.5%, to eradicate Callosobruchus maculatus adults [83]. It was stated that complete insect mortality for 500 g of grain sample (1 cm depth) could be achieved at the microwave power of 2900 W, air temperature of 60 °C, and exposure time of 6 min. Although these process parameters were reported to reduce cooking time, they also reduced grain seeds germination. However, for having better results for all quality aspects of the host, utilizing lower microwave power combined with hot air could be recommended.

Table 11.2 Insect control in grains by microwave heating[a]

Legume/ grain	Initial MC% (wb)	Frequency (MHz)	Specific power (W g^{-1})	T (°C)	Time (s)	Pest	Quality change	Reference
Wheat	14,16, 18	2450	4, 6, 8, 10		28, 56	Insect (Tribolium castaneum, Cryptolestes ferrugineus, and Sitophilus granarius)	100% mortality of insect occurred at 500 W & 28 s but reduced G	[69]
Rice	13–14	2450	0.085–0.68	55	90–720	Rice weevils		[70]
Barley	14–18	2450	4–10	42.6, 53.7, 66.9, 73 (14%MC, 28 s) 57.3, 75.5, 91.2(14% MC, 56 s) for up to 4 W g^{-1}	28, 56	Tribolium castaneum (Coleoptera: Tenebrionidae)	Reduced α-amylase, diastatic power, soluble protein, viscosity at 500 W,28 s but no change at 400 W g^{-1}, 56 s; both were effective on insects	[71]
Barley		2450	14.5		4–8		Decreased hardness & increased malting quality after 4 s; 8 s exposure had an adverse effect	[53]
Chickpea, green pea, lentil	6.19–6.54	27	2	60	600		Reduced moisture content & total weight	[72]
Chickpea		2450	0.7, 1.4, 2.1, 2.8, 3.5	40–80	300, 240, 200, 160, 100	Insect adult (Callosobruchus chinensis)	Reduced G & viability but achieved 100% insect mortality	[73]
Green gram		2450	0.7, 1.4, 2.1, 2.8, 3.5	40–80	300, 240, 160, 120, 70	Insect adult (Callosobruchus chinensis)	Reduced G & viability	[73]

(continued)

Table 11.2 (continued)

Legume/ grain	Initial MC% (wb)	Frequency (MHz)	Specific power (W g^{-1})	T (°C)	Time (s)	Pest	Quality change	Reference
Pigeon pea		2450	0.7, 1.4, 2.1, 2.8, 3.5	40–80	280, 240, 180, 140, 90	Insect adult (Callosobruchus chinensis)	Reduced G & viability	[73]
Lentil	6.9	27	0.938	60	600	Cowpea weevil	No change in MC, G, and color	[74]
Green gram		2450	808 W		80	Callosobruchus sp.		[34]
Mung bean	12	2450	8	68.1	28	Cowpea weevil (Callosobruchus maculatus)	Reduced G by increasing power (200-400 W); 200 W, 42 s did not change G & MC	[75]
Common bean soybean chickpea Wheat, corn		2450	700 W		60, 120, 180	–	Reduced mineral & protein content	[50]
Cowpea	10.67%	2450	~20		120–600	Insect 1–2 day old (Callosobruchus maculatus)	Reduced G, emergence, protein, fat & fiber	[76]
Green gram	8	2450	1.5–13		50, 60, 90, 110, 120	Pulse bruchid	Reduced G and MC; moisture loss was minimum for the 1 cm thickness of grains	[77]
Weak wheat beans	12.2/12.9	2450	1000 W (for 4 cm thickness of the material)	70	75	Infesting fauna	Did not affect G & quality	[78]

Cowpea		2450	1.5		5–25	Insect adult (Callosobruchus maculatus (F.) (Coleoptera: Chrysomelidae: Bruchidae)	25 s exposure time was effective on insect eradication, but reduced germination	[79]
Cowpea		2450	~48		30–150	Larvae cowpea weevil Callosobruchus maculatus (Fabricius) (Bruchidae)	120 and 150 s were effective on insect eradication, but reduced germination	[80]

[a]*T* temperature, *MC* moisture content, *G* germination

11.6.2 Fungi and Bacteria Control (Disinfection)

Fungal contamination is a serious problem of stored products around the world. Not only do they spoil the grains, reduce germination and viability, and degrade nutritious compounds, but some species can also produce toxic components like Mycotoxins, which are poisonous for both humans and animals. Today, 25% of cereals are not rendered fit for human consumption in the world due to mycotoxin contamination [84].

There are two types of grain fungi: field and storage fungi. Field fungi are those that invade the plants and the seeds before harvesting when the moisture content is very high. They survive at a water activity of more than 0.9 and are mostly those, which cause diseases in plants and seeds. Field fungi in grains, which include *Alternaria, Cladosporium, Helminthosporium, and Fusarium,* gradually die when the moisture content is below 13% [85]. However, their spores can remain in the seeds and cause diseases later when the conditions are favorable again. Storage fungi usually attack the grains after harvesting. They cannot grow at a water activity below 0.65 at 20–25$^{\circ}C$ [85], which is equivalent to a moisture content of 12.5–13.5% in wheat and rice. *Aspergillus* and *Penicillium* are the most important storage fungi and can spoil the grains by producing Mycotoxins and reducing their germination and nutritional values.

Therefore, moisture content and corresponding water activity has a great role in the survival of the fungi in grain seeds and likewise on their susceptibility to heat and electromagnetic energy [86–88]. On the other hand, grain seed viability is also more vulnerable at higher moisture contents when treated at the same temperature or electromagnetic power. This contradiction, however, could be solved by optimizing the process parameters such as power, exposure time, seed moisture content, and relative humidity of the process environment. For example, microwave treatment of winter wheat at 15% moisture content for the eradication of *Fusarium culmorum* decreased seed germination before eliminating the fungi while injecting steam during microwave processing, which was also able to make the heat more uniform, could control the pathogen without any reduction in germination [89]. Steam injection raised the relative humidity around the grain seeds and increased fungal susceptibility to electromagnetic heating. Although in some references it was concluded that at higher moisture contents lethality of fungi was higher with the same power and time [90, 91], they cannot be used to draw any conclusions about the pathogen's susceptibility at higher seed moisture contents. The reason is that seeds with higher moisture contents absorb more electromagnetic energy at the same microwave power and exposure time due to their higher dielectric properties [14] and thus seeds' temperature raises to a higher value, which can be the reason for faster or easier pathogen elimination. As a result, the final temperature of the host material should be considered as an important process parameter along with the grain moisture content when the aim of microwave treatment is pathogen control.

Dielectric heating application to eradicate or reduce some of the field and storage fungi in the grains is summarized in Table 11.3. What is obvious from the literature

Table 11.3 Summary of seed fungal and bacterial infection control by microwave heating[a]

Grain	Initial MC% (wb)	Frequency (MHz)	Specific power (W g^{-1})	T°C	Time (s)	Pathogen	Quality change	Reference
Sorghum grain	12,14,16	1250	1.5, 3, 6	30–40; 90–110	30, 60	Fungi (Eurotium spp., Aspergillus candidus, A. niger and Penicillium spp.)	6 W g^{-1}, 60s dramatically reduced seed viability	[90]
Soybean, common bean		2450	1420 W		0–420	Fungal spores	Reduced G	[92]
Wheat	8, 14, 20	2450	0.3,0.4,0.5, 0.6		20, 30, 40, 50s min^{-1}	Fusarium graminearum	Reduced pathogens from 36% to 7%, reduced G from 100 to 85% & seed vigor to 80% of control	[91]
Soybean		2450			30, 45, 60	Inner fungi	30s was effective against fungi & did not affect viability and vigor	[93]
Common bean	9.5	2450	650 W/200 seeds	30.5–62.5	15–120	Fungus (Alternaria alternata, Fusarium spp. and Penicillium spp.)	Was effective against Penicillium spp. & improved seed vigor	[40]
Wheat	12,15,18	2600, 5700, 9700	100, 100, 80 kW		600–1200	Seed-borne fungi (Phaeosphaerianodorum, Pyrenophora tritici-repentis and Fusarium spp.).	Caused abnormally germinated seeds & was just effective against Tilletia caries	[94]
Wheat	10–40	2450	800 W/204 seeds		15, 30, 45	Fungi (saprophyte, Fusarium spp., Microdochium nivale)	Reduced seed viability at high MC	[95]
Dry bean	7.1–8.6	2450	1100 W/ 150 seeds		40	Bacterial blight (Xanthomonas axonopodis pv. Phaseoli)	Reduced seed emergence up to 7%; little control of the disease	[96]
Dry bean	6.6–10.6	2450			40			[97]

(continued)

Table 11.3 (continued)

Grain	Initial MC% (wb)	Frequency (MHz)	Specific power (W g^{-1})	T°C	Time (s)	Pathogen	Quality change	Reference
			1100 W/ 150 seeds			Bacterial blight (Colletotrichum lindemuthianum)	Decreased disease symptoms by 17–23% in combination with chemicals	
Wheat corn	12, 15	27	13.3	65, 70	600	Aspergillus flavus	Did not affect seed vigor, reduced fungi up to 3–4 log at 15%MC & 2–3 log at 12% MC	[87]
Brown rice, barley	7.33, 4.98	2450	70		10–50	Aspergillus flavus & Aspergillus parasiticus	20 s exposure did not affect grain quality with more than 90% reduction in pathogen	[98]
Red lentil	9, 16, 19	2450	4, 9.7	62–99	19–127	Ascochyta lentis	Reduced infected seeds from 17% to 9% at 9% MC with no G loss	[88]

[a]*T* temperature, *MC* moisture content, *G* germination

(Table 11.3) is that higher electromagnetic power, more exposure time, and higher seed moisture contents lead to higher temperatures, which could be the reason for seed viability loss at these conditions. On the other hand, each pathogen can be eradicated at a specific temperature and relative humidity (or seed moisture content/water activity). By considering just the thermal effect of the microwave, this temperature can be reached by absorbance of a specific amount of microwave energy, which corresponds to specific microwave power and exposure time. To investigate grain pathogen control utilizing microwave energy, it seems more reasonable to find the threshold of pathogen susceptibility to heat (temperature) at different seed moisture content or relative humidity followed by reaching that temperature using the proper microwave power and exposure time and controlling the grain temperature so as not to exceed the limitation for the grain seed's quality. It is also worth investigating which of the higher power and lower exposure time or lower power and longer exposure time is best to reach the target temperature, and which would be more beneficial regarding host quality, pathogen control, and energy efficiency. In spite of the attempts to show dielectric heating's potential in grain pathogen control, which is summarized in Table 11.3, there are not any information about important seed-borne diseases of pulses or how much of the pathogens which could be eradicated without a significant effect on the pulse quality. There should also be more investigation on the combination of the microwave with conventional methods of disinfection.

11.7 Challenges of Microwave Processing

11.7.1 Quality Change

One of the most important concerns when exposing grains to microwave heating would be any negative change in qualities such as seed germination and vigor. Thus, to design a proper thermal treatment, the sensitivity of pests and hosts need to be evaluated first and if the pests are more sensitive than the commodity, the process is worth being considered. All agricultural products have a specific quality curve when exposing them to a thermal process. These curves depend on many factors such as properties of the materials or the process parameters. What is crucial in obtaining the curves of quality-temperature/time is examining the proper quality attributes related to the process and the host.

Dielectric heating could be considered as a thermal process for quality evaluation of the treated material. However, this process is not isothermal and usually, temperature rises during the exposure time and thus frequency, input power, and exposure time have been commonly considered as key factors affecting the process and quality of the material. For example, applying microwave radiation at frequencies of 2.6, 5.7, and 9.3 GHz decreased seedling vigor and increased the number of abnormally germinated seeds in wheat [94]. Soybeans, which were treated by microwave at 2450 MHz for removing internal fungi, did not face any quality

change after 30 s of exposure time, but the germination and structure of the seed cell walls were altered after 45 s [93]. Common bean germination improved after a 120-s exposure to microwave with the power of 650 W [40] but exposure to 1420 W for 7 min reduced germination [92]. This could stem from the total energy absorbed by the samples and the final temperature of the seeds, which should also be considered in dielectric heating. The quality change of the grains as a result of considered process parameters in different kinds of grains are represented in Tables 11.2 and 11.3.

Optimization of process parameters is a strategy to find the effective point of the process with maximum pest/pathogen reduction and minimum adverse effect on the quality of the materials. Optimization, however, has been rarely utilized by researchers to report the quality change of grains after microwave treatments. There was a study done by Pande et al. [34] who optimized the power level and exposure time during microwave drying of green gram. The optimum point found through Response Surface Methodology (RSM) was microwave power of 808 W and exposure time of the 80 s, which resulted in 99.5% mortality of *Callosobruchus sp.* and seed moisture content of 8.9%. They concluded that at this optimum condition, in vitro protein digestibility, Zn and Fe contents increased while there was no change in Mg, Mn, Cu, K; and Ca decreased slightly.

The sensitivity of different types of grains to electromagnetic heating is another issue which should be taken into account by thoroughly investigating the effect of process parameters on the quality attributes of different types of the grains after finding the proper process parameters for drying, disinfection, or disinfestation. For instance, while studying the quality attributes of two different types of bean (Bayo and Negro) after microwave treatments with the aim of insect control [99], it was revealed that there was no change in germination of Negro whereas Bayo's germination decreased at higher power levels (370, 510 and 950 W). It is interesting to note that the final temperature in all the treatments was 48.9 $^{\circ}C$. In another study, dry beans, with a moisture content of 18%, were treated at the power level of 1100 W for eliminating bacterial blight (*Colletotrichum lindemuthianum*) and there was less than 10% reduction in germination and viability [97]. Nevertheless, the latter's result cannot be compared with the other two types of beans in the previous research as the seed moisture content and applied microwave power were different. Different cowpea cultivars were also reported to have different germination percentage after treating with the same microwave power and exposure time [80]. The difference in susceptibility of the seed among different cultivars could be an obstacle to generalizing the obtained results for dielectric heating process parameters from a specific grain crop.

Moisture content is a very important factor which needs to be considered when designing a process of thermal treatment. It was reported that by increasing the moisture content of wheat and sorghum grains, adverse effects of microwave treatment on germination and vigor could increase [90, 94]. Germination reduced after Microwave treatment at the final temperature of 40 $^{\circ}$C for chickpea, green gram, and pigeon pea [73], but it did not change during RF treatment at above 60 $^{\circ}$C for chickpea, green pea, and lentil [72]. One reason for this difference in the results

could be different moisture contents of the seeds. Although there was some evidence that insect mortality was more at higher seed moisture contents while treating with microwave [69], treating the dry form of the seeds was mostly preferred (Tables 11.2 and 11.3), probably due to less risk of seed quality alteration.

Moreover, for determination of the effect of microwave processing on quality, the seed size is also of great importance. In thermal treatments, large seeds like soybean could lose their viability before a complete eradication of the pathogen and so their processing for the eradication of pathogens seemed to be more difficult [62]. Therefore, seeds with larger dimensions should not be exposed to higher power levels or longer exposure times, which would result in higher temperatures.

In general, having considered microwave processing for pest and pathogen control or grain drying, a thorough examination of the seed quality needs to be carried out at the optimized process parameters. These quality attributes, which differ among different grains and different end usage, are summarized by Jayas and Ghosh [17]. A possible solution for considering quality change of grains as a result of microwave treatment could be grouping them based on the parameters which affect the proper process parameters such as microwave power and exposure time. These grouping could be based on the seed's size, initial moisture content, seed coat thickness, protein/lipid/starch contents, or physical and dielectric properties of grains. After the grouping, the process parameters could be defined for each to facilitate the industrialization of the process.

One possible explanation for the drastic quality change of the grains before complete control of pests and pathogens could be nonuniformity of heat distribution during microwave processing. Manickavasagan et al. [100] investigated the effect of microwave power and exposure time on wheat seed germination at different moisture contents in a continuous microwave dryer. They stated that germination of the seeds in hot spots was lower than those in other regions and it decreased with increasing power level and moisture contents. They concluded that drying wheat, even at a power level of 100 W, had adverse effects on germination in the hot spots. However, there are some solutions to overcome this problem and make sure that the temperature difference between hot and cold spots is minimum and pests could be eradicated before any adverse effect on the seed quality. These possible solutions will be further discussed in the next section.

The effect of microwave treatment and drying on the sensory aspects of grains has been mentioned in a few studies and needs to be fully discovered. Microwave treatment was reported to increase redness and yellowness of wheat seeds' color but did not affect their odor [101]. A recent study by Adebowale et al. [102] indicated that microwave treatment of sorghum kernels (up to 90 kJ/100 g) improved sensory attributes of the flour during its storage by reducing the fat content through lipase inactivation and preventing the formation of rancid off-flavor.

Different methods of sensory analysis have been developed to evaluate the consumers' responses to food products. The quantitative descriptive analysis (QDA) which includes quantifying the type and intensity of the sensory attributes and temporal dominance of sensations (TDS) which involves the description of the dominant sensation during a specified time were employed for cheese sensory

evaluation [103]. The sensory analysis could also be projective using the descriptive word or image groups [104, 105]. In this technique, the panel selects their first thoughts or feelings toward the food product among the words or images provided for them. Preferred Attribute Elicitation (PAE) is another new rapid sensory method that has been developed for many food products and compared with the conventional descriptive technique [106]. In this method, the untrained panelists are employed to evaluate the characteristics of a product and define which attributes lead to the consumers' preference. All these sensory evaluation techniques could be applied to determine the effect of microwave processing on the grain's sensory attributes including color, texture, odor, and taste.

11.7.2 Heat Uniformity

Microwave radiation is intrinsically nonuniform in heating the materials which cause the existence of cold and hot spots in food materials. For drying grains by means of microwave heating, differences between cold and hot spots reached 59.2, 72.8, and 78.9 °C for Canola, Wheat, and Barley, respectively [107]. This nonuniformity, which was expressed as differences between maximum and minimum temperatures, was also observed in a microwave dryer with moving grains at different seed moisture contents on a conveyor belt [108]. What is obvious is that this nonuniformity of temperature is a major problem which can lead to significant grain viability loss or quality deterioration before completing the microwave processing. The challenge of heating nonuniformity is agreed in all the area of food processing including drying and sterilization of fruits and vegetables, and despite many finding regarding much lower energy consumption and enhancement effect of microwave on food commodities, the issue of nonuniformity of heating is still urged to be investigated more [109] and this creation of hot and cold spots was an issue even in the continuous flow sterilization of solid, semisolid, and heterogenous liquid foods that could cause serious food safety issues [110]. Microwave-assisted thermal sterilization (MATS) [111] has been proposed as the latest development for sterilization of the packaged foods with very short treatment time and improved nutritional and sensory properties. In this process, hot water immersion of the packaged food was employed to overcome the problem of nonuniformity of temperature distribution resulting from microwave radiation.

The position of hot and cold spots directly depends on the shape and size of the material. Hot spots tend to be at the center for small cylinders and spheres with low loss factor. By increasing the dimensions and loss factor, the heating will move from the core to the surface [7, 112]. Some recent studies were carried out on the role of the material's thickness in the dissipation of microwave energy [6, 113]. It was indicated that in thin materials (thickness: 4–6 mm), regardless of the shape, the starting point of heating is the geometrical center of the sample, while in thick materials in which the ratio of thickness to penetration depth is equal to or more than three, sample shape and location inside the microwave cavity affected this location.

Despite the mentioned problems, some solutions have been suggested for the prediction of temperature distribution and boosting its uniformity during irradiation. Lorenson et al. [114] disclosed a method to increase heat uniformity by controlling the thickness of the product which controlled the irradiation modes. Ho and Yam [115] tried different patterns of metal shielding around a cylindrical food model and concluded that heat uniformity could be improved by some special patterns without reducing the amount of absorbed power. For ready meals, it is stated that the heating uniformity is mostly affected by geometry, packaging, and more importantly by the placement of the sample (location) in the cavity [116]. Peyre et al. [117] investigated the impact of changes in dielectric properties on heating patterns of foods in a microwave oven. They showed that materials with low (like ice) or moderate loss factors could be considered as a dielectric cavity and their size significantly affected the heating patterns inside them. Moderate loss materials, however, created more modes resulting in a more uniform heating pattern. Ni et al. [118] showed that heat uniformity improved and the total moisture loss decreased by increasing the surface area for a specific volume. Lee et al. [119] worked on the optimization of the heat/cold cycle for improving heat uniformity. In this method, microwave power was employed to heat the sample, followed by a holding time, which let the heat transfer inside the food by conduction. This heat/hold cycle caused more even temperature distribution. Zhang et al. [120] designed a container in which the frozen food was reheated uniformly when irradiated by microwave.

The more uniform temperature distribution was reported to be achieved by lower microwave power and longer exposure time [121] as well as shielding with aluminum foil [115]. According to Hong et al. [122], for the temperature below 200 °C, less energy input will be required at lower powers. Therefore, at low power not only is the temperature more uniform but also less energy is needed. Law et al. [123] observed that loosely packed oil palm kernels had more heat uniformity than when tightly packed. When the particles were tightly packed, the maximum temperature occurred at the contact points while it was inside the kernels for loosely packed samples.

Regarding the effect of surrounding materials in microwave heating, using a turntable composed of different materials was found to improve the heat uniformity by 26–47% [124]. The materials used in this research were Polyethylene (PE), Alumina, and Aluminum. The highest uniformity was achieved with the combination of PE and Alumina.

Generally, the following list of suggestions from the literature can increase heat uniformity in microwave processing:

- Mode stirrer and turntable.
- Optimally designing the waveguide and the cavity.
- Manipulating the heat cycle, using lower power & longer time.
- Pulsed microwave instead of continuous radiation.
- Designing a special packaging.
- Using metal shielding for the material.
- Controlling the geometry, size, depth, and the location of the material.

- The combination of the microwave with other heating methods.
- Fluidization with air or mechanical mixing of particulate materials.
- Surface temperature controlling.

However, not all these solutions are applicable in microwave processing of grains. In this regard, combining microwave with other conventional methods might be considered a better tool for industrializing grain processing. It is possible to combine microwave with other kinds of irradiation like Gamma and Infrared or processing with a partial vacuum so as to have more uniform heating as well as making the process more effective [82]. For drying purposes, it is beneficial to combine hot air with microwave radiation in order to achieve volumetric, faster, uniform, and energy-efficient heating [125–127]. Fluidization of particulate materials with air during microwave treatment was also recommended to have uniform temperature distribution [128]. However, the susceptibility of the grains to cracking needs to be considered in this process. Microwave fluidized bed was successfully employed for simultaneous drying and disinfection of lentil seeds [129] and was confirmed that by a proper combination of the microwave power (4.8 W g^{-1}) and air temperature (50 °C), the detrimental impacts on the seeds' biochemical characteristics could be avoided [130]. Controlling the surface temperature of the particulate materials by a continuous temperature monitoring was another recommendation to have uniform heating and preserving the grain quality [131, 132].

Process parameters such as microwave power, exposure time, and seed moisture content are other factors which can be considered to study heat uniformity while designing a microwave process for grains. Nonuniformity, expressed as the difference between hot and cold spot, was reported to increase by increasing microwave power and exposure time during treatment of grains in a continuous microwave dryer [107, 108] and remained constant when the microwave power is larger than a specific amount depending on the treated material [133]. However, increasing grain moisture content could lead to an increase or no change in the difference between the maximum and the minimum temperature [39, 107, 108].

An issue raised here is that the definition of heat uniformity is not consistent among researchers in the field of microwave grain processing. As just mentioned, some researchers expressed the difference between hot and cold spot temperatures as an indicator of heat uniformity, while others calculated a Heat Uniformity Index (HUI) [72, 134]. HUI has been expressed as the increase in the standard deviation of material temperature divided by the increase in average material temperature during the treatment time. Temperature can be measured by fiber-optic probes in several points of the product (in the whole volume of the product) or the infrared image (surface temperature of the product) can be taken before and after the treatment followed by exporting the temperature values from different points of the image. Coefficient of Variation (COV) was also considered for expressing heat uniformity of microwave processing [133]. The lower the HUI or COV is, the more uniform the temperature distribution will be.

Nevertheless, temperature difference and HUI are not always positively correlated. Taheri et al. [39] explained that the difference between the maximum and

minimum surface temperature of a single layer of lentil seeds treated in a microwave oven increased by increasing moisture content and input microwave power, while HUI (or temperature uniformity index, TUI) decreased. It means by increasing maximum–minimum temperature difference, the heat uniformity in the whole material does not necessarily get worse. Conclusively, it seems more reasonable to consider both HUI and the difference between maximum and minimum temperature of the whole material for the study of heat uniformity in microwave processing.

To date, the industrial equipment, which has been designed for grain processing, is continuous treatment on a conveyor belt and receiving the radiation from the top through multiple waveguides. This process can be coupled by low-speed hot air flow on or across the bed of the grain to increase the heating uniformity, and in the case of drying, to facilitate moisture removal from the grain's surface. Other lab-scale microwave processing which has been developed for grain treatments with improved heat uniformity is represented in Fig. 11.3. There are also several other systems which have been developed for in-field treatment of grains [32, 33].

11.8 Conclusion and Future Work

Safe storage and safe post-storage usage of grains for sowing and end-user purposes demand that they are free of pest and pathogens, at a safe seed moisture content and have high and desirable quality attributes. All these targets could be achieved by microwave processing as their effectiveness have been evaluated separately. Now the question needs to be focused on how these targets could be achieved in one single process with electromagnetic processing. Insects have been eradicated at a temperature below 60 °C, while fungi and bacteria might tolerate higher temperatures, depending on the availability of water. Therefore, partial control of both pests and pathogens as well as the possibility of quality modifications during grain drying for the reduction of the reliance on chemicals could be examined in future studies. However, it might seem a very challenging work to find an overlap between seed germination enhancement with the other applications, as it could be achievable at a very low microwave power or exposure time, which would not be sufficient for other purposes.

Two major problems related to microwave treatment are highly non-uniform heating and any negative effect on the product. Non-uniformity can be solved by a combination of microwave processing with other methods or designing a proper cavity and process in which temperature could be controlled, as stated for drying purpose, by fluidizing grain bed using hot air or mechanical agitation. Surface temperature control by continuously changing the microwave power during the treatments is another strategy which could help in this regard. By improving heat uniformity and controlling surface temperature, the hot spot temperature could be controlled in order not to increase beyond the product's tolerable limitation and therefore, any negative effect on the seed quality attributes could also be prevented.

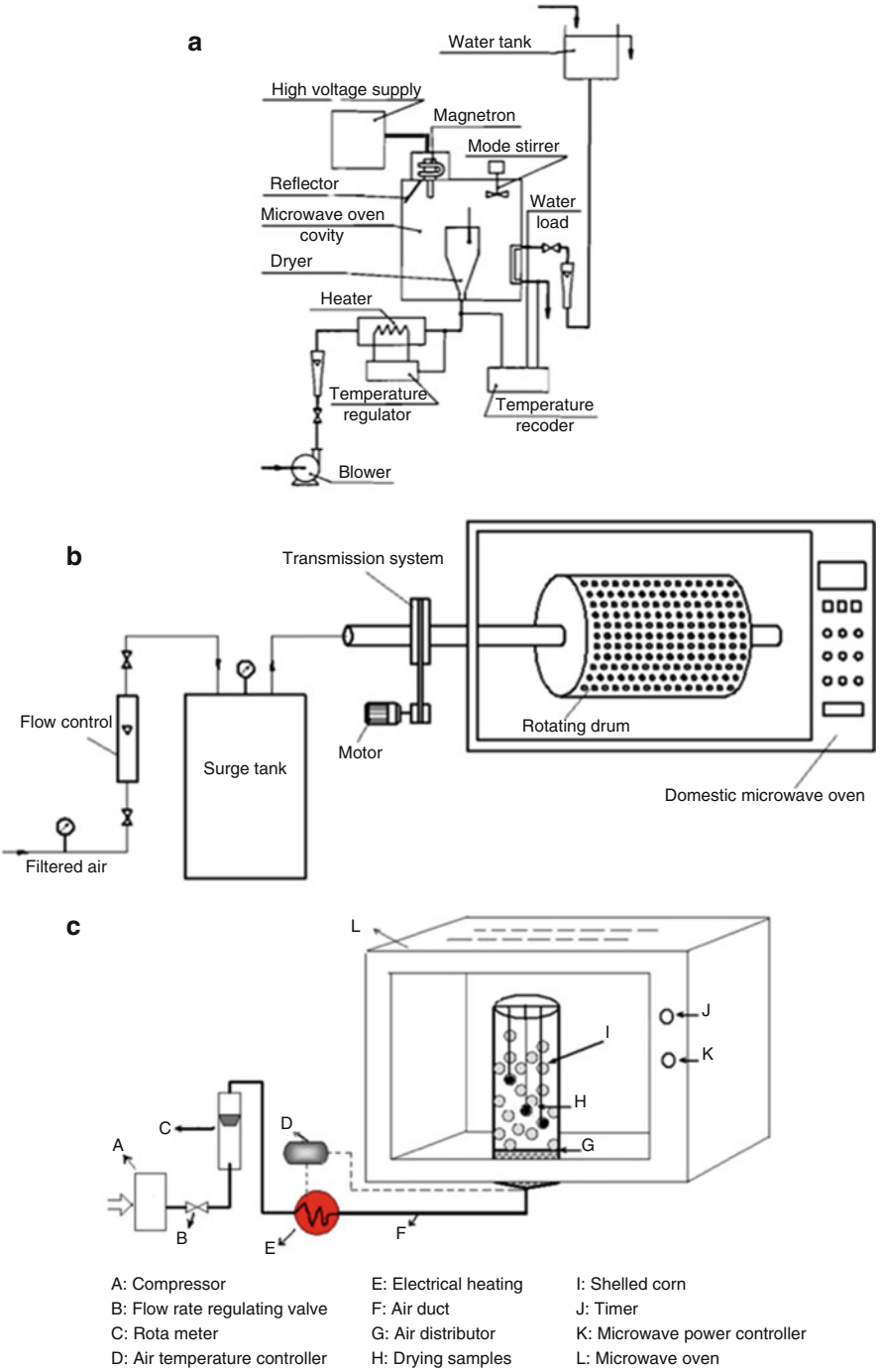

Fig. 11.3 Schematic of three lab-scale apparatus used for microwave processing of grains with improved heat uniformity; (**a**) Microwave spouted bed for drying particulate materials [135], (**b**) Microwave rotary process for soybean drying [19], (**c**) Microwave fluidized bed for drying shelled corn [136]

The other important fact for utilizing microwave treatment is to optimize the process parameters to have the most energy efficiency. These parameters include power, time, and moisture content of the sample. By finding the critical points, the process of microwave heating can be combined with other conventional physical ways to obtain complete pest and pathogen control of stored commodities as well as reducing their moisture content for safe storage and have the best quality for end users. This combination could be designed in a way to overcome the weakness of each method as well as with the aim of reducing the usage of chemical treatments.

References

1. FAO. The future of food and agriculture: trends and challenges. 2017.
2. Alexandratos N, Bruinsma J. World agriculture towards 2030/2050: the 2012 revision. 2012.
3. Misra NN, Koubaa M, Roohinejad S, Juliano P, Alpas H, Inácio RS, et al. Landmarks in the historical development of twenty first century food processing technologies. Food Res Int. 2017;97:318–39. https://doi.org/10.1016/j.foodres.2017.05.001.
4. Ahmad T, Butt MZ, Aadil RM, Inam-ur-Raheem M, Bekhit AED, Guimarães JT, et al. Impact of nonthermal processing on different milk enzymes. Int J Dairy Technol. 2019;72(4):481–95.
5. Nelson SO. Dielectric-properties of agricultural products - measurements and applications. IEEE Trans Electr Insul. 1991;26(5):845–69. https://doi.org/10.1109/14.99097.
6. Bhattacharya M, Basak T. A comprehensive analysis on the effect of shape on the microwave heating dynamics of food materials. Innovative Food Sci Emerg Technol. 2017;39:247–66.
7. Brodie G. The influence of load geometry on temperature distribution during microwave heating. Trans Am Soc Agric Biol Eng. 2008;51(4):1401–13.
8. Guo W, Wang S, Tiwari G, Johnson JA, Tang J. Temperature and moisture dependent dielectric properties of legume flour associated with dielectric heating. LWT Food Sci Technol. 2010;43(2):193–201.
9. Jiao S, Johnson J, Tang J, Tiwari G, Wang S. Dielectric properties of cowpea weevil, black-eyed peas and mung beans with respect to the development of radio frequency heat treatments. Biosyst Eng. 2011;108(3):280–91.
10. Nelson S, Trabelsi S. Models for the microwave dielectric properties of grain and seed. Trans ASABE. 2011;54(2):549–53.
11. Torrealba-Meléndez R, Sosa-Morales ME, Olvera-Cervantes JL, Corona-Chávez A. Dielectric properties of beans at ultra-wide band frequencies. J Microw Power Electromagn Energy. 2014;48(2):104–12.
12. Torrealba-Meléndez R, Sosa-Morales ME, Olvera-Cervantes JL, Corona-Chávez A. Dielectric properties of cereals at frequencies useful for processes with microwave heating. J Food Sci Technol. 2015;52(12):8403–9. https://doi.org/10.1007/s13197-015-1948-3.
13. Torrealba-Meléndez R, Sosa-Morales ME, Olvera-Cervantes JL, Corona-Chávez A. Dielectric properties of beans at different temperatures and moisture content in the microwave range. Int J Food Prop. 2016;19(3):564–77.
14. Taheri S, Brodie G, Jacob MV, Antunes E. Dielectric properties of chickpea, red and green lentil in the microwave frequency range as a function of temperature and moisture content. J Microw Power Electromagn Energy. 2018;52(3):198–214. https://doi.org/10.1080/08327823.2018.1452550.
15. Guo W, Tiwari G, Tang J, Wang S. Frequency, moisture and temperature-dependent dielectric properties of chickpea flour. Biosyst Eng. 2008;101(2):217–24.
16. Bala BK. Drying and storage of cereal grains. Chichester: John Wiley & Sons; 2016.

17. Jayas D, Ghosh P. Preserving quality during grain drying and techniques for measuring grain quality. Paper presented at the 9 th International Working Conference on Stored Product Protection; 2006.
18. Shivhare U, Raghavan V, Bosisio R, Giroux M. Microwave drying of soybean at 2.45 GHz. J Microw Power Electromagn Energy. 1993;28(1):11–7.
19. Wang R, Li Z, Li Y, Ye J. Soybean drying characteristics in microwave rotary dryer with forced convection. Front Chem Eng China. 2009;3(3):289–92.
20. Zare D, Ranjbaran M. Simulation and validation of microwave-assisted fluidized bed drying of soybeans. Dry Technol. 2012;30(3):236–47.
21. Khoshtaghaza MH, Darvishi H, Minaei S. Effects of microwave - fluidized bed drying on quality, energy consumption and drying kinetics of soybean kernels. J Food Sci Technol. 2015;52(8):4749–60. https://doi.org/10.1007/s13197-014-1557-6.
22. Iik E, Izli N, Bayram G, Turgut I. Drying kinetic and physical properties of green laird lentil (Lens culinaris) in microwave drying. Afr J Biotechnol. 2011;10(19):3841–8.
23. Chayjan R, Radmard S. Moisture and thermal diffusivity of lentil seed under convective infrared-microwave: modelling with and without shrinkage. Res Agric Eng. 2016;62 (3):129–40.
24. Wadsworth JI, Koltun SP. Physicochemical properties and cooking quality of microwave-dried rice. Cereal Chem. 1986;63(4):346–8.
25. Kaasova J, Kadlec P, Bubnik Z, Hubackova B, Prihoda J. Physical and chemical changes during microwave drying of rice. Chem Papers-Slovak Acad Sci. 2002;56(1):32–5.
26. Sangdao C, Songsermpong S, Krairiksh M. A continuous fluidized bed microwave paddy drying system using applicators with perpendicular slots on a concentric cylindrical cavity. Dry Technol. 2010;29(1):35–46.
27. Horrungsiwat S, Therdthai N, Ratphitagsanti W. Effect of combined microwave-hot air drying and superheated steam drying on physical and chemical properties of rice. Int J Food Sci Technol. 2016;51(8):1851–9.
28. Smith DL. Development of A one pass microwave heating technology for rice drying and decontamination; 2017.
29. Velu V, Nagender A, Prabhakara Rao PG, Rao DG. Dry milling characteristics of microwave dried maize grains (Zea mays L.). J Food Eng. 2006;74(1):30–6.
30. Song G, Choudhary R, Watson DG. Microwave drying kinetics and quality characteristics of corn. Int J Agric Biol Eng. 2013;6(1):90–9.
31. Hemis M, Choudhary R, Watson DG. A coupled mathematical model for simultaneous microwave and convective drying of wheat seeds. Biosyst Eng. 2012;112(3):202–9.
32. Bensussan A, Azam G. Microwave drying device for drying products in form of grains. Google Patents; 1982.
33. Snaper AA. Method and apparatus for drying harvested crops prior to storage. Google Patents; 2003.
34. Pande R, Mishra HN, Singh MN. Microwave drying for safe storage and improved nutritional quality of green gram seed (Vigna radiata). J Agric Food Chem. 2012;60(14):3809–16.
35. Smith DL, Atungulu GG. Impact of drying deep beds of rice with microwave set at 915 MHz frequency on rice microbial community responses. Cereal Chem. 2018;95(1):130–40.
36. Irfan Afzal HUR, Naveed M, Shahzad MAB. Recent advances in seed enhancements. New Chall Seed Biol. 2016; https://doi.org/10.5772/64791.
37. Araujo SD, Paparella S, Dondi D, Bentivoglio A, Carbonera D, Balestrazzi A. Physical methods for seed invigoration: advantages and challenges in seed technology. Front Plant Sci. 2016;7:646. https://doi.org/10.3389/fpls.2016.00646.
38. Aladjadjiyan A. Effect of microwave irradiation on seeds of lentils (Lens Culinaris, med.). Rom J Biophys. 2010;20(3):213–21.
39. Taheri S, Brodie GI, Gupta D. Heat uniformity study and viability of red lentil at different moisture contents after low dose microwave treatment. Trans ASABE. 2019;62(2):281–8. https://doi.org/10.13031/trans.13002.

40. Tylkowska K, Turek M, Prieto RB. Health, germination and vigour of common bean seeds in relation to microwave irradiation. Phytopathologia. 2010;55:5–12.
41. Jakubowski T. Evaluation of the impact of pre-sowing microwave stimulation of bean seeds on the germination process. Agric Eng. 2015;19
42. Kontar A, Valevakhin G, Buryak YI, Bespalko V, Ogurtsov YY, Onischenko O. Seed pre-treatment of grain and vegetable crops by microwave energy. Paper presented at the Antenna Theory and Techniques (ICATT), 2015 International Conference on; 2015.
43. Food and Nations. Food wastage footprint: impacts on natural resources: summary report: FAO; 2013.
44. Roy F, Boye JI, Simpson BK. Bioactive proteins and peptides in pulse crops: pea, chickpea and lentil. Food Res Int. 2010;43(2):432–42. https://doi.org/10.1016/j.foodres.2009.09.002.
45. Hernandez-Infante M, Sousa V, Montalvo I, Tena E. Impact of microwave heating on hemagglutinins, trypsin inhibitors and protein quality of selected legume seeds. Plant Foods Hum Nutr. 1998;52(3):199–208.
46. Zhong Y, Wang Z, Zhao Y. Impact of radio frequency, microwaving, and high hydrostatic pressure at elevated temperature on the nutritional and antinutritional components in black soybeans. J Food Sci. 2015;80(12):C2732–9.
47. Marconi E, Ruggeri S, Cappelloni M, Leonardi D, Carnovale E. Physicochemical, nutritional, and microstructural characteristics of chickpeas (Cicer arietinum L.) and common beans (Phaseolus vulgaris L.) following microwave cooking. J Agric Food Chem. 2000;48 (12):5986–94.
48. Alajaji SA, El-Adawy TA. Nutritional composition of chickpea (Cicer arietinum L.) as affected by microwave cooking and other traditional cooking methods. J Food Compos Anal. 2006;19(8):806–12. https://doi.org/10.1016/j.jfca.2006.03.015.
49. El-Adawy TA. Nutritional composition and antinutritional factors of chickpeas (Cicer arietinum L.) undergoing different cooking methods and germination. Plant Foods Hum Nutr. 2002;57(1):83–97.
50. Ertas N. Dephytinization processes of some legume seeds and cereal grains with ultrasound and microwave applications. Legum Res. 2013;36(5):414–21.
51. Oomah BD, Kotzeva L, Allen M, Bassinello PZ. Microwave and micronization treatments affect dehulling characteristics and bioactive contents of dry beans (Phaseolus vulgaris L.). J Sci Food Agric. 2014;94(7):1349–58.
52. Divekar MT, Karunakaran C, Lahlali R, Kumar S, Chelladurai V, Liu X, et al. Effect of microwave treatment on the cooking and macronutrient qualities of pulses. Int J Food Prop. 2017;20(2):409–22.
53. López-Perea P, Figueroa J, Sevilla-Paniagua E, Román-Gutiérrez A, Reynoso R, Martínez-Peniche R. Changes in barley kernel hardness and malting quality caused by microwave irradiation. J Am Soc Brew Chem. 2008;66(4):203–7.
54. Velu V, Nagender A, Rao PP, Rao D. Dry milling characteristics of microwave dried maize grains (Zea mays L.). J Food Eng. 2006;74(1):30–6.
55. Purohit P, Jayas DS, Chelladurai V, Yadav BK. Microwave treatment of mung bean (Vigna radiata) for reducing the cooking time. Appl Eng Agric. 2013;29(4):547–56.
56. Randhir R, Shetty K. Microwave-induced stimulation of l-DOPA, phenolics and antioxidant activity in fava bean (Vicia faba) for Parkinson's diet. Process Biochem. 2004;39 (11):1775–84. https://doi.org/10.1016/j.procbio.2003.08.006.
57. Jogihalli P, Singh L, Sharanagat VS. Effect of microwave roasting parameters on functional and antioxidant properties of chickpea (Cicer arietinum). LWT Food Sci Technol. 2017;79:223–33.
58. González Z, Pérez E. Evaluation of lentil starches modified by microwave irradiation and extrusion cooking. Food Res Int. 2002;35(5):415–20. https://doi.org/10.1016/S0963-9969(01)00135-1.
59. Waard M, Georgopoulos S, Hollomon D, Ishii H, Leroux P, Ragsdale N, Schwinn F. Chemical control of plant diseases: problems and prospects. Annu Rev Phytopathol. 1993;31(1):403–21.

60. Athanassiou CG, Arthur FH. Recent advances in stored product protection. Berlin: Springer; 2018.
61. Fallik E, Lurie S. Thermal control of fungi in the reduction of postharvest decay. Wallingford: CABI; 2007.
62. Grondeau C, Samson R. A review of thermotherapy to free plant materials from pathogens, especially seeds from bacteria. Crit Rev Plant Sci. 1994;13(1):57–75. https://doi.org/10.1080/713608054.
63. Hansen J, Johnson J, Winter D. History and use of heat in pest control: a review. Int J Pest Manag. 2011;57(4):267–89.
64. Tang J, Ikediala J, Wang S, Hansen JD, Cavalieri R. High-temperature-short-time thermal quarantine methods. Postharvest Biol Technol. 2000;21(1):129–45.
65. Brodie G. Microwave heating in moist materials. Advances in induction and microwave heating of mineral and organic materials. InTech; 2011.
66. Nelson SO. Review and assessment of radio-frequency and microwave energy for stored-grain insect control. Trans Am Soc Agric Eng. 1996;39:1475–84.
67. Nayak MK, Daglish GJ. Importance of stored product insects. In: Athanassiou CG, Arthur FH, editors. Recent advances in stored product protection. Berlin, Heidelberg: Springer; 2018. p. 1–17.
68. Wang S, Tang J. Radio frequency and microwave alternative treatments for insect control in nuts: a review. Agric Eng J. 2001;10(3&4):105–20.
69. Vadivambal R, Jayas D, White N. Wheat disinfestation using microwave energy. J Stored Prod Res. 2007;43(4):508–14.
70. Zhao S, Qiu C, Xiong S, Cheng X. A thermal lethal model of rice weevils subjected to microwave irradiation. J Stored Prod Res. 2007;43(4):430–4. https://doi.org/10.1016/j.jspr.2006.12.005.
71. Vadivambal R, Jayas D, White NDG. Determination of mortality of different life stages of Tribolium castaneum (Coleoptera: Tenebrionidae) in stored barley using microwaves. J Econ Entomol. 2008;101(3):1011–21.
72. Wang S, Tiwari G, Jiao S, Johnson J, Tang J. Developing postharvest disinfestation treatments for legumes using radio frequency energy. Biosyst Eng. 2010;105(3):341–9.
73. Singh R, Singh K, Kotwaliwale N. Study on disinfestation of pulses using microwave technique. J Food Sci Technol. 2012;49(4):505–9.
74. Jiao S, Johnson JA, Tang J, Wang S. Industrial-scale radio frequency treatments for insect control in lentils. J Stored Prod Res. 2012;48:143–8. https://doi.org/10.1016/j.jspr.2011.12.001.
75. Purohit P, Jayas DS, Yadav BK, Chelladurai V, Fields PG, White NDG. Microwaves to control Callosobruchus maculatus in stored mung bean (Vigna radiata). J Stored Prod Res. 2013;53:19–22. https://doi.org/10.1016/j.jspr.2013.01.002.
76. Echereobia CO, Asawalam EF, Emeasor KC, Nwana IE, Sahayaraj K. Efficacy of microwave irradiation on the postharvest control of cowpea Bruchid, (Callosobruchus maculatus) Coleoptera: Bruchidae on stored cowpea. Am J Exp Agric. 2014;4(11):1305–13.
77. Mohapatra D, Giri S, Kar A. Effect of microwave aided disinfestation of Callosobruchus maculatus on green gram quality. Int J Agric Food Sci Technol. 2014;5(2):55–62.
78. Lamberti G. Microwave technology applied in post-harvest treatments of cereals and legumes. Chem Eng Trans. 2015;44:13–8. https://doi.org/10.3303/CET1544003.
79. Ahmady A, Mousa MA, Zaitoun AA. Effect of microwave radiation on Tribolium confusum Jaquelin du Val (Coleoptera: Tenebrionidae) and Callosobruchus maculatus (F.)(Coleoptera: Chrysomelidae: Bruchidae). Entomol Zool Stud. 2016;4(4):1257–63.
80. Silva Fontes L, Silva PRR, Neves JA, Melo AF, Esteves Filho AB. Microwave radiation to control Callosobruchus maculatus (Coleoptera: Chrysomelidae) larvae in cowpea cultivars. Aust Entomol. 2016;56(1):70–4.
81. Macana R, Baik O. Disinfestation of insect pests in stored agricultural materials using microwave and radio frequency heating: a review. Food Rev Int. 2017:1–28.

82. Yadav DN, Anand T, Sharma M, Gupta R. Microwave technology for disinfestation of cereals and pulses: an overview. J Food Sci Technol. 2014;51(12):3568–76.
83. Mohapatra D, Saha KP, Babu VB. Disinfestation of chickpea and green gram from Callosobruchus maculatus adults through hot-air-assisted microwave heating system. Agric Res. 2018:1–12. https://doi.org/10.1007/s40003-018-0346-2.
84. Hojnik N, Cvelbar U, Tavčar-Kalcher G, Walsh JL, Križaj I. Mycotoxin decontamination of food: cold atmospheric pressure plasma versus "classic" decontamination. Toxins. 2017;9 (5):151.
85. Christensen CM, Kaufmann HH. Grain storage, the role of Fungi in quality loss (NED - new edition ed.). Minneapolis: University of Minnesota Press; 1969.
86. Forsberg G, Andersson S, Johnsson L. Evaluation of hot, humid air seed treatment in thin layers and fluidized beds for seed pathogen sanitation/Bewertung der Saatgutbehandlung mit heißer, feuchter Luft und in einer Verwirbelungskammer zur Eliminierung von samenbürtigen Pathogenen. Zeitschrift für Pflanzenkrankheiten Pflanzenschutz J Plant Dis Prot. 2002;109 (4):357–70.
87. Jiao S, Zhong Y, Deng Y. Hot air-assisted radio frequency heating effects on wheat and corn seeds: quality change and fungi inhibition. J Stored Prod Res. 2016;69:265–71.
88. Taheri S, Brodie GI, Gupta D, Dadu RHR. Effect of microwave radiation on internal inoculum of ascochyta blight in lentil seeds at different seed moisture contents. Trans ASAE. 2019;62 (1):33–43. https://doi.org/10.13031/trans.13088.
89. Hoersten DV, Wolfgang L. Thermal treatment of seeds - comparison of different methods for eradicating Seedborne Fungi. 2001 ASAE Annual Meeting; 2001. https://doi.org/10.13031/2013.4138.
90. Atmaca S, Akdag Z, Dasdag S, Celik S. Effect of microwaves on survival of some bacterial strains. Acta Microbiol Immunol Hung. 1995;43(4):371–8.
91. Reddy MB, Raghavan G, Kushalappa A, Paulitz T. Effect of microwave treatment on quality of wheat seeds infected withFusarium graminearum. J Agric Eng Res. 1998;71(2):113–7.
92. Cavalcante MJB, Muchovej JJ. Microwave irradiation of seeds and selected fungal spores. Seed Sci Technol. 1993;21(1):247–53.
93. Reddy P, Mycock DJ, Berjak P. The effect of microwave irradiation on the ultrastructure and internal fungi of soybean seed tissues. Seed Sci Technol. 2000;28(2):277–89.
94. Gaurilčikienė I, Ramanauskienė J, Dagys M, Simniškis R, Dabkevičius Z, Supronienė S. The effect of strong microwave electric field radiation on:(2) wheat (Triticum aestivum L.) seed germination and sanitation. Zemdirbyste-Agriculture. 2013;100:185–90.
95. Knox OG, McHugh MJ, Fountaine JM, Havis ND. Effects of microwaves on fungal pathogens of wheat seed. Crop Prot. 2013;50:12–6.
96. Friesen AP, Conner RL, Robinson DE, Barton WR, Gillard CL. Effect of microwave radiation on dry bean seed infected with Colletotrichum lindemuthianum with and without the use of chemical seed treatment. Can J Plant Sci. 2014;94(8):1373–84. https://doi.org/10.4141/cjps-2014-035.
97. Friesen AP, Conner RL, Robinson DE, Barton WR, Gillard CL. Effect of microwave radiation on dry bean seed infected with Xanthomonas axonopodis pv. phaseoli with and without the use of chemical seed treatment. Crop Prot. 2014;65:77–85. https://doi.org/10.1016/j.cropro.2014.07.007.
98. Lee S-H, Park S, Byun K-H, Chun H, Ha S-D. Effects of microwaves on the reduction ofAspergillus flavusandAspergillus parasiticuson brown rice (Oryza sativaL.) and barley (Hordeum vulgareL.). Food Addit Contam Part A Chem Anal Control Expo Risk Assess. 2017;34(7):1193–200.
99. Sosa-Morales ME, Aguilar-Morales M, Cerón-García A, Rojas-Laguna R, López-Malo A. Quality of beans (Phaseolus vulgaris L.) after postharvest microwave treatments. J Microw Power Electromagn Energy. 2017;51(3):178–86.
100. Manickavasagan A, Jayas D, White N. Germination of wheat grains from uneven microwave heating in an industrial microwave dryer. Can Biosyst Eng. 2007;49:3.

101. Warchalewski JR, Gralik J, Wojtasiak R, Zabielski J, Kusnnierz R. The evaluation of wheat grain odour and colour after gamma and microwave irradiation. Electron J Pol Agric Univ. 1998;1(1):1–11.
102. Adebowale OJ, Taylor JRN, de Kock HL. Stabilization of wholegrain sorghum flour and consequent potential improvement of food product sensory quality by microwave treatment of the kernels. LWT. 2020;132:109827. https://doi.org/10.1016/j.lwt.2020.109827.
103. Silva HLA, Balthazar CF, Silva R, Vieira AH, Costa RGB, Esmerino EA, et al. Sodium reduction and flavor enhancer addition in probiotic Prato cheese: contributions of quantitative descriptive analysis and temporal dominance of sensations for sensory profiling. J Dairy Sci. 2018;101(10):8837–46. https://doi.org/10.3168/jds.2018-14819.
104. Judacewski P, Los P, Lima L, Alberti A, Zielinski AAF, Nogueira A. Perceptions of Brazilian consumers regarding white mould surface-ripened cheese using free word association. Int J Dairy Technol. 2019;72(4):585–90.
105. Polizer Rocha YJ, Lapa-Guimarães J, de Noronha RLF, Trindade MA. Evaluation of consumers' perception regarding frankfurter sausages with different healthiness attributes. J Sens Stud. 2018;33(6):e12468.
106. da Costa GM, de Paula MM, Costa GN, Esmerino EA, Silva R, de Freitas MQ, et al. Preferred attribute elicitation methodology compared to conventional descriptive analysis: A study using probiotic yogurt sweetened with xylitol and added with prebiotic components. J Sens Stud. 2020;35(6):e12602.
107. Manickavasagan A, Jayas D, White N. Non-uniformity of surface temperatures of grain after microwave treatment in an industrial microwave dryer. Dry Technol. 2006;24(12):1559–67.
108. Vadivambal R, Jayas D, Chelladurai V, White N. Preliminary study of surface temperature distribution during microwave heating of cereals and oilseed. Can Biosyst Eng. 2009;51:3.45–43.52.
109. Guo Q, Sun D-W, Cheng J-H, Han Z. Microwave processing techniques and their recent applications in the food industry. Trends Food Sci Technol. 2017;67:236–47. https://doi.org/10.1016/j.tifs.2017.07.007.
110. Martins CP, Cavalcanti RN, Couto SM, Moraes J, Esmerino EA, Silva MC, et al. Microwave processing: current background and effects on the physicochemical and microbiological aspects of dairy products. Compr Rev Food Sci Food Saf. 2019;18(1):67–83.
111. Tang J. Unlocking potentials of microwaves for food safety and quality. J Food Sci. 2015;80 (8):E1776–93.
112. Remmen HH, Ponne CT, Nijhuis HH, Bartels PV, Kerkhof PJ. Microwave heating distributions in slabs, spheres and cylinders with relation to food processing. J Food Sci. 1996;61 (6):1105–14.
113. Pu Y-Y, Sun D-W. Prediction of moisture content uniformity of microwave-vacuum dried mangoes as affected by different shapes using NIR hyperspectral imaging. Innovative Food Sci Emerg Technol. 2016;33:348–56.
114. Lorenson CP, Hewitt BC, Keefer R, Ball MD. Improved uniformity of microwave heating by control of the depth of a load in a container. Google Patents; 1991.
115. Ho Y, Yam K. Effect of metal shielding on microwave heating uniformity of a cylindrical food model. J Food Process Preserv. 1992;16(5):337–59.
116. Ryynänen S, Ohlsson T. Microwave heating uniformity of ready meals as affected by placement, composition, and geometry. J Food Sci. 1996;61(3):620–4.
117. Peyre F, Datta A, Seyler C. Influence of the dielectric property on microwave oven heating patterns: application to food materials. J Microw Power Electromagn Energy. 1997;32 (1):3–15.
118. Ni H, Datta A, Parmeswar R. Moisture loss as related to heating uniformity in microwave processing of solid foods. J Food Process Eng. 1999;22(5):367–82.
119. Lee DS, Shin DH, Yam KL. Improvement of temperature uniformity in microwave-reheated rice by optimizing heat/hold cycle. Food Serv Technol. 2002;2(2):87–93.

120. Zhang H, Hayert-Bonneveau L, Yout W, Helstern GC, Loizeau G. Uniform microwave heating of food in a container. Google Patents; 2004
121. Vadivambal R, Jayas D. Non-uniform temperature distribution during microwave heating of food materials—A review. Food Bioprocess Technol. 2010;3(2):161–71.
122. Hong Y-D, Lin B-Q, Li H, Dai H-M, Zhu C-J, Yao H. Three-dimensional simulation of microwave heating coal sample with varying parameters. Appl Therm Eng. 2016;93:1145–54. https://doi.org/10.1016/j.applthermaleng.2015.10.041.
123. Law M, Liew E, Chang S, Chan Y, Leo C. Modelling microwave heating of discrete samples of oil palm kernels. Appl Therm Eng. 2016;98:702–26.
124. Ye J, Hong T, Wu Y, Wu L, Liao Y, Zhu H, et al. Model stirrer based on a multi-material turntable for microwave processing materials. Materials. 2017;10(2):95.
125. Gowen A, Abu-Ghannam N, Frias J, Oliveira J. Optimisation of dehydration and rehydration properties of cooked chickpeas (Cicer arietinum L.) undergoing microwave–hot air combination drying. Trends Food Sci Technol. 2006;17(4):177–83. https://doi.org/10.1016/j.tifs.2005.11.013.
126. Pu Y-Y, Sun D-W. Combined hot-air and microwave-vacuum drying for improving drying uniformity of mango slices based on hyperspectral imaging visualisation of moisture content distribution. Biosyst Eng. 2017;156:108–19.
127. Sanga E, Mujumdar A, Raghavan G. Simulation of convection-microwave drying for a shrinking material. Chem Eng Process Process Intensif. 2002;41(6):487–99.
128. Feng H, Tang J. Microwave finish drying of diced apples in a spouted bed. J Food Sci. 1998;63(4):679–83.
129. Taheri S, Brodie G, Gupta D. Microwave fluidised bed drying of red lentil seeds: drying kinetics and reduction of botrytis grey mold pathogen. Food Bioprod Process. 2020;119:390–401. https://doi.org/10.1016/j.fbp.2019.11.001.
130. Taheri S, Brodie G, Gupta D. Fluidisation of lentil seeds during microwave drying and disinfection could prevent detrimental impacts on their chemical and biochemical characteristics. LWT. 2020;129:109534. https://doi.org/10.1016/j.lwt.2020.109534.
131. Poogungploy P, Poomsa-ad N, Wiset L. Control of microwave assisted macadamia drying. J Microw Power Electromagn Energy. 2018;52(1):60–72.
132. Xu W, Song C, Li Z, Song F, Hu S, Li J, et al. Temperature gradient control during microwave combined with hot air drying. Biosystems Eng. 2018;169:175–87. https://doi.org/10.1016/j.biosystemseng.2018.02.013.
133. Zhang Z, Su T, Zhang S. Shape effect on the temperature field during microwave heating process. J Food Qual. 2018;2018:1–24.
134. Wang S, Yue J, Tang J, Chen B. Mathematical modelling of heating uniformity for in-shell walnuts subjected to radio frequency treatments with intermittent stirrings. Postharvest Biol Technol. 2005;35(1):97–107.
135. Kudra T. Dielectric drying of particulate materials in a fluidized state. Dry Technol. 1989;7(1):17–34.
136. Momenzadeh L, Zomorodian A, Mowla D. Experimental and theoretical investigation of shelled corn drying in a microwave-assisted fluidized bed dryer using artificial neural network. Food Bioprod Process. 2011;89(1):15–21.

Part III
Plasma Applications

Chapter 12
Growth Enhancement Effect of Gene Expression of Plants Induced by Active Oxygen Species in Oxygen Plasma

Nobuya Hayashi

Abstract Enhancements of germination and growth of plants are observed after oxygen plasma irradiation to seeds. Gene expressions in plant seeds irradiated by oxygen plasma were investigated using DNA microarray bioinformatics analysis to clarify the pathways responsible for growth enhancement of plants. Gene expressions involved in photosynthesis and energy production by active oxygen species in oxygen plasma are one of the factors for the growth enhancement of plants. The observed growth enhancement effect is not passed on to the next generation by irradiating seeds, and there is no significant change in gene expressions in second-generation seeds. The observed growth enhancement of plants is brought about by epigenetics.

Keywords Plant growth enhancement · Active oxygen species · Oxygen plasma · Gene expression · Epigenetics

12.1 Introduction

The modern agriculture has been supported by the artificial climate for plant growth, which is realized by electricity, fuel, and pesticides. However, there are side effects such as environmental pollution and increase of cost. These issues lead to decline of agriculture and forestry. For example, Japanese forestry is declining and uncontrolled forests are increasing. This leads to pollinosis. Increase of germination rate of cedar and cypress, cost reduction of nursery trees, and then regeneration of Japanese forestry. In order to save the environment and to reduce the cost of cultivation, these fuel and chemicals must be reduced in agriculture. One of the most promising ways to save the environment and cost is to reduce the cultivation

N. Hayashi (✉)
Interdisciplinary Graduate School of Engineering Sciences, Kyushu University, Fukuoka, Japan
e-mail: hayashi.nobuya.056@m.kyushu-u.ac.jp

S. Horikoshi et al. (eds.), *Agritech: Innovative Agriculture Using Microwaves and Plasmas*, https://doi.org/10.1007/978-981-16-3891-6_12

Fig. 12.1 Typical growth enhancement of radish sprout. (**a**) Control samples without plasma irradiation. (**b**) Sprouts from seeds subjected to plasma irradiation. Used with permission from N. Hayashi, R. Ono, M. Shiratani and A. Yonesu (2015). Antioxidative activity of plant and regulation of Brassicaceae induced by oxygen radical irradiation. Jpn. J. Appl. Phys. 54, 06GD01-1 – 06GD01-5. DOI: https://doi.org/10.7567/JJAP.54.06GD01

period of plants. Therefore, enhancement of germination of seeds and growth of plants are required in agriculture.

Enhancement of germination and growth have been investigated, which are induced with plasma irradiation using different discharge types and various gases [1–7]. Recently, plant germination and growth regulations have been observed when plant seeds are irradiated by active oxygen species produced by oxygen plasmas, as shown in Fig. 12.1. Some biochemical reactions that occur inside plant cells are affected by active oxygen species, and photosynthesis and/or protein production are enhanced [8, 9]. The first-stage reactions induced by active oxygen species are the redox reactions of thiol compounds. When plant seeds are irradiated by active oxygen species generated by oxygen plasma, thiol compounds in cells are oxidized, and the thiol bases change into disulfide bonds [10]. The major thiol compound in living organisms is Thioredoxin, which plays roles as an oxygen sensor and scavenger of excess active oxygen species [11, 12]. However, the pathways by which the oxidation of thiol compounds by exterior active oxygens affect growth regulation have not been understood. The oxidation and reduction of thiol compounds should lead to the regulation of enzymatic reactions, including gene expression [13–15]. Clarification of the involved pathways is important to confirm the safety of plasma applications for agriculture, such as the disinfection of agricultural products and sterilization of seeds. However, there is no definite method to clarify the mechanism of plant growth enhancement.

When an external stimulus such as ultraviolet rays or radiation is given to a living body, the expression of a response to them and the inheritance of acquired traits to the next generation are observed. Ultraviolet (UV) rays and radiation with energies of several eV or more can dissociate the bonds between the bases that make up the gene. Therefore, changes in biological functions caused by high-energy external stimuli such as ultraviolet rays and radiation are generally due to changes in protein synthesis and changes in genetic information due to changes in the base sequence of

genes. However, in recent years, the expression and inheritance of functions that are not mediated by mutations in the base sequence of genes have been found. Such a phenomenon is called epigenetics, and it is not a change in the base sequence, but a change in the chromatin structure or nucleosome structure, which is the larger structure of the gene (for example, histone modification and DNA methylation), is thought to be related to changes in functional expression and inheritance of acquired functions. In recent years, it has been found that plasma irradiation of a living body induces a series of biological reactions in cells along with physical changes on the surface of the living body, and exhibits biological functions such as enhancement of plant growth [3, 4, 16, 17], promotion of cell proliferation [18–20], and induction of apoptosis [21]. However, the process of expression of biological functions by plasma irradiation and the mechanism related to its inheritance have not been elucidated so far [3]. In this study, the seeds of Arabidopsis thaliana were irradiated with oxygen plasma, and the gene expression effect was clarified.

In the present study, (i) growth enhancement mechanism of plants and (ii) inheritance mechanism of acquired functions of plants are investigated, when seeds are irradiated with discharge plasmas containing active oxygen species. Gene expressions of plant seeds induced by neutral active oxygen species in plasmas were clarified by functional annotation bioinformatics analysis and gene ontology analysis using microarray.

12.2 Experimental Methods

For irradiation with plasmas, low-pressure [22–25] and atmospheric pressure plasmas [26, 27] have been used. The pure oxygen plasma is generated by the low-pressure radio frequency (RF) discharge as shown in Fig. 12.2. Low-pressure plasmas are able to control particle species in the plasmas by selecting material gas species and the discharge condition precisely. Oxygen gas was introduced into the vacuum chamber with capacity of 20 L, and pressure is set at 60 Pa. The RF antenna is set inside the vacuum chamber along the chamber wall. The shape of the antenna is a wound rod with total length of 200 cm. The RF power with the frequency of 13.56 MHz is varied from 20 to 100 W. Treatment time is ranged from 30 to 120 min. The oxygen plasma generated by the RF discharge localizes around the RF antenna owing to the difficulty of the oxygen discharge at relatively higher-pressure condition. Active oxygen species were confirmed by light emission spectra and a chemical indicator, which were set at the position of the sample seeds. The chemical indicator used in this experiment is designed for the detection of neutral active oxygen species [26, 28]. The seeds were enclosed in a nonwoven bag to avoid stimulation by ion impacts, and were placed at the bottom of the chamber.

Active oxygen species are also generated by the atmospheric dielectric barrier discharge device, which is a popular device in the field of plasma application studies [28, 29], as shown in Fig. 12.3. In atmospheric plasmas, the active oxygen is in the form of ozone that has longer lifetime than atomic oxygen and excited oxygen

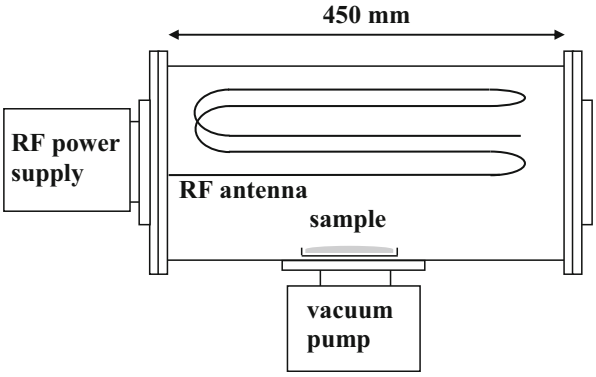

Fig. 12.2 Low-pressure radio frequency discharge plasma production device. Used with permission from Satoshi Watanabe, Reoto Ono, Nobuya Hayashi, Kousuke Tashiro, Satoru Kuhara, Asami Inoue, Kaori Yasuda, and Hiroko Hagiwara (2016). Growth Enhancement and Gene Expression of *Arabidopsis* irradiated by active oxygen species. Jpn. J. Appl. Phys. 55, 07LG10-1 – 07LG10-6. DOI: https://doi.org/10.7567/JJAP.55.07LG10

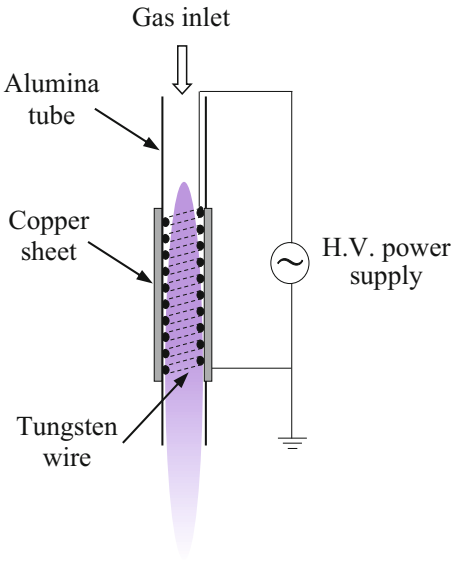

Fig. 12.3 Atmospheric-pressure low-frequency AC discharge plasma production device. Used with permission from N. Hayashi, R. Ono, M. Shiratani and A. Yonesu (2015). Antioxidative activity of plant and regulation of *Brassicaceae* induced by oxygen radical irradiation. Jpn. J. Appl. Phys. 54, 06GD01-1 – 06GD01-5. DOI: https://doi.org/10.7567/JJAP.54.06GD01

molecule. The cylindrical alumina tube with diameter of several mm is sandwiched by a spiral shape stainless wire as a discharge electrode and cupper sheet that wrap around the outer surface of the alumina tube. When the high-voltage AC power is applied to the discharge electrode, the barrier-type discharge occurs around the stainless wire in the tube. When oxygen gas flows into the discharge region in the tube, the oxygen molecule changes into the ozone (O_3). The ozone is decomposed into oxygen molecule and atomic oxygen. Therefore, active oxygen is also obtained by the atmospheric pressure plasmas.

Arabidopsis thaliana (wild type, Columbia-01) and *Raphanus sativus var. longipinnatus* (radish sprout) seeds were irradiated with active oxygen species generated in the oxygen plasma. These plants were utilized for growth observation and gene analysis, respectively. After the plasma irradiation, 50 dried seeds of *Arabidopsis* are ground-up and RNA of 1μg was extracted using the RNA extraction reagent. The quality of the extracted RNA was confirmed by electrophoresis. Gene expression of seeds was analyzed by the microarray method using a microarray scanner (Agilent SurePrint G3 GE 8x60K v2). The obtained gene data were arranged by the functional annotation bioinformatics microarray method and pathway analysis method using the database for annotation, visualization, and integrated discovery (DAVID) [30]. The microarray analyses of the same condition are repeated twice, and repeatability of the result has been confirmed. The antioxidative activity was estimated as the amount of thiol compounds in plants, which is measured using the thiol quantification reagent (ANASPEC, SensoLyteR Thiol Quantitation Assay Kit). The weight of the plant sample is 0.17 g and kept constant throughout the experiments.

12.3 Active Oxygen Irradiation to Seeds

Active oxygen species generated in the oxygen plasma by the RF discharge at low pressure were measured using optical emission spectroscopy. Figure 12.4 shows light emission intensities from atomic oxygen and excited oxygen molecule with their intensity ratio varying the oxygen gas pressure. In the lower pressure region around 20 Pa, atomic oxygen O(^{5}P) at the emission wavelength of 777 nm and oxygen ions tend to be generated. When the pressure increases to 60 Pa, excited oxygen molecules such as O_2 ($^1\Sigma_g^+$) at 761 nm are produced dominantly owing to the lower energy electrons. The lifetime of an excited oxygen molecule is the order of ms in low-pressure conditions. The tendency of $^1\Sigma_g^+$ to O(^{5}P) indicates the effect of $^1\Sigma_g^+$. The effect of $^1\Sigma_g^+$ increases with the oxygen gas pressure till 60 Pa, and saturates with the pressure higher than 60 Pa. Therefore, the pressure in the chamber was varied within a range of several tens of Pa. Also, the chemical indicator shows generation of active oxygen species in the afterglow region of the chamber. In this experiment, seeds of the radish sprout and the *Arabidopsis* are utilized for the growth observation and the gene analysis, respectively. Germination of radish sprouts is observed after one and 2 days from seeding. The germination rate increases significantly after plasma irradiation of seeds. When growth enhancement occurs in plants by irradiating seeds with active oxygen species under particular conditions, stem and root lengths increase compared with those of seeds without irradiation.

Figure 12.5 shows plant seeds irradiated with the low-pressure radio frequency oxygen plasma. To irradiate neutral active oxygen species, those velocity is lower than charged particles, the seeds are placed in the afterglow region of the plasma at approximately 10 cm away from the RF-powered electrode. Then, damages of seeds by ion bombardment can be avoidable. Figure 12.6 shows the growth of *Arabidopsis*

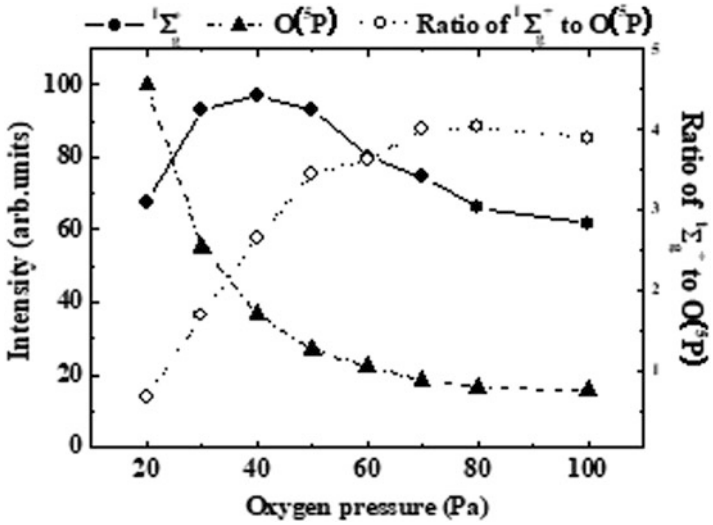

Fig. 12.4 Optical emission intensities from $^1\Sigma_g^+$, O(^{5}P) and intensity ratio of $^1\Sigma_g^+$ to O(^{5}P) varying oxygen gas pressure. Used with permission from Riku Nakano, Kosuke Tashiro, Reona Aijima, and Nobuya Hayashi (2016). Effect of oxygen plasma irradiation on gene expression in plant seeds induced by active oxygen species. Plasma Medicine 6, 303–313. DOI: https://doi.org/10.1615/PlasmaMed.2016019093

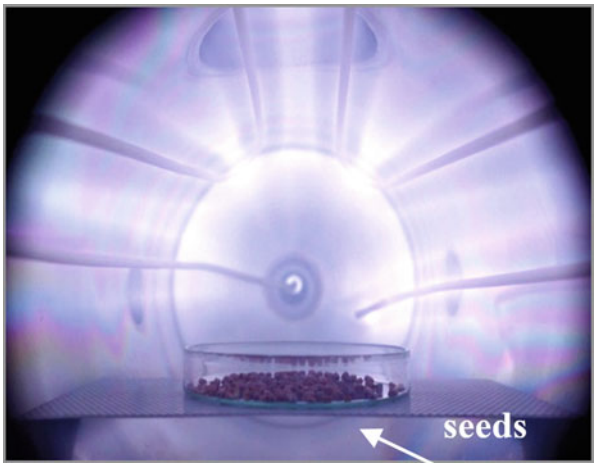

Fig. 12.5 Plant seeds irradiated with active oxygen species in afterglow region in low-pressure oxygen plasma. Used with permission from Nobuya Hayashi, Reoto Ono and Shohei Uchida (2015). Growth Enhancement of Plant by Plasma and UV Light Irradiation to Seeds. J. Photopolym. Sci. Technol. 28**,** 445–448. DOI: https://doi.org/10.2494/photopolymer.28.445

thaliana wild-type by the oxygen plasma irradiating seeds for 3 min with control (untreated). The size of leaves is apparently larger than the control, and the number of leaves does not change. This fact implies that the oxygen plasma irradiation enhances the growth of plant cells. Therefore, the amount of thiol compound in plant cells works as a kind of the indicator of active oxygens in cells.

Fig. 12.6 Growth of *Arabidopsis thaliana* wild-type by oxygen plasma irradiating seeds for 3 min with control

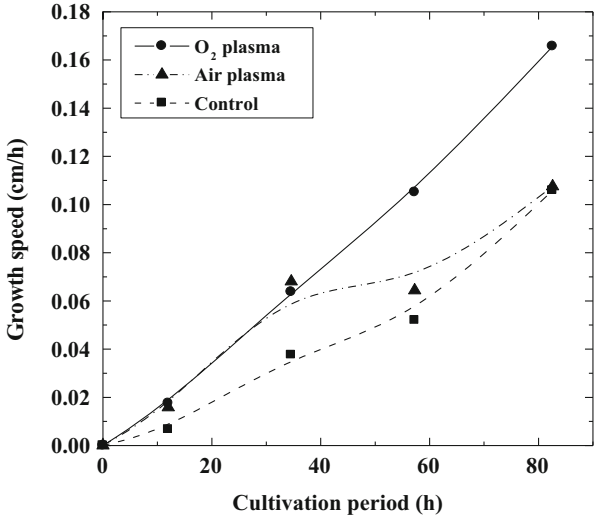

Fig. 12.7 Growth speed of the radish sprout length after the plasma irradiation with control. Used with permission from Riku Nakano, Nobuya Hayashi, Reona Aijima, Yoshio Yamashita, Akira Kobayashi (2018). Gene Expression Effect of Plant Seeds Irradiated by Low Pressure Oxygen Plasma. Journal of IAPS 26, 91–95

Figure 12.7 shows the growth speed of the radish sprout length after the plasma irradiation with control. After irradiations with oxygen plasma and air plasma, the growth speeds become larger than the control. The speed reduces to almost the same as the control in the case of the air plasma after a cultivation period of 60 h. Active oxygen species would be the factor of the plant growth enhancement. When active oxygen species irradiates plants, plants receive active oxygens as a kind of stimulus using thiol compounds such as thioredoxin. When thiol compounds in plant cell are consumed by active oxygen species making disulfide bonds, then the amount of thiol

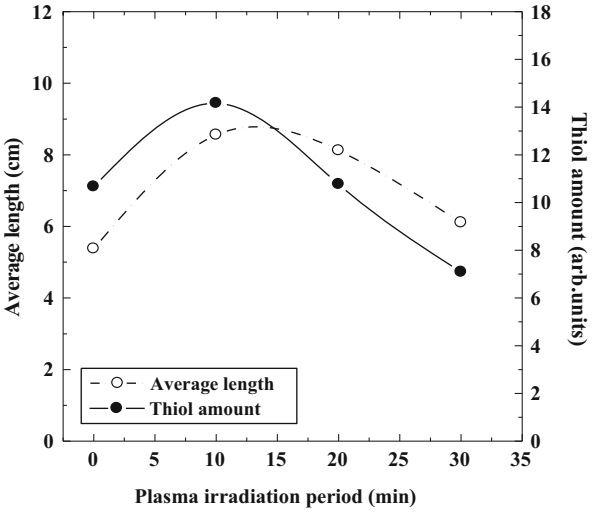

Fig. 12.8 Tendencies of the thiol compounds amount in seeds and the average length of radish sprout varying the plasma irradiation. Used with permission from N. Hayashi, R. Ono, M. Shiratani and A. Yonesu (2015). Antioxidative activity of plant and regulation of *Brassicaceae* induced by oxygen radical irradiation. Jpn. J. Appl. Phys. 54, 06GD01-1 – 06GD01-5. DOI: https://doi.org/10.7567/JJAP.54.06GD01

compounds in plant cells increases to absorb the active oxygens [12, 14, 31]. Figure 12.8 shows tendencies of the thiol compounds amount in seeds and the average length of radish sprout varying the plasma irradiation period. The plant length increases with the plasma irradiation period till 10 min, where the active oxygen species would work as the appropriate stimulus for the plant growth. When the plasma irradiation period is larger than 10 min, the excess amount of active oxygen would cause the oxidation damage on the seeds. Then, the average length of the radish spout decreases monotonically with the irradiation period. Student t-tests are performed between lengths of untreated and plasma-irradiated radish sprouts. p-values of all data used in this manuscript are below 0.05. Population served for the student t-test is 30.

The thiol compounds those are kinds of antioxidative substances contains many SH base in the structure, and reduce the excess amount of active oxygen species in cells, and produce the disulfide bonds. The thiol amount increases with the plasma irradiation period till 10 min, which relates to the dose of active oxygen species. The increase of antioxidative substances, those are reduction-type thiol compounds, would be a counter reaction against the oxidative stresses [32, 33]. When the irradiation period is larger than 10 min, the thiol compound amount in cell decreases with the irradiation period. In this phase, the consumption of the thiol compounds by active oxygen species exceeds its production in cells. The competition between the stimulus and damage to seeds would decide the appropriate irradiation condition of the oxygen plasma. When the oxygen gas pressure increases from 20 to 100 Pa, the maximum length of the plant, which grows from the oxygen plasma irradiated seeds, is obtained around 40 to 60 Pa. This tendency coincides with that of the light emission intensity from the singlet oxygen molecule ($^1\Sigma_g^+$). Therefore, the $^1\Sigma_g^+$ is the best candidate of a factor for the plant growth enhancement. Microscopic observation of plants indicated that the size of cells in stems and leaves grown

from plasma-irradiated seeds was almost the same as in those without plasma irradiation. These results imply that the cell cycle is accelerated owing to excited oxygen molecules, and therefore the cell number in stem and leaf of plant increases.

12.4 Gene Expression Modification of Seeds by Oxygen Plasma Irradiation

Excited oxygen molecules will penetrate into the inner part of seed through seed coat, when seeds are irradiated by the oxygen plasma. Then some counterreactions against oxidation are expected to occur. In order to investigate the mechanism of biological reactions in seeds those were induced by oxygen plasma irradiation, the gene expression analysis is performed using the functional annotation bioinformatics microarray method. Figure 12.9 shows a functional annotation chart of the biological processes in expressed genes obtained by the gene ontology analysis, which was derived from seeds just after being irradiated by oxygen plasma. Functional annotations are obtained by functional analysis of genes whose expression levels were 4 times higher than the original (standard) level. The annotation chart indicates that functions of expressed genes in plasma-irradiated seeds are categorized into cell growth, stress response, photosynthesis, hormone response, and others. Results of the microarray scanning of RNAs of *Arabidopsis* seeds and the gene ontology analysis indicate that the expression of 678 genes increased after oxygen plasma irradiation. When *Arabidopsis* seeds were irradiated by the oxygen plasma, major functional gene categories related to cell growth or cellular metabolism, such as photosynthesis, carbon fixation, glycolysis, and the citrate cycle (TCA cycle), had increased expression by irradiation of active oxygen species.

In order to determine the detailed reactions in plant cell, which are activated by the active oxygen irradiation, signal pathways are constructed from the functional annotation chart obtained by gene ontology analysis [34–36]. Signal pathways are obtained from activated genes concerning (a) carbon fixation in photosynthetic organisms and (b) TCA cycle [37, 38]. In the carbon fixation processes in photosynthetic organs, genes of RuBisCO, GAP, and the malate dehydrogenase (MDH) have been regulated [39, 40]. When seeds are irradiated by active oxygen species, genes coding enzymes such as ribulose 1,5-bisphosphate carboxylase/oxygenase (RuBisCO), which catalyzes the rate-controlling reaction of photosynthesis and carbon fixation, were found to be expressed. Then, carbon fixation processes such as photosynthesis and the Calvin–Benson cycle are activated, which is constructed from the annotation table of the significantly expressed genes. Figure 12.10(a) shows the signaling pathway concerning the photosynthesis on the surface of the thylakoid membrane. The proton pump system on the thylakoid membrane is enhanced to be expressed significantly. Active oxygen species in oxygen plasma should oxidize Thioredoxin system on enzymes causing thiol bases to form disulfide bonds, enhancing their activities owing to the active oxygen irradiation. The RuBisCO

GO	Count	PValue
GO:0009628~response to abiotic stimulus	37	1.55E-08
GO:0006970~response to osmotic stress	17	7.61E-06
GO:0042547~cell wall modification during multidimensional cell growth	6	1.17E-05
GO:0009828~plant-type cell wall loosening	6	3.64E-05
GO:0009409~response to cold	12	5.03E-05
GO:0007047~cell wall organization	13	5.26E-05
GO:0009651~response to salt stress	15	5.31E-05
GO:0045229~external encapsulating structure	13	9.01E-05
GO:0042545~cell wall modification	9	1.16E-04
GO:0009827~plant-type cell wall modification	6	1.25E-04
GO:0009825~multidimensional cell growth	6	1.40E-04
GO:0009831~plant-type cell wall modification during multidimensional cell growth	5	1.70E-04
GO:0009664~plant-type cell wall organization	7	2.08E-04
GO:0060560~developmental growth involved in morphogenesis	9	3.14E-04
GO:0009826~unidimensional cell growth	9	3.14E-04
GO:0006949~syncytium formation	4	4.27E-04
GO:0016049~cell growth	10	5.75E-04
GO:0048589~developmental growth	9	8.14E-04
GO:0008361~regulation of cell size	10	8.48E-04
GO:0032535~regulation of cellular component size	10	0.00122
GO:0040007~growth	10	0.001534
GO:0009266~response to temperature stimulus	12	0.001765
GO:0000902~cell morphogenesis	9	0.002043
GO:0009637~response to blue light	5	0.003036
GO:0010114~response to red light	5	0.003243
GO:0032989~cellular component morphogenesis	9	0.003888
GO:0051258~protein polymerization	4	0.004187
GO:0043094~cellular metabolic compound salvage	5	0.00585
GO:0010033~response to organic substance	23	0.008931
GO:0019253~reductive pentose-phosphate cycle	3	0.009909
GO:0009853~photorespiration	4	0.010763
GO:0009639~response to red or far red light	7	0.010959
GO:0019685~photosynthesis, dark reaction	3	0.011352
GO:0009416~response to light stimulus	12	0.013371
GO:0019252~starch biosynthetic process	3	0.014495
GO:0009415~response to water	7	0.016044
GO:0009314~response to radiation	12	0.016792
GO:0015977~carbon utilization by fixation of carbon dioxide	3	0.019823
GO:0009719~response to endogenous stimulus	18	0.037599
GO:0009725~response to hormone stimulus	17	0.04007
GO:0015979~photosynthesis	6	0.043116

Fig. 12.9 Major functions of expressed genes of *Arabidopsis thaliana* seeds after oxygen plasma irradiation. Used with permission from Nobuya Hayashi, Reoto Ono, Riku Nakano, Masaharu Shiratani, Kosuke Tashiro, Satoru Kuhara, Kaori Yasuda, and Hiroko Hagiwara (2016). DNA microarray analysis of plant seeds irradiated by active oxygen species in oxygen plasma. Plasma Medicine 6, 459–471. DOI: https://doi.org/10.1615/PlasmaMed.2016018933

and GAP genes work in the initial stage of the carbon fixation of plants; therefore, the energy production processes by the photosynthesis are enhanced by plasma irradiation. The enhancement of the photosynthesis would be the one of the mechanisms of the plant growth enhancement. Figure 12.10(b) illustrates the signal pathway diagram of the carbon fixation process and the TCA cycle, respectively, which are figured out from the microarray analysis. The pathway analysis reveals that hydrogen pump on thylakoid and some reactions in TCA circuits are activated by the oxygen plasma irradiation. Also, upregulation of some reactions involved in starch production by the Calvin–Benson cycle leads to an increase in pyruvic acid generation through glycolysis. Enhancement of ATP production leads to increase of growth speed of plants.

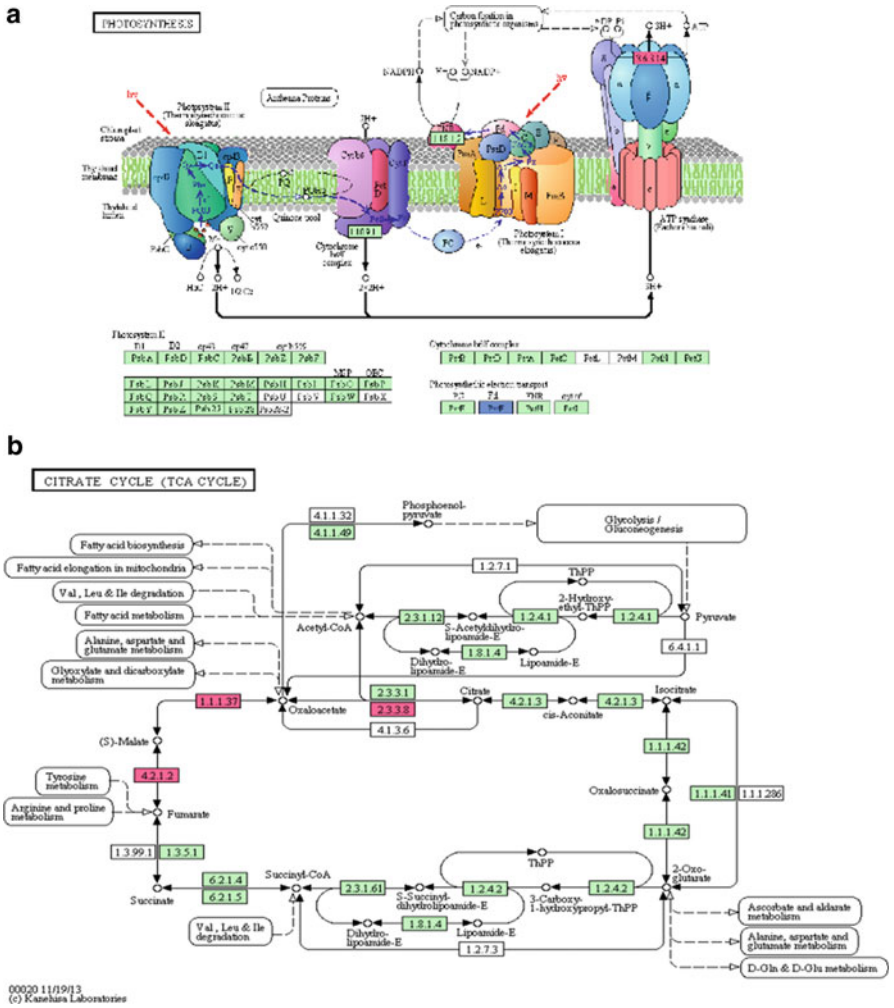

Fig. 12.10 (**a**) Signal pathway on the thylakoid membrane in the plasma-enhanced plant growth. (**b**) Signal pathway of the TCA cycle in the plasma-enhanced plant growth. Used with permission from Nobuya Hayashi, Reoto Ono, Riku Nakano, Masaharu Shiratani, Kosuke Tashiro, Satoru Kuhara, Kaori Yasuda, and Hiroko Hagiwara (2016). DNA microarray analysis of plant seeds irradiated by active oxygen species in oxygen plasma. Plasma Medicine 6, 459–471. DOI: https://doi.org/10.1615/PlasmaMed.2016018933

Also, in the signal pathway diagram of the TCA cycle, the downstream reactions of productions of Oxaloacetate, Marate, Fructose, and Bisphosphorate are upregulated by the plasma irradiation of seeds, and this leads to enhancement of the TCA cycle. Therefore, the production process of the adenosine triphosphate (ATP) in plants is accelerated by oxygen plasma irradiation. In the citrate cycle, genes of MDH and ATP citrate lyase (ACLA), which catalyze the reactions in the

citrate cycle and enhance the generation of ATP, are found to be upregulated by the plasma irradiation to seeds. Genes of the mitochondrial lipoamide dehydrogenase and fumonisin are downregulated. These gene expressions indicate that some reactions in the TCA cycle are enhanced by the oxygen plasma irradiation. Genes such as AT5G43330 and PMD2, which are oxidoreductases of enzymes working in metabolic processes of plant, are found to be upregulated commonly in TCA circuits and carbon fixation process. Finally, an increase in ATP enhances the cell cycle, the number of cells increases, and consequently plant growth is enhanced. Results of the GO analysis indicate gene expressions of cell cycle (GO:0007049) and cell division (GO:0051301). Since upregulation of the gene expression concerning the ATP production, materials for cell production become enriched and the cell division enhances. Also, gene expressions of cell growth (GO:0016049), regulation of cell size (GO:0008361), unidimensional cell growth (GO:0009826), and cell morphogenesis (GO:0000902) are upregulated. This result suggests that size of cells increases as well as the cell division enhancement.

Functional annotation charts and signal pathways also indicate that genes related to Auxin hormone generation were upregulated, as well as those involved in photosynthesis and carbon fixation. Auxins are classes of plant hormone that influence plant growth significantly even in small amounts [41–44]. Increases in auxin in plants leads to enhanced enzyme production and an increase in the cell longitudinal length, and therefore the length of plant is expected to increase. Although the Auxin amount has not been quantified, the genes concerning the Auxin production are found to be upregulated by the oxygen plasma irradiation. Therefore, the enhancement of the Auxin production would be one of the factors for the plant growth enhancement. The gene ontology analysis and pathway analysis indicated that some genes concerning cell elongation proteins were activated when seeds were irradiated by active oxygen species. From the experimental results of plant cultivation after plasma irradiation, the lengths of the leaves and stems of *Arabidopsis* increased approximately 1.5 times over the control. Also, the area of leaves increased two times over the control. On the other hand, the diameter of the stems has not been changed. The above results indicate that the production of plant hormones is enhanced by an increase in the activity of transcription factors that regulate genes concerning hormone production such as L-tryptophan pyruvate aminotransferase (TAA1).

From the above results, the whole picture of estimated pathway from oxygen plasma irradiation to the plant growth enhancement from these expressed genes is figured out, as shown in Fig. 12.11. The growth enhancement of plants owes to (i) enhancement of energy production of plants via photosynthesis and carbon fixation, and (ii) production of Auxins in seeds. Above gene analysis derives one of series reactions from plasma irradiation to growth enhancement, which is activation of energy production system in cells. Figure 12.11 summarizes the sequence of reactions in seeds via reactions (i). The photosynthesis process is enhanced by active oxygen species in plasma owing to activation of enzymes such as the above-described RuBisCO. Activation of the photosynthesis leads to enhancement of the downstream reactions sequentially.

Activation of enzymes such as RubisCO by active oxygen irradiation
↓
Enhancement of photosynthesis
dissociation of water to H+ + OH- + e-
↓
Enhancement of carbon fixation and Calvin-Benson cycle
ribulose-bisphosphate carboxylase large chain
EC:4.1.1.39, starch production
↓
Enhancement of Glycolysis
metabolism to produce pyruvic acid from glucose
↓
Enhancement of TCA cycle (Citric Acid Cycle)
metabolism cycle to produce ATP from pyruvic acid
↓
Acceleration of cell cycle
↓
Growth enhancement

Fig. 12.11 Whole picture of growth enhancement mechanism of the oxygen plasma-irradiating seeds. Used with permission from Nobuya Hayashi, Reoto Ono, Riku Nakano, Masaharu Shiratani, Kosuke Tashiro, Satoru Kuhara, Kaori Yasuda, and Hiroko Hagiwara (2016). DNA microarray analysis of plant seeds irradiated by active oxygen species in oxygen plasma. Plasma Medicine 6, 459–471. DOI: https://doi.org/10.1615/PlasmaMed.2016018933

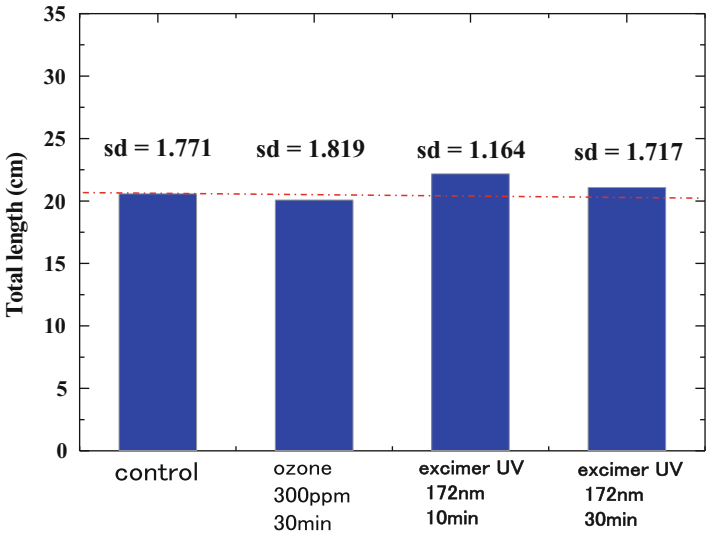

Fig. 12.12 Total length of Arabidopsis thaliana seeds irradiated with the deep UV light. Used with permission from Nobuya Hayashi, Reoto Ono and Shohei Uchida (2015). Growth Enhancement of Plant by Plasma and UV Light Irradiation to Seeds. J. Photopolym. Sci. Technol. 28, 445–448. DOI: https://doi.org/10.2494/photopolymer.28.445

12.4.1 UV Irradiation to Seed

Figure 12.12 shows the total length of *Arabidopsis thaliana* when the plant seeds are irradiated with the deep UV light with the wavelength of 172 nm with the ozone

treatment case. Growth enhancement is observed only in the case of irradiating seeds with ozone. Expressed genes of the seeds irradiated by 172 nm UV light are almost concerning stress responses and cell growth regulation, and there is no gene expression of plant hormone and growth enhancement. The fact that genes of photosynthesis and hormone response are not expressed does not promote growth. When seeds are irradiated by the oxygen plasma, growth enhancement occurs with good repeatability. Genes related to energy production are expressed, and active oxygen species are effective for the growth enhancement.

12.5 Gene Analysis of Second-Generation Seeds

Growth enhancement of plants those are grown from second-generation seeds is used to confirm the inheritance of the growth enhancement effect to nest generations. Second-generation seeds were cropped from plants that grew from the plasma-irradiated seeds (first generation), as illustrated in Fig.12.13. The growth of second-generation plants was almost the same as for seeds without plasma irradiation. Therefore, growth-enhanced effects have not passed on to the next generations. This result implies that there is no mutation on the genes those relate to the growth enhancement. In order to determine influences those are acquired by the second-generation seeds by plasma-irradiating seeds, gene functional annotation analysis of *Arabidopsis* second-generation seeds was performed. Figure 12.14 shows the functional annotation chart of the second-generation seeds. The gene ontology analysis shows that the gene expression of the second-generation seeds was different from that of seeds with the first-generation seeds irradiated by oxygen plasma. There were only 50 genes with genetic variations, which is common when comparing the first generation of seeds irradiated by oxygen plasma with the second generation. In the second-generation seeds, the response to oxidative stress and the secondary metabolism of plants was found to be significant among the expressed genes, which included induction of toxin catabolic processes and phenylpropanoid metabolism.

Fig. 12.13 Growth of the second-generation plant by the plasma-irradiating seeds. Used with permission from Riku Nakano, Nobuya Hayashi, Reona Aijima, Yoshio Yamashita, Akira Kobayashi (2018). Gene Expression Effect of Plant Seeds Irradiated by Low Pressure Oxygen Plasma. Journal of IAPS 26, 91–95

GO	Count	PValue
GO:0019748~secondary metabolic process	19	4.11E-09
GO:0019439~aromatic compound catabolic process	7	6.36E-08
GO:0042545~cell wall modification	11	9.44E-08
GO:0052482~cell wall thickening during defense	5	5.89E-06
GO:0052544~callose deposition in cell wall during defense response	5	5.89E-06
GO:0010200~response to chitin	9	6.49E-06
GO:0052542~callose deposition during defense response	5	9.79E-06
GO:0052543~callose deposition in cell wall	5	9.79E-06
GO:0052386~cell wall thickening	5	1.23E-05
GO:0052545~callose localization	5	1.53E-05
GO:0042343~indole glucosinolate metabolic process	4	1.57E-05
GO:0042434~indole derivative metabolic process	6	1.77E-05
GO:0042430~indole and derivative metabolic process	6	1.77E-05
GO:0033037~polysaccharide localization	5	1.88E-05
GO:0009743~response to carbohydrate stimulus	10	2.48E-05
GO:0006952~defense response	22	3.88E-05
GO:0010033~response to organic substance	22	2.54E-04
GO:0016143~S-glycoside metabolic process	5	3.72E-04
GO:0019760~glucosinolate metabolic process	5	3.72E-04
GO:0019757~glycosinolate metabolic process	5	3.72E-04
GO:0006790~sulfur metabolic process	8	3.76E-04
GO:0042436~indole derivative catabolic process	3	5.92E-04
GO:0009617~response to bacterium	9	6.35E-04
GO:0055114~oxidation reduction	21	7.57E-04
GO:0009723~response to ethylene stimulus	9	8.69E-04
GO:0007047~cell wall organization	9	0.001439
GO:0042219~cellular amino acid derivative catabolic	4	0.001448
GO:0019438~aromatic compound biosynthetic process	8	0.00145
GO:0009808~lignin metabolic process	5	0.001635
GO:0009725~response to hormone stimulus	17	0.001749
GO:0033554~cellular response to stress	11	0.001785
GO:0009698~phenylpropanoid metabolic process	7	0.001881
GO:0006955~immune response	9	0.002048
GO:0045229~external encapsulating structure	9	0.002048
GO:0042435~indole derivative biosynthetic process	4	0.002944
GO:0042742~defense response to bacterium	7	0.003147
GO:0010035~response to inorganic substance	12	0.003208
GO:0009719~response to endogenous stimulus	17	0.00353
GO:0016137~glycoside metabolic process	5	0.004163
GO:0009407~toxin catabolic process	4	0.005467
GO:0009404~toxin metabolic process	4	0.005467
GO:0045087~innate immune response	8	0.005683
GO:0006575~cellular amino acid derivative metabolic	8	0.006256

Fig. 12.14 Major functions of expressed genes of the second-generation seeds. Used with permission from Nobuya Hayashi, Reoto Ono, Riku Nakano, Masaharu Shiratani, Kosuke Tashiro, Satoru Kuhara, Kaori Yasuda, and Hiroko Hagiwara (2016). DNA microarray analysis of plant seeds irradiated by active oxygen species in oxygen plasma. Plasma Medicine 6, 459–471. DOI: https://doi.org/10.1615/PlasmaMed.2016018933

Phenylpropanoids, having a hydroxyl base belonging to polyphenol moieties, indicate reducibility. The expression of genes concerning phenylpropanoids is a reaction against active oxygen irradiation. On the other hand, genes of photosynthesis, carbon fixation, and the TCA cycle did not show differential expression, which was prominent in the first-generation seeds. These results imply that the second-generation plant obtains a resistivity against the active oxygen species. Also, gene

expression related to plant growth in the second-generation seeds was similar to that of the first generation.

The above results indicate that the tendency of gene expression in seeds of the second generation is significantly different from that of the first generation that is irradiated by the plasma. The enhancement of cell growth and cellular metabolism such as photosynthesis and carbon fixation, which are upregulated in the first-generation seeds by oxygen plasma irradiation, was not passed on to the next generation. Since the chemical energy of active oxygen species produced in this experiment is approximately 4 eV, active oxygen species hardly modified DNA sequences and mutations were not expected. These results indicate that DNA concerning energy production was not modified by active oxygen irradiation. Therefore, the growth enhancement has not been observed in plants grown from second-generation seeds. The active oxygen species would enhance some transcription processes in the first generation due to oxidation of enzymes involved in energy production, and then genes concerning energy production are activated. This result implies that the genes concerning the cell growth would be regulated epigenetically. Therefore, the growth enhancement phenomenon observed in the first generation owing to enhancement of gene expressions is likely epigenetic. However, detailed biological functions of those are induced by the observed epigenetic gene expression have been investigated.

12.6 About Epigenetics

When the seeds are irradiated with the active oxygens in the oxygen plasma, counterreactions against the plasma irradiation are induced by the gene expression modification. Gene modification mechanism and inheritance mechanism of acquired functions of plant due to the plasma irradiation is attempted to be clarified. There are two routes to the gene expression modification by plasma-irradiating seeds as indicated in Fig. 12.15; (a) Epigenetics, that is the chemical modification of DNA,

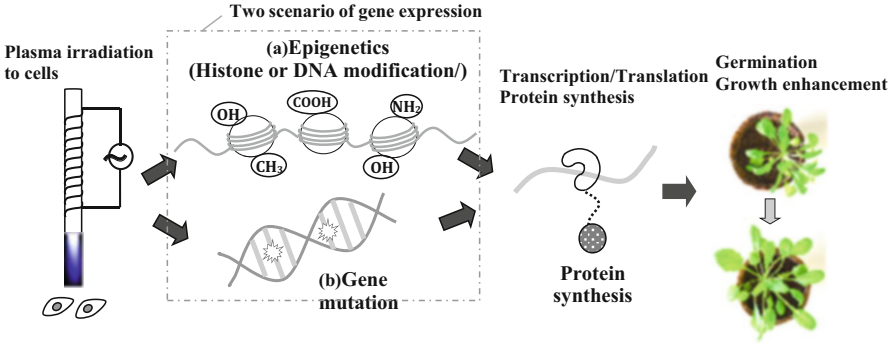

Fig. 12.15 Two scenario of gene expression in seeds irradiated by plasma

makes inheritance within a generation and sometimes over generations. (b) DNA mutation that is the random variation of base sequence makes inheritance beyond generations for positive natural selection.

Short-term irradiation of plant seeds with plasma stimulates the plant and improves growth promotion and antioxidant activity. As a result of cultivating seeds collected from plasma-irradiated plants and investigating the inheritance of the plasma irradiation effect to the second generation, the plasma irradiation effect such as growth promotion is obtained by the plasma parameters (a). As long as the generation is limited, it may return to its original properties after the second generation without being passed on to the next generation, or (b) it may be passed on to the next generation or later. In the case (b) in which the plasma irradiation effect is inherited, germination and growth promotion occur continuously even after cell division during the first generation of germination and growth from the irradiated seed, and the effect of oxygen plasma irradiation is divided. When the effect of the plasma is inherited by next-generation cells, high-energy ions contribute to the effect. On the other hand, in the case of only one generation (a), the genetic information of the seeds obtained from the first generation is initialized by the neutral reactive oxygen species, and the acquired traits such as histone modification and DNA methylation are not inherited, and no plasma irradiation effect such as growth promotion is observed in the second generation.

Epigenetics is the most suitable concept for explaining the inheritance characteristics of acquired characteristics by the oxygen plasma irradiation in such case (a). The epigenetics is change of gene expression that is not along with base sequence variation. Since the growth enhancement effect of plants observed in this study has not been inherited to next generation, the genetic mutation is not induced by the oxygen plasma irradiation. On the other hand, the growth enhancement effect has been preserved during cell divisions in the first generation. Therefore, there is possibility that the observed gene expression is epigenetics. In this case, it is presumed that the information on biological functions such as the growth-promoting effect obtained by plasma irradiation is mainly stored in the chromatin structure of DNA and passed on to the cells after division through cell division. It has been found that the results of comprehensive gene expression analysis of plasma-irradiated plant seeds show the expression of epigenetics-related genes. However, the mechanism of gene expression and biological function generation by plasma irradiation and the mechanism of inheritance of genetic information between cells beyond cell division remain unclear.

12.7 Induction of Epigenetics by Plasma Irradiation

After the plasma irradiation to seeds, sample seeds grow and the growth speed of the plant is measured as one of plant growth characteristics. Within the first generation of the plasma irradiation, the growth speed of plant irradiated with the plasma is constantly higher than that without the irradiation throughout the cultivation period,

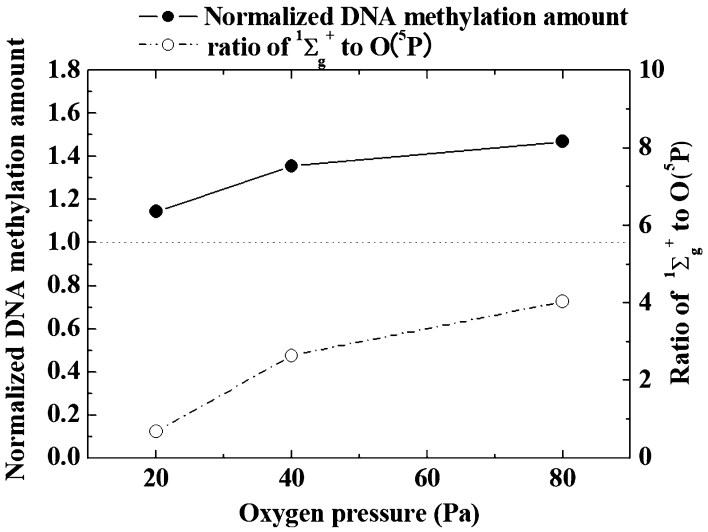

Fig. 12.16 Normalized DNA methylation amount and ratio of $^1\Sigma_g^+$ and O(^{5}P) varying oxygen pressure. Used with permission from Riku Nakano, Kosuke Tashiro, Reona Aijima, and Nobuya Hayashi (2016). Effect of oxygen plasma irradiation on gene expression in plant seeds induced by active oxygen species. Plasma Medicine **6**, 303–313. DOI: https://doi.org/10.1615/PlasmaMed.2016019093

as shown in Fig. 12.7. Growth enhancement effect maintains over the whole period of the plant growth. This indicates that the growth enhancement effect is inherited from cells to daughter cells through cell divisions. The growth enhancement effect has not been passed on to the plant that is grown from second-generation seeds. The growth tendency (length and growth speed) of the second-generation plant is same as that of control, and the growth enhancement effect does not appear on the plant growth characteristics. In this section, the inheritance mechanism of acquired functions within the first generation (e.g., growth enhancement) by the plasma irradiation is investigated.

In order to investigate the epigenetic modifications of the genes in seeds, the methylation of DNA in seeds was evaluated by quantifying the amount of 5-methylcytosine. Seed meth was irradiated with the oxygen plasma changing the oxygen pressure. The oxygen gas pressure dependences of the amount of the modified DNA and the emission intensity ratio of $^1\Sigma_g^+$ and O (^{5}P) are shown in Fig. 12.16 [23]. The above ratio can be regarded as the abundance ratio of $^1\Sigma_g^+$ and O (^{5}P). The methylation of the seed nuclear DNA enhances with increase of the oxygen pressure. Since the pressure dependence of the DNA methylation shows similar tendency with the light emission intensity from $^1\Sigma_g^+$, $^1\Sigma_g^+$ is considered to be an important factor for inducing DNA methylation. It is speculated that methylation has increased in order to stabilize various genes activated by $^1\Sigma_g^+$.

When epigenetic modification, that is the methylation of DNA, occurs in seed genes, recovery reactions for the DNA modification are expected to occur in seed.

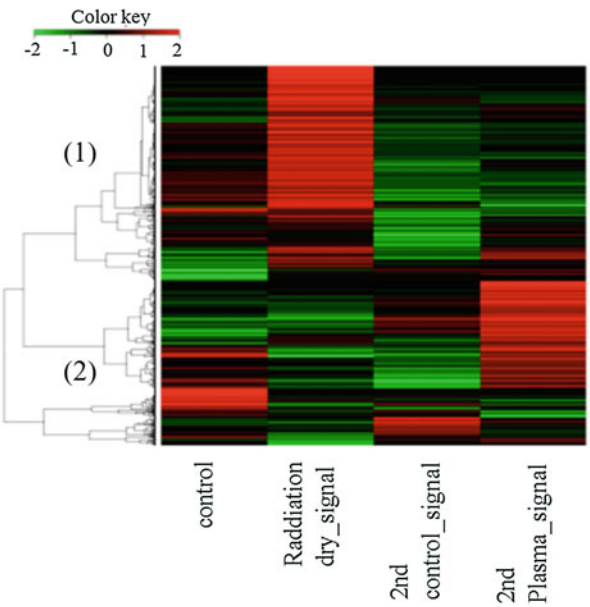

Fig. 12.17 Heat map of gene expression between oxygen plasma irradiation and control. Used with permission from Satoshi Watanabe, Reoto Ono, Nobuya Hayashi, Kousuke Tashiro, Satoru Kuhara, Asami Inoue, Kaori Yasuda, and Hiroko Hagiwara (2016). Growth Enhancement and Gene Expression of *Arabidopsis* irradiated by active oxygen species. Jpn. J. Appl. Phys. 55, 07LG10-1 – 07LG10-6

DNA methylation induced by active oxygen species would modify aspects of chromosome structure related to chromatin remodeling [45]. Remodeling of chromatin regions affect gene expression by control of transcription factors or other DNA-binding proteins to access condensed DNA. Therefore, modification of chromatin and DNA methylation may induce variation in gene expression related to plant growth enhancement.

Arabidopsis thaliana wild-type (Columbia-01) seeds obtained from RIKEN BRC were used for samples to investigate gene expression variations, which are irradiated with the oxygen plasma. For gene expression, RNA was extracted from seeds after irradiation with oxygen plasma using a reagent (DNeasy Plant Mini Kit, Qiagen) to prepare a microarray, and a gene whose expression was fluctuated was found by a microarray scanner (Agilent SurePrint G3 GE 8x60K v2). Variation of gene expressions owing to the change in the structure of chromosome and nucleosome regions in DNA can be specified. When these structures are modified, gene expressions are varied. Epigenetics-related analysis of plant DNA such as (i) gene expression related to epigenetics and (ii) quantification of DNA methylation and histone modification analysis are performed to determine the inheritance mechanism of the plasma irradiation effect. Gene ontology analysis using a bioinformatics database (DAVID [30]) and heat maps identified the functions of genes that changes due to plasma irradiation [46]. Active oxygens tend to bind to and activate the oxygen receptor (-SH) of the transcription factor corresponding to the genes encoding the enzyme that catalyzes the rate-determining reaction of histone modification and DNA methylation. Modification of chromatin structure, Histone loosing, and DNA methylation are proof of epigenetics by active oxygen species. Figure 12.17 shows a typical

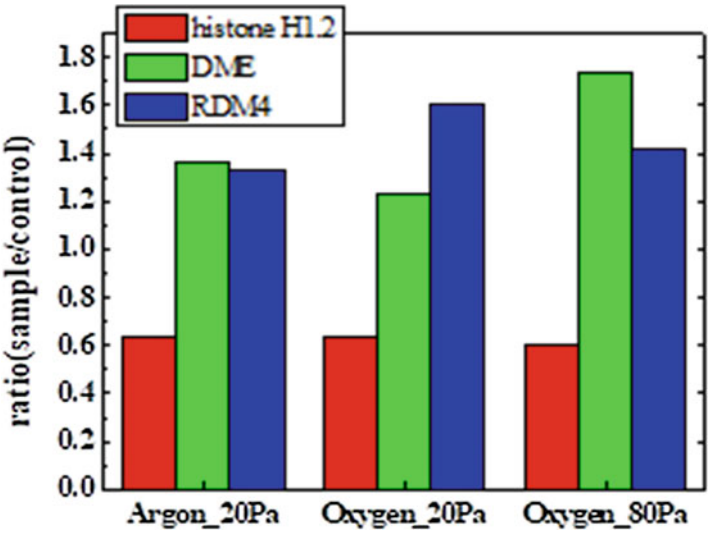

Fig. 12.18 Variation of gene expression related to DNA methylation and histone modification. Used with permission from Riku Nakano, Kosuke Tashiro, Reona Aijima, and Nobuya Hayashi (2016). Effect of oxygen plasma irradiation on gene expression in plant seeds induced by active oxygen species. Plasma Medicine **6**, 303–313. DOI: https://doi.org/10.1615/PlasmaMed.2016019093

example of a heat map obtained from the comprehensive gene expression variation analysis and gene ontology analysis using a microarray [24]. From this heat map above, epigenetics-related genes whose expression levels were changed by oxygen plasma irradiation were identified. Genes of DME and RDM4 those are expressed significantly are located in region (1) in Fig. 12.17, and their expression is upwardly controlled by the oxygen plasma irradiation. On the other hand, linker histone H1.2 is located in the downregulated gene group.

Gene expression amounts concerning chromosome region are estimated quantitatively from the variations of the gene expression level, that is, (1) histone H1.2: histone methylation, (2) DME: DNA demethylation, and (3) RDM4: DNA methylation. The linker histone H1.2 relates to the histone modification and is generally involved in chromatin organization by stabilizing chromatin structure [47, 48]. The role of histone H1.2 protein is as a transcription repressor that prevents the access of transcription factors or DNA-binding proteins.

Genes of DME and RDM4 encode the production of enzymes that catalyze the reaction regulating DNA demethylation and methylation, respectively [49]. Figure 12.18 shows the results of quantifying changes in the expression levels of above genes of histone H1.2, DME, and RDM4 with different plasma irradiation parameters, which are measured using the real-time PCR. Reliability of the data in the figure is checked by the T-test with a p-value of 0.05 or less. When the gas type and plasma conditions are changed, the variation tendency in the expression amount of each gene is different from each other. When the Ar plasma irradiates the seeds,

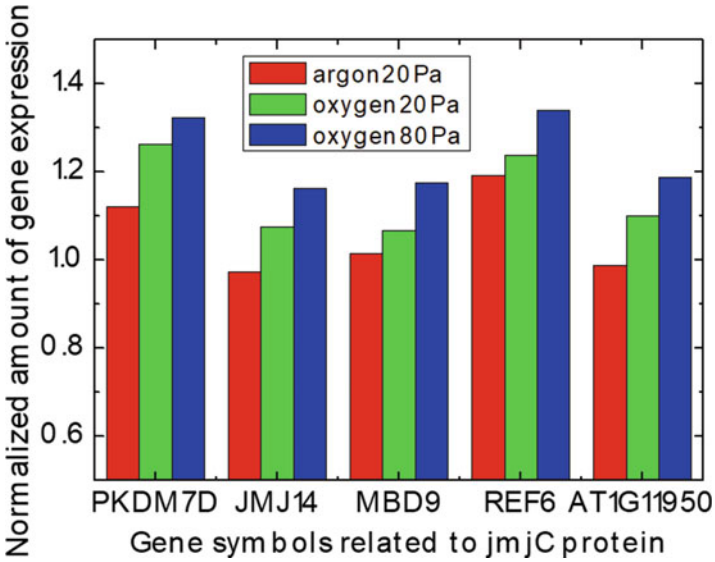

Fig. 12.19 Variation of gene expression amounts related to jmjC protein

the expressions of DME and RDM4 genes increase even though enhancement effects of germination and growth has not been observed. The expression amount of RDM4 gene increases and the DME gene expression decreases with the O_2 plasma case at 20 Pa comparing with that of the Ar plasma case at 20 Pa. This tendency indicates that the lower pressure oxygen plasma, where the atomic oxygen and the oxygen ion irradiate seeds, tends to restrict the epigenetic gene expression. On the other hand, the gene expression enhances owing to the loose histone structure and the demethylation in the higher pressure oxygen plasma, where the excited oxygen molecule is produced. The gene expression level of the linker histone H1.2 is almost constant and lower than the control value, even when the oxygen pressure and gas type are varied. In the case of O_2 plasma at 80 Pa, the expression amount of the DME gene is superior than that of the Ar plasma case, which indicates the enhancement of gene expressions.

Figure 12.19 shows the gene expression amounts related to JmjC proteins. JmjC proteins are catalysts of histone demethylase in gene-coding region and change the chromatin structure. In the Ar plasma case, gene expressions are not significant. All of the listed gene expressions with the oxygen plasma irradiation in the figure increase with the oxygen gas pressure. Increase of gene expression related to JmjC proteins would lead to enhancement of the gene expressions related to the plant growth speed. Above gene expression results imply that the epigenetic gene expressions are enhanced with the irradiation amount of active oxygen species.

Above results shown in Figs. 12.17, 12.18, and 12.19 figure out that gene expressions concerning epigenetics such as DME and JmjC are enhanced in seed DNA to increase epigenetic gene expressions, when active oxygen species have

Table 12.1 Expressed amounts of genes with typical functions treated with different types of plasmas

	O_2 20 Pa	O_2 80 Pa	O_2 80 Pa 2nd gen	Ar 20 Pa
Redox	0	10.6	12.5	7.9
Epigenetics	2.9	2.8	0.4	0
DNA	0.6	0	0	1.2
Hormone	0.6	5.4	6.4	3.5

induced epigenetic DNA modifications those suppress gene expressions. When the seeds germinate and grow, coding of genes concerning energy production and seed growth enhance, and then the plant growth enhancement is observed. Relative amounts of expressed genes concerning the epigenetics and other major effects in plant seeds, which are induced by several types of treatments, are investigated as shown in Table 12.1. Relative gene expression amounts are obtained from the gene expression analysis of plant seeds. When the oxygen plasma with the pressure of 80 Pa irradiates seeds, the redox reactions would be induced by the active oxygen species. And also the plant hormone production is expected. While the pressure reduces to 20 Pa, the oxygen gas changes to oxygen ions owing to the high-energy electron with the lower collision frequency. The oxygen ion would not induce the biological reactions such as redox reactions and plant hormone production. In the case of the second-generation seeds, induction of the redox reaction and plant hormone production are almost the same as the seeds directly irradiated with the oxygen plasma at 80 Pa; however, the epigenetics would not occur in the biological reactions in the second-generation seeds. Therefore, growth enhancement effect appears only on the first-generation plant, which is induced by active oxygen species in the oxygen plasma. This fact supports the observed epigenetic inheritance mechanism of the seeds irradiated with the oxygen plasma. Also, in the genic level, some information concerning redox and hormone generation can inherit to the next generation.

12.8 Summary

The excited oxygen molecules in the oxygen plasma induce gene expressions of photosynthesis and carbon fixation processes concerning the cell growth or cellular metabolism and plant hormone generation. Disappearance of the growth enhancement effect in the second generation indicates that the genetic mutation in the seed DNA has not been induced by the oxygen plasma irradiation, and therefore the epigenetic in the first generation would be one of mechanisms of the plant growth enhancement. When plant seeds are irradiated by oxygen plasma,

1. Growth enhancement occurs and genes related to energy production are expressed.
2. Growth enhancement effects have not passed onto next generations when the oxygen plasma irradiates seeds. Genes involved in epigenetics are expressed.

These results indicate that the growth enhancement effect due to plasma irradiation is induced by epigenetics. It is expected that the histone modification and DNA methylation reaction will be promoted. However, there is no evidence for the relationship between gene expression of the growth enhancement and the epigenetics. The relationship between the growth enhancement effect and epigenetics has to be clarified.

References

1. Kitazaki S, Koga K, Shiratani M, Hayashi N. Redox characteristics of thiol compounds using radicals produced by water vapor radio frequency discharge. Proc AVS 57th Int Symp. 2010;670
2. Dubinov AE, Lazarenko EM, Selemir VD. Effect of glow discharge air plasma on grain crops seed. IEEE Trans Plasma Sci. 2000;28(1):180. https://doi.org/10.1109/27.842898.
3. Hayashi N, Nakahigashi A, Goto M, Kitazaki S, Koga K, Shiratani M. Redox characteristics of thiol compounds using radicals produced by water vapor radio frequency discharge. Jpn J Appl Phys. 2011;50(8S1):08JF04. https://doi.org/10.1143/JJAP.50.08JF04.
4. Kitazaki S, Koga K, Shiratani M, Hayashi N. Growth control of dry yeast using scalable atmospheric-pressure dielectric barrier discharge plasma irradiation. Jpn J Appl Phys. 2013;52(11):11PJ02. https://doi.org/10.1143/JJAP.51.11PJ02.
5. Volin JC, Denes FS, Young RA, Park SMT. Modification of seed germination performance through cold plasma chemistry technology. Crop Sci. 2000;40:1706–18. https://doi.org/10.2135/cropsci2000.4061706x.
6. Jiafeng J, He X, Ling L, Jiangang L, Hanliang S, Xu Q, Renhong Y, Dong Y. Effect of cold plasma treatment on seed germination and growth of wheat. Plasma Sci Technol. 2014;16(1):54–8. https://doi.org/10.1088/1009-0630/16/1/12.
7. Jiayun T, He R, Xiaoli Z, Ruoting Z, Weiwen C, Size Y. Effects of atmospheric pressure air plasma pretreatment on the seed germination and early growth of Andrographis paniculata. Plasma Sci Technol. 2014;16:260–6. https://doi.org/10.1088/1009-0630/16/3/16.
8. Almansouri M, Kinet JM, Lutts S. Effect of salt and osmotic stresses on germination in durum wheat (Triticum durum Desf.). Plant Soli. 2001;231:243–54. https://doi.org/10.1023/A:1010378409663.
9. Song SQ, Lei YB, Tian XR. Proline metabolism and cross-tolerance to salinity and heat stress in germinating wheat seeds. Russian J Plant Physiol. 2005;52:793–800. https://doi.org/10.1007/s11183-005-0117-3.
10. Einaga H, Yoshihara E, Matsuo Y, Yodoi J. Oxidative stress and redox regulation-protein oxidative modification and activation. J Anal Biosci. 2009;32(4):265–72.
11. Rudolph TK, Freeman BA. Transduction of redox signaling by electrophile-protein reactions. Sci Signal. 2009;2:ref7. https://doi.org/10.1126/scisignal.290re7.
12. Winterbourn CC, Hampton MB. Thiol chemistry and specificity in redox signaling. Free Radic Biol Med. 2008;45:549. https://doi.org/10.1016/j.freeradbiomed.2008.05.004.
13. Nordberga J, Arner ESJ. Reactive oxygen species, antioxidants and the mammalian thiredoxin system. Free Radic Biol Med. 2001;31:1287. https://doi.org/10.1016/s0891-5849(01)00724-9.
14. Gelhaye E, Rouhier N, Navrot N, Jacquot JP. The plant thioredoxin system. Cell Mol Life Sci. 2005;62(1):24–35. https://doi.org/10.1007/s00018-004-4296-4.
15. Santosa CVD, Reya P. Plant thioredoxins are key actors in the oxidative stress response. Trends Plant Sci. 2006;11:329. https://doi.org/10.1016/j.tplants.2006.05.005.

16. Kitazaki S, Koga K, Shiratani M, Hayashi N. Growth enhancement of radish sprouts induced by low pressure O2 radio frequency discharge plasma irradiation. Jpn J Appl Phys. 2012;51:01AE01. https://doi.org/10.1143/JJAP.51.01AE01.
17. Akiyoshi Y, Hayashi N, Kitazaki S, Koga K, Shiratani M. MRS Proc. 1469, mrss12-1; 2012.
18. Subaedah S, Uematsu H, Hayashi N. Activation of EL-4 T-cells by irradiation with atmospheric oxygen plasma. Jpn J Appl Phys. 2020;59(SJ):SJJF03. https://doi.org/10.35848/1347-4065/ab83db.
19. Hayashi N, Inoue Y, Kyumoto Y, Kukita T. Characteristics of differentiation of osteoclast cells irradiated with active species in atmospheric oxygen plasma. Jpn J Appl Phys. 2020;59(SJ): SJJF02. https://doi.org/10.35848/1347-4065/ab7ba9.
20. Hayashi N, Yao YC, Matsunaga Y. Regulation of macrophage-like cell activity driven by atmospheric oxygen plasma. Jpn J Appl Phys. 2020;59(SH):SHHF03. https://doi.org/10.35848/1347-4065/ab72cf.
21. Hayashi N, Miyamaru Y, Aijima R, Yamashita Y. Activation of p53-mediated apoptosis pathway in HSC3 cancer cell irradiated by atmospheric DBD oxygen plasma. IEEE Trans Plasma Sci. 2018;47(2):1093–9. https://doi.org/10.1109/TPS.2018.2867431.
22. Hayashi N, Ono R, Uchida S. Growth enhancement of plant by plasma and UV light irradiation to seeds. J Photopolym Sci Technol. 2015;28:445–8. https://doi.org/10.2494/photopolymer.28.445.
23. Nakano R, Hayashi N, Aijima R, Yamashita Y, Kobayashi A. Gene expression effect of plant seeds irradiated by low pressure oxygen plasma. J IAPS. 2018;26:91–5.
24. Watanabe S, Ono R, Hayashi N, Tashiro K, Kuhara S, Inoue A, Yasuda K, Hagiwara H. Growth enhancement and gene expression of arabidopsis irradiated by active oxygen species. Jpn J Appl Phys. 2016;55:07LG10-1–6. https://doi.org/10.7567/JJAP.55.07LG10.
25. Nakano R, Tashiro K, Aijima R, Hayashi N. Effect of oxygen plasma irradiation on gene expression in plant seeds induced by active oxygen species. Plasma Med. 2016;6:303–13. https://doi.org/10.1615/PlasmaMed.2016019093.
26. Hayashi N, Ono R, Shiratani M, Yonesu A. Antioxidative activity of plant and regulation of Brassicaceae induced by oxygen radical irradiation. Jpn J Appl Phys. 2015;54:06GD01-1–5. https://doi.org/10.7567/JJAP.54.06GD01.
27. Hayashi N, Ono R, Nakano R, Shiratani M, Tashiro K, Kuhara S, Yasuda K, Hagiwara H. DNA microarray analysis of plant seeds irradiated by active oxygen species in oxygen plasma. Plasma Med. 2016;6:459–71. https://doi.org/10.1615/PlasmaMed.2016018933.
28. Hayashi N, Akiyoshi Y, Kobayashi Y, Kanda Y, Ohshima Y, GotoM. Inactivation characteristics of Bacillus thuringiensis spore in liquid using atmospheric torch plasma using oxygen. Vacuum. 2013;88:173–6.
29. Ono R, Hayashi N. Variation of antioxidative activity and growth enhancement of Brassicaceae induced by low-pressure oxygen plasma. Jpn J Appl Phys. 2015;54:06GD03-1–5. https://doi.org/10.7567/JJAP.54.06GD03.
30. Huang DW, Sherman BT, Lempicki RA. Systematic and integrative analysis of large gene lists using DAVID bioinformatics resources. Nat Protoc. 2009;4(1):44–57. https://doi.org/10.1038/nprot.2008.211.
31. Holmgren A. Annu. Thioredoxin Rev Biochem. 1985;54:237–71.
32. Rudolph TK, Freeman BA. Transduction of redox signaling by electrophile-protein reactions. Sci Signal. 2009;2(90):re7-1–13.
33. Santos CVD, Reya P. Plant thioredoxins are key actors in the oxidative stress response. Trends Plant Sci. 2006;11(7):329–34.
34. Ashburner M, Ball CA, Blake JA, Butler H, Davis AP, Dolinski K, Dwight SS, Eppig JT, Harris MA, Hill DP, Tarver LI, Kasarskis A, Lewis S, Matese JC, Richardson JE, Ringwald M, Rubin GM, Sherlock G. Gene ontology: tool for the unification of biology. Nat Genet. 2000;25:25–9.
35. Gene Ontology Consortium. The gene ontology (GO) database and informatics resource. Nucl Acids Res. 2004;32(1):D258–61.

36. Huang DW, Sherman BT, Lempicki RA. Bioinformatics enrichment tools: paths toward the comprehensive functional analysis of large gene lists. Nucleic Acids Res. 2009;37(1):1–13.
37. Krebs HA, Johnson WA. The role of citric acid in intermediate metabolism in animal tissues. J Enzymol. 1937;4:148–56.
38. Krebs HA, Johnson WA. Metabolism of ketonic acids in animal tissues. Biochem J. 1937;31 (4):645–60.
39. Andrews TJ, Whitney SM. Manipulating ribulose bisphosphate carboxylase /oxygenase in the chloroplasts of higher plants. Arch Biochem Biophys. 2003;414(2):159–69.
40. Bassham J, Benson A, Calvin M. The path of carbon in photosynthesis VIII. The role of malic acid. J Biol Chem. 1950;185:781–8.
41. Hardtke CS. Transcriptional auxin-brassinosteroid crosstalk: who's talking? BioEssays. 2007;29(11):1115–23.
42. Abel S, Theologis A. Early genes and auxin action. Plant Physiol 1996 May;111(1):9–17.
43. Wang S, Hagen G, Guilfoyle TJ. ARF-aux/IAA interactions through domain III/IV are not strictly required for auxin-responsive gene expression. Plant Signal Behav. 2013;8(6):e24526-1-5.
44. Vanneste S, Friml J. Plant signaling: deconstructing auxin sensing. Nat Chem Biol. 2012;8:415–6.
45. Gilbert N, Thomson I, Boyle S, Allan J, Ramsahoye B, Bickmore WA. DNA methylation affects nuclear organization, histone modifications, and linker histone binding but not chromatin compaction. J Cell Biol. 2007;177(3):401–11.
46. Huang DW, Sherman BT, Lempicki RA. Systematic and integrative analysis of large gene lists using DAVID bioinformatics resources. Na Protoc. Dec 2008;4(1):44–57.
47. Thomas JO. Histone H1: location and role. Curr Opin Cell Biol. 1999;11(3):312–7. https://doi.org/10.1016/S0955-0674(99)80042-8.
48. Croston GE, Kerrigan LA, Lira LM, Marshak DR, Kadonaga JT. Sequence-specific antirepression of histone H1-mediated inhibition of basal RNA polymerase II transcription. Science. 1994;251(4994):643–9. https://doi.org/10.1126/science.1899487.
49. Matzke MA, Matzke AJM, Kooter J. RNA: guiding gene silencing. Science. 2001;293 (5332):1080–3. https://doi.org/10.1126/science.1063051.

Chapter 13
Improvement of Plant Growth and Control of Cultivation Environment Using Electrical Stimuli

Douyan Wang

Abstract Electrical stimuli such as electric fields, currents, and discharge plasma can both enhance and inhibit plant growth. This chapter covers both direct stimuli (electrical energy applied directly to plant seeds, seedlings, or the plant itself) and indirect stimuli (electrical energy applied to the plant cultivation environment). Proper control of applied electrical energy can cause genomic modifications, stimulate enzyme activity, enhance photosynthesis, control pH and bacteria levels in the cultivation environment, and increase nutrient uptake, resulting in increased harvest yield. This chapter summarizes various studies performed using different stimulation methods.

Keywords Electric fields · Magnetic fields · Air ion · Current · DC · AC · Pulse · Discharge plasma · Plasma-treated/activated water · RONS · Hydroponics · Photosynthesis · Plant root · Plant growth control · Growth enhancement · Growth inhibition

13.1 Introduction

Many studies have been performed to examine the effects of applying discharge plasma and electrical fields to improve seed germination and early plant growth [1–6]. However, there is very little research on postgermination effects. The reason for this is difficult to discern, but may be due to the complexities of the mechanisms involved. During plant development, the basic functions of a plant are absorption of nutrients into the plant body via the roots and photosynthesis via the leaves. In some situations, stimuli alter these basic functions to trigger growth enhancement or inhibition. This chapter discusses the enhancement of plant growth via both direct

D. Wang (✉)
Institute of Industrial Nanomaterials, Kumamoto University, Kumamoto, Japan
e-mail: douyan@cs.kumamoto-u.ac.jp

S. Horikoshi et al. (eds.), *Agritech: Innovative Agriculture Using Microwaves and Plasmas*, https://doi.org/10.1007/978-981-16-3891-6_13

stimulation of plants and indirect stimulation via improvement of growth environment.

13.2 Direct Stimulation of Plants Using Electricity and Air Ions

13.2.1 Past Research Up to 2000

Electrical stimuli can sometimes occur naturally, with some examples being charge balance in the ionosphere and electric and magnetic fields from high-voltage transmission lines. Beginning in the middle of the eighteenth century, electric fields and air ions have been applied to plants both in the field and under laboratory conditions [7]. In the 1770s, Beccaria (1775) suggested that electrical currents might influence vegetation [8], and this was tested repeatedly by many researchers. These studies established that applied electric fields can accelerate or inhibit growth in higher plants.

Research continued into the twentieth century. In the early 1960s, Krueger et al. (1963) reported that air ions from an electrostatic precipitator can induce growth in higher plants. Ions of either charge generated in pure air produced statistically significant increases in stem length, integral elongation, and wet and dry weights. A possible mechanism is that air ions enhance the incorporation of Fe into cytochrome c [9]. Cytochrome c is a small hemeprotein that plays a major role in cell apoptosis. It is also an essential component of the electron transport chain, where it carries one electron. When seedlings are grown in a substrate containing Fe and are exposed to ionized air, they do not develop chlorosis but exhibit typical ion-induced increases in growth rate and an increased production of cytochrome c [9].

Kotaka et al. (1968) found that exposure to air ions results in increased swelling and shrinking of isolated chloroplasts in response to light, which may involve the expenditure of energy from ATP hydrolysis. When chloroplasts were incubated in light, dark, and reilluminated environments, the augmented ATP metabolism increased the swelling rate during the period of preincubation and similarly accelerated the shrinking rate during dark incubation. Eventually, there is not enough ATP left to support increased swelling of ion-treated chloroplasts upon reillumination. Air ions affect the ATP energy-yielding reaction that proceeds within the chloroplast and is associated with swelling and shrinking [10]. Smith et al. (1961) indicated that exposure of *Microcoleus vaginatus* (Vaucher) to positively ionized air, especially carbon dioxide, results in increased migration and growth. The hypothesis is that positively ionized air causes increased growth in plants by releasing endogenous bound indoleacetic acid [11].

Murr (1966) conducted a series of experiments on numerous plant species in both electrostatic and electrokinetic fields and summarized the effects of current flow on plant growth response. Murr found that less than 10^{-16} amps per plant resulted in

unstimulated plant growth, 10^{-15}–10^{-9} amps resulted in a general positive response for plant extension and dry weight, 10^{-8}–10^{-6} amps generally resulted in negative effects such as leaf damage and dry weight reduction, and 10^{-5} and higher resulted in plant or leaf destruction [12]. Sidaway et al. (1968) studied electrostatic fields in the range of 5–10 kV/m for alterations in respiration in various types of plant material and found there was a definite electrostatic influence on respiration [13].

In 1971, Black et al. (1971) found small currents could stimulate or inhibit active ion pumps or alter the internal distribution of growth-regulating compounds in tomato plants. Significant increases in growth (5–30%) and K, Ca, and P uptake were obtained when direct currents of 3–15 μA were applied per plant with the plant negative to the ground. Reductions in growth occurred when the plants were treated with 15 μA positive to the ground or with any currents of magnitude greater than 30 μA per plant. It seems likely that the applied electrical current may not only affect ion accumulation but also affect internal auxin or gibberellin activity. The conclusion is that stimulation of ion uptake and growth via electric current is mainly due to neither increased passive cation uptake nor electroosmosis, nor is it closely related to the reduction potential of each cation. The researchers posit that changes in growth and ion uptake are likely due to active ion pump stimulation at the root surface or due to redistribution under the electric field of plant growth-regulating substances inside the living tissue [14].

In 1981, Pohl et al. (1981) reported that a mild current of air anions (4 pA/cm^2) stimulates bean crop growth, encourages earlier blossoming, and increases growth in the annual *Exacum affine* and in seedling geraniums. An increase in average plant height of about 15% among the ion-cultured plants was obtained after 45 days, and the growing period required until the plants reached a saleable stage of maturity could be shortened by about 2 weeks under greenhouse conditions [15]. Goldsworthy et al. (1985) reported that a weak electric current (1 or 2 μA) to tobacco callus cells between the callus and the culture medium caused a many-fold stimulation of shoot formation and a 60–70% stimulation of growth. The callus growth stimulation occurred only when the callus was made negative to the medium and IAA (indole-3-acetic acid) was added. The electrical treatment may have aligned the physiological polarities of the callus cells so as to promote the polar transport of IAA into the tissue when the callus was negative to the medium [16]. IAA is the most common auxin plant hormone, and it regulates various aspects of plant growth and development. Cogalniceanu et al. (1998) subjected *Nicotiana tabacum* morphogenetic callus cells to an electric current (50 Hz, 0.1–50 μA) for 30 days. Shoot number increased by up to 300% for samples stimulated with 50 μA, though no significant changes were noted in total mass, DNA content, or protein content in the stimulated samples compared to control. A series of changes in the activity of membrane components, as a consequence of the modulation of membrane potential by the external electric field, were observed. Therefore, the researchers suggest that in the presence of an external electric current, the callus cells become more sensitive to chemical signals (hormones and/or ions) in the culture medium [17].

A primary site of action may be the plasma membrane, involving a signal transduction process, or changes in electric potential or enzyme activity. Other

models suggest perturbations in the metabolic machinery of the cells including the genomic molecules (DNA, RNA) or proteins. The electromagnetic fields could also interact with ion flows and change the flow of transcellular currents. These might affect growth regulators, leading to the generation of various physiological gradients in the callus or changes in intercellular polarities, causing suitable conditions for cell proliferation, shoot differentiation, and growth. Electromagnetic fields also remove calcium ions from cell membranes, making them more permeable and stimulating enzyme activity via the calcium cascade. Bovelli et al. (2000) observed that treatment of a continuously pulsing electromagnetic field increased seed germination and callus growth of *Nicotiana tabacum* L. A treatment of 5 h per day also caused a significant stimulation of shoot regeneration and development compared with the controls. The researchers concluded that electromagnetic fields may be a useful and inexpensive way to increase the in vitro regeneration of plants after genetic modifications [18].

13.2.2 Electric Field Stimulations

Regarding research trends prior to 2000, electrical stimulation of the plant body was mostly done with weak DC or air ions that were attempts at simulating possible conditions in the natural environment observed in geoelectric field studies. In the years since, more studies have been carried out using higher power electric fields or shorter application durations. Pulsed electric fields and atmospheric plasma are now used as sources of stimuli for plants with the advent of electric power sources for these uses.

Pulsed electric fields (PEFs) have been widely investigated in improving juice extraction and reducing drying time in vegetables [19], which is assumed to be due to electroporation of the cell membrane [20]. In related research, Hohenberger et al. (2011) investigated the role of the actin cytoskeleton in the response of plant cells to both nanosecond range PEF and long pulses typically utilized for classical electroporation [21]. They found that actin bundling stabilizes the membrane against electropermeabilization. Changes in apparent membrane thickness dependent on actin bundling were observed, and TIRF microscopy showed that actin and microtubules are in close physical contact ($<$50 nm) with the membrane. The researchers proposed a model where the plasma membrane is in a dynamic equilibrium with a submembranous tubulovesicular reservoir of membrane material that is maintained and mobilized by actin filaments and that contributes to the resealing of pores induced by nsPEFs through relaxation of mechanical tensions in the membrane. In conclusion, the submembrane cytoskeleton stabilizes the plasma membrane against permeabilization caused by electric pulses.

However, there are not many reports on growth control of vegetables. Ye et al. (2004) reported that PEF (50 Hz, 10 V/m) application can elicit defense responses and stimulate secondary metabolite accumulation in plant cells in suspension cultures of *Taxus chinensis*. A significant increase in intracellular accumulation of

taxuyunnanine C (Tc), a bioactive secondary metabolite, was observed when cells in the early exponential growth phase were exposed to a 30-min PEF. PEF treatment can be optimized to enhance the desired secondary metabolite production without harmful effects on plant cell growth, viability, and biosynthetic capacity. In addition, PEF may change the dielectric properties of the cell membrane and induce the release of intracellular metabolites [22].

Zvitov et al. (2003) observed stomatal opening as a result of low DC electrical field treatment of leaves of *Cucumis sativus* L. and *Commelina communis* L. One possible explanation for stomatal opening is the differential influence of the electrical treatment on guard cell turgor pressure versus the turgor pressure of the surrounding epidermal cells. The applied voltage damages the epidermal cells, causing a decrease in turgor pressure and a loss of pressure against the swelling of the guard cells, leading to the opening of many stomata. In the study, small voltages (~5 V) were sufficient to cause opening of the stomata in the treated leaves, but higher voltages (~20 V) led, in addition to stomatal opening, to guard cell death. Neutral red staining results showed that small voltages damaged the epidermal and subsidiary cells but kept the guard cells viable, whereas high voltages led to the death of the guard cells as well [23].

13.2.3 PEF Stimulation Effect on Photosynthesis

The effects of PEF on photosynthesis in *Auxenochlorella protothecoides* microalgae were explored by Straessner et al. (2013) in 2013 [24]. High-voltage pulse duration was set at 100 ns and 1000 ns for PEF treatment of microalgae suspensions. The treatment energy was varied between 2 and 78 kJ/kg. The electric field amplitude was constant throughout the experiments ($E_{Cuv} = 40$ kV/cm). The imposed stress on photosystem II (PS II) by PEFs was detected in changes in chlorophyll fluorescence. The results showed that *Auxenochlorella protothecoides* was much more sensitive to long rather to short PEFs, in particular at low specific treatment energies. The obtained results showed a significant influence of PEFs on PS II. Compared to the experiments with $t_{Imp} = 100$ ns, microalgae exposed to $t_{Imp} = 1000$ ns pulses started with significantly lower F_v/F_m values and exhibited a notably faster decline over time (F_v/F_m indicates the maximum photochemical quantum yield of PS II chemistry after dark adaption). The paper revealed that intracellular organelles exposed to shorter ($t_{Imp} = 100$ ns) PEFs showed less damage compared to those in longer PEF experiments ($t_{Imp} = 1000$ ns) under identical treatment energy conditions.

Sonoda et al. (2017) also investigated the effect of PEFs on photosynthesis in *Lactuca sativa* L. leaf lettuce in 2017 [25]. Low-intensity PEFs (0.2 kV/cm) and high-intensity PEFs (1.0 kV/cm) at pulse durations of 400 ns and 500 pulse were used. Photosynthetic electron transport rate (ETR), photochemical quenching (qP; related to the redox state of electron acceptors in photosystem II), and non-photochemical quenching (NPQ; related to heat dissipation of light energy) were evaluated after PEF treatment. Experimental results showed that ETR and qP of

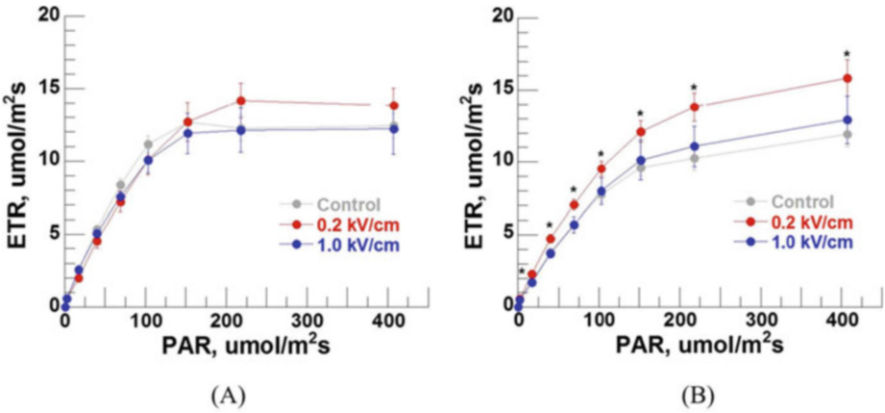

Fig. 13.1 Results of ETR in both conditions (light-acclimated and dark-acclimated) after PEF treatment [25]. (**a**) ETR of light-acclimated samples. (**b**) ETR of dark-acclimated samples. (Reproduced with permission from Sonoda et al. 2017)

dark-acclimated nursery leaf lettuce can be increased through application of 0.2 kV/cm PEF, while 1.0 kV/cm treatment had no significant effect (Fig. 13.1). Conversely, 1.0 kV/cm treatment resulted in a decrease in NPQ, while 0.2 kV/cm treatment had no significant effect. These results suggest that relatively low PEFs may improve the electron transfer flux through PSII in photosynthesis, yet relatively high PEFs may inhibit heat dissipation, which serves as a stress defense. The light-acclimated and dark-acclimated conditions used in this study can be thought of as the light-receiving state of plants in real photosynthesis.

13.2.4 Electrical Stimulation of Plant Rhizomes

A rhizome is the main stem of the plant that runs underground horizontally. Plant root cells produce electric fields through ion transporter activity. This ion movement creates a flow of current through the tissue, generating electrical potentials across the membranes of the root cells. During the growth response of the root to gravity, the electrical patterns change. The application of exogenous electrical fields to the root can be used to investigate the relationship between electrical patterns and root growth [26].

13.2.4.1 Culture in Aqueous Medium

Ishikawa et al. (1990) applied DC voltage to maize (*Zea mays* L.) roots and examined the kinetics of electrotropic curvature in solutions of low electrolyte concentration. When submerged in an oxygenated solution across which an electric

field was applied, the roots curved rapidly and strongly toward the positive electrode (anode). The strength of the electrotropic response increased, and the latent period decreased with increasing field strength. At field strength of 7.5 V/cm, the latent period was 6.6 min and curvature reached 60 degrees in about 1 h. For electric fields greater than 10 V/cm, the latent period was less than 1 min. There was no response to electric fields less than 2.8 V/cm. Both electrotropism and growth were inhibited when indoleacetic acid (10 μM) was included in the medium. The data indicate either that (a) electrotropic stimulation induces the movement of an effector that does not redistribute after removal of the electric field, or that (b) electrotropic stimulation somehow leads to activation of a transport mechanism that continues to maintain an effector gradient after removal of the electric field. The effectiveness of auxin transport inhibitors in blocking electrotropism suggests the possibility that electrotropic stimulation may affect the activity or distribution of an auxin carrier [27]. Stenz et al. (1993) continued this work. Intact and decapped primary roots of maize (*Zea mays* L.) were exposed to DC electric fields of 0.5–8.0 V/cm in low-salinity media to resolve conflicting results about the direction of electrotropism. In DC fields of 0.5 V/cm or 1.0 V/cm, intact roots always curved toward the cathode. In a field of 8.0 V/cm, intact roots curved toward the anode and growth stopped. Decapped roots also curved toward the anode in both weak and strong fields. The results indicate that growth toward the cathode is the true response of healthy roots [28].

Wolverton et al. (2008) found roots respond to an electric field with opposite curvature occurring in two distinct zones of the root. When a DC electric field with 25 V/cm was applied to the *Vigna mungo* L. roots for 30 min, two responses occurred in two different regions of the root: the central elongation zone and the distal elongation zone. Curvatures toward both the anode and the cathode initiated rapidly upon application of the field. The curvature toward the anode is longer-lived, often continuing for several hours following removal of the field. Curvature toward the cathode occurred in the apical segments of the root, comprising the region within 2 mm from the root tip. Both are true responses to the electric field, rather than one being a secondary response to an induced gravitropic stimulation. In the central elongation zone, curvature was driven by inhibition of elongation, whereas curvature in the distal elongation zone was primarily due to stimulation of elongation [29].

Bitonti et al. (2006) investigated the effects of electromagnetic fields (EMFs) on meristem activity and cell differentiation in *Zea mays* roots. Exposure of *Zea mays* seedlings to a continuous electromagnetic field for 30 h induced a 30% stimulation in the rate of root elongation compared with the controls. It also resulted in a significant increase in cell expansion in both the acropetal and basipetal directions. In addition, in EMF-exposed roots, a precocious structural disorder was observed in differentiating both metaxylem cells and root cap cells [30]. Wawrecki et al. (2007) then focused on the root apical meristem response after application of a DC electric field. Roots of *Zea mays* seedlings, grown in liquid medium, were exposed to DC electric fields of differing strengths from 0.5 to 1.5 V/cm with a frequency of 50 Hz for 3 h. DC fields of 1 and 1.5 V/cm resulted in noticeable changes in the cellular pattern of the root apical meristem. The electric field activated the quiescent center, with the

cells of the quiescent center penetrating the root cap junction, disturbing the organization of the closed meristem, and changing it temporarily into the open type. A field of slightly higher strength damages root cap initials, terminating their division [31].

Cakmak et al. (2012) studied the change in enzyme activities of apoplastic and symplastic antioxidant systems in shallot leaves by applying weak static electric and magnetic fields (EF and MF) [32]. Shallot (*Allium ascalonicum* L.) bulbs were chosen and sprouted under weak static MF and EF with the magnitudes 7 mT MF and 20 kV/m EF for 17 days. The results showed root and leaf length increased in response to MF, but these effects were not observed in response to EF application. Moreover, weak MF induced sprouting approximately 1 day earlier than other groups. Root and leaf dry biomass increased in response to EF and MF applications. Despite a lack of visible symptoms of injury, lipid peroxidation and H_2O_2 levels increased in EF applied leaves. In plants, the reactive oxygen species (ROS) production level increased under stress conditions and at some growth stages. At certain levels, increases in ROS production simply either increased metabolic activity or possible redox imbalance depending on changes in the levels of oxidative stress markers such as lipid peroxidation and protein carbonylation. Apoplastic and symplastic antioxidant systems were also evaluated. Certain symplastic antioxidant enzyme activities and nonenzymatic antioxidant levels increased in response to MF and EF applications. Antioxidant enzymes in the leaf apoplast, by contrast, were found to show different regulation responses to EF and MF. This suggests that apoplastic constituents may work as potentially important redox regulators that sense and signal environmental changes. Static continuous MF and EF at low intensities have a distinct impact on growth and antioxidant systems in plant leaves, and weak MF is involved in antioxidant-mediated reactions in the apoplast, resulting in overcoming a possible redox imbalance [32].

Tataranni et al. (2013) applied a DC 12.0 V/m electric field with a current intensity of 10 mA to tomato (*Solanum lycopersicum* L.) seedlings grown hydroponically in a floating system. The tomato plants grown near the positive electrode showed pronounced length, root hair development, and root branching compared to the plants grown at the central area of the container and near the negative electrode. Electric conductivity values of the growing solution did not change after the application of the electric field. There was a change in pH, however, with alkalinization occurring at the positive electrode and acidification at the negative one. Thus, the different growth patterns observed could be related to the different mineral gradients formed by migration of cations toward the negative electrode and anions toward the positive electrode in the water solution under the applied EF. Hypotheses were discussed in which the different growth patterns observed could be related to chemiosmotic-induced activity and/or the distribution of plasma membrane carriers. In conclusion, root growth was affected by positions relative to the EF [33].

Sonoda et al. (2014) applied PEFs (0.2–2.0 kV/cm, 400 ns of pulse width) to the roots of leaf lettuce grown hydroponically. The results showed PEF intensity from 0.2 to 1.0 kV/cm is positive for growth stimulation, with a maximum increase of 20% at 0.4 kV/cm. Conversely, those over 1.0 kV/cm resulted in growth inhibition

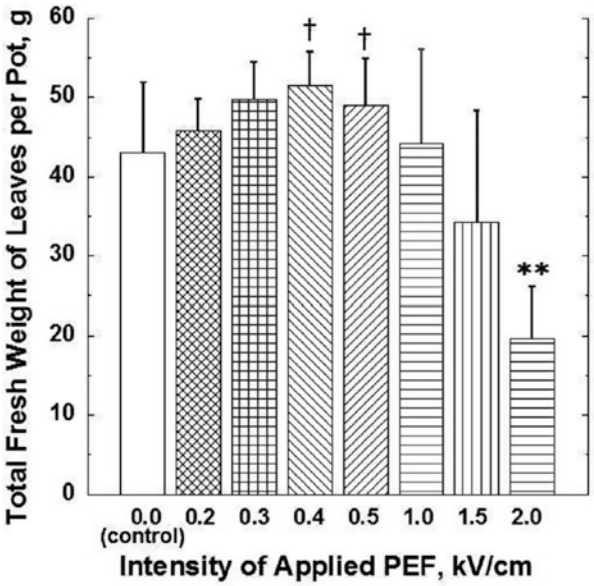

Fig. 13.2 Dependence of fresh weight of leaves on various applied PEFs [34]. The asterisks ** and the dagger † indicate significant growth differences for $P < 0.01$ and $P < 0.1$, respectively. (Reproduced with permission from Sonoda et al. 2014)

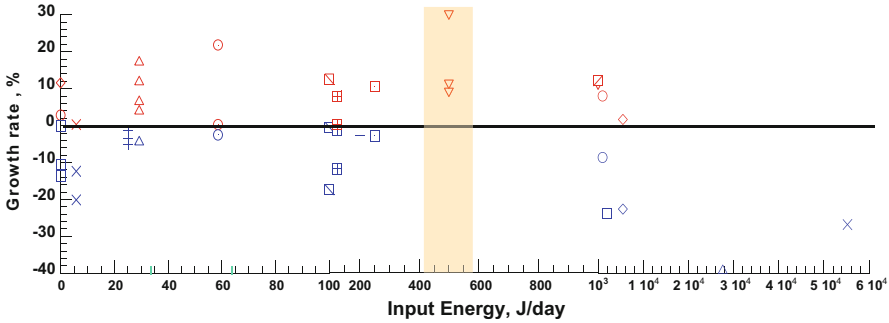

Fig. 13.3 Dependence of growth rate of lettuce leaves on input energy per day [35]. (Reproduced with permission from Wang et al. 2017)

for leaf lettuce (Fig. 13.2). The amount of total nitrogen and liquid components showed no significant difference between the control and PEF-applied sample, thus suggesting that PEF does not affect liquid fertilizer composition but directly influences the growth of leaf lettuce. The possible reason for lettuce growth might be electroporation on the root cells induced by PEF application, or increased activation of ion channels on root cells through the application of PEF [34]. Extended work was carried out in a laboratory-scale plant factory, and it was discovered that the optimum input energy is 500 J/day (Fig. 13.3). Lower input energy shows no significant effect on lettuce growth, while energies exceeding 10^4 J/day inhibit growth [35].

13.2.4.2 Culture in Soil Medium

The studies above on plant rhizome stimulation were all carried out in aqueous solutions. Scopa et al. (2009) applied a weak DC electric field to *Arundo donax* grown in soil and confirmed via morphological analysis a significant increase in growth rate in the shoots and roots of treated plants. A DC electric field of 12.0 V/m with a current intensity of 10 mA was applied to the root primordia of *Arundo donax*, which had been cultivated in an organic compost substrate. The epidermis of the treated sample was heavily covered with root hairs on both the proximal and distal ends of the root. The presence of root hairs alters the environment close to the root by means of carbon dioxide released during respiration, which promotes cation exchange with the soil and nutrient uptake. In addition, active growth of hyphae was observed on the root hair surface in the treated sample. Soil conductivity was 345 and 237 mS/m for treated and control samples, respectively, and pH was 6.58 for both samples. The change in soil conductivity values could likely be linked to the observed differential in root growth development [36].

Yi et al. (2012) investigated both the changes to bacterial community and crop growth in soil treated with PEFs. Electric pulses generated from DC 2, 4, 6, 8, and 10 V of electricity with periodic exchange of the anode and cathode were applied to a culture soil in which lettuce and hot peppers were grown. The distance between electrodes was 120 mm. 16S rDNA amplified from DNA extracted from the culture soil was examined, as the 16S rRNA gene is used in phylogenetic studies because it is highly conserved between different species of bacteria and archaea. The results showed that electric pulse charging did not result in a change to soil bacteria community, though the difference in cultivation time for plant growth did. Growth of lettuce increased in the 4, 6, 8, and 10 V culture soil groups. Growth of hot pepper plants was not activated by electric pulsing; however, growth duration increased and fruiting duration was proportional to growth duration [37].

Plant growth enhancement can sometimes increase phytoremediation in contaminated soil. Here, phytoremediation refers to the use of plants to reduce the concentrations or toxic effects of contaminants in the environment. Cadmium (Cd) is one of the most prominent heavy metal pollutants in contaminated soils and exerts toxic effects on the kidneys and the skeletal and respiratory systems of humans. *Solanum nigrum* L. is a potential Cd hyperaccumulator. Xu et al. (2020) investigated the effects of different electric fields and electrodes on *Solanum nigrum* L. Cd hyperaccumulation in soil [38]. A DC electric field (1 V/cm) for which polarity was switched every 3 h, a DC electric field (1 V/cm) with no polarity switching, and an AC electric field (1 V/cm) were applied to soil where *S. nigrum* were planted. Stainless steel electrodes and graphite electrodes were used to compare differences in electrode type. The results showed that DC and AC electric fields significantly increased *S. nigrum* Cd concentration compared to the control that did not have an electric field applied, and the effect in the group where polarity was switched was greater. On the other hand, the AC electric field significantly increased *S. nigrum*

root and shoot biomass (DC had no affect). The effects of the two different electrode types on *S. nigrum* accumulating Cd were basically same.

13.3 Indirect Stimulation through Improvement of Growth Environment: Plasma Stimulations

13.3.1 Role of Plasma

Nonthermal plasma (NTP) technology has been explored in ozone production, material processing, and environmental improvement studies for many decades. Plasma is a state of matter consisting of partially ionized gas that contains a range of charged and neutral particles. NTP is a nonequilibrium ionized gas where electron temperature is much higher than that of ions and neutrals. Thus, the plasma stays barely above room temperature, in some cases a NTP can even be touched with hands while operating. Therefore, there is less thermodynamic damage to the reaction targets. There are many chemical reactions in plasma which give rise to a wide range of reactive oxygen and nitrogen species (RONS; O_3, $^1O_2$, ·OH, NO_2, N_2O, NO, CO_2, HNO_3, HNO_2, etc.) [39]. Those RONS directly stimulate plants or react with surrounding media to trigger further complex reactions. In the past, generation of NTP required complicated and expensive equipment because it had to be generated in low-pressure conditions where ionization of gas particles is easier. The development of NTP at atmospheric pressure in recent years has increased the options for where it can be utilized and allowed for innovative applications.

Recently, NTP has found utility in biological fields such as plasma medicine [40, 41] and plasma agriculture [39, 42, 43]. NTP can dissociate air molecules and directly fix them into water. This allows the production of both oxidized and reduced forms of nitrogen. It can also help in N transformation. Generally, N is unstable in the soil system, being lost to the atmosphere by ammonia volatilization and N_2O/N_2 denitrification and lost to groundwater via NO_3^- leaching. Due to these losses, the efficiency of N fertilizers is low, and roughly 50% of all applied fertilizers are not used by plants. This suggests that although further N input will increase crop yield slightly, adverse effects on the environment warrant additional strategies to reduce N waste. Here, NTP creates possibilities for NO_3^- and NH_3 production through oxidation and reduction of N_2 after its dissociation [42].

Plasma-treated water (PTW) has been used to pretreat seeds and irrigate seeds, plants, and crops in the field [42]. Acidity plays an important role in the stability of NO_3^-, NO_2^-, and H_2O_2 during PTW storage. When relatively neutral, the end product concentrations show initial decay, but remain stable over time. Although tap water does act as a buffer, prolonged treatment may result in a decreased pH, similar to deionized water. In cases of greater acidity ($pH < 3.5$), NO_2^- is not stable. When NO_2^- concentration is on the same order of magnitude of NO_3^-, NO_3^- concentration increases rapidly according to the following [42]:

$$3NO_2^- + 3H^+ \rightarrow 2NO(aq) + NO_3^- + H_3O \text{ (or } H_2O + H^+)$$

When both NO_2^- and H_2O_2 are present, peroxynitrite reactions must also be considered [44]:

$$NO_2^- + H_2O_2 + H^+ \rightarrow ONOOH + H_2O$$

$$ONOOH \rightarrow OH + NO_2$$

The reactivity of peroxynitrite increases as pH drops, contributing to NO_2^- decay.

Another important issue is that NTP treatment can cause physical destruction of prokaryotes or cell death similar to apoptosis. The reason is that RONS from NTP can interact with peptidoglycan in the cell wall and cause its disruption, which can, in turn, result in the physical destruction of the cell and release of its content, or death due to the oxidation stress caused by RONS that have entered the cell through cracks in the cell wall. Inactivation of prokaryotic organisms is a field that is well-studied, as in research on elimination of the phytopathogenic fungi from seeds, which is sufficient for inactivation of fungal cells while being harmless to plant leaves, etc. [39].

The effects of plasma are not merely limited to surface decontamination, but also include influences on processes inside the cells of given eukaryotic organisms as well. Seed germination enhancement is a common research topic that has been investigated by many researchers on various plant species. Detailed information relating to NTP treatment on plant seeds can be found in Chap. 12 of this book. Other NTP treatment research has been done on changes in the activity of antioxidant enzymes, plant secondary metabolites, gene expression, and plant heat shock factors.

NTP also has the potential to induce adaptive response to abiotic stress. In nature, the ideal conditions for organisms, including plants, occur relatively rarely, with unfavorable conditions being far more common. ROS are produced naturally in plant cells, mainly in chloroplasts from photosynthetic tissues and in mitochondria from nonphotosynthetic tissues due to electron transport systems. In general, ROS can be detrimental to plant growth, as they can damage cellular membranes, proteins, and nucleic acids, and can distort redox homeostasis. Therefore, plants induce antioxidant mechanisms to regulate ROS. Recent studies show that ROS serve as signaling molecules in plants. ROS control plant growth and development by either regulating stress responses or modulating growth parameters. In auxin pathways, which mediate plant growth and development, ROS production has shown effects on auxin homeostasis and flux, which can ultimately affect plant growth [42].

13.3.2 Effects of Plasma-Treated Solutions on Plant Growth—Hydroponics

Plants can be grown hydroponically by suspending the majority of the root system in a hydroponic solution that contains dissolved fertilizer as the main source of nutrients for plant growth. For soilless production, mainly N fertilizers containing N as NO_3^- and NH_4^+ are used. As stated above, RONS can be generated by plasma, which plays an important role in N uptake in the culture medium of plants. Plants take up N in the form of NO_3^- and NH_4^+ at the root plasma membrane, with NO_3^- being a major source for N for most plants [42].

In hydroponic cultivation, pH is an important parameter. The pH value can vary between 5.0 and 6.0, changing often during the growing period due to variations in the uptake of anions and cations by the plant. Uptake of cations such as NH_4^+ is associated with the release of H_3O^+ and thus a decrease in pH. Uptake of anions such as NO_3^- is associated with the release of OH^- by the plant and pH increases [42]. Electrical conductivity (EC) is another important parameter in hydroponics, and it is used to estimate the general nutrient level and to gauge any salinity issues. A reasonable EC range is 1.6–3.0 mS/cm [42].

Many studies have used plasma to investigate changes in plant growth. Takaki et al. (2013) used a magnetic compression pulsed power generator to generate pulsed discharge plasma in air bubbles injected into the drainage water from plant pots. *Brassica rapa var. perviridis* was cultivated using treated drainage water in pots filled with artificial soil. The experimental results showed that the growth rate increased significantly when drainage water was irradiated with plasma. The growth rate increased with plasma irradiation time. Chlorophyll content analysis revealed that nitrogen concentration in the leaves increased as a result of plasma irradiation, and bacteria in the drainage water were also inactivated by plasma irradiation. After a 28-day plant cultivation period, the concentrations of nitrate nitrogen (NO_2^-) and nitrous nitrogen (NO_3^-) in the drainage water were measured for various plasma irradiation times. NO_2^- and NO_3^- were not detected in the nonirradiated drainage water but were found in irradiated water, with concentration increasing with irradiation time. The drainage water was acidified with HNO_2 and HNO_3 as HNO_2 (aq) and HNO_3 (aq) because the Henry constants of HNO_2 and HNO_3 are larger than that of the other species produced with air plasma. The nitrogen concentration of *Brassica rapa var. perviridis* leaves at 28 days of cultivation and the length of cultivated leaves over time were also investigated. Both results showed increases. Therefore, the increase in plant growth rate as a result of plasma irradiation of the water supplied to the soil for plant cultivation is mainly caused by the air plasma-produced NO_3^- (aq) [45]. The same plasma generation method was used for inactivation of *R. solanacearum* bacteria in the liquid fertilizer for a tomato hydroponic culture system by Okumura et al. (2016) [46]. Results showed that the number of colony-forming units (CFUs) of *R. solanacearum* in the liquid fertilizer decreased from 10^7 to 10^2 CFU/mL when treated with discharge plasma. Tomato seedlings

treated with discharge plasma were relatively healthy, while the infected positive controls all wilted and died [46].

Park et al. (2013) used three types of plasmas (thermal spark discharge, gliding arc discharge, and transferred arc discharge) in order to study the effect of plasma-treated water on germination, growth rates, and overall nutritional value of various plants. Nonthermal gliding arc discharge plasma resulted in lower (acidic) pH and the production of a significant number of oxidizing species (e.g., H_2O_2). Gliding arc discharge also caused significant acidification of water, but was accompanied by production of reactive nitrogen species (NO, NO_2^-, and NO_3^-). Spark discharge treatment resulted in neutral or higher (basic) pH depending on initial water composition and in the production of RNS as well. Plant growth evaluation when using plasma-treated water was done on watermelon (*Citrullus lanatus*), zinnia (*Zinnia peruviana*), alfalfa (*Medicago sativa*), pole beans (*Phaseolus coccineus*), and shade champ grass [47].

Ndiffo Yemeli et al. (2020) investigated the influence of plasma-activated water (PAW; the meaning is identical to the abovementioned PTW) generated by two sources of cold atmospheric air plasma (transient spark with water electrospray and glow discharge with water cathode) on maize (*Zea mays* L. var. Saccharata) and barley (*Hordeum vulgare* L.) seedlings. After 4 weeks of plant growth, the effects of PAW were analyzed by measuring plant growth, physiological parameters (plant length and fresh weight), photosynthetic pigment concentration and photosynthesis rate, total soluble proteins, antioxidant enzyme activity, and DNA damage. For plant growth, the average length of barley plants watered with PAW increased by several percentage points compared to the control. The fresh weight of barley plants increased by several 10s of percentage points when cultivated with PAW. Analytical results for RONS in PAW showed increases in concentrations of H_2O_2, NO_2^-, and NO_3^- compared to a tap water control. These results indicate a slight improvement in the plant length for barley, but a considerable improvement to fresh weight of the above-ground plant when treated with PAW and nitric acid. Similar results were observed for maize as well. Photosynthetic pigment concentrations (chlorophyll a, chlorophyll b, and carotenoids) for plants watered with PAW showed some slight increases. Light response curves of photosynthetic rate (P_N) were evaluated, and the results showed significant decreases for barley plants but only a slight decrease for maize plants when both are watered with PAW. The total soluble proteins in the above-ground plants increased by about 20% for both barley and maize plants, which could be due to nitrates in the watering solution. PAW induced changes in the antioxidant enzymes of both plants: a decrease in superoxide dismutase (SOD) activity in both plants; an increase in guaiacol peroxidase (G-POX) activity in barley and a slight decrease in maize; and an increase in catalase (CAT) activity in both plants. Long-lasting RONS (H_2O_2, NO_2^-, NO_3^-), especially H_2O_2, in PAW is probably responsible for these effects. Finally, plant growth enhancement of barley using these air plasma-based PAWs was not accompanied by any DNA damage [48].

Hashizume et al. (2020) verified the effectiveness of cold plasma treatment during rice cultivation in a paddy field used for rice farming using two approaches: direct plasma irradiation and Ringer's lactate solution (PAL). After harvest, plant growth,

grain yield, and grain quality were assessed. With the direct method, rice plants were directly irradiated with cold plasma to stimulate the apical meristem in either the early stage (first month), late stage (second month), or entire growth period (both months). During the early vegetative period, after irradiation for 30 s, the weight of panicles and culms increased along with the number of panicles. In addition, plant height, main stem growth, and panicle weight increased after irradiation for 5 min. Both irradiations led to improvements in brown rice yield (increases of 12% and 15%, respectively). The results suggested that the growth promotion by plasma irradiation in the early period of plant growth induced an increase in the rate of photosynthesis, which increased the grain yield. In rice, the metabolism of the plant hormone cytokinin is particularly important for panicle differentiation and grain yield, and the gene expression of cytokinin-related factors is also altered under stress conditions. From the results, it is believed that the reactive species may promote cell division in the shoot apical meristem by upregulating the cytokinin pathway. In addition, cell division is stimulated due to the relaxation of the cell wall by ROS, e.g., hydrogen peroxide. In contrast, late period plasma irradiation tended to suppress plant growth, particularly irradiation for 5 min. Thirty seconds of plasma irradiation, however, showed no significant effect. In the late period, the rice plants shifted from late vegetative growth to reproductive growth. Grain quality also decreased considerably due to the significant increase in the ratio of immature grains to total grains. Excessive plasma irradiation can damage the formation of late-forming leaves and young panicles, which, in turn, decreases the grain yield and quality. Finally, direct irradiation for 5 min over the entire growth period markedly inhibited plant growth and yields. Excessive plasma doses over a period twice as long (2 months) may have affected the inhibition. In the PAL treatment, the traits related to the growth of the main stem were improved, whereas the grain yield of the whole plant was decreased due to the suppression of tillering shoot growth. For PAL treatment, the treatment period in this study may not be optimal [49].

13.3.3 Effect of Plasma Treatment on Plant Growth—Soil

Soil pH generally ranges from 4.0 to 8.0, but the optimal range for plants is 5.5–6.5. In soils with pH < 5.5, the acidity is too great for plants, which can exacerbate aluminum and manganese toxicity. N fertilizers acidify soil by releasing H^+ during oxidation of NH_4^+ to NO_3^-. NTP-based fertilization will generate acidity in the ratio of 1 mole of H^+ to each mole of NO_3^- produced, equal to other N fertilizers. Therefore, plasma-generated N requires the same soil acidity management as traditional fertilizers [42].

Soil microbes are a category of soil organisms that are particularly important for soil health and resilience. Microbial communities in bulk soil and associated with plant roots are responsible for N cycling, which significantly impacts plant growth dynamics and soil fertility. N cycling is where microbially catalyzed transformations regulate biologically available N through exchange with the atmosphere via N_2

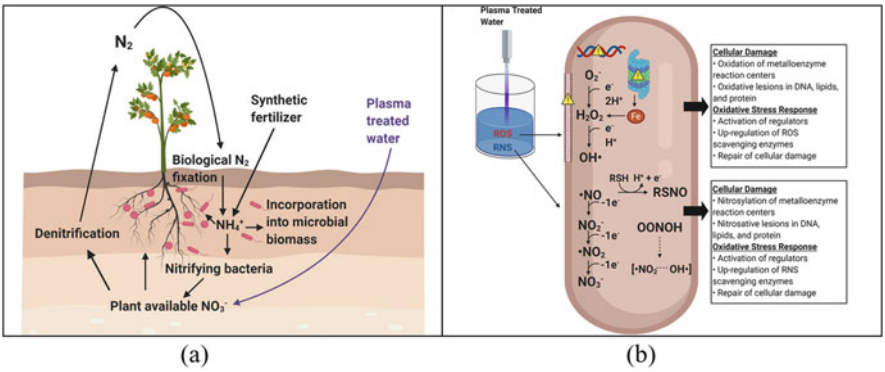

Fig. 13.4 Impact of plasma-treated water (PTW) for plants on soil and microbiome [42]. (**a**) The microbial nitrogen cycle that occurs in agricultural soils. PTW is shown as an additional source of nitrate in this process. (**b**) Molecular responses of bacteria from exposure to ROS and RNS resulting from plasma treatment. (Reproduced with permission from Ranieri et al. 2020)

fixation and denitrification processes and loss by nitrate leaching through the action of nitrifying bacteria (Fig. 13.4a) [42].

In addition to increasing N species concentration through direct and indirect application of plasma to soils, ROS and RNS are generated that can impact microbial viability and function. ROS and RNS damage lipids in cell membranes, membrane-bound and cytoplasmic proteins (especially those containing metal cofactors), and DNA, all of which can impair microbial cell function and act in concert to reduce cell viability. Furthermore, RNS can inhibit cellular respiration, thereby interfering with cellular energy generation, and can disrupt DNA replication through the inactivation of zinc metalloproteins. Both ROS and RNS can also mobilize iron from iron-sulfur-containing dehydratases (e.g., enzymes involved in amino acid synthesis), which further enhances ROS toxicity through Fenton chemistry, resulting in the formation of the extremely reactive hydroxyl radical ($OH^{\bullet}$). The many targets of ROS and RNS acting individually and/or synergistically ultimately result in a broad spectrum of antimicrobial activity, including bacteria, fungi, parasites, and viruses (Fig. 13.4b) [42].

Ozone (O_3) is the strongest commercially available disinfectant and also is very effective at destroying bacteria, viruses, and odors. It has a very short half-life in water and soil, and either decomposes to simple diatomic oxygen or oxidizes other compounds. Ebihara et al. (2012) have studied gaseous ozone sterilization for soil and biomedical prevention for infectious diseases using ozone. Eighty percent of bacteria in the soil were eliminated by 20 min of ozone treatment with 20 gO_3/m^3. The reaction of DNA with ozone is essential to understand sterilization in agricultural soil. Experiment results showed that DNA structures were destroyed through treatment with ozone (100 gO_3, 0.5 L/min, 20 min). Ozone is believed to break up nucleobase hydrogen bonds (thymine–adenine pairs, cytosine–guanine pairs) in DNA [50]. Ebihara et al. (2013) also experimented with ozone mist sterilization for pest control. Ozone mist was produced using a proprietary nozzle system. The

ozone mist generated near the nozzles was sprayed on insects (aphids, tobacco worms, green rice leafhoppers, and caterpillars). This ozone mist treatment (30s) resulted in death of 98% of aphids, with survival rate rapidly decreasing with distance. Gaseous ozone and its derivative radicals are taken into the aphid body through spiracles, travel via the trachea through the body, and reach the cells. As a result, the aphid can be killed by molecular ozone and its derivative radicals acting on the proteins and organelles (e.g., nucleus) of its cells [51].

Mitsugi (2019) found that the generation of radish scab caused by *Streptomyces sp*. bacteria was suppressed by ozone diffusion treatment of the soil [52]. Mitsugi et al. (2016) also investigated the efficacy of ozone for the extermination of soil worms. The influence of ozone on nematodes (*C. elegans*) was studied, and the results showed that ozone worked well in killing nematodes. In addition, the ozone-treated soil also improved germination and fruition of the radishes. The final radish length was, on average, 1.3 times longer than that of the control radishes. Both the leaf and stem lengths grew by a factor of 1.4 when using ozone treatment. Ozone treatment also increased the average total weight by 20% [53]. Mitsugi et al. (2014) further investigated the possibility of using ozone treatment for both disinfection and nitrification of soil. The quantity of hydrogen ions in soil solution increased almost proportionally to the ozone dose. The amount of NO_3-N increased approximately by two orders of magnitude, which could result in a pH(H_2O) decrease of 2 after an 11.6% ozone dose into soil. The amounts of NO_3-N and NH_4-N stayed almost constant after ozone treatment, while the pH(H_2O) recovered to the original value with time due to the buffering function of soil. Most large DNA in the soil had been decomposed and living bacteria were sterilized after 11.6% ozone dose into soil, which caused the immediate generation of nitrogen nutrients. The growth speed of radishes that were seeded in soil treated using the ozone diffusion method was faster than that of radishes seeded in the control soil due to the increased nitrogen nutrients [54].

13.4 Conclusion and Future Work

This chapter summarized research on improving plant growth dating back to the eighteenth century up until today. In early studies, most interest was focused on electrical stimulation that simulated natural phenomena, such as electric fields, air ions, and weak currents. Experiments that resulted in plant growth enhancement or inhibition were observed under laboratory conditions, yet these results lacked a clear understanding of the plant biology involved. Around the twenty-first century, with the development of pulsed voltage generation sources, stimulation trends moved from conventional DC and AC sources toward pulsed electric fields. This opened more possibilities for plant growth enhancement via direct stimulation to plants, resulting in changes to secondary metabolic accumulation, photosynthesis activity, rhizome development, etc. Even with these advances, there is still insufficient understanding of the mechanisms involved in direct electrical stimulation. Indirect

stimulation, in which the plant growth environment is treated with plasma, has been a popular area of study in recent years. In both hydroponic and soil culture environments, plasma plays an important role in improving nutrient uptake (such as NO_3^-), pH regulation, and bacterial management of the cultivation environment.

Electric and magnetic fields, currents, and plasma are promising tools in the enhancement of plant growth. Well-organized elucidation of experimental results from the viewpoints of both electrophysics and plant physiology is expected in the future. Cooperation between researchers in the fields of both electricity and biology is essential to making this a reality.

References

1. Šerý M, Zahoranová A, Kerdík A, Šerá B. Seed germination of Black pine (*Pinus nigra* Arnold) after diffuse coplanar surface barrier discharge plasma treatment. IEEE Trans Plasma Sci. 2020;48(4):939–45.
2. Sera B, Spatenka P, Serý M, Vrchotova N, Hrusková I. Influence of plasma treatment on wheat and oat germination and early growth. IEEE Trans Plasma Sci. 2010;38(10):2963–8.
3. Okumura T, Muramoto Y, Shimizu N. Dependency of *Arabidopsis thaliana* growth on DC electric field intensity. IEEE Trans Dielectr Electr Insul. 2014;21(2):913–7.
4. Songnuan W, Siriwattanakul U, Kirawanich P. Physiological and genetic analyses of Arabidopsis Thaliana growth responses to electroporation. IEEE Trans Nanobioscience. 2015;14(7):773–9.
5. Eing CJ, Bonnet S, Pacher M, Puchta H, Frey W. Effects of nanosecond pulsed electric field exposure on arabidopsis thaliana. IEEE Trans Dielectr Electr Insul. 2009;16(5):1322–8.
6. Sivachandiran L, Khacef A. Enhanced seed germination and plant growth by atmospheric pressure cold air plasma: combined effect of seed and water treatment. RSC Adv. 2017;7 (4):1822–32.
7. Shigemitsu T. Effects of electric fields. Air ion and corona discharge in plants (in Japanese). J Plasma Fusion Res. 1999;75(6):659–65.
8. Beccaria G. Della elettricita terrestre atmosferica a Cielo Sereno. Torino. 1775.
9. Krueger AP, Kotaka S, Andriese PC. A study of the mechanism of air-ion-induced growth stimulation in Hordeum vulgaris. Int J Biometeorol. 1963;7:17–25.
10. Kotaka S, Krueger AP, Andriese PC. The effect of air ions on light-induced swelling and dark-induced shrinking of isolated chloroplasts. Int J Biometeorol. 1968;12(2):85–92.
11. Smith RF, Fuller WH. Identification & mode of action of a component of positively-ionized air causing enhanced growth in plants. Plant Physiol. 1961;36(6):747–51.
12. Murr LE. The biophysics of plant growth in a reversed electrostatic field: a comparison with conventional electrostatic and electrokinetic field growth responses. Int J Biometeorol. 1966;10: 135–46.
13. Sidaway GH, Asprey GF. Influence of electrostatic fields on plant respiration. Int J Biometeorol. 1968;12:321–9.
14. Black JD, Forsyth FR, Fensom DS, Ross RB. Electrical stimulation and its effects on growth and ion accumulation in tomato plants. Can J Bot. 1971;49(10):1809–15.
15. Pohl HA, Todd GW. Electroculture for crop enhancement by air anions. Int J Biometeorol. 1981;25:309–21.
16. Goldsworthy A, Rathore KS. The electrical control of growth in plant tissue cultures: the polar transport of auxin. J Exp Bot. 1985;36(168):1134–41.
17. Cogalniceanu G, Radu M, Fologea D, Moisoi N, Brezeanu A. Stimulation of tobacco shoot regeneration by alternating weak electric field. Bioelectrochem Bioenerg. 1998;44(2):257–60.

18. Bovelli R, Bennici A. Stimulation of germination, callus growth and shoot regeneration of *Nicotiana tabacum* L. by pulsing electromagnetic fields (PEMF). Adv Hortic Sci. 2000;14 (1):3–6.
19. Barba FJ, Parniakov O, Pereira SA, et al. Current applications and new opportunities for the use of pulsed electric fields in food science and industry. Food Res Int. 2015;77(4):773–98.
20. Kandušer M, Miklavčič D. Electroporation in biological cell and tissue: an overview. In: Electrotechnologies for extraction from food plants and biomaterials, Food Engineering Series. New York, NY: Springer; 2009.
21. Hohenberger P, Eing C, Straessner R, Durst S, Frey W, Nick P. Plant actin controls membrane permeability. Biochim Biophys Acta Biomembr. 2011;1808(9):2304–12.
22. Ye H, Huang LL, Chen SD, Zhong JJ. Pulsed electric field stimulates plant secondary metabolism in suspension cultures of *Taxus chinensis*. Biotechnol Bioeng. 2004;88(6):788–95.
23. Zvitov R, Schwartz A, Zamski E, Nussinovitch A. Direct current electrical field effects on intact plant organs. Biotechnol Prog. 2003;19(3):965–71.
24. Straessner R, Eing C, Goettel M, Gusbeth C, Frey W. Monitoring of pulsed electric field-induced abiotic stress on microalgae by chlorophyll fluorescence diagnostic. IEEE Trans Plasma Sci. 2013;41(10):2951–8.
25. Sonoda T, Higashi Y, Yamada Y, Wang D, Namihira T, Akiyama H. Influence of pulsed electric field to leaf lettuce evaluated on chlorophyll fluorescence measurement using pulsed-amplitude-modulated fluorometer. Int J Plasma Environ Sci Technol. 2017;11(1):81–6.
26. Wolverton C, Mullen JL, Ishikawa H, Evans ML. Two distinct regions of response drive differential growth in *Vigna* root electrotropism. Plant Cell Environ. 2000;23(11):1275–80.
27. Ishikawa H, Evans ML. Electrotropism of maize roots. Plant Physiol. 1990;94(3):913–8.
28. Stenz HG, Weisenseel MH. Electrotropism of maize (*Zea mays* L.) roots (facts and artifacts). Plant Physiol. 1993;101(3):1107–11.
29. Wolverton C, Mullen JL, Ishikawa H, Evans ML. Two distinct regions of response drive differential growth in Vigna root electrotropism. Plant Cell Environ. 2008;23(11):1275–80.
30. Bitonti MB, Mazzuca S, Ting T, Innocenti AM. Magnetic field affects meristem activity and cell differentiation in *Zea mays* roots. Plant Biosyst. 2006;140(1):87–93.
31. Wawrecki W, Zagórska-Marek B. Influence of a weak DC electric field on root meristem architecture. Ann Bot. 2007;100(4):791–6.
32. Cakmak T, Cakmak ZE, Dumlupinar R, Tekinay T. Analysis of apoplastic and symplastic antioxidant system in shallot leaves: impacts of weak static electric and magnetic field. J Plant Physiol. 2012;169(11):1066–73.
33. Tataranni G, Sofo A, Casucci C, Scopa A. Different root growth patterns of tomato seedlings grown hydroponically under an electric field. Plant Root. 2013;7:28–32.
34. Sonoda T, Takamura N, Wang D, Namihira T, Akiyama H. Growth control of leaf lettuce using pulsed electric field. IEEE Trans Plasma Sci. 2014;42(10):3202–8.
35. Wang D, Namihira T. Growth control and gene expression of plants using pulsed high electric fields (in Japanese). J Inst Electrosts Jpn. 2017;41(6):249–53.
36. Scopa A, Colacino C, Lumaga MRBL, Pariti L, Martelli G. Effects of a weak DC electric field on root growth in *Arundo donax* (Poaceae), Acta Agriculturae Scandinavica. Sect B Soil Plant Sci. 2009;59(5):481–4.
37. Yi JY, Choi JY, Jeon BY, Jung IL, Park DH. Effects of a low-voltage electric pulse charged to culture soil on plant growth and variations of the bacterial community. Agric Sci. 2012;3 (3):339–46.
38. Xu L, Dai H, Skuza L, Wei S. The effects of different electric fields and electrodes on *Solanum nigrum* L. Cd hyperaccumulation in soil. Chemosphere. 2020;246:125666.
39. Holubová Ľ, Kyzek S, Ďurovcová I, Fabová J, Horváthová E, Ševčovičová A, Gálová E. Non-thermal plasma - a new green priming agent for plants? Int J Mol Sci. 2020;21 (24):9466.
40. Kong MG, Kroesen G, Morfill G, Nosenko T, Shimizu T, Dijk Zimmermann JL. Plasma medicine: an introductory review. New J Phys. 2009;11:115012.

41. Von Woedtke T, Schmidt A, Bekeschus S, Wende K, Weltmann KD. Plasma medicine: a field of applied redox biology. In Vivo. 2019;33(4):1011–26.
42. Ranieri P, Sponsel N, Kizer J, et al. Plasma agriculture: review from the perspective of the plant and its ecosystem. Plasma Process Polym. 2020;18(1):e2000162.
43. Puač N, Gherardi M, Shiratani M. Plasma agriculture: a rapidly emerging field. Plasma Processes Polym. 2018;15:e1700174.
44. Verlackt CCW, Van Boxem W, Bogaerts A. Transport and accumulation of plasma generated species in aqueous solution. Phys Chem Chem Phys. 2018;20:6845–59.
45. Takaki K, Takahata J, Watanabe S, et al. Improvements in Plant Growth Rate Using Underwater Discharge. J Phys Conf Ser. 2013;418:012140.
46. Okumura T, Saito Y, Takano K, et al. Inactivation of Bacteria using discharge plasma under liquid fertilizer in a hydroponic culture system. Plasma Med. 2016;6(3–4):247.
47. Park DP, Davis K, Gilani S, et al. Reactive nitrogen species produced in water by non-equilibrium plasma increase plant growth rate and nutritional yield. Curr Appl Phys. 2013;13:S19–29.
48. Ndiffo Yemeli GB, Švubová R, Kostolani D, Kyzek S, Machala Z. The effect of water activated by nonthermal air plasma on the growth of farm plants: case of maize and barley. Plasma Process Polym. 2020;18(1):e2000205.
49. Hashizume H, Kitano H, Mizuno H, et al. Improvement of yield and grain quality by periodic cold plasma treatment with rice plants in a paddy field. Plasma Process Polym. 2020;18(1): e2000181.
50. Ebihara K, Stryczewska HD, Mitsugi F, Ikegami T, Sakai T, Pawlat J, Teii S. Recent development of ozone treatment for agricultural soil sterilization and biomedical prevention. Przeglad Elektrotechn. 2012;88(6):92–4.
51. Ebihara K, Mitsugi F, Ikegami T, et al. Ozone-mist spray sterilization for pest control in agricultural management. Eur Phys J Appl Phys. 2013;61(2):24318.
52. Mitsugi F. Practical ozone disinfection of soil via surface barrier discharge to control scab diseases on radishes. IEEE Trans Plasma Sci. 2019;47(1):52–6.
53. Mitsugi F, Abiru T, Ikegami T, et al. Influence of ozone generated by surface barrier discharge on nematode and plant growth. IEEE Trans Plasma Sci. 2016;44(12):3071–6.
54. Mitsugi F, Nagatomo T, Takigawa K, et al. Properties of soil treated with ozone generated by surface discharge. IEEE Trans Plasma Sci. 2014;42(12):3706–11.

Chapter 14
Promotion of Reproductive Growth of Mushroom Using Electrical Stimuli

Koichi Takaki

Abstract Electrical stimuli such as electric fields can be used for the promotion of plant growth mode change from vegetative to reproductive. Mushrooms are globally cultivated for fresh food or dried food. Some other mushrooms are cultivated for special medicinal mushroom. Mushroom is fruiting body mainly in basidiomycetous fungi and some ascomycetous fungi. Therefore, mushrooms are developed for spore formation at reproductive growth phase. This chapter covers electrical stimuli which means that the electrical energy is applied directly to mushroom spores, mycelium, or the mushroom itself through the cultivating medium. Proper control of applied electrical energy can cause physical stimulus to the mushroom mycelium in the cultivation environment, resulting in the promotion of fruiting body formation for increasing harvest yield. This chapter summarizes various studies performed at different cultivation environments using high-voltage stimulation methods.

Keywords Electric fields · Mushroom · Electrical stimulation · High voltage · reproductive growth · Fruiting body · Growth enhancement · Artificial lightning

14.1 Introduction

Many studies have been performed to examine the effects of applying discharge plasma and electrical fields in agriculture and food processing including improving seed germination, early plant growth, plant growth mode change from vegetative to reproductive, keeping freshness of agricultural products, and enzyme activity control in food processing [1]. In the applications, the repetitively operated, compact high-voltage power supplies with moderate peak power have been developed for controlling discharge plasmas and electric field distribution. These applications are mainly based on the biological effects of a spatially distributed electric field and the

K. Takaki (✉)
Faculty of Science and Engineering, Iwate University, Morioka, Iwate, Japan
e-mail: takaki@iwate-u.ac.jp

S. Horikoshi et al. (eds.), *Agritech: Innovative Agriculture Using Microwaves and Plasmas*, https://doi.org/10.1007/978-981-16-3891-6_14

chemically active species produced by the plasma [2, 3]. The intense pulse electric fields (PEFs) that have biological effects are caused by applying pulse voltage between the electrodes. When the applied voltage exceeds the corona discharge criterion, discharge plasmas that produce free radicals, ultraviolet (UV) radiation, an intense electric field, and shock waves are generated by the accelerated electrons within the intense electric field in a gas or liquid medium [4]. Different high voltages and plasmas may have different biological effects on substrates via the electric field and reactive species. For instance, intense electric fields form pores on the cell membrane (i.e., electroporation) or influence the nucleus [5]. The agricultural applications of plasma are categorized as seed germination promotion [6], plant growth acceleration [7], the inactivation of bacteria in soil and liquid hydroponic media [5, 8], and the promotion of fruit body formation such as in mushrooms and fruits in the preharvest phase [5, 9]. In the postharvest phase, maintaining the freshness of agricultural products is important for a sustainable food supply chain. High-voltage and plasma technologies can contribute to maintaining freshness by decontaminating the air and liquid in agricultural products storage containers [5, 10]. In the food processing phase, an intense PEF can be used to extract juice, nutritional agents, and antioxidant metabolites such as vitamin, carotenoids, and polyphenols from fruits and vegetables [11]. Some foods and liquors are made by fermenting a food substance. Fermentation is a metabolic process enabled by yeast and bacteria, the activity of which can be controlled by an intense electric field [5, 12].

The number of different mushroom species on earth is estimated at 140000, of which maybe only 10% are known. Meanwhile, of those approximately 14,000 species that we know today, about 50% are considered to possess varying degrees of edibility, more than 2000 are safe, and about 700 species are known to possess significant pharmacological properties. Mushrooms have long been attracting a great deal of interest in many areas of foods and biopharmaceuticals [13]. The production of mushroom was started for the first time in the caves of France. It was then attempted by Chinese in 600 AD. Its production was only 60,000 tons in 1978. Thereafter, cultivation of some mushrooms started artificially in China and Japan. With the passage of time, innovative and easy cultivation technologies were developed resulting in a big jump in production of mushroom from 0.30 million tons in 1961 to 18.58 million tons in 2016 over the period of last 55 years. Mushrooms are now getting significant importance in almost all around the globe, and about 100 countries of the world are cultivating varieties of mushrooms mainly button, shiitake, oyster, wood ear, and paddy straw mushrooms contributing for about 99% of the total world production of mushrooms [14].

Mushrooms such as *Agaricus bisporus* (white button mushroom), *Pleurotus ostreatus* (oyster mushroom), *Lentinula edodes* (*L. edodes*; shiitake mushroom), and *Flammulina velutipes* (enokitake or winter mushroom) are globally cultivated for fresh food or dried food. Some other mushrooms such as *Ganoderma lucidum* are cultivated for special medicinal mushroom. Mushroom is fruiting body mainly in basidiomycetous fungi and some ascomycetous fungi. Therefore, mushrooms are developed for spore formation at reproductive growth phase [13]. Mushroom

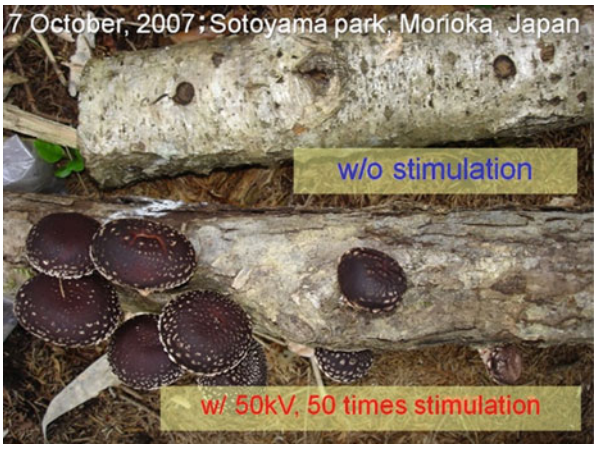

Fig. 14.1 Typical photograph of the cultured *L. edodes* with (**bottom**) and without (**top**) electrical stimulation

farming is mainly based on two methods: log-grown or fungus bed culture using a pot filled with sawdust-based substrate. The later method offers controllable conditions so that effective mushroom growth can be expected. Biological efficiency has been improved by optimizing various factors, such as substrate formula, strain type, culture maturity, water condition, and other environmental conditions of the cultivation room.

Physical phenomena in cells caused by external pulsed electromagnetic energy have a variety of applications on biotechnologies [2]. The electrical stimulation can either destroy the cells and plants or promote its growth rate, depending on the degree of stimulation. In nature, mushrooms' extraordinary grow-up around a hit point of a lightning has been reported by some mushroom farmers. Early studies of mushroom growth promotion by artificial lightning were carried out on edible mushroom cultivation using an impulse generator [15]. The output voltage of the impulse generator was more than 500 kV. After that, the high-voltage pulsed power supplies were designed to generate an output voltage from 50 to 130 kV for the electrical stimulation on mushroom cultivation bed. The promotion effects of high-voltage stimulation on sawdust-based substrate of *L. decastes* and natural logs hosting *L. edodes*, *Pholiota microspora,* and *Hypholoma lateritium* were evaluated using the developed compact pulsed power generator [9]. Typical stimulation effects are shown in Fig. 14.1 as a photograph of cultured *L. edodes* taken on the same day. The upper bed-log was used in cultivation without the high-voltage stimulation. The lower bed-log was used in cultivation, and a 50 kV voltage was applied 50 times as stimulation. *L. edodes* in the stimulated log grew faster than that in the bed-log without stimulation. The high-voltage electrode is located on the left side of the log. The fruiting bodies mainly grow near the high-voltage electrode. In this chapter, the effect of high-voltage electrical stimulation on induction of fruiting body of mushroom is described.

14.2 Mushroom Cultivation and Stimuli for Fruiting Body Development

The life cycle of mushroom is shown in Fig. 14.2 [13]. Mushroom is fruiting body mainly in basidiomycetous fungi and some ascomycetous fungi. Therefore, mushroom fruiting bodies are developed for spore formation. Mushroom-forming fungi differentiate by sensing several environmental factors for fruiting body formation. For fruiting body induction, nutrient, temperature, and light conditions are critical environmental factors. Higher nitrogen and carbon sources in the media will suppress fruiting body induction in many mushroom-forming fungi, with induction being triggered by lower nitrogen and carbon concentrations. Low temperature or temperature downshift is another critical influencing factor for fruiting body induction in many cultivated mushrooms. Fungal response toward starvation and cold involves the production of sexual spores as the next generation.

Condition for fruiting body induction is one of critical factor for mushroom cultivation. To establish high-yield cultivation method, it is very important to understand effects of environmental factors for fruiting body induction. Environmental factors for fruiting body induction are classified into physiological and physical factors. Gaseous condition and nutrient, or hormones are classified as physiological factor, and wounding or striking as physical factors. Light is one of the important factors for fruiting body induction, and blue light is the effective wavelength. For example, light promotes fruiting body induction in *L. edodes*. In contrast, some species can induce fruiting body in complete darkness. Therefore, light can promote fruiting body development in some species, but not really

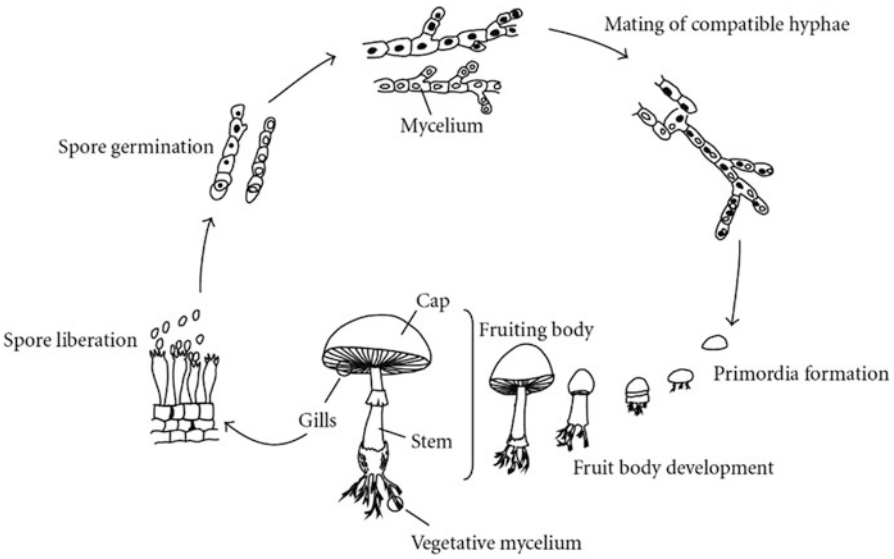

Fig. 14.2 Diagrammatic representation of mushroom life cycle [13]

necessary. Temperature is one of the critical factors for fruiting body induction in basidiomycetes. Especially, downshift of temperature stimulates fruiting body induction in many mushroom species. For example, fruiting body of *Flammulina velutipes* (*F. velutipes*) can induce temperature downshift (e.g., from 23 to 16 °C; degree Celsius) in complete darkness. Interestingly, fruiting body formed in complete darkness has tiny cap on its head [16]. It is revealed that proteins expressed specifically during fruiting body formation are regulated by temperature but not by light in *F. velutipes*. Nutrient is another critical factor for fruiting body induction. Especially, high concentration of carbon and nitrogen sources inhibits fruiting body induction. Wood decay fungi are major species for commercially cultivating mushrooms; therefore, wood decay is closely related to fruiting body induction.

Wounding or striking is used for commercial cultivation in several mushroom species. For example, scrapping mycelia on surface of the media (so-called Kinkaki in Japanese) is used for fruiting body induction in several mushrooms. Striking log wood is used for stimulation of fruiting body induction, especially in *L. edodes.* Electrical stimulation is also a physical factor for fruiting body induction similar to Kinkaki or striking. Japanese farmers have their elders' wisdom that lightning comes crashing into the ground provokes a plentiful mushroom harvest. Electrical stimulation is used for stimulating fruiting body induction by mimicking the effect of lightning in nature.

14.3 History of Electrical Stimuli for Mushroom Fruiting Body Development

The application of a pulsed high voltage to improve the yield in edible mushroom cultivation has also been attempted by some research groups [17]. The fruiting capacity of *L. edodes* (Shiitake mushroom) was remarkably promoted by applying a high voltage to cultivation bed-log (wood) [9]. This effect was also recognized in *L. edodes* fruiting on a mature sawdust substrate [18, 19]. The fruiting body (sporocarp) yield in the electrically stimulated substrate was observed to be 1.7 times more than that without the electrical stimulation [19]. This effect was also confirmed in the fruiting body development of edible mushrooms: *Grifola frondosa, P. microspora, F. velutipes, Hypsizygus marmoreus, P. ostreatus, P. eryngii, P. abalones,* and *Agrocybe cylindracea* [20, 21]. The fruiting body yield in the electrically stimulated substrate was observed to be 130–180% greater than that without the electrical stimulation [20]. The high-voltage stimulation technique was also applied to ectomycorrhizal fungi such as *Laccaria laccata* and *Tricholoma* matsutake [21–23].

Early stage of the study on mushroom fruiting promotion and large-scale impulse generators was used as artificial lightning for stimuli on the mushroom fruiting body development. Figure 14.3 shows typical photograph of an impulse generator [24]. The impulse generator consists of 10–20 capacitors, gap switches, and damping

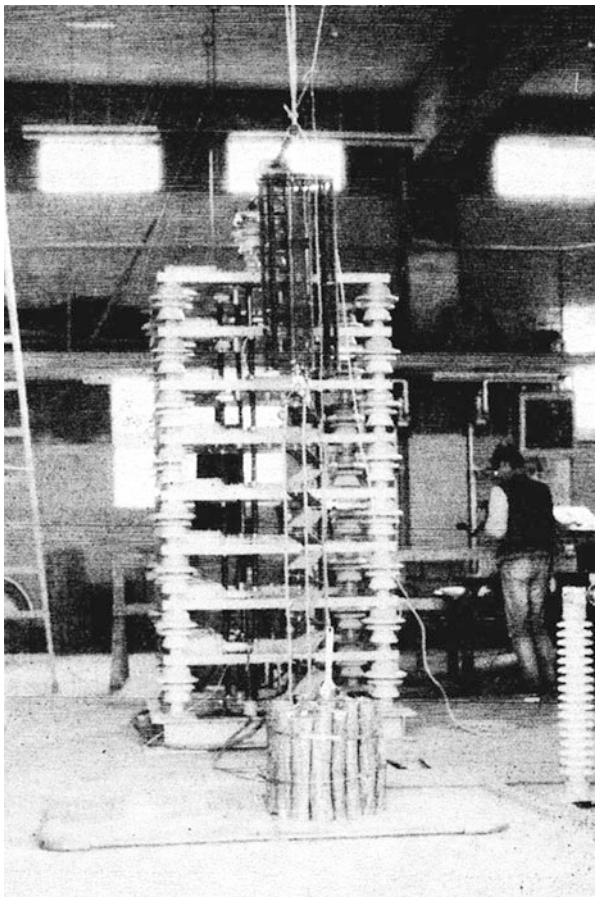

Fig. 14.3 Photograph of impulse generator for stimuli of Shiitake mushroom cultivation bed-log [24]

resistors. The capacitors are connected in parallel at charging phase. After charging up the capacitors, the connection of the capacitors is changed from parallel to series using the gap switches. As a result, the output voltage is multiplied by changing the connection of the capacitors. Typical output voltage is in range from 250 kV to 1 MV. The rise time of the output voltage is controlled around the microsecond order as an artificial lightning stroke voltage. The example of the applied voltage to the bed-log is shown in Fig. 14.4 [15]. The peak voltage of 288 kV is generated by operating the impulse generator. The rise time of the voltage is close to 0.5μs. In experiments, the bed-logs are connected to high-voltage electrode as shown in Fig. 14.3. The bed-logs (Konara oak; Quercus serrata) have dimension of 1 m length. The 5–9 bed-logs are bundled or connected in parallel as shown in Fig. 14.5 for the high-voltage stimulation by impulse generator. The impulse high voltages are applied to the bed-logs bundle or top of the bed-logs connected in parallel. After the stimulation, the bed-logs are cultivated for fruiting body formation. The yielding

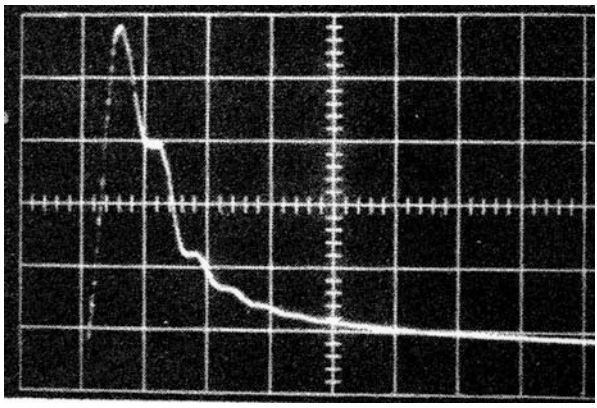

Fig. 14.4 288 kV output voltage of an impulse generator [15]. X: Time (1μs/div.), Y: Voltage (50 kV/div)

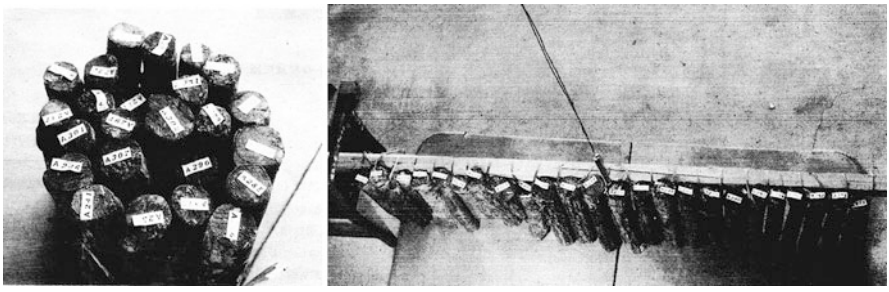

Fig. 14.5 Photographs of setup of bed-logs for impulse high-voltage stimulation [24]

Table 14.1 Fruit body yield of *L. edodes* of bed-logs using high-voltage stimulation without submergence treatment [15, 17]

Exp. group.	Number of exp. bed-logs	Fruit-body yield (per 1 m^3 of wood) number	Dry wt (g)
144 kV	24	505.3	1337.0
288 kV	24	770.1	2171.4
576 kV	24	121.6	558.4
Contd.	24	16.9	55.2

Bed-log age: 38 months after inoculation (Yakult haru 2). Water content of bed-logs: 38.9% (mean value of six samples)
All exp. groups had 34 mm rainfall in a week after discharge

rates of the fruiting bodies on the bed-logs are monitored for each stimulation condition.

Typical results of the stimulation on yielding rate of *L. edodes* fruiting bodies are shown in Tables 14.1 and 14.2 for various amplitudes of applied voltage [15, 17]. The numbers of the bed-logs are 24 and 21 for each experimental condition. The number of fruiting body formation and total harvested yield increase by stimulating high voltage. In both cases, the fruiting body yields increase by applying

Table 14.2 Fruit body yield of *L. edodes* of bed-logs using high-voltage stimulation with submergence treatment [15, 17]

Exp. group	Number of exp. bed logs	Fruit-body yield (per 1 m^3 of wood) number	Dry wt (g)
288 kV	21	650.8	2100.0
576 kV	21	485.8	1648.9
720 kV	21	453.8	1427.4
Cont.	21	276.2	840.6

Bed-log age: 38 months after inoculation (Yakult haru 2). Water content of bed-logs: 42.3% (mean value of six samples)

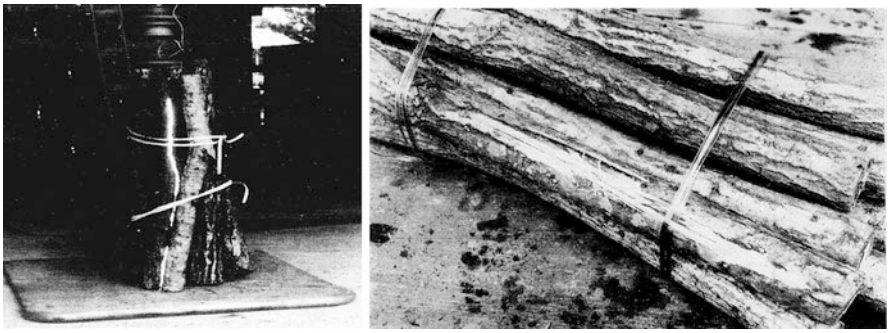

Fig. 14.6 Photographs of electrical discharge on surface of the bed-log and crack of the bed-logs by impulse high-voltage application [24]

impulse high voltages as stimulation for fruiting body forming. However, the optimum amplitude of impulse voltage for improving fruiting body yield exists as shown in Tables 14.1 and 14.2. The fruiting body yield at 288 kV impulse voltage is larger than those at 144 and 576 kV applied voltage as shown in Table 14.1. When an electrical field E is generated by applying impulse high voltage to the bed-logs, hyphae will thus be subjected to a Coulomb force f ($f = qE$; q means total charge of the hypha) from the electrical field. As a result, the hyphae are accelerated toward the positive electrode according to the equation $f = ma$, where m and a mean mass of the hypha and acceleration of the hypha, respectively. The application of electric pulses, resulting in hyphal displacement and sometimes damage, can be considered as a form of physical stress. The physical stress works as trigger to promote the fruiting body formation. However, when the applied voltage is too high compared with the optimum condition, the physical damage of the hypha is too much for stimulation of fruiting body promotion. Sometimes the bed-logs are also damaged by the high-pressure wave (shockwave) caused by electrical discharge and impulse high current as shown in Fig. 14.6 [24].

The frequencies of the fruiting body yield by impulse high-voltage stimulation under same condition as shown in Table 14.1 are shown in Fig. 14.7 [15]. In the control case (without high-voltage stimulation), the fruiting body cannot be harvested for 20 bed-logs (83%). One fruiting body can be harvested from four

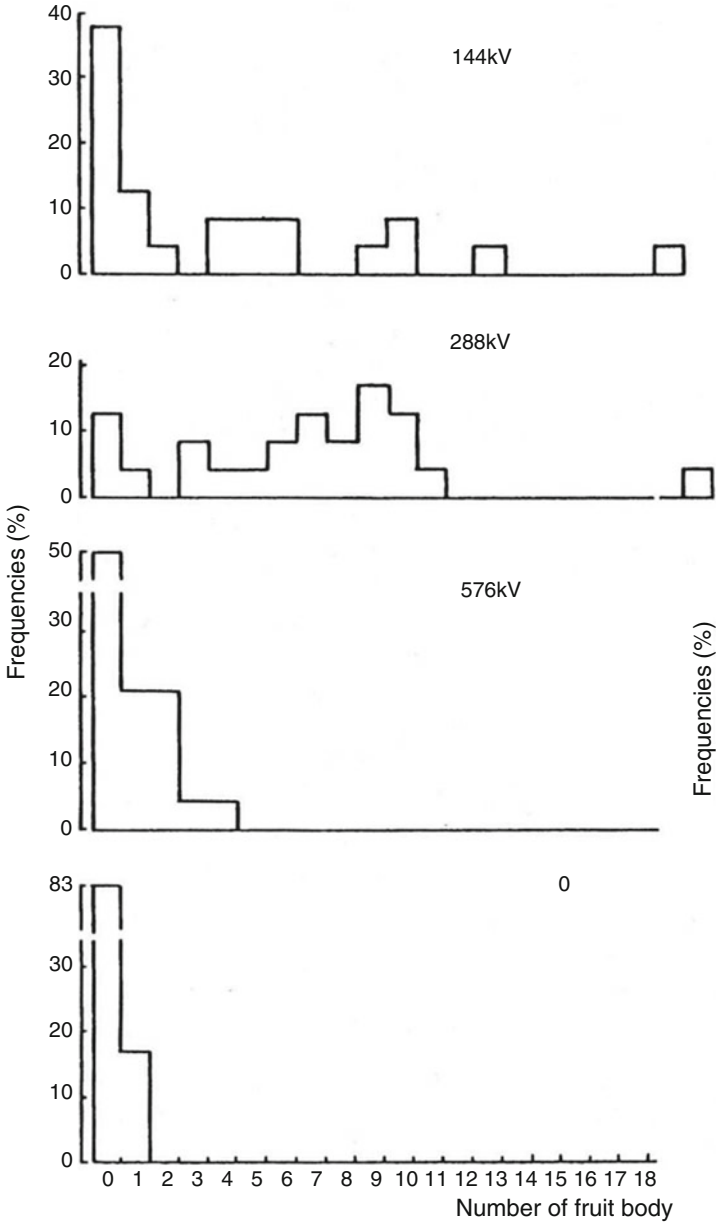

Fig. 14.7 Frequencies of the fruit-body yield by impulse high-voltage stimulation to *L. edodes* of bed-logs without water submerged treatment [15]

bed-logs (17%). However, the fruiting bodies can be harvested from 21 bed-logs (except 3 bed-logs; 12%) at 288 kV impulse voltage applying. The decrease of number of the bed-log without *L. edodes* fruiting bodies mainly contributes to increasing yield of mushroom by applying high-voltage shown in Table 14.1.

14.4 Effect of High-Voltage Stimulation in Bed-Log Cultivation

Several kinds of edible mushrooms are cultivated artificially. Many of them are wood-rotting fungi and so mushrooms grow on dead trunks of wide leaf trees in the forest. *Lentinus edodes* (Shiitake) was localized wild in the southern part of Japan from long time ago, and by the invention of wood-chip spawn by the late Dr. Mori, scientific artificial cultivation started in 1943. They are now cultivated in the forests by inoculated bed-logs of oak trees everywhere in Japan. In 2019, 88,031 tons of fresh Shiitake mushrooms are harvested in a year and 16,901 tons of them are used as dried Shiitake. Beside Shiitake, *Flammulina velutipes* (Enokitake), *Pholiota glutinosa* (Nameko), *Pleurotus ostreatus* (Hiratake), *Grifola frondosa* (Maitake), *Agaricus bisporus*, *Lyophyllum ulmarium* (Shirotamogitake), and others are cultivated commercially. Most of them are cultivated by sawdust culture (bottle or bag culture) in air-conditioned rooms. Many good strains are selected from wild strains, or crossbreeding is carried out by several spawn makers. Now the cultivation of edible mushrooms has grown to a big business for the farmers. The total production of cultivated mushrooms in a year is 456,481 tons, and the market price is about 226 billion Japanese yen.

The bed-log cultivation of mushroom is widely used in the artificial forest and greenhouse as shown in Fig. 14.8. In general, mushrooms such as shiitake are first inoculated into logs, and slowly, the hyphae grow over a period of approximately 1 year. With this growth, the phase changes from hyphal-level vegetative growth to fruiting body (mushroom)-level reproductive growth. At this time, to promote a mushroom outbreak, the bed-log is submerged for 1–2 days, followed by beating several times as physical stimulus. Physiological and biochemical changes occur in the mushroom mycelium owing to the difference between the outside and inside temperature because of the inundation and the stimulus (namely the impact of beating), resulting in a shift from vegetative growth to reproductive growth. Actual shiitake cultivation thus involves artificial stimulation of the bed-logs via mechanical impact. However, the success rates of both methods are highly dependent on the growers' experience, and the expected effects are often not achieved. Furthermore, these aspects make it difficult for elderly or aging producers to maintain production levels.

Figure 14.9 shows the circuit diagram and photograph of pulsed power generator based on Marx generator for electrical stimuli in bed-log cultivation [25–27]. The Marx generator consists of 4 energy storage 0.22μF capacitors (Maxwell, 31160),

Fig. 14.8 Photographs of bed-logs cultivation of *L. edodes* (Shiitake; left) and *Pholiota glutinosa* (Nameko; right). The log length is about 0.9 m

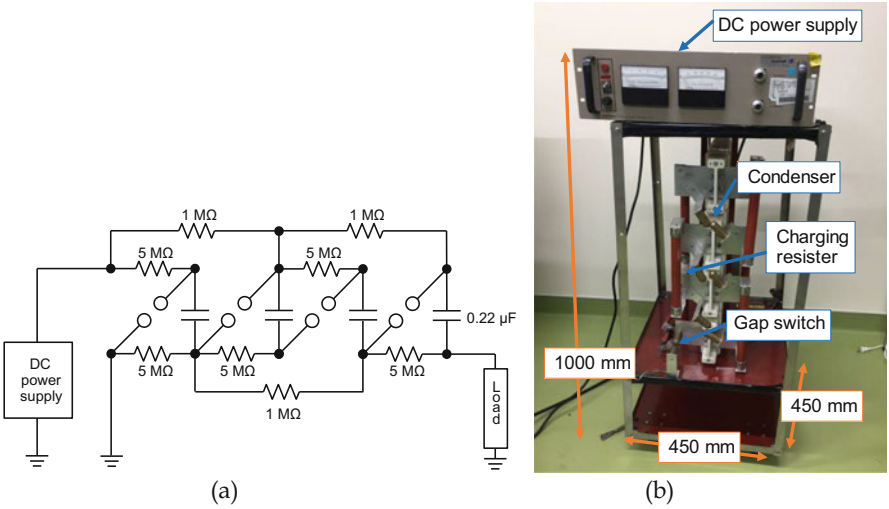

Fig. 14.9 Circuit diagram (**a**) and photograph (**b**) of Marx generator [27]

charging resistors (1 and 5 MΩ) connected to the capacitors, and the spark gap switches. The capacitors are charged up using a high-voltage DC power supply (Gamma high voltage research, RR3-5R/100) up to 12.5 kV. The charging time is required for approximately 10 s because of the output current limit. After charging

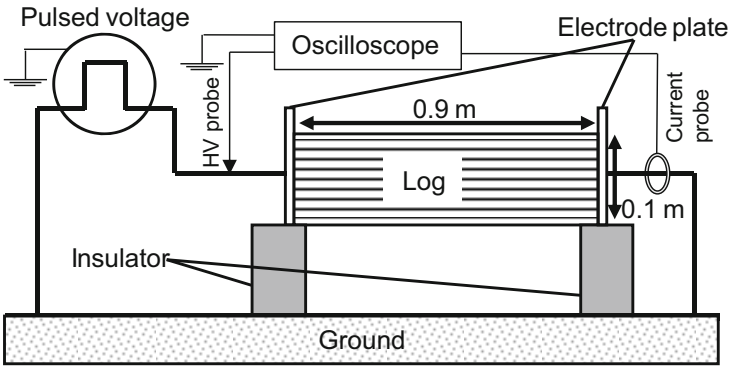

Fig. 14.10 Experimental setup for pulsed voltage stimuli to the *L. edodes* logs [27]

up the capacitors, a spark gap switch is manually closed. When a spark gap switch is closed, the other switches are sequentially closed automatically and the connection of capacitors is changed from parallel to series. The voltage is stepped up and is applied to the load. The Marx generator has 1.0 m × 0.45 m × 0.45 m in sizes and 39.4 kg in weight.

The cultivating mushroom, *L. edodes*, is inoculated on natural logs of *Quercus crispula Blume* 2 years before the experiment. The strain of the fruiting type is Mori#290 (Mori. Co. Ltd., Gunma, Japan). The dimensions of the bed logs are 0.9 m in length and 0.1 m in diameter. The logs are covered with a blackout curtain to maintain the moisture content in the logs hosting the mushroom hyphae. After 2 years incubation, the blackout curtain is unveiled and the logs are placed side by side under environment. The pulsed voltage is applied to the logs 1 month before the date that mushroom fruit body is usually expressed. The fruit body of mushrooms can be cropped from the logs in every two seasons, spring and autumn, over 2 years. Figure 14.10 shows the experimental setup for pulse application to the logs [27]. To apply the pulse voltages to logs, the electrode plate was installed at both ends of logs placed on an insulator. The total input energy into the logs is controlled by the amplitude and the number of the applying.

Figure 14.11 shows the typical waveforms of the applied voltage and output current to the shiitake mushroom logs using the Marx generator [27]. When the gap switch of the circuits is shortened, the voltage charged at the capacitors is applied to the log and then the voltage exponentially decays. The impedance of the log is calculated from the waveforms and is 2.67 kΩ with a standard deviation of 0.64 kΩ in second flush season and 5.29 kΩ with a standard deviation of 1.97 kΩ in fourth flush season. The differences of the impedance could be caused by the moisture contents of the logs and a decay with a hypha filled in the log. The time constant of Marx generator in the case of second flush season is approximately 190μs with a standard deviation of 51μs and that in the case of fourth flush season is approximately 410μs with a standard deviation of 0.41μs, respectively. Although the impedances and the time constants are difference, the total input energy into the

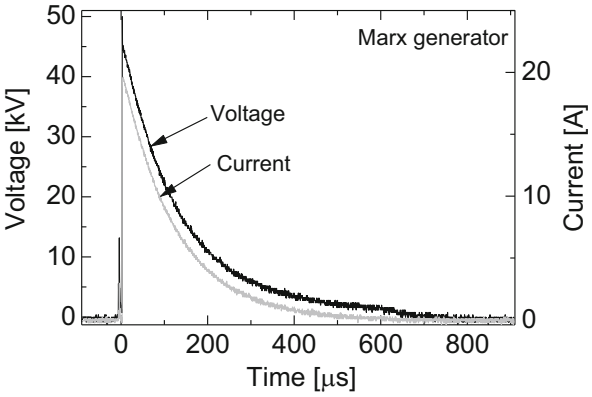

Fig. 14.11 Typical waveforms of applied voltage and current to the *L. edodes* logs using Marx generator [27]

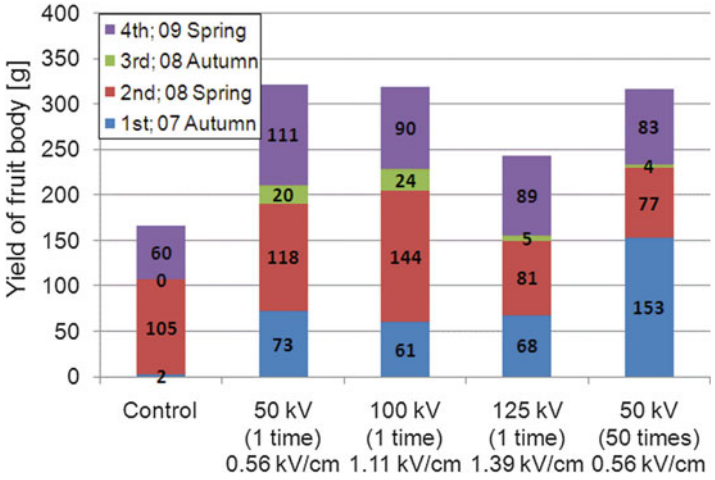

Fig. 14.12 Total weight of cultured *L. edodes* for various electrical stimulation conditions. The total yields are 167, 322, 319, 243, 317 g for control, 50 kV-1 time, 100 kV-1 time, 125 kV-1 time, 50 kV-50 times, respectively [9]

logs is almost same in the two seasons. Assuming that the electric field in the log is uniform, the electric field inside log in the case of 50 kV is 56 kV/m.

Figure 14.12 shows the *L. edodes* yield for different applying voltages [9]. One group is cultured without high-voltage stimulation (control group). Three groups are stimulated by a single high-voltage pulse (one-time application) at three different amplitudes: 50, 90, and 125 kV. The last group is stimulated 50 times with a 50 kV pulsed voltage. The yield of the fruit body is evaluated as the total weight harvested during four seasons. It includes the crops from all 15 logs, appropriately averaged without statistical analysis. The yield of the control group was only 2 g in the first harvesting season, autumn of 2007, because the *L. edodes* species used in the present experiment mainly fruits in the spring. In this case, the 30 g weight of fruit bodies is

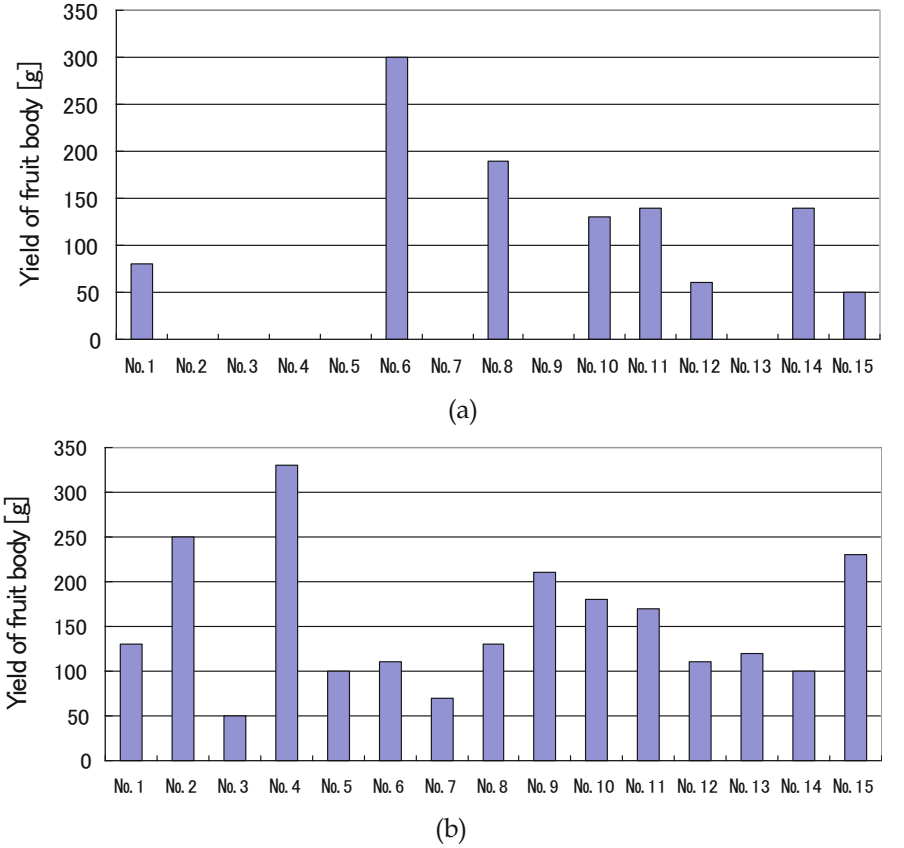

Fig. 14.13 Difference in the yield of fruit bodies of *L. edodes* based on the number of 50 kV applied voltage treatments received. No.1–No.15 indicate labels for each cultivation log. (**a**) one-pulse stimulation; (**b**) 50-pulse stimulation [9]

harvested from only one log. Therefore, the standard deviation is 7.5 g, which is larger than the 2 g average weight. This result indicates that the mushroom species employed in the experiment usually does not develop fruit bodies. However, the yield from the first season increased from 2 to 73 g when a 50 kV pulsed voltage is applied. The yield increased from 73 to 153 g when the number of pulses increased from 1 to 50. In this case, the standard deviation is determined to be 73.0 g, which is lower than the 153 g average weight. This result indicates that the mushrooms develop fruit bodies as the result of applying high voltages. The total harvested weight over four seasons is 167 g in the control group. The yield increases to 322 and 319 g when pulsed voltages of 50 and 100 kV are applied, respectively. However, the yield decreases to 243 g at 125 kV voltage applying. This result indicates that optimum voltage amplitude exists and is estimated in range from 50 to 100 kV/m.

Figure 14.13 shows the weights of *L. edodes* harvested from each log at two different numbers of pulse voltage stimulation [9]. The applied voltage was 50 kV in

Fig. 14.14 Difference in the fruit body developing (**a**) without and (**b**) with 50 kV high-voltage pulse stimulation

all cases. Figure 14.14 shows the photographic image of the difference between harvesting yield with and without electrical stimulation using 50 kV applying voltage. In this experiment, the autumn was chosen as season for evaluation of the electrical stimulation to promote the fruiting body, because the used strain of *L. edodes* was generally suitable for the spring harvest. The applied voltage was 50 kV in all cases. The total weight from the logs after 50-pulse stimulation was 2.29 kg (=153 g × 15), as shown in Fig. 14.12, which is larger than the 1.09 kg (=73 g × 15) harvested after a one-pulse stimulation. The maximum value of the harvested fruiting body from one log after a one-pulse stimulation was 300 g, which is similar to the 320 g obtained after 50-pulse stimulations. Although there were no logs observed without fruiting body formation for 50-pulse stimulation, after a one-pulse stimulation, seven logs contained no fruiting bodies. The average yield for one log was approximately 73 g (=1090/15) after a one-pulse stimulation. Only 6 logs showed a yield larger than the 73 g average value, whereas 14 logs showed a yield larger than 73 g in the case of 50-pulse stimulation. This result indicates that on particular logs, the use of the pulsed voltage decreased the deviation in the mushroom formation. The standard deviations are 27 and 19 g at one- and 50-pulse stimulations, respectively.

Figure 14.15 shows the time history of the amount of mushrooms cultured under various stimulation conditions in the spring of 2009 [9]. The yield is normalized by the total crop weight for one harvesting season and is evaluated as an aggregate of all crops. The total crop weights were 60, 111, 90 and 89 g in the control, 50, 100, and 125 kV stimulation groups, respectively. Compared with the control group, the total yield increased when applying a voltage of 50 and 100 kV. The harvested weight for 15 days after the first crop (day 18) was approximately 50% of the total in the control group. However, the crop weight during this period increased to 86% of the total when applying voltages of 50 and 100 kV. This result indicates that the mushrooms can be harvested in fewer days by applying high voltage as electrical stimulation.

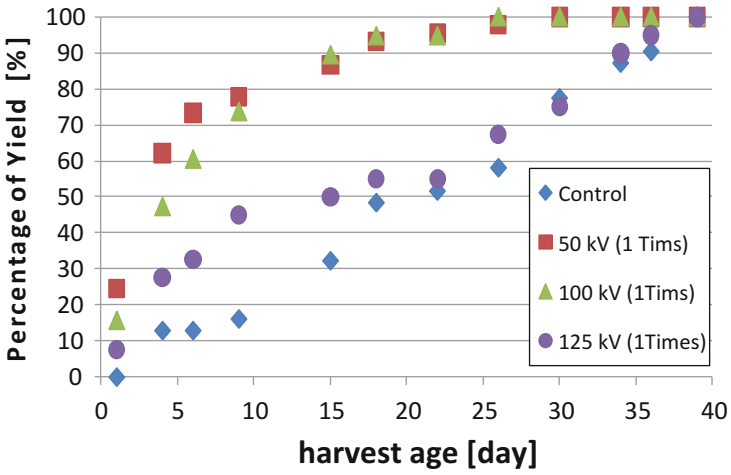

Fig. 14.15 Time history of the total amount of harvested fruit bodies for various stimulation voltages [9]

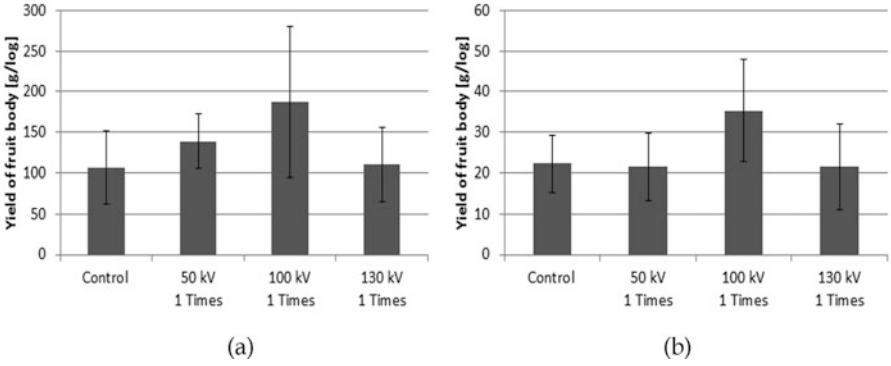

Fig. 14.16 Yield of *Pholiota glutinosa* (Nameko) and (**b**) *Hypholoma sublateritium* (Kuritake) fruit bodies for various amplitudes of applying voltage as stimulation for fruiting body development. Vertical bars indicate the standard errors ($n = 10$ for (**a**) and 13 for (**b**)) [9]

The high-voltage electrical stimuli work for not only *L. edodes* (shiitake) but also many species of mushroom. Figure 14.16 shows the crop weight of (a) *Pholiota glutinosa* (Nameko) and (b) *Hypholoma sublateritium* (Kuritake) harvested at different stimulation voltages [9]. Three groups were stimulated by a single high-voltage pulse with three different amplitudes. The yield of the fruit body at the first flash in bed-log cultivation was used for the evaluation. The yield was obtained by dividing the total weight of the crops from 10 or 13 bed-logs by the number of logs. In Fig. 14.16a, the average *P. glutinosa* yield of the control group is 107 (±45) g/log. The average yield increases to 139 (±33) and 187 (±93) g/log by applying a voltage of 50 and 100 kV, respectively. These yields are 1.3 and 1.7 times larger than

that of the control group by the evaluation using averaged value. The yield decreases to 111 (±46) g/log when the voltage is increased to 130 kV. In Fig. 14.16b, the average yield of *H. sublateritium* increases from 22.3 (±6.9) g/log to 35.4 (±12.4) g/log by applying a voltage of 100 kV, which corresponds to 1.6 times increment compared with that of the control group. The applied voltage of 100 kV corresponds to 1.1 kV/cm in an averaged electric field, which is effective as a stimulation for fruit body development.

14.5 Effect of High-Voltage Stimuli in Bed Sawdust Cultivation

Now a day, many kinds of edible mushrooms are cultivated artificially. Many of them are wood-rotting fungi and are mainly cultivated using bed sawdust (bottle or bag culture) in air-conditioning rooms including greenhouse. Figure 14.17 shows the typical procedure of the bed sawdust cultivation. In general, mushrooms such as shiitake are first inoculated into bed sawdust, and slowly, the hyphae grow over a period of approximately 3 months. With this growth, the phase changes from hyphal-level vegetative growth to fruiting body (mushroom)-level reproductive growth. At this time, to promote a mushroom outbreak, the bed sawdust is submerged for 1 day, followed by beating several times as physical stimulus. Physiological and biochemical changes occur in the mushroom mycelium owing to the difference between the outside and inside temperature because of the inundation and the stimulus, resulting in a shift from vegetative growth to reproductive growth in same manner of the bed-log cultivation.

Figure 14.18 shows circuit diagram and photograph of high-voltage pulsed power supply based on Cockcroft–Walton (C-W) circuit (Green techno, Kanagawa, Japan; GM100) developed for bed sawdust stimulation [27, 28]. The circuit consists of an AC/DC converter, a DC/AC converter, 12 stages of ceramic capacitors and diodes, a

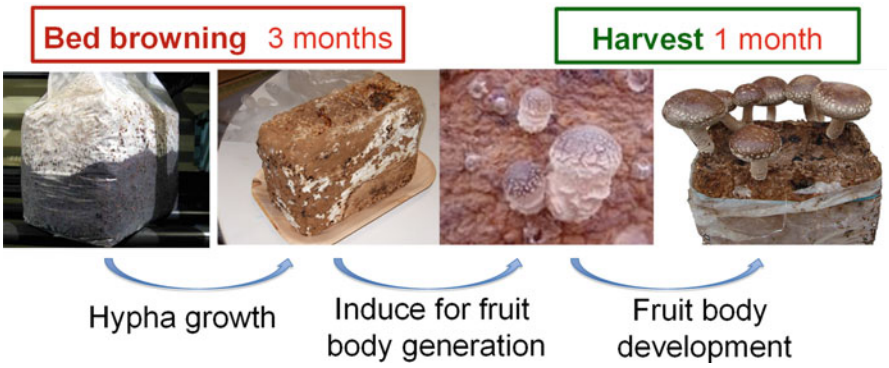

Fig. 14.17 Process of bed sawdust cultivation of *L. edodes* (Shiitake)

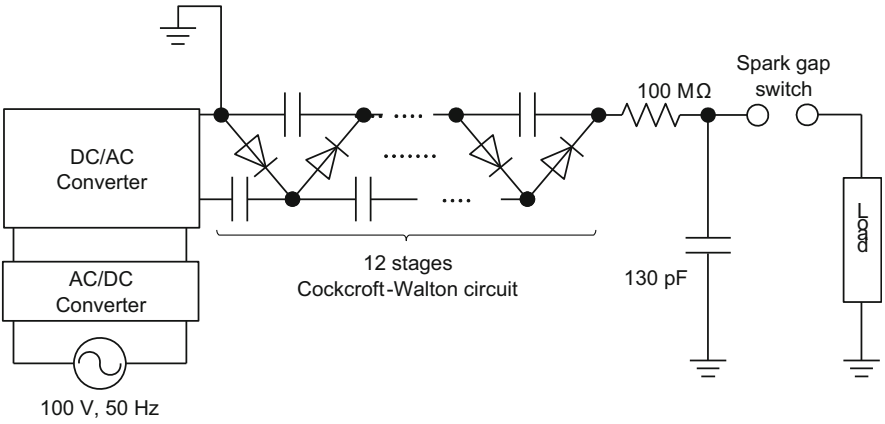

(a)

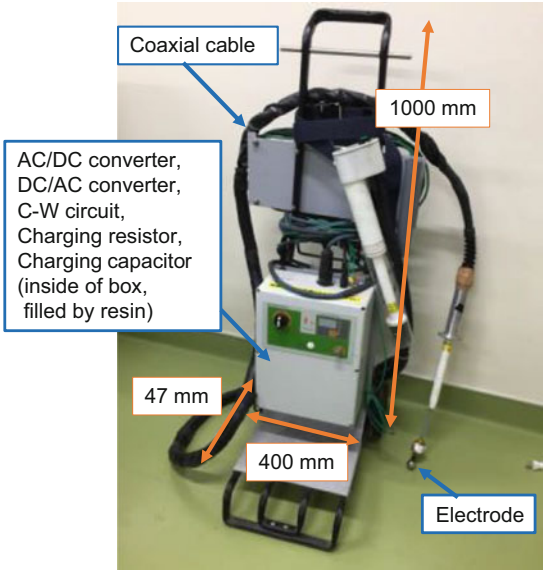

(b)

Fig. 14.18 Circuit diagram (**a**) and photograph (**b**) of C-W circuit [27]

charging capacitor, a 100 MΩ charging resistor, and a spark gap switch. The ceramic capacitors have a capacity of several hundred pF. The DC/AC converter consists of a high-voltage transformer driven by a resonance circuit, and its output voltage of DC/AC converter is 6.2 kV with frequency of 25 kHz. The charging capacitor consists of a 2.6 m coaxial cable with the capacitance of 130 pF (50 pF/m). The

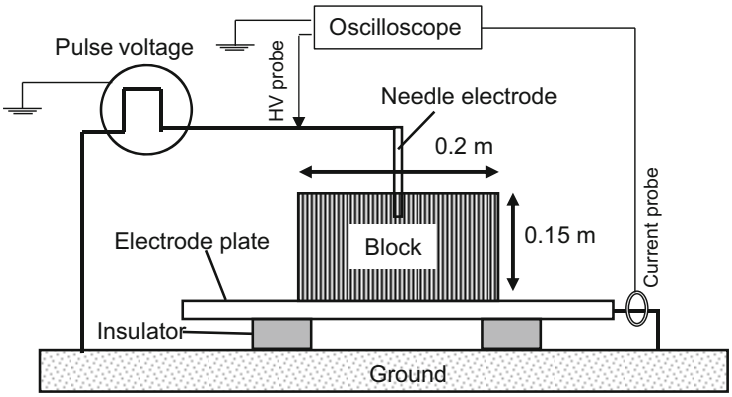

Fig. 14.19 Experimental setup for pulsed voltage stimuli to the bed sawdust [27]

AC/DC and DC/AC converters, C-W circuit, the charging capacitor, and the charging resistor are inside of the box as shown in Fig. 14.1b, which is filled by a resin for insulation. Figure 14.2 shows the charging voltage to the charging capacitor. Although the charging time depends on number of the stages and the frequency, the capacitor is charged during approximately 230 ms after turning the spark gap switch on because the output current of the DC/AC converter is limited. The C-W circuit has 0.4 m × 0.47 m × 1.0 m in sizes and 8.1 kg in weight.

The substrate for *Lyophyllum decastes Sing.* (*L. decastes*; Hatakeshimeji) cultivation consists of sawdust from *Cryptomeria japonica* produced by Kamiyotsuba agricultural cooperative (Kami, Miyagi, Japan). The strain of the fruiting type is Miyagi LD-2 (Tsukidate bio service. Co. Ltd., Miyagi, Japan). The dimensions of the sawdust substrate are 0.12 m × 0.2 m × 0.1 m, and it has a cuboid-block shape. The weight of the substrate was 2.5 kg ± 200 g. *L. decastes* fungus are inoculated on the block and the incubated for 50–60 days under the temperature of 22–23 deg-C with a relative humidity of 65–70%. The blocks are stimulated by the pulsed voltage after the incubation. The pulsed voltage was applied to a needle electrode with a 4 mm diameter driven into the block to a depth of 50 mm, as shown in Fig. 14.19, using C-W circuit [27]. The total input energy into the blocks is.

controlled by the amplitude and number of the applying voltage. Four groups are stimulated by the pulsed voltages with the different amplitudes, 30 kV and 50 kV, and the different numbers of pulses, 100 times and 500 times. The number of blocks for each group is 16 and numbered from 1 to 16.

Figure 14.20 shows waveforms of applied voltage and output current to the *L. decastes* mushroom block [27]. The resistivity of the bed is 45 Ωm, and the impedance of the block is calculated from the waveforms and is 0.35 kΩ with a standard deviation 0.12 kΩ. Because the coaxial cable in the C-W circuit acts as a transmission line, the waveforms of applied voltage and output current are distorted and do not have an exponential shape by the forward and backward transmitted waves. Figure 14.21 shows the electric field distribution analyzed by the finite

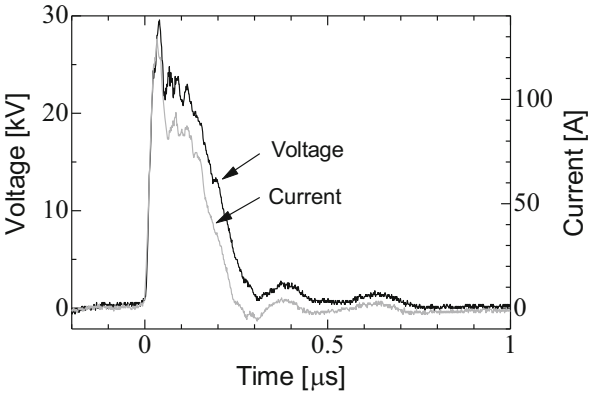

Fig. 14.20 Typical waveforms of applied voltage and current to the *Lyophyllum decastes Sing.* Sawdust block using C-W circuit [27]

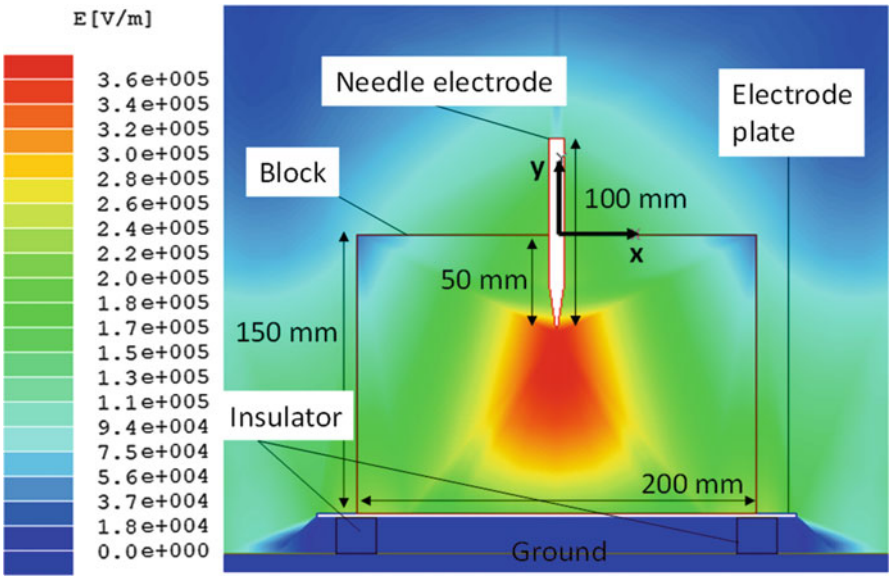

Fig. 14.21 Electric field distribution inside of *Lyophyllum decastes Sing.* Sawdust block for applied voltage of 30 kV [27]

element method (Ansoft Maxwell 2D) [27]. The analysis results show that the electric field inside of the block is concentrated at the tip of the needle and is ranged from 18 to 360 kV/m with the applied voltage of 30 kV. The input energy per a pulse in the cases of 15 and 30 kV applied voltages is 54 mJ and 27 mJ, respectively. The total input energy in the case of 15 kV is 5.4 J for 100 times pulses and 27 J for 500 times pulses and that of 30 kV is 27 J for 100 times pulses and 160 J for 500 times pulses. Figure 14.22 shows the average weight of fruit body cropped per a block for two flush seasons [27]. The error bars represent the standard error. The average weight of fruit body was improved by applying pulse voltages and increased

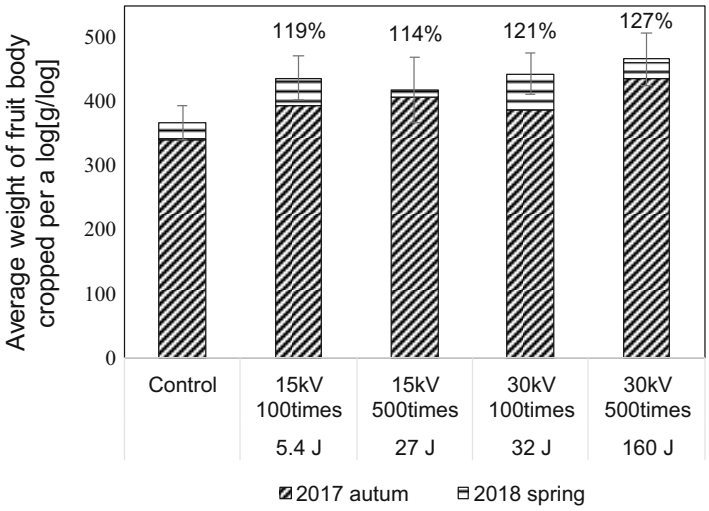

Fig. 14.22 Average yield of fruit body fruitbody of *Lyophyllum decastes Sing.* per a log for 2 flush seasons [27]

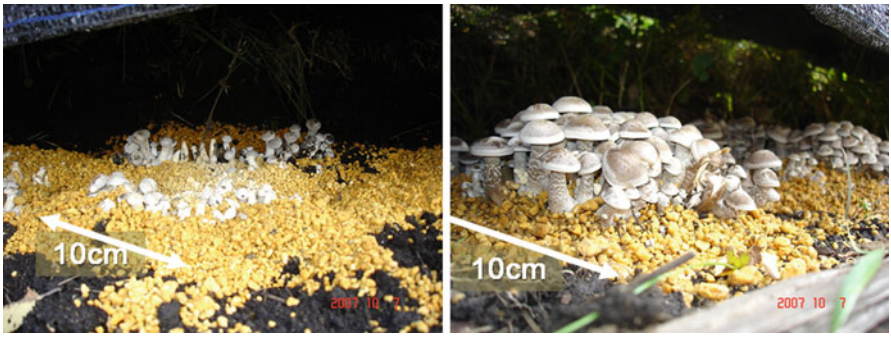

Fig. 14.23 Typical photographs of the cultured *Lyophyllum decastes Sing.* without (left) and with (right) electrical stimulation [9]

with increasing total input energy into the block. Figure 14.23 shows photographs of cultured *L. decastes* taken the same day. The *L. decastes* in the stimulation group grew faster than those in the control group.

14.6 Morphological Changes after Electrical Stimulation

The mechanism driving the increase in the fruiting body formation by applying high voltage is not clear, but researchers have suggested two possible explanations. One is that the mushroom hyphae are ruptured by applying a high voltage. Physical damage

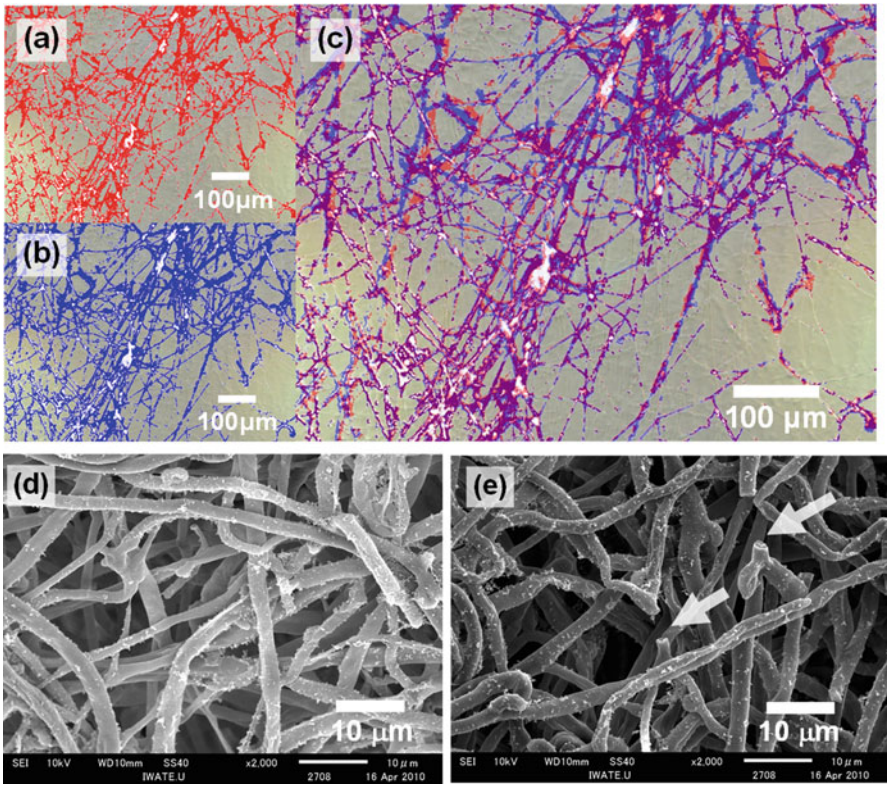

Fig. 14.24 Microscopic images of *Lentinula edodes hypha* (**a**) before and (**b**) after applying 5 kV/cm pulse electric field with pulse width of 100 ns and 500 times of repetition. (**c**) Superimposed image of two images (**a**) and (**b**). (**d**) and (**e**): SEM images of *L. edodes* hyphae before (**d**) and after (**e**) applying 10 kV pulse voltages. White bar indicates 100μm in (**a**), (**b**), (**c**) and 10μm in (**d**) and (**e**)

to the hypha stimulates fruiting body formation in mushrooms [18–20]. The other explanation involves the activation of enzymes. Some enzymes are activated by applying a high voltage, and consequently, mushroom fruiting bodies develop abundantly [15]. Some effects of the high-voltage stimulation were recognized using microscopic observation and chemical analysis. A scanning electron microscope observation indicated that the synthesis of crump connections was accelerated with electrical stimulation [15–18]. Some types of enzymes, including laccase and protease, were activated by the electrical stimulation [17, 18, 22]. It is difficult to reveal how electric stimulation affects fruiting body induction in mushroom clearly based on the experimental results. Therefore, we focus on morphological changes after electrical stimulation.

Figure 14.24a, b shows images of *L. edodes* hyphae before (a, red) and after (b, blue) application of electric pulses. Figure 14.24c shows a superimposed image of (a) and (b) with purple (red + blue) indicating that hyphae retained the same position

before and after applying the pulsed electric fields. Red and blue colored hyphae in Fig. 14.24c show displaced hyphae. Displacement can be explained by the slightly negative charge of mushroom hyphae. When an electrical field E is applied, hyphae will thus be subjected to a Coulomb force f ($f = qE$; q means total charge of the hypha) from the electrical field. As a result, the hyphae are accelerated toward the positive electrode according to the equation $f = ma$, where m and a mean mass of the hypha and acceleration of the hypha, respectively. The application of electric pulses, resulting in hyphal displacement and sometimes damage, can be considered as a form of physical stress. Other physical stresses such as scrapping of surface hyphae (Kinkaki) have been known to induce fruiting body formation in several mushrooms, suggesting that electric pulses that induce fruiting body formation act through a similar mechanism. Figure 14.24d, e shows scanning electron microscope (SEM) images of hyphae before and after applying an electrical pulse of 10 kV between wire electrodes with a gap length of 9 cm. It was observed in the SEM image that after some hyphae were broken by the electric pulse as shown by arrows in Fig. 14.24e. This suggests that the electric pulse will be a similar stimulation as scratching mycelia on the surface of the sawdust media for mushroom production. Furthermore, it would be possible that new hyphae will be generated after electric pulse stimulation and Kinkaki. Hydrophobin, which is involved in hyphal structure and architecture in fungi [29, 30], would be involved in new hyphae generation after pulse stimulation.

14.7 Concluding Remarks

High-voltage electrical stimulation on fruiting body formation in cultivating mushrooms was described. The compact high-voltage pulsed power supplies were developed for the electrical stimulation to promote fruiting body formation on cultivation bed-logs and sawdust substrate (bed-block). The promotion effects of high-voltage stimulation of sawdust-based substrate of *L. decastes* and natural logs hosting *L. edodes*, *P. microspora,* and *H. lateritium* were confirmed through the evaluation using a developed compact pulsed power generator. The fruiting body formation of mushrooms increases 1.3–2.0 times in terms of the total weight. The accumulated yield of *L. edodes* for four cultivation seasons was improved from 160 to 320 g by applying voltages of 50 or 100 kV. However, the yield was decreased from 320 to 240 g upon increasing the applied voltage from 100 to 130 kV. The yield of the other types of mushrooms shows tendencies similar to those of *L. edodes* when voltage was applied. An optimal voltage was confirmed for efficient fruiting body induction. Securing profitability of the electrical stimulation is important for the widespread to the mushroom famers. The pulse voltage stimulation systems for improvement of mushroom yield have been developed and sold by some companies. Typical price of the stimulation system is around 5000 USD. The increment of L. edodes yield is around 155 g/(1-log, 2-year) at 50 kV. The price of the L. edodes is around 20 USD/

1-kg at natural-log cultivation in Japan. If the mushroom farmer uses 1612 logs, the initial cost of 5000 USD can be recovered with increment of the mushroom yield.

Acknowledgements The authors of this chapter confirm that they have received permission to reuse all the tables and figures in their current work.

References

1. Takaki K, Hayashi N, Wang D, Ohshima T. High-voltage technologies for agriculture and food processing. J Phys D Appl Phys. 2019;52:473001.
2. Akiyama H, Heller R, editors. Bioelectrics. Tokyo: Springer; 2017.
3. Graves DB. The emerging role of reactive oxygen and nitrogen species in redox biology and some implications for plasma applications to medicine and biology. J Phys D Appl Phys. 2012;45:263001.
4. Weltmann K, Kindel E, von Woedtke T. Atmospheric pressure plasma sources: prospective tools for plasma medicine. Pure Appl Chem. 2010;82:1223–37.
5. Zimmermann U. Electric field-mediated fusion and related electrical phenomena Biochem. Biophys Acta. 1982;64:227–77.
6. Eing CJ, Bonnet S, Pacher M, Puchta H, Frey W. Effects of nanosecond pulsed electric field exposure on Arabidopsis thaliana. IEEE Trans Dielectr Electr Insul. 2009;16:1322–8.
7. Takahata J, Takaki K, Satta N, Akahashi K, Fujio T, Sasaki Y. Improvement of growth rate of plants by bubble discharge in water. Jpn J Appl Phys. 2015;54:01AG07.
8. Okumura T, Saito Y, Takano K, Takahashi K, Takaki K, Satta N, Fujio T. Inactivation of bacteria using discharge plasma under liquid fertilizer in a hydroponic culture system. Plasma Med. 2016;6:247–54.
9. Takaki K, Yoshida K, Saito T, Kusaka T, Yamaguchi R, Takahashi K, Sakamoto Y. Effect of electrical stimulation on fruit body formation in cultivating mushrooms. Microorganisms. 2014;2:58–72.
10. Koide S, Nakagawa A, Omoe K, Takaki K, Uchino T. Physical and microbial collection efficiencies of an electrostatic precipitator for abating airborne particulates in postharvest agricultural processing. J Electrost. 2013;71:734–8.
11. Yang N, Huang K, Lyu C, Wang J. Pulsed electric field technology in the manufacturing processes of wine, beer, and rice wine: a review. Food Control. 2016;61:28–38.
12. Ohshima T, Tamura T, Sato M. Influence of pulsed electric field on various enzyme activities. J Electrost. 2007;65:156–61.
13. Lull C, Wichers HJ, Savelkoul HFJ. Antiinflammatory and immunomodulating properties of fungal metabolites, mediators of inflammation. Mediators Inflamm. 2005;2:63–80.
14. Thakur MP. Advances in mushroom production: key to food, nutritional and employment security: a review. Indian Phytopathol. 2020;73:377–95.
15. Kaneko S, Yamamoto M, Nakashima Y, Jitsufuji Y. Studies on electrical stimulation on Lentinula edodes bed log (in Japanese). Bull Fukuoka-Ken Forest Exp Stat. 1987;33:1–33.
16. Sakamoto Y. Influences of environmental factors on fruiting body induction, development and maturation in mushroom-forming fungi. Fungal Biol Rev. 2018;32:236–48.
17. Takaki K, Takahashi K, Sakamoto S. High-voltage methods for mushroom fruit-body developments: chapter 7. In: El-Esaw MA, editor. Plant and mushroom development. London: Intech Open Limited; 2018. p. 95–113.
18. Kudo S, Mitobe S, Yoshimura Y. Electric stimulation multiplication of *Lentinulus edodes* (in Japanese). J Inst Electrost Jpn. 1999;23:186–90.
19. Ohga S, Iida S, Koo C-D, Cho N-S. Effect of electric impulse on fruit body production on Lentinula edodes in the sawdust-based substrate. Mushroom Sci Biotechnol. 2001;9:7–12.

20. Ohga S, Cho N-S, Li Y, Royse DJ. Utilization of pulsed power to stimulate fructification of edible mushroom. Mushroom Sci. 2004;16:343–52.
21. Takaki K, Kanesawa K, Yamazaki N, Mukaigawa S, Fujiwara T, Takahasi K, Yamasita K, Nagane K. Effect of pulsed high-voltage stimulation on Pholiota nameko mushroom yield. Acta Phys Pol A. 2004;115:953–6.
22. Ohga S, Iida S. Effect of electric impulse on sporocarp formation of ectomycorrhizal fungus *Laccaria laccata* in Japanese red pine plantation. J For Res. 2001;6:37–41.
23. Islam F, Ohga S. The response of fruit body formation on *Tricholoma* matsutake in situ condition by applying electric pulse stimulator. ISRN Agron. 2012;462724:1–6.
24. Idei T, Yoshizawa N, Tako M. Effects of electric shocks to the bed-logs of Lentinus edodes on fruiting-body production (in Japanese). Bull Utsunomiya Univ Forests. 1988;24:23–38.
25. Takaki K, Kanesawa K, Yamazaki N, Mukaigawa S, Fujiwara T, Takahasi K, Yamasita K, Nagane K. Improvement of edible mushroom yield by electric stimulations. J Plasma Fusion Res Ser. 2009;8:556–9.
26. Mankowski J, Kristiansen M. A review of short pulse generator technology. IEEE Trans Plasma Sci. 2000;28:102–8.
27. Takahashi K, Miyamoto K, Takaki K, Takahashi K. Development of compact high-voltage power supply for stimulation to promote fruiting body formation in mushroom cultivation. Materials. 2018;11:2471.
28. Kobougias IC, Tatakis EC. Optimal design of a half-wave Cockcroft-Walton voltage multiplier with minimum total capacitance. IEEE Trans Power Electron. 2010;25:2460–8.
29. van Wetter M, Schuren F, Schuurs T, Wessels J. Targeted mutation of the SC3 hydrophobin gene of affects formation of aerial hyphae. FEMS Microbiol Lett. 1996;140:265–9.
30. Wessels JGH. Gene expression during fruiting in Schizophyllum commune. Mycol Res. 1992;96:609–20.

Chapter 15
Keeping Freshness of Agricultural Products

Katsuyuki Takahashi

Abstract Keeping freshness of agricultural products such as fruits and vegetables during postharvest period. Various effective methods for keeping freshness have been currently used; problems that cannot be solved using them alone still remain. Nonthermal plasma produces chemical species which has high oxidation potential, such as hydroxyl radicals, and can decompose chemical organic compositions and inactivate microorganisms. The high electric field generated by high voltage can collect floating particles, such as airborne bacteria, by a Coulomb force and allows it to move. These effects can contribute to keep freshness of fruits and vegetables by quickly and high efficiently removing the main factors of their quality deterioration, respiration, and spoilage driven by ethylene and microbial contaminations, which are expected as a new method. In this chapter, mechanisms of degradation of ethylene and microorganisms using atmospheric nonthermal plasma and its practical applications are introduced.

Keywords Fruits and vegetables · Ethylene · Airborne bacteria · Inactivation of bacteria · Nonthermal plasma · Dielectric barrier discharge · Corona discharge · Reactive oxygen species (ROS) · Reactive nitrogen species (RNS)

15.1 Introduction

Keeping freshness of agricultural products such as fruits and vegetables in food supply chain is very important topic for building a sustainable society in the world. The main factors of quality deterioration are respiration and spoilage driven by ethylene (C_2H_4) and microbial contamination. Since these effects can be suppressed in low temperature, a cold chain, a temperature-controlled supply chain, has been

K. Takahashi (✉)
Faculty of Science and Engineering, Iwate University, Morioka, Iwate, Japan

Agri-Innovation Center, Iwate University, Morioka, Iwate, Japan
e-mail: ktaka@iwate-u.ac.jp

S. Horikoshi et al. (eds.), *Agritech: Innovative Agriculture Using Microwaves and Plasmas*, https://doi.org/10.1007/978-981-16-3891-6_15

expanded, especially in developed countries. However, optimum temperature depends on the type of fruits and vegetables, and too low a temperature causes chilling injury. Also, controlled atmosphere (CA) storage and modified atmosphere packing (MAP) are methods to reduce ripening and aging of products by controlling gas composition surrounding fruits and vegetables, which contributes to suppression of C_2H_4 and microbial spoilage. Composition of all gas in the container and storage in the CA storage and the gas inside polymeric film package in the MAP are controlled. Recently, 1-methylcyclopropene (1-MCP), an effective and efficient ethylene inhibitor, has been used for suppression of C_2H_4 spoilage. The microbial spoilage is caused by bacteria and fungi such as mold and yeast. The microorganism contamination in preharvest period causes cultivation environments such as soil, irrigation water, and manure. In postharvest period, some microorganisms can move to other products from the contaminated stuffs via surface contact during storage and distribution [1, 2]. Furthermore, airborne microorganisms such as aerosolized bacteria can adhere on productions. There microorganisms cause not only quality losses but also health hazards by endotoxin and allergy [3]. The damage of products by microorganisms does not appear immediately, but appears over time during storage and distribution in postharvest period. Therefore, treatment of microorganisms after harvesting and during storage and distribution is very important. To control microorganism on the products, ozone and chlorine dioxide have been used as alternative methods to chemical treatments used in the past, such as ethylene oxide, formaldehyde, propylene oxide, and methyl bromide. Ultraviolet ray has been reported as an effective method to inactivate microorganism by inhibiting replication of DNA which has specific absorption at wavelength of 254 nm [4]. As mentioned above, various effective methods to suppress spoilage have been proposed; however, problems that cannot be solved using them alone still remain.

High voltage and plasma have been used for various agriculture and food processing applications such as improvement of plant growth and electrostatic spray of agricultural chemical [5, 6]. The radicals produced by atmospheric nonthermal plasma, which has a high chemical oxidation potential, can contribute to rapid decomposition of C_2H_4 and inactivation of microorganisms. The electric field generated by high-voltage power supply can contribute to collecting airborne bacteria, which can also improve the environment of storage fruits and vegetables. The atmospheric nonthermal plasma can be generated with a compact high-voltage power supply and electrode system, and the generation of it does not require a special environment, which realizes low cost and simple process with compact device. In this chapter, mechanisms of degradation of C_2H_4 and microorganisms using atmospheric nonthermal plasma and its practical applications are introduced.

15.2 Decomposition of Ethylene

C_2H_4 is a hormone in plants. It has an aging effect to fruits and vegetables, and excessive maturation due to prolonged exposure leads to deterioration in their quality. Some fruits and vegetables, such as apples, emit large amount of C_2H_4 into the air. The C_2H_4 emitted from the fruits and vegetables has also autotoxic effects. Thus, the C_2H_4 concentration should be kept low, e.g., less than 1 ppm during the transport of ethylene-sensitive fruits loaded together in one container and the long storage [7–9].

Table 15.1 presents the comparison of the C_2H_4 removal methods. C_2H_4 in the container and storage is usually removed by conventional methods such as venting and absorption. The venting is the easiest way to reduce C_2H_4 concentration. However, to keep freshness, the temperature inside the container and storage should be kept low and its fluctuation should be minimized. The exchange of large amount of gas leads the rapid temperature change, which leads the loos of freshness of fruits and vegetables. The absorption using absorbent materials can reduce C_2H_4 easily; however, its amount of absorption is limited by the size of the absorbent and their regeneration and disposal after use remain an issue. To overcome these limitations of conventional methods, various methods have been proposed. The ozonation is a method using the oxidation reaction of ozone (O_3) generated in an ozonizer. O_3 is a powerful oxidant, and the C_2H_4 in the gas is decomposed into by-products and finally CO_2 and H_2O via oxidation reactions. Although it is effective in removing ethylene, ozone has a harmful effect on not only fruits and vegetables as shown in Fig. 15.1 but also human body and damages the structure of container and storage [10–12]. Photocatalytic reaction is also effective in decomposition of ethylene. The photocatalytic reaction is induced on the surface of photocatalyst such as TiO_2, which is irradiated by ultraviolet lights. H_2O on the surface is reduced by the reaction, and hydroxyl radicals (OH) are produced. OH is one of the most powerful oxidants which can produce in an atmospheric air and has a much higher oxidation potential than O_3. C_2H_4 approached on the reaction zone on the surface can be rapidly decomposed. Because the reaction zone is limited on only the surface, this technology is much safer and less affected on fruits and vegetables. On the other

Table 15.1 Comparison of the C_2H_4 removal methods

	C_2H_4 removal speed	Safety	Size and weight	Performance stability	Operability
Venting	Excellent	Excellent	Good	Excellent	Inferior[a]
Absorption	Excellent	Excellent	Average	Inferior	Inferior
Photocatalyst	Inferior	Good	Inferior	Average	Excellent
Ozone	Inferior	Inferior	Good	Excellent	Inferior[b]
Plasma	Excellent	Good	Good	Excellent	Excellent

[a]Venting leads temperature change, which causes negative effect for keeping freshness of fruits and vegetables

[b]Ozone causeas injury on fruits and vegetables and damage to facility

Fig. 15.1 Apple injured by O_3

hand, since its reaction rate is not high, the large surface area is required for sufficient treatment, which makes the system large and heavy.

Discharges produce instantly nonthermal plasma. In the plasma, various powerful oxidants are produced with high density, and ethylene can be decomposed with very high reaction rate. For instance, the decomposition speed of 200 ppm ethylene by a plasma discharge system is on order of 10^{-7} mol/W s, which is approximately 3 orders higher than that of photocatalytic reactor ($\sim 3 \times 10^{-10}$ mol/W s) [13]. Additionally, the plasma is only produced by electricity, and its energy density in the plasma is very high, which has a high potential to make the system compact and light.

The generation of plasma is initiated by impact of electrons accelerated by electric field to molecules. When the electron has a sufficient energy for dissociation of oxygen molecules, oxygen radicals (O) are produced by following reaction.

$$e + O_2 \rightarrow 2O \tag{15.R1}$$

Since the oxidation potential of O is very high, C_2H_4 can be quickly oxidized as following reactions.

$$O + C_2H_4 \rightarrow CHO + CH_3 \tag{15.R2}$$

$$O + C_2H_4 \rightarrow CH_2CHO + H \tag{15.R3}$$

The rate constants of reactions (15.R2) and (15.R3) are $3.45 \times 10^{-18} \times T^{2.08}$ [cm^3/s] and $2.0 \times 10^{-18} \times T^{2.08}$ [cm^3/s], respectively, where T is a temperature [K]. When the air gas in which plasma is generated does not contain water molecules, above reactions mainly contribute to C_2H_4 decomposition. When the gas contains water molecules, OH is mainly generated by following reactions [14].

$$H_2O + O \rightarrow 2OH \quad (15.R4)$$

$$H_2O + e \rightarrow OH + H \quad (15.R5)$$

$$H_2O + e \rightarrow H^- + OH \quad (15.R6)$$

Here, because rate constant of reaction (15.R4) is $1.0 \times 10^{-11} \times \exp.(-550/T)$ [cm^3/s] and is much higher than that of (15.R5) and (15.R6), (15.R4) is main pathway for OH production in air gas. C_2H_4 can be decomposed by following reactions;

$$OH + C_2H_4 \rightarrow \text{products} \quad (15.R7)$$

The rate constant of (15.R7) is 8.0×10^{-12} [cm^3/s]. The C_2H_4 decomposition rate by the reactions (15.R2) and (15.R3) is expressed as

$$-d[C_2H_4]/dt = 7.7 \times 10^{-13} \times [O] \times [C_2H_4] \quad (15.1)$$

On the other hand, the ethylene decomposition rate by reaction (15.R7) is expressed as.

$$-d[C_2H_4]/dt = 8.51 \times 10^{-12} \times [OH] \times [C_2H_4] \quad (15.2)$$

The OH is short-lived radical; therefore, the ratio of O and OH radicals is estimated as O:OH = 1:0.048 in 80%RH air under the thermally equilibrium condition [15]. Therefore, the reaction rates of Eqs. (15.1) and (15.2) are the same order. As a result, the ethylene decomposition efficiency is almost independent of relative humidity [16].

As the ethylene decomposition process, the direct dissociation of ethylene by energetic electron (>3.5 eV) impact can be considered because the required energy of 3.5 eV to dissociate the C–H bond is lower than that for the O–H bond (4.5 eV). Generally, C_2H_4 concentration in container and storage ranges from several to several tens ppm. Therefore, the decomposition reaction of C_2H_4 caused by direct electron impact is almost negligible [12, 17].

In the plasma, O_3 is also produced by reactions between O and O_2 as a byproduct and also contributes to C_2H_4 decomposition through following reaction.

$$O + O_2 \rightarrow O_3 \quad (15.R8)$$

$$O_3 + C_2H_4 \rightarrow \text{products} \quad (15.R9)$$

Reaction rate of (15.R9) is $1.2 \times 10^{-14} \times (-2630/T)^2$ [cm^6/s] and is much lower than that of O and OH, and the reaction time for C_2H_4 decomposition is on order of several and several 10 s. Thus, to remove C_2H_4 by oxidation reactions induced by O_3, O_3 must be remained in the air gas inside container and storage, which become problem as disadvantage of ozonation already mentioned. In the container and

storage, CO_2 concentration increases with respiration of fruits and vegetables. In the plasma, CO_2 is reduced by electron impact and carbon monoxide (CO), which has a harmful effect on human body, is produced.

$$CO_2 + e \rightarrow CO + O + e \quad (15.R10)$$

These by-products are hazardous to the operator during opening container and storage. Therefore, they should be eliminated after plasma treatment and not be contained in the exhaust gas from the plasma chamber.

The catalysts with nonthermal plasma are effective to the by-products formed in the VOCs degradation [18, 19]. An Ag nanoparticle-loaded zeolite (Ag–zeolite) has high activity and good performance for the removal of CO and O_3. On the surface of Ag–zeolite catalyst, O_3 approached is reduced by Ag, and active oxygen species is formed as an active site [20–22]. In these active oxygen species formed by O_3 decomposition, oxidize CO into CO_2 through the following reactions;

$$O_3 + M* \rightarrow O_2 + M * O \quad (15.R11)$$

$$CO + M * O \rightarrow CO_2 + M* \quad (15.R12)$$

where M* represents the catalyst. The active sites are maintained for a long time. J. Nishimura et al. has performed experiments for removal of 200 ppm C_2H_4 diluted in the gas consisting of 10% O_2, 10% CO, and N2 balance with a gas flow of 5 L/min using dielectric barrier discharges [23]. When the input energy density in the gas is approximately 37 J/L, the almost C_2H_4 is decomposed, but O_3 and CO are produced at concentrations of 200 ppm and 150 ppm, respectively, without the Ag–zeolite catalyst. O_3 and CO concentrations decrease to less than 1 ppm and 100 ppm after the gas has passed through the Ag–zeolite catalyst. Therefore, O_3 and CO can be removed at same time. The active site on the catalyst also contributes to C_2H_4 decomposition. Not only Ag–zeolite but also manganese dioxide (MnO_2) catalyst, which used for O3 decomposition catalyst, has the similar effect for O_3 and C_2H_4 decomposition [14].

Different types of discharges have been used to generate nonthermal plasma. DC or AC corona-type discharge generates small localized nonthermal plasma at needle tips and vicinity of wire electrodes. Because corona electrodes can be easily and simply consisted with needles and conventional DC or AC high-voltage power supply can be adapted, the corona discharge system can be easy to install and robust against contaminations. On the other hand, the volume of plasma is localized, reaction area for C_2H_4 decomposition is limited, and the miniaturization of the system is difficult.

Dielectric barrier discharge (DBD) is one of methods to produce the nonthermal plasma at atmospheric pressure. The DBD is usually generated between two electrodes, of which at least one is covered by a dielectric barrier such as ceramics, with a voltage of AC or pulse applied to these electrodes [24, 25]. The DBD is characterized by a high electron temperature of 10 eV and a high electron density of 10^{20} m^{-3}

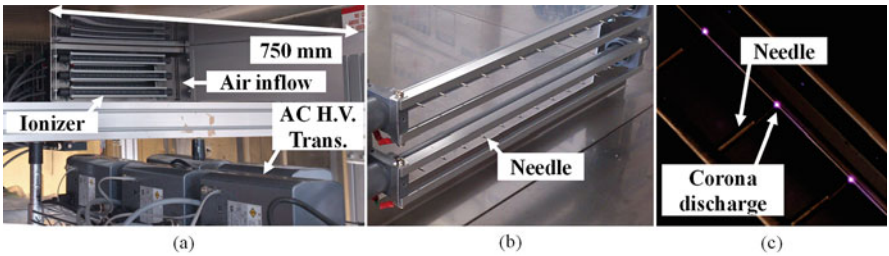

Fig. 15.2 Photographs of corona discharge-type C_2H_4 removal devices (**a**) installed in a container, (**b**) ionizer unit in the device, and (**c**) corona discharges

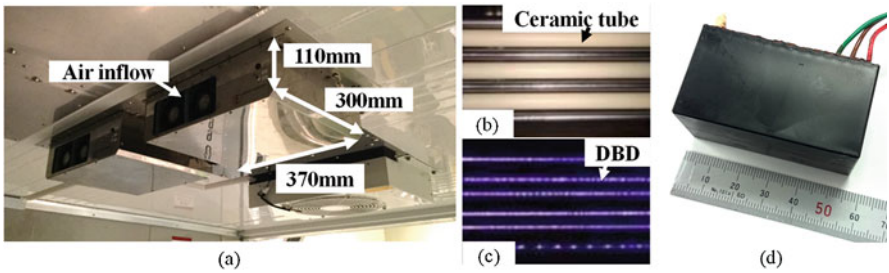

Fig. 15.3 Photographs of DBD-type C_2H_4 removal devices (**a**) installed in a container, (**b**) electrode system, (**c**) DBD, and (**d**) compact winding transformer

in comparison to DC corona discharge [26, 27]. Therefore, the ethylene decomposition efficiency of the DBD is approximately two orders higher than that of the DC corona discharge. Generally, the gap length of the electrodes is usually less than 1 mm. Because the dielectric barrier can inhibit the arc transition by extinguishing the discharges by canceling electric field in the gap with the accumulated charges on it, discharges are steadily generated in the same polarity phase of applied voltage at large area of electrode. In the gap, a lot of discharge columns are generated with slightly low-frequency voltage because of self-organization. The nanosecond pulse voltages with high voltage rise speed can make the discharges uniform [28]. Additionally, the reduced electric field increases with increasing the discharge time lag by increasing voltage rise speed, which enhances the radical production by electron impacts as shown in reactions (15.R1) [28].

Figs. 15.2 and 15.3 show the ethylene removal devices utilizing corona discharge and DBD, respectively, for a 20-ft refer container. The devices are consisted of fans to vacuum air inside container and storage, discharge electrodes, and catalysts. The gas treated by discharges passes through the catalysts to eliminate by-products of plasma treatment such as O_3 and CO_2 in the gas. The corona discharge-type electrode consists of a bar-type ionizer (Shishido electrostatic, BOS-400) driven by AC high-voltage transformer at commercial frequency (Shishido electrostatic, SAT-11) with an amplitude of ± 7.3 kV. The ionizer has 13 corona needles as shown in Fig. 15.2b, and corona discharge occurs at the tip of each electrodes as shown in

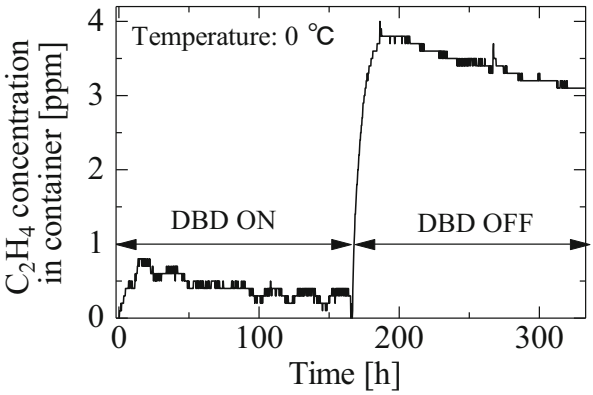

Fig. 15.4 C_2H_4 concentration in container with operation of DBD-type C_2H_4 removal device during transportation

Fig. 15.2c. The number of the ionizer installed in the device is 10. The DBD-type electrode consists of multiparallel rod electrodes covered by ceramic tube with a gap length of 1 mm as shown in Fig. 15.3b, and DBD occurs in the gap as shown in Fig. 15.3c [6]. The AC voltage with an amplitude of ±7.5 kV and a frequency of 500 Hz generated by a compact winding transformer (Shishido electrostatic, Fig. 15.3d) driven by an inverter circuit consisted of MOFETs [29] is applied to the electrodes. The C_2H_4 removal rate of both devices is approximately 60 mg/h with a C_2H_4 concentration of 100 ppm. The corona discharge-type device has approximately a height of 200 mm, a width of 750 mm, and length of 1500 mm, and 5 AC high-voltage transformers, each having a height of 220 mm, a width of 90 mm, and length of 110 mm in size, need to be installed externally. DBD-type device has a height of 110 mm, a width of 370 mm, and length of 300 mm, including internal compact high-voltage power supply system. These indicate that DBD type can be designed to be compact. Figure 15.4 shows the C_2H_4 concentration in the 20-ft container in which fruits and vegetables are mix-loaded and DBD-type C_2H_4 removal system is installed. The C_2H_4 concentration can be kept at low less than 1 ppm with the system operation.

15.3 Removal and Inactivation of Bacteria

In the food industry, foods are contaminated by adhering microorganisms composed of bacteria and fungi via surface contact and via the air, which is composed of bacteria and fungi. The contamination of vegetables surface with bacteria cannot be excluded, because anything that comes into contact with vegetables has the potential to cause contamination. Possible sources of contamination are soil, water, handling of the products, harvesting, processing equipment, and airborne bacteria [30]. For example, in a rice storage facility, the concentration of microorganisms such as aerobic bacteria, molds, and yeasts is 500–2000 CFU/m^3 and increases 10 to 100 times in a harvest season [31], which is a food safety issue.

Thus, it is necessary to reduce the contamination by the inactivation of bacteria to avoid decay. The numbers of viable bacteria and coliform bacteria groups are closely related to potential danger of food poisoning and epidemic diseases. Thus, they are generally treated as the indicator of hygienic quality and environmental pollution [32].

Generally, technologies such as air filtration, UV irradiation, chemical aerosolization, and ozone treatment have been practically used to control microorganisms, while they have limitations on the waste disposal treatment and the inactivation rate and speed. Plasma treatment system using high-voltage power supply can contribute to the quick and efficient control of airborne microorganism contaminations with two effects: microorganism removal by the electrostatic precipitation effect and inactivation by chemical active species reactions.

15.3.1 Removal of Airborne Bacteria

Electrical precipitation is a particle collection technique using electrostatic force with a high collection efficiency and has been widely used in industry for environmental protection [33, 34]. It has been used for cleaning indoor air to collect fungi and pollen dusts in the healthcare applications. The electrical precipitator (ESP) consists of paired high-voltage and grounded electrodes where the electric field is generated between the electrodes. The electrical charged particles between the electrodes move along the electric field toward the electrode surface. When the particle is not naturally charged, the corona discharge is used to charge the particle by diffused ions [35]. The corona discharge occurs around the negative high-voltage wire electrode. Negative ions diffused from the corona discharge charge the particles. The particle collection efficiency can be estimated by the following equation [36]:

$$\eta\,(\%) = 1 - \exp\,(-\omega A/Q)^k \tag{15.3}$$

where ω is the effective migration velocity of particles, A is the total surface area of collecting electrodes, Q is the gas flow rate, and k is a constant value which depends on types of particle and ranges from 0.4 to 0.6. This equation is well-known Deutsch–Anderson equation modified by S. Matt and P.O. Öhnfeldt. ω can be estimated by following equations [37]:

$$\omega = (qE/6\pi\mu a)C_{\mathrm{m}} \tag{15.4}$$

$$C_{\mathrm{m}} = 1 + \alpha\lambda/a \tag{15.5}$$

where q is particle charge, E is electric field, μ is gas velocity, a is particle radius, C_{m} is the Cunningham correction to Stokes's law, λ is the mean free path of the gas molecules, and α is a dimensionless parameter. In the normal temperature and pressure, λ and α are 0.069 μm and 0.86, respectively. Because the estimation of ω

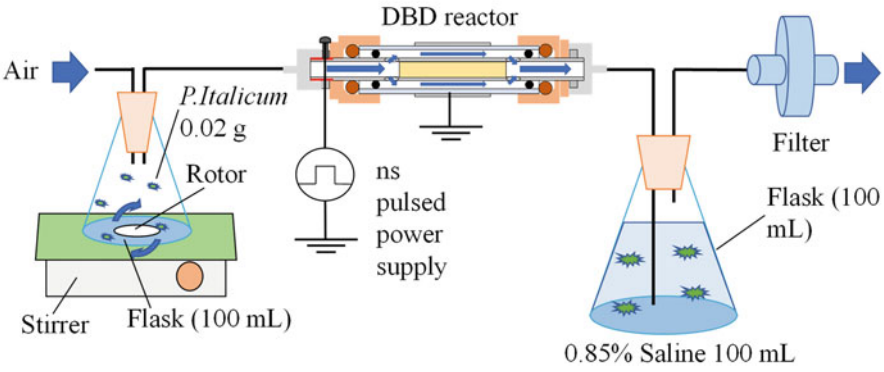

Fig. 15.5 Evaluation system for collecting *P. italicum* spores using DBD

is difficult due to the influence of the ionic wind and complicated calculations of the electric field from the Laplace and Poisson equations considering ions and particles charges, ω is practically estimated from the particle collection efficiency as an apparent velocity. The diameter of airborne microorganism particles ranges from 0.5 to 20 μm, and the airborne microorganism can be efficiently collected by ESP. Because the most of microrganisms are negatively charged [38]. Furthremore, the corona onset voltage of negative polarity is lower than that of positive polarity. Therefore, the negative DC voltage is preferred than the positive for volatage polarity used in ESP for collecting airborne bacteria.

As an example of the use of the ESP, S. Koide et al. have developed an ESP device for collecting ground rice husks contaminated by microorganisms such as bacteria, molds, and yeasts [39]. In the system, ESP consists of wire-to-cylinder electrode with a 36 inner diameter and 300 mm length. A DC high voltage of −6 kV is applied to the wire electrode. The corona current is approximately several μA, and the consumed energy is less than 1 mW. The average size of the particle is 130 μm, and the particle collection efficiency reaches 90%. The microbial removal efficiency which includes microbial collection is approximately 99.95% higher than the collection efficiency. Although the corona discharge is usually used for charging particles, DBD is also effective. T. Kikuchi et al. have reported the DBD reactor for collecting fungal spores [40]. Fig. 15.5 shows evaluation system for collecting *P. italicum* spores using DBD. The spores aerosolized by a rotor rotated by a stirrer are treated by a coaxial cylinder-type DBD as shown in Fig. 15.6a. The DBD reactor has a coaxial cylinder composed of a stainless tube applied high voltage with a 16 mm outer diameter, a glass tube with a 19 mm inner diameter on which 10-mm grounded aluminum tape rapped. *P. italicum* aerosolized in the sample gas is adhered on the surface of the DBD reactor by ESP effects as shown in Fig. 15.6b. The number of colonies of *P. italicum* detected in the flask with and without plasma is 1.7 and 4.2 CFU/mL, respectively, indicating that the spores are adhered to inside of the DBD reactor. These results show that gas treatment system utilizing

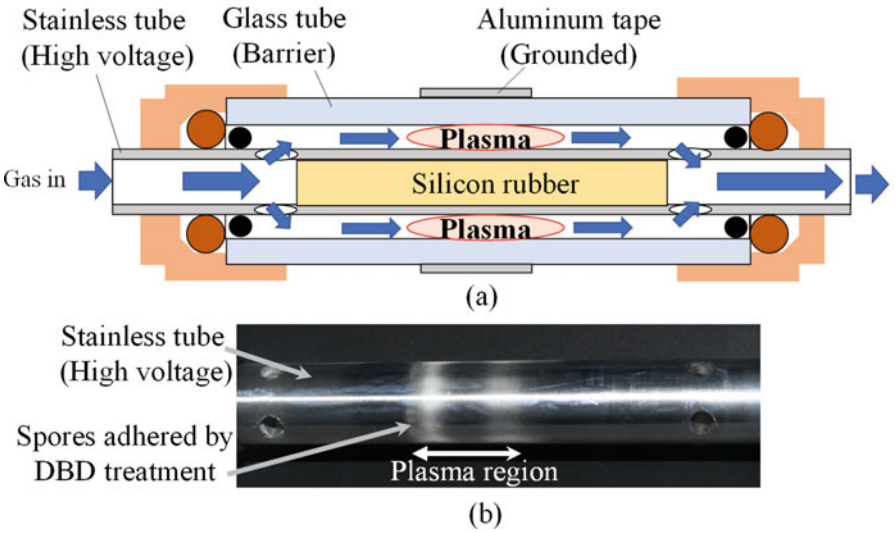

Fig. 15.6 (**a**) Cross-sectional view of DBD reactor and (**b**) photograph of stainless tube used as high-voltage electrode after collecting *P. italicum* spores by plasma

nonthermal plasma generated by DBD is effective for not only C_2H_4 removal as mentioned previously but also removal of airborne bacteria, which can contribute to keeping freshness of fruits and vegetables in container and storage.

15.3.2 Inactivation of Bacteria

Many studies have been performed on the inactivation of bacteria such as *E. Coli, S. Aureus, B. Atrophaeus* and *Salmonella* on agar plates [41–43] and surfaces of fruits and vegetables such as apples [44], using direct plasma irradiation systems with an irradiation time on the order of 10–10^3 s. The nonthermal plasma generated by discharges produces various kinds of chemical species and charged particles instantaneously and emits UV light through chemical reactions inside plasma [45–48]. The diffusion of generated reactive species into the cell leads significant damage to cell membrane and major cell constituent [49]. The reactive oxygen species (ROS) such as the OH, generated by reactions in the plasma as shown in (15.R4), have high oxidation potentials.

Due to the strong oxidizing ability of ROS, various kinds of components of cell react with ROS and cause some irreversible changes in the cell, leading to the destruction of dehydrogenase and breaking respiratory system down of the cell in microorganisms. The main reaction of this phnomenon is the oxidation of SH-group, lipid, protein, DNA and RNA through oxidation reactions by ROS which contributes

to the inactivation of bacteria [50]. The amino acid side chains can be easily oxidized by ROS [51]. When the ROS attack the polyunsaturated fatty acids in the cell membrane, the lipid peroxidation chain reaction is initiated, which causes the membrane rupture [50]. The hydroxyl radical causes the DNA damage through the oxidation of the sugar moiety leading to DNA destruction. Since the life time of hydroxyl radical is very short and its diffusion length is several tens of mm in the gas phase and on the order of 10^{-5}–10^{-6} m in the aqueous phase [52], the hydrogen peroxide produced from the hydroxyl radical and the superoxide in the aqueous phase may mediate the oxidation reaction via Fenton reactions [51]. DNA damage is also caused by the direct attack of ROS through the lipid peroxidation that react with DNA [33, 50]. The DNA damage can lead to necrotic cell death [53]. In addition, the cell membrane disorder happens due to the oxidation of the unsaturated fatty acid residue in the cell wall and the cell membrane, leading the intracellular component leakage.

In the case of airborne bacteria, the inactivatioin of bacetria by ozone takes 10^{2}–10^{3} s because of its low reaction rate and the high concentration of ozone has to be retained, which has same disadvantage of the ozone treatment methods. The reaction rate of hydroxyl radical with bacteria is approximately 10^{3}–10^{4} higher than that of ozone and can be major player for inactivation in plasma with short residence time [54]. Furthermore, the hydroxyl radical reaction can be enhanced by the synergistic effects of other ROS such as the ozone and the atomic oxygen [55]. The humidity is the important factor for not only ROS production but also the inactivation path way. The hydroxyl radical and the superoxide dissolve into the aerosol aqueous solution and are converted to more stable hydrogen peroxide (H_2O_2), which involves the oxidative damage of bacteria, through following reaction.

$$\mathrm{OH} + \mathrm{OH} \rightarrow \mathrm{H_2O_2} \tag{15.R13}$$

Two regulatory oxidation stresses mediated by superoxide dismutase and catalase are suggested for mechanism of efficient inactivation of airborne bacteria [56]. The bacteria can be electrically charged by charged particles generated in the plasma, such as ions of both polarities and electrons. The charged species have significant role in the inactivation via synergy effects of other chemical species. The charged particles damage the membrane by pores opening in order of several microseconds by localized high electric field [57] and/or by the etching effect through ion bombardment at relative high energies [58], which enhances the oxidation reaction by the ROS. This synergy effect also enhances the O_3 reaction and makes the O_3 act on the bacteria [56].

Superoxide anion radical (O_2^-) is generated by electron attachment inside plasma. When O_2^- dissolved into the water under acidic condition, hydroperoxyl radical (HOO) is generated.

$$\mathrm{e} + \mathrm{O_2} \rightarrow \mathrm{O_2}^- \tag{15.R14}$$

Table 15.2 Number of bacteria with various O_3 treatment

Treatment	O_3 concentration	Type of bacteria	Treatment time	Survival rate	Ref.
Treatment on sprout	0.02 ppm	Viable	Until sample sprout	0.01	[60]
		Coliform		0.002%	
Mix with ozone water	0.25 mg/10^9 cells	*E. Coli*	20 s to 5 min	72%	[61]
	0.65 mg/10^9 cells			40%	
	1.9 mg/10^9 cells			6%	[62]
Ozone water sparging	0.68 mg/L (Water)	*E. faecalis*	120s	0.753%	
Surface treatment on broccoli	40 ppm (1.28 mg in 60 s)	Viable	60s	19.95%	[63]
		Coliform		2.51%	

$$O_2^- + H^+ \rightarrow HOO \tag{15.R15}$$

The pKa of this reaction is 4.8. Because HOO is electrically neutral, it easily permeates into the cell membrane and causes damage of lipids and proteins in cells and inactivation of enzymes, which contributes to inactivation of bacteria [33, 59]. Therefore, the solution treated by plasma at low pH has a powerful inactivation effect. In the case of inactivation of bacteria in liquid phase, O_3 contribute to the inactivation because of longer liftime than OH and HOO. Table 15.2 shows the numbers of bacteria with various O_3 treatments [60–63]. From the table, over 99% of the viable bacteria and the coliform bacteria are inactivated by the O_3 treatment, which shows the O_3 is capable of inactivating both of these bacteria. In addition, with the same concentration of O_3, the coliform bacteria have a lower number compared with the viable bacteria which show that the coliform bacteria are weaker than the viable bacteria against ozone. This is because 15% of the dry weight of coliform bacteria is cell wall, and of the cell wall, 23% is lipid and 13% is phospholipid [61]. This ingredient content of coliform bacteria makes them react with O_3 easier than other bacteria.

Not only ROS, but also reactive nitrogen species (RNS) can be key inactivation agents which causes cell damage and inactivation. Because RNS have long lifetime in liquid phase, RNS generated by plasma treatment remain for a long time in the solution after nonthermal plasma irradiation. It has been reported that nonthermal plasma-activated water (PAW), water irradiated by nonthermal plasma, can inactivate bacteria on the surface of fruits and vegetables [64] such as strawberries [65], mushroom [66], and endives [67], which contribute to keep freshness. Various RNS include nitric oxide (NO), nitrites (NO_2^-), nitrates (NO_3^-), peroxynitrite ($ONOO^-$), and peroxynitric acid (O_2NOOH) generated by following equations, which are proposed as the dominant species for bacteria inactivation [68–71].

$$N_2 + e \rightarrow N\left(^4S\right) + N\left(^2D\right) \tag{15.R16}$$

$$H + O_2 \rightarrow HO_2 \quad (15.R17)$$

$$O_3 + OH \rightarrow HO_2 \quad (15.R18)$$

$$N(^2D) + O_2 \rightarrow NO + O(^1D) \quad (15.R19)$$

$$N(^2D) + O_2 \rightarrow NO + O(^3P) \quad (15.R20)$$

$$O(^3P) + NO + N_2 \rightarrow NO_2 + N_2 \quad (15.R21)$$

$$O_3 + NO \rightarrow NO_2 + O_2 \quad (15.R22)$$

$$OH + NO + M \rightarrow HNO_2 \quad (15.R23)$$

$$OH + NO_2 \rightarrow HNO_3 \quad (15.R24)$$

$$3HNO_2 \rightarrow HNO_3 + 2NO + H_2O \quad (15.R25)$$

$$HO_2 + NO_2 \rightarrow O_2NOOH \quad (15.R26)$$

$$H_2O_2 + HNO_2 \rightarrow HOONO + H_2O \quad (15.R27)$$

$$HOONO + H_2O_2 \rightarrow O_2NOOH + H_2O \quad (15.R28)$$

NO_2^- and NO_3^- are produced by dissolving nitrous (HNO_2) and nitrite (HNO_3) acids into the solution through following reactions, which contribute to decrease pH [71, 72].

$$HNO_2 \rightarrow H^+ + NO_2^- \quad (15.R29)$$

$$HNO_3 \rightarrow H^+ + NO_3^- \quad (15.R30)$$

$HOONO_2$ contributes to HOO production via equilibrium decomposition reaction [73].

$$HOONO_2 \rightarrow HOO + NO_2 \quad (15.R31)$$

Therefore, $HOONO_2$ has an important role under acidic conditions.

15.4 Conclusions

The high-voltage and plasma applications to keep the freshness and quality of agricultural products during postharvest period and their mechanisms are described. DBD generates nonthermal plasmas, in which chemical oxidants having high oxidation potential such as oxygen and hydroxyl radicals are generated, and can treat ethylene gas quickly and high efficiently with compact devise size. Not only these radicals but also reactive oxygen and nitrogen species with long lifetime such as ozone and peroxynitric acid can contribute to inactivation of bacteria directly and

indirectly. Electric field generated by high voltage gives a floating particle, such as airborne bacteria, a Coulomb force and allows it to move. The airborne bacteria can be collected by these effects quickly. Although some mechanism such as biological responses to radicals is still an open question, high voltage and plasma show their powerful effects for keeping freshness of agricultural products.

References

1. Pachepsky Y, Shelton DR, McLain JET, Patel J, Mandrell RE. Irrigation waters as a source of pathogenic microorganisms in produce: A review. Adv Agron. 2011;113:73.
2. Castro-Ibáñez MIG, Allende A. Ready-to-eat vegetables: Current problems and potential solutions to reduce microbial risk in the production chain. LWT-Food Sci Technol. 2017;85:284.
3. Dutkiewicz J, Krysińska-Traczyk E, Skórska C, Sitkowska J, Prażmo Z, Golec M. Exposure to airborne microorganisms and endotoxin in herb processing plants. Ann Agric Environ Med. 2001;8:201.
4. Kujundzic E, Matalkah F, Howard CJ, Hernandez M, Miller SL. UV air cleaners and upper-room air ultraviolet germicidal irradiation for controlling airborne bacteria and fungal spores. J Occup Environ Hyg. 2006;3:536.
5. Takaki K, Hayashi N, Wang D, Ohshima T. High-voltage technologies for agriculture and food processing. J Phys D Appl Phys. 2019;52:473001.
6. Takaki K, Takahashi K, Hamanaka D, Yoshida R, Uchino T. Function of plasma and electrostatics for keeping quality of agricultural produce in post-harvest stage. Jpn J Appl Phys. 2021;60:010501.
7. Abeles F, Morgan P, Saltveit M Jr. Ethylene in plant biology. San Diego, CA: Academic Press; 1992. p. 182.
8. Kader A, Zagory D, Kerbel EL. Modified atmosphere packaging of fruits and vegetables. Crit Rev Food Sci Nutr. 1989;28:1.
9. Silva FM, Chau KV, Brecht JK, Sargent SA. Modified atmosphere packaging for mixed loads of horticultural commodities exposed to two postharvest temperatures. Postharvest Biol Technol. 1999;17:1.
10. Moretti CL, Mattos LM, Calbo AG, Sargent SA. Climate changes and potential impacts on postharvest quality of fruit and vegetable crops: A review. Food Res Int. 2010;43:1824.
11. Skog LJ, Chu CL. Effect of ozone on qualities of fruits and vegetables in cold storage. Can J Plant Sci. 2001;81:773.
12. Orlandini I, Riedel U. Chemical kinetics of NO removal by pulsed corona discharges. J Phys D. 2000;33:2467.
13. Yamazaki S, Tanaka S, Tsukamoto H, Photochem J. Kinetic studies of oxidation of ethylene over a TiO_2 photocatalyst. Photobiol-A. 1999;121:55–61.
14. Takahashi K, Motodate T, Takaki K, Koide S. Influence of oxygen concentration on ethylene removal using dielectric barrier discharge. J Jpn Appl Phys. 2017;57:01AG04.
15. Peyrous R. The effect of relative humidity on ozone production by corona discharge in oxygen or air – a numerical simulation – Part II: Air. Ozone Sci Eng. 1990;12:41.
16. Takaki K, Mirura T, Oka A, Takahashi K. Influence of relative humidity on ethylene removal using dielectric barrier discharge. IEEE Trans Plasma Sci. 2021;49:61–8.
17. Takaki K, Urashima K, Cheng JS. Ferro-Electric pellet shape effect on C_2F_6 removal by a packed bed type non-thermal plasma reactor. IEEE Trans Plasma Sci. 2004;32:217.
18. Yu Q, Kong M, Liu T, Fei J, Zheng X. Characteristics of the decomposition of CO_2 in a dielectric packed-bed plasma reactor. Plasma Chem Plasma Process. 2012;32:153–63.

19. Kim HH, Oh SM, Ogata A, Futamura S. Decomposition of gas-phase benzene using plasma-driven catalyst (PDC) reactor packed with Ag/TiO_2 catalystAppl Catal B Environ. 2005;56 (3):213–20.
20. Sano T, Negishi N, Sakai E, Matsuzawa S. Contributions of photocatalytic/catalytic activities of TiO_2 and γ-Al_2O_3 in nonthermal plasma on oxidation of acetaldehyde and CO. J Mol Catal A. 2006;245:235.
21. Teramoto Y, Kim H-H, Ogata A, Negishi N. Study of plasma-induced surface active oxygen on zeolitesupported silver nanoparticles. Catal Lett. 2013;143:1374.
22. Gervasini A, Vezzoli GC, Ragaini V. VOC removal by synergic effect of combustion catalyst and ozone. Catal Today. 1996;29:449.
23. Nishimura J, Takahashi K, Takaki K, Koide S, Suga M, Orikasa T, Teramoto Y, Uchino T. Removal of ethylene and by-products using dielectric barrier discharge with Ag nanoparticle-loaded zeolite for keeping freshness of fruits and vegetables. Trans Mater Res Soc Jpn. 2016;41:41–5.
24. Fang Z, Ji S, Pan J, Shao T, Zhang C. Electrical model and experimental analysis of the atmospheric-pressure homogeneous dielectric barrier discharge in He. IEEE Trans Plasma Sci. 2012;40(3):883–91.
25. Takaki K, Shimizu M, Mukaigawa S, Fujiwara T. Effect of electrode shape in dielectric barrier discharge plasma reactor for NOx removal. IEEE Trans Plasma Sci. 2004;32(1):32–8.
26. Eliasson B, Kogelschatz U. Nonequilibrium volume plasma chemical processing. IEEE Trans Plasma Sci. 1991;19:1063.
27. Wang P, Fan F, Zirilli F, Chen J. A hybrid model to predict electron and ion distributions in entire interelectrode space of a negative corona discharge. IEEE Trans Plasma Sci. 2012;40:421.
28. Miura T, Takahashi K, Takaki K, Nisida Y. Influence of waveform of applied voltage on H_2 production from methane reforming using dielectric barrier discharge. IEEE Trans Plasma Sci. 2021;49:147–53.
29. Takahashi K, Takaki K, Hiyoshi I, Enomoto Y, Yamaguchi S, Nagata H. Modern applications of electrostatics and dielectrics; Chapt. Development of a corona discharge ionizer utilizing high-voltage AC power supply driven by PWM inverter for highly efficient electrostatic elimination. London: IntechOpen Ltd.; 2019. isbn:978-1-78984-557-0.
30. Johannessen GS, et al. Hilde Kruse bacteriological analysis of fresh produce in Norway. Int J Food Microbiol. 2002;77:199–204.
31. Koide S, Yasokawa D, Omoe K, Uchino T. Concentration of airborne microorganisms in a rice storage facility. J JSAM. 2012;74:244.
32. Nakamura H, Ogasawara J, Yasufuku K, Arikawa K, Ohyama M, Abe N, Hase A. Identification and comparison of isolated from several coliform group detection agar medium. Jpn J Food Microbiol. 2012;30(2):164–9.
33. Mizuno A. Electrostatic precipitation. IEEE Trans Dieletr Electr Insul. 2000;7:615.
34. Huang Y, Li S, Zheng Q, Shen X, Wang S, Han P, Liu Z, Yan K. Recent progress of dry electrostatic precipitation for PM2.5 emission control from coal-fired boilers. Int J Plasma Env Sci Technol. 2015;9:69.
35. Sudrajad A, Fitri A. Review of electrostatic precipitator device for reduce of diesel engine particulate matter. Energy Procedia. 2015;68:370.
36. Matts S, Öhnfeldt PO. Efficient gas cleaning with SF precipitators. Flakten Rev. 1964;6:93.
37. White HJ, White HJ. Electrostatic precipitation of fly ash. J Air Pollut Control Assoc. 2012;15:2470.
38. Mainelis G, Adhikari A, Willeke K, Lee S. Collection of airborne microorganisms by electrostatic precipitation. J Aerosol Sci. 2002;33:1417.
39. Koide S, Nakagawa A, Omoe K, Takaki K, Uchino T. Physical and microbial collection efficiencies of an electrostatic precipitator for abating airborne particulates in postharvest agricultural processing. J Electrost. 2013;71:734.

40. Kikuchi T, Guionet A, Takahashi K, Takaki K, Ishida S, Terazawa T. Elimination of airborne fungi using dielectric barrier discharges driven by a pulsed power generator. Plasma Med. 2020;10:169–80.
41. Sun P, Sun Y, Wu H, Zhu W, Lopez JL, Liu W. Atmospheric pressure cold plasma as an antifungal therapy. Appl Phys Lett. 2011;98:021501.
42. Fernández A, Thompson A. The inactivation of Salmonella by cold atmospheric plasma treatment. FRIN. 2012;45:678.
43. Kwon T, Chandimali N, Lee DH, Son Y, Yoon SB, Lee JR, Lee S, Kim KJ, Lee SY, Kim SY, Jo YJ, Kim M, Park BJ, Lee JK, Jeong DK, Kim JS. Potential applications of non-thermal plasma in animal husbandry to improve infrastructure. In Vivo. 2019;1010:999.
44. Kilonzo-nthenge A, Liu S, Yannam S, Patras A. Atmospheric cold plasma inactivation of salmonella and escherichia coli on the surface of golden delicious apples. Front Nutr. 2018;5:120.
45. Herron JT, Green DS. Chemical kinetics database and predictive schemes for humid air plasma chemistry. Part I: Positive ion–molecule reactions. Plasma Chem Plasma Process. 2000;21:235.
46. Herron JT, Green DS. Chemical kinetics database and predictive schemes for nonthermal humid air plasma chemistry. Part II. neutral species reactions. Plasma Chem Plasma Process. 2001;21:459.
47. Nakagawa Y, Ono R, Oda T. Effect of discharge polarity on OH density and temperature in coaxial-cylinder barrier discharge under atmospheric pressure humid air. Jpn J Appl Phys. 2018;57:1.
48. Lowke JJ, Morrow R. Theoretical analysis of removal of oxides of sulphur and nitrogen in pulsed operation of electrostatic precipitators. IEEE Trans Plasma Sci. 1995;23:661.
49. Lu H, Patil S, Keener KM, Cullen PJ, Bourke P. Bacterial inactivation by high-voltage atmospheric cold plasma: influence of process parameters and effects on cell leakage and DNA. J Appl Microbiol. 2014;116:784.
50. Gaunt LF, Beggs CB, Georghiou GE. Bactericidal action of the reactive species produced by gas-discharge nonthermal plasma at atmospheric pressure: A review. IEEE Trans Plasma Sci. 2006;34:1257.
51. Han X, Cantrell W, Escobar EE, Ptasinska S. Plasmid DNA damage induced by helium atmospheric pressure plasma jet. Eur Phys J D. 2014;68:46.
52. Takahashi K, Kawamura S, Yagi I, Akiyama M, Takaki K, Satta N. Influence of reactor geometry and electric parameters on wastewater treatment using discharge inside a bubble. Int J Plasma Env Sci Technol. 2019;13:74.
53. Hirst AM, Simms MS, Mann VM, Maitland NJ, Connell DO, Frame FM. Low-temperature plasma treatment induces DNA damage leading to necrotic cell death in primary prostate epithelial cells. Br J Cancer. 2015;112:1536.
54. Gallagher MJ, Vaze N, Gangoli S, Vasilets VN, Gutsol AF, Milovanova TN, Anandan S, Murasko DM, Fridman AA. Rapid inactivation of airborne bacteria using atmospheric pressure dielectric barrier grating discharge. IEEE Trans Plasma Sci. 2007;35:1501.
55. Liang Y, Sun YWK, Chen Q, Shen F, Zhang J, Yao M, Zhu T, Fang J. Rapid inactivation of biological species in the air using atmospheric pressure nonthermal plasma. Environ Sci Technol. 2012;46:3360.
56. Vaze ND, Park S, Brooks AD, Fridman A, Joshi G. Involvement of multiple stressors induced by non-thermal plasma-charged aerosols during inactivation of airborne bacteria. PLoS One. 2017;12:e0171434.
57. Noyce JO, Hughes JF. Bactericidal effects of negative and positive ions generated in nitrogen on Escherichia coli. J Electrost. 2002;54:179.
58. Hyuk J, Han I, Baik HK, Lee MH, Han DW, Park JC, Lee IS, Song KM, Lim YS. Analysis of sterilization effect by pulsed dielectric barrier discharge. J Electrost. 2006;64:17.
59. Takai E, Kitamura T, Kuwabara J, Ikawa S, Yoshizawa S, Shiraki K, Kawasaki H, Arakawa R, Kitano K. Chemical modification of amino acids by atmospheric-pressure cold plasma in aqueous solution. J Phys D Appl Phys. 2014;47:285403.

60. Naito S, Shiga I. Studies on utilization of ozone in feed preservation. 9. Effect of ozone treatment on elongation of hypocotyl and microbial counts of bean sprouts. Nippon Shokuhin Kagaku Kaishi. 1989;36:181–8.
61. Scott M, et al. Effect of ozone on survival and permeability of Escherichia coli. J Bacteriol. 1963;85:567–76.
62. Hems RS, Gulabivala K, Ng YL, Ready D, Spratt DA. An in vitro evaluation of the ability of ozone to kill a strain of Enterococcus faecalis. Int Endod J. 2005;38:22.
63. Hui Y, Oikawa R, Takahashi K, Takaki K, Aoki H. Inactivation of bacteria adhering to vegetables using discharge in water. IJPEST. 2019;12:97–102.
64. Schnabel U, Andrasch M, Weltmann K. Inactivation of vegetative microorganisms and Bascillus atrophaeus endospores by reactive nitrogen species (RNS). Plasma Process Polym. 2014;11:110–6.
65. Ma R, Wang G, Tian Y, Wang K, Zhang J, Fang J. Non-thermal plasma-activated water inactivation of food-borne pathogen on fresh produce. J Hazard Mater. 2015;300:643–51.
66. Xu Y, Tian Y, Ma R, Liu Q, Zhang J. Effect of plasma activated water on the postharvest quality of button mushrooms, Agaricus bisporus. Food Chem. 2016;197:436–44.
67. Andrasch M, Stachowiak J, Schlüter O, Schnabel U, Ehlbeck J, Scale-up to pilot plant dimensions of plasma processed water generation for fresh-cut lettuce treatment. Food Pack J. Shelf Life. 2017;14:40–5.
68. Kim HN, Prieto G, Takashima K, Katsura S, Mizuno A. Performance evaluation of discharge plasma process for gaseous pollutant removal. J Electrost. 2002;55:25.
69. Soloshenko IA, Tsiolko VV, Pogulay SS, Kalyuzhnaya AG, Bazhenov VY, Shchedrin AI. Effect of water adding on kinetics of barrier discharge in air. Plasma Sources Sci Technol. 2009;18:045019.
70. Komuro A, Ono R, Oda T. Behavior of OH radicals in an atmospheric-pressure streamer discharge studied by two-dimensional numerical simulation. J Phys D Appl Phys. 2013;46:175206.
71. Machala Z, Tarabova B, Hensel K, Spetolikova E, Sikurova L, Lukes P. Formation of ROS and RNS in water electro-sprayed through transient spark discharge in air and their bactericidal effects. Plasma Process Polym. 2013;10:649–59.
72. Warneck P. Chemical reactions in clouds. Fresenius J Anal Chem. 1991;340:585.
73. Regimbal JM, Mozurkewich M, Phys J. Peroxynitric acid decay mechanisms and kinetics at low pH. Chem A. 1997;101:8822–9.

Chapter 16
Enzyme Activity Control and Protein Conformational Change

Takamasa Okumura

Abstract Controlling the enzyme activity shows potential for significant contributions to the pre−/postharvest food industry. In this chapter, the physicochemical factors of plasma mainly in terms of reactive species, taking into account electric fields, and the effects of each element on enzyme activity are discussed. The mechanism will be discussed from multiple angles, centring on conformational changes in proteins. Appropriate plasma control based on quantitative studies on the enzymatic activity and protein conformation of each plasma-induced factor has the potential to greatly contribute to innovative agricultural applications.

Keywords Plasma · Enzyme activity · Protein conformation · Amino acid · Electric field

16.1 Introduction

One of the most attractive ways to apply plasma to agriculture is enzyme control. This chapter reviews the effects of plasma irradiation on the enzyme activity and protein structures that are important in pre-harvest and postharvest in agriculture. Enzyme control can be expected to make a great contribution to maintaining the freshness of foods and ensuring safety, but it can also be expected to be applied to various uses such as functional chemicals, and has the potential to lead to disruptive innovation. Enzymes exhibit a substantial degree of conformational variability in the folded state, and they are sensitive to environmental changes. Since the enzyme activity is determined by the oxidation/reduction modification of amino residues constituting the protein and some fragmentation, the conformational change of the protein with respect to plasma irradiation is also discussed. Enzyme activity control by plasma has been mainly discussed in terms of reactive oxygen species (ROS),

T. Okumura (✉)
Graduate School and Faculty of Information Science, and Electrical Engineering, Kyushu University, Fukuoka, Japan
e-mail: t.okumura@plasma.ed.kyushu-u.ac.jp

S. Horikoshi et al. (eds.), *Agritech: Innovative Agriculture Using Microwaves and Plasmas*, https://doi.org/10.1007/978-981-16-3891-6_16

reactive nitrogen species (RNS) and reactive oxygen and nitrogen species (RONS); however, the electric fields during plasma irradiation are also crucial for its activity control and thus protein conformation, so that this chapter begins with enzymatic activity change by plasma followed by that by electric fields.

Proteins are understood at each stage organized at a conceptual level. Due to the structure of the protein, four levels are generally defined. All covalent bonds (mainly peptide bonds and disulphide bonds) that connect amino acid residues in a polypeptide chain are primary structures. The most important element of the primary structure is the sequence of amino acid residues. The secondary structure is a sequence of extremely stable amino acid residues that results in a repeating structural pattern. Tertiary structure refers to all aspects of the three-dimensional folding of a polypeptide. When a protein has two or more polypeptide subunits, its spatial arrangement is called the quaternary structure. The difference in primary structure is especially important. Each protein has a unique number and sequence of amino acid residues. The primary structure of a protein determines how it folds into a unique three-dimensional structure, which in turn determines the function of the protein. Every protein has its own three-dimensional structure, which gives it its own function.

Some proteins with catalytic activity are simpler biological compounds, namely enzymes. When the protein is an enzyme, the amount of protein in a solution or tissue extract is measured by the catalytic action of the enzyme, i.e. the increased rate at which the substrate is converted to the products in the presence of the enzyme (assay). A more practical and commonly used value to express the enzyme activity is unit (U) = 1 μmol/min. 1 U corresponds to 16.67 nanokatals in SI units.

16.2 Enzyme Activity Change by Plasma Irradiation

Enzyme activity change by plasma irradiation begins with enzymes included in plasma-irradiated biomaterial and then plasma-irradiated single protein. Table 16.1 lists the summary of enzymatic activity change by plasma treatment.

16.3 Enzymes Included in Plasma-Irradiated Biomaterial

The enzymes polyphenol oxidase (PPO, also known as tyrosinase) and peroxidase (POD) can be particularly found in agricultural products. PPO and POD give rise to enzymatic browning and thus play a key role in a quality loss during postharvest handling and processing. Except for some cases such as the production of raisins, cocoa and fermented tea leaves, the activity of PPO should be suppressed in lower level ([31]). PPO and POD belong to a group of plant-based oxidoreductases and just begin to act by operations such as peeling, slicing and cutting as well as impacts during transportation, where they are separated from the membranes and thus come

Table 16.1 Summary of enzymatic activity change by plasma treatment

Enzyme	Sample state	Plasma source	Plasma parameters	Salient results	References
Glucose oxidase	Dried after poured solution (water) on microscopic slide	RF glow discharge	Gas: Ar, air and ethylenediamine, mode: Glow, frequency: 13.56 MHz, pressure (base): 5 (1 × 10–3 Pa), air and Ar with 0.24 cm^3 STP/min and 0.45 cm^3 STP/min, respectively. Ethylenediamine (EDA) vapours with 1.42 cm^3 STP/min. Power: 10, 20, 30 and 40 W, operation time: 20 min. Time course: 40 W for 10, 20 and 30 min	Activity loss was 50%, no remarkable change found in the activity as a function of power, and air seems to be slightly most effective	Dudak et al. [1]
Lipase	Solution (buffer) on a SUS substrate	RF He jet	Gas: He, flow rate: 10 slpm, RF power: 180 W, pressure (downstream): ~1 Pa, temperature: ~57 °C	Relative activity of lipase increased as 1.4 times larger by 50-min treatment, and the buffer itself treated by the plasma jet had no effects on the activity	Li et al. [2]
Lysozyme (hen egg white)	Solution (buffer)	Low-frequency He/O_2 plasma jet	Gas: He/O_2, voltage: −3.5 to +5.0 kV with 13.9 kHz, flow rate: He and O_2 gas were 0.50 and 0.15 L/min, respectively	Residual activity decreased with time, about one-third after the plasma treatment for 30 min	Takai et al. [3]
Peroxidase (tomato)	Filtered supernatant after homogenized	DBD plasma	Voltages: 30, 40 and 50 kV, relative humidity: 42%Rh, temperature: 25 °C, operation time: 0–5 min	Reduction by 71, 67 and 43% at 1 min and 21, 17 and 8% at 2 min by 30, 40 and 50 kV treatment, respectively, and by several % in all conditions after 3 min	Pankaj et al. [4]
Polyphenol oxidase	Solution (buffer)	Plasma jet	Voltage: 1.1 MHz, 2–6 kVpp, gases: Ar, Ar/O_2 0.01–0.1%, flow rate: 5 slm, operation time: 0–360 s	Combination of Ar and O_2 more inactivated polyphenoloxidase than pure Ar and reduction by 70% was achieved at 60 s exposure using Ar with 0.01% O_2	Surowsky et al. [5]

(continued)

Table 16.1 (continued)

Enzyme	Sample state	Plasma source	Plasma parameters	Salient results	References
Peroxidase	Solution (buffer)	Plasma jet	Voltage: 1.1 MHz, 2–6 kVpp, gases: Ar, Ar/O_2 0.01/0.1%, flow rate: 5 slm, operation time: 0–360 s	Ar with 0.1% O_2 was the most suitable gas composition, leading to 68% reduction of activity and the activity decreased only by Ar with 0.05% O_2 to 85%	Surowsky et al. [5]
Polyphenol oxidase (apple)	Cut apple	Air DBD plasma	Gas: Air, flow rate: 1.5 and 0.8 m/s at electrodes and apple surface, power: 150 W, voltage: 15 kVpp with 12.7 kHz. Operation time: 10, 20, 30 min	Polyphenol oxidase activities were about 88, 68 and 42%, respectively, for 5 + 5,10 + 10 and 15 + 15 min treatment times	Tappi et al. [6]
α-Amylase	Dry brown rice	Air DC glow	Gas: Air, pressure: 800 Pa, voltage: 1–3 kV, current: 1.2 mA, operation time: 30 min	α-Amylase activity most decreased to 10.8 units/g, after 3-month storage after plasma treatment with 3 kV	Chen et al. [7]
Lipooxygenase	Dry brown rice	Air DC glow	Gas: Air, pressure: 800 Pa, voltage: 1–3 kV, current: 1.2 mA, operation time: 30 min	Lipooxygenase activity most decreased to 197 AU/min for 3 kV treatment and increase level during storage only increased to 226 AU/min after the exposure	Chen et al. [7]
Lactate dehydrogenase	Dry brown rice	He atmospheric-pressure DBD plasma	Gas: He, flow rate: 80 L/h, voltage: 12 kVpp with 24 kHz, power density: 0.9 W/cm^2, operation time: 300 s, storage time: 24 h	Activity quickly declined in the first 3 h after exposure and then gradually from 3 to 12 h storage	Zhang et al. [8]
Peroxidase	Melon pieces	Air DBD plasma	Voltage: 15 kVpp with 12.5 kHz, gas: Air, temperature: 22 °C, relative humidity: 60%Rh, flow rate 7 × 10^{-3} m3 s^{-1}, operation time: 30–60 min	Peroxidase activity was linearly reduced with plasma treatment time, as the residual activity was 91 and 82% by 15 + 15 min and 30 + 30 min treatment	Tappi et al. [9]

(continued)

Table 16.1 (continued)

Enzyme	Sample state	Plasma source	Plasma parameters	Salient results	References
Pectin methylesterase	Melons	Air DBD plasma	Voltage: 15 kVpp with 12.5 kHz, gas: Air, temperature: 22 °C, relative humidity: 60%Rh, flow rate 7×10^{-3} m3 s^{-1}, operation time: 30–60 min	Pectin methylesterase activity nonactivated at 15 + 15 min treatment but decreased to be 94% by 30 + 30 min treatment	Tappi et al. [9]
α-amylase	Dry brown rice	Atmospheric pressure DBD plasma	Power: 250 W, frequency: 15 kHz, pressure: atmospheric pressure, operation time: 5, 10 and 20 min	α-Amylase activity most increased as 1.21-fold greater than controls by 5-min exposure	Lee et al. [10]
Alkaline phosphatase	Solution (buffer)	Air atmospheric pressure DBD plasma	Gas: Air, voltage: 40, 50, 60 kV, pressure; atmospheric pressure, operation time 15 s to 5 min, temperature: Room temperature	Alkaline phosphatase activity decreased to be below 10% after 180 s of treatment	Segat et al. [11]
Superoxide dismutase (button mushrooms; A. bisporus)	From A. bisporus treated with PAW	Ar/O_2 plasma jet	Voltage: 18 kVpp with 10 kHz. Gas: Ar/O_2 98/2%, flow rate: 5 L/min, operation time: 20 min, temperature: 32.7 °C	Superoxide dismutase activity was most increased during storage after immersing in PAW for 15 min	Xu et al. [12]
Peroxidase (tomato extract)	Supernatant of milled tomato juice	He and Ar DBD plasma	Voltage: 10 kV, power: 20 W, respectively. Gas: He and Ar, flow rate: 3 L/min, temperature: 30 °C, operation time: 1–6 min	Peroxidase activity drastically decreased to 5.67% by 1 min treatment, using air, compared to He	Khani [13]
Peroxidase (tomato extract)	Supernatant of milled tomato juice	Air gliding arc	Voltage: 14 kV, frequency: 20 kHz, power: 50 W, gas: Air, flow rate: 3 L/min, temperature: <350 K	Peroxidase activity reached 7.32% within 7-min treatment	Khani et al. [13]
Lysozyme	Solution (buffer)	DBD and jet	Gas, voltage, current and frequency: (a) air (DBD): 1.23 kV, 7 mA, 16 kHz, (b) N_2(DBD): 0.9 kV, 1.5 mA, 16 kHz, (c) air (jet): 0.6 kV, 32 mA, 24 kHz and (d) N_2 (jet): 0.4 kV, 20 mA, 23 kHz pressure: Atmospheric, operation time; 8 and 12 min	Lysed cell percentage by plasma-treated lysozyme was the smallest in (d) N_2 (jet)	Choi et al. [14]

(continued)

Table 16.1 (continued)

Enzyme	Sample state	Plasma source	Plasma parameters	Salient results	References
Lipase (wheat)	Germ	DBD plasma	Voltage and frequency: 10 kV with 6 kHz applied to an upper electrode and 20 or 24 kV with 50 Hz to a lower electrode, temperature was 30 °C, operation time: 5–35 min	Lipase activity most decreased 39.97 and 36.45 at 5 min, and 27.11 and 25.03% at 25-min treatment with 20 and 24 kV, respectively	Tolouie et al. [15]
Lipoxygenase (wheat)	Germ	DBD plasma	Voltage and frequency: 10 kV with 6 kHz applied to an upper electrode and 20 or 24 kV with 50 Hz to a lower electrode, temperature was 30 °C, operation time: 5–35 min	Lipoxygenase activity was 97.8 and 92.3% at 5 min and 55.18 and 49.98% at 35-min treatment with voltages of 20 and 24 kV, respectively	Tolouie et al. [15]
Glucose oxidase	Dried drop onto a glass slide	Atmospheric-pressure DBD	Gas: He, He/O_2, He/C_2H_4, flow rate: 8 slm, voltage: 0.85 and 1.1 kVrms, frequency: 20 kHz, operation time: 10–60 min, pressure: 105 Pa	Activity of 30 μg of glucose oxidase drastically decreased to 38% after 10-min exposure, dropped to 15% after 30 min and levels off to such a value for longer exposure times by of He/O_2-fed DBD	Fanelli et al. [16]
Lactate dehydrogenase	Solution (buffer)	Atmospheric-pressure DBD	Gas: He, flow rate: 80 L/h, voltage: 12 kVpp, frequency: 24 kHz, power density: 0.9 W/cm^2	Lactate dehydrogenase activity was reduced to 84.1%, 79.2%, 76%, 73% and 67.5% after direct exposure and diminished to 86%, 82.1%, 78.3%, 77% and 71.14%, respectively, after the indirect treatment for 60, 120, 180, 240 and 300 s, respectively	Zhang et al. [17]
Phytase (A. niger)	Solution in a 96-well plate (buffer)	He plasma jet	Gas: He, flow rate: 2 L/min, voltage: Pulsed DC 0–15 kV, frequency: 10 kHz, operation time: 1, 2, 4 and 6 min. Temperature: 4 °C	48% and 53% increase in phytase activity at 360-s treatment	Farasat et al. [18]
Peroxidase (fresh tender coconut; Cocos nucifera L.)	Solution (water and soluble solids content)	Atmospheric-pressure DBD	Voltage: 18, 23 and 28 kV, frequency: 50 Hz, pressure: 1 bar, humidity: 58% Rh, temperature: 27 °C	90% reduction in polyphenol oxidase activity at 3 min	Chutia et al. [19]

(continued)

Table 16.1 (continued)

Enzyme	Sample state	Plasma source	Plasma parameters	Salient results	References
Polyphenol oxidase (fresh tender coconut; Cocos nucifera L.)	Solution (water and soluble solids content)	Atmospheric-pressure DBD	Voltage: 18, 23 and 28 kV, frequency: 50 Hz, pressure: 1 bar, humidity: 58% Rh, temperature: 27 °C	85% reduction in POD activity at 4-min treatment	Chutia et al. [19]
Polyphenol oxidase	Carrot juice	Air DBD plasma	Voltage: 60, 70 and 80 kV, operation time: 3 and 4 min with a 30-s break interval in every treatment, gas: Air	11.2% at minimum observed at 70 kV for 4-min treatment	Umair et al. [20]
Peroxidase	Carrot juice	Air DBD plasma	Voltage: 60, 70, and 80 kV, operation time: 3 and 4 min with a 30-s break interval in every treatment, gas: Air	15.73% at minimum observed at 70 kV for 4-min treatment	Umair et al. [20]
Pectin methylesterase	Carrot Juice	Air DBD plasma	Voltage: 60, 70 and 80 kV, operation time: 3 and 4 min with a 30-s break interval in every treatment, gas: Air	10.21% at minimum observed at 70 kV for 4-min treatment	Umair et al. [20]
Lipoxygenase	Carrot juice	Air DBD plasma	Voltage: 60, 70 and 80 kV, operation time: 3 and 4 min with a 30-s break interval in every treatment, gas: Air	13.42% at minimum observed at 70 kV for 4-min treatment	Umair et al. [20]
Polyphenol oxidase (apple)	Cut apple	Air atmospheric pressure DBD plasma	Temperature: 22 °C, humidity: 60% Rh, voltage: DC, power: 150 W, gas: Air, flow rate: 1.5 and 0.8 m/s at the electrodes the and apple surface	Polyphenol oxidase was most inhibited in Fuji apple, showing an activity of 50 and 10% by 15+ 15 and 30 + 30 min treatment	Tappi et al. [21]
Polyphenol oxidase	Solution on Teflon plate (buffer)	Microwave cold plasma treatment	Gas: Air, N_2, O_2, Ar or He, pressure: 667 Pa, flow rate: 1 L/min, power: 900 W, operation time: 40 min	Polyphenol oxidase activity most decreased by air plasma for extract and effectively decreased as the surface-to-volume ratio increased for potato slices	Kang et al. [22]

(continued)

Table 16.1 (continued)

Enzyme	Sample state	Plasma source	Plasma parameters	Salient results	References
Polyphenol oxidase (Pacific white shrimp (*Litopenaeus vannamei*)	Harvested shrimp	Cold plasma	Operation time: 45, 90 and 150 s	Polyphenol oxidase activity decreased to be 50% at 150-s treatment	Zouelm et al. [23]
Peroxidase (tiger nut milk)	Solution (deionized water)	DBD plasma	Voltage: 10 kHz, frequency: 14 kV, power: 40–60 W, operation time: 0, 2, 4, 6, 8 and 12 min	Peroxidase activity was 5.6, 8.4, 11.5, 3.2 1.3 and 0.54/min· mg protein at 0, 2, 4, 6, 8 and 12 min, showing a peak at 4-min treatment	Muhammad et al. [24]
Peroxidase (horseradish)	Solution (buffer)	Ar/O_2 DBD jet	Gas: Ar/O_2: 98/2%, flow rate: 26–30 L/min, voltage: 7 kV, operation time: 2 min with an interval for a duration of up to 10 min	Peroxidase activity decreased to be 54, 42, 20% by 2, 4 and 10 min.	Han et al. [25]
Glutamic acid	Soil on SUS mesh	Air atmospheric pressure DBD	Voltage: 16 kV, frequency: 50 Hz AC, gas: Air, flow rate: 3 L/min, operation time: 120 min	Glutamic acid activity decreased from 1.72 to 1.22 and 0.21 nmol/g· h within 10- and 120-min treatment, respectively	Wang et al. [26]
Arylsulphatase	Soil on SUS mesh	Air atmospheric pressure DBD	Voltage: 16 kV, frequency: 50 Hz AC, gas: Air, flow rate: 3 L/min, operation time: 120 min	Arylsulphatase activity decreased from 0.0191 to 0.0081 and 0.0099 nmol/g· h within 10- and 120-min treatment, respectively	Wang et al. [26]
Leucine	Soil on SUS mesh	Air atmospheric pressure DBD	Voltage: 16 kV, frequency: 50 Hz AC, gas: Air, flow rate: 3 L/min, operation time: 120 min	Leucine activity decreased from 1.77 to 1.16 and 0.27 nmol/g· h within 10- and 120-min treatment, respectively	Wang et al. [26]
Acetyl glucosaccharase	Soil on SUS mesh	Air atmospheric pressure DBD	Voltage: 16 kV, frequency: 50 Hz AC, gas: Air, flow rate: 3 L/min, operation time: 120 min	Acetyl glucosaccharase activity decreased from 0.155 to 0.037 and 0.031 nmol/g· h within 10- and 120-min treatment, respectively	Wang et al. [26]

(continued)

Table 16.1 (continued)

Enzyme	Sample state	Plasma source	Plasma parameters	Salient results	References
Cellulase	Soil on SUS mesh	Air atmospheric pressure DBD	Voltage: 16 kV, frequency: 50 Hz AC, gas: Air, flow rate: 3 L/min, operation time: 120 min	Cellulase activity decreased from 0.065 to 0.038 and 0.037 nmol/g· h within 10- and 120-min treatment, respectively	Wang et al. [26]
Glucosaccharase	Soil on SUS mesh	Air atmospheric pressure DBD	Voltage: 16 kV, frequency: 50 Hz AC, gas: Air, flow rate: 3 L/min, operation time: 120 min	Glucosaccharase activity decreased from 0.304 to 0.128 and 0.124 nmol/g· h within 10- and 120-min treatment, respectively	Wang et al. [26]
Ligninase	Soil on SUS mesh	Air atmospheric pressure DBD	Voltage: 16 kV, frequency: 50 Hz AC, gas: Air, flow rate: 3 L/min, operation time: 120 min	Ligninase activity decreased from 0.035 to 0.009 and 0.008 nmol/g· h within 10- and 120-min treatment, respectively	Wang et al. [26]
Phosphatase	Soil on SUS mesh	Air atmospheric pressure DBD	Voltage: 16 kV, frequency: 50 Hz AC, gas: Air, flow rate: 3 L/min, operation time: 120 min	Phosphatase activity decreased from 0.337 to 0.267 and 0.139 nmol/g· h within 10- and 120-min treatment, respectively	Wang et al. [26]
Polyphenol oxidase	Cut apple and juice with water	Air DBD plasma	Gas: Air, voltage: 20 kV, frequency: 50, 200, 400, 600, 900 Hz, operation time: 15 min	Polyphenol oxidase activity increased for cubes (1.5 times larger with 600 Hz treatment) but decreased in juice at these frequencies	Farias [27]
Peroxidase	Cut apple and juice with water	Air DBD plasma	Gas: air, voltage: 20 kV, frequency: 50, 200, 400, 600, 900 Hz, operation time: 15 min	Peroxidase activity increased for cubes (9.7 times larger with 900 Hz treatment) but decreased in juice at these frequencies except for 600 Hz	Farias [27]

(continued)

Table 16.1 (continued)

Enzyme	Sample state	Plasma source	Plasma parameters	Salient results	References
Polyphenol oxidase (from avocado pulp)	w/ and w/o lime extract	DBD plasma	No information	Polyphenoloxidase, in sample w/o lime extract, an increase in the enzymatic activity of polyphenoloxidase compared to the control was found in all treatments. In sample w/ lime extract, despite an increase in the enzymatic activity in relation to the control, for almost all treatments applied, compared to w/o lime extract, we observed a lower enzyme activity under the same treatment conditions	Batista et al. [28]
Peroxidase (from avocado pulp)	w/ and w/o lime extract	DBD plasma	No information	For POD, the use of cold plasma in the two pulps showed the reduction of peroxidase, except for sample w/o lime extract subjected to 10 min with 20 ml/min gas flow plasma treatment	Batista et al. [28]
Tyrosinase (from mushroom)	Dried by vacuum (buffer)	DBD plasma	Gas: He, He/O_2 (99/1%), and He/C_2H_4 (0.1–1/99.9–99%) mixtures, flow rate: 8 slm, voltage: 0.85 or 1.1 kVrms, frequency: 20 kHz, pressure: 100 MPa, operation time: 10–60 min	He-DBD has a lower impact on the activity than with O_2 contamination	Lapenna et al. [29]
Crude protease (hairtail fish; Trichiurus lepturus)	Solution (buffer)	DBD plasma	Voltage: 50 kV, operation time: 30, 60, 120, 180, 240 and 300 s	A significant decrease in enzyme activity was observed with the treatment time, where the lowest activity was 0.035 units/mg at 240 s of treatmen	Koddy et al. [30]

into contact with polyphenolics [32]. In the case of PPO, monophenolics or *o*-diphenols are usually dehydrated to instable *o*-diquinones, depending on the availability of oxygen. This triggers the formation of melanins and causes the affected areas to become a brownish colour [33, 34]. Enzymatic browning is also associated with POD, primary function of which is to oxidize phenolic compounds at the expense of H_2O_2, leading to undesirable flavour during storage. POD is the most heat-stable enzyme of agricultural product and thus is used as an indicator for successful blanching [35]. Sensorial losses such as browning and an off-flavour owing to the degradation of phenolic compounds are also associated with losses of nutritional value [36]. Therefore, the inactivation of PPO and POD is a crucial indicator of quality in the processing of fruits and vegetables.

Tappi et al. [6] reported a linear decrease in PPO activities of cut apples with DBD treatment time. Taking 100% PPO activity of each specific control sample (fresh tissue), treated sample residual activities were about 88, 68 and 42%, respectively, for 5 + 5, 10 + 10 and 15 + 15 min treatment times. Plasma condition was150W, 15kVpp and 12.7 kHz, and the treatment time was 10, 20 and 30 min. Air speed was about 1.5 m/s at the electrodes and 0.8 m/s at the apple surface.

Umair et al. [20] reported the inactivation of POD, PPO, pectin methylesterase (PME) and lipoxygenase (LOX) of carrot juice by air DBD plasma treatment operated with 60, 70 and 80 kV for 3 and 4 min with three-time repetitions and a 30-s break interval in every treatment. PME is a cell-wall-bound enzyme, which is able to de-esterify pectins producing methanol and pectins with a lower degree of esterification that are further degraded by other pectolitic enzymes, causing tissue softening, and the activity often increases as ripening continues. LOX is a pathogenicity factor in plant, in that increasing LOX activity during fruit ripening contributes to the destruction of anti-fungal dienes and enhances the susceptibility of fruit to disease [37–39]. Results indicated that less effect was noticed in HVCP at 60 kV for 3 min. A slight change in the effects was observed at 60 kV for 4 min, whereas a significant effect was noticed at 80 kV for 3 and 4 min. However, the effect of HVCP at 70 kV for 4 min was most prominent as compared to other combinations. It suggested that cold atmospheric plasma has the potential to inhibit the formation of alkaline compounds from the decomposition of protein during the storage period through decreasing microbial growth and retarding endogenous protease activity.

PPO inactivation for three apples (Pink Lady apple, Fuji, Red Delicious and Modì) was also shown by S. Tappi et al. [21], using DBD plasma treatment. In Pink Lady apple, the effect seemed proportional to treatment time as in their previous research [6]. PPO residual activity was reduced to 79% after 30 + 30 min. The highest inhibition level was observed in Fuji apple, showing a residual activity of 50 and 10% after, respectively, the 15 + 15 and the 30 + 30 min treatment. On the contrary, in Modì, after 15+ 15 min, the PPO activity was not significantly affected by the treatment, while with a longer exposure, it was reduced to about 50%. Generally, Red Delicious did not show a significant reduction in PPO at 15 + 15 and however showed a PPO activity of over 120% by 30 + 30 plasma treatment at 60%Rh (22 °C). The gas plasma generator was a double barrier discharge type consisting of three parallel pairs of brass electrodes (supplied by a DC power supply

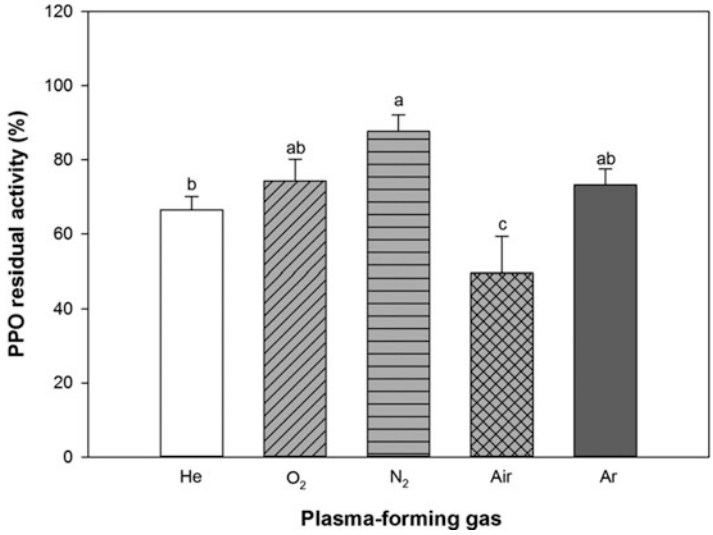

Fig. 16.1 Effect of plasma-forming gas on the residual activity of polyphenol oxidase (PPO) extract after cold plasma treatment at 900 W for 40 min [22]

consuming 150 W powered by high-voltage transformers) placed at the top of a hermetic chamber of 29 dm3 internal volume. The dielectric material used was a 5-mm-thick glass. Over the electrodes, three fans were directing the discharge towards the samples, placed at 9 cm away. The measured air speed was 1.5 m/s at the electrodes and 0.8 m/s at the apple surface.

Kang et al. [22] showed the inactivation of PPO of a sliced potato treated with microwave plasma treatment with 900 W for 40 min, using air, N_2, O_2, Ar or He as a feeding gas at a flow rate of 1 L/min. Typical result is illustrated in Fig. 16.1. The relative activity of extracted PPO treated with N_2, O_2, Ar, He and air plasma at 667 Pa was 87.6 ± 4.4%, 74.3 ± 5.9%, 73.2 ± 4.2%, 66.5 ± 3.6% and 49.5 ± 9.9%, respectively. The degree of enzyme inactivation increased as the surface-to-volume ratio of the potato slices increased. When the surface-to-volume ratios were 7.1 (3.2 × 0.8 × 0.5 cm) and 9.0 (0.8 × 0.8 × 0.5 cm), the relative activity of PPO in the CP-treated potato slices were 72.4 ± 10.9 and 59.0 ± 8.9%, respectively.

Surowsky et al. [5] reported the inactivation of PPO and POD by plasma jet for 360 s. The working gases were pure Ar as well as mixtures of Ar and 0.01 to 0.1% O_2 with 5 slm, using 1.1 MHz, 2–6 kVpp. For PPO, after an early decrease of activity within 120 s, the residual activity slowly approaches around 10%. Using a concentration of 0.01% O_2, a reduction about 70% was already achieved after 60 s of plasma exposure. The combination of Ar and O_2 also showed better inactivation results than pure Ar. For POD, representing a rapid loss of enzyme activity was slightly shorter (60 s). Ar with 0.1% O_2 was the most suitable gas composition, leading to reductions of about 68%. When further extending the treatment time, only

a combination of Ar and 0.05% O_2 was able to significantly decrease the activity by about 85% in total.

Inactivation of PPO and POD by DBD air plasma treatment was also reported for apple juice and cubes by Farias et al. [27]. PPO was partially inactivated in the juice at all plasma excitation frequencies and in apple cubes at excitation frequencies between 50 and 200 Hz. By examining, they found that the POD activity in apple cubes increased, whereas that in juice decreased except for the assay carried out at 600 Hz. The treatment carried out at 200 Hz presented the highest decrease in PPO activity in apple cubes (−46%), and the treatment carried out at 50 Hz also presented the highest decrease in apple juice (−50%). At these frequencies, POD activity increased in apple cubes and decreased in apple juice. For apple juice, the excitation frequency of 50 Hz seems to be a satisfactory compromising point where a decrease in both PPO (−50%) and POD (−56%) could be achieved.

Chutia et al. [19] irradiated the POD and PPO activities of fresh tender coconut (*Cocos nucifera L.*) water at a pH of 5.20 ± 0.2 and soluble solids content of 3.95 ± 0.25 °Brix with DBD plasma using 18, 23 and 28 kV with 50 Hz at 1 bar. Relative humidity and temperature were 58%Rh and 27 °C, respectively. The residual activity of POD and PPO was decreased to 44.4, 69.4 and 77.8% at 1 min and 19.4, 29.2 and 38.9% at 2 min irradiation of plasma in 18-, 23- and 28-kV exposure, respectively. Finally, there was a reduction of 90% in the PPO activity after cold plasma treatment for 3 min and that of 85% in the POD activity after 4 min of treatment.

Batista et al. [28] showed an activation of PPO and POD w/ (with) and w/o (without) lime extract from avocado pulp by DBD plasma. For PPO, in sample w/o lime extract, an increase in the enzymatic activity of PPO compared to the control was found in all treatments. In sample w/lime extract, despite an increase in the enzymatic activity in relation to the control, for almost all treatments applied, compared to w/o lime extract, a lower enzyme activity was observed under the same treatment conditions. For POD, the use of cold plasma in the two pulps showed the reduction of POD, except for sample w/o lime extract subjected to 10 min with 20 ml/min gas flow plasma treatment. These results suggest that the enzymatic activity of avocado pulp is enhanced by the synergistic effect of using lime extract with cold plasma.

Chen et al. [7] reported the inactivation of α-amylase and LOX of brown rice by a DC glow plasma using a DC high-voltage supply operated at 1–3 kV with a constant current of 1.2 mA in air at 800 Pa for 30 min. α-Amylase, a starch-hydrolysing enzyme retaining significant activity after harvest of rice [40, 41], is responsible for the decrease in amylopectin fraction and apparent amylose content, and increase in the amount of low-molecular-weight saccharides in the rice flour [42]. Plasma treatment at 1 kV and 30 min did not affect the α-amylase activity, but the activity declined significantly in early storage period, and the activity is about 26 units/g after 3-month storage, which is similar to that of unexposed brown rice. Plasma treatment at 2 kV significantly decreased the α-amylase activity, and the activity declined to about 23.4 units/g after 1-month storage; the activity did not change after 2- and 3-month storage. After plasma treatment with 3 kV, the α-amylase activity revealed the minimal value, about 10.8 units/g, after 3-month storage. Therefore, plasma

significantly decreased the α-amylase activity. The α-amylase activity in unexposed brown rice significantly decreased from 40.7 to 24.4 units/g after storage. On the other hand, the inactivation of lipooxygenase is one of the most important aims of brown rice preservation operations because it plays an important role in the formation of desirable or undesirable flavour and aroma in many plant products. Lipooxygenase activity is localized in bran fraction in rice seeds, where unsaturated fatty acids represent the normal substrates that are oxidized to hydroperoxides [43]. By increasing the treatment voltage, a significant decrease in the lipooxygenase activities of brown rice was measured, and the residual activities were about 214, 210 and 197 AU/min for 1, 2 and 3 kV, respectively. After storage, the lipooxygenase activity increased to 239 AU/min by 1- and 2-kV exposure, whereas in rice with 3-kV exposure, the levels only increased to 226 AU/min. Lipooxygenase activity in unexposed brown rice increased from 217 to 251 AU/min after storage.

Tappi et al. [9] studied the activity change of POD and PME of melon juice using air DBD plasma with 20 kV and 50, 200, 400, 600 and 900 Hz for 15 min. POD activity underwent a significant reduction in plasma-treated melon samples proportional to the treatment time, as the residual activity was found to be 91% (15 + 15) and 82% (30 + 30) compared to the control sample. PME activity was not affected by the 15 + 15 min treatment, but after the 30 + 30 min treatment, the residual activity was found to be 94%. However, the reduction observed in the enzymatic activity did not seem to have any relationship with colour and textural results.

Lee et al. [44] also irradiated brown rice with an atmospheric pressure DBD plasma with 15 kHz and 250 W for 5, 10 and 20 min. The activity of α-amylase of plasma-exposed brown rice significantly increased at 5, 10 and 20 min, with a maximum value 1.21-fold greater than the controls after 5 min of exposure. The contradictory experimental results of α-amylase reported by Chen and Lee's group may have been caused by differences in plasma temperature and composition of produced active species.

POD inactivation of tomato extracts was reported by Khani et al. [13]. They used DBD plasma for 1–6 min with 20 W and 10 kV at 30 °C. Gases were air and He with 3 L/min. Air gas more decreased the residual activity of POD. The residual activity at 1-, 2-, 3-, 4-, 5- and 6-min treatment was decreased to 5.7, 5.2, 4.8, 3.7, 3.6 and 3.7% by air DBD plasma and 92.0, 80.7, 36.4, 26.2, 24.0 and 4.8% by He DBD plasma, respectively. When air was used as the plasma-forming gas, the required time to reduce the enzyme by 90% rapidly reduces to 60 s. Nevertheless, when He was used by itself, even at 300 s, 90% enzyme deactivation was not obtained. Khani et al. [13] also used gliding arc. The percentage of the remaining enzyme became equal to 32.11% at 1-min processing (30 s for each side of the sample). Increasing the processing time had a great impact on the reduction of the remaining enzyme. This value reached the acceptable percentage of 7.32 within 7 min. The notable point was the lack of increase in the sample temperature to more than 40 °C, which could help to maintain nutrient content.

Tolouie et al. [15] showed the inactivation of lipase and LOX of wheat germ by DBD plasma with 10 kV with 6 kHz applied to the upper electrode and 20 or 24 kV with 50 Hz to the lower electrode, and the plasma temperature was 30 °C. The

inactivation rate of LOX shown was lower compared to lipase inactivation by plasma treatment. The inactivation rate of lipase at 24 kV was higher than that at 20 kV. The residual activities of lipase after 5-min treatment at 20 and 24 kV were 39.97% and 36.45%, respectively. Lipase activity was reduced continuously during 25 min and reached to 27.11% and 25.03% of initial amounts at 20 and 24 kV, respectively. The enzyme inactivation rate was not the same at two applied voltages. No significant inactivation of lipase was observed for treatments longer than 25 min, suggesting an optimum treatment time of 25 min. Despite the rapid inactivation of lipase at a short period of treatment (5 min), LOX activity was only reduced by 2.2% and 7.7% at 20 and 24 kV, respectively. Further inactivation of LOX was observed by increasing the treatment time and after 25 min, the residual activities of LOX were 55.18% and 49.98% at voltages of 20 and 24 kV, respectively. Similar to lipase inactivation, treatments longer than 25 min did not change the residual activity of LOX significantly.

Muhammad et al. [24] showed the inactivation of POD extracted from tiger nut milked by DBD plasma operated at 30 V and a resonance balancing of 1.22 A 10 kHz and a high voltage of 14 kV with 40 60 W for 12 min under continuous stirring. POD activity/min mg protein was approximately 5.6, 8.4, 11.5, 3.2 1.3 and 0.54/min mg at 0, 2, 4, 6, 8 and 12 min, showing a peak at 4-min treatment.

Han et al. [25] reported the POD inactivation of horseradish by DBD jet with pre-mixed gas (98% Ar and 2% O_2) at 26–30 L/min nozzle, using a 220 V AC single-phase power source with an output voltage of 7 kV DC and a current of 10 A for 2-min interval for a duration of up to 10 min. The residual activity was decreased to 54 and 42% by the early 2, 4 min and to 20% in 10-min irradiation.

Cut hairtail (*Trichiurus lepturus*) fish was irradiated with air DBD plasma at atmospheric pressure, with 50 kV for 30, 60, 120, 180, 240 and 300 s done by Koddy et al. [30]. A significant decrease in the enzyme activity was observed with increasing treatment time, where the lowest enzyme activity value of 0.035 units/mg was recorded after 240 s of treatment.

Lapennas et al. [29] treated dried tyrosinase from mushroom with DBD plasma, generated by 0.85 and 1.1 kVrms with 20 kHz at 100 MPa. Working gases were He, He/O_2 and He/C2H4 mixtures at 8 slm. O_2 concentration in He/O_2 mixture was 1% (hereafter referred to as He/1% O_2 mixture), and ethylene concentration ([C_2H_4]) in He-C_2H_4 mixtures was varied in the range 0.1%–1%. Plasma exposure time was 10–60 min. He/1% O_2-fed DBD has no effect on Tyr activity when the exposed amount is 10 μg, while it leads to similar values of residual activity in the case of 2 and 5 μg of Tyr (70 ± 5% and 67 ± 2%, respectively); (ii) exposure of both 2 and 5 μg of Tyr to the pure He DBD leads to a residual activity of about 85%, which is greater than that observed in the case of the O_2-containing plasma, revealing that the He DBD has a lower impact on the enzyme activity than the He/1% O_2-fed DBD. The activity of 5 μg of tyrosinase is reduced with increasing exposure time to the He/1% O_2-fed DBD. Tyr residual activity decreases to ~85% upon 10-min exposure, drops to ~65% when the exposure time is increased to 30 min, while remains constant for longer process duration. Very similar results are obtained as a function of the exposure time, further decreasing the enzyme amount to 2 μg. Moreover,

when the plasma treatment is carried out using a pure He DBD, a residual activity of ~85% is obtained, regardless of the process duration. Therefore, Tyr seems to display remarkable resistance upon plasma exposure; i.e., considerable activity retention is also observed when very low enzyme amounts are used, with very weak dependence on the exposed amount.

Plasma activated water (PAW), often used for inactivating bacteria, was also used to sustain superoxide dismutase contents of mushroom. Xu et al. [12] immersed Button mushrooms (*Agaricus bisporus*) in PAW obtained by treating water with an atmospheric pressure plasma jet, using 8 kVpp AC with 10 kHz for 20 min. Pre-mixed Ar and O_2 (98% Ar and 2% O_2 per volume) are used the working gases at a flow rate of 5 L/min. The mean temperature of the nonthermal plasma near the water surface was 32.7 °C. On the seventh day of storage, superoxide dismutase contents of the PAW-5 min, PAW-10 min and PAW-15 min groups were 23.29%, 25.06% and 47.25%, which are higher than those of the unprocessed group, respectively. The PAW-15 min group manifested the greatest superoxide dismutase content and exceeded the distilled-water-soaked group, which was attributed to the combined effect of water soaking and PAW generating ROS in the beginning. On the last day of the postharvest storage period, the superoxide dismutase content of the PAW-processed groups decreased compared with previous days potentially due to the decay of PAW, which would thus generate fewer ROS.

16.4 Plasma-Irradiated Single Protein

The plasma effects can be selective not only to complex biomaterial, such as agricultural products, but also to simpler enzymes. Dudak et al. [1] reported a relative activity decrease of a model protein (glucose oxidase, GOx) by an RF glow discharge plasma. Argon, air and ethylenediamine (Acros Organics) were used as the working gases in the glow discharge with 13.56 MHz operation. The samples were treated with air and argon (working pressure 5 Pa; flow rates 0.24 cm^3 STP/min and 0.45 cm^3 STP/min, respectively). They were also modified with ethylenediamine (EDA) vapours (working pressure 5 Pa, flow rate 1.42 cm^3 STP/min). The samples were exposed to plasma at 140 W power for 10, 20 and 30 min. The relative activity was decreased to approximately 60 and 50% at 10 and 20 min for air, Ar and EDA, respectively.

Li et al. [2] showed lipase activation, using RF plasma jet at 180 W and He as working gas at a flow rate of 10 slpm. The pressure at plasma downstream was lower than 1 Pa, and the temperature was lower than 57 °C. The relative activity of lipase was 1.0, 1.11, 1.22, 1.28, 1.33 and 1.44 at 0-, 10-, 20-, 30-, 40- and 50-min treatment, respectively. Moreover, the buffer itself treated by the plasma jet has no effects on the enzyme activity.

Lysozyme (Hen egg white) was irradiated with low-frequency (LF) plasma Jet with He gas for 0–30 min by Takai et al. [3]. They used −3.5 to +5.0 kV AC with 13.9 kHz. The flow rates of He and O_2 gas were, respectively, 0.50 and 0.15 L/min.

Time course of residual activity of lysozyme after treatment of the LF plasma jet showed 88, 74, 63, 52, 50, 41 and 33% at 2, 5, 10, 15, 20, 25 and 30 min, respectively. They also used hot-air treatment as the control experiment with air at 80 °C instead of LF plasma jet blown on the samples. The plasma treatment through a quartz glass plate was performed as the control experiment that LF plasma jet irradiated on the samples through a UV-permeability glass vial to confirm the effect of UV alone. As expected, the enzymatic activity and concentration of lysozyme did not change in these control experiments. These data indicate that the decrease in the residual activity results from chemical modification and/or unfavourable denaturation of the enzymes by treatment of LF plasma jet.

Pankaj et al. [4] reported the availability for inactivating tomato POD with in-package DBD plasma technology and showed that POD activity was reduced with increasing treatment time and voltage. They used voltages 30, 40 and 50 kV at 42% relative humidity (RH) and 25 °C for 5 min and found that the residual activity of the POD was 71, 67 and 43% at 1 min and 21, 17 and 8% at 2 min by 30, 40 and 50 kV treatment, respectively. After 3 min, the residual activity showed several % in all conditions.

H. Zhang et al. reported an activity inhibition of LDH dissolved in PBS buffer at the initial concentration of 5 mg/mL by direct and indirect irradiation with atmospheric pressure DBD plasma. After direct exposure to the helium plasma for 60, 120, 180, 240 and 300 s, LDH activity is reduced to 84.06%, 79.23%, 75.98%, 73% and 67.5% compared to the control, respectively. After the indirect treatment, the activity diminishes to 86%, 82.1%, 78.32%, 77% and 71.14%, respectively. The degree of inhibition increases with plasma treatment time. The direct treatment seems to inhibit the LDH activity more effectively than the indirect one [17]. Interestingly, the activity of the LDH with plasma decreases within 12 h and slightly recovered from 12 to 24 h. After the treated LDH solution is stored for 1, 3, 6, 12 and 24 h, the LDH activity after the direct treatment drops from 67.5% to 58.48%, 52.22%, 49.7% and 57.05%, respectively, whereas that of the indirect treatment diminishes from 71.14% to 61.72%, 57.59%, 51.95% and 59.32%, respectively. To determine the role of H_2O_2 in plasma-induced LDH inactivation, they used 129.5-μM of H_2O_2 to mimic the effects of H_2O_2 produced by the 300-s plasma treatment. The results show that H_2O_2-triggered inactivation is weaker than that of the DBD plasma. The LDH activity decreases from 100% to 64.43% after the H_2O_2 treatment in 24 h, but there is no recovery. They concluded that the inactivation of LDH induced by H_2O_2 is not reversible and the plasma-generated H_2O_2 constitutes just one of the effective factors.

Inactivation of alkaline phosphatase was reported by Segat et al. [11]. They used atmospheric pressure DBD plasma, generated by 40, 50 and 60 kV in air at room temperature for 15 s to 5 min. A rapid inactivation of the enzyme was noticed at all the applied voltages. After 120 s of treatment, the activity losses were found around to be 45–50% for all the voltages applied, and beyond this time, the differences were further minimized. However, independent of the voltage used, after 180 s of treatment the activity of the enzyme was found to be below 10%. Both treatment

duration and applied voltage had a significant effect on the inactivation of ALP. The interaction between voltage and time was also found to be significant.

Choi et al. [14] treated lysozyme with (a) Air-DBD: 1.23 kV, 7 mA, 16 kHz, (b) N2-DBD: 0.9 kV, 1.5 mA, 16 kHz; (c) Air-APPJ: 0.6 kV, 32 mA, 24 kHz; and (d) N2-APPJ: 0.4 kV, 20 mA, 23 kHz at an atmospheric pressure for 8 and 12 min. The residual activity was evaluated with bacterial cells as a substrate for the lysozyme. The percentage of lysed cell values were 63, 71, 78, 81 and 58% at 1-min digestion and 56, 63, 69, 71 and 54% at 2-min digestion, and 51, 54, 60, 62 and 49% at 5-min digestion for (a), (b), (c), (d) and control (untreated lysozyme), respectively.

Fanelli et al. [16] irradiated GOx with DBD plasma fed i) He; ii) He/1% O_2(He/O_2) mixture, that could induce considerable enzyme etching; and iii) He/C_2H_4 mixtures to obtain PE-CVD and overcoat the enzyme with a polyethylene-like thin film. Plasma was generated by 0.85 and 1.1 kVrms with 20 kHz at 10^5 Pa for 10–60 min, and flow rate was 8 slm. For He/O_2-fed DBD, the activity of 30 μg of GOx drastically decreased to 38% after 10-min exposure, and it dropped to 15% after 30 min and levels off to such a value for longer exposure times. The effect was dependent on the amount of dry enzyme exposed to the DBD. In the case of 100 μg, the activity after 10 min in He/O_2 plasma was 87%, and upon increasing the exposure time to 60 min, it levels off at 85%. Leaving unchanged the GOx loading, the exposure to the pure He plasma up to 60 min did not affect the enzyme activity. By trebling the amount of exposed enzyme (300 μg), inactivation became negligible and the activity was fully preserved also after 60 min in He/O_2 plasma.

Phytase (Aspergillus niger) activation was suggested by Farasat et al. [18] by direct and indirect plasma jet treatment for 1, 2, 4 and 6 min, generated with a pulsed DC 0–15 kV with 10 kHz and He with 2 L/min as a working gas. Indirect treatment was done by exposing the plasma to the reaction buffer immediately before enzyme addition and direct one by exposing the plasma to the enzyme solution kept at 4 °C during ACP treatment. They found 48% and 53% increase in the enzyme activity at exposure time of 6 min. The persistence of ACP intensification effects on enzymatic activity (ageing time) was investigated for 6 min of exposure and followed for 18 hours. The enzyme activity showed a sharp rise for the next 4 hours, resulting in 125% increase compared to the control. After that, a decreasing trend began. Considering the control protein activity trend, this reduction was mainly related to the intrinsic protein half-life.

Wang et al. [26] reported a decrease of activity for eight enzymes, glutamic acid, arylsulphatase, leucine, acetyl glucosaccharase, cellulase, glucosaccharase, ligninase and phosphatase originally included in soil by DBD plasma treatment. The discharge plasma was triggered using an AC high-voltage power source (50 Hz and 0–30 kV). The discharge spacing was maintained at 8 mm. In a beach processing, 60-g fresh and uncontaminated soil sample was put on the stainless steel mesh, and dry air with a flow rate of 3.0 L/min was injected into the reaction container, and then, a voltage of 16 kV was applied between the two electrodes to trigger the nonthermal discharge plasma. Soil was treated with plasma for 120 min. Then, the glutamic acid enzymatic

activities significantly decreased from 1.72 to 1.22 nmol g-1 h-1 within 10 min's treatment; and further treatment would still lead to its decrease (only 0.21 nmol g-1 h-1 within 120 min's treatment). Leucine enzyme, acetyl glucosaccharase, glucosaccharase, cellulose, phosphatase and ligninase all decreased after the non-thermal discharge plasma treatment; that is, there was appropriately 84.7%, 80.0%, 59.1%, 42.4%, 58.7% and 77.3% decline after 120 min's treatment, respectively.

16.5 Enzyme Activity Change by Electric Field Application

Plasma not only generates RONS but also brings about intense electric field. Here, the enzymatic activity and protein conformational changes induced by electric field (EF) application are briefly provided.

Ertugay et al. [45] reported PPO inactivation of apple juice by using electric field of 30 and 40 kV/cm with a pulse width of 2.0 μs and 200 pulse per second, and flow rate of juice was 500 mL/min at 40 °C. PPO was not completely inactivated at 30 kV/cm. However, the activity decreased up to 32.1%, 7.0%, 2.9% and 1.6% at 50, 100, 150 and 200 pulses, respectively. The residual activity decreased up to 6.2% for 50 pulses at 40 kV/cm and was completely inactivated after 100 pulses. Thus, the inactivation rate obtained at 30 kV/cm for 100 pulses was reached at 50 pulses with 40 kV/cm. These results indicated that PPO activity of apple juices significantly decreased as electrical field intensity and the number of pulses increased.

Okumura et al. [46] applied a pulsed EF (PEF) of 4 MV/m with a pulse width of 10 μs and frequency of 1 Hz to unpasteurized sake and evaluated the activity of α-amylase, glucoamylase and acid carboxypeptidase at 4 and 25 °C. At 4 °C, the α-amylase activity seemed to decrease at 300 PEF applications but not decrease afterward. At 25 °C, the α-amylase activity seemed to decrease with the number of PEF applications. Since the α-amylase activity was maintained under 35 °C, it was found that PEF application inactivated the α-amylase of unpasteurized sake without temperature effect and that the inactivation effect differs with temperature. The glucoamylase activity seemed to decrease at 300 PEF applications but not decrease afterward at 4 °C, as same as the result for α-amylase. The result at 25 °C had a similar trend with that at 4 °C, but a significance decrease in the glucoamylase activity was found with 100 PEF applications. These results suggest that the inactivation effect of PEF is independent of the number of PEF applications and temperature. At 4 °C, the acid carboxypeptidase activity seemed to decrease with 300 PEF applications, but the inactivation effect was suggested to decrease afterward. Nevertheless, at 25 °C, the acid carboxypeptidase activity seemed to increase by PEF application, and a significant increase was observed with 300 PEF applications. These results show that the effect of PEF application differs with temperature on the acid carboxypeptidase of unpasteurized sake. From the above results, the sensitivity of enzyme to PEF application differs depending on the types of enzyme. Similar results can be found in previous research [47, 48].

16.6 Protein Conformational Change

Table 16.2 lists the summary of conformational change in enzyme and protein of biomolecule or single molecules by plasma treatment.

16.7 Plasma Irradiation-Induced Conformational Change

To understand protein conformational changes induced by plasma irradiation is also crucial. This is because the function of the enzyme is provided by its conformational characteristics. This section reviews studies on conformational changes of mainly enzyme proteins by plasma.

Dudak et al. [1] reported an increase in OH/NH groups signal (peak centred near 3400 cm^{-1}), more random C=O bonds (broadening of amide I peak, 1600–1700 cm^{-1}) and some decrease in CH2, CH3 groups signal (relative to OH/NH bonds) for air and Ar plasma. Sodium dodecyl sulphate polyacrylamide gel electrophoresis (SDS-PAGE) revealed that the intensity of low molecular weight protein band increased with the glow discharge treatment. This suggests the fragmentation of the protein in the plasma. Similar changes were observed in SDS-PAGE analysis of GOx samples treated with air, Ar and EDA.

Hayashi and Yagyu [49] irradiated casein protein with RF O_2 ICP glow discharge plasma. The decomposition of β-sheet and α-helix of the protein second-order structure was confirmed by the second derivative of FTIR spectral peaks at 1635 cm^{-1} and 1655 cm^{-1}, respectively. The complete decomposition of casein at the initial concentration of 0.21 mg/cm^2 required approximately 1.5 h. The decomposition efficiency was larger than that at 0.63 mg/cm^2. Both peaks of C–H and N–H bonds of amide structure in protein at 2925 cm^{-1} and 3332 cm^{-1}, respectively, reduced with treatment time, and α-helix and β-sheet, respectively, also decreased with operation time. Structures of amide almost diminished after treatment for 8 h, while the second-order structure remains approximately 15% of original.

Li et al. [2] used RF He jet onto lipase. Irregular structures found in plasma-treated proteins and/or structural transitions during processes, based on α-helical, mainly β-pleated sheet, separate α-helix and β-sheet regions (α/β), intermixed α-helix and β-sheet regions (α/β). Fluorescent spectroscopy revealed that the tryptophan residues in the lipase are affected by the helium plasma jet because of the increase of the emission intensity around 348 nm with increasing plasma treatment time. Since the lipase concentration in the solutions remains almost unchanged after the plasma jet treatment, the increase of the lipase activity is possibly due to the changes of the molecular structures of the lipase. In order to verify the stability of the alterations of the protein structures, the enzyme solution is held overnight at 4 °C after treated by the plasma jet. Not only the fluorescence intensity but also CD spectrum of the lipase changes was significant with increasing plasma treatment time. On the one hand, five different structural classes can be identified based on CD

Table 16.2 Summary of conformational change in enzyme and protein by plasma treatment

enzyme/protein	Sample state	Plasma source	Plasma parameters	Salient results	References
Glucose oxidase	Dried solution (water) on microscopic slide	Glow discharge	Gas: Ar, air and ethylenediamine, frequency: 13.56 MHz, pressure: 5 Pa, power: 10, 20, 30 and 40 W, operation time: 20 min, time course: 40 W for 10, 20 and 30 min	Increase in OH/NH groups signal, more random C=O bonds and some decrease in CH_2, CH_3 groups signal was observed for air and Ar, and fragmentation was observed for all gas components	Dudak et al. [1]
Casein protein	Solution (water) on CaF_2 plate	RF O_2 ICP glow discharge plasma	Gas: O_2, frequency: 13.56 MHz, pressure: 3–10^2 Pa (repeatedly)	β-Sheet and α-helix were decomposed and both peaks of C–H and N–H bonds of amide structure reduced with treatment time. Structures of amide almost diminished after treatment for 8 h, whereas the second-order structure remains approximately 15% of original	Hayashi and Yagyu [49]
Lipase	Solution (buffer) on SUS substrate	RF He jet	Gas: He, flow rate: 10 slpm, RF power: 180 W, pressure (downstream): ~1 Pa, temperature: ~57 °C	Irregular structures found in plasma-treated proteins and/or structural transitions during processes, based on α-helical, mainly β-pleated sheet, separate α-helix and β-sheet regions (α/β), intermixed α-helix and β-sheet regions (α/β). Tryptophan residues were affected	Li et al. [2]
Lysozyme (hen egg white)	Solution (buffer)	Low-frequency (LF) plasma jet	Gas: He/O_2, voltage: −3.5 to +5.0 kV with 13.9 kHz, flow rate: He and O_2 gas were 0.50 and 0.15 L/min, respectively	The secondary structure of lysozyme subjected to with hot air (heat) and plasma jet through the quartz glass plate (UV) did not change but changed by plasma treatment. Fluorescence intensity at 340 nm decreased with plasma treatment time. The peaks of MS spectrum after plasma treatment for 30 min were shifted to high molecular weight	Takai et al. [3]

(continued)

Table 16.2 (continued)

enzyme/protein	Sample state	Plasma source	Plasma parameters	Salient results	References
α-Chymotrypsin	Solution (buffer)	Atmospheric pressure plasma jets	Gas: Air, power supply: Neon light trans, operation time; 5 min	Decrease in transition temperature, calorimetric enthalpy change and Gibbs free energy change values; α-helix increase from 0.08 to 0.09; β-structure decrease from 0.45 to 0.36; and fluorescence wavelength (red shift) increase at ≈346 nm were found in treated α-chymotrypsin, indicating plasma changed the secondary conformation of the protein	Attri et al. [50]
Polyphenoloxidase	Solution (buffer)	Plasma jet	Voltage: 1.1 MHz, 2–6 kVpp, gases: Ar, Ar/O_2 0.01–0.1%, flow rate: 5 slm, operation time: 0–360 s	α-Helix and β-sheet contents changed from 36.9% to 17.8% and 15.2% to 29.4% after the treatment at 360 s and relative fluorescence intensity decreased from 58.61 to 24.76 units by 360-s plasma exposure, whereas the maximum intensity shifted by 5 nm from 341 nm to 336 nm	Surowsky et al. [5]
Peroxidase	Solution (buffer)	Plasma jet	Voltage: 1.1 MHz, 2–6 kVpp, gases: Ar, Ar/O_2 0.01–0.1%, flow rate: 5 slm, operation time: 0–360 s	α-Helix content decreased from 34.9% to 5%, whereas the β-sheet content increased from 15.6% to 39.9% and relative fluorescence intensity decreased from 62.59 units to 40.18 units by 360-s plasma exposure, while the maximum intensity shifted by 5 nm from 335 to 348 nm	Surowsky et al. [5]
Alkaline phosphatase	Solution (buffer)	Air atmospheric pressure DBD plasma	Gas: Air, voltage: 40, 50, 60 kV, pressure; atmospheric pressure, operation time 15 s to 5 min, temperature: Room temperature	α-Helix and β-sheets structures of alkaline phosphatase decreased by ACP treatment and treatment time had a stronger effect than voltage	Segat et al. [11]

(continued)

Table 16.2 (continued)

enzyme/protein	Sample state	Plasma source	Plasma parameters	Salient results	References
Lysozyme	Solution (buffer)	DBD plasma	Gas, voltage, current and frequency: 0.6 kV, 32 mA, 24 kHz for air, 0.4 kV, 20 mA, 23 kHz for N_2; pressure: Atmospheric, operation time: 8 and 12 min	For DBD treatment, the α-helix structure decreases and β-sheet increases for the lysozyme. For DBD treatment with air as feeding gas for the 8 min and 12 min, the α-helix decreases to 49.7% and 48.3%, respectively. Whereas for N_2 gas DBD treatment for 8 min and 12 min, the α-helix decreases to 31.0% and 27.1%, respectively. This shows that α-helical decreases as compared to the control lysozyme α-helix that is 51.3%	Choi et al. [14]
Lysozyme	Solution (buffer)	Plasma jet	Gas: He, flow rate: 80 L/h, voltage: 12 kVpp, frequency: 24 kHz, power density: 0.9 W/cm^2	After the treatment for the 8 and 12 min, for both air and N_2 plasma, showed that the α-helix increases and β-sheet structure decreases. The higher decrease in β-sheet is observed for the N_2-APPJ as compared to the air-APPJ. The α-helix structure increased to 58.2% and 62.0%, in the presence of air APPJ for 8-min and 12-min treatment, respectively. Whereas for N_2 gas APPJ treatment for 8 min and 12 min, the α-helical increases to 59.5% and 70.4%, respectively	Choi et al. [14]

(continued)

Table 16.2 (continued)

enzyme/protein	Sample state	Plasma source	Plasma parameters	Salient results	References
Lactate dehydrogenase	Solution (buffer)	Atmospheric-pressure DBD	Gas: He, flow rate: 80 L/h, voltage: 12 kVpp, frequency: 24 kHz, power density: 0.9 W/cm^2	α-Helix content decreased from 33.20% to 32.20%, 31.60% and 29.30%, whereas β-sheet content increases from 12.30% to 17.30%, 19.40% and 23% by direct treatment at 0, 60, 180 and 300 s. in the indirect treatment, β-helix content decreased from 33.10% to 31.50%, and β-sheet content increased from 12.30% to 20.40% by 300-s treatment	Zhang et al. [17]
Peroxidase (horseradish)	Solution (buffer)	DBD jet, <40 °C	Gas: Ar/O_2: 98/2%, flow rate: 26–30 L/min, voltage: 7 kV, operation time: 2 min with an interval for a duration of up to 10 min	The contents of α-helix were decreased from 39.89% to 29.5% after plasma exposure for 10 min, and the contents of β-sheet were increased from 15.32% to 22.28%, whereas the contents of random coils showed no remarkable change	Han et al. [25]

spectra, i.e. mainly α-helical and β-pleated sheet, separate α-helix and β-sheet regions (α/β), intermixed α-helix and β-sheet regions (α/β), and predominantly unordered (B. [51, 52]), and thus, the changes of the positions corresponding to negative peaks in CD spectra indicate that there are irregular structures in plasma-treated proteins and/or structural transitions during the plasma treatment processes. On the other hand, a peak around 348 nm in the fluorescence spectra represents the tryptophan so that the increase in the emission intensity around 348 nm with increasing plasma treatment time compared to control suggests that tryptophan residues in lipase are affected by He plasma jet.

Takai et al. [3] reported a change in the secondary structure of lysozyme (Hen egg white) by plasma jet. Low-frequency (LF) plasma jet-treated lysozyme showed the secondary structure of lysozyme changed slightly upon treatment with LF plasma jet for far-UV CD spectra. The CD spectrum of lysozyme treated with LF plasma jet for 30 min was close to that of the random coil structure in 6.0 M guanidine HCl. The far-UV ellipticity of lysozyme decreased steeply with plasma treatment time and then reached a plateau for 10 min. They also showed that the far-UV CD spectra did not change in the control experiments of hot air (heat) and plasma jet treated through the quartz glass plate (UV). The results indicate that lysozyme is denatured by the plasma treatment. Consequently, the inactivation of lysozyme by LF plasma jet results from the structural change of lysozyme. After the plasma treatment, lysozyme from hen egg white shows an intrinsic fluorescence by tryptophan residues with excitation at 295 nm. The fluorescence intensity of lysozyme at 340 nm decreased with the plasma treatment, although the maximum wavelength of the fluorescence spectra did not change. It was also confirmed that the control experiments of both hot air (heat) and plasma treated through quartz glass plate (UV) did not affect the fluorescence spectra. Because the fluorescence intensity of tryptophan is unaltered in the range of 25–95 °C, the decrease in the fluorescence intensity may result from the change of chemical structure of tryptophan by LF plasma jet. To investigate the change of chemical structure of lysozyme, mass spectroscopy (MS) was performed. Matrix-assisted laser desorption/ionization time-of-flight (MALDI–TOF) MS of the samples after plasma treatment for 0 or 30 min showed the peak shifts of MS spectrum after plasma treatment for 30 min to high molecular weight; plasma-treated lysozyme increased the mass of about 90, suggesting that LF plasma jet modifies some amino acid side chains in lysozyme. The chemical modification of 20 naturally occurring amino acids by plasma treatment in aqueous solution was well investigated using high-resolution mass spectrometry by their further research [53]. The experimental results that the sensitivity to plasma varies greatly depending on the type of amino acid could be essential for investigating the enzyme activity control and protein conformational change mechanism.

Attri et al. [50] irradiated α-chymotrypsin with atmospheric pressure air plasma jet. Transition temperature, Tm, calorimetric enthalpy change, ΔH, and Gibbs free energy change, ΔG_U, values are decreased for the treated α-chymotrypsin compared to native one. Before treatment of α-chymotrypsin with the plasma jet, the Tm was 315.15 K, whereas after treatment, it was 313.15 K. Hence, there was a decrease of 275.15 K in Tm value after treatment. A similar trend was found for the ΔG_U value;

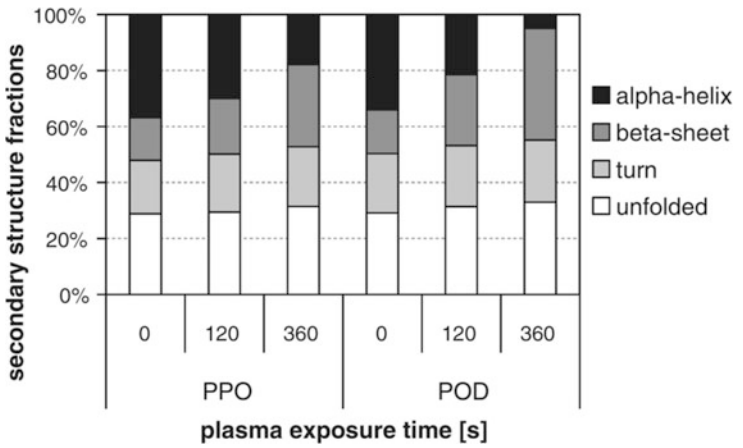

Fig. 16.2 Relative contents of α-helix, β-sheet and unfolded structures and turns in treated (120 and 360 s, pure argon) and untreated Agaricus bisporus polyphenoloxidase and horseradish peroxidase [5]

before treatment, it was 424 kJ/mol, whereas after treatment, it was 299 kJ/mol. After treatment, sharp decrease occurred in value from 18.15 kJ/mol to 11.72 kJ/mol. β-Structure was decreased from 0.45 to 0.36 by treatment, indicating plasma changed the secondary conformation of the protein. The treatment of α-chymotrypsin with plasma jet leads to an increase in fluorescence wavelength (red shift) at ≈346 nm. That leads them to conclude that plasma jet acts as denaturation agents for enzymes.

Surowsky et al. [5] provided the conformational change of PPO by Ar and Ar/O_2 plasma jet. CD-spectrometry revealed that α-helix content decreased from 36.9% to 17.8%, whereas the β-sheet content increased from 15.2% to 29.4% after a treatment time of 360 s for PPO as shown in Fig. 16.2. Regarding POD, the α-helix content decreased from 34.9% to 5%, whereas the β-sheet content increased from 15.6% to 39.9%. Regarding both enzymes, longer plasma exposure times led to greater losses of fluorescence emission intensity as well as to a slight red shift. For PPO, the relative fluorescence intensity decreased from around 58.61 units to 24.76 units after 360 s of plasma exposure (POD: 62.59 units to 40.18 units), while the maximum intensity shifted by 5 nm from 341 nm to 336 nm (POD: 335 nm to 348 nm).

Segat et al. [11] used air atmospheric pressure DBD plasma onto alkaline phosphatase and showed a decrease in α-helix and β-sheets structures by the treatment. The information on the pattern and extent to which plasma treatments cause changes in the enzymes structure were obtained by multivariate chemometric methods, and then, the samples treated for 300 s were very distinct compared to all samples treated for relatively shorter treatment time, but samples treated at different voltages for 300 s were closely related, indicating that treatment time had a stronger effect than voltage for extended treatments durations.

Lysozyme solution was irradiated with DBD plasma and atmospheric pressure plasma jet (APPJ) by Choi et al. [14] with the following specifications:: (i) Air-DBD: 1.23 kV, 7 mA, 16 kHz; (ii) N2-DBD: 0.9 kV, 1.5 mA, 16 kHz; (iii) Air-APPJ: 0.6 kV, 32 mA, 24 kHz; and (iv) N2-APPJ: 0.4 kV, 20 mA, 23 kHz. These results are quite different that the percentage of α-helix decreased for the DBD, while for the APPJ, the percentage of α-helix increased for the same enzyme. DBD treatment decreased α-helix structure and increased β-sheet of the lysozyme. For DBD treatment with air for the 8 min and 12 min, α-helix decreased to 49.7% and 48.3%, respectively. Whereas for N_2 gas DBD treatment for 8 min and 12 min, α-helix decreased to 31.0% and 27.1%, respectively. This shows that α-helix decreases as compared to the control lysozyme α-helix that is 51.3%. However, after APPJ treatment for 8 and 12 min, for both Air and N_2 plasma, it is showed that the α-helix increases and β-sheet structure decreases. The higher decrease in β-sheet was observed for the N_2-APPJ as compared to Air-APPJ. The α-helix structure increased to 58.2% and 62.0%, in the presence of Air APPJ for 8-min and 12-min treatment, respectively, whereas for N_2 gas APPJ treatment for 8 min and 12 min, α-helix increased to 59.5% and 70.4%, respectively. These results were quite different for both devices in which for the DBD, the percentage of α-helix decreased, whereas it increased for APPJ for the same enzyme. The intrinsic tryptophan emission intensity of fluorescent spectrometry provides the change in the structural information of the aromatic environment of the lysozyme before and after plasma treatment. The fluorescence intensities depend on tryptophan environment as well as the structure of tryptophan. Therefore, the change in intensity or shifts in wavelength are due to the change in the solvent environment around the tryptophan residue in the enzymes. Lysozyme showed intrinsic fluorescence from the tryptophan residues with excitation at 295 nm, with a decrease of fluorescence intensity at 340 nm after plasma treatment. However, they did not observe any shift in the maximum wavelength of the fluorescence spectra.

Zhang et al. [17] reported conformational change in lactate dehydrogenase (LDH) using He DBD plasma. In LDH solutions after the direct treatment, the α-helix content decreases from 33.20% to 32.20%, 31.60% and 29.30%, whereas the β-sheet content increases from 12.30% to 17.30%, 19.40% and 23%. In the indirect treatment, the β-helix content decreases from 33.10% to 31.50%, and the β-sheet content increases from 12.30% to 20.40% after treatment for 300 s. The CD spectra acquired after the 300-s direct and indirect plasma treatment and storage for different times revealed that the DBD plasma and H_2O_2 modified the secondary structure of LDH protease continuously. In LDH solutions after direct or indirect treatment, LDH is partially changed after storage for 24 h, especially the β-sheet content, and the DBD-induced modification of LDH is reversible due to change in the secondary structure. In the H_2O_2-treated LDH solutions, the structure changes gradually with storage time, but no renaturation is observed indicating that the modification of LDH by H_2O_2 alone is not reversible. Tertiary structure was also evaluated using dynamic light scattering (DLS) spectrum. The hydrodynamic radius of LDH protease solution is determined after different treatments for 0, 180 and 300 s. An obvious increase in the hydrodynamic radius is observed after plasma exposure for 1 h regardless of the

treatment methods which is direct or indirect. There are some supramolecules with different sizes and distribution in the plasma-treated LDH solution. The hydrodynamic radius of the LDH protease after the direct treatment increases from 4.9 to 7.4, 32.3, 10.7 and 46.2 nm after the LDH solutions have been exposed to the helium plasma for 180 and 300 s, respectively, and after the indirect treatment, it increases to 7.4, 31.9, 10 and 41 nm, respectively. Hence, the DBD plasma modifies the tertiary structure of LDH as well. The DBD plasma can trigger molecular aggregation between LDH molecules to generate larger and more complex supramolecules. Such polymerization increases in the initial 12 h, and the hydrodynamic radius of the supramolecules increases gradually in both plasma- and H_2O_2-treated LDH solutions, indicating that plasma can promote and sustain the polymerization of LDH for a relatively long time. The plasma-induced polymerization of LDH is not caused by H_2O_2 alone.

Han et al. [25] also provided the conformational change of POD (horseradish) by O_2/Ar plasma jet treatment as well as the inactivation. The contents of α-helix were decreased from 39.89% to 29.5% after plasma exposure for 10 min, and the contents of β-sheet were increased from 15.32% to 22.28%, while the contents of random coils showed no remarkable change. A maximum red shift of 7 nm after plasma treatment for 10 min was observed ($\lambda_{ex} = 280$ nm), which implied the unfolding behaviour of enzyme with the exposure of hydrophobic portions. Furthermore, the fluorescence emission spectra at about 430 nm ($\lambda_{ex} = 330$ nm) showed no shift but increase in fluorescence intensity after plasma treatment.

Attri et al. [54] reported the conformational change of mainly secondary structure for larger proteins, i.e. haemoglobin (Hb) and myoglobin (Mb) by plasma jet using different feeding gases such as air, N_2 and Ar. The results clearly revealed that after air plasma treatment, the α-helical structure of both Hb and Mb increases and β-sheet decreases, whereas after the N_2 and Ar plasma treatment, there were a decrease in α-helical structure and an increase in β-sheet as compared to without treated proteins. Furthermore, a closer look at the observations reveals that the decrease in α-helical structure is more for Mb than Hb in the presence of N_2 plasma. After the exposure of air plasma to both proteins (Hb and Mb), their structure becomes compact and percentage of α-helical structure increases, whereas in the case of N_2 and Ar plasma, the modification of α-helix to β-sheet or random coil occurs. We also checked the structural changes of Hb and Mb at pH 4.8 and did not observe any significant structural changes; hence, the observed structural changes after the plasma treatment are not due to the pH change in water. While comparing H_2O_2 effect with N_2 plasma, we observed that N_2 plasma has much more influence on the secondary structure of Hb and Mb as compared to 200 mM H_2O_2. The maximum concentration of H_2O_2 was 60 mM for N_2 plasma. This shows that other radicals (O_2^-, NO, OH and $ONOO^-$) also have a strong influence on the structural modification of proteins. A deeper study of interaction of H_2O_2 with the binding pocket amino acid residues of the target proteins Hb and Mb, using in silico molecular docking, revealed that the H_2O_2 showed molecular interaction with conserved hydrophobic amino acid residues, in Hb and Mb active pocket, thus leading to more stability and potency. However, other radicals as well as H_2O_2 for conformational change are important.

Attri et al. further checked these docking results at molecular level, using 1D NMR for Mb and Hb proteins, and concluded that there are important contributions from the other radicals for the conformational changes of Hb and Mb after the plasma treatment since that amino acid peaks were altered much by plasma treatment but not with the presence of H_2O_2.

16.8 Electric Field-Induced Conformational Change

Bekard and Dunstan [55] applied electric field strengths of 78, 150, 300 and 500 V/m with 10 and 500 Hz to hen egg white lysozyme and bovine serum albumin (BSA) solution. Representative data from the lysozyme sample showed a time-dependent irreversible decrease in the tryptophan fluorescence emission intensity as well as a weak, yet apparent, red shift of the emission wavelength maximum. A decrease in the relative fluorescence emission intensity of lysozyme was observed for all field strengths applied and was more pronounced as the field strength was increased up to 500 V/m. The electric field exposure destabilized the helical segments of lysozyme, with a concomitant increase especially in the β-strand fraction.

Okumura et al. [56] also studied trypsin-digestion process of BSA solution subjected to an external electric field of 66.7 kV/m with 50 Hz for 3 days. The relative BI of the tryptic peptides treated without the AC electric field was higher compared with the specimen treated with the AC electric field. Consistently, the relative BI of the BSA band treated without the AC electric field treatment was lower compared with specimens treated with the AC electric field. The digestion was suppressed by the application of the AC electric field, indicating the conformational change by the electric field.

Prolonged electric field application induces continuous conformational changes, reported by De et al. [57]. They applied a constant static EF of different amplitudes (120 and 200 V/cm) for 5 days to elastin (from bovine neck ligament) in order to investigate the effect of EF on the transport and structural properties. The result showed fibrils of unexposed elastin with ageing, whereas the disruption of fibril formation with EF exposed elastin. First, the elastin size with EF increased, exhibited an apex and subsequently decreased with ageing. The decrease rate of the size by EF was faster for the higher EF. FTIR spectra showed the elastin unfolding by EF. The EF of 120 V/cm facilitated the decrease in the content of β-sheets (5%) and turns (20%) at the cost of increasing α-helix (26%). In contrast, for a higher EF such as 200 V/cm, the content of turns in the protein structure increased (13%) at the cost of β-sheets. They concluded that EF has induced a significant conformational change in elastin and masked the aggregation.

16.9 Key Factors Affect Enzyme Activity and Protein Conformation by Plasma

Since the enzymatic inactivation and conformational change for lysozyme by LF plasma jet were caused by neither UV light nor heat from plasma as shown in the study by Takai et al. [53], the reactive species generated by LF plasma jet may affect lysozyme. One possible mechanism of LF plasma jet on protein is that hydroxyl radicals ($OH^{\cdot}$), superoxide anion radicals ($O_2^{-\cdot}$), hydroperoxyl radicals ($HOO^{\cdot}$) and nitric oxide ($NO^{\cdot}$) result in chemical modifications of chemically reactive sidechain of the amino acids, such as cysteine, aromatic rings of phenylalanine, tyrosine and tryptophan.

The molecular mechanism of LDH modification by plasma irradiation is provided by Zhang et al. [17]. First, the plasma-induced changes of the activity and structure modification can be ascribed to reactive species (RS) especially ones with a long lifetime. The plasma-produced RS modify the secondary and tertiary structures of LDH leading to the deactivation of LDH. Second, the DBD plasma imposes continuous modification effects on LDH in spite of storage for a long time, and there are synergistic effects involving some RS working concert with H_2O_2 to further change the secondary structure and polymerization. These undetermined RS play an important role in renaturation of the secondary structure and disintegration of supramolecules. The changes in the secondary structure and hydrodynamic radius coincide with the loss and recovery of the enzymatic activity. H. Zhang et al. illustrated the schematic of plasma-induced modification. The plasma modifies the structure and polymerization and activity changes of LDH are primarily mediated by plasma-generated RS. The RS act directly on the active sites in the molecule to inhibit the catalytic functions of LDH and also accelerate the aggregation of the LDH molecules leading to inactivation. Plasma-induced aggregation decreases the enzymatic activity and protects the active sites from being modified by RS. When the supramolecules disintegrate after storing for a long time, the protected active sites are exposed again causing recovery as aforementioned. In addition, H_2O_2 modifies the structure and polymerization resulting in inactivation of LDH but without disintegration and reactivation. The experimental results reveal that H_2O_2 plays an important role in plasma-induced modification on LDH, but it is not the sole factor and some synergistic effects of various RS especially long-lived ones can be observed by Attri [54].

16.10 Key Factors Affect Enzyme Activity and Protein Conformation by Electric Field

The mechanism of effect of electric field is most often discussed using MD simulations. Ojeda-May and Garcia [58] demonstrated that an external constant electric field is able to modify the secondary structure of a protein and induces a transition

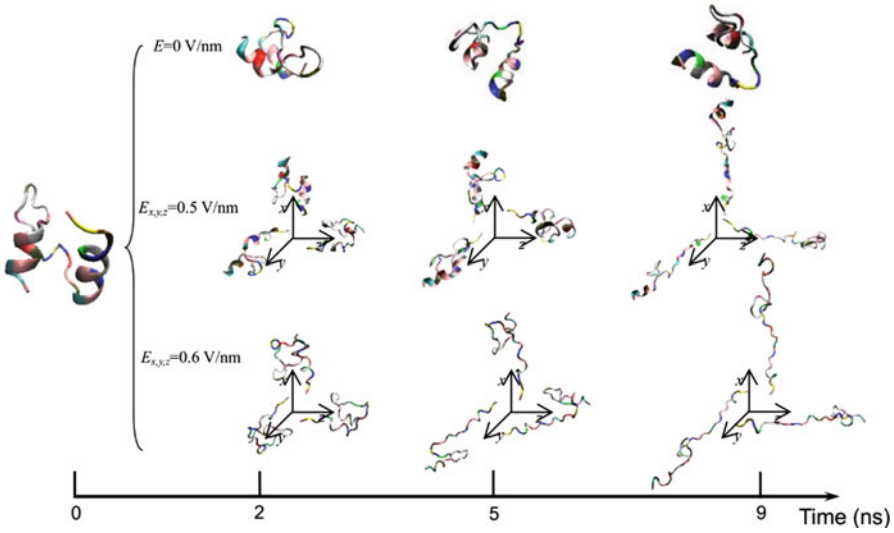

Fig. 16.3 Typical conformation of the protein 1BBL exposed in the electric fields with the strength $E_{x,y,z} = 0$ V/nm, 0.5 V/nm and 0.6 V/nm during the simulation process. [59]

from a β-sheet into a helix-like conformation. This dramatic change is driven by a global rearrangement of the dipole moments at the amide planes. We also predict electric-field-induced modifications of the intermediate states of the protein.

Although relatively strong electric field intensities were used, but Jiang et al. [59] provided useful models to visually understand the effects of electric fields on conformational change of protein as shown in Fig. 16.3. They used protein 1BBL and clearly captured the structural transitions of the protein from helix to turn or random coil conformation induced by the increasing strength of electric field. During the analysis, the conformational stability was weakened, and the protein was stretched as an unfolded structure when it was exposed in a sufficiently high electric field. The characteristic time when the jump occurs in the time evolution curves of root mean square deviation (RMSD) and radius of gyration Rg decreased with electric strength, which demonstrated the rapidly conformational transition that occurred. The number of intra-protein hydrogen bonds, which is a key factor for stabilizing the protein structure, is related to the overall size of the protein. The value of the dipole moment and characteristic time were both influenced by the strength but were independent of the direction of the external electric field. The protein sample becomes rotated with the electric field direction. These conclusions provide a theoretical realization of understanding the protein conformational transition in an electric field and the guidance for anticipative applications.

16.11 Summary

This chapter provided a summary of enzyme activity controls and protein conformational changes using plasma. While previously some studies that reduce the activity of the target enzyme by various gases and plasma generation methods have been of most interest, the effect of RONS generated by plasma has been investigated independently of the effects of temperature increases, UV irradiation and pH decreases associated with plasma generation in the last 10 years. These studies are positioned as very important areas that are expected to contribute not only to the pre- and post-treatment of agricultural products but also to the pharmaceutical and processed food industries.

Further research has to be taken into account for a quantitative discussion of plasma-induced RONS and electric fields. In other words, the effects of RONS and EF on enzymes and proteins should be treated quantitatively, and the effects corresponding to them should be experimentally and precisely advanced, and cross-checks by numerical analysis should be also promoted, with the help of MD simulation. So far there are many cases where existing highly versatile MD simulation software requires new algorithms to deal with RONS and electric fields at the same time. Such researches will be achieved through multiple interdisciplinary studies in the field of electrochemical engineering, protein engineering, molecular biology and computational science.

References

1. Dudak FC, Kousal J, Seker UÖŞ, Boyacı İH, Choukourov A, Biederman H. Proceedings of 28th ICPIG, July 15–20, 2007, Prague, Czech Republic; 2007
2. Li H-P, Wang L-Y, Li G, Jin L-H, Le P-S, Zhao H-X, Xing X-H, Bao C-Y. Manipulation of Lipase Activity by the Helium Radio-Frequency, Atmospheric-Pressure Glow Discharge Plasma Jet. Plasma Process Polym. 2011;2011(8):224–9.
3. Takai E, et al. Protein Inactivation by Low-temperature Atmospheric Pressure Plasma in Aqueous Solution. Plasma Process Polym. 2012;2012(9):77–82.
4. Pankaj SK, et al. Kinetics of tomato peroxidase inactivation by atmospheric pressure cold plasma based on dielectric barrier discharge. Innov Food Sci Emerg Technol. 2013;19 (2013):153–7.
5. Surowsky B, Fischer A, Schlueter O, Knorr D. Cold plasma effects on enzyme activity in a model food system. Innov Food Sci Emerg Technol. 2013;19(2013):146–52.
6. Tappi S, Berardinelli A, Ragni L, Rosa MD, Guarnieri A, Rocculi P. Atmospheric gas plasma treatment of fresh-cut apples. Innov Food Sci Emerg Technol. 2014;21(2014):114–22.
7. Chen HH, Hung CL, Lin SY, Liou GJ. Effect of Low-Pressure Plasma Exposure on the Storage Characteristics of Brown Rice. Food Bioprocess Technol. 2014;8:471–7.
8. Zhang H, Xu Z, Shen J, Li X, Ding L, Ma J, Lan Y, Xia W, Cheng C, Sun Q, Zhang Z, Chu PK. Effects and Mechanism of Atmospheric-Pressure Dielectric Barrier Discharge Cold Plasmaon Lactate Dehydrogenase (LDH) Enzyme. Sci Rep. 2015;5:10031. https://doi.org/10.1038/srep10031.

9. Tappi S, Gozzi G, Vannini L, Berardinelli A, Romani S, Ragni L, Rocculi P. Cold plasma treatment for fresh-cut melon stabilization. Innov Food Sci Emerg Technol. 2016;33 (2016):225–33.
10. Lee K, Kim H, Woo K, Jo C, Kim J, Kim S, Park H, Oh S, Kim W. Evaluation of cold plasma treatments for improved microbial and physicochemical qualities of brown rice. Food Sci Technol. 2016;73:442–7. https://doi.org/10.1016/j.lwt.2016.06.055.
11. Segat A, Misra NN, Cullen PJ, Innocente N. Effect of atmospheric pressure cold plasma (ACP) on activity and structure of alkaline phosphatase. Food Bioprod Process. 2016;98:181–8.
12. Xu Y, Tian Y, Ma R, Liu Q, Zhang J. Effect of plasma activated water on the postharvest quality of button mushrooms, Agaricus bisporus. Food Chem. 2016;197(2016):436–44.
13. Khani MR, Shokri B, Khajeh K. Studying the performance of dielectric barrier discharge and gliding arc plasma reactors in tomato peroxidase inactivation. J Food Eng. 2017;197:107e112.
14. Choi S, Attri P, Lee I, Oh J, Yun J-H, Park JH, Choi EH, Lee W. Structural and functional analysis of lysozyme after treatment with dielectric barrier discharge plasma and atmospheric pressure plasma jet. Sci Rep. 2017;7:1027. https://doi.org/10.1038/s41598-017-01030-w.
15. Tolouie H, Mohammadifar MA, Ghomi H, Yaghoubi AS, Hashemi M. The impact of atmospheric cold plasma treatment on inactivation of lipase and lipoxygenase of wheat germs. Innov Food Sci Emerg Technol. 2018;47(2018):346–52.
16. Fanelli F, Fracassi F, Lapenna A, Angarano V, Palazzo G, Mallardi A. Atmospheric Pressure Cold Plasma: A Friendly Environment for Dry Enzymes. Adv Mater Interf. 2018;2018 (5):1801373.
17. Zhang H, Ma J, Shen J, Lan Y, Ding L, Qian S, Cheng C, Xia W, Chu PK. Comparison of the Effects Induced by Plasma Generated Reactive Species and H2O2 on Lactate Dehydrogenase (LDH) Enzyme. IEEE Trans Plasma Sci. 2018;46(8)
18. Farasat M, Arjmand S, Ranaei Siadat SO, Sefidbakht Y, Ghomi H. The effect of non-thermal atmospheric plasma on the production and activity of recombinant phytase enzyme. Sci Rep. 2018;8:16647. https://doi.org/10.1038/s41598-018-34239-4.
19. Chutia H, Kalita D, Mahanta CL, Ojah N, Choudhury AJ. Kinetics of inactivation of peroxidase and polyphenol oxidase in tender coconut water by dielectric barrier discharge plasma. LWT Food Sci Technol. 2019;101:625–9.
20. Umair M, Jabbar S, Nasiru MM, Sultana T, Senan AM, Awad FN, Hong Z, Zhang J. Exploring the potential of high-voltage electric field cold plasma (HVCP) using a dielectric barrier discharge (DBD) as a plasma source on the quality parameters of carrot juice. Antibiotics. 2019;8:235.
21. Tappi S, Tappi S, Ragni L, Tylewicz U, Romani S, Ramazzina I, Rocculi P. Browning response of fresh-cut apples of different cultivars to cold gas plasma treatment. Innov Food Sci Emerg Technol. 2019;53:56–62.
22. Kang JH, Roh SH, Min SC. Inactivation of Potato Polyphenol Oxidase Using Microwave Cold Plasma Treatment. J Food Sci. 2019;84(5)
23. Zouelm F, Abhari K, Hosseini H, Khani M. The Effects of Cold Plasma Application on Quality and Chemical Spoilage of Pacific White Shrimp (Litopenaeus vannamei) during Refrigerated Storage. J Aquatic Food Prod Technol. 2019;28(6)
24. Muhammad AI, Li Y, Liao X, Liu D, Ye X, Chen S, Hu Y, Wang J, Ding T. Effect of dielectric barrier discharge plasma on background microflora and physicochemical properties of tiger nut milk. Food Control. 2019;96:119–27.
25. Han Y-X, Cheng J-H, Sun D-W. Changes in activity, structure and morphology of horseradish peroxidase induced by cold plasma. Food Chem. 2019;301:125240.
26. Wang T, Wu Y, Li Z, Sha X. Potential impact of active substances in non-thermal discharge plasma process on microbial community structures and enzymatic activities in uncontaminated soil. J Hazard Mater. 2020;393:122489.
27. Farias TRB, Rodrigues S, Fernandes FAN. Effect of dielectric barrier discharge plasma excitation frequency on the enzymatic activity, antioxidant capacity and phenolic content of apple cubes and apple juice. Food Res Int. 2020;136:109617.

28. Batista JDF, Dantas AM, dos Santos FJV, Madruga MS, Fernandes FAN, Rodrigues S, Borges GSC. Effects of cold plasma on avocado pulp (Persea americana Mill.): Chemical characteristics and bioactive compounds. J Food Process Preserv. 2020:e15179.
29. Lapenna A, Fanelli F, Fracassi F, Armenise V, Angarano V, Palazzo G, Mallardi A. Direct exposure of dry enzymes to atmospheric pressure non-equilibrium plasmas: The case of tyrosinase. Materials. 2020;2020(13):2181. https://doi.org/10.3390/ma13092181.
30. Koddy JK, Miao W, Hatab S, Tang L, Xu H, Nyaisaba BM, Chen M, Deng S. Understanding the role of atmospheric cold plasma (ACP) in maintaining the quality of hairtail (Trichiurus Lepturus). Food Chem. 2021;343:128418.
31. Seo SY, Sharma VK, Sharma N. Mushroom tyrosinase: recent prospects. J Agric Food Chem. 2003;51:2837–53.
32. Baltes W. Lebensmittelchemie. 5th ed. Berlin: Springer; 2000.
33. Boonsiri K, Ketsa S, van Doorn WG. Seed browning of hot peppers during low temperature storage. Postharvest Biol Technol. 2007;45:358–65.
34. Valentines MC, Vilaplana R, Torres R, Usall J, Larrigaudière C. Specific roles of enzymatic browning and lignification in apple disease resistance. Postharvest Biol Technol. 2005;36:227–34.
35. Hendrickx M, Ludikhuyze L, Van den Broeck I, Weemaes C. Effects of high pressure on enzymes related to food quality. Trends Food Sci Technol. 1998;9:197–203.
36. Vámos-Vigyázó L. Prevention of enzymatic browning in fruits and vegetables. A review of principles and practice. In: Lee CY, Whitaker JR, editors. Enzymatic browning and its prevention. Washington, DC: American Chemical Society; 1995. p. 49–62.
37. Gardner HW. Biological roles and biochemistry of the lipoxygenase pathway. HortScience. 1995;30:2.
38. Kausch KD, Handa AK. Molecular Cloning of a Ripening-Specific Lipoxygenase and Its Expression during Wild-Type and Mutant Tomato Fruit Development. Plant Physiol. 1997: 11. https://doi.org/10.1104/pp.113.4.1041.
39. Rogiers SY, Mohan Kumar GN, Knowles NR. Maturation and Ripening of Fruit of Amelanchier alnifolia Nutt. are Accompanied by Increasing Oxidative Stress. Ann Bot. 1998;81(2):203–11. https://doi.org/10.1006/anbo.1997.0543.
40. Chrastil J. Influence of storage on enzymes in rice grains. J Agric Food Chem. 1990;38 (5):1198–202. https://doi.org/10.1021/jf00095a008.
41. Chrastil J. Enzyme activities in preharvest rice grains. J Agric Food Chem. 1993;41 (12):2245–8. https://doi.org/10.1021/jf00036a004.
42. Wang YJ, Wang L, Shephard D, Wang F, Patindol J. Properties and Structures of Flours and Starches from Whole, Broken, and Yellowed Rice Kernels in a Model Study. Cereal Chem J. 2002;79(3):383–6. https://doi.org/10.1094/CCHEM.2002.79.3.383.
43. Suzuki Y, Ise K, Li C, Honda I, Iwai Y, Matsukura U. Volatile components in stored rice [Oryza sativa (L.)] of varieties with and without lipoxygenase-3 in seeds. J Agric Food Chem. 1999;47 (3):1119–24. https://doi.org/10.1021/jf980967a.
44. Lee KH, Kim HJ, Woo KS, Jo C, Kim JK, Kim SH, Park HY, Oh SK, Kim WH. Evaluation of cold plasma treatments for improved microbial and physicochemical qualities of brown rice. LWT Food Sci Technol. 2016;73:442e447.
45. Ertugay M, et al. Effect of pulsed electric field treatment on polyphenol oxidase, total phenolic compounds, and microbial growth of apple juice. Turk J Agric For. 2013;37:772.
46. Okumura T, Yaegashi T, Fujiwara T, Takahashi K, Takaki K, Kudo T. Influence of pulsed electric field on enzymes, bacteria and volatile flavor compounds of unpasteurized sake. Plasma Sci Technol. 2018;20:4.
47. Ohshima T, Tamura T, Sato M. Influence of pulsed electric field on various enzyme activities. J Electrost. 2007;65:156.
48. Zhao W, Yang R. The effect of pulsed electric fields on the inactivation and structure of lysozyme. Food Chem. 2008;110:334.
49. Hayashi N, Yagyu Y. Treatment of protein using oxygen plasma produced by RF discharge. J Plasma Fusion Res. 2008;33(3):791–4.

50. Attri P, Venkatesu P, Kaushik N, Han YG, Nam CJ, Choi EH, Kim KS. Effects of atmospheric-pressure non-thermal plasma jets on enzyme solutions. J Korean Phys Soc. 2012;60(6):959–64.
51. Czarnik-Matusewicz B, Pilorz S. 2DCOS and MCR-ALS as a combined tool of analysis of β-lactoglobulin CD spectra. J Mol Struct. 2006;799:211.
52. Manavalan P, Johnson WC Jr. Sensitivity of circular dichroism to protein tertiary structure class. Nature. 1983;305:831.
53. Takai E. Chemical modification of amino acids by atmospheric-pressure cold plasma in aqueous solution. J Phys D Appl Phys. 2014;47:285403.
54. Attri P, Kumar N, Park JH, Yadav DK, Choi S, Uhm HS, Kim IT, Choi EH, Lee W. Influence of reactive species on the modification of biomolecules generated from the soft plasma. Sci Rep. 2015;5:8221. https://doi.org/10.1038/srep08221.
55. Bekard I, Dunstan DE. Electric field induced changes in protein conformation. Soft Matter. 2014;10(3):431–7.
56. Okumura T, Yamada K, Yaegashi T, Takahashi K, Syuto B, Takaki K. External AC electric field-induced conformational change in bovine serum albumin. IEEE Trans Plasma Sci. 2017;45(3):489–94.
57. De D. Electric field-driven conformational changes in the elastin protein. Phys Chem Chem Phys. 2021;23:4195.
58. Ojeda-May P, Garcia ME. Electric Field-Driven Disruption of a Native β-Sheet Protein Conformation and Generation of a Helix-Structure. Biophys J. 2010;99:595–9.
59. Jiang Z, You L, Dou W, Sun T, Xu P. Effects of an Electric Field on the Conformational Transition of the Protein: A Molecular Dynamics Simulation Study. Polymers. 2019;2019 (11):282. https://doi.org/10.3390/polym11020282.

Chapter 17
Plasma Applications in Microalgal Biotechnology

Anh Dung Nguyen, Matteo Scarsini, Fabienne Poncin-Epaillard, Olivier Noel, Justine Marchand, and Benoît Schoefs

Abstract Microalgae are very important organisms for the biosphere because they are at the basis of most of the food chains. Some taxa can also bloom and release dangerous toxins in the environment. Microalgae are also very promising for industrial applications in various sectors, including food, feed, pharmaceutical, wellness, energy, building, space, water treatment, biosensing, and biotechnology. The development of these applications requires in many cases the optimization of processing steps. Plasma technology has already been applied on biomolecules, proteins, enzymes, and peptides in the biomedical field, for the preparation of bioactive compounds and antifouling surfaces. Nowadays, the research prospective deals with the agriculture domain in the purpose of cleaning, sterilizing, or fertilizing the soil. However, plasma technology was also explored for enhancing bioadhesion and bioproduction without destroying microalgae. This chapter gives illustrations on this new application of plasma technology.

Anh Dung Nguyen and Matteo Scarsini contributed equally with all other contributors.

A. D. Nguyen
Institut des Molécules et Matériaux du Mans (IMMM)—UMR 6283 CNRS, Le Mans Université, Le Mans, France

Metabolism, Engineering of Microalgal Molecules and Applications (MIMMA), Mer Molécules Santé, IUML—FR 3473 CNRS, Le Mans University, Le Mans, France
e-mail: Anh_Dung.Nguyen.Etu@univ-lemans.fr

M. Scarsini · J. Marchand · B. Schoefs (✉)
Metabolism, Engineering of Microalgal Molecules and Applications (MIMMA), Mer Molécules Santé, IUML—FR 3473 CNRS, Le Mans University, Le Mans, France
e-mail: justine.marchand@univ-lemans.fr; benoit.schoefs@univ-lemans.fr

F. Poncin-Epaillard · O. Noel
Institut des Molécules et Matériaux du Mans (IMMM)—UMR 6283 CNRS, Le Mans Université, Le Mans, France
e-mail: Fabienne.Poncin-Epaillard@univ-lemans.fr; olivier.noel@univ-lemans.fr

S. Horikoshi et al. (eds.), *Agritech: Innovative Agriculture Using Microwaves and Plasmas*, https://doi.org/10.1007/978-981-16-3891-6_17

Keywords Plasma · Microalgae · Biotechnology · Microalga immobilization · Metal analysis

17.1 Introduction

17.1.1 The Microalgal World

Microalgae are eukaryotic unicellular or colonial eukaryotic microorganisms differing from cyanobacteria, which are prokaryotic, by the presence of a nucleus and semi-autonomous organelles. In this chapter, both types of organisms will be designated as microalgae. Microalgae represent a polyphyletic group. Microalgae differ by the type of cell wall, pigment composition and metabolism. Being photosynthetic, microalgae contribute to circa half of the world's oxygen emission and carbon dioxide capture. The generated biomass plays a significant role in the benthic food web because microalgae are enriched in several key ingredients such as vitamins, polyunsaturated fatty acids, magnesium, iron and calcium, antioxidants, and other biologically active compounds [1]. Thanks to their powerful adaptive capacity to stress conditions, microalgae have colonized every type of ecological niche [2, 3]. Consequently, they are abundantly found in rivers, oceans, lakes, sea, and moist soil. Beside their natural content made using the inorganic capture carbon, microalgae can take up, store, or transform other inorganic forms of elements such as metals [4].

17.1.2 Microalgae: Development in Unfavorable Environment

The natural environment is usually rather poor in crucial elements for cell development [5], and therefore, microalgae develop in unfavorable conditions. Fortunately, the complex evolutionary story of microalgae resulted in organisms exhibiting a tremendous metabolic flexibility [2, 6]. This includes the reorientation of the carbon metabolism toward the accumulation of energy inside intracellular compounds such as lipids or carbohydrates [7]. Exploiting all of these possibilities perfectly, microalgae are able to occupy every type of ecological niche as well as degraded environments such as those enriched in nitrogen, phosphorus, and other nutrients triggering the eutrophication of lakes [3, 4].

17.1.3 Microalgae and Biotechnology

During the last centuries, the intensification of the utilization of fossil gas and oil reserves as a main source of energy for world development has generated more CO_2

than the environment can absorb causing CO_2 accumulation in the atmosphere at the origin of global warming [8]. This, together with the eventual reduction of fossil fuel reserves, drove an intensive research for new energy sources. Because photosynthesis allows the production of lipids from atmospheric CO_2 photosynthetic organisms constitute the best possibility to produce biofuels. The history of biofuels has been divided into four "generations" [9]. The first and second generations were based on feedstock derived mainly from terrestrial plant waste streams whose productions compete with food production. In contrast, the third and fourth generations are based on microalgae, thereby reducing the food *versus* fuel concerns. From the combustion point of view, the utilization of lipids as biofuel generates CO_2, and therefore, they are not solving the CO_2 emission in the atmosphere. From this point of view, biohydrogen looks more interesting because it is a zero-carbon fuel and produces water [10, 11]. Therefore, hydrogen is considered as a clean, versatile, and promising alternative fuel with high energy density (142 MJ/kg) [12]. Because hydrogen is not readily available in nature, one of the main recent challenges is hydrogen production, including the production by microalgae [12]. Besides fuels, microalgae synthesize other metabolites of interest for food, health, cosmetic, energy, or pharmaceutical industries [1, 13]. Most of these compounds are high-value molecules. For instance, the price of the natural carotenoid astaxanthin is over \$14,000 US kg^{-1} [14]. Microalgae can also be used in phytoremediation process or in the preparation of element-enriched biomass for nutritional purposes [15] or biofertilizers [16].

From the biotechnological point of view, most of the processes comprise two steps. The first one aims at growing microalgae in favorable conditions in order to obtain biomass. The biomass is then placed in unfavorable growth conditions in order to induce the metabolic reorientation that ends by the accumulation of the desired compounds. Because the compounds accumulate inside the cells, they need to be extracted. Downstream processes are either destructive for the biomass that should be regrown after each extraction or nondestructive, offering the possibility of a milking process [17].

This contribution deals with the use of plasma in microalgal biotechnology. First, notions of plasma physics and chemistry are briefly presented, and then, plasma technology development in microalgal biotechnology is reviewed. This chapter ends with the applications of plasma in the field of water treatment and compound analyses.

17.2 Plasma: The Basic Side

Plasma physics usually describes one of the four fundamental states of matter consisting of neutral, positively, and negatively charged atoms and molecules. The densities of charged particles are equal, and therefore, the overall medium is electrically neutral. Non-thermal Ar/O_2, N_2/O_2, He/air, etc. plasmas at working pressure comprised between atmospheric pressure, and few Torr are applied in the

biotechnology field since the associated species energy and temperature are suitable for soft organic matter. But these plasma phases remain an effective source of reactive nitrogen or oxygen species (RNS and ROS, respectively) toward biomolecules and living tissues. Therefore, such a gaseous state was recently applied to biology, medicine, and agriculture fields despite its complex chemical pathway. Applications of non-thermal plasmas have been therefore developed into several active research areas. Plasma medicine generates several chemical pathways, which can trigger cell functions [18, 19]. Furthermore, in agriculture, plasma has been applied recently for the germination of seeds and growth of farm products [20].

Radicals, ions, excited atoms and molecules, and photons formed in the plasma phase are able to (de)activate microorganisms, and their reactivity was first applied to the sterilization and disinfection processes of inert liquid and solid materials [21]. The survival kinetic to exposition to plasma mixtures typically comprised 2 or 3 decreasing phases characterized by different rates: The first phase, the fastest, corresponds to the stacked microorganisms killed by plasma-generated UV; the second phase, the slowest is due to physical erosion by the atomic oxygen bombardment. It is sometimes one with the lowest kinetics rate and is sometimes combined with the third phase. Reactive neutral species generated from the plasma (O, O_3, OH, NO, NO_2...), the so-called ROS and RNS, are the major source of active species for tissue engineering including sterilization, microorganisms' adhesion, and culture. ROS are double-sided with biological cells. On the one hand, they act as cellular signaling molecules triggering important physiological responses such as carotenogenesis in green microalgae [22], while on the other hand, ROS are able to oxidize any type of biological compounds, creating deleterious oxidative burst.

The plasma treatment efficiency is mostly bound to the formed ROS and RNS, atoms, and UV radiations. However, the other plasma species also interact with any (bio)organic material. Electrons driving the plasma physics impact the surface chemistry of polymers and therefore have a chemical effect on microorganisms on quite thick penetration (μm scale: Rusanov et al. [23]). Moreover, at the interface of plasma and aqueous microorganisms' solution, the hydrated electrons convert the oxygen dissolved in water into superoxide O_2^-, involved in various biological processes. Positive ions, predominant as charged plasma species, also interact and transfer their charge to solvated molecules until forming H_3O^+ with water altering the lipid layer of cellular membrane. Plasma phase is initiated from an electrical discharge at variable frequency and power, which controls the ionic motion in the gaseous phase but which may also create electrostatic force by charge accumulation on the insulating materials as cells and then causes the cell membrane rupture [24]. Furthermore, even if the heat effect is negligible with non-thermal plasma, some local and short-time but intensive heating may appear, especially with atmospheric plasma that alters the microorganism in contact.

17.3 Plasma Treatment and Microalgal Biotechnology

17.3.1 Preparation of Dedicated Nutrients for Microalgal Culture

Because microalgae are often grown out of their natural environment, synthetic medium mimicking it more or less adequately is required. The ability of the artificial growth medium to support algal development depends on its composition, and taxa may have particular requirements. For instance, the mixotrophic strains of *Haematococcus pluvialis* grow better on acetate than on carbon dioxide [25]. This is also the case of diatoms that usually cannot develop in the absence of silicium [26, 27], an element required to build their highly decorated cell wall. Using inductively coupled plasma (ICP)-synthesized nanosilica, Saxena et al. [28] recorded a better biomass productivity and pigment content of three diatoms than with nonplasma-synthesized Si. The authors attributed this result to the lower cell adhesion and aggregation that would impact positively the flow ability of nanosilica throughout the media because of its improved homogenous nature.

17.3.2 Plasma-Modified Surface for Microalga Immobilization

Microalgal biotechnology requires cultivating a large volume of microalgal biomass. For this purpose, microalgae are grown in either open ponds or closed photobioreactor. Sometimes both systems are combined, and recently, new cultivation ways have been proposed. Because the cell density remains rather weak (<0.5 kg m^{-3}), microalgal biotechnology usually faces a challenging downstream process that is microalgae harvesting. From the economic point of view, harvesting may represent as much as 20–30% of the production costs [29].

17.3.2.1 Algal Immobilization

One way to reduce the harvesting cost consists in immobilizing microalgae, which avoids regrowing microalgae after each harvesting/extraction cycle used by traditional process. This has been developed since the 1980s and is currently used by pharmaceutical, aquaculture, food and cosmetic industries, wastewater treatment and preconcentration of trace substances, and energy production, including biohydrogen (for a review, see Barros et al. [29]). Recently, we estimated the adhesion of *Phaeodactylum tricornutum* diatom on N_2, O_2, or CO_2 plasma-modified polyethylene terephthalate (PET) surfaces by developing an original protocol using an atomic force microscopy (AFM) (Fig. 17.1). Measurements reported in this section were carried out using a commercial Si_3N_4 probe (DNP10 probes, Bruker) whose

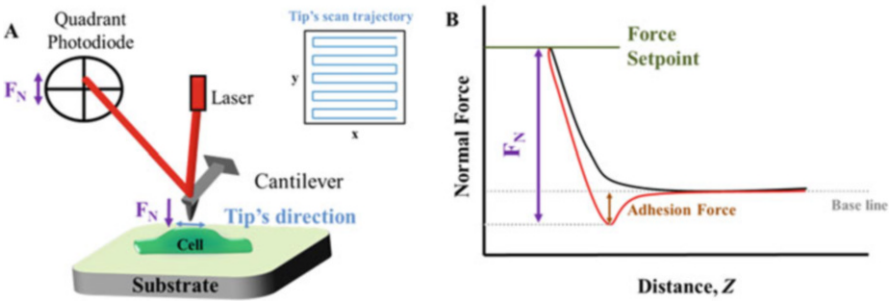

Fig. 17.1 Methodology for determining the adhesion force between the cell and the specific substrate. (**a**) Schematic illustration of the AFM imaging in contact mode. The AFM tip scans the sample surface (x, y) at a constant applied normal force by using a servo-loop system. (**b**) A typical force curve obtained on the cell in force spectroscopy mode in air. The applied normal force in imaging mode for the adhesion force measurement was determined by registering a force curve. The value of the applied force (F_N) expressed in newton is defined as the force difference in between the force setpoint (top) and minimum force of the curve corresponding to the adhesion force in between the AFM probe and the microalga (bottom)

cantilever has a nominal stiffness of 0.58 N m^{-1}. The principle of the method consisted in imaging microalga in AFM contact mode imaging and using the probe for scratching the microalga under a definite constant applied force load to the contact. Depending on the plasma treatment, the number of scans required to completely remove the cell varied. If the cell or a part of the cell was not totally removed from the substrate, a gradual increase of the applied force was adjusted until the cell was completely removed from the substrate. Finally, the adhesion force of the cell with the substrate was assessed by a specific parameter, which was defined by the product of the applied force with the number of scans needed to completely remove the cell from the substrate.

Our results show that the diatom *P. tricornutum* had a better adherence to the plasma-treated PET substrates compared to the untreated PET substrate (Fig. 17.2). The microalga adherence was however different according to the plasma treatment (Fig. 17.3). N_2 plasma- and O_2 plasma-treated PET substrates improved only slightly the adherence, whereas it was strongly increased on CO_2 plasma-treated PET substrate (after 32 scans, the cell is still on the substrate) (Fig. 17.2). The differences in adherence can be explained by the different types and the diversity of functions created at the PET surface during the plasma treatment: O_2 and CO_2 treatments have generated -CO_2-, -CO-, -CHO, and -OH functions, whereas N_2 treatment allowed the creation of amine (-NH_x) and amide (CO-N_x-) functional groups; the two latter rendering the surface more hydrophilic [30]. The extracellular matrix of diatoms is mostly composed by polar polymeric substances, and they can strongly interact with the hydrophilic substrates *via* van der Waals interactions and/or physical and/or chemical bonds. Consequently, *P. tricornutum* cells have a greater adherence with the plasma-treated substrate generating hydrophilic chemical groups. The adhesion

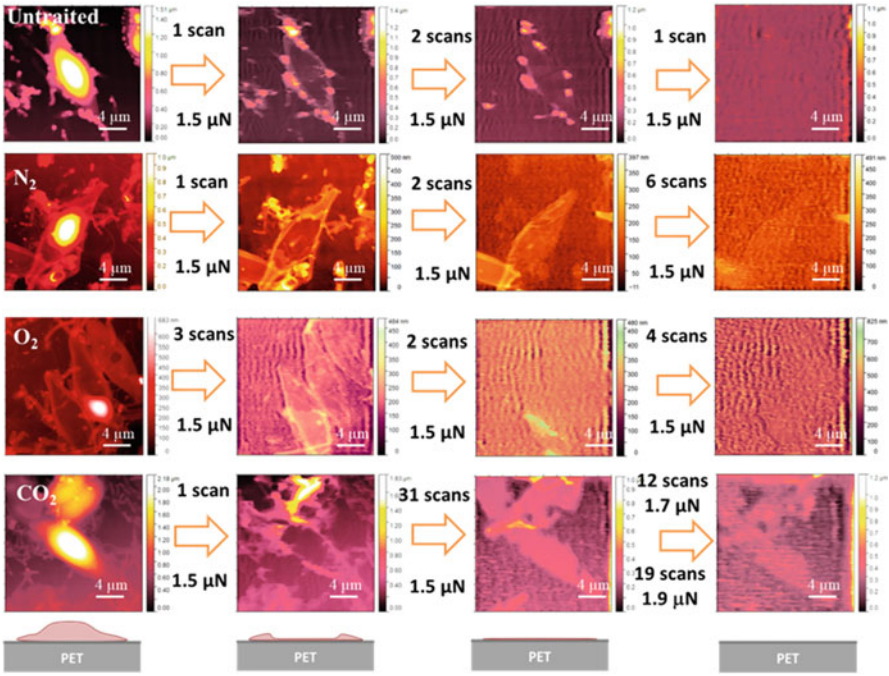

Fig. 17.2 AFM images of *P. tricornutum* cells immobilized on untreated and plasma-treated PET surfaces obtained in contact mode AFM in air during scratching. For completely removing the microalga from the substrate, it needs 4 scans at an applied normal force of 1.5µN for untreated PET substrate: (**a**) 9 scans at an applied normal force of 1.5µN for N_2 plasma-treated PET substrate, (**b**) 9 scans at an applied normal force of 1.5µN for O_2 plasma-treated PET substrate, (**c**) 32 scans at an applied normal force of 1.5µN, 12 scans at an applied normal force of 1.7µN, and (**d**) 19 scans at an applied normal force of 1.9µN for CO_2 plasma-treated PET substrate

force parameter of the microalgae cell with different treated substrates presents a similar trend than that of the surface energy (Fig. 17.3).

17.3.3 Plasma Treatment as a Mean to Improve Algal Productivity

A explained previously, plasma treatment generates both chemical (ROS, RNS, UV, and charged particles) and physical (shock waves and electric field) stresses able to modify or even deactivate, i.e., kill, microorganisms, including microalgae, notably through their mutagenesis capacity or/and the eventual dramatic pH decrease of the growth medium [31, 32]. The acidification of the growth medium during the plasma treatment may be responsible for the spectacular modification of microalga aspect at least for dinoflagellates [32]. There are only a few studies dedicated to the impact of

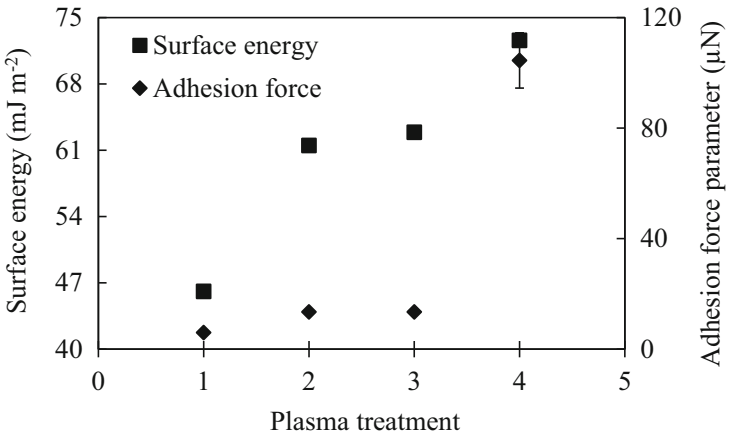

Fig. 17.3 Evolution of the surface energy (determined by measuring contact angles with water and dichloromethane and di-iodide methane and of the adhesion force of the *P. tricornutum* for different PET substrates

a plasma treatment on the physiology of algae. Microalgae respond to the oxidative stress generated by the plasma treatment by activating antioxidant defense mechanisms (superoxide dismutase and catalase) and producing signaling molecules such as NOx [31]. During long-term plasma treatment, these mechanisms may become inoperative, contributing to cell death (Table 17.1). Interestingly, and despite the fragility of chlorophyll (Chl) pigments [38, 39], the cellular quota in Chl was not too much affected by a cold plasma treatment (120 s), allowing an effective photosynthesis in the cells having survived to the plasma treatment and thus biomass development. Longer treatments induced Chl bleaching and cell death [38]. Microalgal movements as well as the metabolism ending with the accumulation of products such as lipids might be affected because running defense mechanisms consume energy that is no longer available for running flagella motors and the activity of metabolic pathways [32]. Accordingly, Almarashi et al. [31] observed a decrease of the cellular lipid quota, lipid productivity, and lipid quality in plasma-treated microalgae (more than 30 s) with the formation of peroxided products and a modified fatty acid composition. The fatty acid being more saturated, their nutritional interest is reduced but could be used to produce biofuels. When compared to other microorganisms, microalgae appeared as rather resistant to the cumulative stresses induced by a plasma treatment, probably because they can rely on specific and efficient morphologic (rigid cell wall), enzymatic (ROS: Nguyen-Deroche et al. [40]) and biophysical [41] defense mechanisms, and also a wonderful plasticity of their metabolism [7, 42].

The success of algal biotechnology resides partly on the obtention of very productive strains. For this purpose, biodiversity can be used, but the process is long and uncertain [17]. To speed up the process of tailoring microalgae for specific applications (biodiesel, biohydrogen, etc.), the creation of mutants using targeted or

Table 17.1 Summary of the effects of ARTP on different microalgae

Algal category	Genus	Species	Original strain	Mutant strain	Genetic stability (generation)	Characteristics						References
						Morphologic change	Growth rate	Biochemistry				
								Chlorophyll (per unit cell volume)	Fatty acid methyl ester	Exopolysaccharides	Lipid	
Cyanobacteria	*Spirulina*	*platensis*	FACHB-904	3-A10 3-B2 4-B3	>9	No Linear No	69 93 110			140% 178% 70%	– – –	[33]
Green microalgae	*Scenedesmus*	*dimorphus*		Sd-Pm210		Yes	Yes		×1.4	–		[34]
	Chlorella	*pyrenoidosa*	FACHB-8 HIT9	II-H6	> 10	–	Yes		–	–	+16.85%	[35]
		vulgaris					–					[31]
	Chlamydomonas	*reinhardtii*	FACHB-265	A4		Twice larger		5–6 times lower				[36]
Dinoflagellate	*Crypthecodinium*	*cohnii*	ATCC 30556	M7	> 9	–	–			+160%		[37]

nontargeted approaches can be used [43, 44]. Among the nontargeted approaches, atmospheric temperature plasma mutagenesis was developed recently for mutating microorganisms such as microalgae [45]. Ar/O_2 atmospheric pressure dielectric barrier discharge can cause mutations, but the method presents numerous shortcomings, such as low mutation controllability, high operating voltage, inhomogeneous discharge, and low mutation efficiencies as demonstrated with the yeast *Saccharomyces cerevisiae* [46]. More recently, atmospheric pressure and room temperature plasma (ARTP) were introduced to induce mutations in microorganisms [47]. According to Cao et al. [35], the particles produced by ARTP would activate the global response to DNA damage, the so-called SOS repair mechanism, with high fault tolerance level, producing a variety of mismatch sites in the repair process. Compared with the traditional targeted mutation methods (chemical or physical such as the use of UV), ARTP presents several advantages: (1) It diversifies DNA damages, thus increasing the mutation rates, and (2) ARTP is not toxic, and no harmful matter is involved in the mutation process. The rate of mutation is dependent on the power source, gas flow, the distance between the emission source and carrier, and the processing time [48]. The latter parameter is the most flexible. The longer the treatment, the higher the mutation and death rates (*Chlorella*: Cao et al. [35], *Crypthecodinium*: Liu et al. [37]). Because cell permeability changes according to cell development stage [25], the death rate varies accordingly as exemplified with the dinoflagellate *Crypthecodinium cohnii* [37]: it is higher when cells divide actively like during the exponential phase of growth. According to Wang et al. [48], the mutation rate and the positive mutation rate were calculated using the following equations:

$$\text{Mutation rate (RM)}\ (\%) = \text{M/T} \times 100 \tag{17.1}$$

and

$$\text{Positive mutation rate (RP)}\ (\%) = P/M \times 100 \tag{17.2}$$

where M is the total colony-forming unit of the mutant strains with changed phenotype compared with the wild strain, and P is the CFU of the mutants with an improved phenotype.

As high as 96% of the hydrogen energy is generated from fossil fuels, tarnishing its low-carbon image. It is known from a long time that microalgae such as *Chlamydomonas*, *Scenedesmus* or *Chlorella* are able to produce hydrogen, the so-called biohydrogen [49]. Such a possibility looks great because the process involves the photosynthetic machinery that also consumes CO_2, reinforcing the low-carbon potential of biohydrogen production. The protons and electrons needed by the biological process may be provided indirectly, i.e., through the degradation of intracellular carbon storage compounds such as starch (direct biophotolysis), or directly, i.e., from water splitting by water oxidase (direct biophotolysis) [49]. The former possibility will not be considered here because no paper describing the involvement of plasma treatment was reported. The bottleneck of the latter process

is the relatively low efficiency of the conversion of the energy associated with the absorbed photons into electrons and protons. One possibility for removing the bottleneck consists in reducing the cellular quota in Chl. This possibility has been successfully tested in land plants [50] and microalgae using targeted mutagenesis. Ban et al. [36] used the nontargeted mutagenesis capacity of ARTP to select mutants of the green microalga *Chlamydomonas reinhardtii* with a reduced Chl cellular quota to serve as biohydrogen producer. A mutant, named A4, presents a strongly reduced Chl content, probably ensuring a better light transmittance in the culture and within the cells (Table 17.1) allowing an increase in biohydrogen production. These results are in line with those obtained with mutants obtained using other methods (DNA insertion: Kosourov et al. [51], RNAi: Oey et al. [52], and targeted mutagenesis: Esquível et al. [53]).

17.3.4 Plasma and Downstream Processing

Regardless of the biotechnological process used and the final products obtained from algae, they all start with growing algae to obtain biomass. The interest of plasma technologies in this respect has been described above. Once produced, the biomass is harvested and processed according to a dedicated downstream program generally involving dewatering, drying, grinding, extraction, and purification steps: Drying, grinding, and extraction are the most popular steps. A critical assessment of current microalga bioprocessing technology reveals that downstream processing also poses a number of important technical and economic challenges [17]. There are several publications reporting the use of plasma technologies in different steps of the downstream process.

17.3.4.1 Algal Harvesting

In most cases, the biomass contained in a photobioreactor or in an open pond is rather diluted. Consequently, the first step of a downstream process consists in microalga harvesting. Traditionally, biomass dewatering is achieved using continuous centrifugation of the culture, yielding an alga paste [54]. Because this step is time- and energy-consuming i.e., it is costly and not friendly from the environment point of view, alternative processes, including flocculation, have been developed [55]. Flocculation uses polymers as flocculants to harvest the cultivated microalgae. Chitosan, a naturally large molecule with many functional groups such as free amino groups and hydroxyl groups has been considered as a possible flocculant [56]. Actually, cationic active groups in chitosan chains can neutralize negatively charged algal cells resulting in adsorption [57]. Unfortunately, chitosan is poorly soluble under neutral conditions [58], and grafted copolymers are used to improve water solubility and effectiveness of flocculation [59]. Copolymer rafting is usually initiated by chemical and radiation methods [60]. Recently, plasma-initiated polymerization

was introduced to prepare chitosan-based flocculants [61]. Using this method, Sun et al. [62] prepared an acrylamide and dimethyl diallyl ammonium chloride-grafted chitosan [CSg-P(AM-DMDAAC)] that was tested for its capacity to remove low-density microalgae. The flocculation performance of CS-gP(AM-DMDAAC) was found to be higher than those of other flocculants such as cationic polyacrylamide and polymeric aluminum and iron. Optimal flocculation (better than the commercially available) was obtained with a polymer composed of 20% monomer concentration and 7:3 polyacrylamide:chitosan ratio (40 W discharge power, 90 s discharge time, 50 °C post-polymerization temperature, and 24 h post-polymerization time) [63].

17.3.4.2 Dry Matter Treatment

The next steps in biomass processing consist in drying and extracting compounds from the biomass. As mentioned above, biohydrogen can be produced along different processes. Beside the nondestructive possibilities described in Sect. 17.3.3, biohydrogen can also be obtained through microalgal biomass destruction. The latter possibility may involve microwave-induced pyrolysis i.e., a thermal decomposition of organic components in an oxygen-free atmosphere to produce bio-oil, gas mixture (syngas), and charcoal (coal made by burning photosynthetic organisms) [64]. During pyrolysis, microwave heating may stimulate the breaking of compounds into gaseous molecules such as hydrogen. Many studies have been carried out in recent years to characterize the pyrolysis behavior of microalgae biomass [65]. Using an atmospheric pressure microwave plasma, Lin et al. [65] succeeded to pyrolyze the unicellular cyanobacterium *Spirulina* sp. Interestingly, the duration of the plasma treatment required for complete conversion of algae to hydrogen is almost independent of the reaction temperature. In contrast, the microwave power used in the reaction was found to be proportional to the rate of hydrogen production. The optimal hydrogen production rate was obtained with 1000 W discharge power. In this condition, 60 mg of hydrogen was produced from 1 g DW of *Spirulina* sp. [65].

17.4 Water and Wastewater Treatment

Global warming, anthropic activities, water pollution, and eutrophication of water bodies have increased the occurrence of algal and cyanobacterial blooms, degrading the quality of freshwater sources worldwide [66, 67]. Beside blocking filter beds in water supply treatment processes, deteriorating plug or corroding pipelines and increasing the amount of chlorination by-products, algal and cyanobacterial blooms are frequently associated with the accumulation in the water bodies (including drinking water reservoirs) of dangerous toxins and taste-and-odor-compounds [68]. Therefore, before further use, these types of water need to be treated. A first possibility consists in harvesting microalgae, a difficult task with low-algal load

waters. Among the different possibilities, coagulation–flocculation is the safest, most effective, and widely used because this treatment does not destroy algal cells, avoiding the eventual release of toxins in the medium [69]. Removing microalgae from water may however not be sufficient because during the process, toxins and taste-and-odor-compounds, including geosmin and 2-methylisoborneol, that are semi-volatile metabolites, might be released. Consequently, to avoid any risk, these compounds need to be destroyed. Beside physical methods such as activated carbon adsorption and filtration [69] and biological methods such as adsorption by tolerant organisms that are often affected by environmental factors [70], chemical methods involving advanced oxidation processes (photocatalysis, UV photolysis, ultrasonication, and ozone-based processes) appear as alternative methods. Dielectric barrier discharge (or DBD plasma) has been used to produce long lifetime ozone in air and short lifetime ROS in water or water vapor [71]. The capacity of ROS to oxidize any type of biological compounds can be exploited for developing a process aiming at inactivating microalgae that would pollute water bodies and/or water reservoirs [72]. For instance, Kim et al. [73] calculated a 89% efficiency in eliminating microalgae after a 24-h treatment of plasma. Using a similar method, Nisol et al. [74] eliminated the toxic filamentous cyanobacterium *Dolichospermum* sp. after a 6-min treatment (Table 17.2). A better understanding of the ROS action mechanism(s) on microalgae would greatly help in optimizing the process. Electronic microscope pictures showed surface modification, i.e., shrinkage before disruption [73] (Fig. 17.4).

Zhang et al. [75] degraded the cyanobacterial toxin microcystin-LR, using glow discharge plasma generated above the water surface. In this process, reactions occur only at the gas-solution interface, resulting in a limitation on the rate of degradation. In the same manner, Jo et al. [76] applied atmospheric pressure underwater plasma system for decomposing two odorous organic compounds, geosmin and 2-methyl isoborneol, from cyanobacteria. Chlorinated volatile organic compounds (CleVOCs) such as chloromethane, chloroethane, chloroethylene and aromatic chlorides belong to an another family of compounds produced directly or indirectly by microalgae [77]. Beside their unpleasant smell, these compounds are harmful for the environment and health [78, 79]. Chemical, physical and biological methods have been proposed for air treatment [78–80]. Biological processes involve several steps such as absorption, diffusion, and biodegradation. The efficiency of the process requires the involvement of resistant microorganisms as well as a good mass transfer between the different steps, a transfer that can be difficult when less-water-soluble CleVOCs are considered [81]. Non-thermal plasma (NTP), eventually coupled to another method, has been proposed as a pretreatment step to facilitate the mass transfer because it could convert less-water-soluble CleVOCs to more soluble intermediates [82]. Coupling DBD with biotrickling filters allowed Jiang et al. [83] to reduce significantly the number of by-products and to improve both the water solubility and biodegradability of the intermediates of waste air containing 1,2-dichloroethane.

Table 17.2 Summary of the effectiveness of plasma treatment for the eradication of microalgae from wastewater

		Plasma type	Time of exposure	Efficiency (%)	Remaining nonviable (%)	References
Groups	Taxa					
Cyanobacteria	–	Cold plasma	24 h	88.8–94		[73]
Cyanobacteria	*Dolichospermum* sp.	Cold plasma	6 min	87.0	80	[74]
Green alga	*Scenedesmus* sp.	Cold plasma	6 min	< 87.0	–	[74]

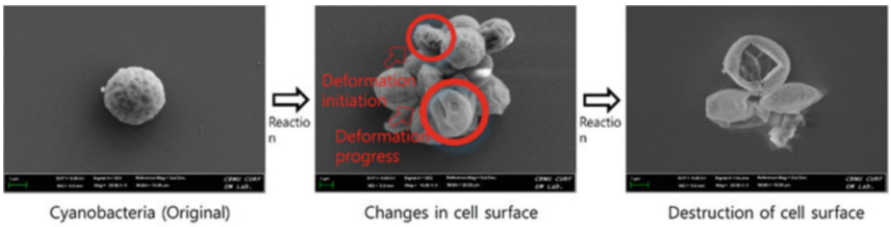

Fig. 17.4 Scanning electron microscopy image showing the morphological modifications induced by the plasma treatment of blooming cyanobacteria. Reprinted from Kim et al. [73]

Because NTP can be lethal (see above), the treatment was also limiting the biodiversity and abundance of the microbial community involved in the process. Metals and especially heavy metals are another kind of water pollutants needed to be removed because they are toxic for living organisms [4]. Dead microalgal biomass has been considered as a mean for water decontamination of polluting metals [84]. Mahan et al. [85] tested three taxa belonging to green algae (i.e., *Stichococcus bacillaris*, *Chlamydomonas reinhardtii*, and *Chlorella pyrenoidosa*) for their capacity to quench heavy metals. The determination of metal bound to the dead biomass using ICP coupled to different ionization processes revealed the high binding capacity of microalgae for Pb, Fe, Cu, Ni, Zn, Cd, Sr [85], Hg [86], and Au [87].

17.5 Plasma and Intracellular Metal Analysis

It is well established that an unbalance in metal elements may cause severe troubles to cells, including microalgae [4, 88]. It is thus crucial in many studies to quantify the cellular composition in metals, heavy metals, and other nonmetal elements. The determination of the intracellular metal quota usually involves sample digestion [41] for further analyses using total reflection X-ray fluorescence (TXRF), particle-induced X-ray fluorescence (PIXE) [89], electrothermal atomic absorption spectrometry (ETAAS), inductively coupled plasma-atomic emission spectrometry (ICP-AES), and/or inductively coupled plasma-mass spectrometry (ICP-MS) [90]. Commonly, ICP-MS is hyphenated with a tool that is used to separate the compounds of interest from the other compounds before MS analysis. For instance, Bednarik et al. [91] used thin-layer chromatography as an alternative to HPLC to determine the selenoamino acids by diode laser thermal vaporization ICP MS (DLTV ICP MS), whereas Li et al. [92] used capillary electrophoresis-coupled IPC (CE-IPC MS) to determine Pb(II) ions, trimethyl lead, and triethyl lead in seaweeds. These tools are however inadequate for individual cell study. This limitation has recently been overcome through the emergence of single cell-inductively coupled plasma-mass spectrometry (SC-ICP-MS). SC-ICP-MS

technology consists in the introduction of cells into the ICP-MS system using a modified nebulizer working in conjunction with a peristaltic pump delivering small volumes of a cell suspension into the spray chamber. Optimizing cell concentration and flow rate allows individual cells to enter the plasma. Cells become ionized in the plasma as discrete plumes that are subsequently detected as pulsed signals by the mass spectrometer. Three types of information are derived from the signal: (1) the elemental mass of compounds in an individual (proportional to the pulsed signal), (2) the cell concentration within the cell suspension (related to the pulse signal frequency), and (3) the extracellular concentration of an analyte within the cell suspension (the baseline signal in the absence of a pulse) [93]. Using SC-ICP-MS, Shen et al. [93] monitored the cell status and quantified copper uptake and accumulation by the toxic cyanobacterium *Microcystis aeruginosa* following exposure to copper-based algaecides. The optimized protocol allows the detection of cell suspensions directly after suitable dilution avoiding cell preparation steps such as washings and re-suspensions, allowing fast time-course measurement (1–4 h depending on the concentration) after the herbicide application [93]. Developments of SC-ICP-MS will probably make this technique a major tool for microalgal components analysis. Table 17.3 summarizes the type of components addressed by this method in microalga.

17.6 Conclusions and Perspectives

In this chapter, we summarized how plasma technology can be combined with different fields dealing with microalgae. Clearly, plasma technology is a very promising tool for the optimization of microalga technology and biotechnology. The introduction of plasma in biology is rather recent. A literature search revealed a first publication early in the twenty-first century (Fig. 17.5). Since then, the field is developing slowly but regularly (Fig. 17.5) and arouses interest as the yearly citation number increases. Let's bet it will continue, making the combination of plasma technology and microalgae a major interface between biology, chemistry, and physics.

Table 17.3 Intracellular metal and metal complexes quantification using ICP-MS

		Heavy metals						
		Cu	Mg	Cell concentration	Selenomethionine	Selenocysteine	As (III)	As (V)
Extracellular		1μg L^{-1} [93]	0.2μg L^{-1} [93]					
Cyanobacteria	*Microcystis aeruginosa*	65 ag $cell^{-1}$ [93]	98 ag $cell^{-1}$	3000 mL^{-1} [93]				
Chlorophyta	*Chlorella vulgaris, strain R117*	–	–	–	161–197μg g^{-1} [91]	196–247μg g^{-1} [91]		
	Chlorella vulgaris						6.1 ± 0.4μg g^{-1} [94]	11.8 ± 0.5μg g^{-1} [94]

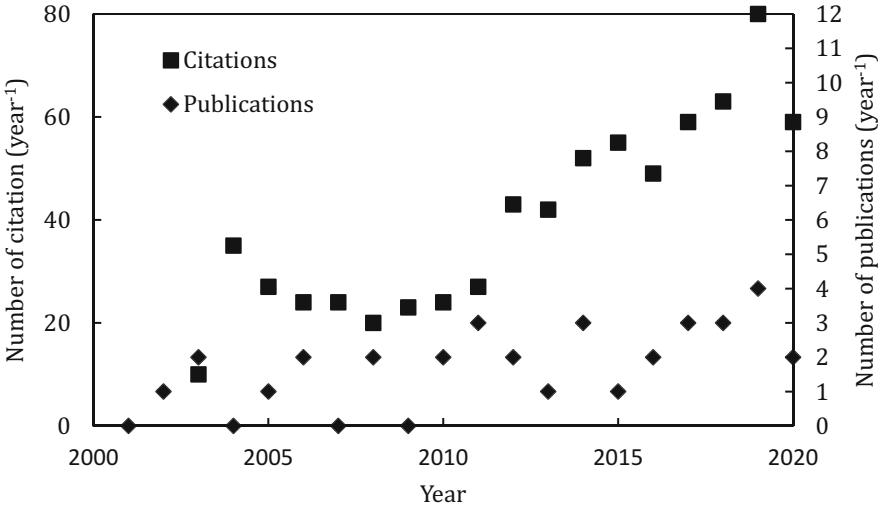

Fig. 17.5 Bibliometry data concerning the field "plasma and microalgae." The data obtained after interrogating Web of Science with the question "TITLE: (plasma* not (membrane* or plasma-lemma*)) AND TITLE: (alga or algae or algal)" (September 2020)

References

1. Mimouni V, Ulmann L, Pasquet V, Mathieu M, Picot L, Bougaran G, Cadoret J-P, Morant-Manceau A, Schoefs B. The potential of microalgae for the production of bioactive molecules of pharmaceutical interest. Curr Pharm Biotechnol. 2012;13:2733–50.
2. Hopes A, Mock T. Evolution of microalgae and their adaptations in different marine ecosystems. eLS. 2015:1–9.
3. Schoefs B, van de Vijver B, Wetzel C, Ector L. From diatom species identification to ecological and biotechnological applications. Bot Lett. 2020;167:2–6.
4. Masmoudi S, Nguyen-Deroche N, Caruso A, Ayadi H, Morant-Manceau A, Tremblin G, Bertrand M, Schoefs B. Cadmium, copper, sodium and zinc effects on diatoms: from heaven to hell - a review. Cryptogam Algol. 2013;34:185–223.
5. Coale KH, Johnson KS, Fitzwater SE, Gordon RM, Tanner S, Chavez FP, Ferioli L, Sakamoto C, Rogers P, Millero F, Steinberg P, Nightingale P, Cooper D, Cochlan WP, Landry MR, Constantinou J, Rollwagen G, Trasvina A, Kudela R. A massive phytoplankton bloom induced by an ecosystem-scale iron fertilization experiment in the equatorial Pacific Ocean. Nature. 1996;383:495–501.
6. Parker MS, Mock T, Armbrust EV. Genomic insights into marine microalgae. Annu Rev Genet. 2008;42:619–45.
7. Heydarizadeh P, Veidl B, Huang B, Lukomska E, Wielgosz-Collin G, Couzinet-Mossion A, Bougaran G, Marchand J, Schoefs B. Carbon orientation in the diatom Phaeodactylum tricornutum: the effects of carbon limitation and photon flux density. Front Plant Sci. 2019;10:471.
8. Moss R, Edmonds J, Hibbard K, Manning M, Rose S, Vuuren D, Carter T, Emori S, Kainuma M, Kram T, Meehl G, Mitchell J, Nakicenovic N, Riahi K, Smith S, Ronald S, Thomson A, Weyant J, Wilbanks T. The next generation of scenarios for climate change research and assessment. Nature. 2010;463:747–56.

9. Gordon D, Merz CR, Gurke S, Schoefs B. Bubble farming: scalable microcosms for diatom biofuel and the next green revolution. In: Seckbach J, Gordon R, editors. Diatoms: fundamentals & applications. Beverly, MA: Wiley-Scrivener; 2019.
10. Kirubakaran A, Jain S, Nema RK. A review on fuel cell technologies and power electronic interface. Renew Sust Energ Rev. 2009;13:2430–40.
11. Verhelst S, Wallner T. Hydrogen-fueled internal combustion engines. Prog Energy Combust Sci. 2009;35:490–527.
12. Ainas M, Hasnaoui S, Bouarab R, Abdi N, Drouiche N, Mameri N. Hydrogen production with the cyanobacterium Spirulina platensis. Int J Hydrog Energy. 2017;42:4902–7.
13. Heydarizadeh P, Poirier I, Loizeau D, Ulmann L, Mimouni V, Schoefs B, Bertrand M. Plastids of marine phytoplankton produce bioactive pigments and lipids. Mar Drugs. 2013;11:3425–71.
14. Scarsini M, Marchand J, Schoefs B. Carotenoid overproduction in microalgae: biochemical and genetic engineering. In: Jacob-Lopes E, Queiroz MI, Zepka LQ, editors. Pigments from microalgae handbook. Cham: Springer International Publishing; 2020.
15. Babaei A, Ranglová K, Malapascua JR, Masojídek J. The synergistic effect of selenium (selenite, $-SeO_3^{2-}$) dose and irradiance intensity in Chlorella cultures. AMB Express. 2017;7:56.
16. Gojkovic Ž, Vílchez C, Torronteras R, Vigara J, Gómez-Jacinto V, Janzer N, Gómez-Ariza J-L, Márová I, Garbayo I. Effect of selenate on viability and selenomethionine accumulation of Chlorella sorokiniana grown in batch culture. Sci World J. 2014;2014:401265.
17. Vinayak V, Manoylov KM, Gateau H, Blanckaert V, Herault J, Pencreac'h G, Marchand J, Gordon R, Schoefs B. Diatom milking: a review and new approaches. Mar Drugs. 2015;13:2629–65.
18. Graves DB. The emerging role of reactive oxygen and nitrogen species in redox biology and some implications for plasma applications to medicine and biology. J Phys D Appl Phys. 2012;45:263001.
19. Okada T, Chang C-Y, Kobayashi M, Shimizu T, Sasaki M, Kumagai S. Plasma-on-chip device for stable irradiation of cells cultured in media with a low-temperature atmospheric pressure plasma. Arch Biochem Biophys. 2016;605:11–8.
20. Kitazaki S, Koga K, Shiratani M, Hayashi N. Growth enhancement of radish sprouts induced by low pressure O_2 radio frequency discharge plasma irradiation. Jpn J Appl Phys. 2012;51:01AE01.
21. Straňák V, Špatenka P, Tichý M, Koller J, Kříha V, Scholtz V. Surfatron plasma-based sterilisation. Czechoslov J Phys. 2006;56:B843–7.
22. Lemoine Y, Schoefs B. Secondary ketocarotenoid astaxanthin biosynthesis in algae: a multifunctional response to stress. Photosynth Res. 2010;106:155–77.
23. Rusanov VD, Fridman AA, Sholin GV. The physics of a chemically active plasma with nonequilibrium vibrational excitation of molecules. Soviet Phys Uspekhi. 1981;24:447–74.
24. Laroussi M, Mendis DA, Rosenberg M. Plasma interaction with microbes. New J Phys. 2003;5:41.
25. Gateau H, Blanckaert V, Veidl B, Burlet-Schiltz O, Pichereaux C, Gargaros A, Marchand J, Schoefs B. Application of pulsed electric fields for the biocompatible extraction of proteins from the microalga Haematococcus pluvialis. Bioelectrochemistry. 2021;137:107588.
26. Bachrach E, Lefèvre M. Contribution à l'étude du rôle de la silice chez les êtres vivants. Observ Biol Diat J Physiol Pathol Gén. 1929;27:241–9.
27. Martin-Jézéquel V, Hildebrand M, Brzezinski MA. Silicon metabolism in diatoms: implications for growth. J Phycol. 2000;36:821–40.
28. Saxena A, Prakash K, Phogat S, Singh PK, Tiwari A. Inductively coupled plasma nanosilica based growth method for enhanced biomass production in marine diatom algae. Bioresour Technol. 2020:314.
29. Barros AI, Gonçalves AL, Simões M, Pires JCM. Harvesting techniques applied to microalgae: a review. Renew Sust Energ Rev. 2015;41:1489–500.

30. Tarrade J, Darmanin T, Taffin de Givenchy E, Guittard F, Debarnot D, Poncin-Epaillard F. Texturation and superhydrophobicity of polyethylene terephthalate thanks to plasma technology. Appl Surf Sci. 2014;292:782–9.
31. Almarashi JQM, El-Zohary SE, Ellabban MA, Abomohra AE-F. Enhancement of lipid production and energy recovery from the green microalga Chlorella vulgaris by inoculum pretreatment with low-dose cold atmospheric pressure plasma (CAPP). Energy Convers Manag. 2020;204:112314.
32. Tang YZ, Lu XP, Laroussi M, Dobbs FC. Sublethal and killing effects of atmospheric-pressure, nonthermal plasma on eukaryotic microalgae in aqueous media. Plasma Process Polym. 2008;5:552–8.
33. Fang M, Jin L, Zhang C, Tan Y, Jiang P, Ge N, Heping L, Xing X. Rapid mutation of Spirulina platensis by a new mutagenesis system of atmospheric and room temperature plasmas (ARTP) and generation of a mutant library with diverse phenotypes. PLoS One. 2013;8:e77046.
34. Choi JI, Yoon M, Joe M, Park H, Lee SG, Han SJ, Lee PC. Development of microalga Scenedesmus dimorphus mutant with higher lipid content by radiation breeding. Bioprocess Biosyst Eng. 2014;37:2437–44.
35. Cao S, Zhou X, Jin W, Wang F, Tu R, Han S, Chen H, Chen C, Xie GJ, Ma F. Improving of lipid productivity of the oleaginous microalgae Chlorella pyrenoidosa via atmospheric and room temperature plasma (ARTP). Bioresour Technol. 2017;244:1400–6.
36. Ban S, Lin W, Luo Z, Luo J. Improving hydrogen production of Chlamydomonas reinhardtii by reducing chlorophyll content via atmospheric and room temperature plasma. Bioresour Technol. 2019;275:425–9.
37. Liu B, Sun Z, Ma X, Yang B, Jiang Y, Wei D, Chen F. Mutation breeding of extracellular polysaccharide-producing microalga Crypthecodinium cohnii by a novel mutagenesis with atmospheric and room temperature plasma. Int J Mol Sci. 2015;16:8201–12.
38. Schoefs B. Chlorophyll and carotenoid analysis in food products. A practical case-by-case view. Trends Anal Chem. 2003;22:335–9.
39. Schoefs B. Determination of pigments in vegetables. J Chromatogr A. 2004;1054:217–26.
40. Nguyen-Deroche TLNN, Caruso A, Le TT, Viet Bui T, Schoefs B, Tremblin G, Morant-Manceau A. Zinc affects differently growth, photosynthesis, antioxidant enzyme activities and phytochelatin synthase expression of four marine diatoms. Sci World J. 2012;15:982957.
41. Roháček K, Bertrand M, Moreau B, Jacquette J, Caplat C, Morant-Manceau A, Schoefs B. Relaxation of the non-photochemical chlorophyll fluorescence quenching in diatoms: kinetics, components and mechanisms. Philos Trans R Soc B Biol Sci. 2014;369:20130241.
42. Heydarizadeh P, Boureba W, Zahedi M, Huang B, Moreau B, Lukomska E, Couzinet-Mossion-A, Wielgosz-Collin G, Martin-Jezequel V, Bougaran G, Marchand J, Schoefs B. Response of CO_2-starved diatom Phaeodactylum tricornutum to light intensity transition. Philos Trans R Soc B Biol Sci. 2017;372:20160396.
43. Wang M, Yang Y, Chen Z, Chen Y, Wen Y, Chen B. Removal of nutrients from undiluted anaerobically treated piggery wastewater by improved microalgae. Bioresour Technol. 2016;222:130–8.
44. Zhang Y, He M, Zou S, Fei C, Yan Y, Zheng S, Rajper AA, Wang C. Breeding of high biomass and lipid producing Desmodesmus sp. by ethylmethane sulfonate-induced mutation. Bioresour Technol. 2016;207:268–75.
45. Xu Z. Recent progress on atmospheric and room temperature plasma mutation breeding technology and its applications. CIESC J. 2014;65:2676–84.
46. Chen H, Bai F, Xiu Z. Oxidative stress induced in Saccharomyces cerevisiae exposed to dielectric barrier discharge plasma in air at atmospheric pressure. IEEE Trans Plasma Sci. 2010;38:1885–91.
47. Li X, Liu R, Li J, Chang M, Liu Y, Jin Q, Wang X. Enhanced arachidonic acid production from Mortierella alpina combining atmospheric and room temperature plasma (ARTP) and diethyl sulfate treatments. Bioresour Technol. 2015;177:134–40.

48. Wang LY, Huang ZL, Li G, Zhao HX, Xing XH, Sun WT, LI HP, Gou ZX, Bao CY. Novel mutation breeding method for Streptomyces avermitilis using an atmospheric pressure glow discharge plasma. J Appl Microbiol. 2010;108:851–8.
49. Khetkorn W, Rastogi RP, Incharoensakdi A, Lindblad P, Madamwar D, Pandey A, Larroche C. Microalgal hydrogen production – A review. Bioresour Technol. 2017;243:1194–206.
50. Jenkins CL, Edwards GE, Andrews J. Reduction in chlorophyll content without a corresponding reduction in photosynthesis and carbon assimilation enzymes in yellow-green oil yellow mutants of maize. Photosynth Res. 1989;20:191–205.
51. Kosourov SN, Ghirardi ML, Seibert M. A truncated antenna mutant of Chlamydomonas reinhardtii can produce more hydrogen than the parental strain. Int J Hydrog Energy. 2011;36:2044–8.
52. Oey M, Ross IL, Stephens E, Steinbeck J, Wolf J, Radzun KA, Kügler J, Ringsmuth AK, Kruse O, Hankamer B. RNAi knock-down of LHCBM1, 2 and 3 increases photosynthetic H_2 production efficiency of the green alga Chlamydomonas reinhardtii. PLoS One. 2013;8:e61375.
53. Esquível MG, Amaro HM, Pinto TS, Fevereiro PS, Malcata FX. Efficient H_2 production via Chlamydomonas reinhardtii. Trends Biotechnol. 2011;29:595–600.
54. Singh M, Shukla R, Das KC. Harvesting of microalgal biomass. In: BUX F, editor. Biotechnological applications of microalgae: biodiesel and value added products. Boca Raton: Taylor and Francis Group; 2013.
55. Pugazhendhi A, Shobana S, Bakonyi P, Nemestóthy N, Xia A, Banu JR, Kumar G. A review on chemical mechanism of microalgae flocculation via polymers. Biotechnol Rep. 2019;21:e00302.
56. Lu Y, Shang Y, Huang X, Chen A, Yang Z, Jiang Y, Cai J, Gu W, Qian X, Yang H, Cheng R. Preparation of strong cationic chitosan-graft-polyacrylamide flocculants and their flocculating properties. Ind Eng Chem Res. 2011;50:7141–9.
57. Thakur VK, Thakur MK. Recent advances in graft copolymerization and applications of chitosan: a review. ACS Sustain Chem Eng. 2014;2:2637–52.
58. Jia S, Yang Z, Ren K, Tian Z, Dong C, Ma R, Yu G, Yang W. Removal of antibiotics from water in the coexistence of suspended particles and natural organic matters using amino-acid-modified-chitosan flocculants: A combined experimental and theoretical study. J Hazard Mater. 2016;317:593–601.
59. Wang J-P, Chen Y-Z, Ge X-W, Yu H-Q. Gamma radiation-induced grafting of a cationic monomer onto chitosan as a flocculant. Chemosphere. 2007;66:1752–7.
60. Wang J-P, Chen Y-Z, Zhang S-J, Yu H-Q. A chitosan-based flocculant prepared with gamma-irradiation-induced grafting. Bioresour Technol. 2008;99:3397–402.
61. Yu J, Gege Y, Yuanpei P, Quanfang L, Wu Y, Jinzhang G. Poly (acrylamide-co-acrylic acid) hydrogel induced by glow-discharge electrolysis plasma and its adsorption properties for cationic dyes. Plasma Sci Technol. 2014;16:767.
62. Sun YJ, Zhu CY, Sun WQ, Xu YH, Xiao XF, Zheng HL, Wu HF, Liu CY. Plasma-initiated polymerization of chitosan-based CS-g-P(AM-DMDAAC) flocculant for the enhanced flocculation of low-algal-turbidity water. Carbohydr Polym. 2017;164:222–32.
63. Sun YJ, Ren MJ, Sun WQ, Xiao XF, Xu YH, Zheng HL, Wu HF, Liu ZY, Zhu H. Plasma-induced synthesis of chitosan-g-polyacrylamide and its flocculation performance for algae removal. Environ Technol. 2019;40:954–68.
64. Brennan L, Owende P. Biofuels from microalgae—A review of technologies for production, processing, and extractions of biofuels and co-products. Renew Sust Energ Rev. 2010;14:557–77.
65. Lin KC, Lin YC, Hsiao YH. Microwave plasma studies of Spirulina algae pyrolysis with relevance to hydrogen production. Energy. 2014;64:567–74.
66. Paerl HW, Paul VJ. Climate change: links to global expansion of harmful cyanobacteria. Water Res. 2012;46:1349–63.

67. Zamyadi A, Mcquaid N, Dorner S, Bird D, Burch M, Baker P, Hobson P, Prevost M. Cyanobacterial detection using in vivo fluorescence probes: managing interferences for improved decision-making. J Am Water Works Assoc. 2012;104:E466–79.
68. Lawton LA, Robertson PKJ, Robertson RF, Bruce FG. The destruction of 2-methylisoborneol and geosmin using titanium dioxide photocatalysis. Appl Catal B Environ. 2003;44:9–13.
69. Rashid N, Rehman SU, Han J-I. Rapid harvesting of freshwater microalgae using chitosan. Process Biochem. 2013;48:1107–10.
70. Chen X, Yang X, Yang L, Xiao B, Wu X, Wang J, Wan H. An effective pathway for the removal of microcystin LR via anoxic biodegradation in lake sediments. Water Res. 2010;44:1884–92.
71. Lebout H. Fifty years of ozonation at nice. Ozone Chemistry and Technology. Washington, DC: American Chemical Society; 1959.
72. Mizukoshi Y, Matsuda Y, Yamanaka S, Ikeno T, Haraguchi K, Goda N, Nishimura Y, Yamamoto K. Deactivation of algae by plasma generated in seawater flow. Chem Lett. 2018;47:116–8.
73. Kim HJ, Nam GS, Jang JS, Won CH, Kim HW. Cold plasma treatment for efficient control over algal bloom products in surface water. Water. 2019;11:1513.
74. Nisol B, Watson S, Leblanc Y, Moradinejad S, Wertheimer MR, Zamyadi A. Cold plasma oxidation of harmful algae and associated metabolite BMAA toxin in aqueous suspension. Plasma Processes Polymers. 2019;16:e1800137.
75. Zhang H, Huang Q, Ke Z, Yang L, Wang X, Yu Z. Degradation of microcystin-LR in water by glow discharge plasma oxidation at the gas–solution interface and its safety evaluation. Water Res. 2012;46:6554–62.
76. Jo JO, Kim SD, Lee HJ, Mok YS. Decomposition of taste-and-odor compounds produced by cyanobacteria algae using atmospheric pressure plasma created inside a porous hydrophobic ceramic tube. Chem Eng J. 2014;247:291–301.
77. Achyuthan KE, Harper JC, Manginell RP, Moorman MW. Volatile metabolites emission by in vivo microalgae-an overlooked opportunity? Meta. 2017;7:39.
78. Li T, Li H, Li C. A review and perspective of recent research in biological treatment applied in removal of chlorinated volatile organic compounds from waste air. Chemosphere. 2020;250:126338.
79. Tsai WT. Fate of chloromethanes in the atmospheric environment: implications for human health, ozone formation and depletion, and global warming impacts. Toxics. 2017;5:23.
80. Li C, Zhao Y, Song H, Li H. A review on recent advances in catalytic combustion of chlorinated volatile organic compounds. J Chem Technol Biotechnol. 2020;95:2069–82.
81. Ye J-X, Lin T-H, Hu J-T, Poudel R, Cheng Z-W, Zhang S-H, Chen J-M, Chen D-Z. Enhancing chlorobenzene biodegradation by Delftia tsuruhatensis using a water-silicone oil biphasic system. Int J Environ Res Public Health. 2019;16:1629.
82. Schiavon M, Torretta V, Casazza A, Ragazzi M. Non-thermal plasma as an innovative option for the abatement of volatile organic compounds: A review. Water Air Soil Pollut. 2017;228:388.
83. Jiang L, Li S, Cheng Z, Chen J, Nie G. Treatment of 1,2-dichloroethane and n-hexane in a combined system of non-thermal plasma catalysis reactor coupled with a biotrickling filter. J Chem Technol Biotechnol. 2018;93:127–37.
84. Lin Z, LI J, Luan Y, Dai W. Application of algae for heavy metal adsorption: A 20-year meta-analysis. Ecotoxicol Environ Saf. 2020;190:110089.
85. Mahan CA, Majidi V, Holcombe JA. Evaluation of the metal uptake of several algae strains in a multicomponent matrix utilizing coupled plasma emission spectrometry. Anal Chem. 1989;61:624–7.
86. Mitchell PG, Greene B, Sneddon J. Direct determination of mercury in solid algal cells by direct-current argon-plasma emission-spectrometry with sample introduction by electrothermal vaporization. Mikrochim Acta. 1986;1:249–58.

87. Greene B, Mitchell PG, Sneddon J. Direct determination of gold in solid algal cells by direct-current argon plasma emission-spectrometry with introduction by electrothermal atomization. Spectrosc Lett. 1986;19:101–11.
88. Bertrand M, Schoefs B, Siffel P, Rohacek K, Molnar I. Cadmium inhibits epoxidation of diatoxanthin to diadinoxanthin in the xanthophyll cycle of the marine diatom Phaeodactylum tricornutum. FEBS Lett. 2001;508:153–6.
89. Bertrand M, Weber G, Schoefs B. Metal determination and quantification in biological material using particle-induced X-ray emission. TrAC Trends Anal Chem. 2003;22:254–62.
90. Cerchiaro G, Manieri TM, Bertuchi FR. Analytical methods for copper, zinc and iron quantification in mammalian cells. Metallomics. 2013;5:1336–45.
91. Bednarik A, Kuta J, Vu DL, Ranglova K, Hrouzek P, Kanicky V, Preisler J. Thin-layer chromatography combined with diode laser thermal vaporization inductively coupled plasma mass spectrometry for the determination of selenomethionine and selenocysteine in algae and yeast. J Chromatogr A. 2018;1533:199–207.
92. Li JX, Sun CJ, Zheng L, Jiang FH, Yin XF, Chen JH, Wang XR. Determination of lead species in algae by capillary electrophoresis-inductively coupled plasma-mass spectrometry. Chin J Anal Chem. 2016;44:1659–64.
93. Shen X, Zhang HT, He XL, Shi HL, Stephan C, Jiang H, Wan CH, Eichholz T. Evaluating the treatment effectiveness of copper-based algaecides on toxic algae Microcystis aeruginosa using single cell-inductively coupled plasma-mass spectrometry. Anal Bioanal Chem. 2019;411:5531–43.
94. Salgado SG, Nieto MAQ, Simon MMB. Determination of soluble toxic arsenic species in alga samples by microwave-assisted extraction and high performance liquid chromatography-hydride generation-inductively coupled plasma-atomic emission spectrometry. J Chromatogr A. 2006;1129:54–60.